Nucleophilic Fluorination Under Synergistic Hydrogen Bonding Phase-Transfer Catalysis

A thesis submitted to the Board of the Faculty of Physical Sciences, in partial fulfilment of the requirements for the degree of Doctor of Philosophy at the University of Oxford.

Claire Dooley

Balliol College

University of Oxford

Hilary Term 2025

Author's Declaration

The work presented in this thesis was conducted under the supervision of Prof. Véronique Gouverneur at the Department of Chemistry, University of Oxford. All of the work is my own, unless otherwise stated, and has not been submitted for any other degree at this or any other university.

Claire Dooley

January 2025

Table of Contents

Abstract v
Acknowledgements vii
Abbreviations ix

1. Introduction 1
1.1. Fluorine in Modern Day Chemistry 1
1.2. Properties of the C–F Bond 3
1.2.1. Acidity and Metabolic Stability 3
1.2.2. Bioisosterism 4
1.2.3. Conformational Properties 6
1.2.3.1. Dipole-dipole Interactions 6
1.2.3.2. Gauche Effect 7
1.2.4. Hydrogen Bonding 9
1.3. Natural Occurrence of Fluorine 11
1.4. Fluorine in Organic Synthesis 13
1.5. Fluorinating Reagents in Asymmetric Synthesis 15
1.5.1. Prologue to Asymmetric Synthesis 15
1.5.2. Asymmetric Electrophilic Fluorination 16
1.5.3. Asymmetric Nucleophilic Fluorination 24
1.5.4. Asymmetric Biocatalytic Fluorination 33
1.5.5. Nucleophilic Fluorination with Alkali Metal Fluoride Salts 34
1.6. Conclusions 39
1.7. References 40

2. Development of a Strategy for Nucleophilic Fluorination under Synergistic Hydrogen Bonding Phase Transfer Catalysis 46
2.1. Introduction 46
2.1.1. Hydrogen Bonding Phase Transfer Catalysis (HBPTC) 46
2.1.2. Extension of the Electrophilic and Nucleophilic Scope of HBPTC 51
2.1.3. New Approach for the Fluorination of Neutral, Unsymmetrical Electrophiles 53
2.2. Results and Discussion 55
2.2.1. Preliminary Investigations 55
2.2.2. Lewis Base Additives 58
2.3. Phosphonium Salts as Phase Transfer Catalysts 63

2.3.1. Role of the Phosphonium Salt 65
2.4. Reaction Development of Urea-Onium PT System 70
2.4.1. Optimisation of Onium Salt Co-catalyst 70
2.4.2. Evaluation of Fluoride Sources 72
2.4.3. Synthesis and Optimisation of Urea HBD Catalysts 73
2.4.4. Solvent Effect 79
2.4.5. Temperature Effect 82
2.4.6. Scope – Benzylic Fluorination 84
2.5. Evaluation of Other Electrophiles under S-HBPTC 87
2.5.1. Introduction to Asymmetric α-Halogenation of Ketones 87
2.5.2. Optimisation for the Fluorination of α-Bromoketones under S-HBPTC 89
2.5.3. Scope – Fluorination of α-Bromoketones 94
2.6. Conclusions 96
2.7. References 97

3. Mechanistic Investigations into Fluorination Under Synergistic HBPTC 99
3.1. Introduction 99
3.2. NMR Study of Complexes Between Urea HBD Catalysts and Onium Salts with KF 100
3.2.1. Characterisation of Unbound Urea Catalyst 101
3.2.2. Characterisation of a Ternary Urea-Phosphonium-Fluoride Complex 104
3.2.3. Elucidation of Ion-Pair Structure in Solution 110
3.2.4. Urea-Phosphonium-Fluoride Complexes Formed with Tetradentate Catalyst 114
3.2.5. Urea-Phosphonium-Fluoride Complexes as Reactive Fluorinating Reagent 118
3.3. Effect of Catalytic Iodide on Reaction Rate 119
3.4. Kinetics 126
3.4.1. Introduction to Kinetic Isotope Effects 126
3.4.2. Aims of the Experiment 128
3.4.3. Design of Experimental Set-up 129
3.4.4. Results and Discussion 130
3.4.5. Kinetic Isotope Effect Employing TBAF as Fluoride Source 135
3.4.6. Summary of Results 136
3.5. Mechanistic Investigations into Enantioconvergence 137
3.5.1 Introduction to Enantioconvergent Nucleophilic Substitution Reactions 137
3.5.2. Monitoring Enantiomeric Ratios Over Time 142
3.5.3. Racemisation of Enantioenriched Substrate 147
3.5.4. Non-linear Effect Studies 150

3.5.5. Transition State Analyses 153
3.6. Conclusions and Implications on Catalysis 155
3.7. References 157

4. Experimental 158
4.1. General Information 158
4.2. Urea Catalyst Synthesis and Characterisation 160
4.2.1. Synthesis of Alkylated BINAM Intermediates 160
4.2.2. Catalyst Synthesis 163
4.3. Substrate Synthesis and Characterisation 184
4.3.1. Synthesis of Benzylic Bromide Precursors 184
4.3.2. Synthesis of Benzylic Bromides 198
4.3.3. Synthesis of α-Bromoketones 213
4.4. Synthesis of Onium Salts 218
4.5. General Procedure for Fluorination under S-HBPTC 220
4.5.1. General Procedure for Enantioselective Benzylic Fluorination 220
4.5.2. General Procedure for Enantioselective Fluorination of α-Haloketones 220
4.5.3. General Procedure for Synthesis of Racemic Standards 220
4.5.4. Synthesis and Characterisation of Benzylic Fluoride Products 221
4.5.5. Synthesis and Characterisation of α-Fluoroketone Products 239
4.6. Synthesis of Deuterated Precursors and Substrates 247
4.7. Synthesis of Enantioenriched Precursors and Substrates 250
4.8. NMR Investigations 251
4.8.1. Assignment of Urea Catalyst (*S*)-**3u** and Copies of NMR Spectra 251
4.8.2. Assignment of UPF Complex and Copies of NMR Spectra 258
4.8.3. HOESY 267
4.8.4. $^{1}H–^{19}F$ CLIP-HSQC 269
4.9. Kinetics 270
4.9.1. Kinetic Isotope Effect Study 270
4.9.2. Calculation of KIE Values 280
4.10. References 288

Abstract

Chapter 1 – Introduction

This chapter aims to highlight the importance of fluorination in modern life science with emphasis to its presence in the pharmaceutical, agrochemical and materials industry. Fluorine's unique properties and the effect of its substitution within molecules is described, as well as the origins of the fluorinating reagents which are prevalent in organic synthesis. Finally, the chapter provides a concise overview of asymmetric fluorination methodologies, covering both electrophilic and nucleophilic fluorine sources.

Chapter 2 - Development of an Enantioconvergent Nucleophilic Substitution under Synergistic Hydrogen Bonding Phase Transfer Catalysis with Potassium Fluoride

Chapter 2 outlines the discovery and development of a nucleophilic fluorination strategy for neutral electrophiles, benzylic bromides, using potassium fluoride (KF). Motivated by the Gouverneur group's interest in Hydrogen Bonding Phase-Transfer Catalysis (HBPTC) led to the development of a synergistic approach employing two-phase transfer agents, an onium halide salt and chiral *bis*-urea hydrogen bond donor catalysts. This combination of catalysts was critical for the solubilisation and subsequent reactivity of KF for the fluorination of a scope of benzylic halides providing fluorinated products in high yields and enantioselectivities. Furthermore, this method was demonstrated to be applicable towards a second class of neutral electrophiles – α-bromoketones.

Chapter 3 - Mechanistic Investigations into Fluorination under Synergistic HBPTC

Chapter 3 describes the mechanistic investigations that were undertaken on the novel catalytic manifold entitled Synergistic HBPTC (S-HBPTC). A detailed spectroscopic NMR investigation highlighted the synergistic role of the urea and onium catalysts for the solubilisation of KF. The preparation of the resultant urea-onium-fluoride complexes allowed for their evaluation as reactive fluorinating species. A kinetic isotope effect study deciphered the mode of substitution on the benzylic substrate class and key control experiments were performed to gain understanding of the mechanisms at play which allowed for enantioconvergence to be achieved within the system.

Acknowledgements

First and foremost, I would like to thank Prof Véronique Gouverneur for all her support over the past four years. Véronique's passion and determination to find solutions for the big questions within fluorination chemistry has been a great source of inspiration. I am grateful for all the discussions and advice she has given me over the past years, and for working with and supporting me through challenging projects which allowed me to constantly learn and grow as a scientist.

I would also like to express my gratitude to Prof Guy Lloyd Jones for his invaluable advice and support over the past couple of years with regards to the kinetic studies performed. I feel very grateful for all his contributions to the work and am inspired by his ability to see reactions through data alone. I also extend thanks to Prof Robert Paton for his continuing collaboration and dedication to the work performed within the Gouverneur group and the scientific contributions he made toward my own project.

A big thanks goes to the members of the VG group who made a difference every day. From those who were present in the lab when I joined under the lockdown rules of 2020 and made me feel instantly welcomed, to those I am leaving behind here, I feel honoured to have spent so much time around amazing scientists. A particular mention goes to the brilliant masters' and DPhil students I worked closely with over the years Bence, Louis, Jess, Zian and Chiara, I learnt so much from all of you. As well as notable mentions to Artemis, Maddison and Zijun for being great friends and always available for a good chat over coffee. Thanks to Sofia, an honorary member of the group who provided beautiful figures of my NMR tubes which are displayed within this thesis. The warmest thanks go to Calum, Joe and Seb, some of my best friends in and out of the lab. I couldn't have chosen a better group of people to go through the DPhil years with, you guys made the everyday more achievable and I am very proud of all of you.

I would like to thank the great group of friends I have around me. Including all of those I met here in Oxford, with particular mention to Lauren whose friendship was invaluable to me over the first years of my DPhil. I still hold our friendship and memories we have together very close to my heart. Alongside all my friends from Leeds and London, who understood my radio silence at points during this degree and provided me with much needed escapes from the lab.

A warm thanks to my brilliant family; my Mum and Dad, sister Siobhan and brothers Ryan and Joe, for their unconditional support and love, it wouldn't have been possible without all of you.

Finally, I would like to thank Francesco, my partner and best friend, as well as being my co-author and one of the first members of the VG group I met! You have been a constant source of inspiration, not only as a scientist but even more so as a person. Thank you for your kindness and support, which included proofreading this entire thesis when I realise it was sometimes the last thing you wanted to do after work. I will never be able to express in words my gratitude and how important your contributions have been to making the past four years possible.

Abbreviations

α-SKIE	Alpha Secondary Kinetic Isotope Effect
α-PKIE	Alpha Primary Kinetic Isotope Effect
β-SKIE	Beta Secondary Kinetic Isotope Effect
5’-FDA	5'-fluoro-5'-deoxyadenosine
Å	Angstrom, 1 $x10^{-10}$ m
BINAM	[1,1'-binaphthalene]- 2,2'-diamine
BINAP	2,2’-bis(diphenylphosphino)-1,1’-binaphthyl
Br	Broad (NMR signals)
CCl_4	Tetrachloromethane
CPME	Cyclopentyl methyl ether
CsF	Cesium fluoride
DCM	Dichloromethane
DCA	Dichloroacetate
DCE	Dichloroethane
DFB	Difluorobenzene
DFT	Density Functional Theory
DKR	Dynamic Kinetic Resolution
DMAP	4-Dimethylaminopyridine
DYKAT	Dynamic Kinetic Asymmetric Transformation
ε	Dielectric Constant
ee	Enantiomeric Excess
e.r.	Enantiomeric Ratio
ED_{50}	Median effective dose
E1	Unimolecular elimination
E2	Bimolecular elimination
FDA	Food and Drugs Administration
HB	Hydrogen bond
HBC	Hydrogen bond contact
HBD	Hydrogen bond donor
HBPTC	Hydrogen Bonding Phase Transfer Catalysis
hERG	human Ether-a-go-go-Related Gene
HFIP	Hexafluoroisopropanol
HMBC	Heteronuclear Multiple Bond Correlation
HOESY	Heteronuclear nuclear Overhauser Effect SpectroscopY
HSQC	Heteronuclear Single Bond Correlation
IC_{50}	Half Maximal Inhibitory Concentration
IR	Infra-red
KBr	Potassium Bromide
KF	Potassium Fluoride
KI	Potassium Iodide
KIE	Kinetic Isotope Effect
KR	Kinetic Resolution
LB	Lewis Base
$LiPF_6$	Lithium Hexafluorophosphate

mCPBA	*meta*-chloroperoxybenzoic acid
MD	Molecular Dynamics
MeCN	Acetonitrile
MF	Metal Fluoride
ms	milliseconds
MTBE	methyl *tert*-butyl ether
NFSI	N-fluorobenzenesulfonimide
NLE	Non-linear effect
NMR	nuclear magnetic resonance
nOe	nuclear Overhauser effect
NOESY	Nuclear Overhauser Effect SpectroscopY
pKa	acid dissociation constant, -log10
PPh_3	Triphenylphosphine
PTFE	Polytetrafluoroethylene
PVDF	Polyvinylidene
PT	Phase transfer
PTC	Phase transfer catalysis
rt	Room temperature
ROESY	Rotating frame nuclear Overhauser Effect SpectroscopY
rpm	revolutions per minute
SAM	S-adenosylmethionine
S-HBPTC	Synergistic Hydrogen Bonding Phase Transfer Catalysis
SN1	Unimolecular nucleophilic substitution
SN2	Bimolecular nucleophilic substitution
SN2X	Halogenophilic nucleophilic substitution
STU	Schreiner's thiourea
SU	Schreiner's urea
TBAF	Tetrabutylammonium fluoride
THF	Tetrahydrofuran
TLC	Thin Layer Chromatography
TS	Transition State
UPBr	Urea-phosphonium-bromide complex
UPF	Urea-phosphonium-fluoride complex
UPI	Urea-phosphonium-iodide complex
v.	Vide (refer to)
VT	Variable temperature
µM	Micromolar

1. Introduction

1.1. Fluorine in Modern Day Chemistry

"*If you are the monovalent element at the end of the electronegativity universe, your presence in a molecule could prove absolutely crucial for function. A stand in for a C–F group might suffice in some applications but, wishful thinking aside, an honest surrogate for a C–F unit does not exist – nothing even comes close" – Barry Sharpless*[1]

Fluorinated molecules have an unmistakeable presence in modern day science, particularly within the pharmaceutical, agrochemical and materials industry. Historical developments in fluorination chemistry depict many important scientific discoveries of the 20th century, from advancements in pharmaceutical science and medical imaging (e.g. [^{18}F]-FDG for Positron Emission Tomography) to the developments of refrigerants and materials that have now become crucial to our everyday life (e.g. $LiPF_6$, PTFE and PVDF). In the 1950s the first fluoropharmaceutical, Florinef, was developed which possessed beneficial biological activity over non-fluorinated analogues. Since this, fluorine substitution in biologically active compounds has become common practice, which has resulted in the development of blockbuster drugs and agrochemicals (e.g. Lipitor, Prozac, Indaziflam and tetraconazole). It is estimated that 20 % of pharmaceuticals and 50 % of agrochemicals registered in the past two decades contain at least one fluorine atom.[2] The steady increase in number of fluoro-organic compounds is matched with increased demand for the development of synthetic methodologies for fluorine incorporation. Fluorine chemistry, once regarded as a niche field of organic chemistry, has evolved into a vibrant and expansive area of research. However, the discipline remains shadowed by a reputation as inherently dangerous with a historically challenging past.

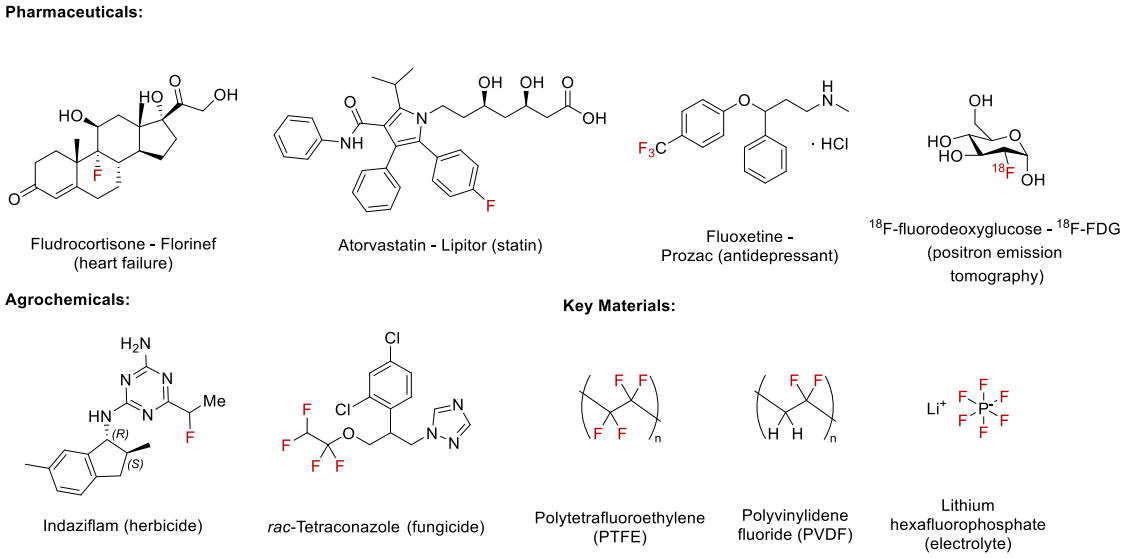

Scheme 1.1: Examples of important fluorinated motifs in modern science

Fluorine is naturally abundant on the Earth's crust, as fluorite (CaF_2) and fluorapatite ($Ca_5(PO_4)_3F$), stable minerals which were described as early as 1529 by Georgius Agricola, who noted their usefulness as fluxing agents facilitating the smelting of iron ores.[3] However, the emergence of fluorine chemistry relied on the discovery and isolation of the two highly toxic gases which sit at its core, hydrogen fluoride (HF) and elemental fluorine (F_2). Many chemists of the 18th and 19th century sought to isolate fluorine hypothesising a missing element at the top of group 17, however the discovery of fluorine and birth of fluorine chemistry can perhaps be credited to two specific scientists, Carl Wilhelm Scheele and Henri Moissan. It was Scheele who first in 1771 described the process of treating CaF_2 with sulfuric acid to from HF and Moissan who throughout the 1880s sought for the isolation of elemental fluorine (F_2), and in 1886, succeed *via* the electrolysis of HF and potassium bifluoride (KHF_2).[4, 5] The fluorine chemists of this era are often named 'the fluorine martyrs', as many of them suffered severe injuries in the pursuit of isolating toxic fluorine gases. Such injures included poisoning and blindness, and many individuals faced premature deaths, due to the lack of awareness around the dangers associated with such fluorinated gases, as well as insufficient equipment for their handling.[6] Moissan was awarded the 1906 Nobel prize in chemistry, a year before his death at 55 years old, in acknowledgment of his success in identifying elemental fluorine after decades of effort.

1.2. Properties of the C–F Bond

Fluorine substitution has been shown to affect almost all pharmacokinetic properties (e.g. adsorption, distribution, metabolism, excretion) of a compound, making it an attractive modification in analogue development of biologically relevant molecules. Fluorine's exceptional electronegativity (χ_p = 4.0) and small Van der Waals radius (r_{VDW} = 1.47 Å), makes it an especially electron-dense atom and in consequence the C–F bond remarkably strong, with high ionic character in comparison to other carbon-halogen, oxygen, or nitrogen bonds (Table 1.1).[7, 8] Incorporation of a C–F bond in a molecule can increase the strength of adjacent C–C bonds and alter the pK_a of neighbouring functionalities which can improve bioavailability. Fluorine is commonly employed as a bioisosteric replacement for hydrogen, carbonyl or hydroxyl groups, with organofluorine compounds exhibiting increased metabolic stability and reduced clearance *in vivo*.[9] Furthermore, incorporation of highly polarising C–F bonds can have profound influence on stereoelectronic and conformational effects due to the influence of the low-lying anti-bonding (σ*) orbital of the C–F bond, which can proficiently accept electron-density from nearby donating groups.[10]

Table 1.1: Properties of selected elements and their bonds to carbon[7]

	H	**F**	O	N	C	Cl	Br
Van der Waals radius (Å)	1.20	**1.47**	1.52	1.55	1.70	1.75	1.85
Pauling Electronegativity	2.1	**4.0**	3.5	3.0	2.5	3.2	2.8
C–X bond length (Å)	1.09	**1.40**	1.43	1.47	1.54	1.77	1.97
C–X bond strength (kcal mol^{-1})	98	**105**	84	70	83	77	66

1.2.1. Acidity and Metabolic Stability

Fluorine, the lightest element of the group 17 halogens, is most recognised for having the highest electronegativity on the Pauling scale.[11] Fluorine substitution on a molecule can contribute to increased Brønsted acidity of neighbouring functionalities, as a result of fluorine's inductive withdrawing effect. The effect of fluorine substitution on the basicity of cyclic amines is a particularly well studied phenomenon; the introduction of a single fluorine on piperidine reduces the basicity of the amine by 1.7 pK_a units and further substitution of fluorine atoms has additive effects diminishing basicity further (Scheme 1.2a).[12-14] Modulating the pK_a of basic functionalities through fluorine substitution is a well-

established and reported strategy in medicinal chemistry shown to achieve improved distribution and bioavailability of drug compounds. Compound **1.1** possessing a piperidine core was identified as a lead in a medicinal chemistry programme of adenosine monophosphate-activated kinase (AMPK) regulators. However, **1.1** suffered from high *in vivo* clearance (rat) as well as significant inhibition of the human ether-a-go-go-related gene (hERG), which can be fatal as its obstruction slows down the repolarisation of cardiac muscle.[15, 16] Analogue development of **1.1** demonstrated that fluorine substitution on the piperidine unit (**1.2**) attenuated basicity, which was postulated to be the basis for a much improved hERG profile. Furthermore, fluorinated analogue **1.2** demonstrated a much lower clearance *in vivo* from 150 mL/min/kg to 19 mL/min/kg (Scheme 1.2b).[17]

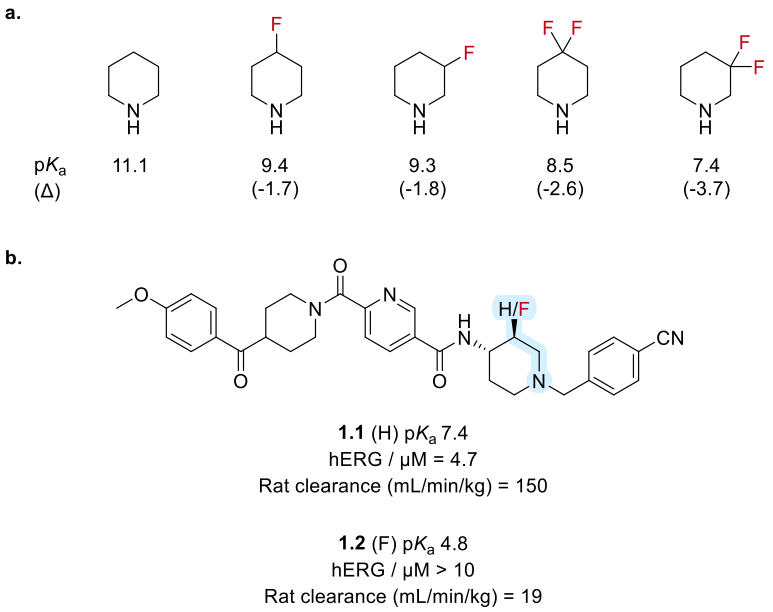

Scheme 1.2: a. Effect fluorine substitution has on the pK_a (conjugate acid) on piperdines; b. Effect of fluorine substitution on pK_a, hERG inhibition and clearance on **1.1** and **1.2**

1.2.2. Bioisosterism

Bioisosterism is a popular concept within medicinal chemistry whereby functional groups of a similar size or chemical function can be interchanged to give improved biological or pharmacokinetic properties.[18] Bioisosteres can be employed to improve binding affinity, potency or overcome issues associated with resistance or poor bioavailability. Fluorine's unique electronic properties matched with

its small size has made it a versatile bioisostere demonstrating wide applicability in medicinal chemistry campaigns.

Fluorine is commonly employed as a bioisosteric replacement for hydrogen atoms.[9] This H/F exchange can probe the benefit of electronegativity changes in a molecule with minimal effect on steric requirements, considering the similarities in size between H and F (Table 1.1). The increased strength of the C–F bond often serves as a strategy to develop more potent molecules which are more resistant to metabolism *in vivo*, this can be illustrated in the molecule Ezetimibe **1.4**, a medication for the treatment of high cholesterol. Analysis of the metabolites of lead compound **1.3** identified the demethylation of methoxy functionalities and aromatic hydroxylation. Analogue development showcased that the substitution of aromatic C–H and C–OMe bonds with C–F bonds increased potency ultimately leading to compound **1.4**, which demonstrated significantly lower median effective dose (ED_{50}) values across a series of animal models (Scheme 1.3).[19]

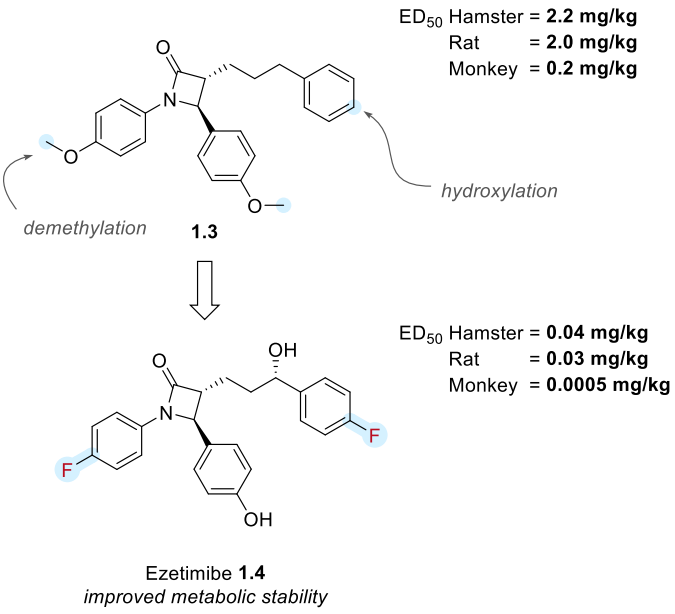

Scheme 1.3: Development of Ezetimibe **1.4** as fluorinated analogue of **1.3** with ED_{50} values for different animal models[19]

An interesting example of fluorinated bioisosteres was found during the development of a series of nicotinonitrile derivatives (**1.5**) where a trifluoromethyl (CF_3) substituted cyclopropyl served as an

isostere for a *tert*-butyl group. This substitution extended the biological half-life of the molecule in both rat and human liver microsomes (RLM/HLM) (Scheme 1.4).[20]

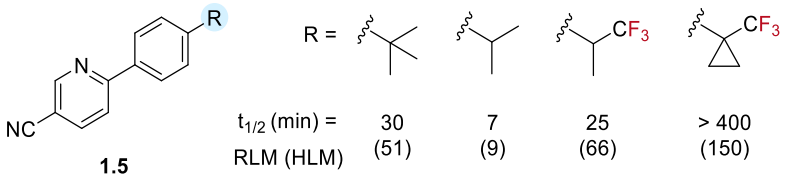

Scheme 1.4: Selected isosteres prepared for **1.5** and half-lives in RLM/HLM[20]

1.2.3. Conformational Properties

1.2.3.1. Dipole-dipole Interactions

The strongly ionic nature of the C–F bond gives rise to a large dipole moment, which can have substantial effects on the conformational behaviour of fluorinated compounds. For example, α-fluoroamides (**1.6**) have a conformational preference to position the C–F bond *anti*-planar to the dipole of the amide carbonyl (~7.5 kcal mol^{-1}) (Scheme 1.6a). This preference steadily reduces in compounds with weaker dipoles (e.g. esters, aldehydes and ketones).[21-23] Vinylfluorides have emerged as bioisosteres for amides, despite being structurally very different, specifically considering the loss of their hydrogen-bonding ability. However, the success of vinylfluorides as bioisosteres is considered to be related not only to the superior lipophilicity of the fluorine atom, but also to the dipole of vinylfluorides, which although is weaker than that of the amides (~0.97 vs 3.7 D), is orientated in the same direction (Scheme 1.5b).[21-23]

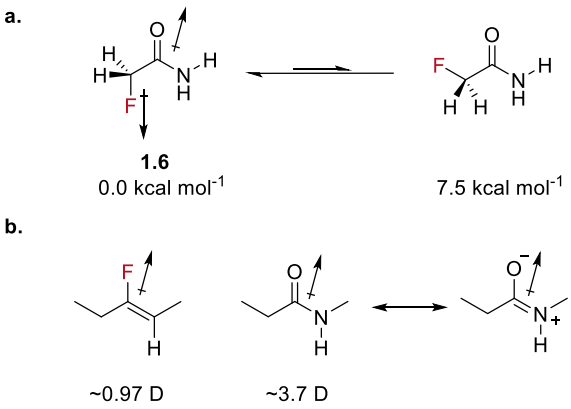

Scheme 1.5: a. Conformational preference of fluoroamides and calculated energy difference; b. Dipole of amides and vinylfluoride compounds

1.2.3.2. Gauche Effect

The gauche effect, a concept introduced by Wolfe in 1972, refers to the now well-recognised phenomenon in which the stability of the gauche conformation of X–CH_2–CH_2–X (where X substituents are separated by a dihedral angle of approximately 60°) increases, surpassing that of the more usually favourable anti-conformation (180°), as the electronegativity of the substituent X increases.[27]

Seminal work in the 1960s described this effect in difluoroethane, where the gauche disposition of the fluorine atoms is favoured by ~1 kcal/mol compared to the anti-conformation. Preference for the gauche conformer is rationalised considering the stabilisation gained by hyperconjugation, where the low-lying antibonding orbital (σ*) of the C(sp^3)–F bond can accept electron density from the electron rich C(sp^3)–H bond when correctly aligned (Scheme 1.6a). This is not observed for other 1,2-dihaloethanes which experience larger steric clashes and preferentially place halogens (Br, I) anti- to each other, further highlighting the unique properties of size and electronegativity that distinguishes fluorine amongst the halogens.[25-27] The gauche effect is also observed when one fluorine atom is positioned beta to an electron-withdrawing group (e.g. esters, amides, sulfones etc.). In this case favourable electrostatic interactions between this substituent and fluorine also plays a significant role in stabilisation, as was first discussed in seminal works by Lankin and Synder (Scheme 1.6b).[13, 28, 29]

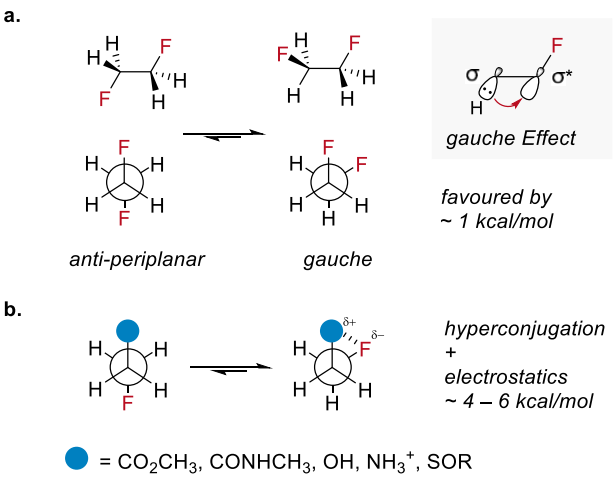

Scheme 1.6: Gauche effect observed on fluorinated motifs; a. in difluoroethane; b. organofluorine molecules with differing EWGs

The gauche effect has been used as a tool in the design of organocatalysts, for example the combination of a β-fluoroamine catalyst with an aldehyde yields iminium intermediates which adopt a gauche conformation.[33] This fluorine-iminium gauche effect has been widely studied by Gilmour and co-workers; an example includes the investigation (*S*)-2-(fluorodiphenylmethyl)-pyrroline catalysts (**1.7**) for stereoselective epoxidation of α,β-unsaturated aldehydes.[31, 32] The condensation of the proline catalyst with the aldehyde substrate switches on the gauche effect, resulting in a highly preorganised transition state consisting of hyperconjugative ($\sigma_{C\text{-}H} \rightarrow \sigma_{C\text{-}F}^*$), electrostatic ($N^+\cdots F^{\delta-}$) as well as π-stacking interactions which favours the *syn-clincal exo* conformation (Scheme 1.7). High selectivity was observed under this regime for the epoxidation of enal substrates employing H_2O_2 as an oxidant, as the incoming nucleophile is directed towards the lower face of the transient *E*-iminium ion providing enantioselectivities of up to 96% *ee*. To validate the importance of the gauche effect for stereocontrol, deletion experiments were performed removing the β-fluorine atom, as well as the phenyl rings on the catalyst **1.7** which demonstrated that the corresponding epoxide products were formed in diminished enantioselectivities (**1.7**—**1.11**).

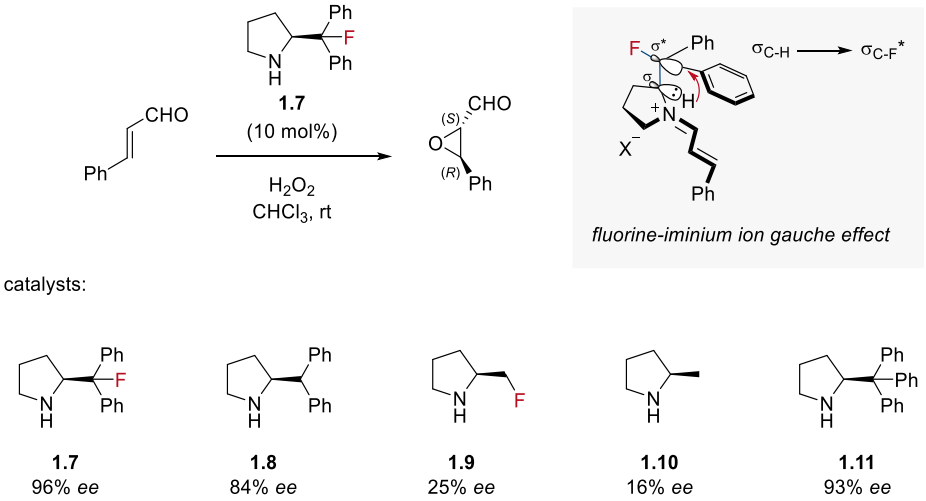

Scheme 1.7: Fluorine-iminium ion gauche effect in the catalytic epoxidation of enals by Gilmour and co-workers[35]

1.2.4. Hydrogen Bonding

Defined by IUPAC, a hydrogen bond is 'a form of association between an electronegative atom and a hydrogen atom attached to a second, relatively electronegative atom.'[36] Hydrogen bonds are recognised as electrostatic interactions and can vary in terms of strength and directionality as a reflection of the different proton donors or acceptors which participate in this phenomenon (Table 1.2).

Table 1.2: Properties of Hydrogen Bonds[37]

	Strong	**Moderate**	**Weak**
nature of bonding	mostly covalent	mostly electrostatic	electrostatic
H-bond length (Å)	1.2 – 1.5	1.5 – 2.2	2.2 – 3.2
bond angle (°)	175 – 180	130 – 180	90 – 150

Hydrogen bonding plays a significant role in biological systems including stabilising and in promoting drug-target interactions. The widespread benefit of fluorine atoms within biologically active compounds may be expected to stem from increased interaction (e.g. hydrogen bonding) between electronegative fluorine and protein targets. However, whilst the C–F bond is highly polarised, and the presence of three lone-pairs on fluorine might suggest its likelihood to act as a hydrogen-bond acceptor, this has been historically controversial.[38, 39] Organic fluorine is weakly polarisable, and evaluation of X-ray crystal structures of fluorinated drugs bound to their target receptors, suggest that C–F bonds preferentially engage in 'multipolar' interactions to carbonyl groups (C–F···C=O) rather than hydrogen bonding (e.g. C–F···H–N).[8, 24] Such multipolar interactions were illustrated during the development of a series of p38a inhibitors by Roche, where fluorination on the phenoxy unit of lead compound **1.12** resulted in a ten-fold decrease in IC_{50} value. The improved potency of **1.13** was attributed to the close contact between the fluorine atom and carbonyls on leucine and valine units of the target protein (Scheme 1.8).[37]

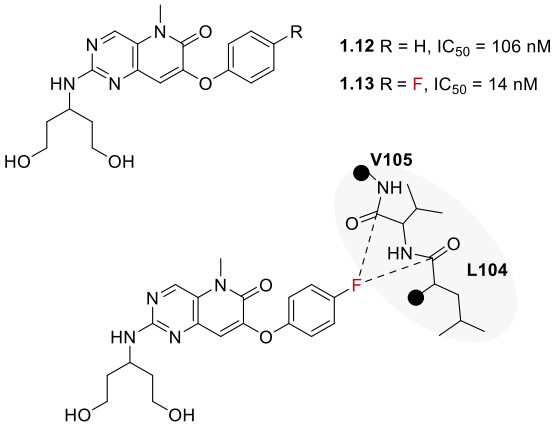

Scheme 1.8: Multipolar interactions of C–F bond in compound **1.13**[37]

In 2009, the group of Takemura investigated hydrogen bonding within the small molecule compound 8-fluoro-4-methyl-1-naphthol (**1.14**). In the solid-state intramolecular hydrogen bonds were not formed, and the compound underwent intermolecular tetramisation, with measured O–H···F bond distances on the upper limits of a hydrogen bond (2.41 Å). However different behaviour was observed in solution ($CDCl_3$), with spectroscopic analysis by NMR revealing the dissociation of the tetramer and the formation of intramolecular hydrogen bonds between the fluoride and O–H donor. Evidence for this interaction included the high chemical shift of the OH resonance compared to other isomers of **1.13**, and the signal appearing as a doublet due to scalar coupling of the O–H proton to fluorine ($^{1h}J_{(H,F)}$ = 28.4 Hz in $CDCl_3$) (Scheme 1.9). This study highlighted that X-ray crystallography alone may not be sufficient to determine the presence of hydrogen bonding in organofluorine compounds and NMR spectroscopy can serve as an important tool to identify key changes in both chemical shift and scalar coupling as evidence of hydrogen bonding in solution.[41, 42] Experimental evidence for intermolecular hydrogen bonding involving the C–F bond has also been reported by the groups of Gouverneur and Linclau.[40-42]

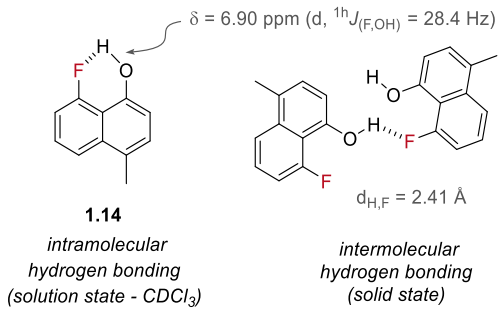

Scheme 1.9: Hydrogen bonding interactions observed in solution and in solid state for **1.13**[41]

1.3. Natural Occurrence of Fluorine

Fluorine atoms are naturally found in a handful of stable mineral compounds namely, fluorspar (CaF_2), fluorapatite ($Ca_5(PO_4)_3F$).[46] The natural existence of elemental fluorine (F_2) was heavily debated for over 200 years, however recent evidence suggests its natural occurrence in a radioactive variety of fluorspar, called antozonite or "Stinkspar". The origin of elemental fluorine within antozonite is thought to be a result of radiolysis by β-radiation of CaF_2 into elemental calcium and fluorine due to the trace quantities of uranium which is found within the ore. The odour of fluorine was noted to be liberated upon fracture of Antozonite, and its presence was further validated by the identification of a characteristic F_2 signal observed by ^{19}F MAS NMR spectroscopy (δ = 425 ppm).[47]

Fluorine is the 13th most abundant element on the Earth's crust, and whilst it is present in significantly larger quantities than the other halogens (Cl – 20th, Br – 62nd, I – 64th), the biochemistry of fluorine is very limited. In fact, there are only six discrete fluorinated natural products, out of more than the approximately 130,000 natural products which have been characterised in the literature.[45-47] This is in part a consequence of the low abundance of fluoride in oceans as a result of the scarce solubility of CaF_2 (solubility in water: 0.0016 g/100 g H_2O).[51] More so, much of the biochemistry of the halogens involves oxidation to the corresponding halonium ions (X^+) by hydrogen peroxide (H_2O_2) dependent enzymes (*haloperoxidases*). Fluoride's oxidation potential (E°= 2.87 V), which is lower than H_2O_2 (E°= 1.76 V) makes this oxidation process unfeasible, prohibiting this key enzymatic halogenation pathway.[52] Therefore, fluoride biochemistry is limited to nucleophilic strategies, which face challenges as it requires the evolution of an enzyme capable of desolvating the fluoride anion.

For many years the origin and biosynthesis of the few naturally occurring organofluorine compounds remained a mystery until in 2002, the first natural occurring enzyme capable of catalysing the formation of C–F bonds was discovered and characterised by O'Hagan and co-workers.[53] This enzymatic process was observed in strains of the bacterium *Strepomyces cattleya* and catalyses C–F bond formation through the nucleophilic attack of fluoride ion onto *S*-adenosylmethionine (SAM) yielding 5'-fluoro-5'-deoxyadenosine (5'-FDA). This enzyme has become more commonly named

fluorinase and is still the only known natural biosynthetic route to forming C–F bonds. 5'-FDA is considered as the precursor for other biogenic organofluorine compounds through the intermediacy of 2-fluoroacetaldehyde. However, this pathway cannot account for presence of compounds such as fluoroacetone, fluorouracils or fluoroaryl propionic acids, where their existence is either misidentified, deemed as a result of industrial contamination, or so far unreported (Scheme 1.10).[54] The biosynthesis of nucleocidin, an antibiotic produced by bacterium *Strepomyces calvis*, is distinct and not traced to the common 5-FDA precursor. Whilst significant interest and research including gene-disruption experiments have provided clues towards the enzymatic requirements to make nucleocidin, the biochemical mechanism of this C–F bond formation remains unclear.[52, 53]

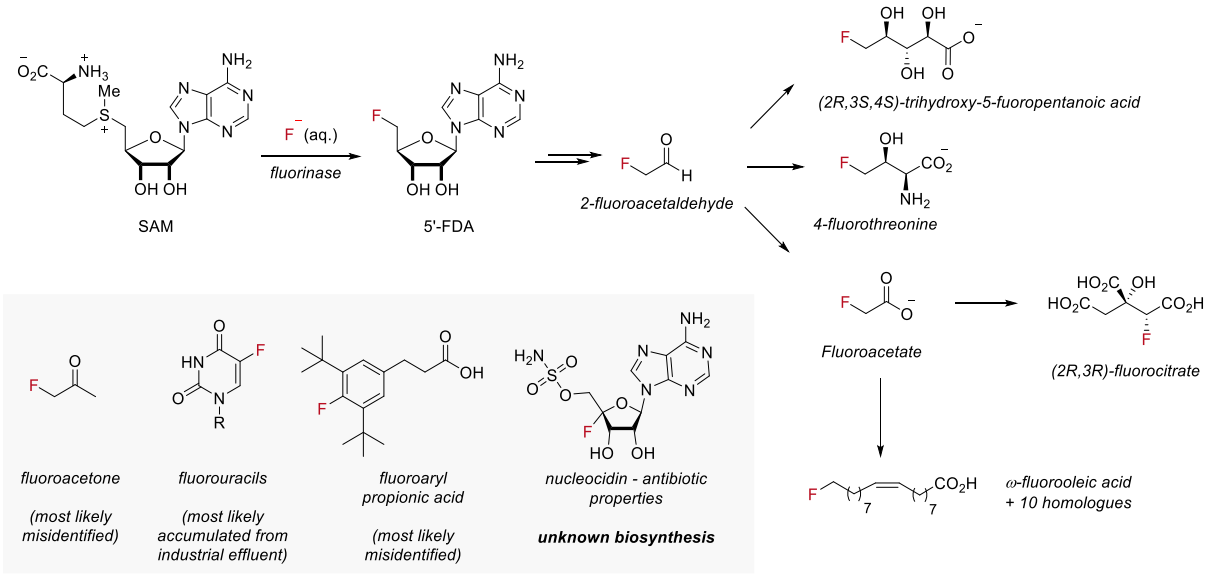

Scheme 1.10: Biosynthetic pathway for biogenic organofluorine compounds

Fluorinase is reported to increase the rate of fluorination between 10^6 to 10^{15} times, however its turnover rate (k_{cat}) of 0.06 /min, makes it an exceptionally slow enzyme, with the average turnover rates of enzymes lying in the region of $10^3 - 10^7$/s. This slow turnover rate is considered to be associated with the high kinetic barrier of fluoride desolvation (heat of hydration ~120 kcal/mol). *Fluorinase* achieves desolvation by the exchange of water molecules within fluoride's hydration shell, with hydrogen bond contacts to the serine and threonine residues which is further compensated and driven by the electrostatic stabilisation provided by the SAM electrophile, poising the 5'-carbon for nucleophilic attack (Scheme 1.11).[57]

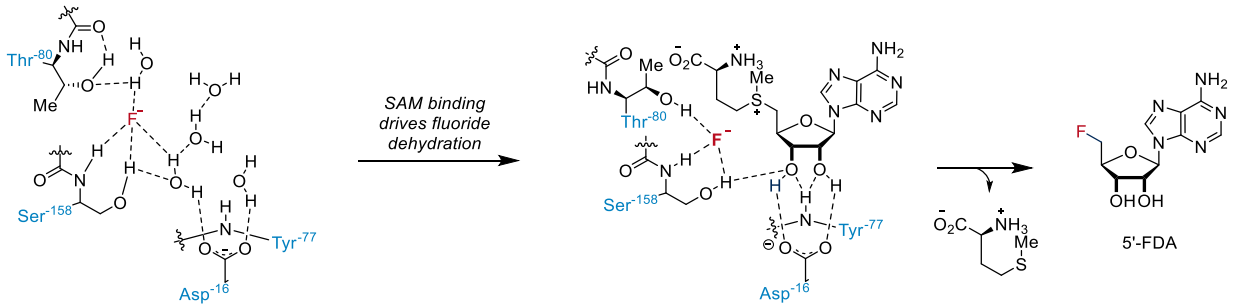

Scheme. 1.11: Desolvation and hydrogen bonding of fluoride anion in fluorinase active site

1.4. Fluorine in Organic Synthesis

Whilst fluorine is abundant on Earth as CaF_2, its low solubility and high stability renders its direct use towards C–F bond formation challenging. Industrially fluorine atoms are released from fluorite ores through an energy intensive process *via* treatment with sulfuric acid at exceptionally high temperatures, releasing hydrogen fluoride (HF). Hydrogen fluoride, a gas with a boiling point of 19.5 °C, sits at the core of the fluorochemical industry and is the starting point for the synthesis and preparation of all commercially available fluorinating reagents (Scheme 1.12).[58]

Approximately half of the anhydrous HF that is produced is used for the preparation of chlorofluoro- and hydrochlorofluorocarbons (CFCs and HCFCs), which were prepared first by Frédéric Swarts in the 1890s *via* halogen exchange.[59] CFCs and HCFCs had early applications as refrigerants prior to knowledge of their harmful environmental impact and have now replaced by hydrofluorolefins (HFOs) which have a significantly shorter atmospheric lifetimes.[50] Fluorinated hydrocarbons are still critical materials employed as building blocks for commonly used fluoropolymers (e.g. Teflon).[60, 61] The electrolysis of HF to form F_2 is the primary step in the production of electrophilic sources of fluorine. This process, first reported by Moissan in 1886, is now utilised on an industrial scale through electrolysing a mixture of anhydrous HF with potassium fluoride (KF) (2:1) at 70 – 130 °C.[5] F_2 can be subsequently reacted with nucleophiles accessing a host of electrophilic fluorinating reagents including the important class of "N–F" reagents, 1-chloromethyl-4-fluoro-1,4-diazoniabicyclo[2.2.2]octane *bis*(tetrafluoroborate) (Selectfluor®), *N*-fluorobenzenesulfonimide (NFSI) and *N*-fluoropyridinium salts, all of which have found great application in modern organic synthesis.[62-65] These N–F reagents, disclosed between 1986

– 1992, have shown great applicability through their swift implementation in asymmetric C–F bond formation, which can be rationalised considering their compatibility with established catalytic strategies. Whilst the use of electrophilic fluorinating reagents for enantioselective catalysis has become common practice, there are some key disadvantages that cannot be overlooked; including their syntheses, reliant on the handling of F_2 gas, which is reflected downstream in the great expense of these reagents. Also, the highly oxidising properties of the N–F reagents, whilst beneficial in transition metal catalysis, can be problematic considering the fragility of some functional groups towards oxidation. Finally, there are sustainability implications considering the large molecular weight and poor atom economies of these reagents. For example, in the case of Selectfluor®, which possesses tetrafluoroborate counter anions, a total of nine fluorine atoms is employed to, in most cases, form a single C–F bond. In contrast, nucleophilic fluorine sources are more cost-effective and atom economical. In particular the alkali metal fluoride salts (e.g. NaF, KF, CsF), which are prepared *via* the neutralisation of HF with hydroxide salts, could be considered the preferred option for the introduction of a fluorine atom through displacement reactions, as they are easy to handle, widely available and have a much lower environmental impact than electrophilic counterparts.

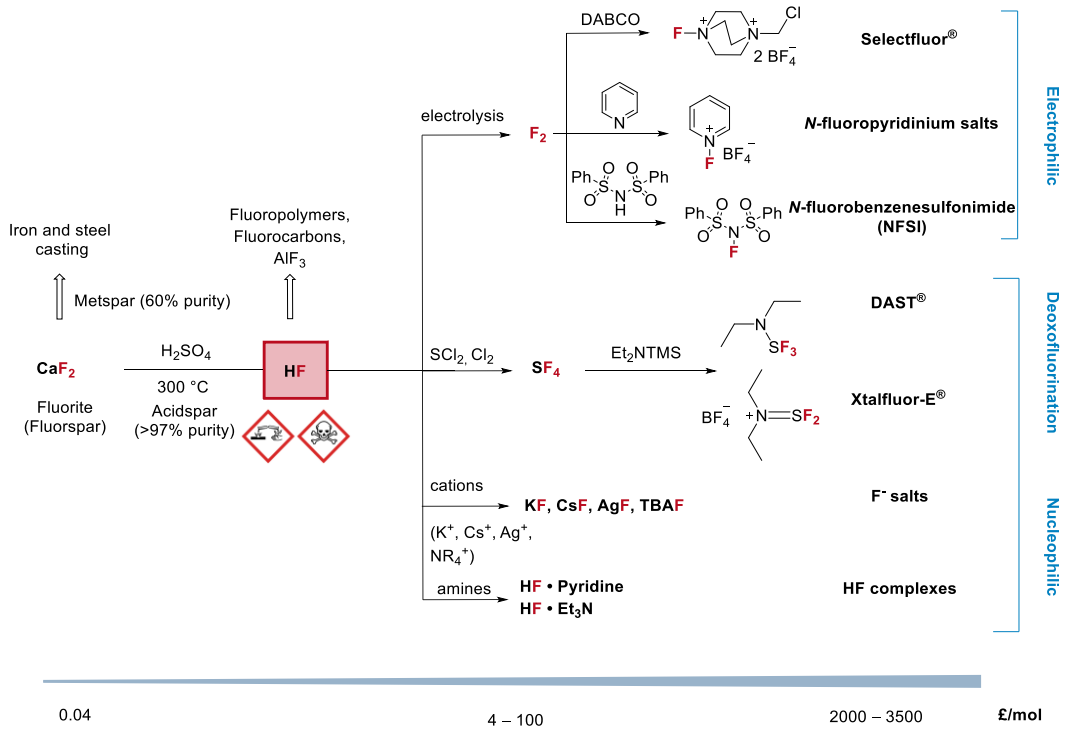

Scheme 1.12: Fluorochemical supply chain[58]

1.5. Fluorinating Reagents in Asymmetric Synthesis

1.5.1. Prologue to Asymmetric Synthesis

The importance of chirality in the natural world has influenced the way that chemists conceptualise and design molecules, yet the synthesis of compounds in their enantiomerically pure forms is still one of the most sought-after challenges in organic chemistry today.

Whilst nature has provided access to enantiomerically pure compounds denoted as our "chiral pool", industrially chiral separation of racemic mixtures is still commonly performed to access single enantiomers, regardless of the high waste associated with the disposal of the undesired enantiomer.[66] Asymmetric catalysis has provided the greatest potential for chemists to formulate strategies towards the synthesis of enantiomerically pure compounds, avoiding the need for chiral separation. The first illustration of asymmetric catalysis dates back to 1912 by Bredig and Fiske, who employed a quinine cinchona alkaloid organocatalyst (**1.15**) towards the addition of hydrogen cyanide to benzyaldehyde (Scheme 1.13).[67] Since this earliest disclosure, the past century represents a period of rapid growth in the development of asymmetric catalysis, particularly in the advent of transition metal catalysis and the renaissance of organocatalysis since the millennium. This pillar of organic chemistry in the design of chiral molecules and continuous development of new organocatalysts and ligands has given chemists the power to synthesise a broad range of enantioenriched molecules that nature itself cannot make.

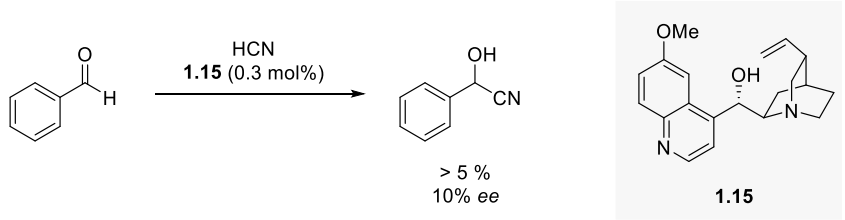

Scheme 1.13: First demonstration of asymmetric organocatalysis by Bredig and co-workers[67]

1.5.2. Asymmetric Electrophilic Fluorination

1.5.2.1. Transition Metal Mediated Asymmetric Electrophilic Fluorination

The development of "N–F" reagents as electrophilic sources of fluorine atoms initiated the significant advances that were made in the field of metal catalysed asymmetric fluorination. Seminal work reported in 2000 by Togni and co-workers demonstrated that chiral titanium catalysts (**1.16**) can engage in two-point binding to β-ketoesters acting as Lewis acids, generating metal enolate nucleophiles poised to react with Selectfluor® forming C–F bond in up to 90% *ee* (Scheme 1.14).[68] Soon after this formative study, several protocols for enantioselective α-fluorination of dicarbonyl compounds emerged employing similar transition metal strategies with electrophilic fluorinating reagents.[69]

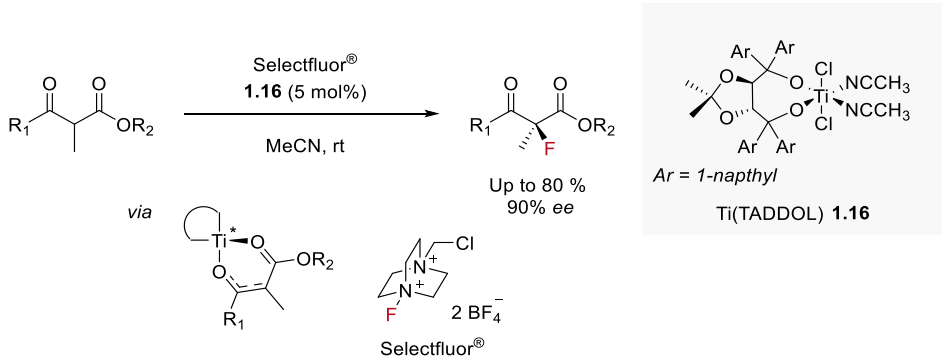

Scheme 1.14: Seminal report of catalytic asymmetric fluorination by Togni and co-workers[68]

Diverting from electrophilic α-fluorination of 1,3-dicarbonyls species, which is by and large the most common transformation reported in the field, Toste and co-workers achieved a palladium directed fluoroarylation of styrenes accessing stereogenic C–F bonds at the benzylic position.[70] Based on understanding that C–F bonds could be forged from the reductive elimination from high-valent palladium species,[70-73] Toste reported a three-component system involving styrene substrates possessing an amide directing group, boronic acids and Selectfluor®. The reaction proceeded through a Pd(IV) species, accessed through oxidation of a Pd(II) species by Selectfluor®, followed by a regio- and stereoretentive reductive elimination furnishing C–F bonds in up to 96% *ee* (Scheme 1.15).

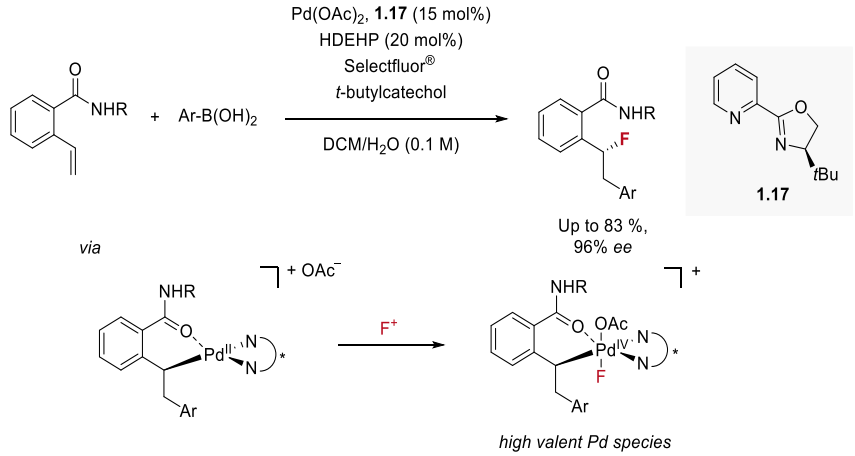

Scheme 1.15: Asymmetric fluoroarylation of styrenes by Toste and co-workers[70]

Yu and co-workers also investigated this reductive elimination strategy from Pd(IV) species towards C(sp^3)–H benzylic fluorination reactions *via* a transient directing group approach.[74] Here, bulky amino amide directing group **1.18** proved critical for selectivity. This approach promoted C(sp^3)–F reductive elimination from Pd(IV) intermediates *via* an inner sphere mechanism outcompeting the undesired outer sphere C(sp^3)–O bond formation by attack of acetate ligands. *N*-Fluoro-2,4,6-trimethylpyridnium tetrafluoroborate was employed as the fluorinating reagent and oxidant required to access the high valent Pd(IV) species, and this methodology allowed for a scope of benzaldehyde substrates to be fluorinated in good yields and excellent enantioselectivities (up to 61 %, 99% *ee*) (Scheme 1.16).

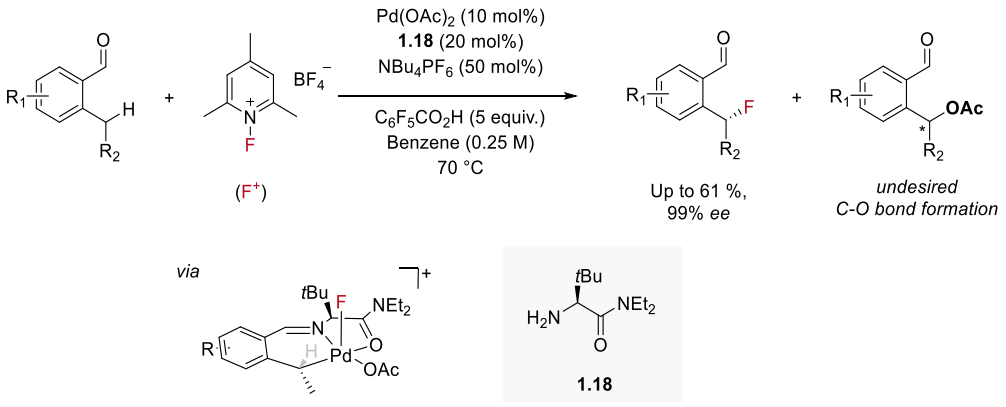

Scheme 1.16: Reductive elimination from Pd(IV) to access benzylic fluorides by Yu and co-workers[74]

1.5.2.2. Organocatalytic Asymmetric Electrophilic Fluorination

Disclosures of organocatalysis were sporadically published throughout the 20th century, from the earliest work of Bredig and Fiske (Scheme 1.13)[67], to seminal work by Hajos and Parrish who recognised the power of *L*-proline as a catalyst.[75] Other very notable milestones include the use of enantiomerically pure ketones for the enantioselective epoxidation of alkenes (e.g. Shi oxidation), and early examples of hydrogen bond donor (HBD) catalysis developed by the groups of Jacobsen and Corey towards asymmetric Strecker reactions.[76-89] These seminal reports all demonstrated the ability of small organic molecules to catalyse reactions and impart their chirality onto substrates in high selectivity. However, as a field, organocatalysis had significant resurgence and interest following reports of Enders, Barbas, List and MacMillan who concomitantly published the discovery of enantioselective enamine and iminium catalysis.[80, 81] These works demonstrated broader applicability of organocatalysts towards functionalisation of carbonyl compounds and consequently, List and MacMillan were recognised and awarded the Nobel prize in chemistry for their contributions to this work in 2021.[82]

In 2005, several groups investigated the application of organocatalysts, specifically proline catalysts to furnish enantioenriched C–F bonds with electrophilic sources of fluorine. Seminal work by Enders and co-workers demonstrated the feasibility using proline catalyst **1.19** for the α-fluorination of cyclohexanone substrates in moderate yields and enantioselectivities (up to 56 %, 36% *ee*) with Selectfluor® as the fluorinating reagent (Scheme 1.17).[83]

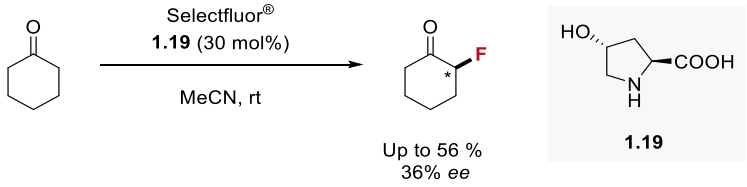

Scheme 1.17: First proline catalysed asymmetric α-fluorination of ketones by Enders and co-workers[83]

Jørgensen and co-workers reported the application of silylated proline derivative **1.20** as a catalyst for the α-fluorination of aldehydes with NFSI, yielding β-fluorinated alcohols following reduction *in situ*.[84]

This protocol furnished fluorinated products in excellent yields and enantioselectivies (up to 95 %, 97 % *ee*). Mechanistically the stereocontrol was proposed to be a consequence of forming a more stable *E*-enamine with the sterically demanding substituent on the catalyst blocks the *Re* face of enamine for reactivity with "F^+" (Scheme 1.18b). This methodology was also shown amenable towards the formation of a quaternary stereocentre **1.22**, employing modified catalyst **1.21**, in good yield 78 % albeit lower enantioselectivity (78 %, 48% *ee*) (Scheme 1.18c).

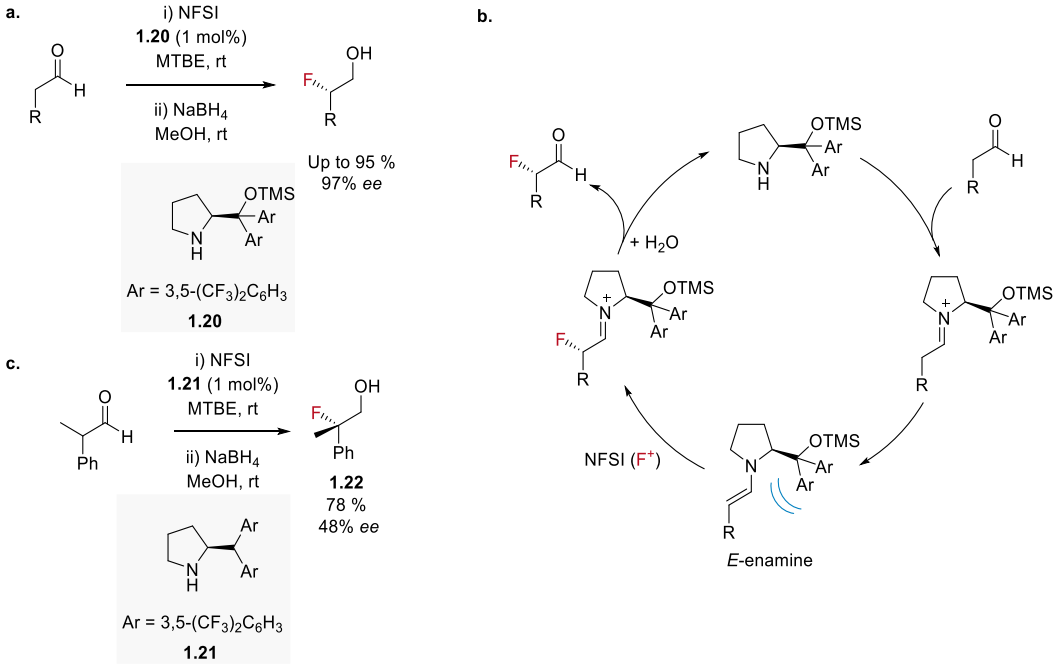

Scheme 1.18: a. α-Fluorination of aldehydes by Jørgensen and co-workers[84]; b. Proposed catalytic cycle; c. Application towards synthesis of a fluorinated quaternary stereocentre

In a similar period, Barbas and co-workers reported an enantioselective α-fluorination of branched aldehydes using a related proline-derived catalyst (**1.23** or **1.24**), with products formed in good yields and enantioselectivities (up to 98 %, 66 % *ee*) (Scheme 1.19a).[85] MacMillan and co-workers also disclosed an imidazolidinone catalyst **1.25** employed for the fluorination of a broad scope of linear aldehydes, which following reduction, yielded fluorinated alcohols in excellent yields and enantioselectivies (up to 96 %, 99% *ee*) (Scheme 1.19b).[86]

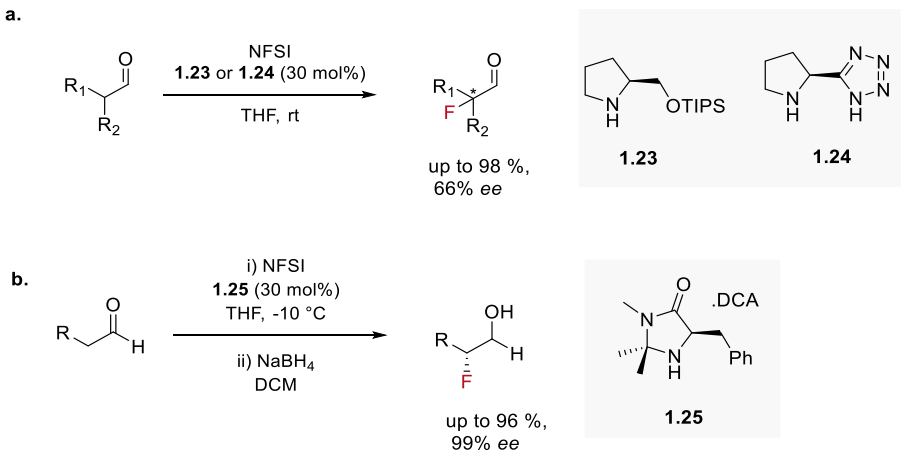

Scheme 1.19: a. α-Fluorination of branched aldehydes by Barbas and co-workers[85]; b. α-Fluorination linear aldehydes by MacMillan and co-workers[86]

It is noteworthy that research in this area heavily focused on the α-fluorination of aldehydes, which condense more readily with secondary amine catalysts compared to ketones. In addition, ketone-derived enamines exist as mixtures of rotational isomers as there is less distinction between the R group of ketones compared to aldehydic substrates.[87] This inherently lower order of organisation results in lower enantiocontrol which is demonstrated in the seminal works of Enders (Scheme 1.17).[79] In 2011, MacMillan and co-workers investigated what they described as this "ketone fluorination problem" which demonstrated that a high-throughput evaluation of chiral amine catalysts identified an optimal cinchona alkaloid derived amine catalyst **1.26** amenable for the fluorination of cyclic ketones. This methodology employing catalyst **1.26,** trichloroacetic acid (TCA) as a co-catalyst and NFSI furnished α-fluorinated ketones in excellent yields and enantioselectivity (up to 88 %, 99% *ee*).[88] Lam and Houk undertook detailed computational analysis of MacMillan's findings to determine the origins of enantioselectivity.[89] The authors proposed the initial fluorination of the quinuclidine of catalyst **1.25** which is followed by an enantiodetermining intramolecular fluorine transfer onto the enamine, rather than an intermolecular reaction with NFSI. It was determined that the preferred chair conformation of this seven membered TS, as well as the equatorial preference for the sterically bulky aryl group on the catalyst were key for enantiocontrol (Scheme 1.20).

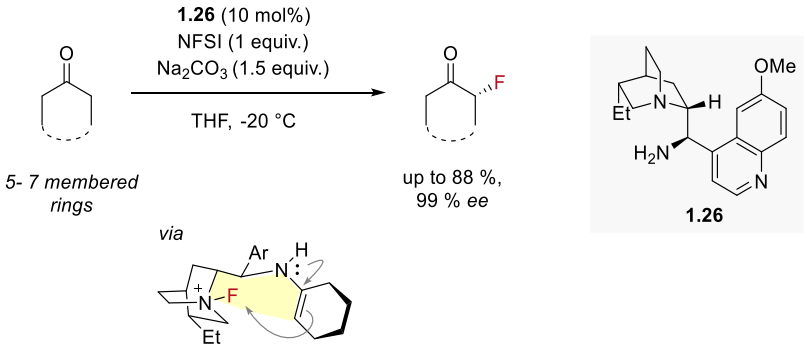

Scheme 1.20: Fluorination of cyclic ketones by MacMillan and co-workers[88, 89]

1.5.2.3. Phase-Transfer Catalysis

Phase-transfer catalysis (PTC), first introduced in the 1970s by Starks and co-workers, has recently flourished in terms of its capabilities in enantioselective synthesis.[90] Starks found that in a biphasic solution the substitution of a lipophilic alkyl halide with inorganic sodium cyanide only occurred in the presence of a quaternary ammonium or phosphonium salt ($^*Q^+ X^-$). Onium salt catalysts are capable of shuttling reagents between aqueous and organic phases permitting reactivity (Scheme 1.21).[91] Whilst homogeneity is preferred in most organic reactions, PTC can exploit the insoluble nature of reagents which can be advantageous, particularly in the context of asymmetric synthesis. If the reactivity of a reagent is unlocked solely in the presence of a chiral PT catalyst, bringing it into the organic phase, high selectivity can be achieved with little to no undesired uncatalysed background reaction. PTC has also received attention beyond academic research, as its mild reaction conditions and use of more environmentally friendly solvent systems can enhance the sustainability of industrial processes.[92]

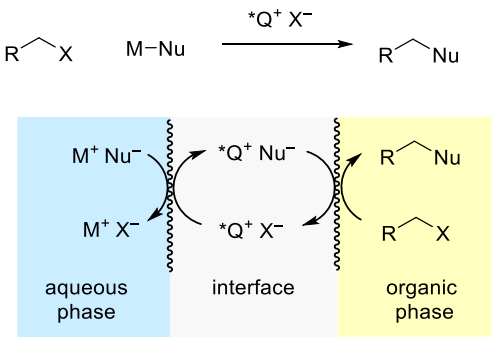

Scheme 1.21: General mechanism for PTC

The first example of fluorination under PTC was reported by Kim and Park in 2002 who achieved the fluorination of cyclic β-ketoesters with NFSI in the presence of a chiral ammonium salt based on a cinchona alkaloid **1.27**.[93] This liquid-liquid PTC manifold yielded fluorinated quaternary centres in moderate enantioselectivities (48 – 69% *ee*) and demonstrated for the first time the viability of PTC for enantioselective fluorination. For a decade, this concept went somewhat unnoticed by the scientific community, until 2010, when Maruoka and co-workers showed improvements on this catalytic mode through the introduction of a novel class of axially chiral bifunctional ammonium catalysts (**1.28**).[94] Such catalysts allowed for the fluorination of cyclic β-ketoesters in excellent enantioselectivities with NFSI at low catalyst loadings (2 mol%). **1.28** was proposed to act as a bifunctional catalyst, with the tertiary alcohols present at the 3,3'- positions providing additional stabilisation to the enolate oxygen through hydrogen bonding (Scheme 1.22).

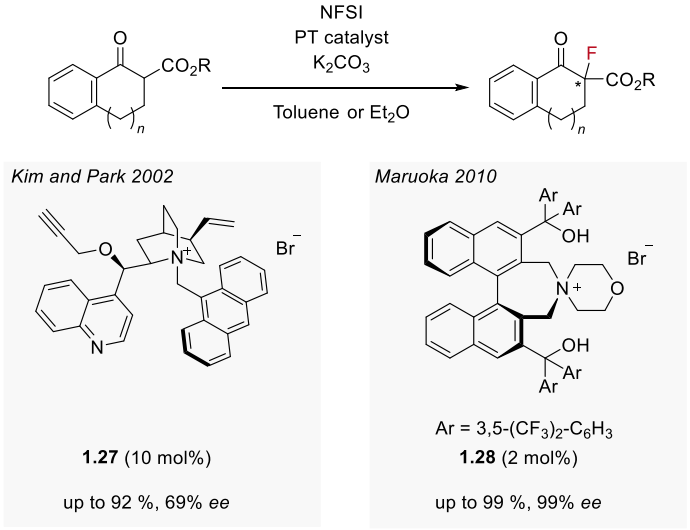

Scheme 1.22: Enantioselective fluorination of cyclic β-ketoesters under PTC by Kim and Park[93], and Maruoka[94]

The fluorination of acyclic β-ketoesters was achieved only recently, due to the outstanding challenge of controlling the formation of single enolate species, which ultimate dictates stereocontrol. Arimitsu and co-workers however reported the enantioselective fluorination of α-branched β-ynone esters to yield the corresponding quaternary fluorinated products.[95] Previous studies have reported that the higher *s*-character of β-ynone's is beneficial for the deprotonation of the α-proton to form the

corresponding enolate intermediates.[93] Researchers in this study however also noted the importance of the rod-like and rigid structure of the alkyne for the formation of a single enolate species, forming products in good yields and enantioselectivities (up to 93 %, 90 % *ee*) in the presence of the cinchona alkaloid catalyst **1.29** (Scheme 1.23).

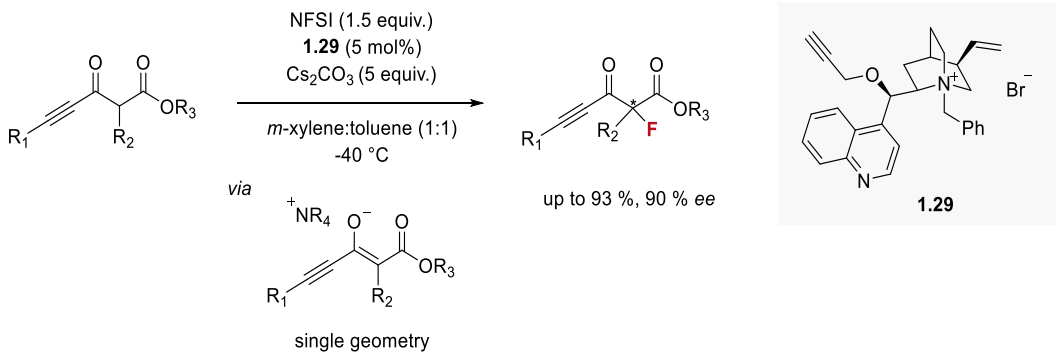

Scheme. 1.23: Enantioselective fluorination of α-branched β-ynone by Arimitsu and co-workers[95]

A charge inverted approach towards PT fluorination was considered by Toste and co-workers who employed a chiral anionic PT catalyst, more specifically a BINOL derived phosphoric acid **1.30**.[96] The phosphoric acid pre-catalyst, activated in solution through deprotonation, yields a chiral lipophilic phosphate anion **1.31**, which forms an intimate ion pair with the cationic electrophilic fluorinating reagent, Selectfluor®. This was demonstrated successfully in the context of a fluorocyclisation of olefins possessing a pendant amide nucleophilic site to obtain spiro-fused fluorotetrahydrofuran oxazolines in high yields, diastereo- and enantioselectivity (up to 90 %, 20:1 d.r., 97% *ee*). Hydrophobic alkyl chains on the BINOL backbone of catalyst (R_1) proved beneficial for PT and to achieve high enantioselectivity. A positive non-linear effect (NLE) suggested that two molecules of chiral **1.31** were involved in the enantiodetermining fluorination, and were required for the solubilisation of Selectfluor® as an ion-pair (2:1 **1.31**: Selectfluor®).

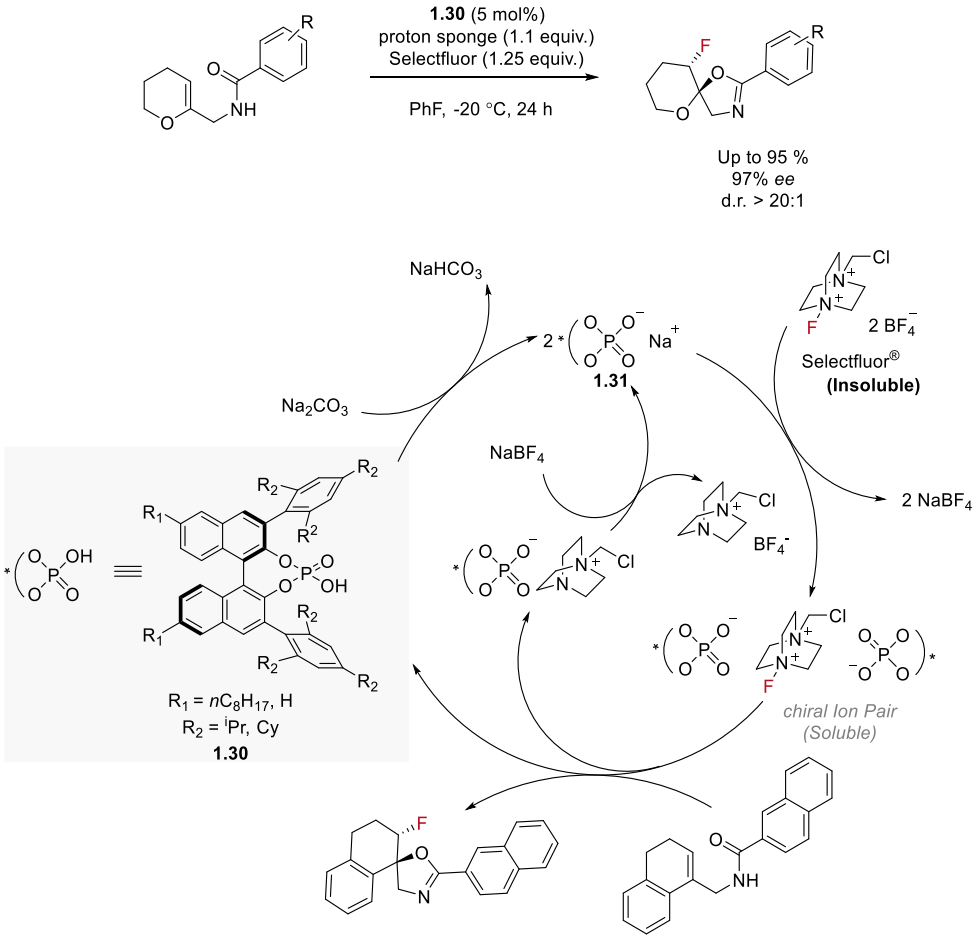

Scheme 1.20: Anionic PTC strategy by Toste and co-workers[96]

1.5.3. Asymmetric Nucleophilic Fluorination

In contrast to their electrophilic counterparts, there are less reports of asymmetric nucleophilic fluorination. This is surprising considering the historical presence of fluoride and nucleophilic reagents within organofluorine chemistry, in comparison to the newer N–F electrophilic reagents. However, challenges attributed to low nucleophilicity, and high basicity of fluoride has limited its use in fluorination. The success of electrophilic reagents, a result of their compatibility with common catalytic manifolds, has somewhat eclipsed the contributions made in the field of asymmetric nucleophilic fluorination by number. The next section highlights the advancements which has been made and demonstrate how researchers have overcome the intrinsic difficulties in employing fluoride as a nucleophile.

1.5.3.1. Transition Metal Mediated Asymmetric Nucleophilic Fluorination

The earliest asymmetric nucleophilic fluorination reactions focused on the ring opening of strained systems with transition metal catalysts as activators. A seminal report by Haufe and co-workers in 2002 demonstrated that the employment of ((*S*,*S*)-(+)-salen)chromium chloride catalyst **1.32** with silver fluoride (AgF) allowing for the ring-opening of cyclic *meso*-epoxides in up to 66 % *ee*.[97] Very high catalyst loadings (80–100 mol%) were required for product formation due to substantial poisoning of the catalyst **1.32** with fluoride (Scheme 1.21). For this reason, as well as increased background reactivity, highly reactive sources of fluoride such as HF complexes or potassium bifluoride (KHF_2) were deemed unsuitable, resulting in poor yield and selectivity of products.[98]

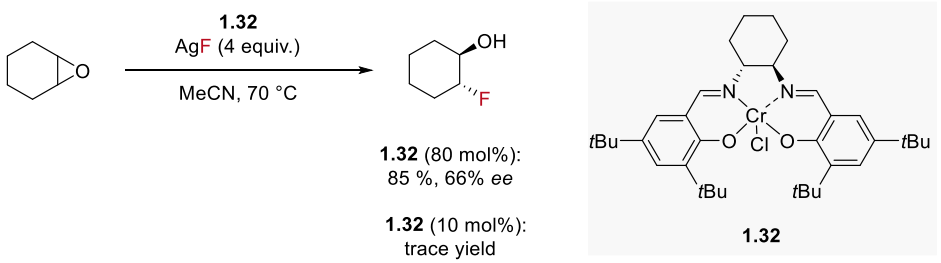

Scheme 1.21: Seminal work towards asymmetric nucleophilic fluorination of epoxides by Haufe and co-workers[97]

In 2010, Doyle and co-workers ameliorated this asymmetric ring-opening strategy, developing a catalytic variant. Key to this was the generation of a latent HF source from benzoyl fluoride and hexafluoroisopropanol (HFIP).[99] Maintaining a low concentration of fluoride ensured the absence of uncatalysed background reactivity or catalyst degradation, which allowed for the ring-opening of epoxides to proceed in high yields and enantioselectivities with a catalytic loading of cobalt salen catalyst **1.33** (10 mol%) and amidine co-catalyst **1.34** (8 mol%). The requirement for the chirality to be present on the cobalt catalyst **1.33** was demonstrated as employing only a chiral amine **1.33** did not induce measurable enantioselectivity in products (< 5% *ee*). Furthermore, a significant matched/mismatched effect for both the yield and enantioselectivity was observed between the two catalysts **1.33** and **1.34** (Scheme 1.22).

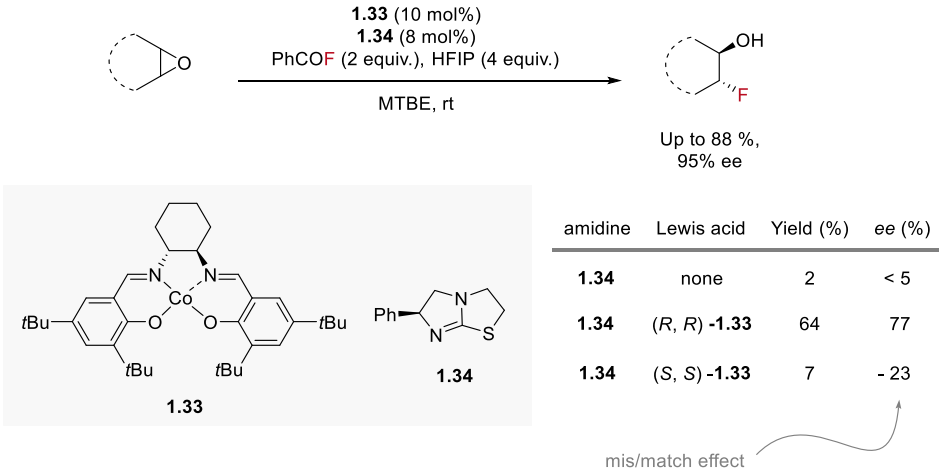

Scheme 1.22: Enantioselective catalytic ring-opening of epoxides with latent HF source by Doyle and co-workers[99]

Investigations into the mechanism of Doyle's ring-opening of epoxides uncovered a bimetallic mechanism, deciphered by an observed positive NLE between the enantiomeric ratio of product and the cobalt catalyst (**1.32**).[100] It was proposed that the cobalt catalyst (**1.33**) activates the epoxide substrate following the formation of a bimetallic [Co-FHF] intermediate prepared by acyl transfer between benzoyl fluoride and HFIP. The role of the amidine co-catalyst **1.34** was deciphered to be as a Lewis basic ligand which following attack onto the cobalt centre of this dimeric complex, reveals an active fluorinating monomeric species, which subsequently opens the epoxide. Based on the understanding of this bimetallic mechanism, Doyle and co-workers further developed a dimeric cobalt catalyst **1.35** which showed a significant rate enhancement for the ring opening of epoxides and accessed an expanded substrate scope compared to the use of monomeric catalyst **1.33** (Scheme 1.23b).

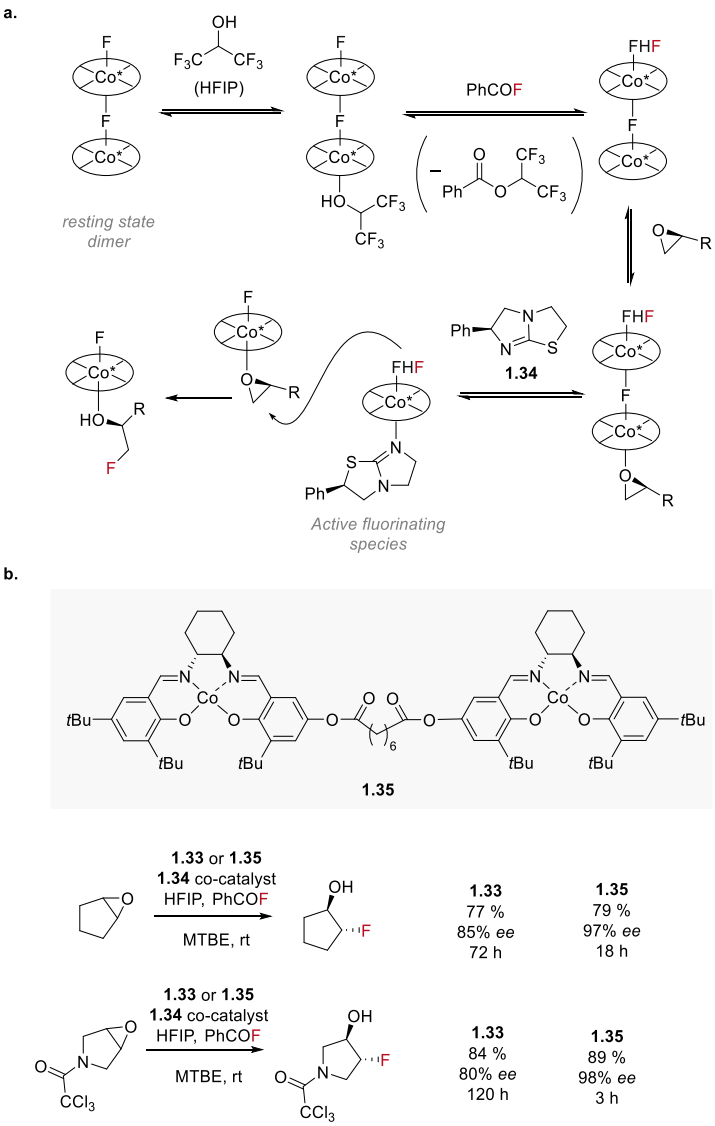

Scheme 1.23: a. Mechanistic understanding for enantioselective ring opening of epoxides by Doyle and co-workers; b. Design of dimeric cobalt catalyst **1.35** for ring opening improving selectivity and reaction times[100]

Doyle and co-workers further expanded the scope of their latent HF strategy to the ring-opening of azirdines yielding enantioenriched β-fluoroamines.[101] In contrast to the epoxide substrate class, an achiral Ti(IV) co-catalyst was also required for the activation of the aziridine. Furthermore, the protecting group on the nitrogen was deemed critical for the observed enantioselectivity, with 2-picolinamide acting as a chelating ligand onto Ti(IV) activating the aziridine which is subsequently opened by nucleophilic attack from the [Co-FHF] species (Scheme 1.24).

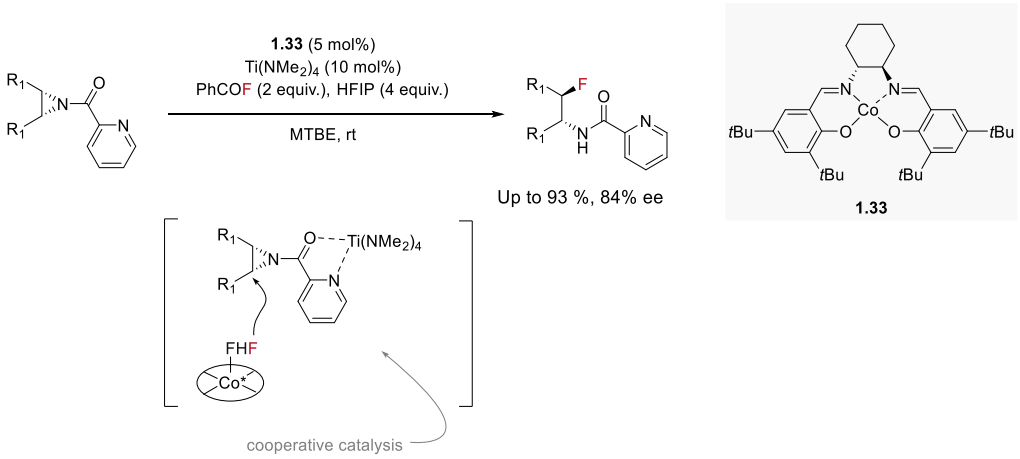

Scheme 1.24: Enantioselective ring-opening of aziridines with latent HF source by Doyle and co-workers[101]

Aside from ring-opening strategies, another substrate class which is well studied for asymmetric C–F bond are allylic (pseudo)halides. Seminal work by Doyle and co-workers reported the fluorination of cyclic allylic chlorides achieved under palladium catalysis with a chiral (Trost) bisphosphine ligand **1.36** and AgF.[102] Here, it was envisaged that allylic C–F bonds could be formed following a nucleophilic attack of fluoride onto a chiral Pd(II)-allyl species, which is a well-established mechanism for allylic functionalisation. The choice of fluorinating reagent was critical for reactivity within the system, and replacing AgF with alkali metal fluoride salts (KF or CsF) resulted in predominant elimination forming the diene side product. Doyle and co-workers also demonstrated that their methodology was amenable towards the fluorination of acyclic allylic chlorides in good regio- and moderate enantioselectivities under modified conditions, employing bulkier ligand **1.37** (Scheme 1.25a).[103] It is notable that substantial differences in reactivity were observed upon altering the leaving group. Acetates or carbonates, which are commonly employed in palladium-catalysed alkylation chemistry, were seen to be unreactive towards this fluorination protocol. Mechanistic investigations proposed that the importance of the chloride leaving group is related to the precipitation of AgCl, which provides a thermodynamic driving force towards C–F bond formation (Scheme 1.25b).

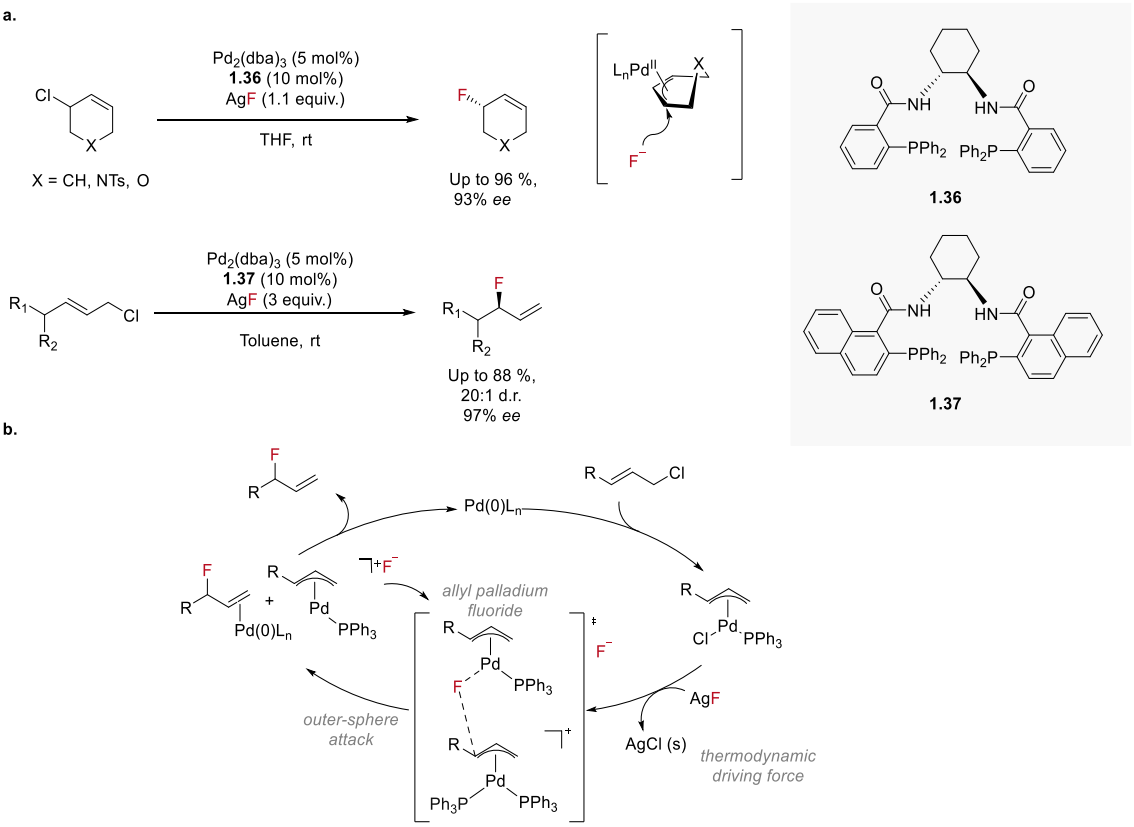

Scheme 1.25: a. (A)Cyclic allylic fluorination with AgF by Doyle and co-workers[102, 103]; b. Proposed catalytic cycle

In 2015, Nguyen and co-workers reported an enantioselective fluorination of secondary allylic trichloroacetimidiates with $Et_3N{\cdot}3HF$ under iridium catalysis using chiral diene ligand **1.38**.[104] A range of α-heteroatom and linear substrates were fluorinated under the optimised conditions in excellent regio- and enantioselectivity (branched: linear > 99:1, up to 97 % *ee*). Interestingly, benzylic substrates were fluorinated in 65 % yield however showed no induced enantioselectivity, with the hypothesis that the formation of discrete benzylic carbocations make enantiocontrol in these positions very challenging. The authors proposed enantioconvergence achieved *via* a dynamic kinetic asymmetric transformation (DYKAT) where epimerisation of a π-allyl-iridium intermediate by π-σ-π interconversion occurs at a faster rate than nucleophilic substitution with fluoride, allowing for racemic substrates to be converted into a single enantiomer of fluoride product (Scheme 1.26b).

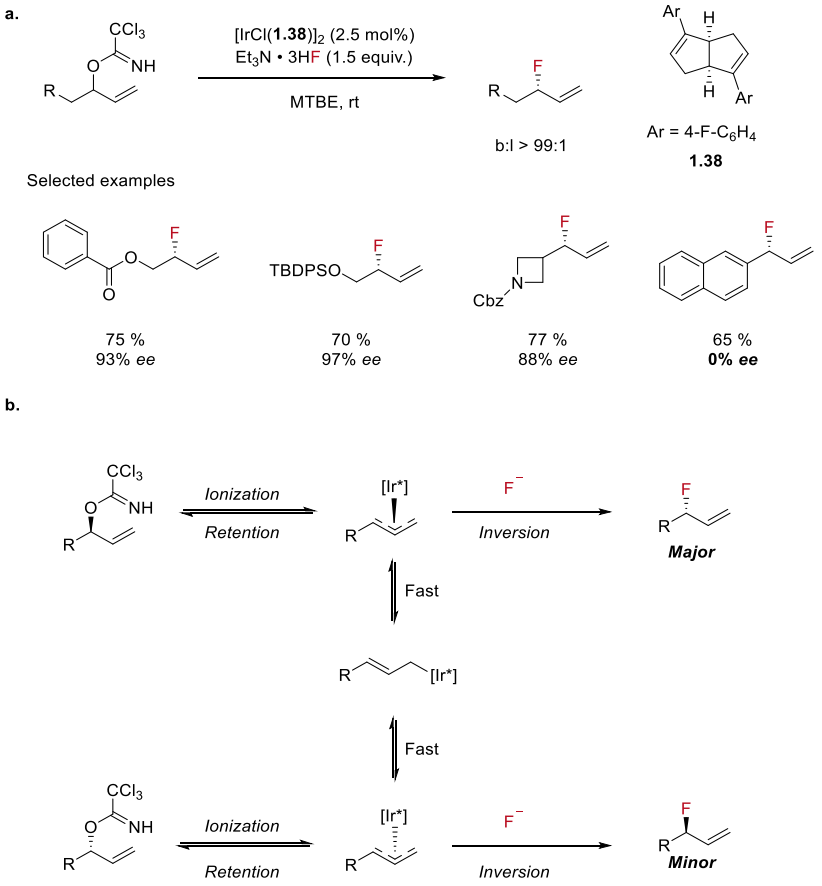

Scheme 1.26: a. Nguyen's iridium catalysed allylic fluorination of trichloroacetimidates and selected scope; b. Proposed mechanism for DYKAT[104]

In 2013, Groves and co-workers disclosed a manganese catalysed oxidative fluorination of benzylic C–H bonds with $Et_3N{\cdot}3HF$.[105] The use of a chiral manganese salen catalyst **1.39** in the presence of an external oxidant, iodosylbenzene (PhIO), and fluoride allowed for selective C–H fluorination and scope of benzylic fluorides could be prepared in up to 70 % yield. Mechanistically it was proposed that a Mn(III)salenF species formed *in situ* from **1.39** and HF is oxidised to Mn(V)(salen)O species by PhIO which is responsible for the abstraction of a hydrogen atom from the substrate forming a radical on the benzylic carbon. The benzylic radical was proposed to subsequently react with a Mn(IV)(salen)F_2 complex forming fluoride product and regenerating the Mn(II) catalyst. Analysis of the compounds **1.40** and **1.41** on a chiral stationary phase showed detectable enantioselectivities of 20% and 40% *ee* respectively, providing mechanistic evidence that the chiral salen catalyst (**1.39**) is involved in the fluoride transfer step to form products (Scheme 1.27b). The following year this methodology was

further developed and shown amenable for late stage benzylic C–H fluorination employing [^{18}F]fluoride.[106]

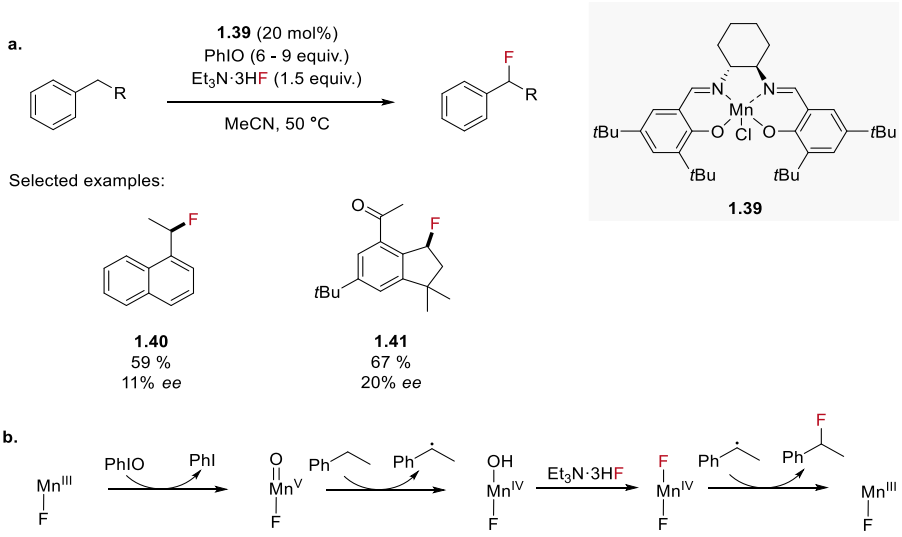

Scheme 1.27: a. Grove's oxidative fluorination catalysed by manganese salen catalyst; b. Proposed mechanistic hypothesis[105]

In 2020, Fürstner and co-workers disclosed a copper catalysed asymmetric fluorination of α-diazoesters, employing bisoxazole (BOX) ligand **1.42** and CsF.[107] This work was inspired by the racemic nucleophilic (radio)fluorination of such substrates published by Doyle and co-workers in 2016, where α-fluoroester products were prepared employing ([^{18}F])KF, however only modest enantioselectivities (31% *ee*) of products were disclosed (Scheme 1.27a).[108] The design and synthesis of bulkier BOX ligand **1.43** by Fürstner and co-workers, as well as changing the fluoride source from KF to CsF, allowed for the reaction to proceed at room temperature and accessed a scope of enantioenriched α-fluoroesters in up to 96 %, 95% *ee* (Scheme 1.28b). Mechanistically, copper insertion into diazo compounds forms electrophilic metal carbenoids; computational studies suggested an initial attack of fluoride onto the copper centre, rather than electrophilic carbon atom, which followed by a 1,2-fluoride shift delivers the fluorinated product.

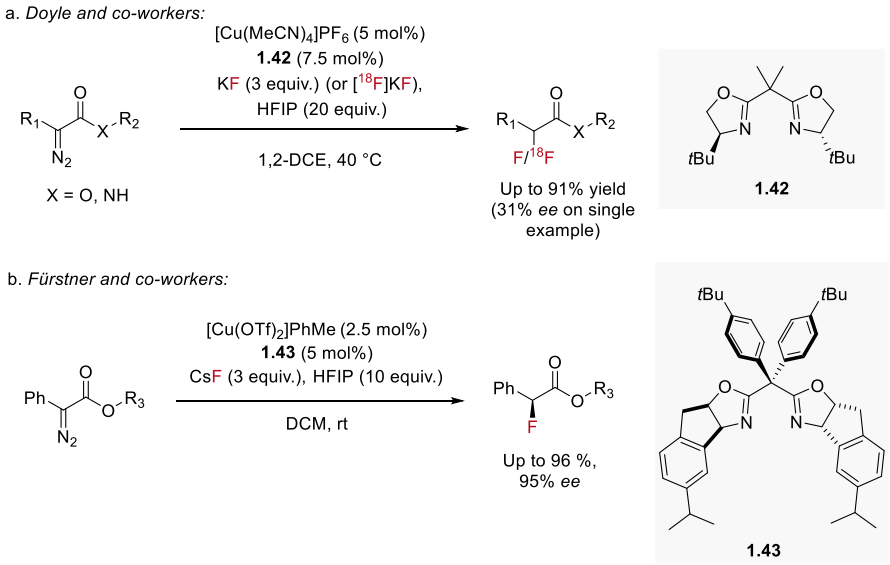

Scheme 1.28: a. Nucleophilic (radio)fluorination of α-diazoesters by Doyle and co-workers[108]; b. Enantioselective fluorination of α-diazoesters by Fürstner and co-workers[107]

1.5.3.2. Organocatalytic Asymmetric Nucleophilic Fluorination

Prior to the seminal work of Gouverneur and co-workers (*v. infra* 2.1.1. *Hydrogen Bonding Phase Transfer Catalysis*), which sits at the foundation of the work described in this thesis, there were only a handful of organocatalysed asymmetric fluorination reports where a nucleophilic approach was employed. Shibata and co-workers presented the first attempts towards enantioselective nucleophilic fluorination of β-ketoesters and the fluorocyclisation of γ-aminoalkenes employing hypervalent iodine catalysis.[109] This study built on seminal work by Nevado and co-workers who demonstrated the feasibility of iodoarene difluorides ($ArIF_2$) as stoichiometric fluorinating reagents.[110] Shibata's catalytic system consisted of chiral binaphthyl iodoarene catalyst **1.43**, HF·pyridine and *m*CPBA as an external oxidant, critical for the regeneration of the $ArIF_2$ species. Fluorinated products for both transformations were isolated in good yields and moderate enantioselectivities (Scheme 1.29).

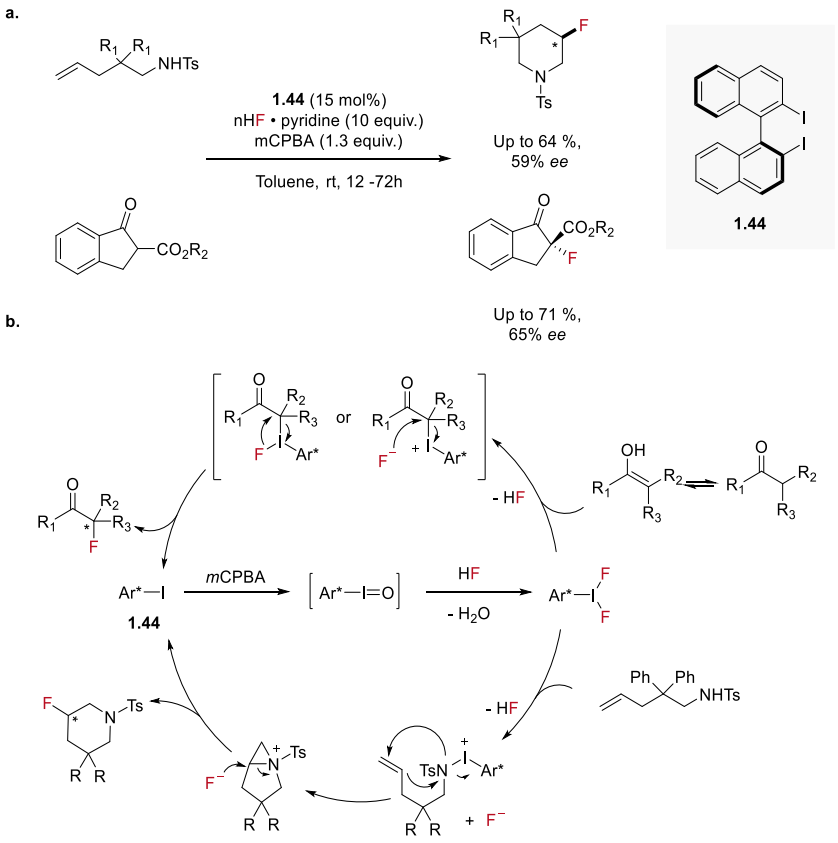

Scheme 1.29: a. Organocatalytic fluorination of β-fluoroesters and fluorocyclisation of γ-aminoalkenes; b. proposed catalytic cycle(s)[109]

This concept of using hypervalent iodine organocatalysts with HF as a fluorine source has been widely explored following this first disclosure, and an increase range of novel iodoarene catalysts have been reported which have allowed for the synthesis of a broader scope of fluorinated products to be synthesised in high enantiopurity,[111-113] including examples of asymmetric difluorinations by the groups of Jacobsen and Gilmour.[114, 115]

1.5.4. Asymmetric Biocatalytic Fluorination

Recently efforts have been made towards the development of biocatalytic strategies for fluorination. Concurrently, Huang, Yang, Garcia-Borras and co-workers, and Liu, Yang and co-workers reported the discovery and development of non-haem iron enzymes capable of enantioselective C(sp^3)–H benzylic fluorination *via* a radical fluorine transfer from *N*-fluoroamide substrates.[116, 117] Huang, Yang and Garcia-Borrás identified a (*S*)-2-hydroxypropylphosphonate epoxidase from *Streptomyces viridochromogenes* (SvHppE-Fluor) which allowed access to (*R*)-configured chiral benzylic fluorides in up to 94% *ee.*

Meanwhile Liu and Yang reported an engineered variant of 1-aminocyclopropane-1-carboxylic acid oxidase from *Petunia hybrida* ($ACCO_{CHF}$), which accessed the (*S*)-configured fluoride product in up to 94% *ee*. Mechanistically these two complimentary approaches were both proposed to involve a rate determining activation of the N–F bond of the fluoroamide substrate is followed by a 1,5-hydrogen atom abstraction to yield a benzylic radical, which following the fluorine atom rebound forms corresponding C–H fluorination product (Scheme 1.30).

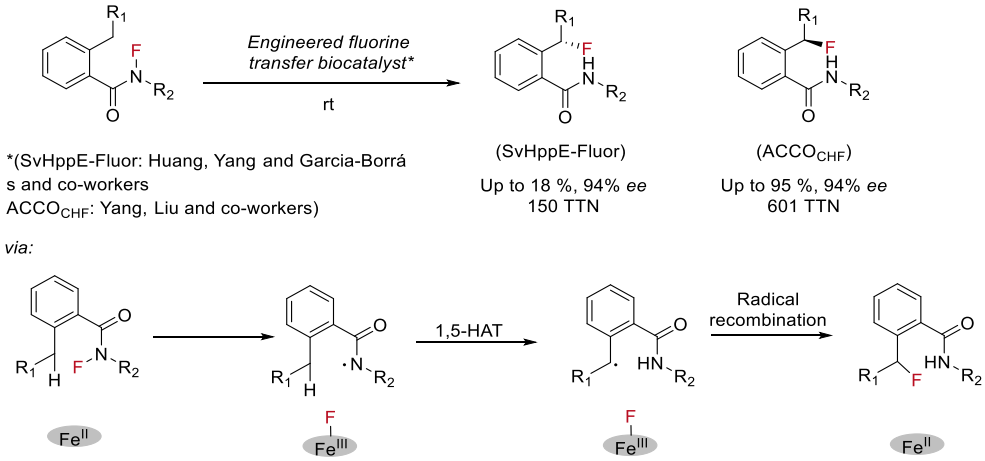

Scheme 1.30: Two approaches to biocatalytic C(sp^3)–F bond formation *via* radical fluorine transfer from *N*-fluoroamides[116, 117]

1.5.5. Nucleophilic Fluorination with Alkali Metal Fluoride Salts

Alkali metal fluoride salts, particularly potassium fluoride (KF), could be considered as optimal sources of fluorine atoms in organic synthesis. KF is a safer and easier to handle fluorinating reagent than HF and its complexes, which are associated with a multitude of safety concerns and have been responsible for many industrial scale disasters in recent years.[118, 119] KF is cost-effective, particularly in comparison to its electrophilic counterparts (e.g., KF - \$8 mol^{-1}, Selectfluor® - \$407 mol^{-1}). However, the predominate factor making the alkali metal fluoride salts unfavourable as fluorinating reagents is their lack of solubility in organic solvents. This property is on account of their high lattice energy, which decreases upon increasing cationic radius, with CsF having the weakest crystalline lattice of the alkali metals (Table 1.3). Hygroscopity and the propensity of fluoride to form strong hydrogen bonds with water, or any capable hydrogen-bond donor, is also a challenge in the employment of alkali metal fluorides as reagents. CsF, which has a lattice energy of 181 kcal/mol, is highly hygroscopic making it a

challenging to handle and the presence of water difficult to avoid. Moreover, the hydration shell formed around fluoride dampens its nucleophilicity, further complicating its use.

Table 1.3: Cationic radius and lattice energy of alkali metal fluoride salts[120]

Entry	Fluoride Salt	Cation radius (Å)	Lattice energy (kcal/mol)
1	LiF	0.79	251
2	KF	1.38	198
3	RbF	1.52	190
4	CsF	1.67	181

Methods of improving the reactivity of alkali metal fluoride salts can be divided into two key strategies: (i) modulation/sequestration of the alkali metal cation, weakening ionic interactions to release the fluoride anion, (ii) modulation/sequestration of the fluoride anion through hydrogen bonding. Liotta and co-workers investigated the former through use of 18-crown-6 to improve the solubility of KF in acetonitrile and benzene.[121] Sequestration of the potassium cation by the crown ether resulted in the generation of, in the authors words, a "naked" fluoride anion. Liotta and co-workers evaluated the reactivity of the "naked" fluoride anion towards fluorination of different substrate structures. Whilst primary fluorination under this strategy provided quantitative yield of fluorinated product, the highly basic nature of fluoride in its unsolvated form, resulted in competitive elimination pathways being favoured for secondary and tertiary alkyl halides (Scheme 1.31).

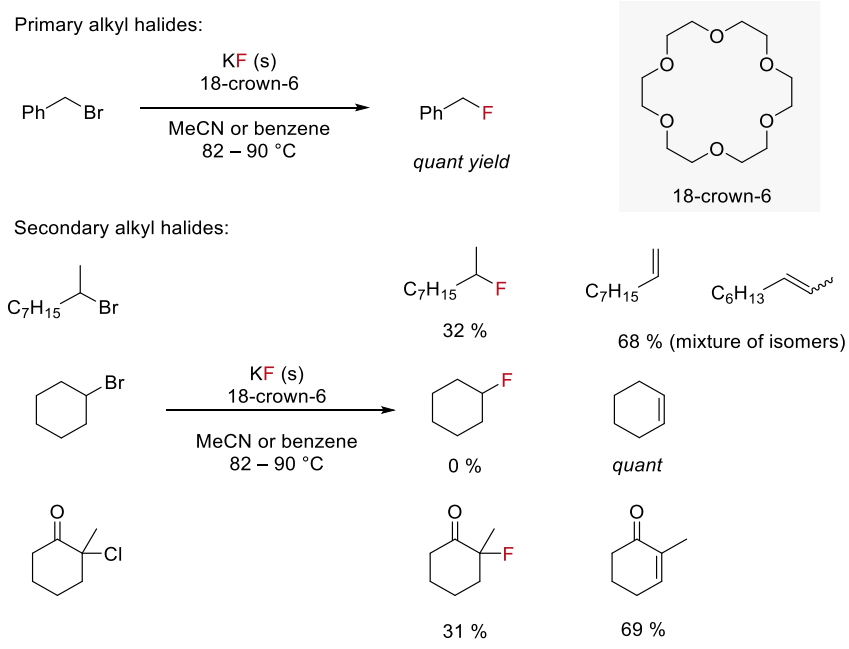

Scheme 1.31: The use of 18-crown-6 to increase reactivity of KF for the fluorination of alkyl halides by Liotta and co-workers[121]

It is notable that chiral polyether-based PT catalysts have been reported for the solubilisation of KF, however they have largely been employed for asymmetric desilylative resolution processes rather than towards nucleophilic fluorination.[122]

Kim and co-workers were the first to report the use of bulky alcohol solvents to increase the rate and selectivity of S_N2 fluorination reactions with CsF. The model mesylate substrate **1.46** could only be fluorinated in 7 % yield in MeCN, however the modulation of the fluoride anion with hydrogen bonding interactions of *t*BuOH as a solvent increased the yield of fluorinated product **1.47** to 92 % (Scheme 1.32a).[123] Furthermore, the authors described the preparation of a complex of TBAF(*t*-BuOH)$_4$ which could be used as a stoichiometric reagent giving analogous results to employing CsF in *t*-BuOH as a solvent. TBAF(*t*-BuOH)$_4$, a stable solid of lower hygroscopicity than TBAF·3H$_2$O, has been widely employed as a reagent, an example of this is the transition metal mediated fluorination of allylic carbonates by Gouverneur and co-workers (Scheme 1.32b).[124]

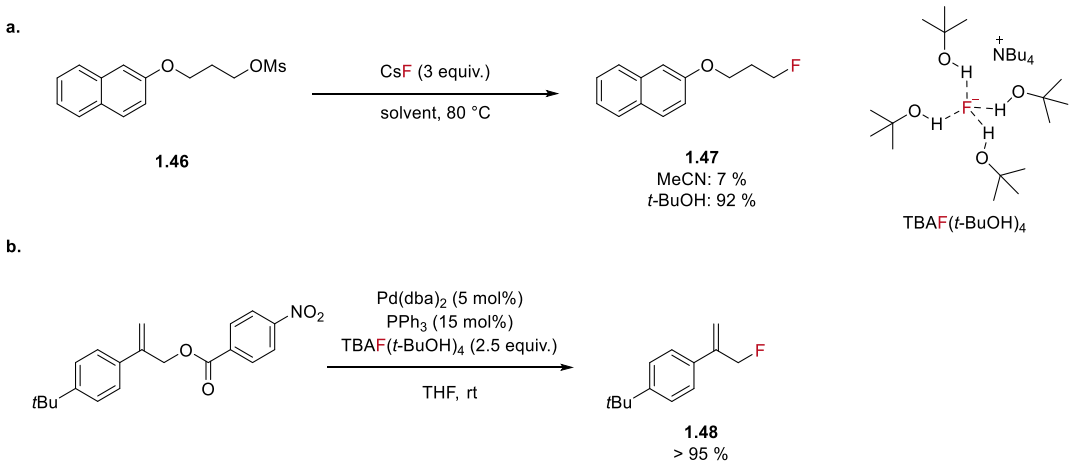

Scheme 1.32: a. Fluorination of primary mesylates with CsF in MeCN/*t*-BuOH by Kim and co-workers[123]; b. The use of TBAF(*t*-BuOH)$_4$ as a stochiometric reagent in allylic fluorination by Gouverneur and co-workers[124]

These seminal reports encouraged further investigation on how hydrogen bonding can be used to increase the reactivity of fluoride, but unlike crown ethers, also allow for selective fluorination over elimination. In 2015, Gouverneur and co-workers studied fluoride-alcohol complexes and the impact of coordination and hydrogen bonding on reactivity.[125] A series of fluoride-alcohol complexes were prepared and characterised through X-ray crystallography. It was observed that fluoride coordination

ranged from two to four alcohols, depending on the steric bulk of the alcohol employed. In general, it was seen that more coordination around the fluoride resulted in slower reaction rates however also a more favourable distribution between substitution and elimination (Scheme 1.33).

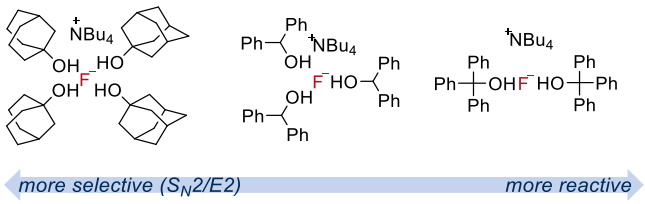

Scheme 1.33: Alcohol-TBAF complexes prepared by Gouverneur and co-workers[125]

Gouverneur and co-workers further investigated the hydrogen bonding ability of diphenylureas to fluoride. A series of electronically diverse diphenyl urea HBDs were synthesised and their TBAF complexes prepared and characterised *via* X-ray crystallography and neutron scattering.[126] A diverse array of structural arrangements were observed for urea-fluoride complexes including di-, tetra-, and even hexa- coordination depending on the size of ammonium counter cation. Urea-fluoride complexes could also be co-crystallised with water yielding higher order structures possessing bridging water molecules (Scheme 1.34).

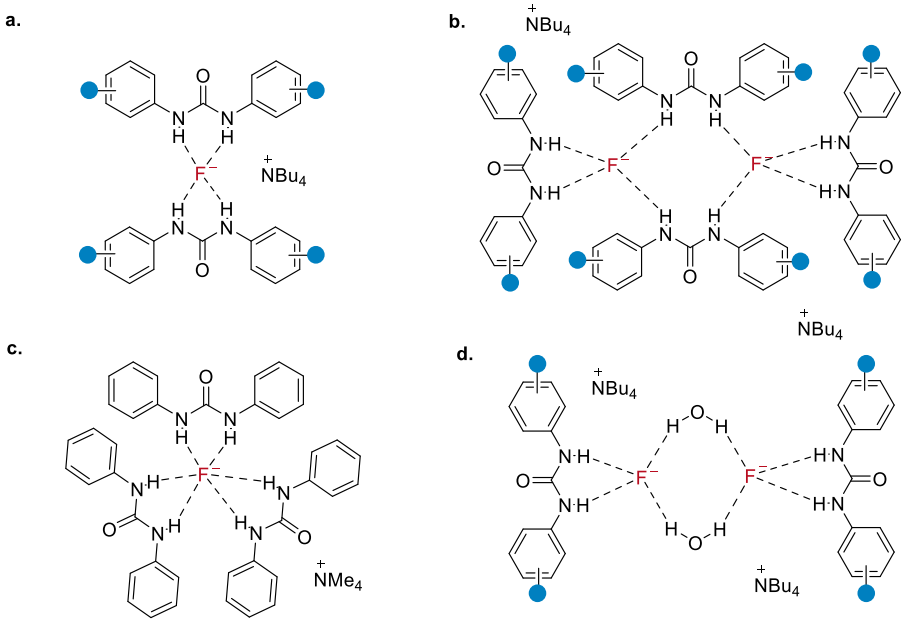

Scheme 1.34: Diversity of coordination modes observed for urea-fluoride complexes by Gouverneur and co-workers[126]

The fluorinating ability of diphenylurea-fluoride complexes were investigated on model alkyl bromide **1.49**. Diphenylurea complexes were found to be efficient fluorinating reagents, however showed significantly lower reactivity than the previously disclosed alcohol-TBAF complexes and soluble fluoride source TBAF·3H_2O (Table 1.4, entry 8).

Investigations into the electronic properties of the aryl rings on diphenyl ureas demonstrated that complexes derived from electron-deficient ureas were less reactive than the corresponding electron-neutral or rich as a consequence of increased hydrogen bonding. However, electron poor ureas also showed improved S_N2/E2 selectivity in favour of fluorination of **1.48**. 1,3-*bis*(4-fluorophenyl) urea performed best within the series, with an S_N2/E2 ratio of 8.7 (Table 1.4, entry 7). Spectroscopic studies provided evidence that urea-fluoride species exists as both 1:1 $[UF]^-$ and 2:1 $[U_2F]^-$ complexes as a function of fluoride concentration, however kinetic data demonstrated that increased second order rate constants were measured at higher dilution. This indicated that reactivity proceeds by a pre-equilibrium dissociation to the more reactive 1:1 $[UF]^-$ species for fluorination.

Table 1.4: Relative rates of fluorination / elimination for diarylurea HBD catalysts[126]

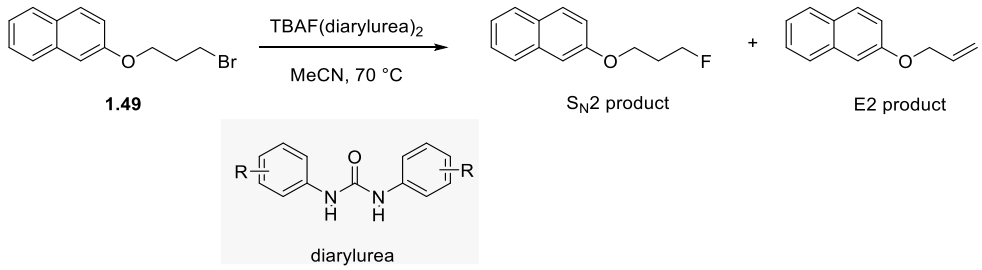

Entry	R	*k* (relative)	*k* (S_N2)/ k (E2)
1	4-OMe	7.7	5.2
2	4-Me	6.0	5.7
3	4-H	3.5	6.8
4	4-F	3.4	7.1
5	4-Cl	3.5	6.9
6	4-NO_2	2.0	8.4
7	4-CF_3	1.0	8.7
8	TBAF·3H_2O	227	1.6

1.6. Conclusions

Fluorine's significance in modern science has generated considerable interest in developing methods to incorporate it into organic molecules. This chapter provided an overview of how fluorine substitution uniquely impacts molecules, and explores the fascinating origins of fluorine on Earth examining the contrast between its absence in biochemistry and its current importance in organic synthesis, particularly towards pharmaceutical design. Additionally, the chapter offers a prelude to the synthesis of asymmetric carbon-fluorine bonds, covering key developments from early electrophilic fluorination under enamine or transition metal catalysis to more recent advances in both phase transfer and organocatalysis.

The next chapters will introduce and focus on the developments made within the Gouverneur group on asymmetric fluorination under Hydrogen Bonding Phase Transfer Catalysis (HBPTC) where alkali metal fluoride salts are used as fluorinating reagents. This thesis will specifically highlight the recent advancements which have been made possible through a synergistic approach that combines the principles of hydrogen bonding and onium salt phase transfer catalysis.

1.7. References

(1) Roesky, H. W.; *Efficient Preparations of Fluorine Compounds;* John Wiley & Sons, Inc., 2012.
(2) Inoue, M.; Sumii, Y.; Shibata, N. Contribution of Organofluorine Compounds to Pharmaceuticals. *ACS Omega* **2020**, *5* (19),10633–10640.
(3) Agricola, G. Bermannus sive de re metallica; Hieronymus Froben, 1530.
(4) Scheele, C. W. Undersökning om fluss-spat och dess syra (Investigation of fluorite and its acid). *Kongl. Vetenskaps Akademiens Handlingar* **1771**, *32*, 129–138.
(5) Moissan, H. Action d'un courant électrique sur l'acide fluorhydrique anhydre. Comptes rendus hebdomadaires des séances de l'Académie des sciences **1886**, 1543–1544.
(6) Wisniak, J. The History of Fluorine - from Discovery to Commodity. *IJCT*, **2002**, *9,* 363–372.
(7) Hunter, L. The C–F bond as a conformational tool in organic and biological chemistry. *Beilstein J. Org. Chem.* **2010**, *6* (38).
(8) Müller, K.; Faeh, C.; Diederich, F. Fluorine in Pharmaceuticals: Looking Beyond Intuition. *Science* **2007**, *317* (5846), 1881–1886.
(9) Meanwell, N. Fluorine and Fluorinated Motifs in the Design and Application of Bioisosteres for Drug Design. *J. Med. Chem.* **2018**, *61* (14), 5822–5880.
(10) Thiehoff, C.; Rey, Y. P.; Gilmour, R. The Fluorine Gauche Effect: A Brief History. *Irs. J. Chem.* **2017**, *57*, 92–100.
(11) Pauling, L.; *The Nature of the Chemical Bond and the Structure of Molecules and Crystals*; Cornell University Press, 1939.
(12) Gillis, E.; Eastman, K.; Hill, M.; Donnelly, D.; Meanwell, N.; Applications of Fluorine in Medicinal Chemistry. *J. Med. Chem.* **2015**, *58* (21), 8315–8359.
(13) Lankin, D; Chandrakumar, N.; Rao, S.; Spangler, D.; Snyder, J. Protonated 3-Fluoropiperidines - An Unusual Fluoro Directing Effect and a Test for Quantitative Theories of Solvation. *J. Am. Chem. Soc.* **1993**, *115* (8), 3356–3357.
(14) Snyder, J.; Chandrakumar, N.; Sato, H.; Lankin, D. The Unexpected Diaxial Orientation of *cis*-3,5-difluoropiperdine in Water: A potent CF---NH Charge-Dipole Effect. *J. Am. Chem. Soc.* **2000**, *122* (3), 544–545.
(15) Trudeau, M.; Warmke, J.; Ganetzky, B.; Robertson, G. HERG, A Human Iward Rectifier in the Voltage-Gated Potassium Channel Family. *Science* **1995**, *269* (5220), 92–95.
(16) Sanguinetti, M.; Jiang, C.; Curran, M.; Keating, M. A Mechanistic Link Between an Inherited and an Acquired Cardiac-Arrhythemia - HERG Encodes the IKR Potassium Channel. *Cell* **1995**, *81* (2), 299–307.
(17) Shaw, S.; Goff, D.; Boralsky, L.; Singh, R.; Sweeny, D.; Park, G.; Sun, T.; Jenkins, Y.; Markovtsov, V.; Issakani, S.; Payan, D. G.; Hitoshi, Y. Optimization of Pharmacokinetic and In Vitro Safety Profile of a Series of Pyridine Diamide Indirect AMPK Activators. *J. Med. Chem.* **2023**, *66* (24), 17086–17104.
(18) Thornber, C. Isosterism and Molecular Modification in Drug Design. *Chem. Soc. Rev.* **1979**, *8*, 563–580.
(19) Clader, J. W. The Discovery of Ezetimibe: A View from Outside the Receptor. *J. Med. Chem.* **2004**, *47* (1), 1–9.
(20) Barnes-Seeman, D.; Jain, M.; Bell, L.; Ferreira, S.; Cohen, S.; Chen, X.; Amin, J.; Snodgrass, B.; Hatsis, P. Metabolically Stable tert-Butyl Replacement. *ACS Med. Chem. Lett.* **2013**, *4* (6), 514–516.
(21) Banks, J.; Batsanov, A.; Howard, J.; O'Hagan, D.; Rzepa, H.; Martin-Santamaria, S. The preferred conformation of α-fluoroamides. *J. Chem. Soc., Perkin Trans. 2* **1999**, (11), 2409–2411.
(22) Vanderveken, B.; Truyen, S.; Herrebout, W.; Watkins, G. Vibrational Conformational-Analysis of Methyl Fluoroacetate and Methyl Difluoroacetate. *J. Mol. Struct.* **1993**, *293*, 55–58.
(23) Abraham, R. J.; Jones, A. D.; Warne, M. A.; R., R.; Tormena, C. F. Conformational Analysis. Part 27. NMR, Solvation and Theoretical Investigation of Conformational Isomerism in Dluoro- and 1,1-Difluoro-Acetone. *J. Chem. Soc., Perkin Trans. 2* **1996**, *2*, 533–539.
(24) O'Hagan, D. Understanding Organofluorine chemistry. An introduction to the C–F bond. *Chem. Soc. Rev.* **2008**, *37*, 308–319.

(25) McKinney, B.; Urban, J. Fluoroolefins as Peptide Mimetics. 2. A Computational Study of the Conformational Ramifications of Peptide Bond Replacement. *J. Phys. Chem.* **2010**, *114* (2), 1123–1133.
(26) Abraham, R. J.; J, A. R.; Ellison, S. L. R.; Schonholzer, P.; Thomas, W. A. A. Theoretical and Crystallographic Study of the Geometries and Conformations of Fluoro-olefins as Peptide Analogues. *Tetrahedron* **1986**, *42* (7), 2101–2110.
(27) Wolfe, S. Gauche Effect - Some Stereochemical Consquences of Adjacent Electron Pairs and Polar Bonds. *Acc. Chem. Res.* **1972**, *5* (3), 102–111.
(28) Martins, F.; Freitas, M. The Fluorine Gauche Effect and a Comparison with Other Halogens in 2-Halofluoroethanes and 2-Haloethanols. *Eur. J. Org. Chem.* **2019**, *2019* (37), 6401–6406.
(29) Akkerman, F.; Buschmann, J.; Lentz, D.; Luger, P.; Rödel, E. Crystal and Molecular Structure of 1,2-Difluoroethane and 1,2-Diiodoethane. *J. Chem. Crystallogr.* **2003**, *33*, 969–975.
(30) Silva, D.; Santos, L.; Hamlin, T.; Guerra, C.; Freitas, M.; Bickelhaupt, F. The Gauche Effect in XCH2CH2X Revisited. *ChemPhysChem.* **2021**, *22* (7), 641–648.
(31) Sugiura, K.; Nagano, K.; Hirabayashi, K.; Nishinaga, T.; Shimizu, T. The Gauche Effect in 1,2-Bis(arylsulfonate)ethanes. *Eur. J. Org. Chem.* **2024**. e202400781.
(32) Briggs, C. R. S.; Allen, M. J.; O'Hagan, D.; Tozer, D. J.; Slawin, A. M. Z.; Goeta , A. E.; Howard, J. A. K. The Observation of a Large Gauche Preference when 2-Fluoroethylamine and 2-Fluoroethanol Become Protonated. *Org. Biomol. Chem.* **2004**, *2*, 732–740.
(33) Sparr, C.; Schweizer, W.; Senn, H.; Gilmour, R. The Fluorine-Iminium Ion Gauche Effect: Proof of Principle and Application to Asymmetric Organocatalysis. *Angew. Chem. Int. Ed.* **2009**, *48* (17), 3065–3068.
(34) Marigo, M.; Franzén, J.; Poulsen, T. B.; Zhuang, W.; Jørgensen, K. A. Asymmetric Organocatalytic Epoxidation of α,β-Unsaturated Aldehydes with Hydrogen Peroxide. *J. Am. Chem. Soc.* **2005**, *127* (19), 6964–6965.
(35) Aufiero, M.; Gilmour, R. Informing Molecular Design by Stereoelectronic Theory: The Fluorine Gauche Effect in Catalysis. *Acc. Chem. Res.* **2018**, *51* (7), 1701–1710.
(36) Arunan, E.; Desiraju, G.; Klein, R.; Sadlej, J.; Scheiner, S.; Alkorta, I.; Clary, D.; Crabtree, R.; Dannenberg, J.; Hobza, P.; Kjaergaard, H. G.; Legon, A. C.; Mennucci, B.; Nesbitt, D. J. Definition of the Hydrogen Bond (IUPAC Recommendations 2011). *Pure Appl. Chem.* **2011**, *83* (8), 1637–1641.
(37) Steiner, T. The Hydrogen Bond in the Solid State. *Angew. Chem. Int. Ed.* **2002**, *41* (1), 48–76.
(38) Howard, J.; Hoy, V.; OHagan, D.; Smith, G. How Good is Fluorine as a Hydrogen Bond Acceptor? Tetrahedron. **1996**, *52*, 12613–12622.
(39) Dunitz, J.; Taylor, R. Organic Fluorine Hardly Ever Accepts Hydrogen Bonds. Chem. Eur. J. **1997**, *3* (1), 89–98.
(40) Goldstein, D.; Soth, M.; Gabriel, T.; Dewdney, N.; Kuglstatter, A.; Arzeno, H.; Chen, J.; Bingenheimer, W.; Dalrymple, S.; Dunn, J.; Farrell, R.; Frauchiger, S.; La Fargue, J.; Ghate, M.; Graves, B.; Hill, R. J.; Li, F.; Litman, R.; Loe, B.; McIntosh, J.; McWeeny, D.; Papp, E.; Park, J.; Reese, H. F.; Roberts, R. T.; Rotstein, D.; San Pablo, B.; Sarma, K.; Stahl, M.; Sung, M. L.; Suttman, R. T.; Sjogren, E. B.; Tan, Y.; Trejo, A.; Welch, M.; Weller, P.; Wong, B. R.; Hasim, Z. Discovery of 6-(2,4-Difluorophenoxy)-2[3-hydroxy-1-(2-hydroxyethyl)propylamino]-8-methyl-8*H*-pyrido[2,3-*d*]pyrimidin-7-one (Pamapimod) and 6-(2,4-Difluorophenoxy)-8-methyl-2-(tetrahydro-2*H*-pyran-4-ylamino)pyrido[2,3-*d*]pyrimidin-7(8*H*)-one (R1487) as Orally Bioavailable and Highly Selective Inhibitors of p38α Mitogen-Activated Protein Kinase. *J. Med. Chem.* **2011**, *54* (7), 2255–2265.
(41) Takemura, H.; Ueda, R.; Iwanaga, T. C-F···HO Hydrogen Bond in 8-fluoro-4-methyl-1-naphthol. J. Fluor. Chem. **2009**, *130* (7), 684–688.
(42) Champagne, P.; Desroches, J.; Paquin, J. Organic Fluorine as a Hydrogen-Bond Acceptor: Recent Examples and Applications. *Synthesis* **2015**, *47* (3), 306–322.
(43) Giuffredi, G. T.; Gouverneur, V.; Bernet, B. Intramolecular OH···FC Hydrogen Bonding in Fluorinated Carbohydrates: CHF is a Better Hydrogen Bond Acceptor than CF_2. *Angew. Chem. Int. Ed.* **2013**, *52* (40), 10524–10528.

(44) Graton, J.; Wang. Z.; Brossard, A. M.; Monteiro, D. G.; Le Questel, J. Y.; Linclau, B. An Unexpected and Significantly Lower Hydrogen-Bond-Donating Capacity of Fluorohydrins Compared to Nonfluorinated Alcohols. *Angew. Chem. Int. Ed.* **2012**, *51* (25), 6176–6180.
(45) Linclau, B.; Peron, F.; Bogdan, E.; Wells, N.; Wang. Z.; Compain, G.; Fontenelle, C. Q.; Galland, N.; Le Questel, J. Y.; Graton, J. Intramolecular OH···Fluorine Hydrogen Bonding in Saturated, Acyclic Fluorohydrins: The γ-Fluoropropanol Motif. *Chem. Eur. J.* **2015**, *21* (49), 17808–17816.
(46) Greenwood, N. N.; Earnshaw, A.; *Chemistry of the Elements 2nd Edition;* Butterworth-Heinemann, 1998.
(47) Günne, J.; Mangstl, M.; Kraus, F. Occurrence of Difluorine F2 in Nature-In Situ Proof and Quantification by NMR Spectroscopy. *Angew. Chem. Int. Ed.* **2012**, *51* (31), 7847–7849.
(48) Chan, K.; O'Hagan, D. The Rare Fluorinated Natural Products and Biotechnological Prospects for Fluorine Enzymology. Methods in Enzymology. **2012**, *516,* 219–235.
(49) Sorokina, M.; Merseburger, P.; Rajan, K.; Yirik, M.; Steinbeck, C. COCONUT online: Collection of Open Natural Products database. *J. Cheminf.* **2021**, *13*.
(50) Rosén, J.; Gottfries, J.; Muresan, S.; Backlund, A.; Oprea, T. Novel Chemical Space Exploration via Natural Products. *J. Med. Chem*. **2009**, *52* (7), 1953–1962.
(51) Haupt, A.; *Organic and Inorganic Fluorine Chemistry*; De Gruyter, 2021.
(52) Zechel, D. L.; Reid, S. P.; Nashiru, O.; Mayer, C.; Stoll, D.; Jakeman, D. L.; Warren, P. A. J.; Withers, S. G. Enzymatic Synthesis of Carbon-Fluorine Bonds. *J. Am. Chem. Soc.* **2001**, *123* (18), 4350–4351.
(53) O'Hagan, D.; Schaffrath, C.; Cobb, S.; Hamilton, J.; Murphy, C. Biosynthesis of an Organofluorine Molecule. *Nature* **2002**, *416*, 279–279.
(54) Petkowski, J.; Seager, S.; Bains, W. Reasons Why Life on Earth Rarely Makes Fluorine-Containing Compounds and Their Implications for the Search for Life Beyond Earth. *Scientific Reports* **2024**, *14*, 15575.
(55) Motter, J.; Benckendorff, C.; Westarp, S.; Sunde-Brown, P.; Neubauer, P.; Kurreck, A.; Miller, G. Purine Nucleoside Antibiotics: Recent Synthetic Advances Harnessing Chemistry and Biology. *Nat. Prod. Rep.* **2024**, *41* (6), 863–884.
(56) O'Hagan, D.; Deng, H. Enzymatic Fluorination and Biotechnological Developments of the Fluorinase. *Chem. Rev.* **2015**, *115* (2), 634–649.
(57) Harper, D.; O' Hagan D. The Fluorinated Natural-Products. *Nat. Prod. Rep.* **1994**, *11*, 123–133.
(58) Harsanyi, A.; Sandford, G. Organofluorine Chemistry: Applications, Sources and Sustainability. *Green Chem.* **2015**, *17* (4), 2081–2086.
(59) Filler, R.; Saha, R. Fluorine in Medicinal Chemistry: A Century of Progress and a 60-year Retrospective of Selected Highlights. *Future Med. Chem.* **2009**, *1* (5), 777–791.
(60) Villalba, G.; Ayres, R.; Schroder, H. Accounting for Fluorine - Production, Use, and Loss. *J. Ind. Ecol.* **2007**, *11* (1), 85–101.
(61) Caron, S. Where Does the Fluorine Come From? A Review on the Challenges Associated with the Synthesis of Organofluorine Compounds. *Org. Process Res. Dev.* **2020**, *24* (4), 470–480.
(62) Umemoto, T.; Kawada, K.; Tomita, K. N-fluoropyridinium Triflate and its Derivatives: Useful Fluorinating Agents. *Tetrahedron Lett.* **1986**, *27* (37), 4465–4468.
(63) Umemoto, T.; Harasawa, K.; Tomizawa, G.; Kawada, K.; Tomita, K. Syntheses and Properties of N-Fluoropyridinium Salts. BCSJ. **1991**, *64* (4), 1081–1092.
(64) Banks, R. Selectfluor™ reagent F-TEDA-BF_4 in Action: Tamed Fluorine at Your Service. *J. Fluor. Chem.* **1998**, *87* (1), 1–17.
(65) Differding, E.; Ofner, H. N-Fluorobenzenesulfonimide - A Practical Reagent for Electrophilic Fluorinations. *Synlett*. **1991**, *3*, 187–189.
(66) Brill, Z.; Condakes, M.; Ting, C.; Maimone, T. Navigating the Chiral Pool in the Total Synthesis of Complex Terpene Natural Products. *Chem. Rev.* **2017**, *117* (18), 11753–11795.
(67) Bredig, G.; Fiske, P. S. Durch Katalysatoren Bewirkte Asymmetrische Synthese. *Biochem. Z.* **1912**, *46*, 7–23.
(68) Hintermann, L.; Togni, A. Catalytic Enantioselective Fluorination of β-Ketoesters. *Angew. Chem. Int. Ed.* **2000**, *39* (23), 4359–4362.

(69) Yang, X. Y.; Wu, T.; Phipps, R. J.; Toste, F. D. Advances in Catalytic Enantioselective Fluorination, Mono-, Di-, and Trifluoromethylation, and Trifluoromethylthiolation Reactions. *Chem. Rev.* **2015**, *115* (2), 826–870.
(70) Talbot, E. P. A.; Fernandes, T. D.; McKenna, J. M.; Toste, F. D. Asymmetric Palladium-Catalyzed Directed Intermolecular Fluoroarylation of Styrenes. *J. Am. Chem. Soc.* **2014**, *136* (11), 4101–4104.
(71) Furuya, T.; Kaiser, H. M.; Ritter, T. Palladium-Mediated Fluorination of Arylboronic Acids. *Angew. Chem. Int. Ed.* **2008**, *47* (32), 5993–5996.
(72) Ball, N. D.; Sanford, M. S. Synthesis and Reactivity of a Mono-sigma-Aryl Palladium(IV) Fluoride Complex. *J. Am. Chem. Soc.* **2009**, *131* (11), 3796–3797.
(73) Engle, K.; Mei, T.; Wang, X.; Yu, J. Bystanding F+ Oxidants Enable Selective Reductive Elimination from High-Valent Metal Centers in Catalysis. *Angew. Chem. Int. Ed.* **2011**, *50* (7), 1478–1491.
(74) Park, H.; Verma, P.; Hong, K.; Yu, J. Q. Controlling Pd(IV) Reductive Elimination Pathways Enables Pd(II)-Catalysed Enantioselective C(sp^3)–H Fluorination. *Nat. Chem.* **2018**, *10* (7), 755–762.
(75) Hajos, Z.; Parrish, D. Asymmetric Synthesis of Bicyclic Intermediates of Natural Product Chemistry. *J. Org. Chem.* **1974**, *39* (12), 1615–1621.
(76) Tu, Y.; Wang, Z.; Shi, Y. An Efficient Asymmetric Epoxidation Method for Trans-Olefins Mediated by a Fructose-Derived Ketone. *J. Am. Chem. Soc.* **1996**, *118* (40), 9806–9807.
(77) Denmark, S.; Wu, Z.; Crudden, C.; Matsuhashi, H. Catalytic Epoxidation of Alkenes with Oxone .2. Fluoro Ketones. *J. Org. Chem.* **1997**, *62* (24), 8288–8289.
(78) Sigman, M.; Jacobsen, E. Schiff Base Catalysts for the Asymmetric Strecker Reaction Identified and Optimized from Parallel Synthetic Libraries. *J. Am. Chem. Soc.* **1998**, *120* (19), 4901–4902.
(79) Corey, E.; Grogan, M. Enantioselective Synthesis of α-Amino Nitriles from N-Benzhydryl Imines and HCN with a Chiral Bicyclic Guanidine as Catalyst. *Org. Lett.* **1999**, *1* (1), 157–160.
(80) List, B.; Lerner, R.; Barbas, C. I. Proline-Catalyzed Direct Asymmetric Aldol Reactions. *J. Am. Chem. Soc.* **2000**, *122* (10), 2395–2396.
(81) Ahrendt, K.; Borths, C.; MacMillan, D. New strategies for Organic Catalysis: The First Highly Enantioselective Organocatalytic Diels-Alder Reaction. *J. Am. Chem. Soc.* **2000**, *122* (17), 4243–4244.
(82) Krämer, K. Explainer: Why Has Asymmetric Organocatalysis Won the Chemistry Nobel Prize? In Chemistry World, 2021.
(83) Enders, D.; Hüttl, M. Direct Organocatalytic α-Fluorination of Aldehydes and Ketones. Synlett. **2005**, *2005* (6), 991–993.
(84) Marigo, M.; Fielenbach, D.; Braunton, A.; Kjoersgaard, A.; Jorgensen, K. Enantioselective Formation of Stereogenic Carbon-Fluorine Centers by a Simple Catalytic Method. *Angew. Chem. Int. Ed.* **2005**, *44* (24), 3703–3706.
(85) Steiner, D.; Mase, N.; Barbas, C. Direct Asymmetric α-Fluorination of Aldehydes. *Angew. Chem. Int. Ed.* **2005**, *44* (24), 3706–3710.
(86) Beeson, T.; MacMillan, D. Enantioselective Organocatalytic α-Fluorination of Aldehydes. *J. Am. Chem. Soc.* **2005**, *127* (24), 8826–8828.
(87) Gurowitx, W. D.; Joseph, M. A. Enamines. II. Factors Determining the Structure of Enamines of 2-Substituted Ketones. *J. Org. Chem*. **1967**, *32* (11), 3289–3292.
(88) Kwiatkowski, P.; Beeson, T.; Conrad, J.; MacMillan, D. Enantioselective Organocatalytic α-Fluorination of Cyclic Ketones. *J. Am. Chem. Soc.* **2011**, *133* (6), 1738–1741.
(89) Lam, Y.; Houk, K. How Cinchona Alkaloid-Derived Primary Amines Control Asymmetric Electrophilic Fluorination of Cyclic Ketones. *J. Am. Chem. Soc.* **2014**, *136* (27), 9556–9559.
(90) Starks, C. M. Phase-Transfer Catalysis 1. Hetereogeneous Reactions Involving Anion Transfer by Quaternary Ammonium and Phosphonium Salts. *J. Am. Chem. Soc.* **1971**, *93* (1), 195–199.
(91) Lee, H.; Maruoka, K. Asymmetric Phase-Transfer Catalysis. *Nat. Rev. Chem.* **2024**, *8* (11), 851–869.
(92) Makosza, M. Phase-Transfer Catalysis. A General Green Methodology in Organic Synthesis. *Pure Appl. Chem.* **2000**, *72* (7), 1399–1403.
(93) Kim, D. Y.; Park, E. J. Catalytic Enantioselective Fluorination of β-Keto Esters by Phase-Transfer Catalysis using Chiral Quaternary Ammonium Salts. *Org. Lett.* **2002**, *4* (4), 545–547.

(94) Wang, X. S.; Lan, Q.; Shirakawa, S.; Maruoka, K. Chiral Bifunctional Phase Transfer Catalysts for Asymmetric Fluorination of Beta-Keto Esters. *Chem. Comm.* **2010**, *46* (2), 321–323.
(95) Arimitsu, S.; Iwasa, S.; Arakaki, R. Enantioselective Fluorination of α-Branched β-Ynone Esters Using a Cinchona-Based Phase-Transfer Catalyst. *J. Org. Chem.* **2020**, *85* (19), 12804–12812.
(96) Rauniyar, V.; Lackner, A. D.; Hamilton, G. L.; Toste, F. D. Asymmetric Electrophilic Fluorination Using an Anionic Chiral Phase-Transfer Catalyst. *Science* **2011**, *334* (6063), 1681–1684.
(97) Haufe, G.; Bruns, S. (Salen)chromium Complex Mediated Asymmetric Ring Opening of Meso- and Racemic Epoxides with Different Fluoride Sources. *ACS*. **2002**, *344* (2), 165–171.
(98) Bruns, S.; Haufe, G. Enantioselective Introduction of Fluoride into Organic Compounds: First Asymmetric Ring Opening of Epoxides by Hydrofluorinating Reagents. *J. Fluor. Chem.* **2000**, *104* (2), 247–254.
(99) Kalow, J. A.; Doyle, A. G. Enantioselective Ring Opening of Epoxides by Fluoride Anion Promoted by a Cooperative Dual-Catalyst System. *J. Am. Chem. Soc.* **2010**, *132* (10), 3268–3269.
(100) Kalow, J. A.; Doyle, A. G. Mechanistic Investigations of Cooperative Catalysis in the Enantioselective Fluorination of Epoxides. *J. Am. Chem. Soc.* **2011**, *133* (40), 16001–16012.
(101) Kalow, J. A.; Schmitt, D. E.; Doyle, A. G. Synthesis of Beta-Fluoroamines by Lewis Base Catalyzed Hydrofluorination of Aziridines. *J. Org. Chem.* **2012**, *77* (8), 4177–4183.
(102) Katcher, M. H.; Doyle, A. G. Palladium-Catalyzed Asymmetric Synthesis of Allylic Fluorides. *J. Am. Chem. Soc.* **2010**, *132* (49), 17402–17404.
(103) Katcher, M. H.; Sha, A.; Doyle, A. G. Palladium-Catalyzed Regio- and Enantioselective Fluorination of Acyclic Allylic Halides. *J. Am. Chem. Soc.* **2011**, *133* (40), 15902–15905.
(104) Zhang, Q.; Stockdale, D. P.; Mixdorf, J. C.; Topczewski, J. J.; Nguyen, H. M. Iridium-Catalyzed Enantioselective Fluorination of Racemic, Secondary Allylic Trichloroacetimidates. *J. Am. Chem. Soc.* **2015**, *137* (37), 11912–11915.
(105) Liu, W.; Groves, J. T. Manganese-Catalyzed Oxidative Benzylic C–H Fluorination by Fluoride Ions. *Angew. Chem. Int. Ed.* **2013**, *52* (23), 6024–6027.
(106) Huang, X.; Liu, W.; Ren, H.; Neelamegam, R.; Hooker, J. M.; Groves, J. T. Late Stage Benzylic C–H Fluorination with [^{18}F]Fluoride for PET Imaging. *J. Am. Chem. Soc.* **2014**, *136* (19), 6842–6845.
(107) Buchsteiner, M.; Martinez-Rodriguez, L.; Jerabek, P.; Pozo, I.; Patzer, M.; Nöthling, N.; Lehmann, C.; Fürstner, A. Catalytic Asymmetric Fluorination of Copper Carbene Complexes: Preparative Advances and a Mechanistic Rationale. *Chem. Eur. J.* **2020**, *26* (11), 2509–2515.
(108) Gray, E.; Nielsen, M.; Choquette, K.; Kalow, J.; Graham, T.; Doyle, A. Nucleophilic (Radio)Fluorination of α-Diazocarbonyl Compounds Enabled by Copper-Catalyzed H–F Insertion. *J. Am. Chem. Soc.* **2016**, *138* (34), 10802–10805.
(109) Suzuki, S.; Kamo, T.; Fukushi, K.; Hiramatsu, T.; Tokunaga, E.; Dohi, T.; Kita, Y.; Shibata, N. Iodoarene-Catalyzed Fluorination and Aminofluorination by an Ar-I/HF.pyridine/mCPBA System. *Chem. Sci.* **2014**, *5* (7), 2754–2760.
(110) Kong, W. Q.; Feige, P.; de Haro, T.; Nevado, C. Regio- and Enantioselective Aminofluorination of Alkenes. *Angew. Chem. Int. Ed.* **2013**, *52* (9), 2469–2473.
(111) Pluta, R.; Krach, P. E.; Cavallo, L.; Falivene, L.; Rueping, M. Metal-Free Catalytic Asymmetric Fluorination of Keto Esters Using a Combination of Hydrogen Fluoride (HF) and Oxidant: Experiment and Computation. *ACS Catal.* **2018**, *8* (3), 2582–2588.
(112) Wang, Y.; Yuan, H.; Lu, H.; Zheng, W. Development of Planar Chiral Iodoarenes Based on [2.2]Paracyclophane and Their Application in Catalytic Enantioselective Fluorination of β-Ketoesters. *Org. Lett.* **2018**, *20* (9), 2555–2558.
(113) Feng, Y.; Huang, R.; Hu, L.; Xiong, Y.; Coeffard, V. Chiral C2-Symmetric Iodoarene-Catalyzed Asymmetric α-Oxidation of β-Keto Esters. *Synthesis* **2016**, *48* (16), 2637–2644.
(114) Banik, S. M.; Medley, J. W.; Jacobsen, E. N. Catalytic, Diastereoselective 1,2-Difluorination of Alkenes. *J. Am. Chem. Soc.* **2016**, *138* (15), 5000–5003.
(115) Scheidt, F.; Schäfer, M.; Sarie, J. C.; Daniliuic, C. G.; Molloy, J.J.; Gilmour, R. Enantioselective, Catalytic Vicinal Difluorination of Alkenes. *Angew. Chem. Int. Ed.* **2018**, *57* (50), 16431–16435.

(116) Zhao, Q.; Chen, Z.; Soler, J.; Chen, X.; Rui, J.; Tianlin Ji, N.; Yu, Q. E.; Yang, Y.; Garcia-Borrás, M.; Huang, X. Engineering Non-Haem Iron Enzymes for Enantioselective C(sp^3)–F Bond Formation via Radical Fluorine Transfer. *Nature Synth.* **2024**, *3* (8), 958-966.
(117) Zhao, L.; Mai, B.; Cheng, L.; Gao, F.; Zhao, Y.; Guo, R.; Wu, H.; Zhang, Y.; Liu, P.; Yang, Y. Biocatalytic Enantioselective C(sp^3) –H Fluorination Enabled by Directed Evolution of Non-Haem Iron Enzymes. *Nature Synth.* **2024**, *3* (8), 967–975.
(118) Yoo, S.; Yoon, S.; Woo, K.; Kim, J.; Cho, S.; Lee, S.; Lim, H.; Ahn, Y.; Yang, W. Psychological Effects of a Disastrous Hydrogen Fluoride Spillage on the Local Community. *Ann. Occup. Environ. Med.* **2017**, *29*.
(119) Park, S. Alert over South Korea Toxic Leaks. *Nature* **2013**, *494* (7435), 15–16.
(120) Learner, R.; *CRC Handbook of Chemistry and Physics,* 84th Edition; Lide, D. R., Ed.; CRC Press, 2003.
(121) Liotta, C.; Harris, H. Chemistry of Naked Anions 1. Reactions of 18-Crown-6 Complex of Potassium Fluoride with Organic Substrates in Aprotic Organic-Solvents. *J. Am. Chem. Soc.* **1974**, *96* (7), 2250–2252.
(122) Yan, H.; Bin Jang, H.; Lee, J. W.; Kim, H. K.; Lee, S. W.; Yang, J. W.; Song, C. E. A Chiral-Anion Generator: Application to Catalytic Desilylative Kinetic Resolution of Silyl-Protected Secondary Alcohols. *Angew. Chem. Int. Ed.* **2010**, *49* (47), 8915–8917.
(123) Kim, D.; Jeong, H.; Litn, S.; Sohn, M.; Katzenellenbogen, J.; Chi, D. Facile Nucleophilic Fluorination Reactions Using *tert*-Alcohols as a Reaction Medium: Significantly Enhanced Reactivity of Alkali Metal Fluorides and Improved Selectivity. *J. Org. Chem.* **2008**, *73* (3), 957–962.
(124) Hollingworth, C.; Hazari, A.; Hopkinson, M.; Tredwell, M.; Benedetto, E.; Huiban, M.; Gee, A.; Brown, J.; Gouverneur, V. Palladium-Catalyzed Allylic Fluorination. *Angew. Chem. Int. Ed.* **2011**, *50* (11), 2613–2617.
(125) Engle, K.; Pfeifer, L.; Pidgeon, G.; Giuffredi, G.; Thompson, A.; Paton, R.; Brown, J.; Gouverneur, V. Coordination Diversity in Hydrogen-Bonded Homoleptic Fluoride-Alcohol Complexes Modulates Reactivity. *Chem. Sci.* **2015**, *6*, 5293–5302.
(126) Pfeifer, L.; Engle, K.; Pidgeon, G.; Sparkes, H.; Thompson, A.; Brown, J.; Gouverneur, V. Hydrogen-Bonded Homoleptic Fluoride-Diarylurea Complexes: Structure, Reactivity, and Coordinating Power. *J. Am. Chem. Soc.* **2016**, *138* (40), 13314–13325.

2. Development of a Strategy for Nucleophilic Fluorination under Synergistic Hydrogen Bonding Phase Transfer Catalysis

The experimental work described in this chapter was carried out in collaboration with Dr. Francesco Ibba, Bence Botlik and Chiara Palladino. Dr. Francesco Ibba assisted with the interpretation of spectroscopic NMR studies. Bence Botlik was involved in preliminary optimisation of the benzylic system, and Chiara Palladino collaborated on the extension of this methodology towards the fluorination of α-bromoketones, and prepared molecules **12e-m** and **13b-m**. The interpretation of the kinetic studies and calculations of KIE values, discussed within Chapter 3, were performed by Yuan Gao and Professor Guy Lloyd Jones. All computational work discussed within this thesis was performed by Dr. Christopher Goult and Professor Robert Paton.

The results reported in this thesis are included within the publication *'Enantioconvergent Nucleophilic Substitution under Synergistic Phase Transfer Catalysis'* C. Dooley, F. Ibba, B. B. Botlik, C. Palladino, C. A. Goult, Y. Gao, A. Lister, R. S. Paton*, G. C. Lloyd-Jones* and V. Gouverneur* *Nature Catalysis*, **2025**, *8* (2), 107–115.[1]

2.1. Introduction

2.1.1. Hydrogen Bonding Phase Transfer Catalysis (HBPTC)

In 2018, Gouverneur and co-workers reported a new approach towards asymmetric nucleophilic fluorination coined 'Hydrogen Bonding Phase Transfer Catalysis (HBPTC)'.[2] Encouraged by the understanding that hydrogen bond donors (HBDs) such as alcohols or achiral ureas can modulate the reactivity of fluoride to act as nucleophile or a base (*v. 1.4.5. Nucleophilic Fluorination with Alkali Metal Fluoride Salts*), it was hypothesised that the use of chiral HBD catalysts could allow for the enantioselective installation of C–F bonds directly from alkali metal fluoride salts.

Foundational research in the field of anion-binding catalysis demonstrated the ability for chiral HBD catalysts to abstract halide ions resulting in the formation of chiral ion pairs that can be trapped with

an external nucleophile to fashion stereogenic C–Nu bonds.[3, 4] Whilst in this scenario the halide is a non-reactive component, Gouverneur and co-workers envisaged the use of chiral HBD donor catalysts to bring insoluble fluoride salts into solution through HB interactions which subsequently can engage in ion pairs with electrophilic species resulting in the formation of stereogenic C–F bonds.

As a proof-of-concept Gouverneur and co-workers investigated the fluorination of β-bromosulfides, which generate reactive *meso*-episulfonium ions *in situ* and engage in ion-pairing interactions with a hydrogen-bonded fluoride anion.[2] This work was reminiscent of Nature's method for C–F bond formation and the enzyme *fluorinase*, where the sulfonium electrophile (SAM) is critical to reactivity, providing electrostatic stabilisation with hydrogen bound fluoride (*v. 1.2. Natural Occurrence of Fluorine*) (Figure 2.1).[5, 6]

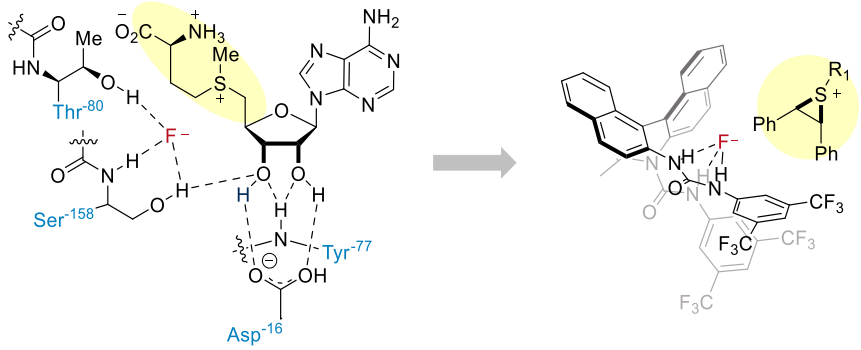

Figure 2.1: Comparison between binding mode of fluoride in the catalytic pocket of fluorinase enzyme[5] and urea-fluoride interaction[2]

Preliminary experiments were performed on an achiral system which demonstrated that stilbene derived β-bromosulfides could be fluorinated with cesium fluoride (CsF) in the presence of HBD catalyst Schreiner's urea (**SU**), in dichloromethane. In the absence of the HBD catalyst, no formation of the β-fluorosulfide was observed in line with the poor solubility of CsF in organic solvents.[2] Reactivity was also achieved using **SU** with potassium fluoride (KF) as the fluoride source, however, this required elongated reaction times (24 h), as a result of the increased lattice energy of KF (CsF – 759 kJ/mol, KF – 829 kJ/mol).[7] It is noteworthy that analogous Schreiner's thiourea HBD catalyst (**STU**) did not allow for fluorination, regardless of its stronger hydrogen-bonding ability compared to **SU** (**STU** $pK_{a\,(DMSO)}$ =

8.5, **SU** p$K_{a\,(DMSO)}$ = 13.8). This was explained considering the superior nucleophilicity of the thiourea over the fluoride, which resulted in the formation of a C–S bond over a C–F bond, consuming the catalyst (Scheme 2.1).

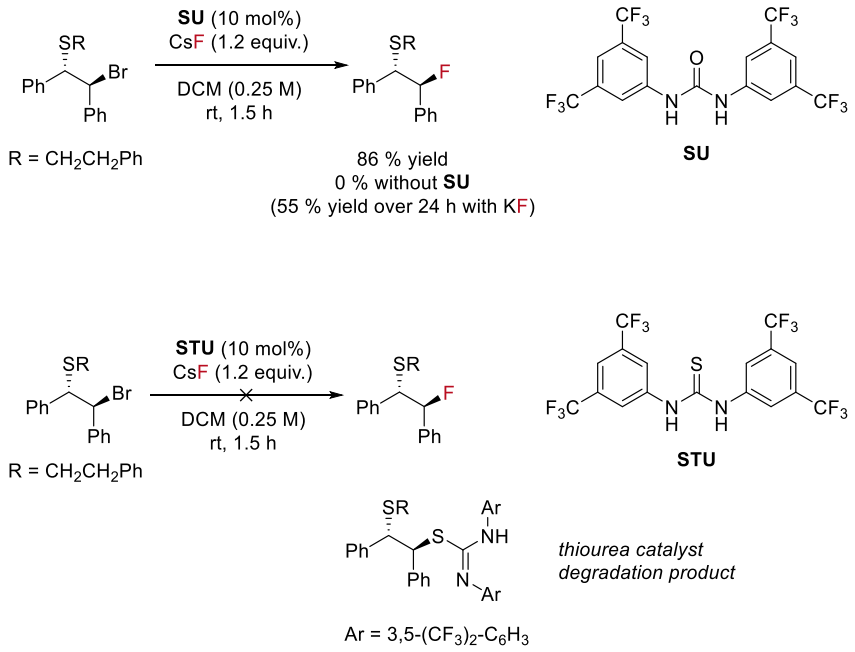

Scheme 2.1: Fluorination of β-bromosulfides with achiral HBD catalysts and CsF[2]

Progression towards an asymmetric variant of this transformation led to the development of a class of axially chiral, 1'-binaphthyl-2,2'-diamine (BINAM) derived *bis*-urea HBD catalysts. BINAM and biaryl structures are considered privileged scaffolds in asymmetric catalysis and simple stepwise synthesis forming ureas *via* isocyanate addition allowing for a broad range of HBDs to be accessed with different electronic and steric properties.[8] During the development of BINAM derived *bis*-urea catalyst libraries, mono-*N*-alkylation was seen to be beneficial, achieving higher enantioselectivities of fluorinated products. This design was guided by molecular dynamics (MD) simulations which indicated that *bis*-urea motifs engaged favourably in a tridentate NH binding mode to the fluoride anion, with one non-participating NH. *Anti-anti* to *syn-anti* urea isomerisation of the C(O)–N bond proximal to the BINAM backbone was observed displaying binding reminiscent of the fluorinase enzyme (Scheme 2.2).[2]

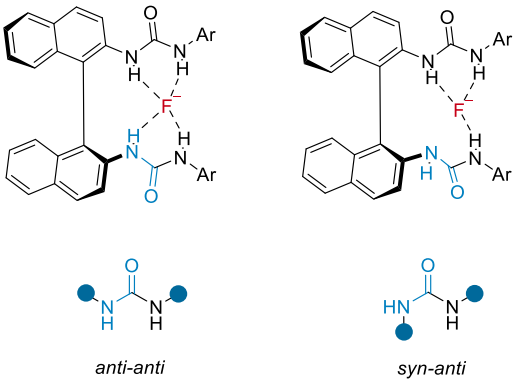

Scheme 2.2: Isomerisation of urea motifs[2]

Experimentally mono-*N*-alkylated catalysts afforded β-fluorosulfide products in increased selectivity, and the final reaction conditions for this transformation consisted of an *N*-isopropylated urea (*S*)-**3d**, CsF (1.2 equiv.) in halogenated aromatic solvents (e.g. 1,2-difluorobenzene), allowing for the fluorination of scope of stilbene-derived β-bromosulfides in excellent yields and enantioselectivities (up to 98 %, 94% *ee*) (Scheme 2.3).[2]

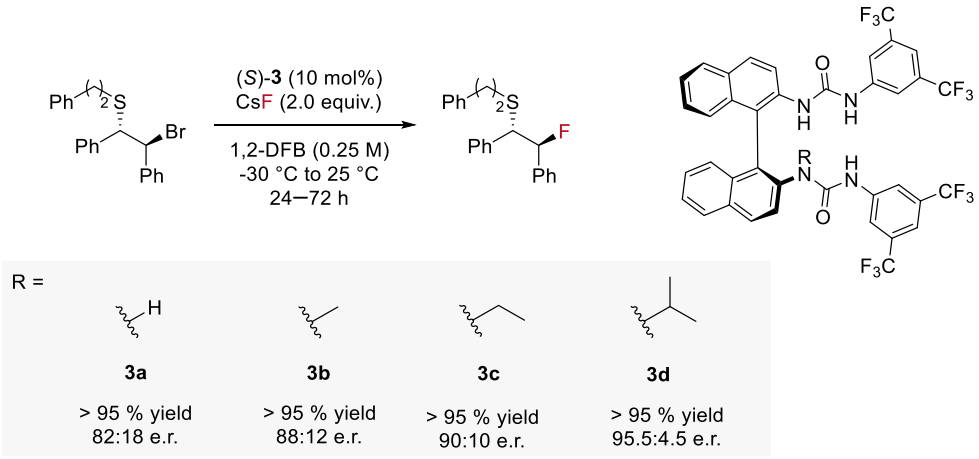

Scheme 2.3: Fluorination of β-bromosulfide with chiral HBD catalysts and CsF[2]

Mechanistically the catalytic cycle for this novel fluorination manifold, HBPTC, comprised of three fundamental steps: (i) The solubilisation of metal fluoride (MF) salt by the HBD catalyst, (ii) the formation of an ion-pair between the hydrogen-bonded fluoride and the charged electrophile formed *in situ*, (iii) collapse of the reactive ion-pair to form the stereogenic C–F bond and regenerate the HBD catalyst.[2]

Whilst the ultimate step of the catalytic cycle is always the irreversible collapse of the key ion-pair between electrophile and hydrogen-bonded fluoride to form the fluorinated product, two distinct scenarios were envisaged to arrive at such point. It was proposed that the urea could initiate the reaction through the solubilisation of MF salt from the solid phase, forming a $M^+[UF]^-$ ion pair, which subsequently undergoes a cationic exchange with the electrophile (E^+ = episulfonium ion) (Figure 2.2a). Alternatively, the urea could directly interact and potentially aid the ionisation of the substrate forming an $E^+[UBr]^-$ ion pair which then undergoes an anionic exchange with MF, precipitating the metal bromide salt (MF) out of solution (Figure 2.2b). Computationally, barriers towards the formation of episulfonium ions were close in energy when calculated with or without the assistance of urea catalyst (**SU**) suggesting the possibility for auto-ionisation of substrates.[2] However, without detailed kinetic analysis it is difficult to explicitly say which catalytic cycle is more persistent under HBPTC.

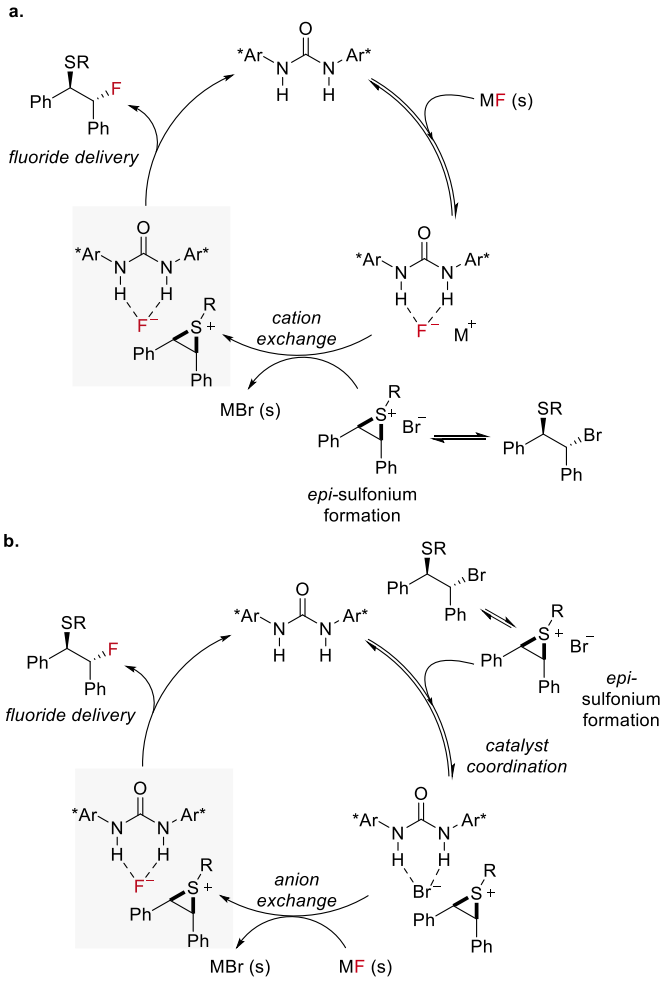

Figure 2.2: Scenarios for the catalytic cycle of HBPTC[2]; a. Initial MF solubilisation; b. Initial ionisation of substrate

2.1.2. Extension of the Electrophilic and Nucleophilic Scope of HBPTC

Following the seminal study of the asymmetric fluorination of β-bromosulfides, the concept of HBPTC to construct highly enantiopure fluorinated products with MF salts was extended to a larger substrate scope. In 2019, Gouverneur and co-workers achieved the desymmetrisation of aziridinium ions, formed *in situ* from β-chloroamines in an analogous system to the sulfide substrate class (Scheme 2.4).[9] A scope of enantioenriched and pharmaceutically relevant β-fluoroamine compounds were synthesised, including a multi-decagram scale synthesis of fluorinated diphenidine in 66 % yield (31.1 g) and 94% *ee* employing **3z** at a reduced catalyst loading (3 mol%). The scope was also extended to demonstrated applicability of HBPTC towards non-stilbene derived substrates in good yield and moderate enantioselectivity (up to 69 %, 71% *ee*). A standout difference in this study, compared to the previous report, was the success of employing potassium fluoride (KF) as the fluorinating reagent. The use of CsF gave excellent yields and enantioselectivity under the optimised conditions with catalyst **3z**, however comparable results were obtained with the more economical and abundant KF, regardless of the additional barriers associated with its higher lattice energy.[9]

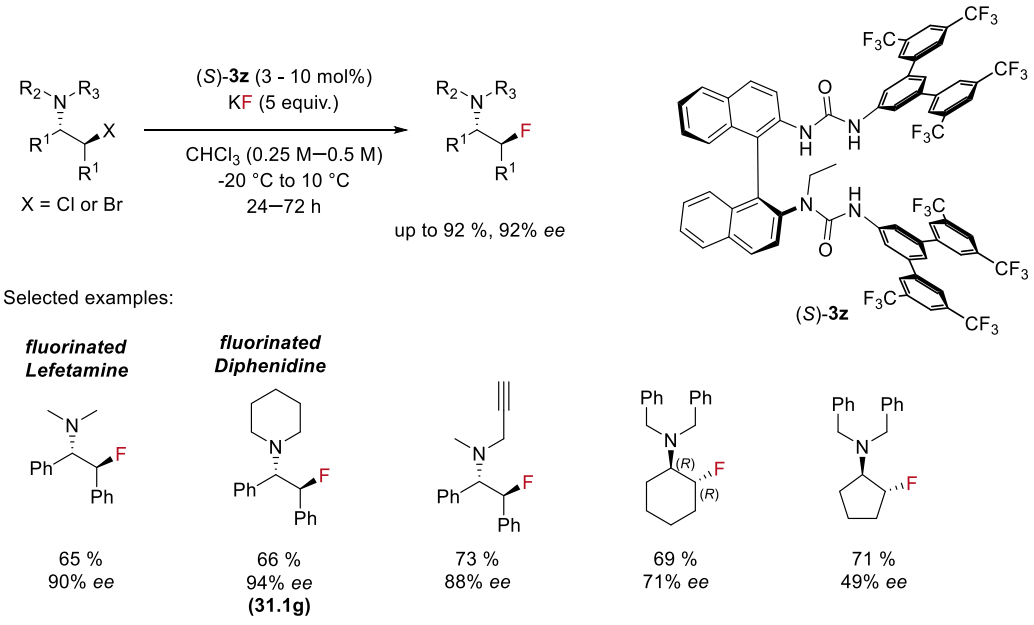

Scheme 2.4: HBPTC with KF for the enantioselective synthesis of β-fluoroamines[9]

In 2020, Gouverneur and co-workers investigated the fluorination of pre-formed azetidinium salts, under HBPTC.[10] Here, *bis*-urea catalyst (*S*)-**3d** was shown to provide enantioenriched γ-fluoroamines in up to 99 % yield and 97.5:3.5 e.r. (Scheme 2.5a). Notably, the HBD catalyst (**3d**) was able to outcompete the background reactivity which arises from the substrate-mediated phase-transfer solubilisation of CsF by means of electrostatic interactions. The subjection of diastereomerically pure samples of achiral azetidinium starting materials gave the fluorinated amine in comparable yield and enantioselectivity, suggesting that this process allowed for the enantioconvergence of diastereomers. This was rationalised through DFT calculations which demonstrated that the projection of the azetidinium *N*-substituents away from the catalyst binding site led to indifference upon fluoride attack and therefore mixtures of diastereomers were subjected to the standard conditions to give single products.[10] This methodology was applied towards the gram scale synthesis of fluorinated Lorcaserin, a selective serotonin 2C receptor agonist which has been FDA-approved for chronic weight management, in good yields and selectivity (86 %, 96:4 e.r.) (Scheme 2.5b).[11, 12]

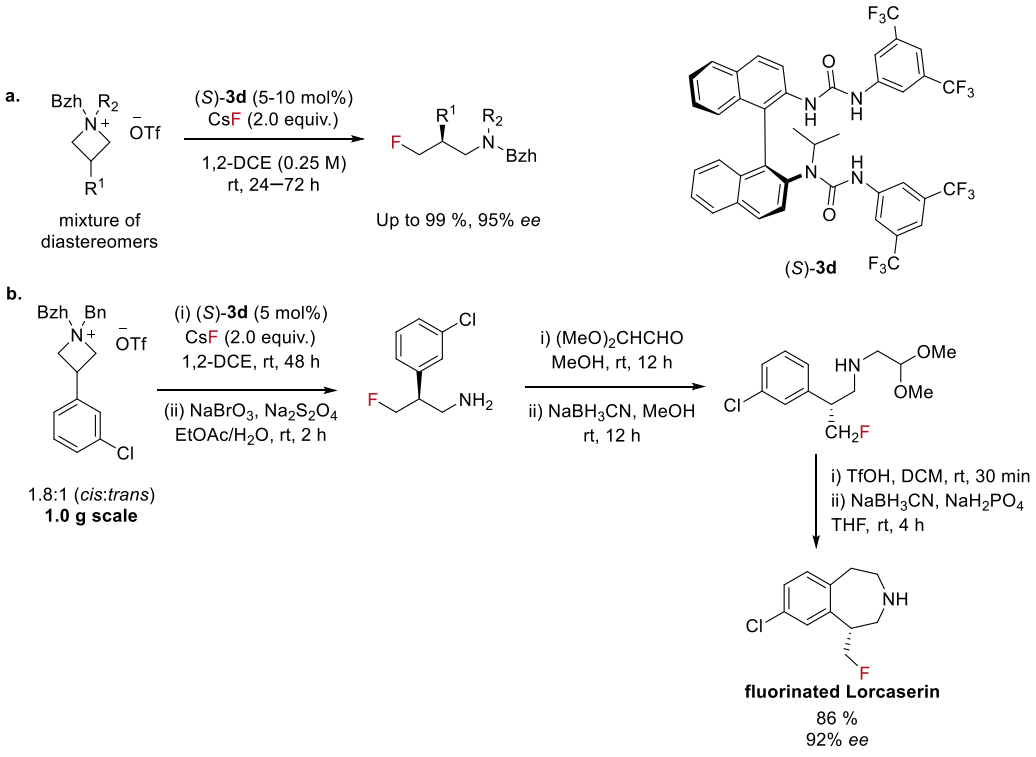

Scheme 2.5: a. HBPTC with ionic reagents: enantioselective synthesis of γ-fluoroamines; b. Gram-scale synthesis of fluorinated Lorcaserin[10]

The diversification of the nucleophile scope under HBPTC has also been explored and Gouverneur and co-workers disclosed an asymmetric azidation of the β-chloroamine substrate class employing NaN_3. Subsequent azide substitution products were isolated in high yields and enantioselectivity using *bis*-urea catalyst (*S*)-**3d** (up to 94 %, 96:4 e.r.) (Scheme 2.6a).[13] Furthermore, Gouverneur and co-workers recently reported the regiodivergent fluorination of dissymmetric aziridinium salts with CsF, where selective α- or β- fluorinated products were obtained depending on the modulation of fluoride's charge density with or without a HBD catalyst (**SU**) (Scheme 2.5b).[14]

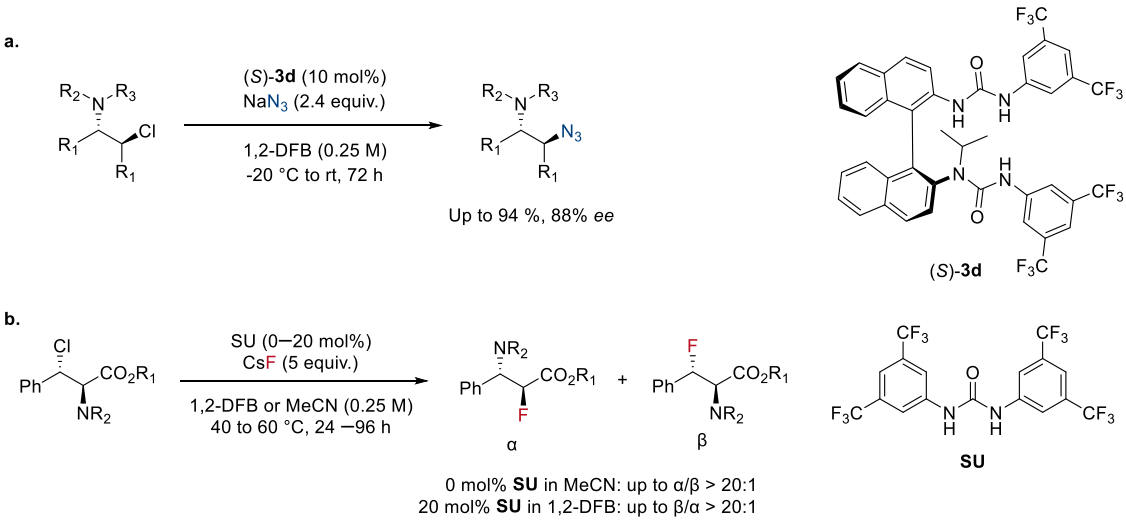

Scheme 2.6: a. Asymmetric azidation with NaN_3 under HBPTC[13]; b. Regiodivergent fluorination of dissymmetric β-chloroamines with CsF[14]

2.1.3. New Approach for the Fluorination of Neutral, Unsymmetrical Electrophiles

The aim of the project described within this thesis was to develop a novel catalytic strategy to further expand the scope of HBPTC beyond the desymmetrisation of highly reactive and charged electrophiles, thus enabling the fluorination of neutral, and unsymmetrical electrophiles with KF. Several questions and challenges had to be addressed to achieve this target: (i) currently, success under HBPTC is reliant on ion-pairing interactions between fluoride bound to the urea catalyst and a charged electrophile, which raises concern that reactivity may not be attainable with neutral electrophiles (Figure 2.3), (ii) the propensity of alkali metal fluoride salts such as KF to act as a base rather than a nucleophile may

result in challenging chemoselectivity depending on the electrophile chosen, (iii) HBPTC is limited to desymmetrisation chemistries, the progression to unsymmetrical electrophiles also raises questions on developing an enantioselective process and whether a kinetic resolution or enantioconvergence can be achieved.

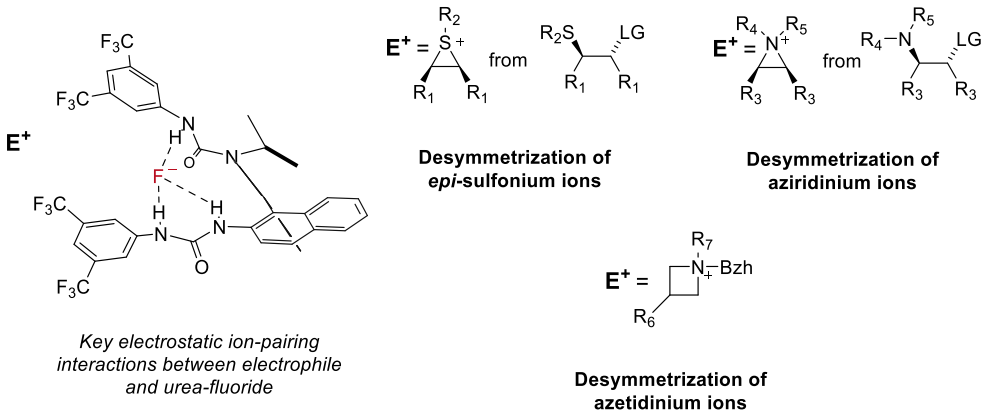

Figure 2.3: Ion-pairing interactions between urea-fluoride species and cationic electrophiles (E^+)

It was a key goal of the project to achieve good reactivity and selectivity employing KF as the fluorinating reagent considering its profile as a safe and cost-effective reagent. Moreover KF is advantageous compared to other alkali metal fluoride salts including CsF, which is of higher cost in line with concerns associated with the global depletion of cesium reverses.[15]

To investigate possibility of translating the concepts of HBPTC to the fluorination of neutral electrophiles the benzylic halide was selected as a starting point, with reason that an activated substrate was necessary to address the low nucleophilicity of hydrogen-bound fluoride. However, substitution with fluoride at the benzylic position faces challenges considering the likelihood for competitive elimination to form stable styrene by-products and stereocontrol around the secondary benzylic carbon centres is a notorious challenge.[16] The formation of benzylic carbocations has been hypothesised to be the cause of diminished or no enantioinduction in asymmetric substitution literature including previous studies in fluorination, which makes a benzylic substitution an interesting mechanistic uncertainty (Scheme 2.4).[17, 18] Furthermore, the lack of synthetic methods to access enantioenriched secondary benzylic fluorides, none of which employ alkali metal fluoride salts, would

render this transformation a significant advance in asymmetric nucleophilic fluorination and expanding the toolbox of enantioselective transformations that can be achieved with KF.

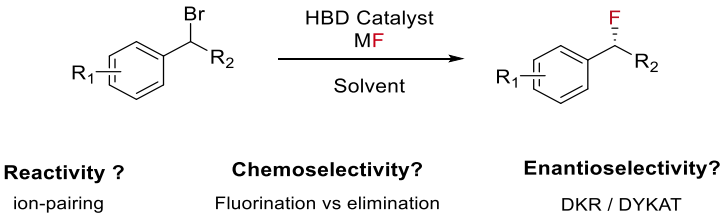

Scheme 2.4: Project scope and challenges

2.2. Results and Discussion

2.2.1. Preliminary Investigations

Initially, the benzylic bromide motif was investigated, establishing its reactivity with different nucleophilic sources of fluorine with and without HBD catalysts. (*S*)-**3d** was selected as the catalyst for all preliminary investigations into the system considering its success in the seminal report of HBPTC for the asymmetric fluorination of β-bromosulfides.[1] Furthermore, previous studies have highlighted the superiority of urea catalysts over other classes of HBD catalyst including thioureas, squaramides and guanidines.[2] (*S*)-**3d** was readily prepared through a two-step reported synthesis: (i) reductive amination of acetone onto (*S*)-BINAM to prepare *N*-isopropylated BINAM intermediate (**15b**), (ii) refluxing **15b** with 3,5-*bis*(trifluoromethyl)phenyl isocyanate in anhydrous DCM to give (*S*)-**3d** in 91 % yield (Scheme 2.5).

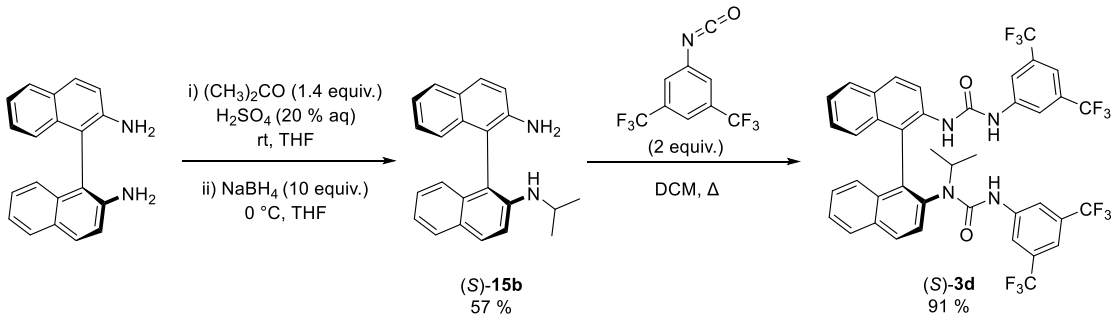

Scheme 2.5: Preparation of *bis*-urea HBD catalyst (*S*)-**3d**

It is critical that the reaction of *N*-isopropylated BINAM (**15b**) with 3,5-*bis*(trifluoromethyl)phenyl isocyanate is performed under anhydrous conditions to ensure minimal formation of achiral Schreiner urea (**SU**). **SU** can be formed following the hydrolysis of 3,5-*bis*(trifluoromethyl)phenyl isocyanate and subsequent decarboxylation to afford the corresponding aniline which can react with another equivalent of the isocyanate. It is vital to avoid the formation of this by-product and ensure it is not present in batches of (*S*)-**3d**, considering its potential ability to act as a catalyst and mediate a competitive non-enantioselective fluorination process, which could diminish the measured enantioselectivities of fluorination products (Scheme 2.6).[2]

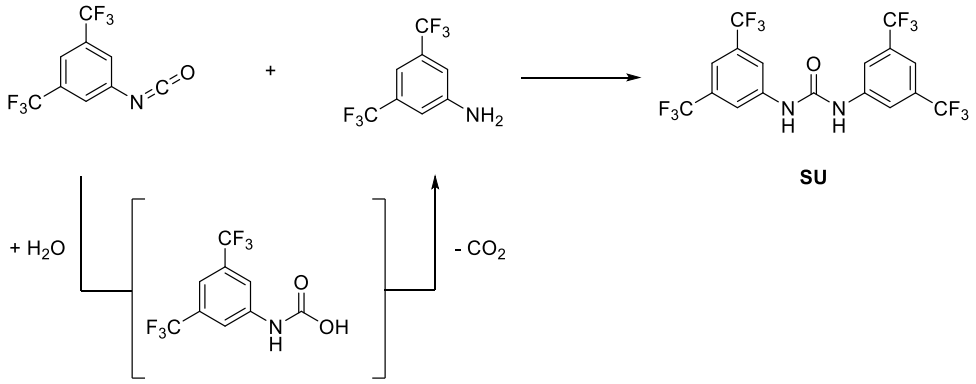

Scheme 2.6: Formation of SU from hydrolysis of 3,5-*bis*(trifluoromethyl)phenylisocyanate

4-(1-Bromoethyl)-1-1'-biphenyl **1a** was selected as a model substrate for preliminary optimisation. **1a** can be quantitively prepared without the need for purification from the corresponding alcohol through bromination with phosphorus tribromide (PBr_3), or under Appel halogenation conditions (PPh_3, CBr_4) (Scheme 2.7).

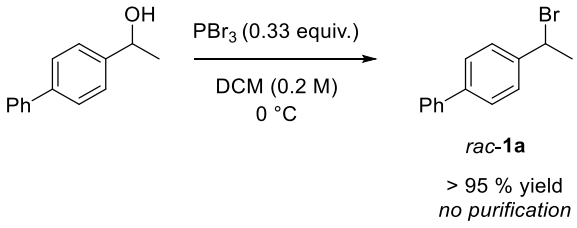

Scheme 2.7: Synthesis of *rac*-**1a** from deoxybromination of corresponding alcohol

Preliminary reactions of **1a** in toluene with different nucleophilic fluorinating reagents, KF, CsF and tetrabutylammonium fluoride trihydrate (TBAF·3H_2O or TBAF) were performed. In the absence of a HBD catalyst no conversion was observed using KF or CsF with **1a**, consistent with the insolubility of alkali metal fluoride salts in organic solvents. In contrast soluble TBAF allowed for conversion of **1a** to both fluoride **2a** in 48 % yield and elimination by-product **4a** in an equal ratio. Addition of HBD catalyst (*S*)-**3d** (20 mol%) saw reactivity restored for CsF, allowing the conversion of **1a** to **2a** in 38 % and 74:26 e.r., however significant elimination was also observed (1:1 **2a**: **4a**). It is noteworthy that when (*S*)-**3d** was added to the reaction employing TBAF no enantioinduction was measurable, suggesting that the uncatalysed background reactivity of TBAF cannot be controlled by (*S*)-**3d** in toluene. In contrast to CsF, the reaction employing (*S*)-**3d** with KF led to no conversion of **1a** even at elevated temperatures, and only remaining starting material detected by ^{1}H NMR. Different leaving groups were evaluated which demonstrated that the reaction also proceeded from benzylic chlorides and CsF, however in diminished yields (7 %). The evaluation of pseudohalides such as tosylates was also investigated, however no conversion of the substrate to fluorinated product was observed with KF or CsF.

Table 2.1: Preliminary screening of fluoride sources with benzylic (pseudo)halides

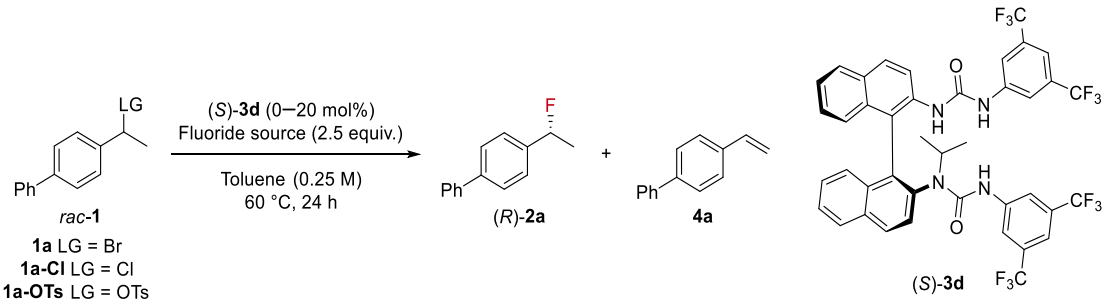

Entry	Fluoride Source	LG	(*S*)-**3d** (mol%)	Yield **2a** (%)[a]	Ratio **2a**:**4a**	e.r. [b]
1	KF	Br	0	0	-	nd
2	CsF	Br	0	0	-	nd
3	TBAF·3H_2O	Br	0	48	1:1	nd
4	KF	Br	20	0	-	nd
5	CsF	Br	20	38	1:1	74:26
6	TBAF·3H_2O	Br	20	59	1.5:1	50:50
7	KF	Cl	20	0	-	nd
8	CsF	Cl	20	7	1:2	80:20
9	TBAF·3H_2O	Cl	20	50	1.5:1	50:50
10	KF	OTs	20	0	-	nd
11	CsF	OTs	20	0	-	nd

General conditions: 0.05 mmol substrate, stirring at 1200 rpm. [a]Determined by ^{19}F NMR using 4-fluoroanisole as internal standard, [b]e.r. determined by HPLC analysis using a chiral stationary phase, nd = not determined.

With a determination to establish reactivity with KF, these unsuccessful results were investigated. In 2019, HBPTC was successfully extended to the fluorination of β-chloroamines employing KF, highlighting the possibility of harnessing its potential as a reagent.[9] It was hypothesised that the lower reactivity of the benzylic electrophile could be the origin for the lack of reactivity observed with KF, which is more demanding than CsF considering its lattice energy (KF lattice energy, 829 kJ/mol, CsF lattice energy, 759 kJ/mol).[7] In order to investigate whether increasing the electrophilicity of the substrate could unlock reactivity with KF the addition of Lewis base (LB) additives which could act as nucleophilic catalysts were considered within the system. It was envisaged that the combination of a neutral electrophile such as the benzylic halide with a Lewis base could lead to the formation of a positively charged adduct which could engage in ion-pairing with a urea-fluoride species improving the likelihood for reactivity (Scheme 2.8).

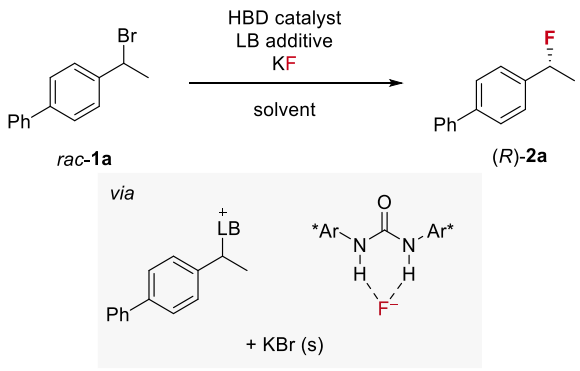

Scheme 2.8: Envisaged reactivity of **1a** with LB additives

2.2.2. Lewis Base Additives

Preliminary screening was performed on a range of additives such as DMAP, imidazole, sulfides and phosphines. One equivalent of a LB was added to bromide **1a** and (*S*)-**3d** with KF in toluene and heated to 60 °C for 24 hours. Pleasingly, reactivity of **1a** and fluorination with KF as the fluorinating reagent was observed upon the addition of LBs into the system (Table 2.2). The best result was seen with triphenylphosphine (PPh_3), allowing fluorination with KF in 67 % yield and 75:25 e.r. (Table 2.2, entry 5). The addition of PPh_3 to the system also improved the chemoselectivity, with fluorination favoured over the competing elimination pathway (4:1 **2a**:**4a**). The addition of PPh_3 into the reaction employing

CsF also saw over a two-fold increase in the yield of **2a** to 86 %, compared to 38 % without, however with a diminished enantioselectivity of 59:41 e.r. (Table 2.2, entry 6). Other additives such as DMAP and imidazole did also allow for reactivity with KF, however in lower yields than PPh_3 (Table 2.2, entries 3 and 9).

Table 2.2: Screening of Lewis bases with **1a**

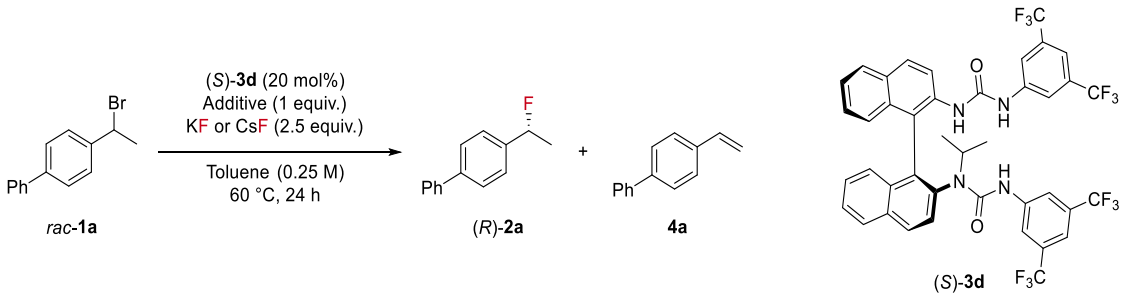

Entry	Additive	Fluoride Source	Yield **2a** (%)[a]	Ratio **2a**:**4a**	R.S.M **1a** (%)	e.r. [b]
1	-	KF	0	-	100	-
2	-	CsF	38	1:1	12	74:26
3	DMAP	KF	4	1:2	1	nd
4	DMAP	CsF	10	1.5:3	0	61:39
5	PPh_3	KF	67	4:1	8	75:25
6	PPh_3	CsF	86	6:1	0	59:41
7	SPh_2	KF	0	0:1	0	-
8	SPh_2	CsF	2	1:10	20	nd
9	Imidazole	KF	3	1:1	74	nd
10	Imidazole	CsF	7	1:2	69	74:26

General conditions: 0.05 mmol substrate, stirring at 1200 rpm. [a]Determined by ^{19}F NMR using 4-fluoroanisole as internal standard, [b]e.r. determined by HPLC analysis using a chiral stationary phase. R.S.M = remaining starting material, nd = not determined.

It is important to highlight that no fluorination was observed when either PPh_3 or the urea catalyst (*S*)-**3d** was removed from the system (Table 2.3, entries 2 and 3). Moreover, catalytic quantities (20 mol%) of PPh_3 were shown to give similar results to its stochiometric use (Table 2.3, entries 1 and 4). Pleasingly the loading of both the urea catalyst (*S*)-**3d** and PPh_3 could be reduced to 10 mol% and fluoride **2a** was still obtained in 42 % yield and 76:24 e.r. (Table 2.3, entry 5).

Table 2.3: Screening of (*S*)-**3d** and PPh_3 loading with **1a**

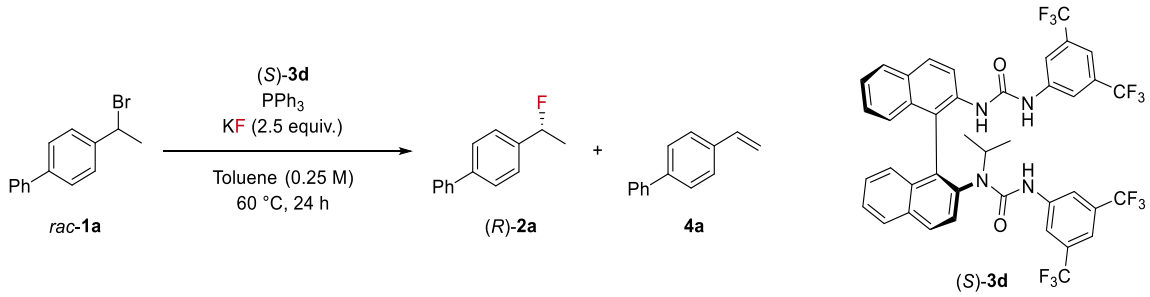

Entry	(*S*)-**3d** (mol%)	PPh_3 (mol%)	Yield **2a** (%)[a]	Ratio **2a**:**4a**	R.S.M **1a** (%)	e.r. [b]
1	20	100	67	4:1	8	75:25
2	0	100	0	-	100	-
3	20	0	0	-	100	-
4	20	20	70	3:1	0	76:24
5	10	10	42	2:1	22	76:24

General conditions: 0.05 mmol substrate, stirring at 1200 rpm. [a]Determined by ^{19}F NMR using 4-fluoroanisole as internal standard, [b]e.r. determined by HPLC analysis using a chiral stationary phase. R.S.M = remaining starting material.

A range of phosphines were screened to determine if structure and electronic property could impact the outcome of the reaction. No clear trend could be drawn from the screening results (Scheme 2.9), since electron-withdrawn phosphine **7b** performed comparably to electron-donating phosphines **7f** and **7g** (22 %, 29 %, and 33 % respectively). Sterically hindered phosphines possessing larger cone angles such as **7e** (Tolman cone angle **7a**: 145°, **7e**: 194°) were unsuccessful in the reaction resulting in a shutdown of reactivity.[19] Interestingly bidentate phosphines performed well within the reaction (**7h**-**j**), however, when chiral variants such as (*R*)- or (*S*)- BINAP (**7i**), were employed there was no direct effect on the absolute configuration of the fluorinated product, both providing **2a** in comparable yield and enantioselectivity (50 %, 76:24 e.r. and 54 %, 74:26 e.r. respectively) (Scheme 2.9).

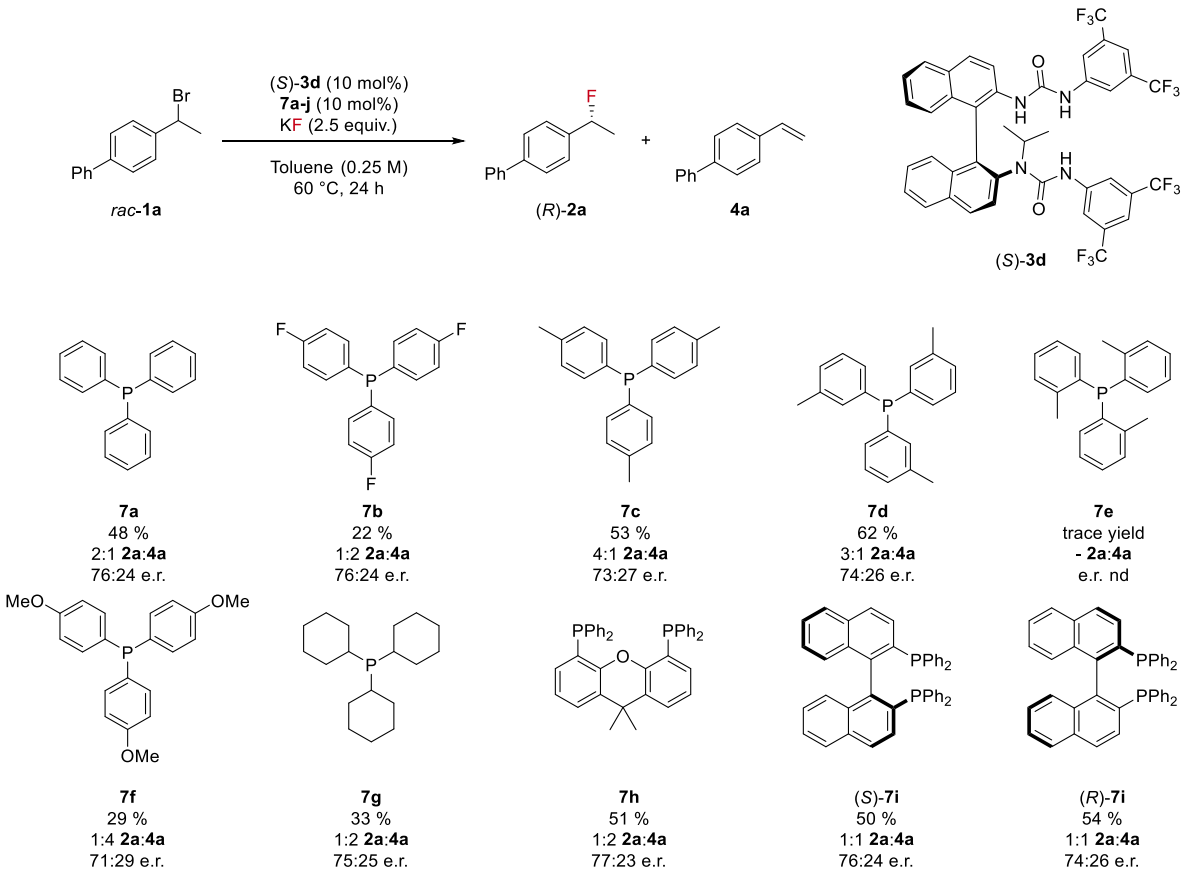

Scheme 2.9: Screening of phosphine catalysts (**7**) with **1a**, nd = not determined.

Spectroscopic analysis of the reaction mixture determined the formation of a phosphonium species, indicated by the presence of a broad signal at δ = 27 ppm in ^{31}P NMR ($CDCl_3$). The identity of species **8a** was further confirmed through a spiking experiment in which an independently synthesised aliquot of **8a** was added to the NMR sample of the reaction mixture. NMR control experiments demonstrated the importance of the urea catalyst (*S*)-**3d** for the formation of **8a**; the addition of PPh_3 (1 equiv.) to **1a** in toluene-d_8 saw no spectroscopic changes or formation of the phosphonium species, however, upon the addition of (*S*)-**3d**, signals corresponding to **8a** became visible.

Time course investigations, whereby identical reactions were set up and analysed by NMR at different points, elucidated that the concentration of the phosphonium species **8a** increased over 2–6 hours of monitoring, then stayed at a constant concentration over the remainder of the reaction, and was not consumed (~ 10 % of the total reaction mixture) (Table 2.4, Figure 2.4).

Table 2.4: Time course study for the conversion of **1a**

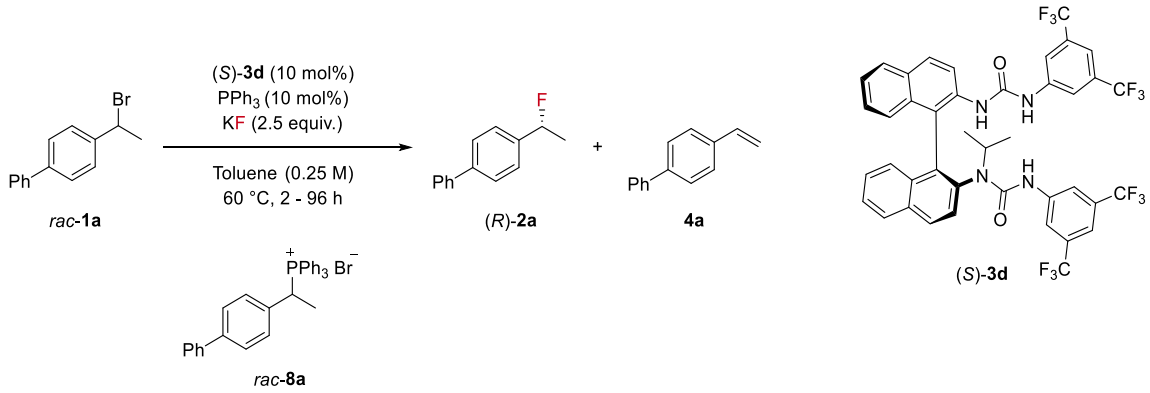

Entry	Time (h)	Yield **2a** (%)[a]	Yield **4a** (%)	Yield **8a** (%)	R.S.M **1a** (%)	e.r. [b]
1	2	6	9	6	77	79:21
2	4	14	15	6	63	78:22
3	6	26	17	7	50	78:22
4	8	28	19	7	46	77:23
5	24	44	26	9	21	76:24
6	48	63	25	9	3	76:24
7	72	66	26	9	0	76:24
8	96	66	26	9	0	76:24

General conditions: 0.05 mmol substrate, stirring at 1200 rpm. [a]Determined by ^{19}F NMR using 4-fluoroanisole as internal standard, [b]e.r. determined by HPLC analysis using a chiral stationary phase. R.S.M = remaining starting material.

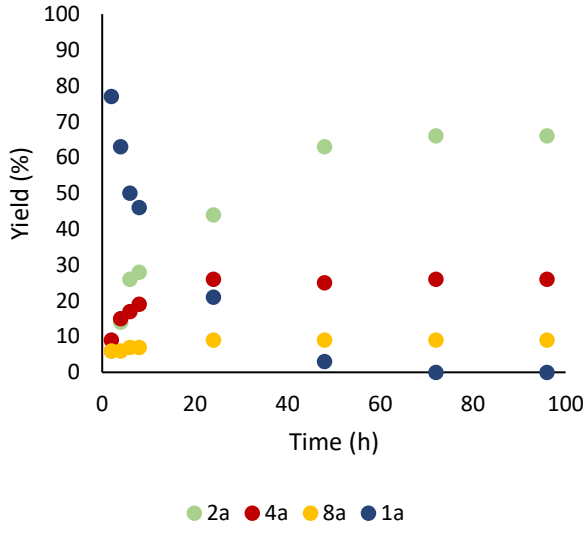

Figure 2.4: Graphical plot of components of reaction mixture over time

To verify whether the phosphonium species **8a**, formed through nucleophilic attack of PPh_3 onto bromide **1a,** could be an intermediate in the system, it was independently prepared and purified following a literature procedure.[20] Subjection of **8a** to the reaction conditions, employing (*S*)-**3d** (10 mol%) and KF (2.5 equiv.) in toluene, resulted in no formation of fluoride product **2a**, and only the

starting material **8a** was observed in ^{1}H NMR. Moreover, under a range of different fluorinating conditions, including employing CsF, or soluble TBAF, fluorination of **8a** could not be achieved, negating its role as a reactive intermediate (Scheme 2.10).

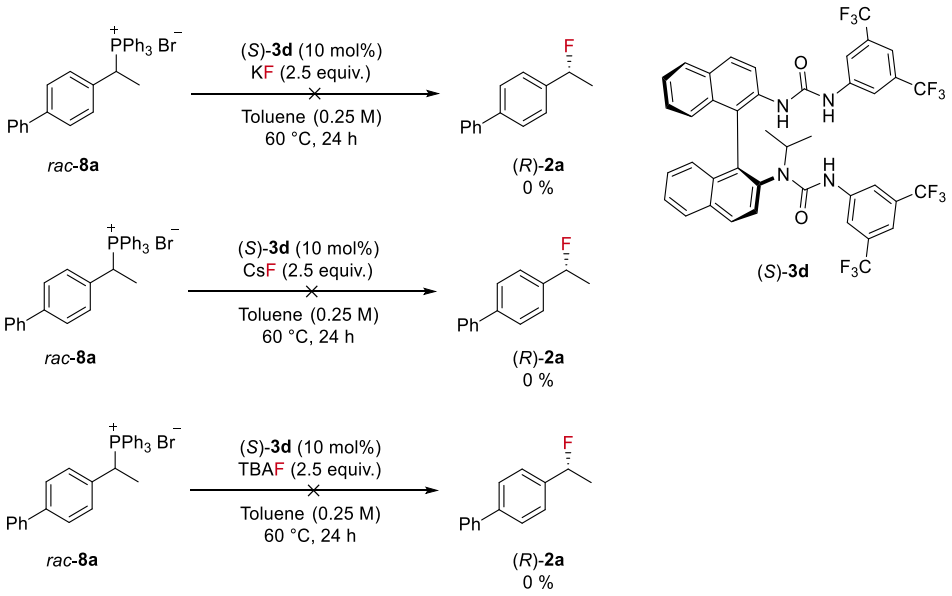

Scheme 2.10: Control reactions performing reactions with phosphonium **8a** as substrate

These results are corroborated by the poor leaving group ability of phosphines, which has excluded their use in the literature as nucleophilic catalysts.[21] Considering that there was no evidence that **8a** was an intermediate within the reaction, alternative roles for the phosphonium species within the system were considered.

2.3. Phosphonium Salts as Phase Transfer Catalysts

The possibility that the phosphonium species formed within the reaction could serve as a phase-transfer co-catalyst, rather than an intermediate was considered. The participation of phosphonium salts as phase-transfer catalysts has been widely reported since the seminal work of Starks, where tetraalkyl phosphonium bromide salts were employed as PT catalysts to shuttle cyanide anions (NaCN) across the organic-aqueous phase barrier (Scheme 2.11).[22]

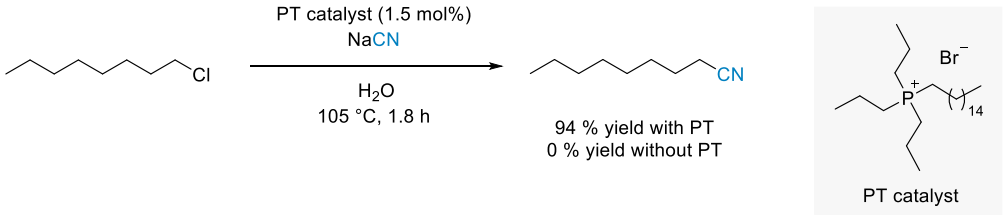

Scheme 2.11: Stark's cyanation of 1-chlorooctanol with phosphonium PT catalyst[22]

To investigate this hypothesis, a control reaction was performed where phosphonium **8a** was added as a co-catalyst (10 mol%) with (*S*)-**3d** (10 mol%) and KF to **1a**. Fluorination was observed in 54 % yield, 76:24 e.r. Notably removing either **8a** or (*S*)-**3d** was detrimental to reactivity (Scheme 2.12).

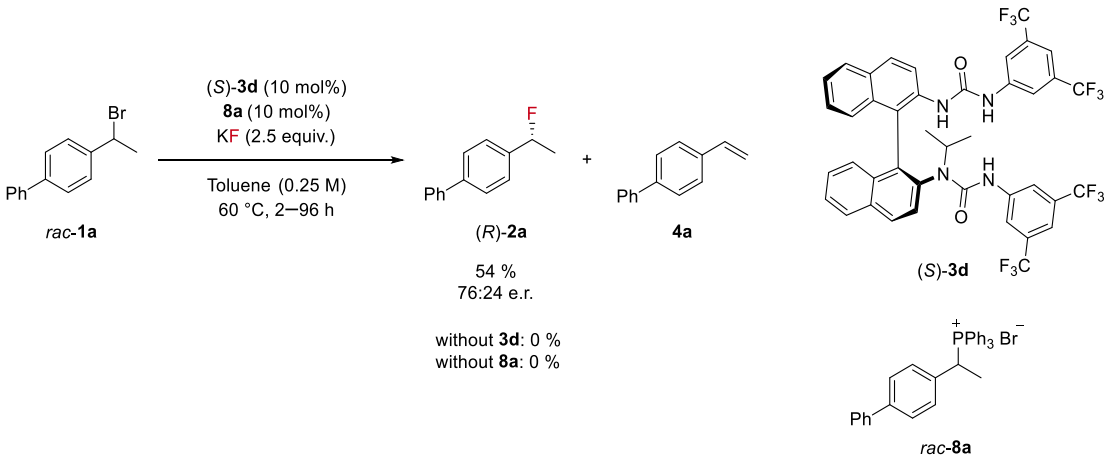

Scheme 2.12: Reaction employing **8a** as a co-catalyst with (*S*)-**3d**

These data support the hypothesis that the addition of PPh_3 into the reaction with benzylic bromide **1a**, urea catalyst (*S*)-**3d** and KF led to the formation of phosphonium **8a**, which acted to proficiently co-catalyse the fluorination of **1a** with KF. Reflecting on the screening results of the LB additives (Table 2.2), the low yield of product as well as poor mass balance observed for DMAP and diphenylsulfide, correlates with how well the nucleophile consumes substrate **1a** to form the corresponding onium salts. Control reactions indicated that the addition of PPh_3 (1 equiv.) to **1a** in the presence of urea (*S*)-**3d** in toluene only yielded ~ 7 % phosphonium **8a** at elevated temperatures (60 °C). This quantity of **8a** could suitably co-catalyse the fluorination of the remaining bromide starting material **1a**, rather than fully consuming it, which would be unproductive for fluorination. For comparison a control experiment

investigated the addition of DMAP (1 equiv.) to **1a** in the presence of (*S*)-**3d** which yielded ~ 20 % of the corresponding ammonium salt (**9a**) as well as significant yields of the elimination product **4a** (17 %) (Scheme 2.13).

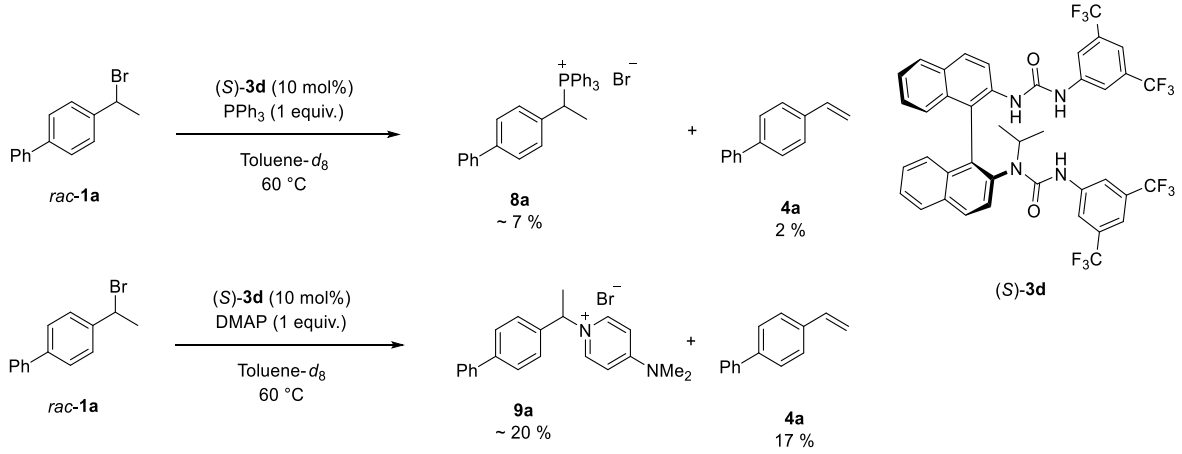

Scheme 2.13: Control reactions forming onium salts **8a** or **9a**

The next section of the results and discussion describe how these preliminary findings led to the development of Synergistic HBPTC (S-HBPTC) whereby urea HBD catalysts and onium halide salts co-catalysts were employed which allowed for the asymmetric fluorination of neutral alkyl halides with KF.

2.3.1. Role of the Phosphonium Salt

To elucidate the necessity of the onium salt to permit reactivity with KF, but not CsF, preliminary NMR experiments were performed to investigate the phase transfer ability of urea (*S*)-**3d**. The addition of CsF to (*S*)-**3d** in DCM-d_2 revealed significant changes in the ^{1}H NMR spectra. Deshielding of urea NH resonances (Figure 2.5a, blue circles) as well as the presence of ^{1}H–^{19}F scalar coupling constants ($^{1h}J_{NH\text{-}F}$ = 59, 36, 35 Hz) indicated strong binding of the fluoride anion to the catalyst, as noted in previous studies.[23] Moreover, a broad fluoride signal at -96.8 ppm is suggestive of the formation of a urea-fluoride complex with CsF (Figure 2.5a). In contrast, in an analogous experiment where KF was added to a solution containing (*S*)-**3d**, no spectroscopic changes were observed. The urea NH resonances remained visible and unchanged suggesting that the catalyst remained in a conformational unbound

state (Figure 2.5b, blue circles). Furthermore, no signal indicative of fluoride solubilisation was observed by ^{19}F NMR (Figure 2.5b). When the equivalent experiment was carried out in toluene-d_8, the same results were obtained.

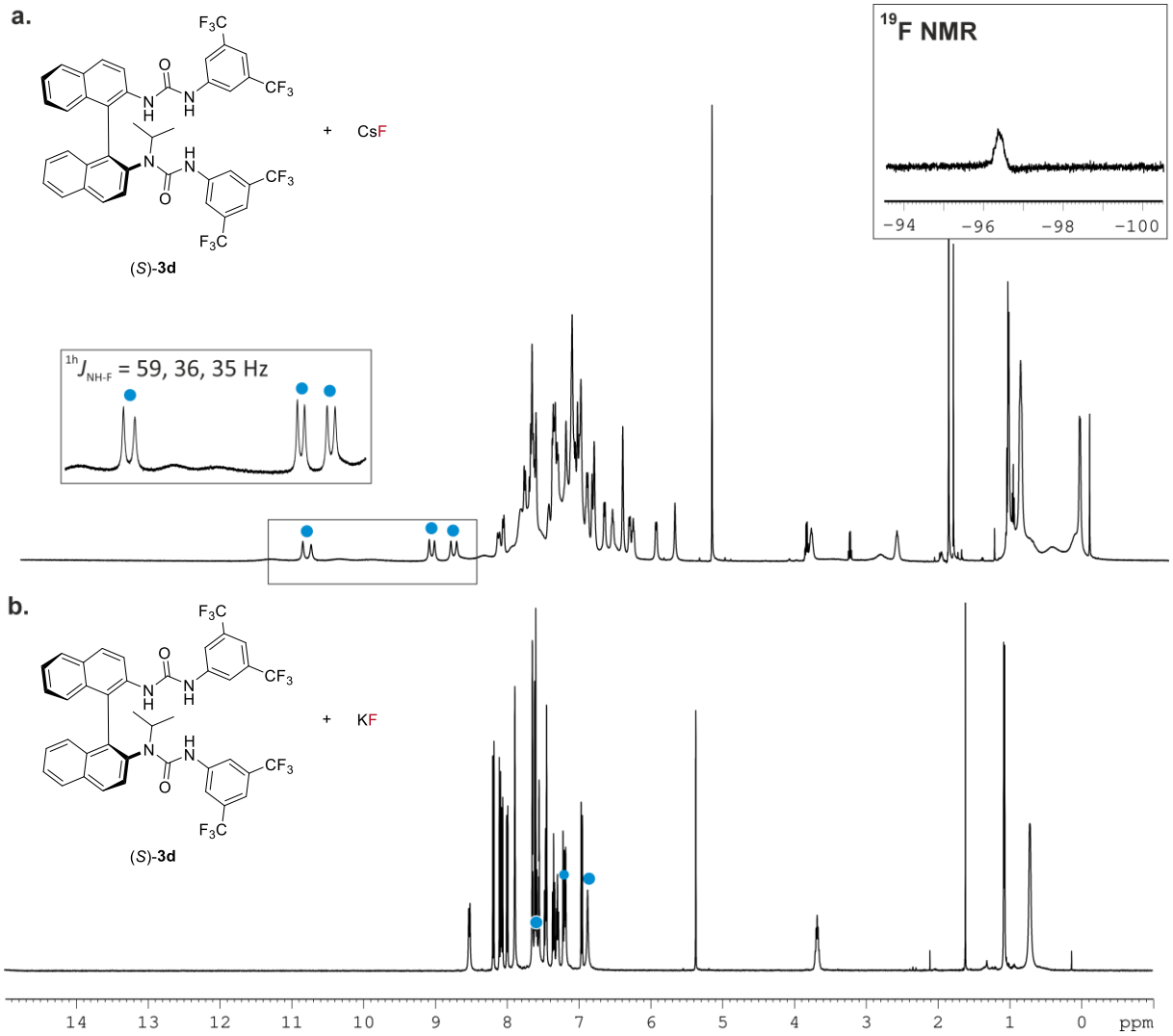

Figure 2.5: a. ^{1}H NMR spectra of **3d** and CsF (500 MHz, DCM-d_2, 25 mM, 298 K), inset ^{19}F NMR spectra showing urea bound fluoride (F^-) signal; b. ^{1}H NMR spectra of **3d** and KF (500 MHz, DCM-d_2, 25 mM, 298 K).

These experiments suggest that (*S*)-**3d** is unable to bind fluoride from KF in DCM or toluene. This result stood contradictory to the reported catalytic cycle for the fluorination of β-chloroamines achieved with KF under HBPTC in DCM.[9] Considering that the urea catalyst appeared incapable of KF solubilisation, a catalytic cycle initiating with this step seemed unlikely (Figure 2.6a). This prompted a putative hypothesis that in this instance the transient onium electrophile, the aziridinium ion, may act as a second phase-transfer agent allowing for KF solubilisation (Figure 2.6b). Here, ion-pairs between the reactive aziridinium and fluoride (or bromide) could not be spectroscopically observed, as the

electrophile is swiftly opened with fluoride to form the product. However, as phosphonium species have been shown to be unreactive to nucleophilic attack with fluoride (*v*. Scheme 2.10), this allowed for an opportunity to study their interaction with urea catalysts and KF.

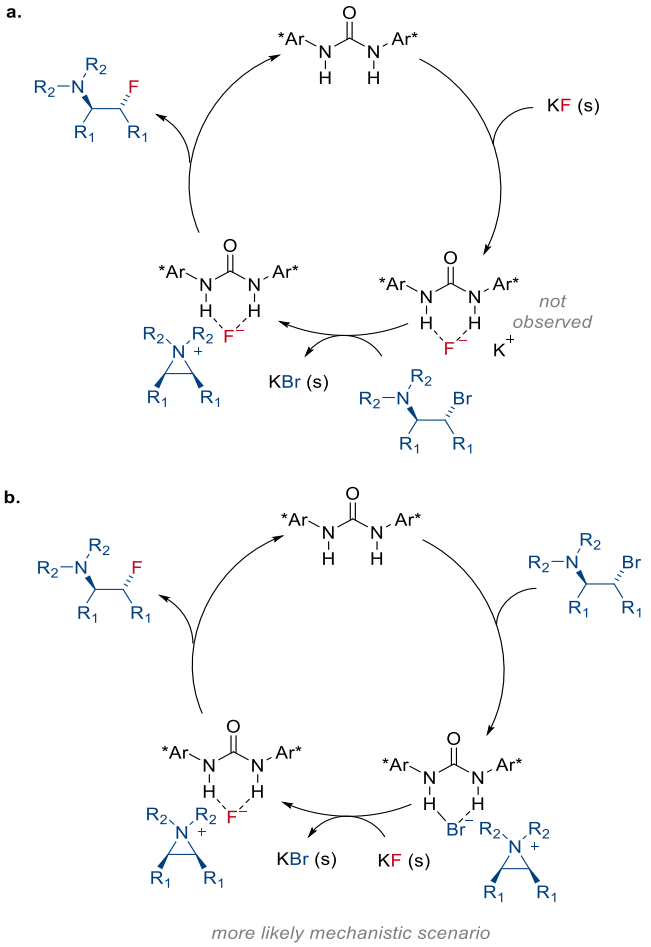

Figure 2.6: Possible mechanistic scenarios for the fluorination of β-bromoamines under HBPTC with KF

Distinctive changes were observed upon the addition of phosphonium bromide **8b** to solution containing catalyst (*S*)-**3d** and KF in DCM-d_2. Deshielding of urea NH resonances as well as substantial line-broadening downfield was observed in ^{1}H NMR, suggesting the presence of multiple species equilibrating in solution (Figure 2.7a). Variable temperature (VT) NMR experiments (293–193 K) revealed the detection of two defined species, characterised by the presence of two sets of urea NH signals, confirmed by ^{1}H–^{13}C HSQC (green and blue circles) (Figure 2.7b). The ^{19}F NMR spectra also showed a broad peak at -86.8 ppm, indicative of fluoride solubilisation, which sharpened upon cooling (Figure 2.7 inset).

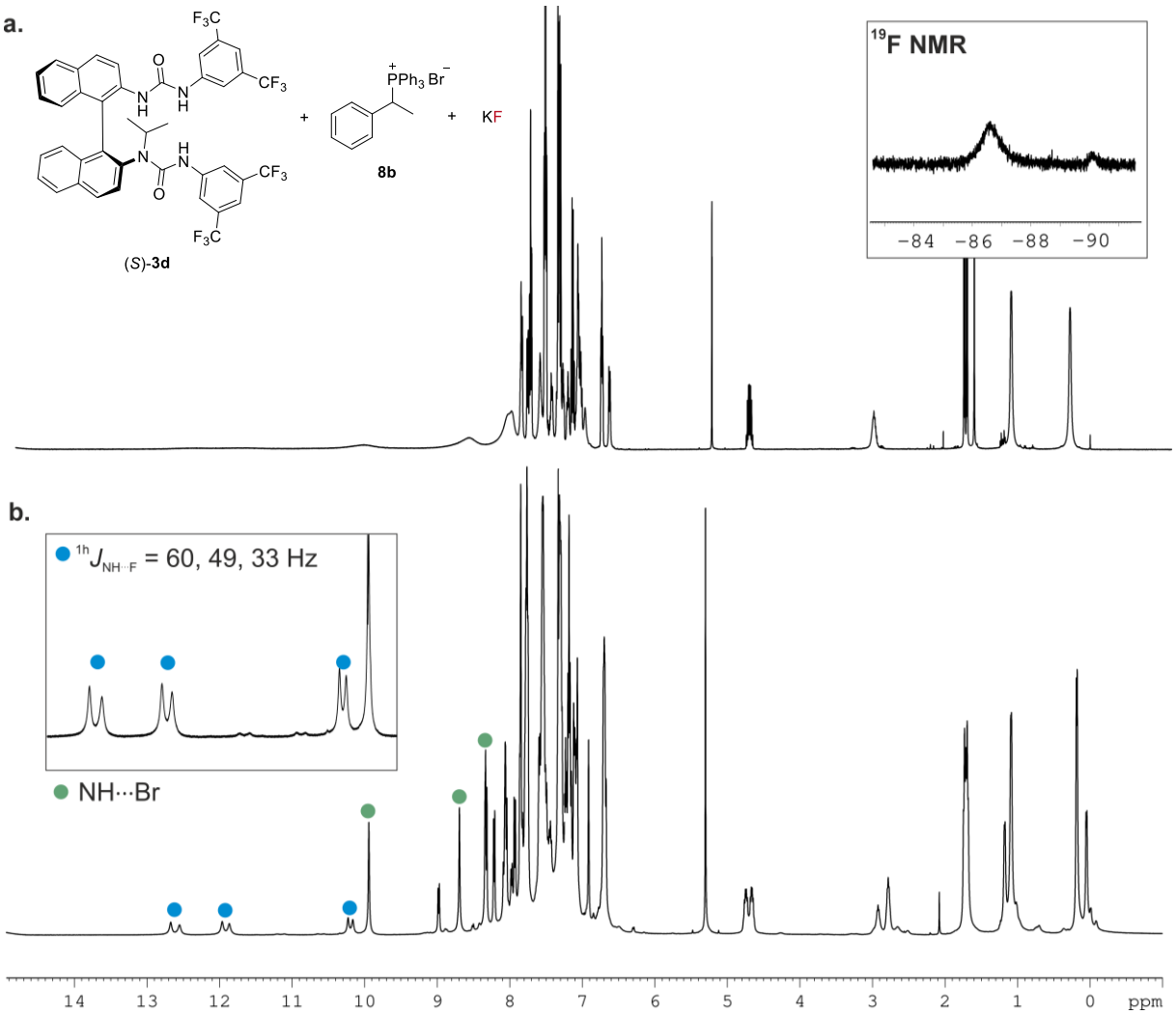

Figure 2.7: a. ^{1}H NMR spectra of **3d**, **8b** and KF (500 MHz, DCM-d_2, 25 mM, 298 K), inset ^{19}F NMR spectra showing fluoride (F^-) signal; b. ^{1}H NMR spectra of **3d**, **8b** and KF (500 MHz, DCM-d_2, 25 mM, 193 K)

One set of urea signals could be ascribed to the NH protons binding to fluoride (Figure 2.7b blue circles), evident from significant deshielding of the resonances ($\Delta\delta_{NH}$ ~ + 3–6 ppm) as they bind to the highly electronegative fluoride anion. Additionally, each NH signal appeared as a doublet in ^{1}H NMR. When the spectrum was obtained with fluorine decoupling, all three NH signals collapsed into singlets. This multiplicity is a result of scalar coupling which develops between ^{19}F and ^{1}H across hydrogen bonds ($^{1h}J_{NH\cdots F}$ = 60, 49, 33 Hz). The coupling constants observed were in line with data previously reported for this class of urea catalysts and provide unambiguous evidence of hydrogen bonding interactions between urea NH protons and fluoride.[23] A smaller subset of NH resonances which showed binding to fluoride were also observed, which may be related to higher order species of urea-fluoride (e.g. 2:1 urea:fluoride complexes). Another species was observed where the urea NH resonances were

deshielded singlets ($\Delta\delta_{NH}$ ~ + 1–3 ppm), which corresponded to the binding of a bromide anion to the urea catalyst (Figure 2.7b green circles).

Noteworthy changes were also observed for signals corresponding to phosphonium **8b**. Principally, the chemical shift and the multiplicity of the resonance corresponding the benzylic proton (Figure 2.8 purple circle) changed from a doublet of quartets at 6.35 ppm to a higher ordered multiplet with a complex splitting pattern at 4.84 ppm. From decoupling ($^1H\{^{31}P\}$ and $^1H\{^1H\}$) and VT NMR experiments, it could be deduced that the multiplicity of the signal was a result of close proximity of this proton to the chiral urea (*S*)-**3d**. The chiral environment of the urea induces asymmetry upon the chiral carbon of **8b** resulting in the formation of two diastereomeric complexes (Figure 2.8).

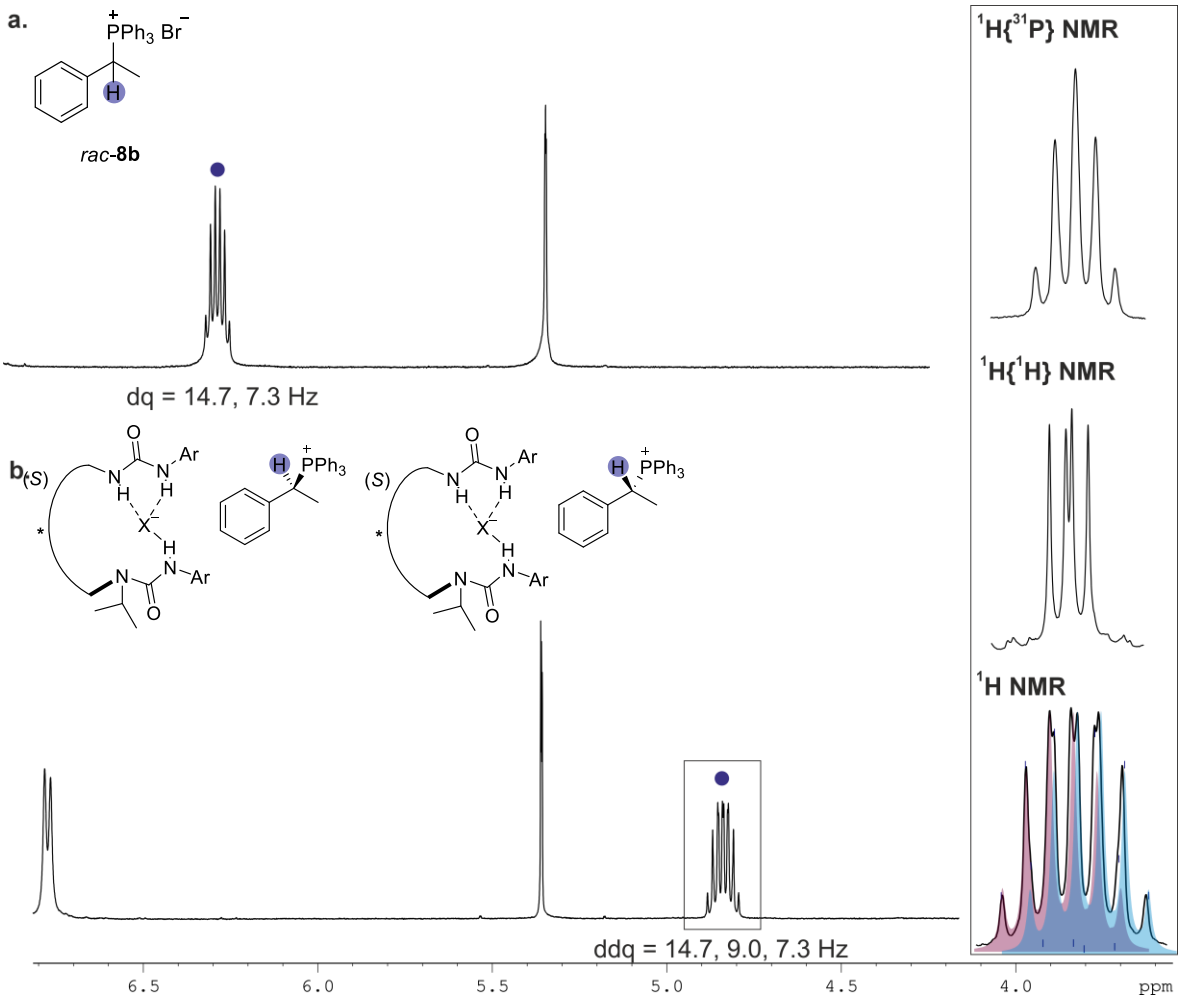

Figure 2.8: a. ^1H NMR spectra of **8a** (500 MHz, DCM-d_2, 25 mM, 298 K); b. ^1H NMR spectra of **8a** in the presence of (*S*)-**3d** and KF (500 MHz, DCM-d_2, 25 mM, 298 K), inset – ^1H and ^{31}P decoupling experiments on benzylic proton (purple circle)

These experiments comprehensively underlined the difference between the solubilisation of KF and CsF by HBD urea catalysts. Whilst (*S*)-**3d** was shown to be an efficient catalyst for CsF solubilisation through hydrogen-bonding forming a urea-cesium-fluoride complex, which has been previously reported and well-understood *via* NMR studies and X-ray crystallographic evidence, this is not the case for the more demanding fluoride salt, KF.[23] Here, it was shown that the introduction of a second cationic catalyst, a phosphonium halide, permitted the solubilisation of potassium fluoride as a urea-phosphonium-fluoride [UPF] ion pair. Within this experiment the use of a phosphonium bromide halide additionally resulted in the formation of a urea-phosphonium-bromide ion pair [UPBr] which exists concurrently in solution and has also been shown to form exclusively in the absence of KF.

2.4. Reaction Development of Urea-Onium PT System

2.4.1. Optimisation of Onium Salt Co-catalyst

The effect of different onium salts within the reaction was evaluated. Whilst the reaction discovery stemmed from the *in situ* formation of phosphonium salt **8a**, the reaction also proceeded in the presence of a range of structurally different phosphonium, ammonium and sulfonium salts (Scheme 2.14). Tetraphenylphosphonium salts (**8c** and **8d**) performed best, ensuring a higher level of enantiocontrol for the formation of **2a** than alkyl onium counterparts (**8k**–**8m**). When enantiopure ammonium catalysts (*S*)-**8o** and (*R*)-**8o** were employed, there was no significant (mis)match effect and the absolute configuration of fluoride product **2a** was the same (71:29 and 73:27 e.r.). Control reactions demonstrated that the removal of the urea catalyst (**3d**) resulted in a loss of reactivity for all onium salt co-catalysts employed. A beneficial effect in yield and minor increase in enantioselectivity, was observed when the counter-anion of onium salts was changed from bromide, chloride or tetrafluoroborate to iodide, and commercially available $Ph_4P^+ I^-$ (**8d**) selected as the optimal co-catalyst giving 61 % yield of **2a** in 77:23 e.r. at 60 °C for 24 hours.

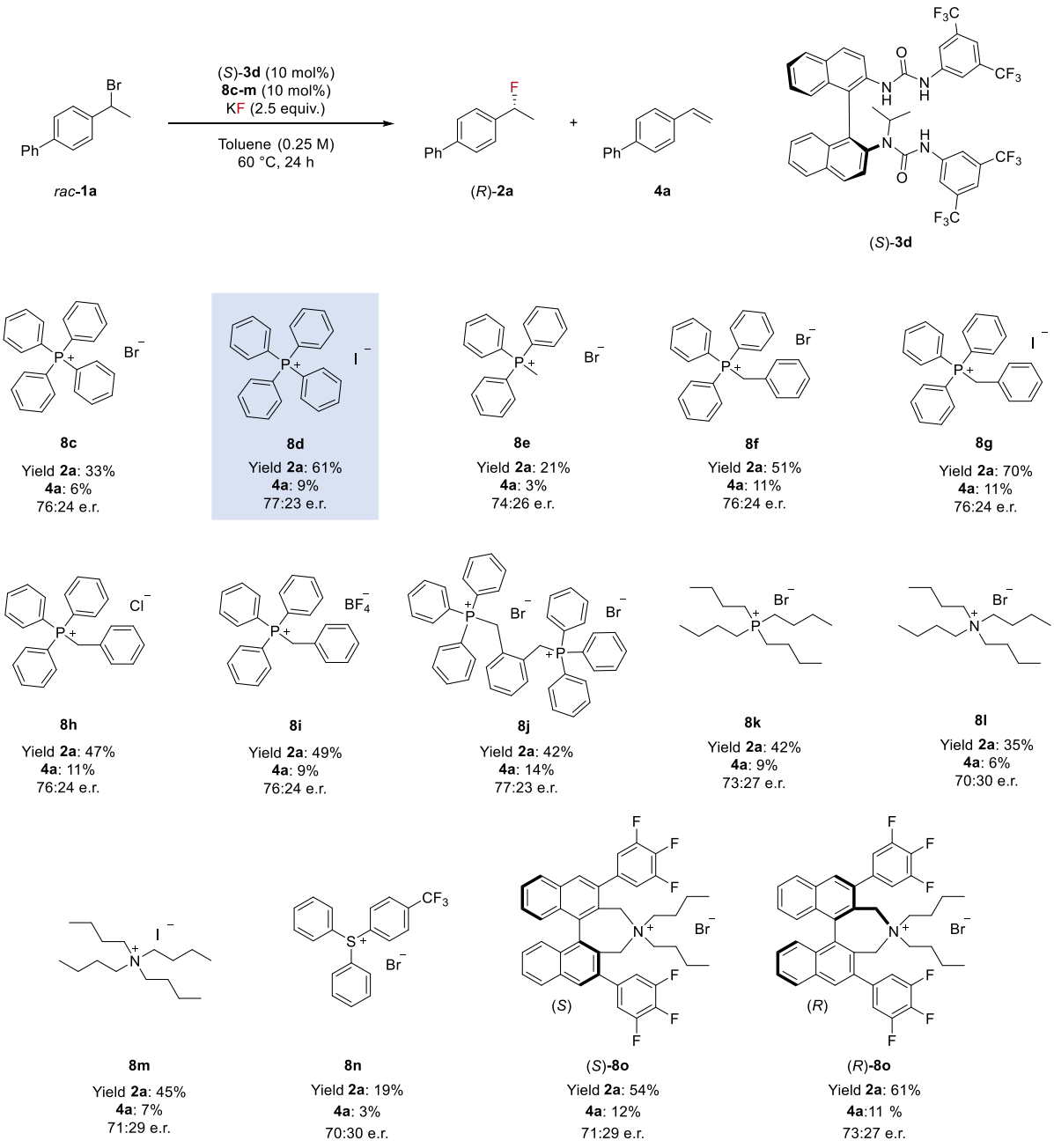

Scheme 2.14: Screening of onium catalysts with (*S*)-**3d** and **1a**

Increasing the loading of $Ph_4P^+ I^-$ from 10 mol% up to (super)stochiometric equivalents was not seen to benefit the yield or enantioselectivity of **2a** (Table 2.5). Lowering the temperature to 40 °C and performing the reaction for 48 hours allowed for the conversion of **1a** into **2a** in 32 % yield with improved chemoselectivity (8:1 **2a**:**4a**) and higher enantiomeric ratio of 80:20 (Table 2.5 entry 6).

Table 2.5: Screening of tetraphenylphosphonium iodide loading with **1a**

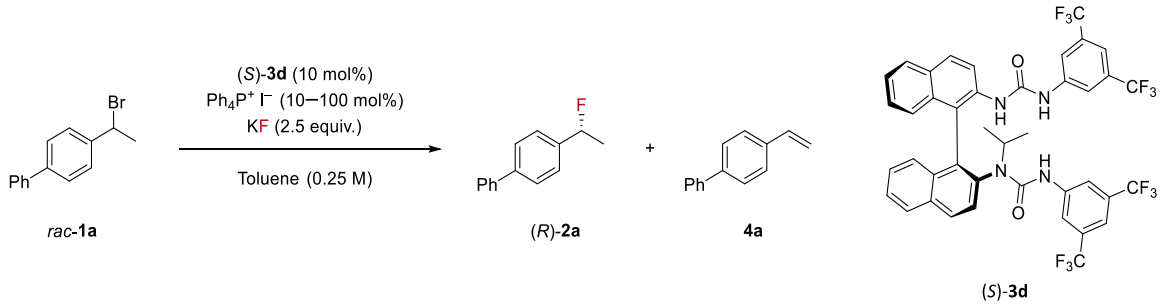

Entry	$Ph_4P^+ I^-$ (mol%)	Conditions	Yield **2a** (%)[a]	Ratio **2a**: **4a**	e.r.[b]
1	10	60 °C / 24 h	61	7:1	77:23
2	20	60 °C / 24 h	59	7:1	77:23
3	50	60 °C / 24 h	64	7:1	77:23
4	100	60 °C / 24 h	57	7:1	77:23
5	200	60 °C / 24 h	61	7:1	77:23
6	10	40 °C / 48 h	32	8:1	80:20

General conditions: 0.05 mmol substrate, stirring at 1200 rpm. [a]Determined by ^{19}F NMR using 4-fluoroanisole as internal standard, [b]e.r. determined by HPLC analysis using a chiral stationary phase

2.4.2. Evaluation of Fluoride Sources

The effect of employing different fluoride sources was also evaluated. It was previously demonstrated that unlike CsF, the use of KF for the fluorination of **1a** required the addition of onium salt co-catalyst. Spectroscopic data suggested that the higher lattice energy of KF made solubilisation through hydrogen-bonding alone unfeasible and the addition of a secondary cationic PT catalyst aided solubilisation through additional electrostatic stabilisation as a urea-onium-fluoride ion pair. Therefore, other alkali metal fluoride salts, such as NaF and LiF, of higher lattice energies were investigated to determine if their reactivity could also be harnessed under this strategy.

Substrate **1a** underwent fluorination with KF, optimal onium salt $Ph_4P^+ I^-$ and KF in toluene providing fluoride **2a** in 61 % yield and in 77:23 e.r. at 60 °C. Employing CsF gave a slightly improved yield of fluorinated product in 68 % in comparable enantioselectivity of 76:24 e.r. however also resulted in a higher yield of elimination side product (13 %).

In contrast, NaF and LiF were both seen to be unsuitable fluoride sources for this transformation, providing no yield of the desired fluorinated product **2a** and only elimination to **4a** (up to 12 %) (Table 2.6 entries 3 and 4). Exploratory NMR experiments were undertaken which demonstrated there was no spectroscopic evidence that the urea catalyst **3d** could solubilise either LiF or NaF in the presence of an onium salt co-catalyst, as was observed with KF.

Table 2.6: Evaluation of different alkali metal fluoride salts with **1a**

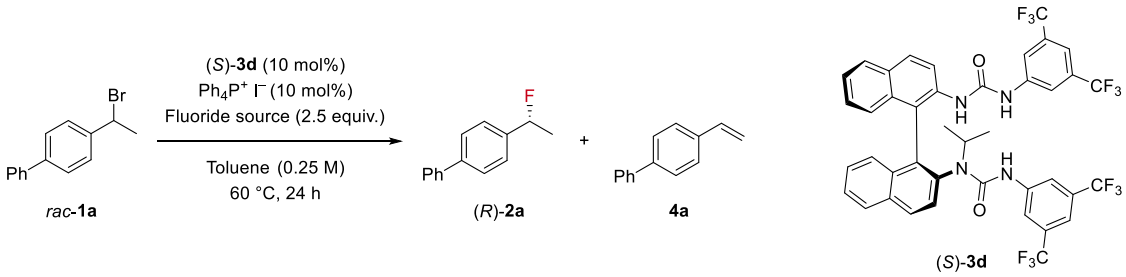

Entry	Fluoride Source	Lattice energy kcal/ mol[7]	Yield **2a** (%)[a]	Yield **4a** (%)	e.r. [b]
1	CsF	181	68	13	76:24
2	KF	198	61	9	77:23
3	NaF	222	0	12	nd
4	LiF	254	0	5	nd

General conditions: 0.05 mmol substrate, stirring at 1200 rpm. [a]Determined by ^{19}F NMR using 4-fluoroanisole as internal standard, [b]e.r. determined by HPLC analysis using a chiral stationary phase. nd = not determined.

2.4.3. Synthesis and Optimisation of Urea HBD Catalysts

The structure and electronic properties of urea HBD catalysts is understood to exert the most prominent effects in both the yield and stereochemical outcome of fluorinated products synthesised under HBPTC.[23] BINAM ([1,1'-binaphhalene]-2,2'-diamine) is commercially available as both enantiomers and can be easily modified in several ways. Backbone modification of the naphthalene rings can be performed allowing for 3,3' or 6,6' halogenation (at R_4 and R_5) which can act as functional handles for further modification (e.g. cross-couplings). Such modifications have been previously explored for this class of catalysts with minimal impacts on their performance and therefore was not considered as a promising option for future catalyst design.[24, 25]

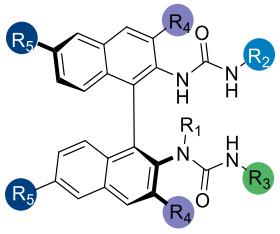

Scheme 2.15: Sites of functionalisation for BINAM derived *bis*-urea catalysts

Urea mono-*N*-alkylation has been demonstrated as an impactful modification for this class of catalysts (*v. 2.1.1. Hydrogen Bonding Phase Transfer Catalysis (HBPTC)*) considering their tendency to bind fluoride in a tricoordinate fashion. Mono-*N*-alkylation also allows for the synthesis of unsymmetrical *bis*-urea catalysts possessing different R_2 and R_3 substitutions, as the less sterically hindered unalkylated amine reacts first. Mono-urea catalysts could be isolated and subsequently reacted with a different isocyanate (R_3NCO). This process was also shown to be amenable to a telescoped synthesis whereby isocyanates were sequentially added to form *bis*-urea catalysts (Scheme 2.16).

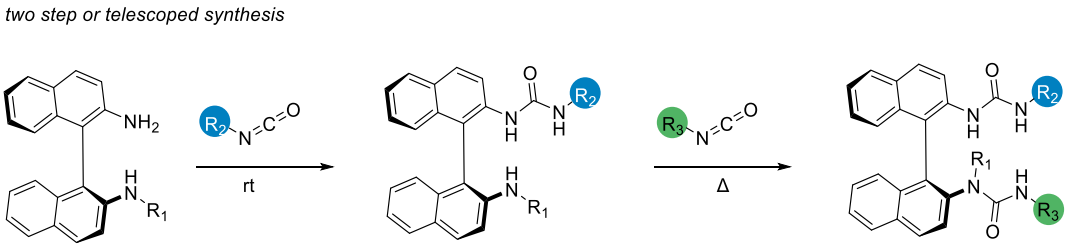

Scheme 2.16: Strategy for the synthesis of dissymmetric BINAM derived *bis*-urea catalysts

Preliminary catalyst screening demonstrated that the replacement of the highly electron-withdrawn 3,5-*bis*(trifluoromethyl)phenyl ring with an unsubstituted phenyl ring on the unalkylated urea (R_2) had substantial benefit on the yield and enantioselectivity of **2a** (63 %, 83:17 e.r.). In contrast the opposite modification and replacement with an unsubstituted phenyl ring at R_3 showed drastically diminished reactivity and enantioselectivity of **2a** (6 %, 56:44 e.r.) (Scheme 2.17). This is consistent with previous results obtained for the asymmetric fluorination of β-bromosulfides under HBPTC, which highlights the importance of the NH proximal to the *N*-alkylation on *bis*-urea catalysts.[23]

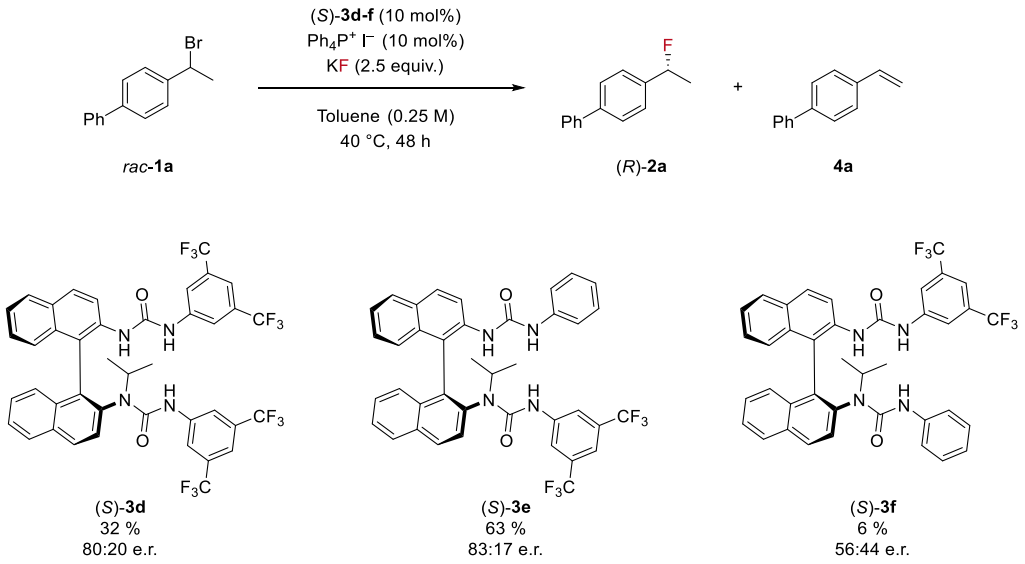

Scheme 2.17: Preliminary screening of electronics on urea HBD catalysts with **1a**

Functionalisation of the unalkylated urea was investigated next (Scheme 2.18). Catalysts **3g**-**j** where halogen atoms were substituted on the aryl ring at R_1, furnished fluorinated product **2a** in comparable yields and improved enantiocontrol (86:14 e.r.) to **3e** (83:17 e.r.). It is notable that para-fluoro substituted catalyst (**3g**) performed best in this series giving a yield of 64 %. Difluorination at the meta and para-position of this aryl ring (**3k**) further increased the yield of **2a** and enantioselectivity (79 % yield, 87:13 e.r.), however trifluorinated aryl substitution (**3l**) did not present further benefits to the yield of **2a** (46 %) and only marginally improved the enantioselectivity (88:12 e.r.). Catalysts with *ortho*-substitution such as **3m** resulted in trace product formation, consistent with previous data which describe the ortho C–H protons on the urea aryl rings as hydrogen bond contacts (HBC) to fluoride. Catalysts which possessed more electron-donating functionalities were also investigated, with para-methyl (**3o**) and methoxy (**3p**) derivatives synthesised. These catalysts however resulted in diminished yields and enantioselectivity of the product **2a** (58 % 85:15 e.r., and 55 % 85:15 e.r. respectively), as well as reduced chemoselectivity (7:1 **2a**: **4a**).

Finally, *bis*-urea catalysts with structurally different functionality were evaluated such as **3q** with a fused cyclopentane which gave lower yield and enantioselectivity (44 %, 85:15 e.r.) and **3r** with an

extended aryl ring system, which gave a lower yield of fluorinated product (25 %) at an equivalent enantioselectivity (87:13 e.r.) to the best performing catalyst **3k**.

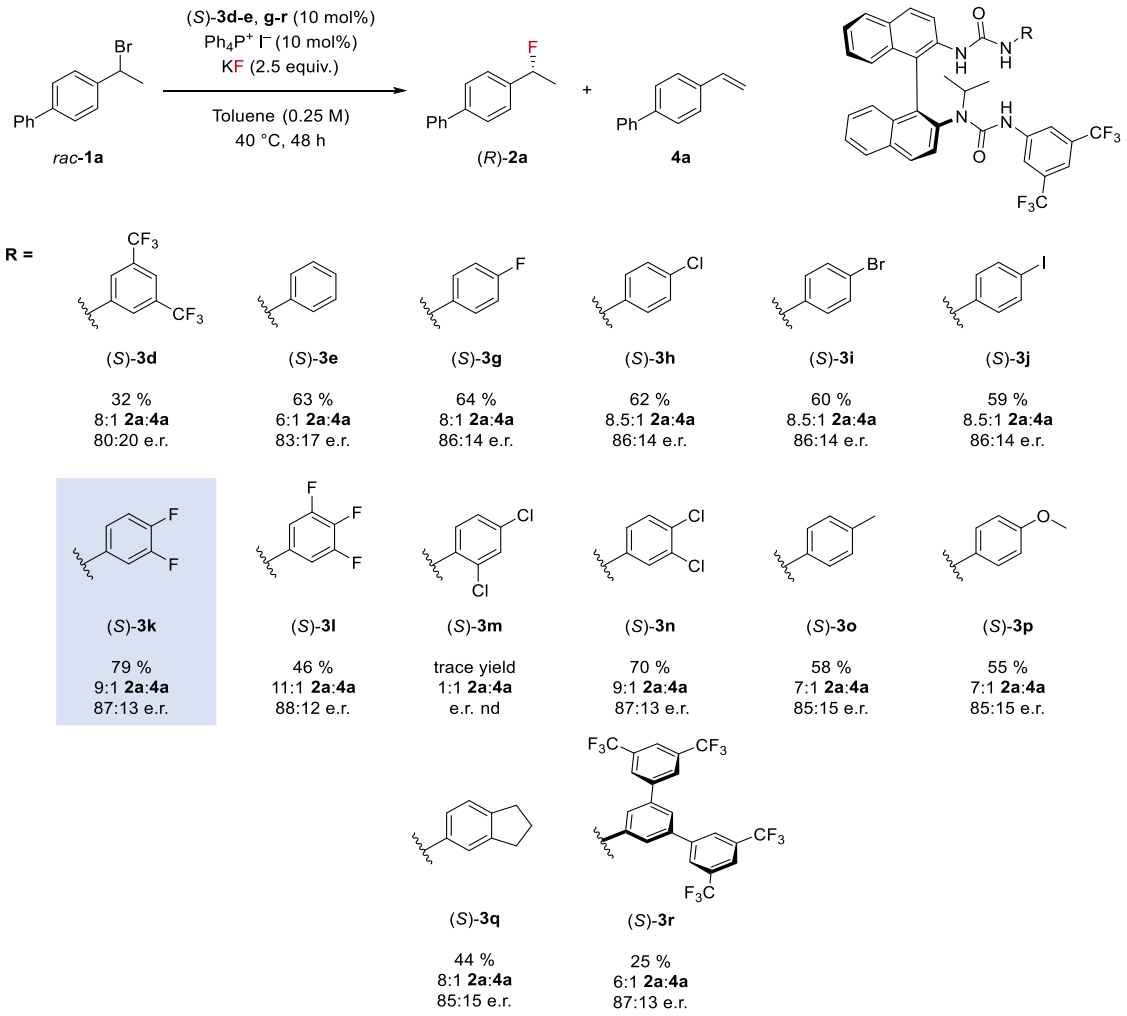

Scheme 2.18: Screening of *bis*-urea catalysts **3d-e**, **g-r**

Given the importance of the NH adjacent to the *N*-alkyl group on the urea (Scheme 2.17), efforts were made to increase the acidity of this NH by the introduction of stronger electron-withdrawing groups, such as 3,5-*bis*(pentafluorosulfanyl). The preparation of this catalyst required the synthesis of 3,5-*bis*(pentafluorosulfanyl)phenyl isocyanate. This was initiated through the synthesis of 3,5-*bis*(pentafluorosulfanyl)aniline **10** which could be prepared from the commercially available aryl bromide following a literature procedure.[26] The synthesis of the corresponding isocyanate was attempted *in situ* from **10** and triphosgene, and the consumption of aniline **10** was monitored by TLC and when complete, catalyst intermediate **11** was added and the reaction was set to reflux. However,

this synthesis failed to deliver the final catalyst with the hypothesis that the very electron-withdrawn isocyanate was highly sensitive and decomposed rapidly under the reaction conditions (Scheme 2.19).

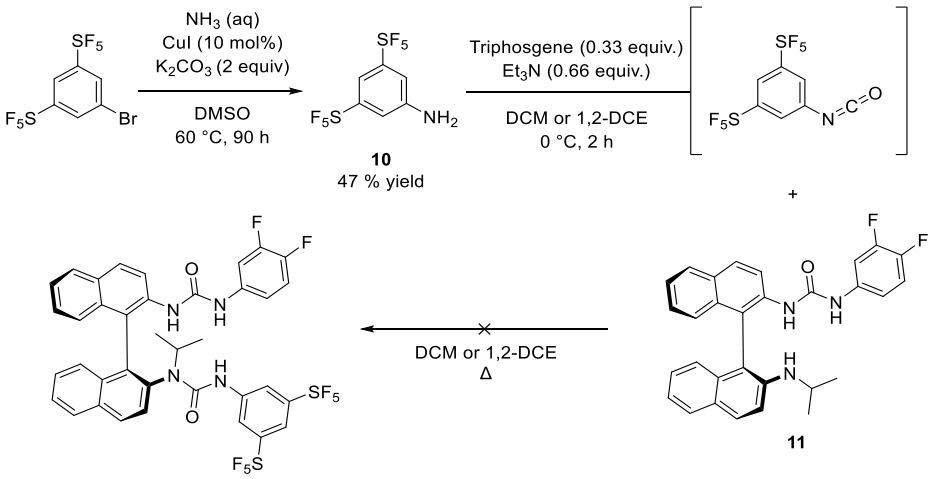

Scheme 2.19: Investigation into the synthesis of a 3,5-*bis*(pentafluorosulfanyl) substituted catalyst

Attention was turned to investigating *N*-alkylation of catalysts considering the great impact this exerted on reaction outcomes within previous studies of HBPTC (*v. 2.1.1 Hydrogen Bonding Phase Transfer Catalysis (HBPTC)*). Interestingly tetradentate *bis*-urea catalyst (*S*)-**3a** was not an efficient catalyst for the fluorination of **1a**, and only trace elimination (**4a**) was observed. (Scheme 2.20)

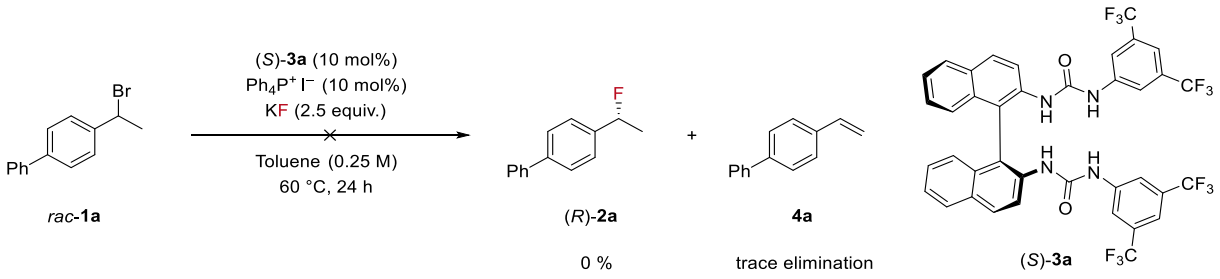

Scheme 2.20: Reaction performed with tetradentate *bis*-urea catalyst **3a**

Investigating less bulky *N*-alkyl groups such as the replacement of the *N*-iPr (**3k**) for an *N*-Et group (**3s**) resulted in a decrease in yield of **2a** from 81 % to 28 %. In contrast, increasing the bulk of the *N*-alkylation from *i*Pr to 3-pentyl (**3t**) and 4-heptyl (**3u**) showed minor improvements in the yield of **2a** at 40 °C to 79 and 85 % respectively, with no change in the enantioselectivity observed (87:13 e.r.). Increasing the *N*-alkylation to 5-nonyl demonstrated a limit on the benefit of this modification to reactivity, with lower yields of 65 % observed, however also at the same level of enantioselectivity

(87:13 e.r.). Further investigations into catalysts possessing cyclic alkyl groups, for example cyclohexane **3w** and indane **3x**, did not show benefit to reactivity or enantioselectivity which gave fluorinated product **2a** in 54 %, 87:13 and 28 %, 88:12 e.r. respectively (Scheme 2.21).

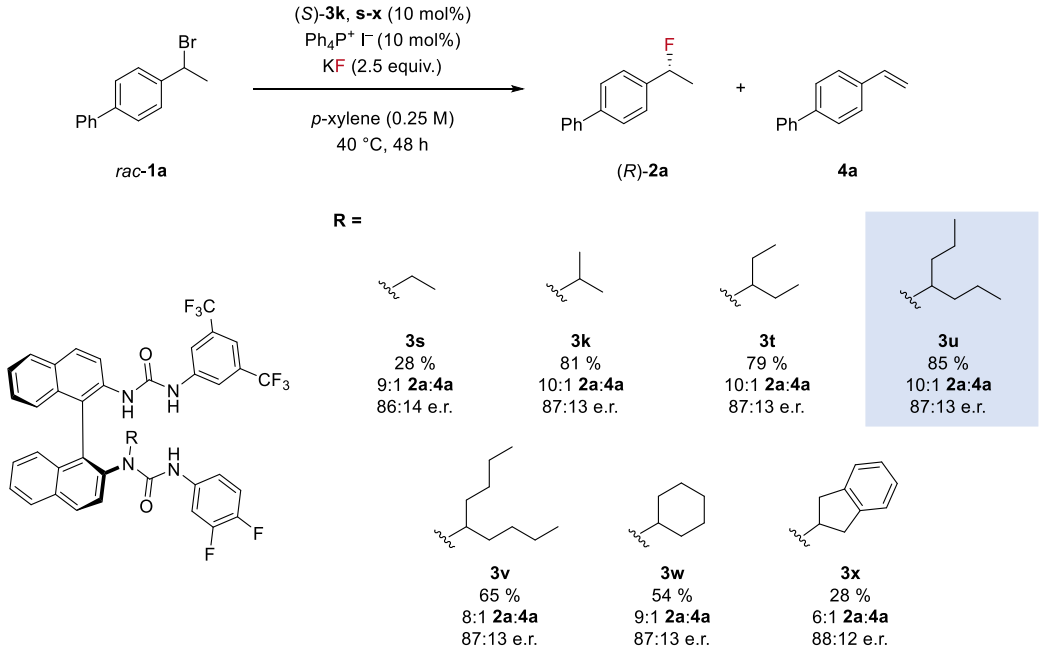

Scheme 2.21: Screening of *bis*-urea catalysts possessing different *N*-alkylations **3k**, **s-x**

The minimal impact that catalyst *N*-alkylation has on the enantioselectivity of **2a** can be rationalised through analysis of X-ray crystal structures of catalyst **3d**, which show that the *N*-alkylation is positioned outside of the binding pocket when the urea is bound to fluoride (Figure 2.9). Increasing the steric bulk at this nitrogen is not expected to affect the position of fluoride or the overall transition state. Improved reactivity as a factor of urea catalyst *N*-alkylation may stem from enhanced catalyst-fluoride stability or an increased population of reactive conformers of catalyst-fluoride species.

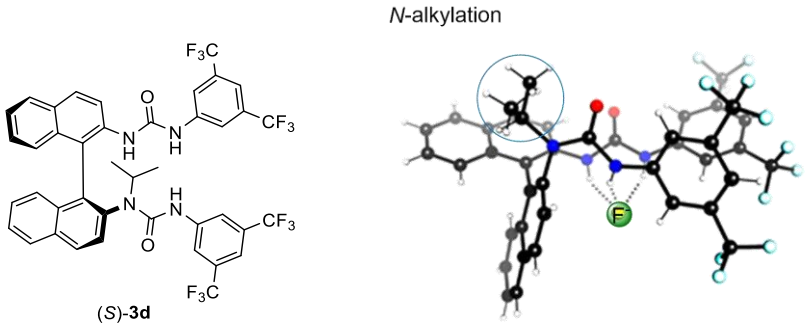

Figure 2.9: Crystal structure of catalyst (*S*)-**3d** bound to fluoride (TBAF), tetrabutylammonium cation omitted for clarity. Adapted with permission from reference[2, 23]

2.4.4. Solvent Effect

Solvation effects are crucial in understanding the behaviour and reactivity of ion-pairs. The strength of ionic interactions is dependent on Coulomb's law, where attractive forces are a function of the polarity of medium they are present in.[27] Stronger electrostatic interactions and tighter, contact, ion pairs are formed in apolar solvents possessing low dielectric constants (ε). In contrast, polar solvents facilitate ion dissociation to solvent-shared or solvent-separated ion-pairs (Figure 2.10).[28] Therefore, it is common to see chemistry which utilises and exploits the properties of ion-pairing to be performed in solvents such as 1,4-dioxane, toluene or MBTE, which possess low dielectric constants.

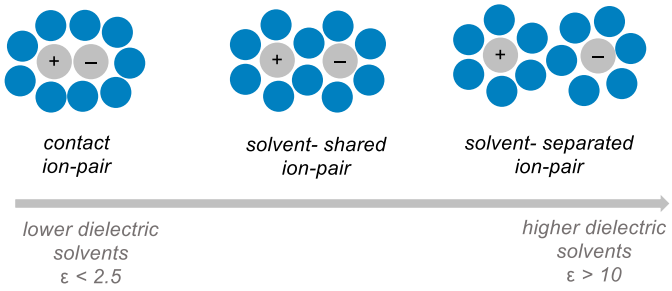

Figure 2.10: Effect of solvation on ion-pairs

Investigations into the solvent effect for the fluorination of benzylic bromides under S-HBPTC elucidated a clear trend between the dielectric constant (ε) of the reaction solvent and the enantiopurity of fluoride product **2a**. Preliminary reaction development was performed in toluene (ε = 2.38), yielding **2a** in 64 %, 87:13 e.r. (Table 2.7, entry 11), however other non-polar aromatic solvents such as benzene and xylenes performed equally with *p*-xylene (ε = 2.37) providing an increase in reaction yield of **2a** to 81 % in comparable enantioselectivity (87:13 e.r.) (Table 2.7, entry 13). Non-aromatic solvents, that are also of low dielectric constants such as ethereal solvent MTBE or halogenated CCl_4 also ensured a high level of enantiocontrol, however lower yields of fluorinated product **2a** were obtained compared to *p*-xylene (Table 2.7, entries 7–9 and 16). These results indicated that the polarity of the solvent, rather than structure was the important factor for controlling the enantioselectivity. This correlation was hypothesised to be related to an increased strength of ion-pairing interactions between the urea-fluoride anion and onium cation in apolar solvents. In contrast

solvents of high polarity including DCM, trifluorotoluene, 1,2-DCE and 1,2-DFB all provided fluorinated product **2a** in diminished enantioselectivity (Table 2.7, entries 2–5, Figure 2.11a).

Table 2.7: Solvent Screening for fluorination of **1a**

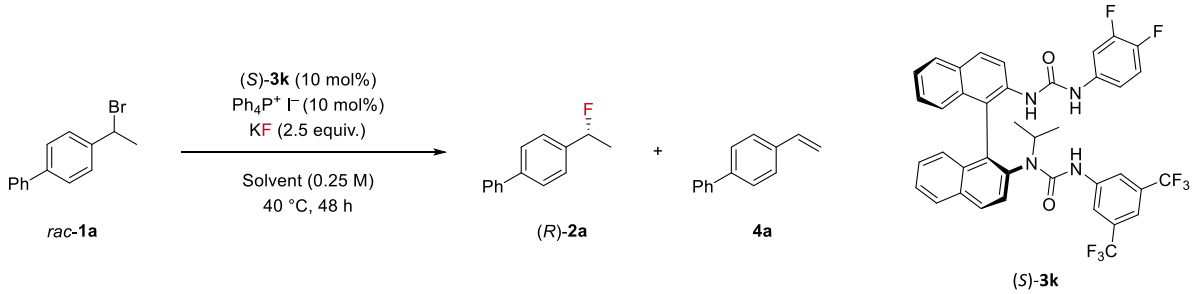

Entry	Solvent	Dielectric Constant (ε)	Yield **2a** (%)[a]	Ratio **2a**: **4a**	e.r.[b]
1	MeCN	37.5	6	1:8	nd
2	1,2-DFB	14.3	44	6:1	69:31
3	1,2-DCE	10.4	24	2:1	74:26
4	$PhCF_3$	9.18	41	7:1	81:19
5	DCM	8.93	24	1:1	71:29
6	THF	7.52	15	4:1	78:22
7	CPME	4.76	51	7:1	82:18
8	MTBE	4.50	74	8:1	84:16
9	Isopropyl ether	3.80	65	7:1	83:17
10	*o*-Xylene	2.50	59	7:1	86:14
11	Toluene	2.38	64	9:1	87:13
12	*m*-Xylene	2.37	56	8:1	87:13
13	*p*-Xylene	2.37	81	10:1	87:13
14	Benzene	2.28	44	8:1	84:16
15	Cyclohexane	2.02	3	1:1	nd
16	CCl_4	1.34	66	8:1	86:14

General conditions: Substrate (0.05 mmol), urea (10 mol%), $Ph_4P^+ I^-$ (10 mol%) and KF (2.5 equiv.) in 200 µL of solvent stirred at 1200 rpm. [a]Determined by ^{19}F NMR using 4-fluoroanisole as internal standard, [b]e.r. determined by chiral HPLC.

It is important to emphasise that the trend observed was between the polarity of the solvent and the enantioselectivity of **2a**, and similar correlations could not be drawn relating dielectric constant to the yields of fluorinated product (Figure 2.11b). For example, reactions performed in low polarity alkane solvents (e.g. cyclohexane ε = 2.02) exhibited substantially reduced reactivity (**2a**: 3 %) (Table 2.7, entry

15). This is however thought to be related to the visibly low solubility of both the bromide substrate and the urea and onium catalysts in these solvents. Furthermore, diminished yields of fluorinated products were observed in reaction solvents such as MeCN, 1,2-DCE and DCM, which promoted the competitive elimination pathway to form **4a** (Table 2.7, entries 1, 3 and 5). Low yields and poor chemoselectivity in these cases may be related to an increased basicity of the fluoride anion in polar aprotic solvents such as MeCN or uncontrolled factors such as differing concentrations of water present within different solvents.[29]

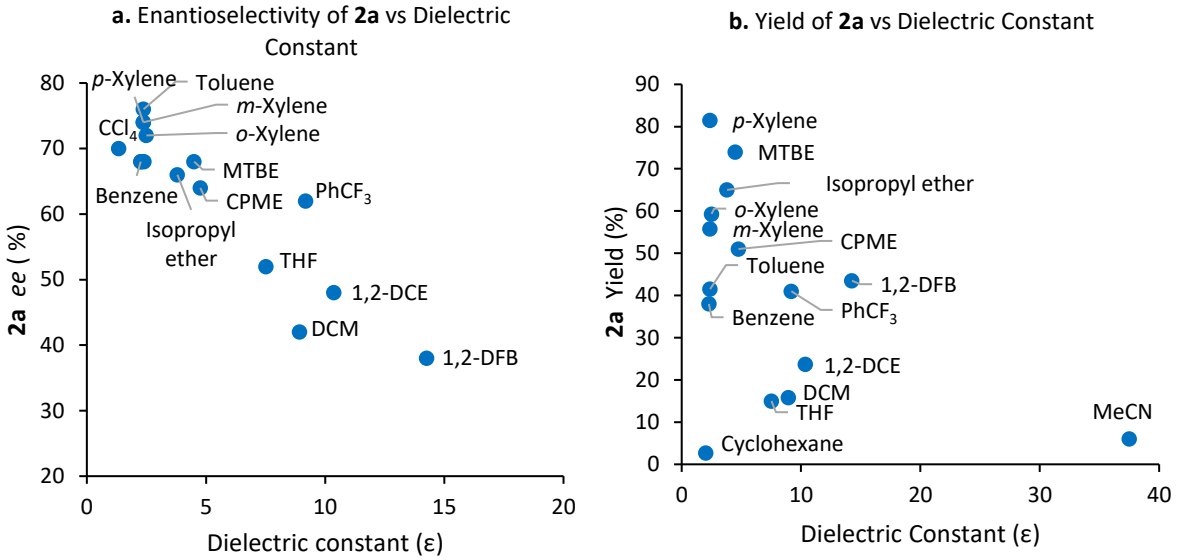

Figure 2.11: a. Graphical plot of product (**2a**) *ee* vs dielectric constant (ε) of solvent; b. Graphical plot of product (**2a**) yield vs dielectric constant of solvent (ε).

It is worth highlighting that this solvent effect follows a recognised trend in asymmetric ion-pairing catalysis where solvents of low polarity correlate with high enantioselectivity.[28, 30] This however stands juxtaposed to the previous data collected for fluorination reactions performed under HBPTC, where the preferred solvents included DCM or 1,2-DFB.[2,9,10] In this case, it was hypothesised that increased polarity of the solvent may have a beneficial effect on the solid-liquid phase transfer process.[31] This divergence for the fluorination of benzylic bromides under a synergistic phase transfer system could foreshadow distinct differences in mechanism between previous HBPTC systems with cationic electrophiles to that described here.

2.4.5. Temperature Effect

It is a well-known phenomenon that enantioselectivity generally increases with decrease in temperature, as enantiodiscrimination is determined by differences in the relative rates between the competing transition states leading to either enantiomeric product. Decreasing the temperature of a reaction can greatly affect the rate difference and therefore, the overall selectivity of a transformation.

Throughout the optimisation studies of the fluorination of benzylic bromides under S-HBPTC it was noted that the reaction suffered from poor reactivity at low temperatures. The fluorination of **1a** with catalyst (*S*)-**3k** and $Ph_4P^+ I^-$ in *p*-xylene, yielded 81 % of fluorinated product **2a**, in good chemoselectivity (10:1 **2a**:**4a**) and enantioselectivity of 87:13 e.r. at 40 °C, over 48 hours. However, reducing the reaction temperature to 25 °C for 48 hours, or to 15 °C for an extended 72 hours, drastically diminished the yields obtained for **2a**, to 25 % and 11 % respectively, albeit with promising increases in enantioselectivity (89:11 e.r. and 92:8 e.r. respectively) (Table 2.8, entries 1–3). Evaluation of different catalysts deduced that ureas which possessed larger *N*-alkylations allowed for higher reactivity to be obtained at reduced temperatures (Table 2.8). The final conditions for fluorination of **1a** under S-HBPTC employed *N*-heptyl derived catalyst (*S*)-**3u** with $Ph_4P^+ I^-$ in *p*-xylene, where at 15 °C for 72 hours yielded fluorinated product **2a** in 75 % yield and 92.5:7.5 e.r. At this lower temperature the chemoselectivity was also improved, with a ratio of fluorination (**2a**) to elimination (**4a**) of 15:1 (Table 2.8, entry 9).

The lower limit of temperature selected for this transformation was 15 °C considering the relatively high freezing point of *p*-xylene (mp = 13 °C). Performing the reaction in *p*-xylene and reducing the temperature below 15 °C resulted in solidifying of the reaction mixture. Changing solvent to other isomers of xylene which have lower freezing points (mp = -48 °C (*m*-xylene), -25 °C (*o*-xylene)), did not benefit the selectivity of the reaction and **2a** was obtained in very low yields (> 10 % over 72 hours). Furthermore, modifying the concentration at which reactions were performed did not improve reactivity; lower concentrations led to lower yields of fluorinated product over the same time-periods,

while increasing the concentration resulted in poorer stirring of the heterogeneous mixture and lower overall conversion.

Table 2.8: Screening of *N*-alkylated *bis*-urea catalysts at differing temperatures

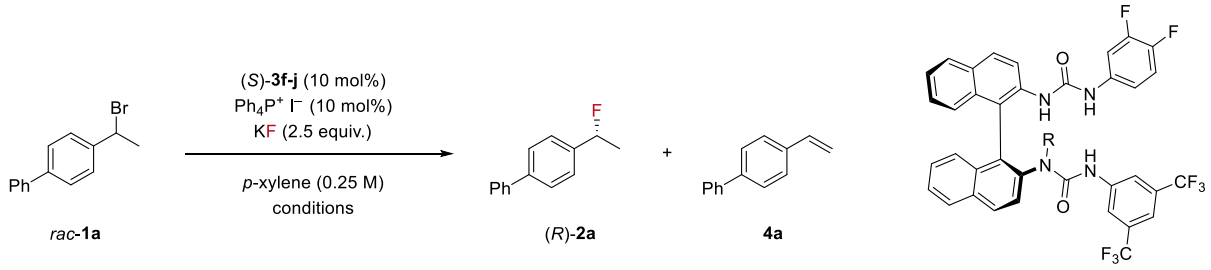

Entry	Urea catalyst	R	Temp/time	Yield **2a** (%)[a]	Ratio **2a**: **4a**	e.r.[b]
1	(*S*)-**3k**	*i*Pr	40 °C/ 48 h	81	10:1	87:13
2	(*S*)-**3k**	*i*Pr	25 °C/ 48 h	35	10:1	89:11
3	(*S*)-**3k**	*i*Pr	15 °C/ 72 h	11	6:1	92:8
4	(*S*)-**3t**	3-pent	40 °C/ 48 h	79	10:1	87:13
5	(*S*)-**3t**	3-pent	25 °C/ 72 h	57	11:1	90:10
6	(*S*)-**3t**	3-pent	15 °C/ 72 h	43	14:1	92:8
7	(*S*)-**3u**	4-hept	40 °C/ 48 h	83	10:1	87:13
8	(*S*)-**3u**	4-hept	25 °C/ 48 h	63	11:1	90:10
9	(*S*)-**3u**	4-hept	15 °C/ 72 h	75	15:1	92.5:7.5
10	(*S*)-**3v**	5-nona	40 °C/ 48 h	65	8:1	87:13
11	(*S*)-**3v**	5-nona	25 °C/ 48 h	57	11:1	90:10
12	(*S*)-**3v**	5-nona	15 °C/ 72 h	36	16:1	92:8
13	(*S*)-**3w**	cyclohex	40 °C/ 48 h	54	9:1	87:13
14	(*S*)-**3w**	cyclohex	25 °C/ 48 h	60	12:1	90:10
15	(*S*)-**3w**	cyclohex	15 °C/ 72 h	47	12:1	93:7
16	(*S*)-**3x**	indane	40 °C/ 48 h	28	6:1	88:12
17	(*S*)-**3x**	indane	25 °C/ 48 h	16	10:1	91:9
18	(*S*)-**3x**	indane	15 °C/ 72 h	12	12:1	91:9

General conditions: 0.05 mmol substrate, stirring at 1200 rpm. [a]Determined by ^{19}F NMR using 4-fluoroanisole as internal standard, [b]e.r. determined by HPLC analysis using a chiral stationary phase

2.4.6. Scope – Benzylic Fluorination

The scope of S-HBPTC was next evaluated with a range of benzylic bromide substrates under the optimised conditions: (*S*)-**3u** and $Ph_4P^+ I^-$ as catalysts in equal loadings (10 mol%) using KF (2.5 equiv.) in *p*-xylene.

Substrates based on the biphenyl motif, afforded products in good yields and enantioselectivities comparable to that of **1a**. Electron-rich benzylic fluorides such as methoxy substituted **2c** were isolated in slightly diminished yields but comparable selectivity (64 %, 92:8 e.r.) to electron-poor or neutral substrates. The reaction also tolerated functionality in the meta- position such as the 3-biphenyl motif **2g** which underwent fluorination 80 % yield and 90.5:9.5 e.r. The scope was further extended which highlighted that 1-naphthalene substituted benzylic bromides provided fluorinated product **2h** in excellent yields and enantioselectivities of up to 95 % and 95.5:4.5 e.r. Alkyl chain length was investigated which demonstrated increasing R_1 from methyl to *n*-propyl had a minimal effect on substitution versus elimination, with **2p** isolated in 59 % yield and 89:11 e.r. Common functional groups including halides (**2b**, **2d**, **2n**, **2o**), ethers (**2c**, **2w**), sulfonate esters (**2v**) and amides (**2f**) were tolerated in the reaction which could serve as handles for further functionalisation. The mild reactions conditions employing KF were highlighted by the tolerance of fluorophilic functionalities such as trimethylsilyl (**2u**) and boron pinacol esters (**2t**) which would be cleaved in the presence of more reactive and soluble fluorine sources such as HF (Scheme 2.22).

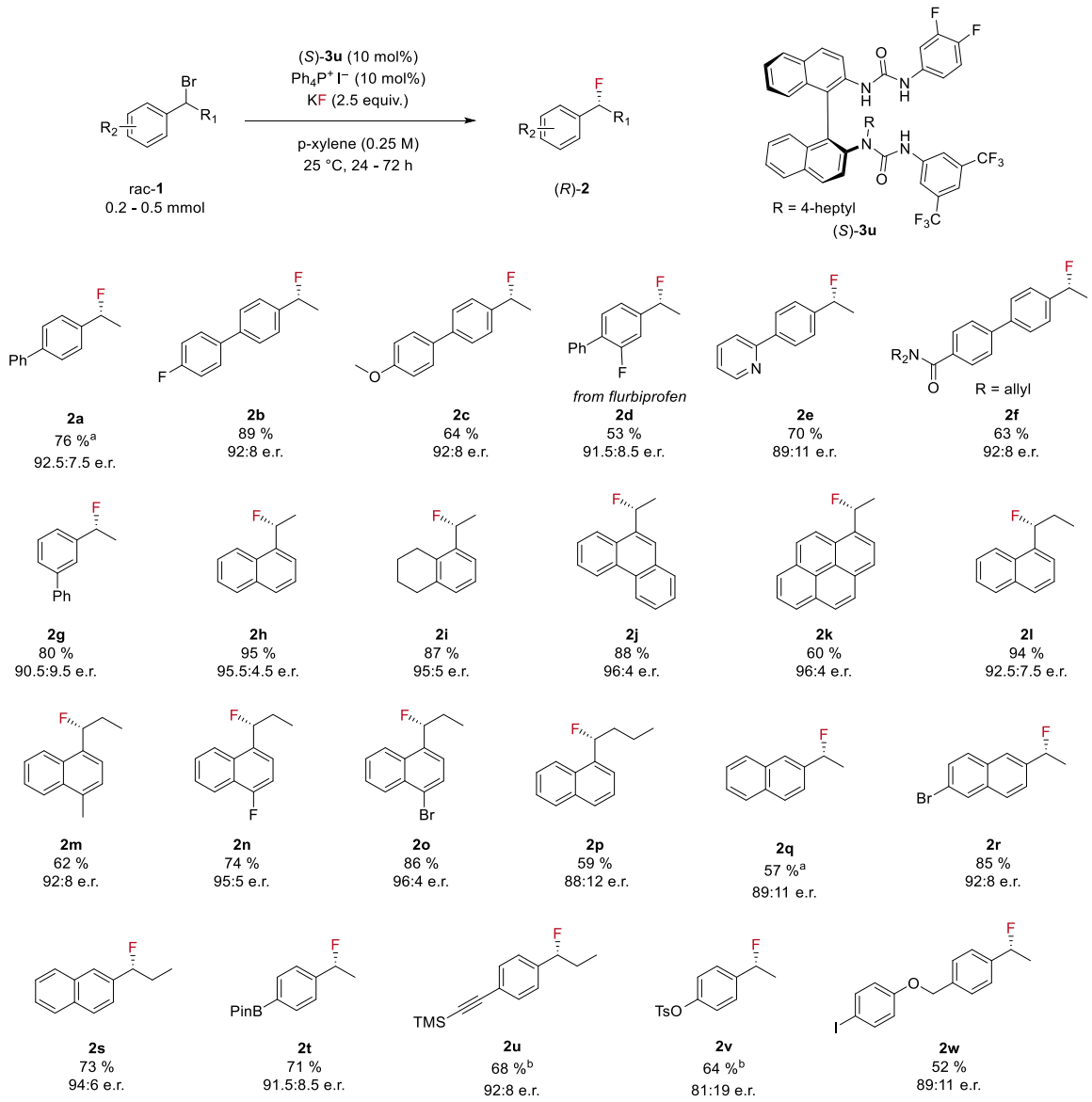

Scheme 2.22: Evaluation of scope for phenyl substrates **1a**-**w**. Isolated yields reported [a]performed at 15 °C, [b]performed at 40 °C

Pleasingly departure from phenyl-based structures allowed for the synthesis of a range of enantioenriched heterobenzylic motifs, including quinolines (**2x**, **2y**) which could be isolated in excellent yields and enantioselectivities (up to 99 %, 97:3 e.r), as well as indole (**2z**), indazole (**2aa**), benzofuran (**2ab**, **2ac**) and benzothiophene motifs (**2ad**). Finally, the applicability of the methodology was demonstrated to the fluorination of more complex bioactive scaffolds. Fluorinated analogues of quazoline[32] **2af** (65 %, 78:22 e.r.), fenofibrate **2ag** (54 % yield, 93:7 e.r.) and celestolide **2ah** (83 % yield, 93.5:6.5 e.r.) were prepared under the standard conditions (Scheme 2.23).

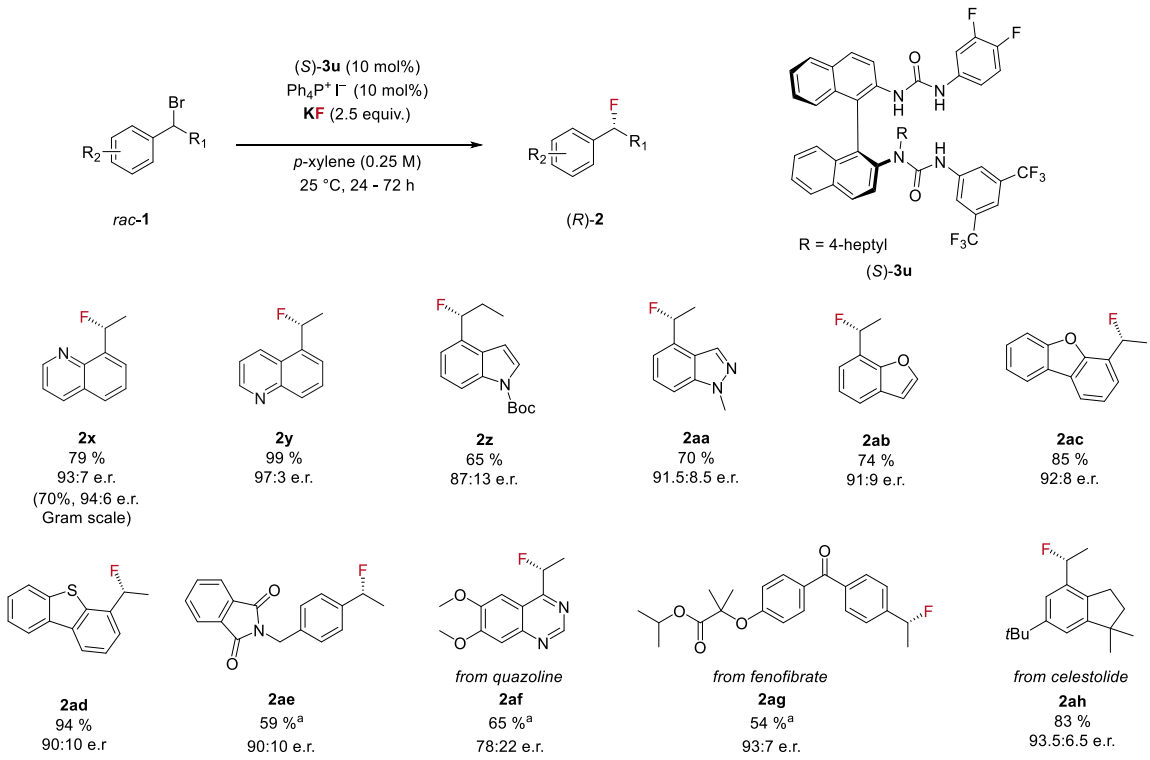

Scheme 2.23: Evaluation of heterocyclic substrates and biorelevant substrates **1x**-**1ah**. Isolated yields reported

[a]performed at 40 °C

During the development of the reaction scope, several scaffolds were found to be challenging or not amenable to fluorination under the standard conditions, providing insight into the limitations of the system as well as some preliminary mechanistic understanding. Low reactivity and poor conversion were observed for bromides which possessed large substituents ortho to the benzylic position, such as 2-biphenyl motif which was fluorinated in 6 % yield (**2ai**). Furthermore, bromides bearing steric bulky groups at the α-position such as phenyl (**1aj**) or *t*-butyl (**1ak**) were not competent substrates for this transformation. Finally, the subjection of a tertiary benzylic bromide (**1al**) to the reaction conditions resulted in no fluorination. These unsuccessful results may shed light on the mode of substitution with fluoride, where significant steric hinderance about the benzylic carbon and the inability to fluorinate a tertiary bromide may suggest the presence of an S_N2, rather than S_N1 pathway. However, it should be noted that for tertiary bromide **1al**, substantial conversion to a highly stable elimination by-product was observed, therefore a more thorough detailed mechanistic investigation is required to underpin the pathway of substitution (Scheme 2.24).

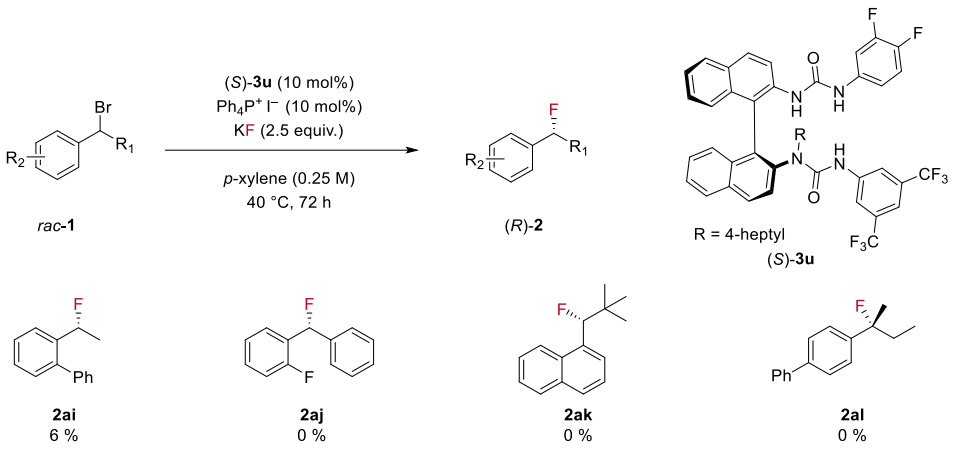

Scheme 2.24: Evaluation of challenging substrates **1ai**-**1al**. ^{19}F NMR yield reported employing 4-fluoroanisole as an internal standard.

2.5. Evaluation of Other Electrophiles under S-HBPTC

2.5.1. Introduction to Asymmetric α-Halogenation of Ketones

The successful implementation of S-HBPTC towards the fluorination of benzylic bromides prompted evaluation of other neutral electrophiles under our synergistic phase transfer system. Of particular interest was the synthesis of α-fluorocarbonyls under S-HBPTC considering the synthetic utility of the carbonyl unit which can be further functionalised to access a broad range of enantioenriched fluorinated products. Whilst the α-fluorination of aldehydic carbonyls with electrophilic fluorinating reagents under organocatalytic enamine strategies is widely reported, the translation of this chemistry to ketones has been more challenging.

As described in *1.4.2.2. Organocatalytic Asymmetric Electrophilic Fluorination*, MacMillan and co-workers were the first to report a highly enantioselective fluorination of cyclic ketones with NFSI, achieved through high-throughput evaluation of amine catalysts. This high throughput platform screened a library of 250 organocatalysts for the fluorination of a cyclohexanone model substrate, achieving high enantio-, diastero- and regioselectivity employing a cinchona-alkaloid based amine catalyst **1.25**. Whilst this work demonstrates the success of intensive catalyst screening, the limitation of this methodology to cyclohexanone derivatives was evident, and changing substrate structure to

cycloheptanones demonstrated lower reactivity (45 % yield) and cyclopentanones suffered with lower enantioselectivity (88 % *ee*) (Scheme 2.28).[33]

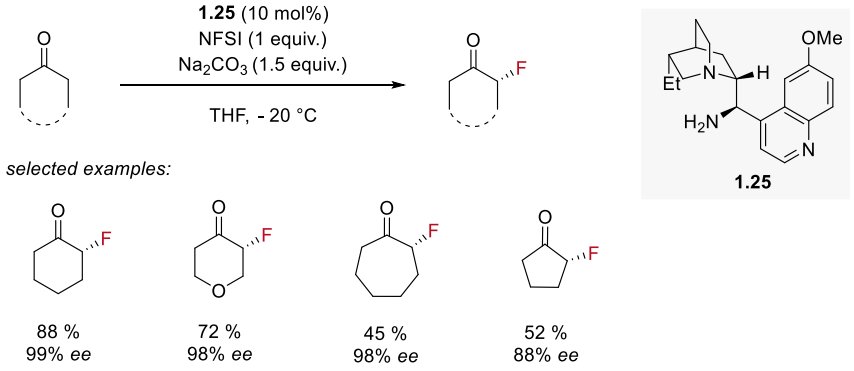

Scheme 2.28: Macmillan's fluorination of cyclic ketones under secondary amine catalysis with NFSI

In the context of halogenation, Sun and co-workers recently reported an organocatalytic chlorination of α-keto sulfonium salts under a liquid-liquid phase transfer mechanism with NaCl (sat aq.) and chiral thiourea HBD catalyst (**TU**). The charged sulfonium leaving group played a crucial role both in aiding reactivity through ion-pairing with a chloride bound thiourea species, and in increasing the acidity of the α-proton permitting a dynamic kinetic resolution (DKR) process *via* facile racemisation of the substrate (Scheme 2.29).[34]

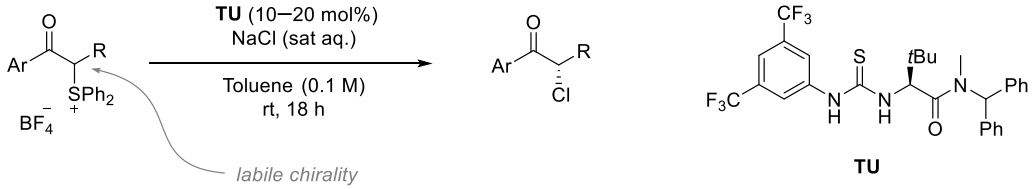

Scheme 2.29: Chlorination of α-keto sulfonium salts by Sun and co-workers

Inspired by the work of Sun and co-workers, preliminary studies were performed to evaluate α-keto sulfonium salts as potential substrates for fluorination. It was validated that sulfonium **18a** underwent chlorination under liquid-liquid phase transfer with saturated NaCl (aq) and thiourea catalyst **TU** in 57 % yield and good enantioselectivity (88:12 e.r.) as reported by Sun and co-workers (Table 2.9, entry 1).[34] Furthermore, chlorination of **18a** also proceeded under a solid-liquid phase transfer system employing NaCl (s) albeit in a diminished enantioselectivity of 67:33 e.r. (Table 2.9, entry 2). In contrast,

when KF or CsF (s) were employed, only trace yield of α-fluoroketone **13a** was observed under either a solid-liquid or liquid-liquid phase transfer system with either the thiourea catalyst **TU** reported by Sun and co-workers (Table 2.9, entries 3–5). Furthermore, no fluorination occurred when BINAM derived *bis*-urea catalyst **3d**, optimised for fluorination under HBPTC, was employed (Table 2.9, entries 6–8), with only significant decomposition of the sulfonium salt observed by ^{1}H NMR.

Table 2.9: Evaluation of α-keto sulfonium salts as a substrate for fluorination

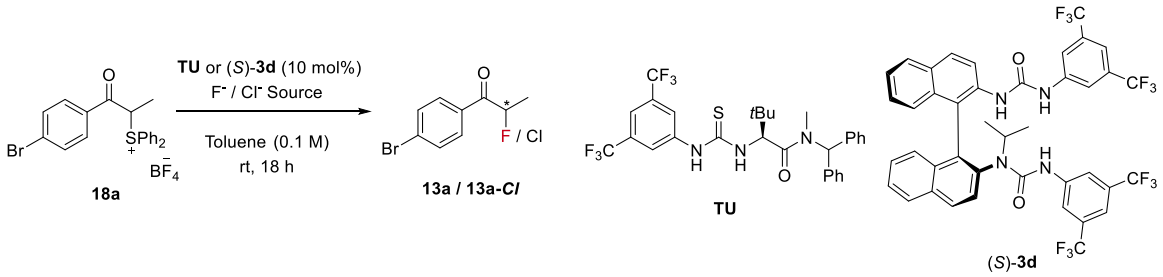

Entry	Catalyst	Fluoride / Chloride source	Yield **13**[a]	e.r.[b]	**Reference**
1	**TU**	NaCl (sat aq)	57	88:12	Sun and co-workers[34]
2	**TU**	NaCl (s)	61	67:33	This work
3	**TU**	KF (s)	0	-	This work
4	**TU**	CsF (s)	1	nd	This work
5	**TU**	KF (sat aq)	0	-	This work
6	(*S*)-**3a**	KF (s)	0	-	This work
7	(*S*)-**3a**	CsF (s)	0	-	This work
8	(*S*)-**3a**	KF (sat aq)	0	-	This work

General conditions: Substrate (0.05 mmol), HBD catalyst (10 mol%), KF, CsF or NaCl (2.5 equiv.) or KF or NaCl (sat aq) (0.5 mL) in toluene (0.1 M). [a]Determined by quantitative ^{19}F using 4-fluoroanisole as internal standard, [b]e.r. determined by HPLC analysis using a chiral stationary phase. nd = not determined.

2.5.2. Optimisation for the Fluorination of α-Bromoketones under S-HBPTC

Unsuccessful fluorination of α-keto sulfonium salt **18a** (Table 2.9) prompted investigations into whether S-HBPTC, developed for the fluorination of benzylic bromides with KF, was also amenable to the direct fluorination of α-bromoketones. Preliminary screening with bromide **12a** under the previously optimised conditions with catalysts (*S*)-**3u** and Ph_4P^+ I^-, and KF in *p*-xylene afforded α-fluoroketone product **13a** in 46 % yield and 70:30 e.r. at 60 °C for 24 hours (Scheme 2.30). It is notable

that this reaction exclusively formed the fluorinated product and no elimination side-product was observable by ^{1}H NMR.

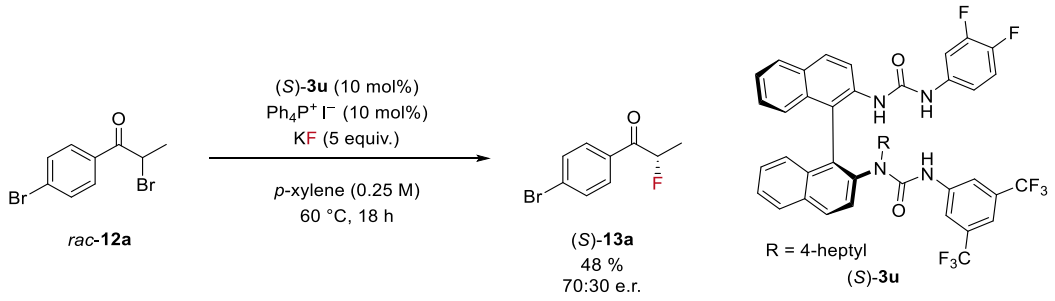

Scheme 2.30: Preliminary investigation of S-HBPTC conditions on **12a**

The fluorination of **12a** also proceeded with urea catalyst (*S*)-**3d** and at room temperature in toluene afforded fluoride **13a** in 21 % yield and 63:37 e.r. (Table 2.10, entry 1). Control experiments demonstrated that analogously to the benzylic bromide substrate class, the removal of either the urea catalyst **3d** or onium salt, Ph_4P^+ I^-, in toluene was detrimental to fluorination of **12a** with KF as the fluorinating reagent (Table 2.10, entry 2 and 3).

Table 2.10: Control experiments for α-bromoketone substrates under S-HBPTC

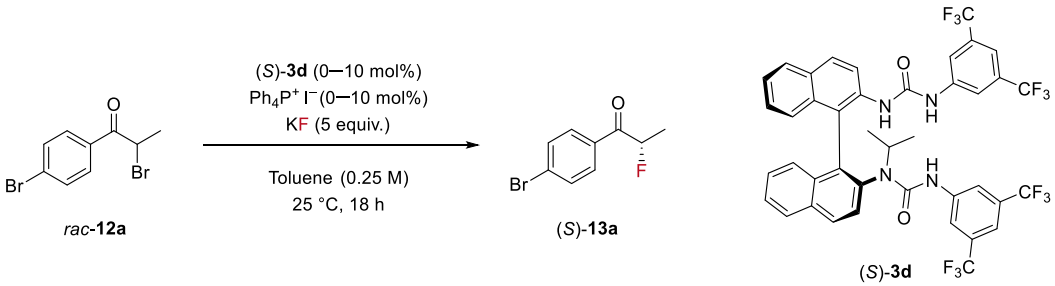

Entry	(*S*)-**3d** (mol%)	Ph_4P^+ I^- (mol%)	Yield **13a** (%)[a]	R.S.M **12a** (%)	**13a e.r.**[b]
1	10	10	21	70	63:37
2	10	0	0	100	-
3	0	10	0	100	-

General conditions: 0.05 mmol substrate, stirring at 1200 rpm. [a]Determined by ^{19}F NMR using 4-fluoroanisole as internal standard, [b]e.r. determined by HPLC analysis using a chiral stationary phase.

A screening of solvents was performed for this transformation as the substrates were visibly insoluble in apolar aromatic solvents, such as toluene or *p*-xylene, which were previously favourable for benzylic substrates. The fluorination of α-bromoketone **12a** performed best in polar aprotic solvent acetonitrile (ε = 37.5), giving an improved yield and enantioselectivity of fluorinated product **13a** (28 %, 71:29 e.r.) (Table 2.11, entry 6). It is noteworthy that, unlike the benzylic halide, no competitive elimination pathway was observed for **12a** even when reactions were performed at elevated temperatures (60 °C), which provided near to full conversion to fluorinated product (Table 2.11, entry 7). In contrast, acetonitrile promoted the competitive elimination pathway of the benzylic substrate **1a**, resulting in very poor yields of fluoride product and poor chemoselectivity (1:8 fluorination **2a**: elimination **4a**) (*v.* Table 2.7, entry 1). Furthermore, the observed enantioselectivity of the fluorinated product **13a**, was not influenced by the dielectric constant of the reaction solvent, as was observed for the benzylic scaffold. Data in Table 2.11 and Figure 2.12 indicate that solvents of differing polarity, e.g. toluene (ε = 2.38) and acetone (ε = 20.7), achieved product **13a** at the same enantioselectivity (63:37 e.r.).

Table 2.11: Solvent effect for the fluorination of **12a**

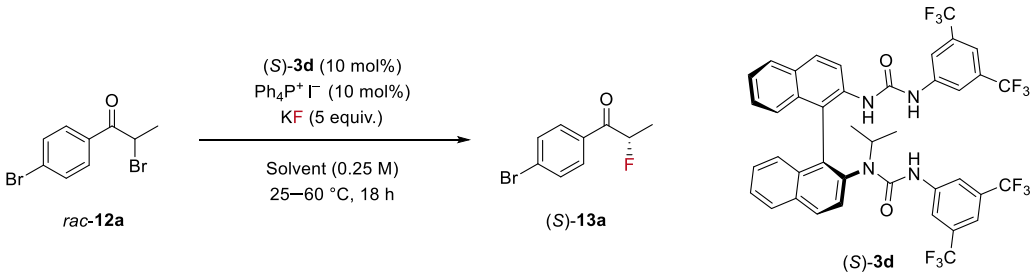

Entry	Solvent	Dielectric Constant (ε)	Temperature	Yield **13a** (%)[a]	R.S.M **12a** (%)	**e.r.**[b]
1	Toluene	2.38	25 °C	21	70	63:37
2	EtOAc	6.02	25 °C	18	73	60:40
3	THF	7.58	25 °C	16	74	56:44
4	DCM	8.93	25 °C	17	73	60:40
5	Acetone	20.7	25 °C	24	66	63:37
6	MeCN	37.5	25 °C	28	62	71:29
7	MeCN	37.5	60 °C	94	2	67:33

General conditions: 0.05 mmol substrate, stirring at 1200 rpm. [a]Determined by ^{19}F NMR using 4-fluoroanisole as internal standard, [b]e.r. determined by HPLC analysis using a chiral stationary phase

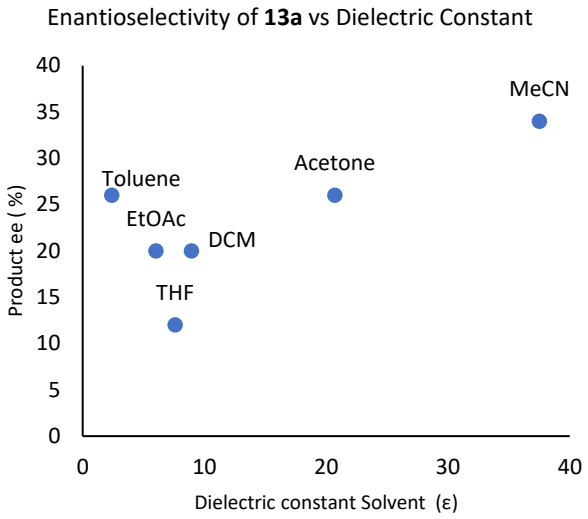

Figure 2.12: Graphical plot of product (**13a**) *ee* and dielectric constant (ε) of solvent

Screening of urea HBD catalysts demonstrated that increasing the steric bulk of urea motifs improved enantioselectivity. The presence of a larger aromatic substituent on the unalkylated urea (*S*)-**3r** improved reactivity achieving a 55 % yield of **13a** at the same level enantioselectivity as catalyst (*S*)-**3d** (70:30 e.r.). The contrasting modification whereby the alkylated urea possessed a bulkier aromatic substituent (*S*)-**3y** significantly improved the enantioselectivity of **13a** to 87:13 e.r., albeit at reduced yield of 19 %. When *N*-ethylated urea (*S*)-**3z**, which has bulky aromatic substitution on both urea motifs, was employed α-fluoroketone product **13a** was obtained in a moderate yield of 44 % with the highest enantioselectivity of 92:8 e.r. (Scheme 2.31).

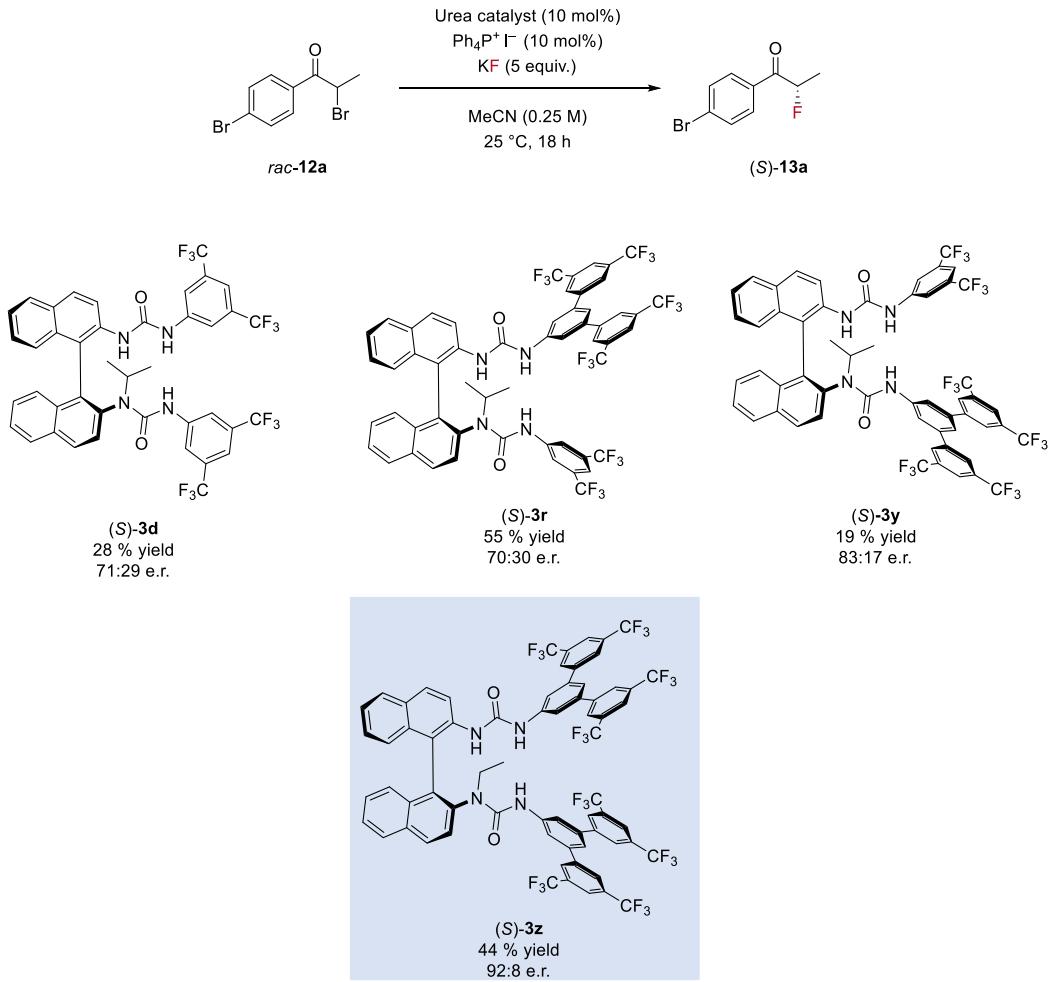

Scheme 2.31: Screening of *bis*-urea catalysts for the fluorination of **12a**

Finally, investigation into the optimal onium salt for the fluorination of **12a** demonstrated that ammonium co-catalysts, such as $Bu_4N^+ I^-$, were also seen to be efficient for the reaction to proceed giving similar results in terms of reactivity and enantioselectivity to using $Ph_4P^+ I^-$ (Table 2.12, entries 1 and 2). Tetraethylammonium iodide ($Et_4N^+ I^-$) was shown to be the optimal co-catalyst, providing **13a** in a yield of 60 % and 92:8 e.r. when reactions were performed in MeCN over 18 hours at room temperature (Table 2.12, entry 4). Minor modifications of the reaction conditions including increasing the concentration to 0.5 M and reducing the temperature to 5 °C for 96 hours allowed for **13a** to be isolated in 65 % yield with improved enantioselectivity of 95:5 e.r. (Table 2.12, entry 6).

Table 2.12: Optimisation of onium co-catalysts for fluorination of **12a**

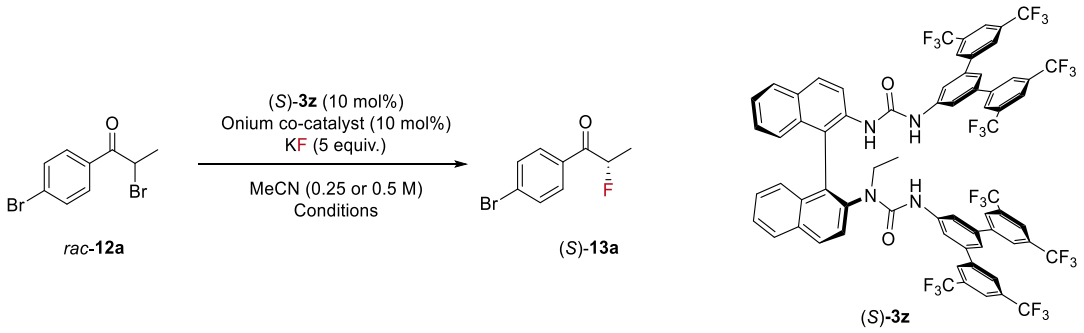

Entry	Onium co-catalyst	Concentration (M)	Conditions	Yield **13a** (%)[a]	R.S.M **12a** (%)	**e.r.**[b]
1	$Ph_4P^+ I^-$	0.25	25 °C, 18 h	44	47	92:8
2	$Bu_4N^+ I^-$	0.25	25 °C, 18 h	39	51	91:9
3	$Bu_4N^+ Br^-$	0.25	25 °C, 18 h	41	59	92:8
4	$Et_4N^+ I^-$	0.25	25 °C, 18 h	60	31	92:8
5	$Et_4N^+ I^-$	0.25	5 °C, 96 h	43	55	95:5
6	$Et_4N^+ I^-$	0.5	5 °C, 96 h	73 (65)	26	95:5

General conditions: 0.05 mmol substrate, stirring at 1200 rpm. [a]Determined by ^{19}F NMR using 4-fluoroanisole as internal standard (isolated yield), [b]e.r. determined by HPLC analysis using a chiral stationary phase.

2.5.3. Scope – Fluorination of α-Bromoketones

With optimised conditions for the fluorination of α-bromoketone **12a** under S-HBPTC in hand, the scope of the reaction was evaluated. A scope of 13 α-fluoroketones were accessed with reactivity and enantioselectivity maintained across a range of electron-withdrawing and donating functionalities (**13a**–**i**). Scaffolds based on 1-naphthalene scaffold (**13j**–**k**) were fluorinated in the highest yields and enantioselectivities of up to 97 % yield and 98:2 e.r., corroborating the results obtained on the benzylic motif. Investigations into the alkyl chain length (R_1), demonstrated that reactivity was lower than that of the model substrate, however, increasing the reaction temperature to 40 °C for these compounds allow them to be isolated in good yields and enantioselectivity (**13l** and **13m**) (Scheme 2.32).

The limitations for the fluorination of α-bromoketones under S-HBPTC were also explored demonstrating that reactivity suffered upon increasing the alkyl chain length beyond 4-carbons, with

fluoride **13n** formed in good selectivity 84:16 e.r. however at diminished yields of 11 % over 96 hours. Furthermore, fluorination did not occur at tertiary carbon centres (**13o**), or alpha to amides or ester functionalities under the standard conditions (**13p** and **13q**) (Scheme 2.32).

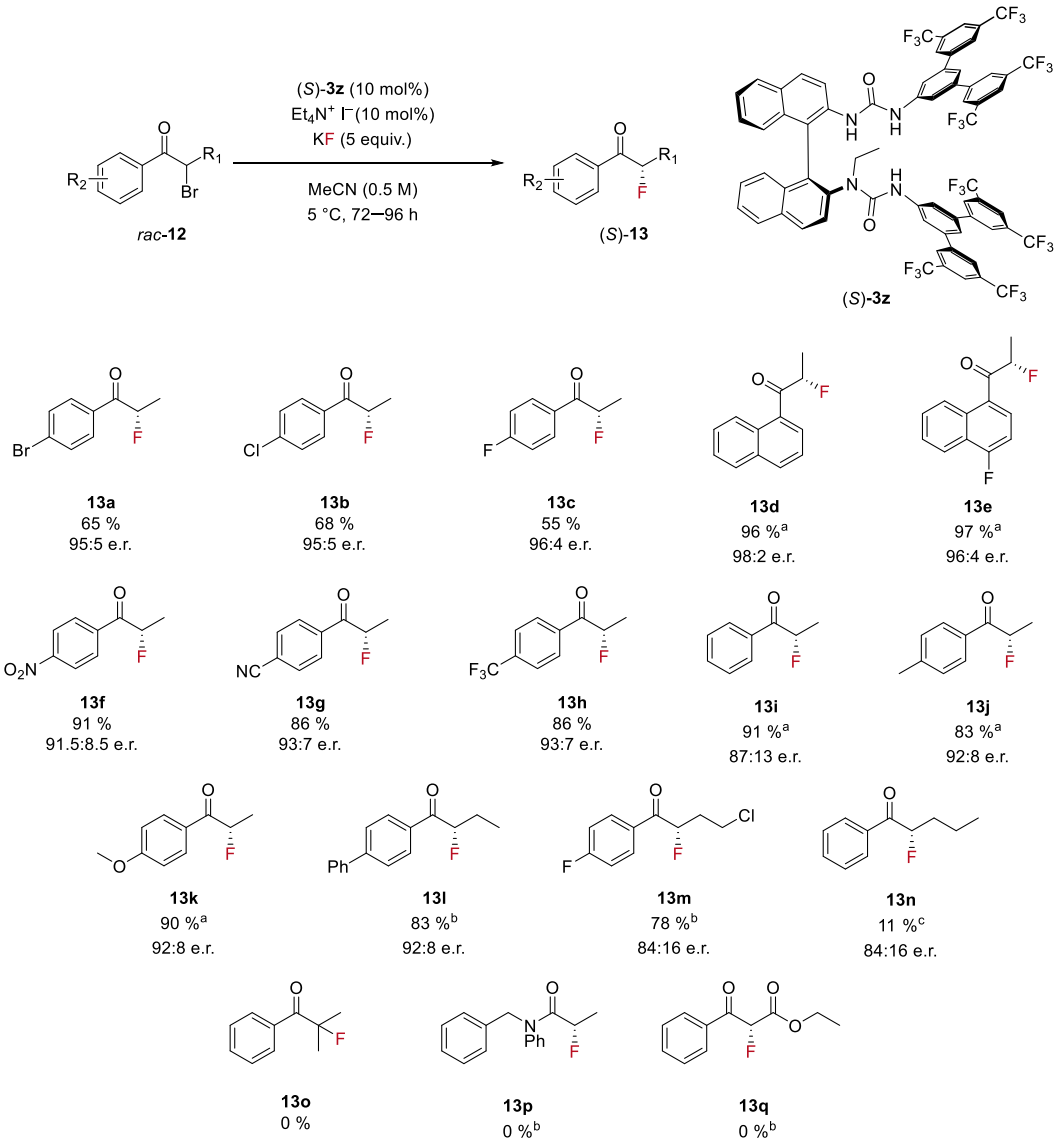

Scheme 2.32: Scope of α-fluoroketones. [a]performed at 25 °C, [b]performed at 40 °C, ^{19}F NMR yield reported employing 4-fluoroanisole as an internal standard

2.6. Conclusions

Herein, is described the reaction discovery and optimisation of Synergistic HBPTC (S-HBPTC), a conceptually novel catalytic manifold featuring both a urea HBD catalyst and an onium salt co-catalyst to facilitate the fluorination of neutral, unsymmetrical electrophiles with KF.

The preliminary findings described within this chapter demonstrate that the fluorination of neutral electrophiles with KF was made possible only through the addition of a second PT catalyst, an onium salt, in combination with the chiral urea HBD catalyst. This understanding was gained fortuitously through the generation of a catalytic quantity of a phosphonium halide *in situ* from the substrate and a phosphine additive. However, key control experiments underpinned the true role of the formed onium species as a co-phase transfer agent, investigated *via* spectroscopic NMR studies.

Optimisation of the reaction conditions including modifying the structure and electronic properties of urea catalyst as well as screening onium co-catalysts, solvent and temperature allowed for the fluorination of a scope of benzylic bromides in high yields and enantioselectivity (up to 99 % yield, 97:3 e.r.). Furthermore, the extension of S-HBPTC towards the synthesis of enantioenriched α-fluorocarbonyls demonstrated the applicability of this new organocatalytic manifold beyond benzylic fluorination. Pleasingly minor modifications in reaction conditions allowed a second class of compounds to be isolated in excellent yields and enantioselectivities (up to 98 % yield, 98:2 e.r.).

2.7. References

(1) Dooley, C.; Ibba, F.; Botlik, B.; Palladino, C.; Goult, C.; Gao, Y.; Lister, A.; Paton, R.; Lloyd-Jones, G.; Gouverneur, V. Enantioconvergent Nucleophilic Substitution via Synergistic Phase-Transfer Catalysis. *Nature Catal.* **2025**, *8* (2), 107–115.

(2) Pupo, G.; Ibba, F.; Ascough, D. M. H.; Vicini, A. C.; Ricci, P.; Christensen, K. E.; Pfeifer, L.; Morphy, J. R.; Brown, J. M.; Paton, R. S.; Gouverneur, V. Asymmetric Nucleophilic Fluorination Under Hydrogen Bonding Phase-Transfer Catalysis. *Science* **2018**, *360* (6389), 638–642.

(3) Ford, D.; Lehnherr, D.; Kennedy, C.; Jacobsen, E. Anion-Abstraction Catalysis: The Cooperative Mechanism of α-Chloroether Activation by Dual Hydrogen-Bond Donors. *ACS Catal.* **2016**, *6* (7), 4616–4620.

(4) Mancheño, O. G. *Anion Binding Catalysis*; Wiley-VCH GmbH, 2022.

(5) O'Hagan, D.; Schaffrath, C.; Cobb, S.; Hamilton, J.; Murphy, C. Biosynthesis of an Organofluorine Molecule. *Nature* **2002**, *416*, 279.

(6) O'Hagan, D.; Deng, H. Enzymatic Fluorination and Biotechnological Developments of the Fluorinase. *Chem. Rev.* **2015**, *115* (2), 634–649.

(7) Haynes, W. M.; Lide, D. R.; Bruno, T. J. *CRC Handbook of Chemistry and* Physics, 97th Edition; Taylor & Francis Inc., 2017.

(8) Xiang, S.; Tan, B. Advances in Asymmetric Organocatalysis Over the Last 10 Years. *Nature Commun.* **2020**, *11* (1), 3786.

(9) Pupo, G.; Vicini, A. C.; Ascough, D. M. H.; Ibba, F.; Christensen, K. E.; Thompson, A. L.; Brown, J. M.; Paton, R. S.; Gouverneur, V. Hydrogen Bonding Phase-Transfer Catalysis with Potassium Fluoride: Enantioselective Synthesis of β-Fluoroamines. *J. Am. Chem. Soc.* **2019**, *141* (7), 2878–2883.

(10) Roagna, G.; Ascough, D. M. H.; Ibba, F.; Vicini, A. C.; Fontana, A.; Christensen, K. E.; Peschiulli, A.; Oehlrich, D.; Misale, A.; Trabanco, A. A.; Paton, R. S.; Pupo, G.; Gouverneur, V. Hydrogen Bonding Phase-Transfer Catalysis with Ionic Reactants: Enantioselective Synthesis of γ-Fluoroamines. *J. Am. Chem. Soc.* **2020**, *142* (33), 14045–14051.

(11) Smilovic, I.; Cluzeau, J.; Richter, F.; Nerdinger, S.; Schreiner, E.; Laus, G.; Schottenberger, H. Synthesis of Enantiopure Antiobesity Drug Lorcaserin. *Bioorg Med Chem.* **2018**, *26*, 2686–2690.

(12) Zhu, Q.; Wang, J.; Bian, X.; Zhang, L.; Wei, P.; Xu, Y. Novel Synthesis of Antiobesity Drug Lorcaserin Hydrochloride. *OPR&D* **2015**, *19* (9), 1263–1267.

(13) Wang, J.; Horwitz, M.; Dürr, A.; Ibba, F.; Pupo, G.; Gao, Y.; Ricci, P.; Christensen, K.; Pathak, T.; Claridge, T.; Lloyd-Jones, G. C.; Paton, R. S.; Gouverneur, V. Asymmetric Azidation under Hydrogen Bonding Phase-Transfer Catalysis: A Combined Experimental and Computational Study. *J. Am. Chem. Soc.* **2022**, *144* (10), 4572–4584.

(14) Horwitz, M. A.; Durr, A. B.; Afratis, K.; Chen, Z. J.; Soika, J.; Christensen, K. E.; Fushimi, M.; Paton, R. S.; Gouverneur, V. Regiodivergent Nucleophilic Fluorination under Hydrogen Bonding Catalysis: A Computational and Experimental Study. *J. Am. Chem. Soc.* **2023**, *145* (17), 9708–9717.

(15) Vidal, R.; Alberola-Borràs, J.; Mora-Seró, I. Abiotic Depletion and the Potential Risk to the Supply of Cesium. Resour. Policy **2020**, *68*.

(16) Singh, V. K.; Zhu, C.; Kanta De, C.; Leutzch, M.; Baldinelli, L.; Mitra, R.; Bistoni, G.; List, B. Taming Secondary Benzylic Cations in Catalytic Asymmetric SN1 Reactions. *Science* **2023**, *382* (6668), 325–329.

(17) Zhang, Q.; Stockdale, D. P.; Mixdorf, J. C.; Topczewski, J. J.; Nguyen, H. M. Iridium-Catalyzed Enantioselective Fluorination of Racemic, Secondary Allylic Trichloroacetimidates. *J. Am. Chem. Soc.* **2015**, *137* (37), 11912–11915

(18) Katcher, M. H.; Sha, A.; Doyle, A. G. Palladium-Catalyzed Regio- and Enantioselective Fluorination of Acyclic Allylic Halides. *J. Am. Chem. Soc.* **2011**, *133* (40), 15902–15905.

(19) Jover, J.; Cirera, J. Computational Assessment on the Tolman Cone Angles for P-Ligands. *Dalton Trans.* **2019**, *48* (40), 15036–15048.

(20) Chalikidi, P. N.; Magkoev, T. T.; Gutnov, A. V.; Demidov, O. P.; Uchuskin, M. G.; Trushkov, I. V.; Abaev, V. T. One-Step Synthesis of Triphenylphosphonium Salts from (Het)arylmethyl Alcohols. *J. Org. Chem.* **2021**, *86* (14), 9838–9846.

(21) Aggarwal, V.; Harvey, J.; Robiette, R. On the Importance of Leaving Group Ability in Reactions of Ammonium, Oxonium, Phosphonium, and Sulfonium Ylides. *Angew. Chem. Int. Ed.* **2005**, *44* (34), 5468–5471.
(22) Starks, C. M. Phase-Transfer Catalysis 1. Heterogeneous Reactions Involving Anion Transfer by Quaternary Ammonium and Phosphonium Salts. *J. Am. Chem. Soc.* **1971**, *93* (1), 195–199.
(23) Ibba, F.; Pupo, G.; Thompson, A. L.; Brown, J. M.; Claridge, T. D. W.; Gouverneur, V. Impact of Multiple Hydrogen Bonds with Fluoride on Catalysis: Insight from NMR Spectroscopy. *J. Am. Chem. Soc.* **2020**, *142* (46), 19731–19744.
(24) Ibba, F. Hydrogen Bonding Phase-Transfer Catalysis: A New Approach to Asymmetric Fluorination. DPhil Thesis, University of Oxford, 2020.
(25) Vicini, A., C. Hydrogen Bonding Phase-Transfer Catalysis with Alkali Metal Fluorides: Enantioselective Synthesis of β-Fluoroamines from Reaction Development to Scale-up. DPhil Thesis, University of Oxford, 2020.
(26) Yang, Y.; Tokunaga, E.; Akiyama, H.; Saito, N.; Shibata, N. Bis(pentafluorosulfanyl)phenyl Azide as an Expeditious Tool for Click Chemistry Toward Antitumor Pharmaceuticals. *ChemMedChem.* **2014**, *9* (5), 913–917.
(27) Anslyn , E. V.; Dougherty , D. A. Modern Physical Organic Chemistry; Murdzek, J., Ed.; *University Science Books*, 2006.
(28) Brak, K.; Jacobsen, E. N. Asymmetric Ion-Pairing Catalysis. *Angew. Chem. Int. Ed.* **2013**, *52* (2), 534–561.
(29) Kim, D.; Jeong, H.; Lim, S.; Sohn, M. Tetrabutylammonium Tetra(tert-Butyl Alcohol)-Coordinated Fluoride as a Facile Fluoride Source. *Angew. Chem. Int. Ed.* **2008**, *47* (44), 8404–8406.
(30) Ovian, J.; Vojácková, P.; Jacobsen, E. Enantioselective Transition-Metal Catalysis via an Anion-Binding Approach. *Nature* **2023**, *616* (7955), 84–89.
(31) Starks, C. M.; Liotta, C. L.; Halpern, M. E. *Phase-transfer catalysis: Fundamentals, Applications and Industrial Perspectives*; Springer Dordrecht, 1994.
(32) Meanwell, M.; Adluri, B. S.; Yuan, Z. L.; Newton, J.; Prevost, P.; Nodwell, M. B.; Friesen, C. M.; Schaffer, P.; Martin, R. E.; Britton, R. Direct Heterobenzylic Fluorination, Difluorination and Trifluoromethylthiolation with Dibenzenesulfonamide Derivatives. *Chem. Sci.* **2018**, *9* (25), 5608–5613.
(33) Kwiatkowski, P.; Beeson, T.; Conrad, J.; MacMillan, D. Enantioselective Organocatalytic α-Fluorination of Cyclic Ketones. *J. Am. Chem. Soc.* **2011**, *133* (6), 1738–1741.
(34) Li, Z. Y.; Wang, B. C.; Zhang, C. S.; Lo, W. Y.; Yang, L. L.; Sun, J. W. Catalytic Enantioselective Nucleophilic α-Chlorination of Ketones with NaCl. *J. Am. Chem. Soc.* **2024**, *146* (4), 2779–2788.

3. Mechanistic Investigations into Fluorination Under Synergistic HBPTC

3.1. Introduction

Chapter 2 describes the discovery and development of Synergistic Hydrogen Bonding Phase Transfer Catalysis (S-HBPTC), a novel methodology for the fluorination of neutral and unsymmetrical electrophiles. Building on seminal work in nucleophilic fluorination under HBPTC which focused on charged, meso-electrophiles (Figure 3.1a), this work demonstrated that in the absence of a substrate which can ionise to form a cationic electrophile, a cationic co-catalyst (onium halide) is required to fulfil the ion-pairing requirements for the solubilisation of KF, permitting reactivity with a wider scope of electrophiles, including benzylic bromides or α-bromoketones (Figure 3.1b).

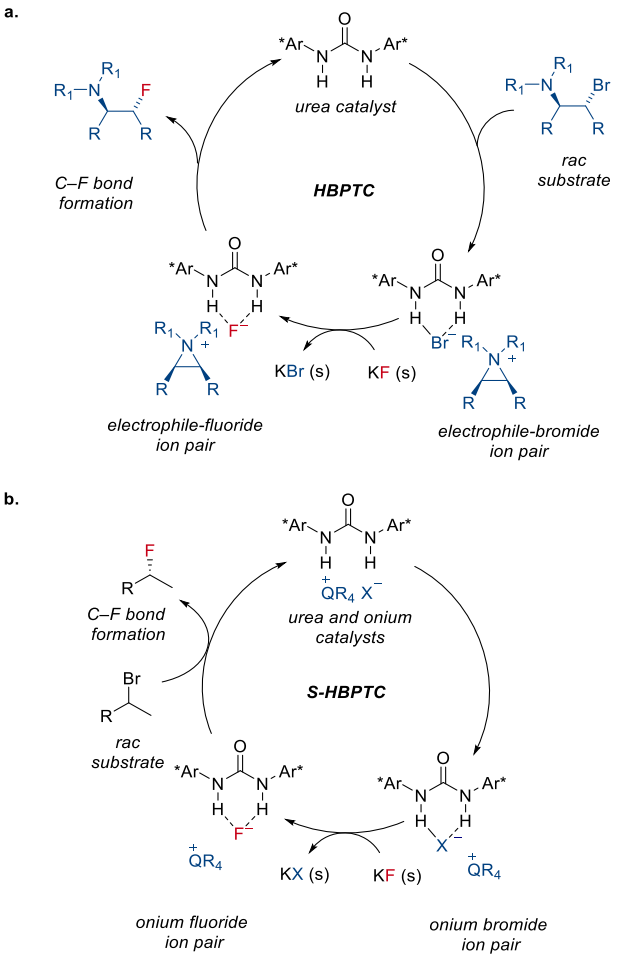

Figure 3.1: Proposed catalytic cycles of a. Hydrogen Bonding Phase Transfer Catalysis (HBPTC); b. Synergistic Hydrogen Bonding Phase Transfer Catalysis (S-HBPTC)

The development of this novel catalytic manifold prompted a thorough mechanistic investigation particularly considering the following questions:

1. Building on preliminary experiments described in Chapter 2, can the putative ternary urea HBD-phosphonium-fluoride complexes be independently prepared, characterised and validated as reactive fluorinating reagents within the reaction system?
2. What is the basis for rate acceleration observed when onium iodide salts were used as co-catalysts instead of onium bromides?
3. What is the mechanism for nucleophilic substitution? In particular the mechanistic complexity around the benzylic centre raises questions on whether an S_N1 or S_N2 pathway is occurring.
4. What is the mode of racemisation or ionisation of the substrate, and what is the mechanism which allows for enantioconvergence of racemic halide starting materials into enantioenriched fluoride products?

3.2. NMR Study of Complexes Between Urea HBD Catalysts and Onium Salts with KF

Preliminary investigations demonstrated that onium halide salts and urea HBD catalysts act synergistically permitting the solubilisation of KF through the formation of stabilised ion-pairs (*v. 2.3.1. Role of Phosphonium Salt*). Whilst there is considerable evidence for solubilisation of CsF forming urea-CsF complexes *via* NMR and X-ray crystallography, this was not observed for KF, suggesting the inability of urea catalysts to solubilise KF solely through hydrogen-bonding.[1] Initial insights gained through NMR spectroscopy were described in Chapter 2, however a more detailed spectroscopic investigation was desired to increase the understanding of the ion-pairing interactions between urea-onium-fluoride species and establish their ability to perform as reactive fluorinating reagents.

3.2.1. Characterisation of Unbound Urea Catalyst

Spectroscopic investigations were performed on the optimised catalyst for the fluorination of benzylic bromides (*S*)-**3u.** A detailed assignment of this novel catalyst was required prior to undertaking further NMR analysis.

The ^{1}H and ^{13}C spectra of **3u** present conformational information which is in line with previous observations made for *bis*-urea catalysts.[1] Such observations include: the characteristic deshielding and line-broadening of signals of protons H3' and H17, at the ortho position of BINAM naphthyl and the aryl ring of the alkylated urea (Figure 3.2). This is a result of the orientation of the adjacent carbonyl C9, which can affect the chemical shift by anisotropic electron currents. Line-broadening of carbonyl C9 present is also evident in ^{13}C spectra (Figure 3.3).

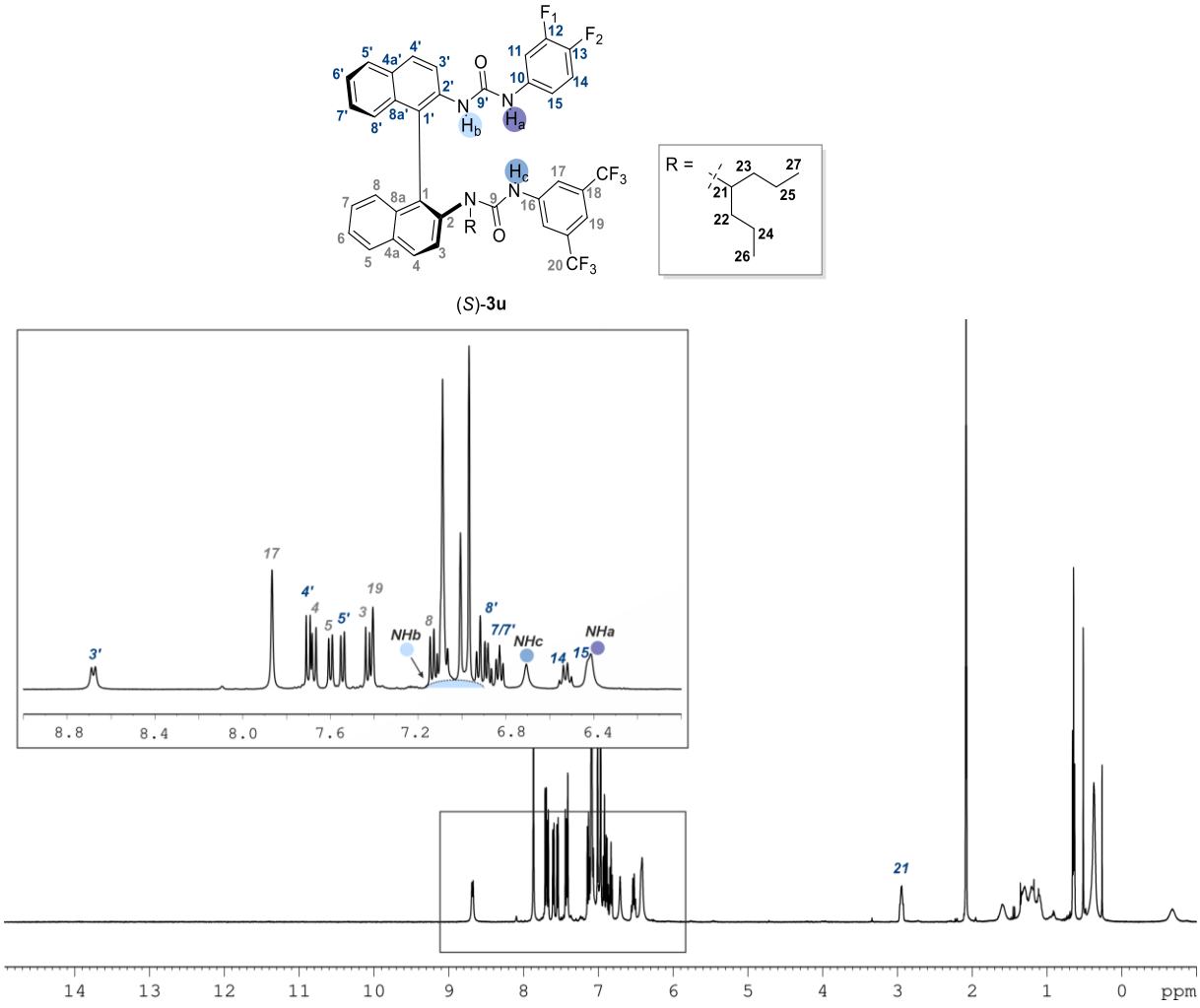

Figure 3.2: ^{1}H NMR of (*S*)-**3u** (600 MHz, Toluene-d_8, 25 mM, 298 K)

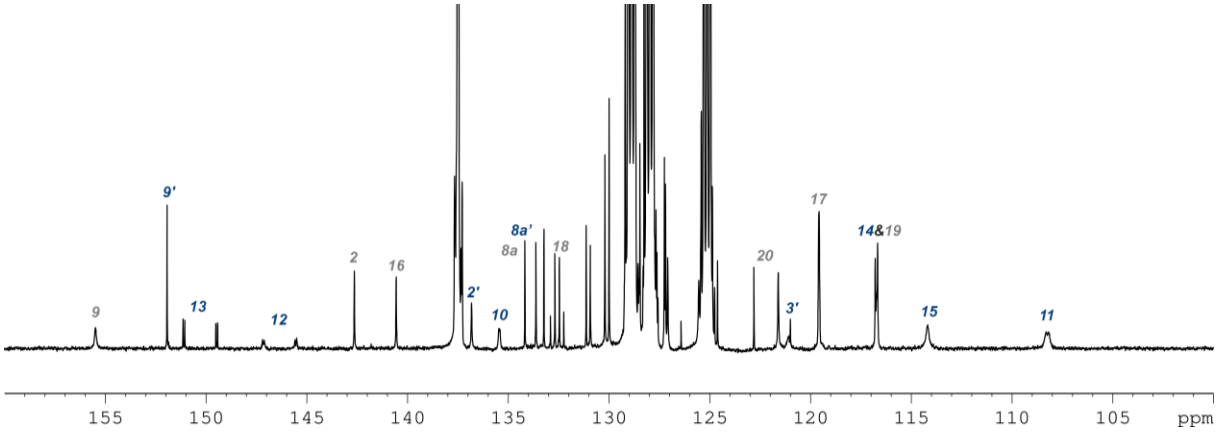

Figure 3.3: ^{13}C NMR of (*S*)-**3u** (151 MHz, Toluene-d_8, 25 mM, 298 K)

^{1}H–^{13}C HMBC correlations were observed between the CH proton of the *N*-heptyl alkyl group (H21) and the carbonyl of the alkylated urea (C9, δ = 155.5 ppm), and between H21 and the quaternary carbon on BINAM backbone (C2, δ = 142.6 ppm, Figure 3.4)

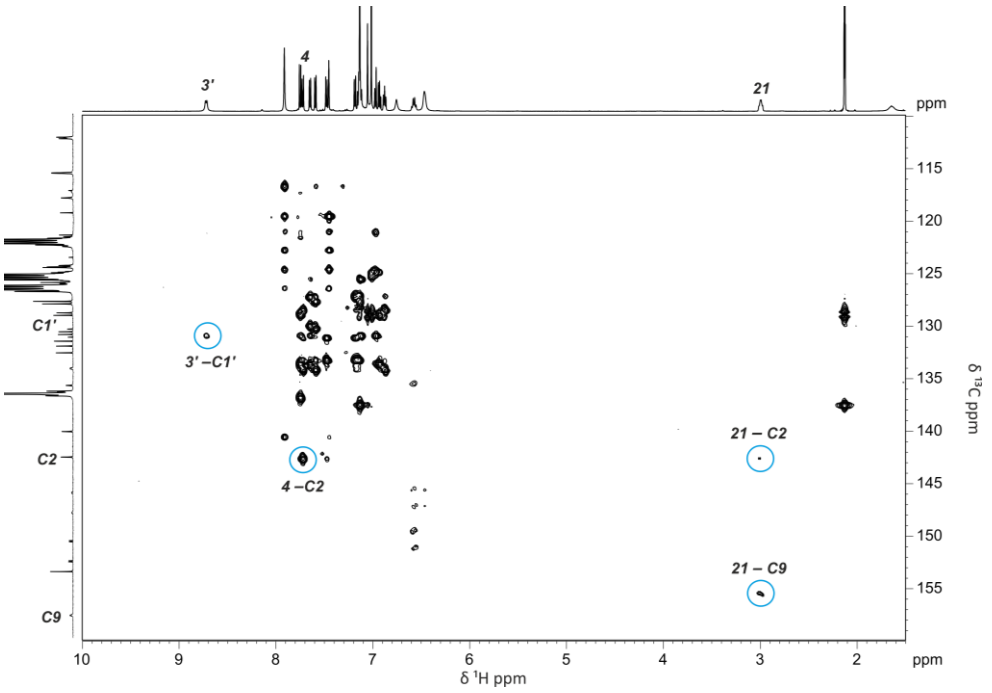

Figure 3.4: ^{1}H–^{13}C HMBC of (*S*)-**3u** (600 MHz, Toluene-d_8, 25 mM, 298 K).

^{1}H–^{13}C HSQC and ^{1}H–^{1}H NOESY analysis subsequently allowed for the full assignment of urea NH resonances: NHc could be assigned through the observation of nOe cross-peaks to H17, H21 and H8'; NHa was assigned at δ = 6.41 ppm which allowed for the detection of NHb, a signal masked within the aromatic signals and toluene solvent peaks, identified by the presence of a broad nOe. NHb is the most

deshielded urea resonance (δ = 7.04 ppm), in line with previous assignments of *N*-isopropylated urea catalysts (Figure 3.5).[1] Whilst NHb is less electron-withdrawn than both NHc and NHa, the deshielding and broadness of this resonance has been rationalised due to the existence of a dynamic intramolecular hydrogen bond which forms between NHb and the carbonyl C9 of the opposite urea (Figure 3.6).

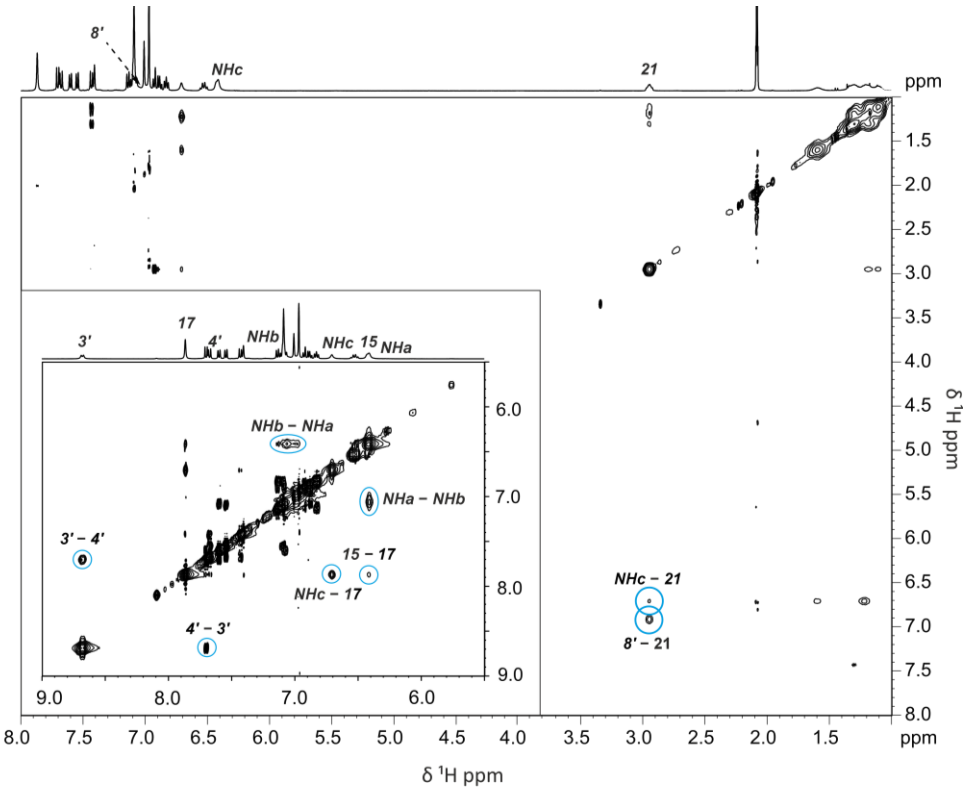

Figure 3.5: ^{1}H–^{1}H NOESY of (*S*)-**3u** (600 MHz, Toluene-d_8, 25 mM, 298 K).

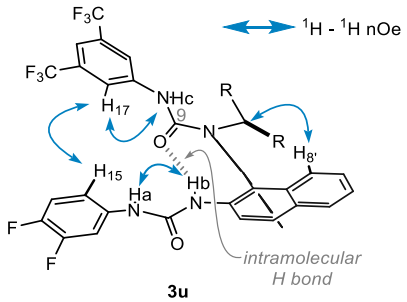

Figure 3.6: Proposed structure of **3u** in toluene-d_8 based on ^{1}H-^{1}H nOe correlations

3.2.2. Characterisation of a Ternary Urea-Phosphonium-Fluoride Complex

As described in Chapter 2 *(v. 2.3.1. Role of the Phosphonium Salt)*, urea-phosphonium-fluoride [UPF] species could be formed *via* the addition of urea HBD catalyst, phosphonium bromide salt (**8b**) and KF to an NMR tube, however this UPF species also existed concurrently with a urea-phosphonium-bromide species [UPBr] (Scheme 3.1).

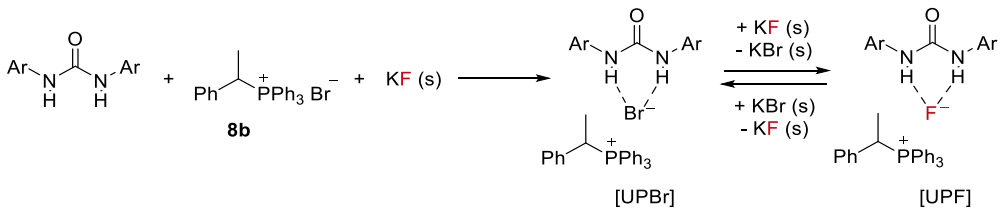

Scheme 3.1: Addition of onium **8b** and KF to urea catalysts forming both UPF and UPBr complexes

In order to fully characterise UPF complexes, forming them as singular species was required and alternative routes towards their preparation were considered. It was hypothesised that the employment of a phosphonium tetrafluoroborate salt (**8i**), rather than a phosphonium bromide salt, would allow for the formation a singular UPF species by NMR, considering the non-coordinating nature of the BF_4 anion to *bis* urea HBD catalysts.[2] Moreover, the presence of methylene protons on **8i** could serve as a spectroscopic probe for determining urea-phosphonium or phosphonium-fluoride interactions. The synthesis of **8i** was facile and could be performed on gram scale performing an anion exchange from commercially available benzyltriphenylphosphonium chloride with $NaBF_4$ in water.[3] The product (**8i**) precipitated out of solution as a white solid and could be isolated in 85 % yield following filtration (Scheme 3.2).

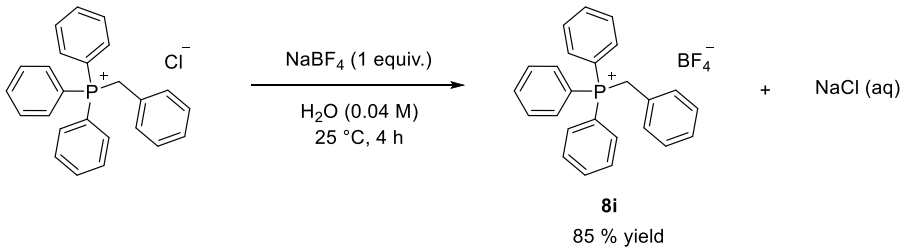

Scheme 3.2: Synthesis of phosphonium salt **8i**

The subjection of either catalysts (*S*)-**3u** or **8i** to sonication with KF (s) in toluene-d_8 independently did not show evidence of fluoride solubilisation within ^{1}H or ^{19}F NMR spectra in line with previous data which was collect in DCM-d_2 (*v. 2.3.1 Role of Phosphonium Salt*). The urea NH resonances of (*S*)-**3u** remained visible in their conformationally unbound state with ^{1}H spectra indistinguishable to the catalyst alone.

When all three components, (*S*)-**3u**, **8i** and KF, were added to an NMR tube and sonicated in toluene-d_8, changes were observed within ^{1}H NMR spectrum consistent with the formation of a singular UPF species following the precipitation of KBF_4 (s), and *de novo* assignment was performed (*v. 4.8 NMR Investigations*). Notable changes to several signals on the urea catalyst **3u** were observed, including the significant deshielding of the urea NH signals, which appear as doublets in ^{1}H NMR spectra, as well as deshielding of protons H3' and H17. The solubilisation of fluoride was evident in the ^{19}F NMR spectra by the presence of a broad signal at -74.2 ppm (Figure 3.8). When the ^{1}H spectrum was acquired with ^{19}F decoupling set to -74.2 ppm, all three urea NH resonances collapsed into singlets (Figure 3.7 inset). This multiplicity is indicative of scalar coupling which develops across hydrogen bonds and has been reported for urea-TBAF and urea-CsF complexes but never with KF as the fluoride salt. Scalar coupling provides unambiguous proof of hydrogen bonding interactions and have been considered a measure of strength where larger coupling constants ($J_{NH\cdots F}$) are related to stronger NH···F interaction. The sharp lines in ^{1}H, ^{19}F and ^{13}C spectra suggest that the species formed between urea catalyst **3u**, onium salt **8i** and KF in toluene-d_8 is singular and dynamically stable, this was further indicated by the presence of a single phosphonium cation observed by $^{31}P\{^{1}H\}$ at 22.3 ppm ($\Delta\delta_P \approx$ -0.6 ppm from Ph_3BnP^+ BF_4^-) (*v. 4.8 NMR Investigations* for all spectra).

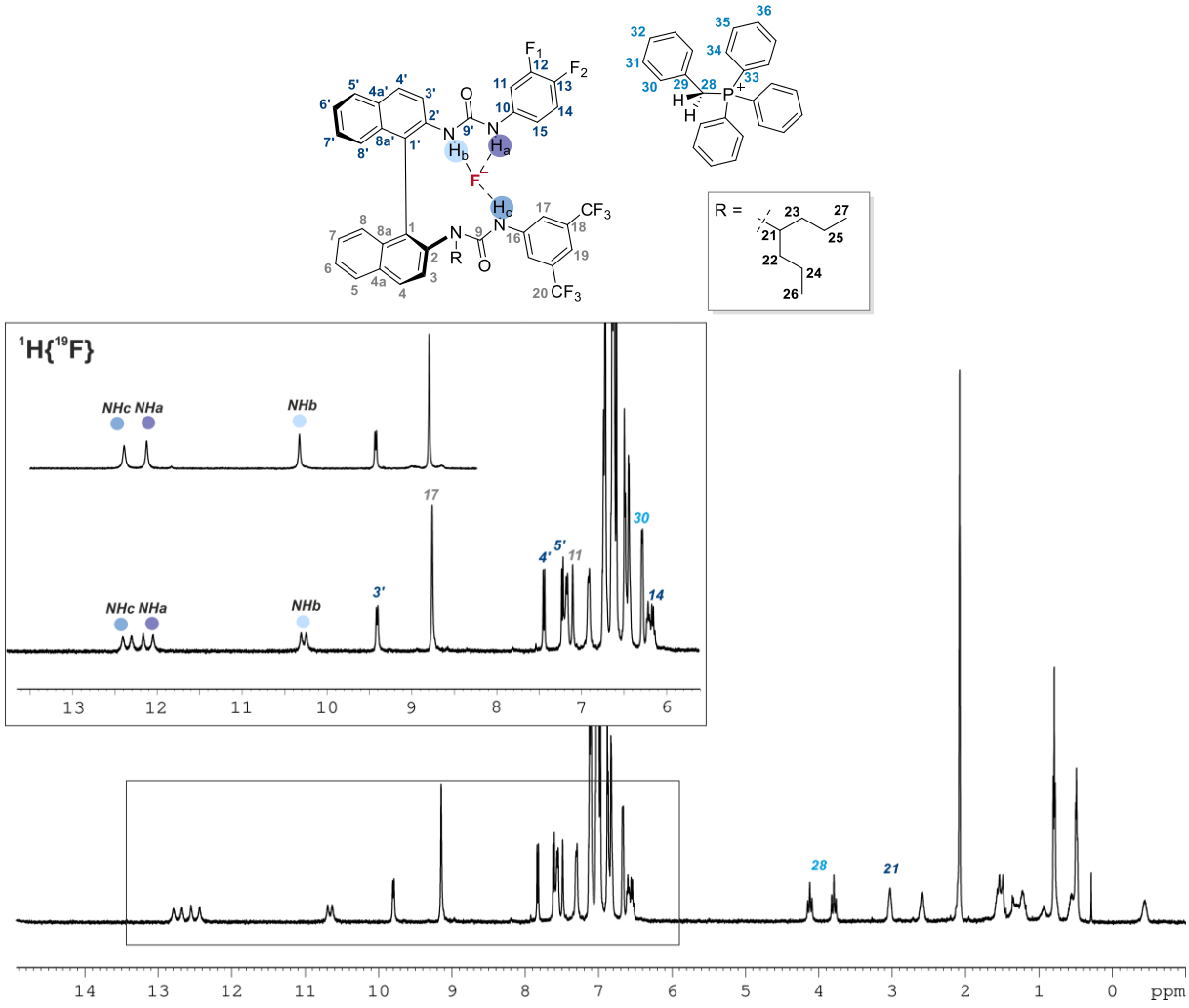

Figure 3.7: ^{1}H NMR of UPF species (*S*)-**3u**: Ph_3BnP^+: F^- (500 MHz, Toluene-d_8, 25 mM, 298 K)

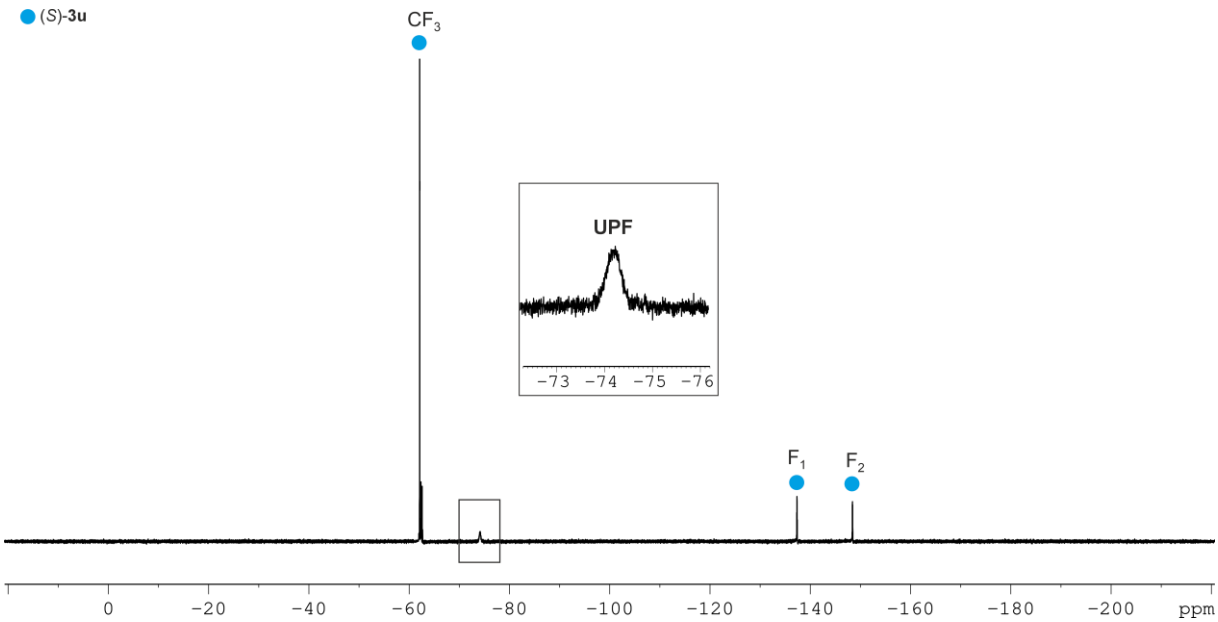

Figure 3.8: ^{19}F NMR of UPF species (*S*)-**3u**: Ph_3BnP^+: F^- (471 MHz, Toluene-d_8, 25 mM, 298 K)

The identities of the NH resonances were assigned based on nOe correlations obtained from ^{1}H–^{1}H Rotating Frame Overhauser Enhancement Spectroscopy (ROESY) experiments, since Nuclear Overhauser Enhancement Spectroscopy (NOESY) experiments failed to give clear indication of cross-peaks between the urea resonances. ROESY spectra displayed correlations between NHc ↔ H17 and NHb ↔ NHa, which were used to unambiguously identify the NH protons as they bind to fluoride (Figure 3.9). This deciphered that NHc and NHa exhibited the highest degree of deshielding upon fluoride binding, with chemical shifts of δ = 12.7 ppm ($\Delta\delta_{NHc}$ = 6.0 ppm) and δ = 12.4 ppm ($\Delta\delta_{NHa}$ = 6.0 ppm) respectively, demonstrating comparable magnitudes of interaction. Whilst NHb, proximal to the BINAM backbone was more shielded with a chemical shift of δ = 10.6 ppm ($\Delta\delta_{NHb}$ = 3.6 ppm) indicating weaker binding to the fluoride anion. It is notable that this pattern of NH deshielding differs from previously studied TBAF complexes formed with *N*-isopropylated urea catalyst (*S*)-**3d**, featuring 3,5-*bis*(trifluoromethyl)phenyl substituents on both urea motifs. In this case NHa was seen to be the most deshielded (12.8 ppm, $\Delta\delta_{NHa}$ = 5.7 ppm), followed by NHc (12.2 ppm, $\Delta\delta_{NHc}$ = 5.3 ppm) and NHb (10.5 ppm, $\Delta\delta_{NHb}$ = 3.0 ppm).[1]

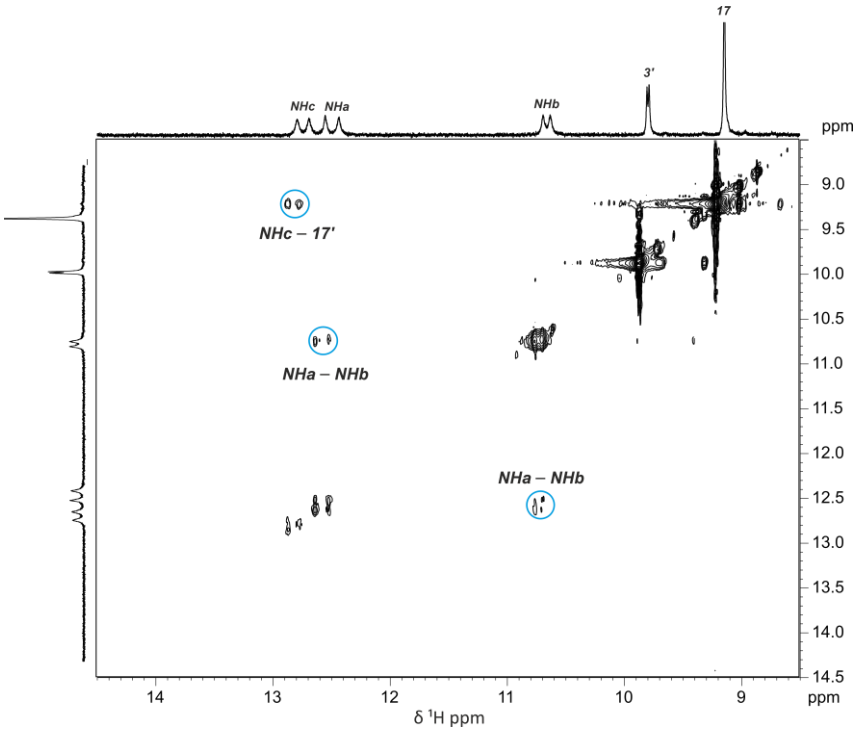

Figure 3.9: ^{1}H–^{1}H ROESY of UPF species (*S*)-**3u**: Ph_3BnP^+: F^- (500 MHz, Toluene-d_8, 25 mM, 298 K)

Significant changes were also seen within ^{1}H NMR spectra for signals ascribed to the phosphonium cation. Particularly, the chemical shift and multiplicity of methylene protons H28 changed from a doublet at δ = 4.47 ppm to two doublets of doublets at δ = 4.25 and 3.82 ppm, upon formation of the UPF complex. The enantiotopic methylene protons H28 experience coupling to phosphorus in their conformationally free state ($^{2}J_{H28\text{-}P}$ = 14.5 Hz), however upon the formation of a UPF complex, these protons, placed in a chiral environment, become diastereotopic, experiencing coupling to phosphorus $^{2}J_{H28\text{-}P}$ = 14.8 Hz as well as to each other $^{2}J_{H28\text{-}H28}$ = 15.1 Hz. Decoupling ^{1}H NMR spectra from the phosphonium signal (^{31}P δ = 22.3 ppm) presents exclusively the ^{1}H–^{1}H coupling constants between the protons (Figure 3.10). This data illustrates the proximity between the chiral urea-fluoride anionic species and the phosphonium cation which form an intimate ion pair in toluene. In this case, the fluoride bound urea catalyst resembles a chiral shift or solvating agent (CSA), and interaction between the phosphonium cation and the enantiopure urea-fluoride anion by means of non-covalent electrostatic interactions gives rise to a chiral ion-pair.[4] Collectively these data indicate that the solubilisation of KF is reliant on the interaction between both the urea and phosphonium catalysts forming a dynamically stable ternary urea-phosphonium-fluoride [UPF] species in toluene (Figure 3.11).

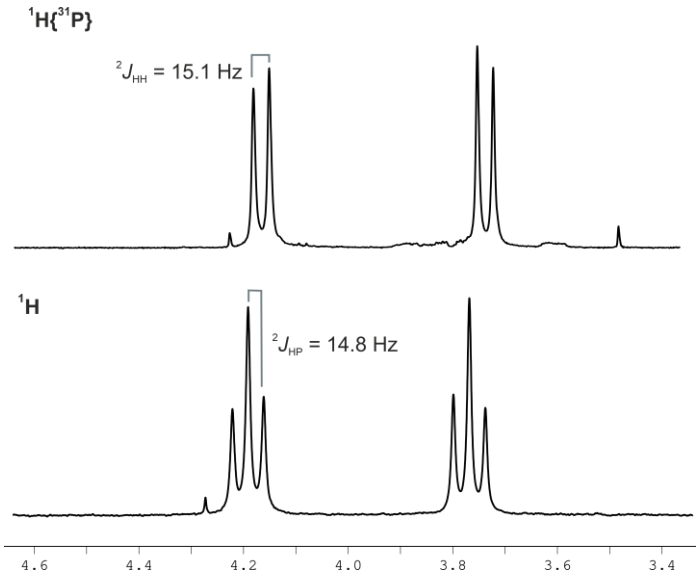

Figure 3.10: Section of ^{1}H NMR and ^{1}H{^{31}P} of UPF Complex (*S*)-**3u**: Ph_3BnP^+: F^- (500 MHz, Toluene-d_8, 25 mM, 298 K)

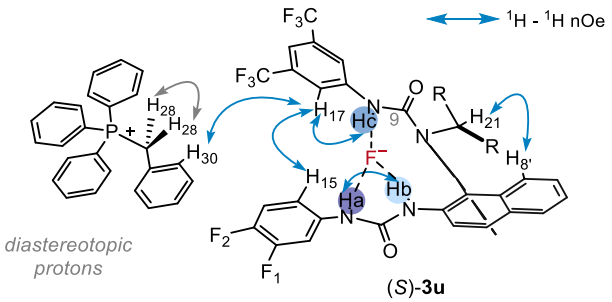

Figure 3.11: Proposed structure of UPF complex

Hydrogen bond correlations were investigated through Clean In Phase-HSQC (CLIP-HSQC), a sequence which can be used to obtain accurate one-bond coupling constants.[5] Whilst HSQC experiments are often employed to identify covalently linked nuclei, the CLIP-HSQC sequence has been previously reported for the detection of $^{1h}J_{NH\cdots F}$ coupling which forms across hydrogen bonds. The obtained 2D spectra reports ^{1}H chemical shifts against ^{19}F chemical shift and the magnitude of $^{1h}J_{NH\cdots F}$ can be measured from the cross peaks (Figure 3.12). For the complex (*S*)-**3u**: Ph_3BnP^+: F^- the three hydrogen bond coupling constants were measured to be $^{1h}J_{NHc\cdots F}$- = 51, $^{1h}J_{NHa\cdots F}$- = 57 and $^{1h}J_{NHb\cdots F}$- = 31 Hz. The measured NH coupling constants correlate with the change in NH chemical shift, with NHa and NHc which have the largest coupling constants to fluoride of 57 Hz and 51 Hz respectively, also experiencing increased deshielding upon binding to fluoride ($\Delta\delta_{NH}$ = 6.0 ppm), compared to NHb which is significantly less deshielded ($\Delta\delta_{NH}$ = 3.6 ppm) and has a smaller coupling constant of 31 Hz.

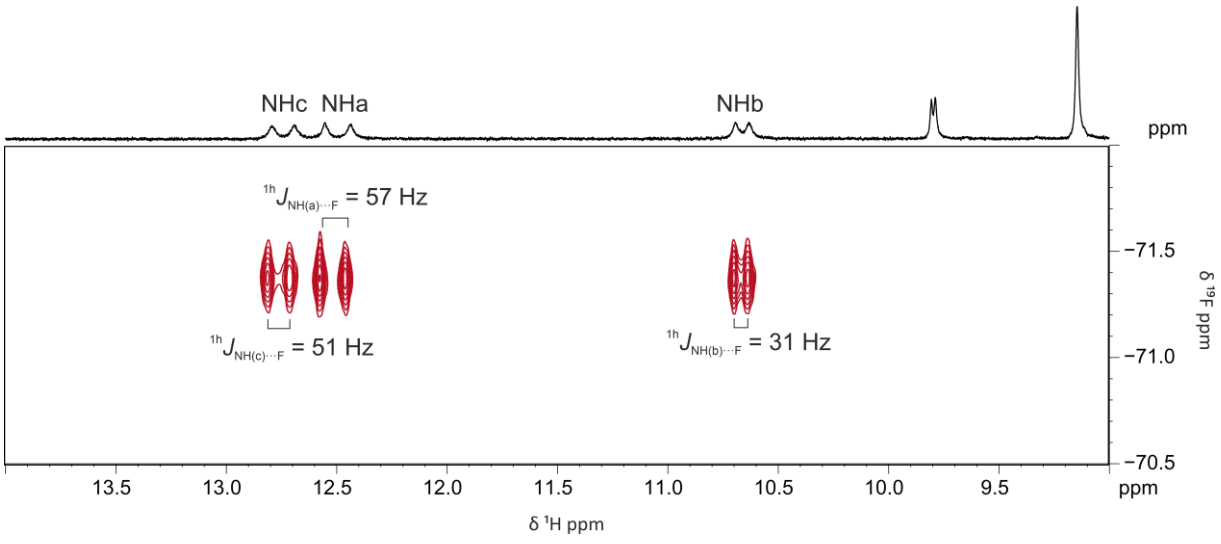

Figure 3.12: ^{1}H–^{19}F CLIP HSQC spectrum of (*S*)-**3u**: Ph_3BnP^+: F^- (500 MHz, Toluene-d_8, 25 mM, 298 K)

3.2.3. Elucidation of Ion-Pair Structure in Solution

To further study intranuclear distances between the urea NH protons and fluoride, and gain structural information about the binding pocket of the fluoride anion, nOes were measured by means of ^{1}H–^{19}F heteronuclear Overhauser spectroscopy (HOESY).[6] Nuclear Overhauser effects (nOes) occur where the perturbation of nuclear spin polarization (e.g. through irradiation) is transferred to another nuclear spin population through dipolar cross-relaxation. HOESY experiments allow for quantification of nOe signals, assuming the initial rate approximation is valid, considering that nOe intensity is inversely proportional to internuclear distance ($\propto r^{-6}$). The initial rate approximation states that nOe intensities build up linearly with the mixing time parameter (τ_m), providing that it is shorter than the longitudinal relaxation T_1.[7]

A series of 1D-HOESY experiments irradiating the signal corresponding to the fluoride anion (^{19}F δ = -74.2 ppm) were collected varying the mixing time parameter (τ_m) between 10 – 400 ms (Figure 3.13). This allowed for the construction of nOe build up curves which were used to calculate relative distances between protons and the fluoride anion (Figure 3.14). This indicated that NHa and NHc were the closest to the fluoride anion, with NHa being ~2 % longer than NHc. NHb was seen to have a longer contact to fluoride (~10 % longer than NHc), which is in agreement with the lower magnitude of the coupling constant to fluoride ($^{1h}J_{NH\cdots F}$) and smaller changes in chemical shift ($\Delta\delta_{NH}$) upon binding to fluoride. A fourth correlation was observed on the urea catalyst from fluoride to H17, which is corroborated by its significant deshielding upon complex formation ($\Delta\delta_{CH}$ = 1.2 ppm). The importance of the ortho protons on the urea aryl ring systems is further illustrated by the diminished reactivity of urea catalysts where this proton is substituted by a halide (*v. 2.4.3. Synthesis and Optimisation of Urea HBD Catalysts*). Whilst there is no evidence that hydrogen bonding between these ortho protons and fluoride takes place, it has been hypothesised that they may participate in the solubilisation or stabilisation of fluoride complexes.[1] Other than correlations between fluoride and the urea HBD catalyst, nOe signals were also observed between the fluoride and protons assigned to the phosphonium cation including methylene protons H28 and aromatic protons H30, H34/35. The

magnitude of the nOe enhancements were weaker than those to protons on the urea catalyst structure (~20–30 % longer than NH distances), however this data provides further evidence of close proximity between the fluoride anion and the phosphonium cation (Figure 3.13). Overall, the relative distance between fluoride and protons follows pattern NHc~NHa > NHb >> H17 > H28 > H34/35 > H30, where the known hydrogen bond contacts (HBCs) between the urea catalyst and fluoride are significantly closer in distance than the ortho proton H17 and the protons on the phosphonium cation.

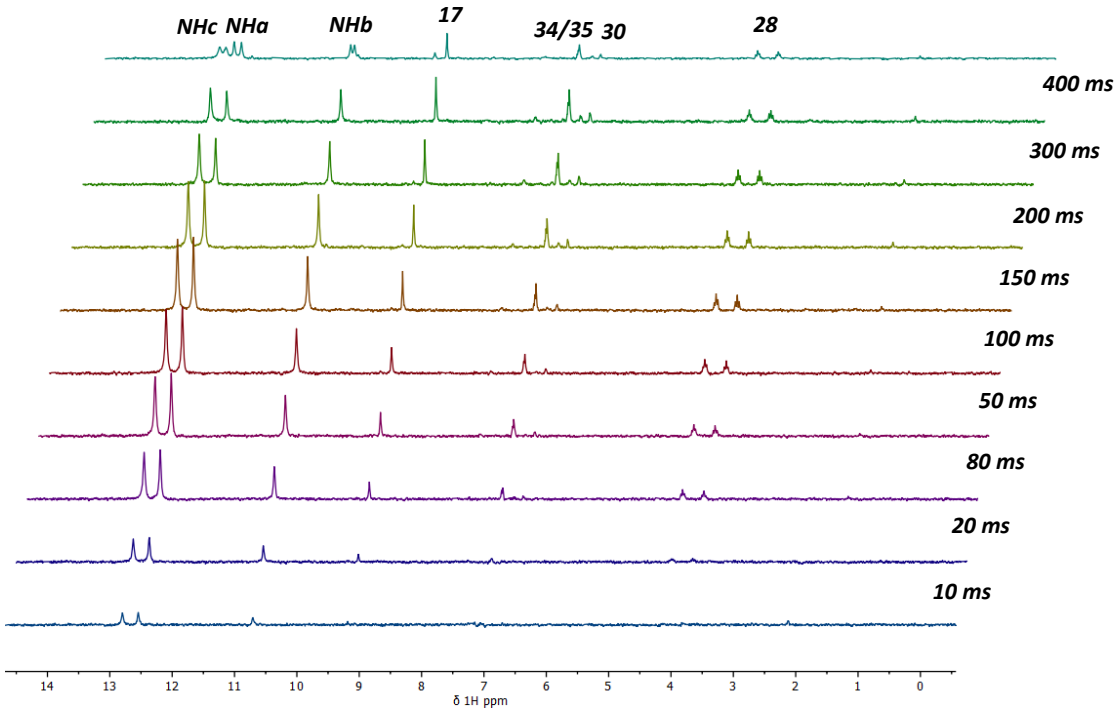

Figure 3.13: Overlay of ^{19}F selective ^{1}H HOESY spectra of UPF complex (*S*)-**3u**: Ph_3BnP^+: F^- performed at different mixing times (τ_m) (500 MHz, Toluene-d_8, 25 mM, 298 K)

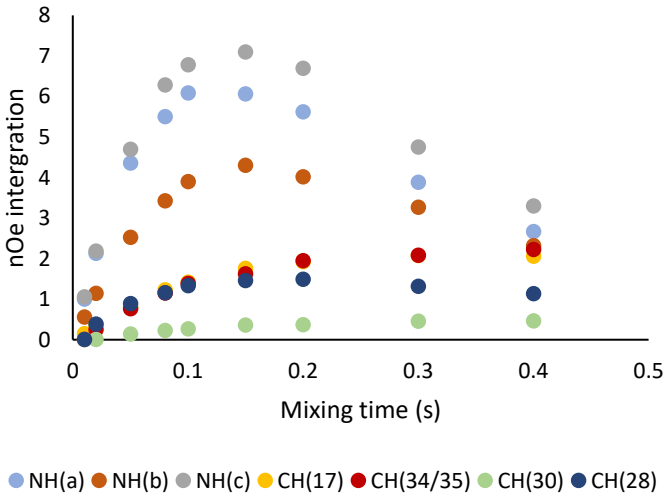

Figure 3.14: Graphical representation of ^{19}F selective ^{1}H HOESY data, comparing nOe intensity to mixing time (τ_m)

Absolute distances can also be extracted from nOe build up curves by comparison to the internal reference distance of 2.60 Å between aryl fluorine (F2) and H14, which was previously determined by X-ray crystallography and neutron diffraction.[18] The comparison of the nOe intensity between F2 and H14 to the intensity of nOes between the fluoride anion and signals of interest, at a uniform mixing time, allows for the estimation of absolute distance values. A mixing time of 50 ms, within the linear growth of nOe build up curves, was selected ensuring the validity of the initial rate approximation (Figure 3.14).[7]

The results for the absolute distances between fluoride and proton resonances are shown in Table 3.1. This data demonstrates that NHa and NHc are near equidistant to the fluoride anion with measured distances of 1.72 and 1.70 Å respectively, whereas the internal NHb has a longer hydrogen bonding interaction with fluoride measured at 1.88 Å. As expected, other non-hydrogen bonding protons had increased distances to the fluoride anion and signals corresponding to protons on the phosphonium cation were shown to be within ~3 Å, lying within the limits expected of ion-pairing interactions.[9]

Table 3.1: Determination of absolute distances for (*S*)-**3u**: Ph_3BnP^+: F^-

nOe correlation	I_{XH-F}	Absolute H–F distance (Å)
NH(a)–F	1.00	1.72
NH(b)–F	0.59	1.88
NH(c)–F	1.08	1.70
CH(17)–F	0.18	2.28
P-CH(30)–F	0.03	3.05
P-CH(28)–F	0.20	2.24
CH(14)–F_2 *(Reference)*	0.08	2.60

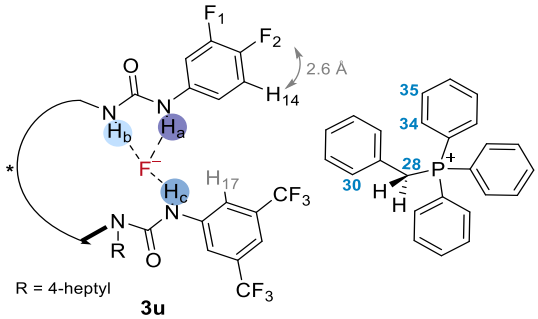

3u

Figure 3.15: Highlighted ^1H – ^{19}F nOe from Ph_3BnP^+ and **3u** to fluoride

Whilst attempts to grow crystals suitable for X-ray diffraction of UPF complexes were unsuccessful, the visualisation of the ion-pair was achieved using the relative distance data gained from HOESY experiments to build a DFT-derived structure. UPF complex (*S*)-**3k**: Ph_4P^+: F^- was selected, with **3k** possessing a less complex *N*-isopropyl alkylation compared to the heptyl alkylation on **3u** (Figure 3.16). Conformational sampling was performed with Conformer-Rotamer Ensemble Sampling Tool, CREST, software, which identified 10 lowest energy conformers for UPF complex. This elucidated that UPF species favoured two distinct binding modes denoted as A or B type. These structures differed the location of the phosphonium cation, which either covered the fluoride binding pocket (A-type) or showed π–π stacking interactions with the aryl rings on the urea catalyst (B-type) (Figure 3.17).

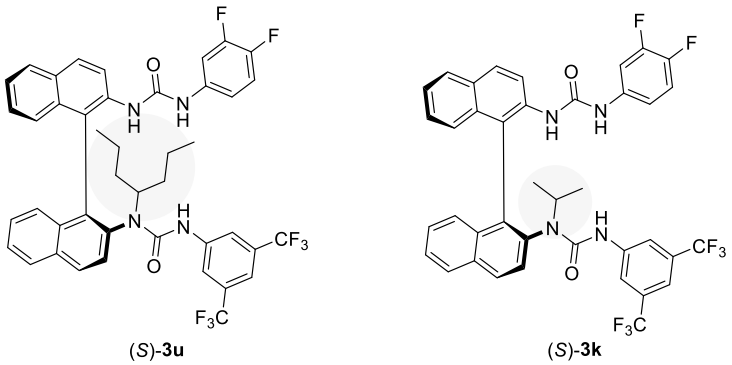

Figure 3.16: Structures of urea catalysts **3u** and **3k**

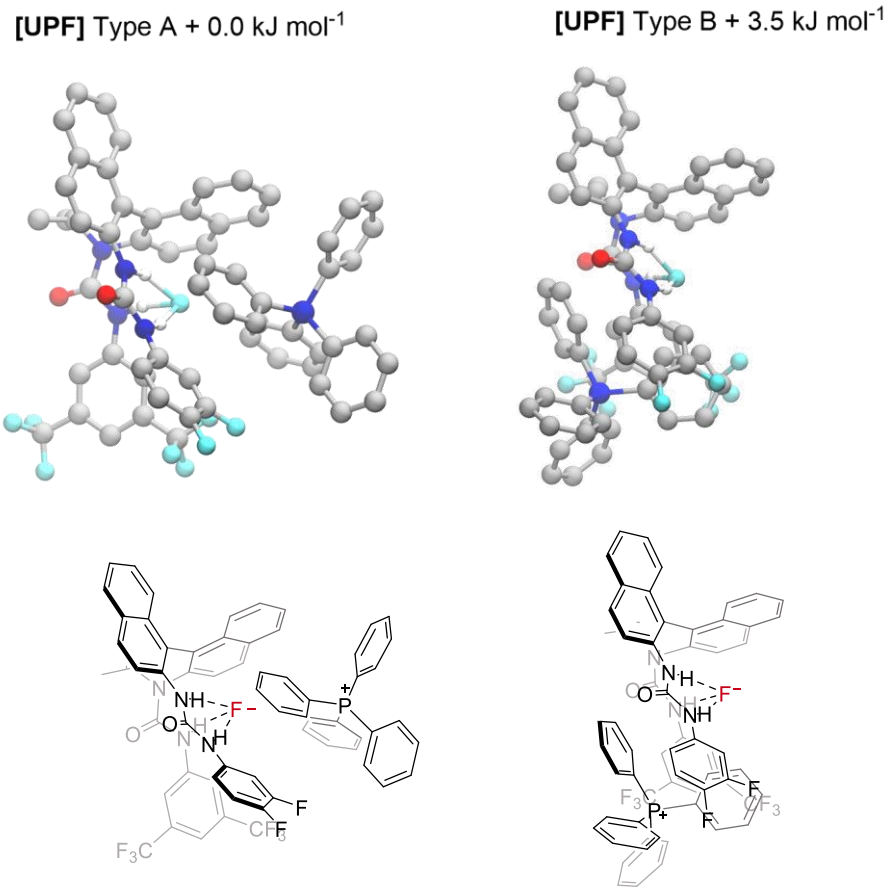

Figure 3.17: Lowest energy structures calculated for (*S*)-**3k:** Ph_4P^+: F^- from HOESY NMR data, type A and type B, showing different positions of phosphonium cation. (Computational work performed by Dr. Christopher Goult and Professor Robert Paton)

3.2.4. Urea-Phosphonium-Fluoride Complexes Formed with Tetradentate Catalyst

Contrary to the fluorination of *meso* electrophiles, such as episulfonium ions, under HBPTC, no fluorination of benzylic bromide **1a** was observed under the standard S-HBPTC conditions, with Ph_4P^+ I^- and KF, or with CsF, when tetradentate urea (*S*)-**3a** was employed (Scheme 3.3).[10] Moreover, urea catalysts possessing 3-pentyl or 4-heptyl *N*-alkylation allowed for benzylic fluorides to be produced in higher yields than catalysts with a smaller *N*-alkylation (e.g. ethyl or isopropyl) (*v. 2.4.3. Synthesis and Optimisation of Urea HBD Catalysts*). In order to investigate this, the binding of (*S*)-**3a** to fluoride was studied in the presence of an onium co-catalyst (**8i**) to gain understanding of how it differs from alkylated catalyst (*S*)-**3u**.

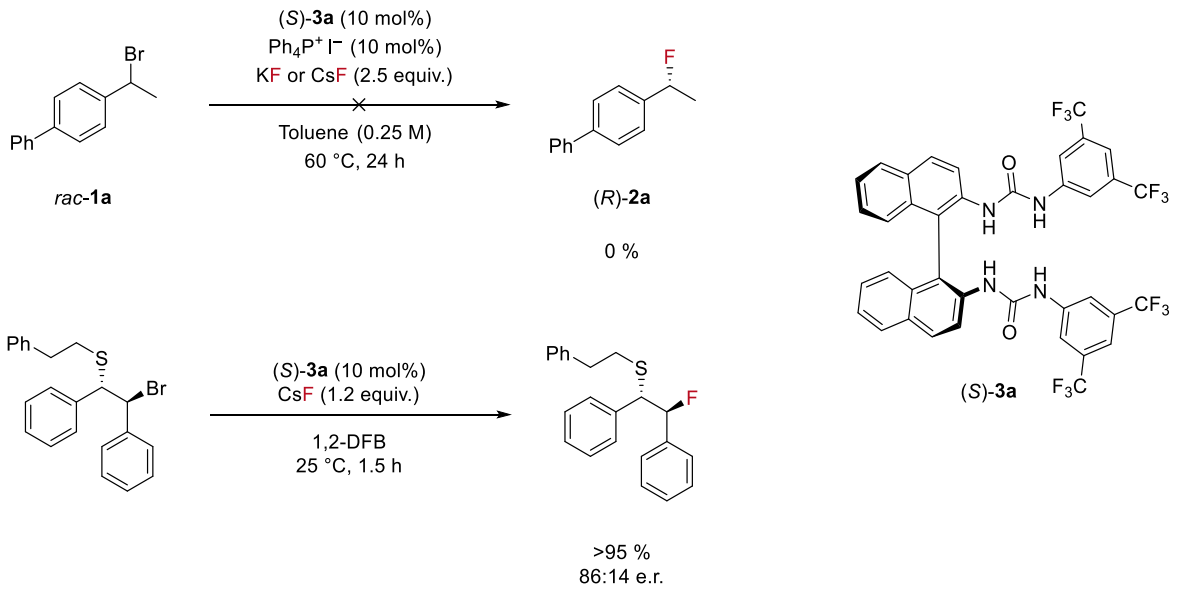

Scheme 3.3: Reactions of **1a** and β-bromosulfide substrate with tetradentate urea catalyst (*S*)-**3a**

Tetradentate urea catalyst (*S*)-**3a**, onium salt **8i** and KF were added to an NMR and sonicated in toluene-d_8 for spectroscopic analysis. The ^{1}H spectra obtained at 298 K showed similarities to those reported for (*S*)-**3u**: Ph_3BnP^+: F^- complexes, where significant line-broadening is observed. Variable temperature NMR spectra obtained at 273 K revealed the presence of two particularly deshielded signals assigned to the NH resonances of the urea catalyst (NHa and NHb), exhibiting scalar coupling to fluoride ($^{1h}J_{NH\text{-}F}$ = 59, 20 Hz), suggesting a tetradentate binding mode of (*S*)-**3a** to fluoride. Solubilisation of fluoride was further evident from the presence of a weak resonance at -96 ppm in the ^{19}F NMR spectrum, which sharpened upon decoupling to ^{1}H. Similarly, to the UPF complex formed between urea **3u**, phosphonium **8i** and KF, the enantiotopic methylene protons (H28) of the phosphonium cation became diastereotopic upon complex formation, ratifying their proximity to the chiral urea-fluoride species held within an ion-pair. It is notable that the two chemical environments for the trifluoromethyl groups of **3a**, as well as the broad aromatic region of the catalyst in ^{1}H NMR suggests the likelihood of dynamic exchange between two equilibrating UPF species (Figure 3.18 and 3.19).

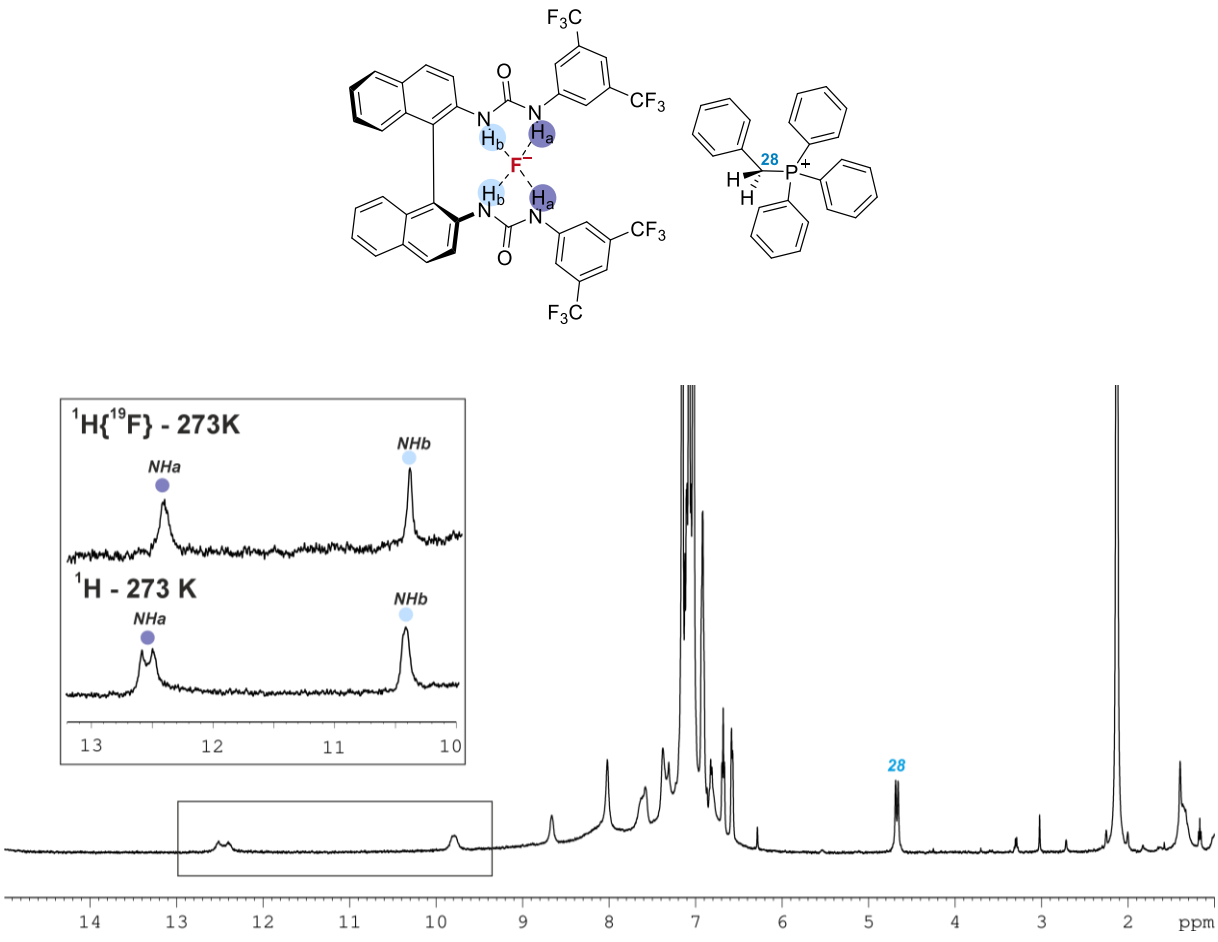

Figure 3.18: ^{1}H NMR of UPF species (*S*)-**3a**: Ph_3BnP^+: F^- (500 MHz, Toluene-d_8, 25 mM, 298 K)

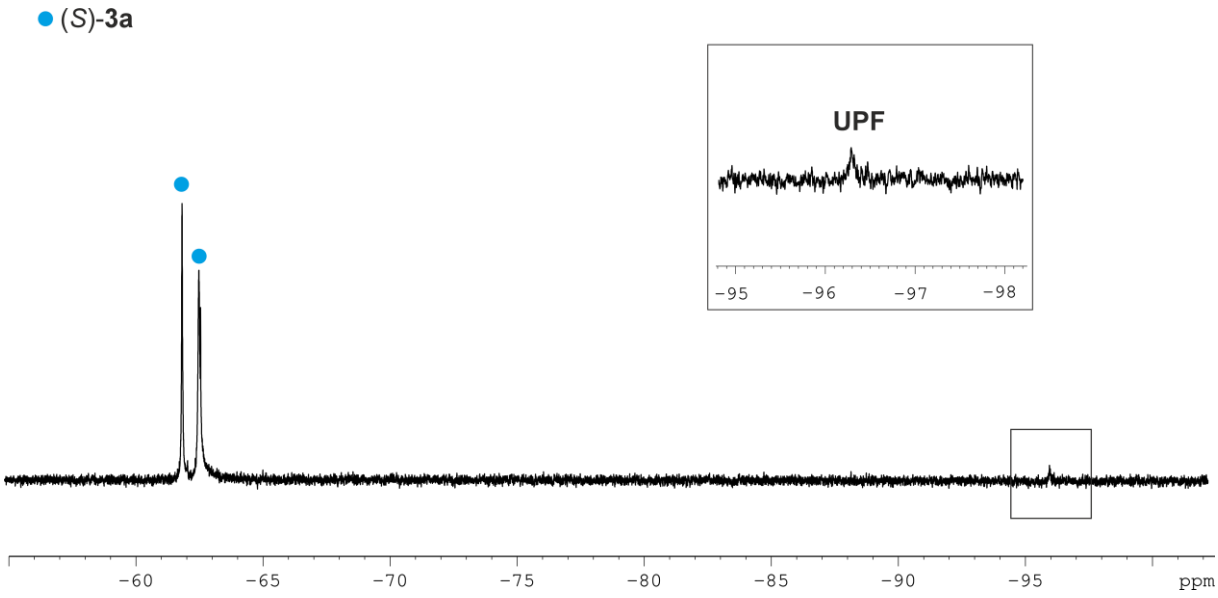

Figure 3.19: ^{19}F NMR spectra of UPF species (*S*)-**3a**: Ph_3BnP^+: F^- (471 MHz, Toluene-d_8, 25 mM, 298 K)

This tetradentate binding mode of fluoride by (*S*)-**3a** was not spectroscopically observed during NMR titration studies, previously published with tetrabutylammonium fluoride (TBAF) solutions.[1, 11] Here, bidentate binding of the distal NHa was dominant and the NHb protons, adjacent to the BINAM backbone, did not experience substantial deshielding upon fluoride addition. Tetradentate was considered as a potential binding mode of **3a** in the seminal report of HBPTC, which was investigated through molecular dynamics simulations with CsF at 373 K. Here, 58 % of the population favoured tetradentate binding to fluoride with the other 42 % tridentate, following an isomerisation of one urea from anti-anti to syn-anti (*v. 2.1.1. Hydrogen Bonding Phase Transfer Catalysis (HBPTC)*). However, TS analysis for the fluorination of episulfonium electrophiles in this study demonstrated that tridentate binding was energetically favoured, with the isomerisation of the urea improving the geometry of HBCs to fluoride. In addition, it was seen that **3a** could not maintain all four HBCs in TSs suggesting that tricoordinate binding of urea catalysts to fluoride is the active mode for fluorination (Scheme 3.4).[10, 12]

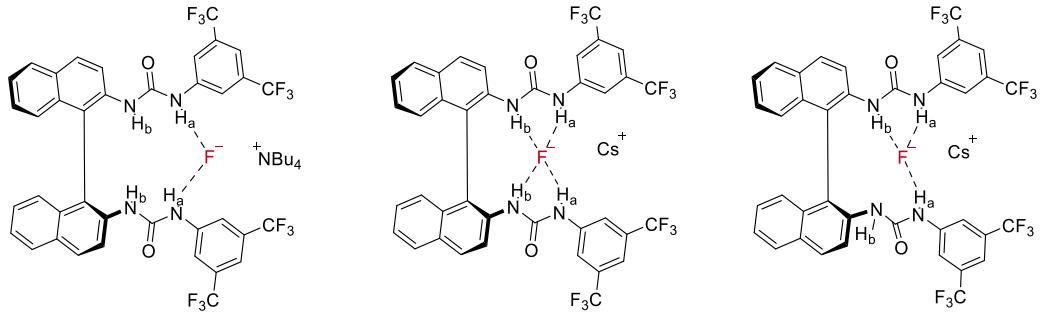

Scheme 3.4: Proposed binding modes of tetradentate catalyst **3a**

These data collectively suggest that tetradentate binding of urea catalysts to fluoride, which occurs upon the solubilisation of KF under the current co-catalytic manifold (urea and phosphonium salt), is detrimental for reactivity of the benzylic bromide **1a**, a less electrophilic substrate than the ones previously studied under HBPTC (Scheme 3.3). Accordingly, the alkylation of one urea nitrogen, preventing it from participating in hydrogen-bonding was beneficial for reactivity of the benzylic scaffold (*v. 2.4.3. Synthesis and Optimisation of Urea HBD Catalysts*). This may be related to the formation of a more favourable and singular UPF species displaying tridentate binding to fluoride which are more reactive towards fluorination.

3.2.5. Urea-Phosphonium-Fluoride Complexes as Reactive Fluorinating Reagent

To determine whether UPF complexes could act as effective fluorinating reagents, model benzylic bromide **1a** was added to an NMR tube containing the UPF complex (*S*)-**3u**: Ph_4P^+: F^- in toluene-d_8 and sonicated for 30 minutes. Reacquisition of the ^1H spectrum showed the formation of fluoride product **2a** as well as elimination product **4a**. A diminished signal corresponding to the UPF species was also observed in ^{19}F NMR (Figure 3.20 and 3.21).

(*S*)-**3u**: Ph_4P^+: F^- [UPF] complex + *rac*-**1a** → **2a** + **4a**

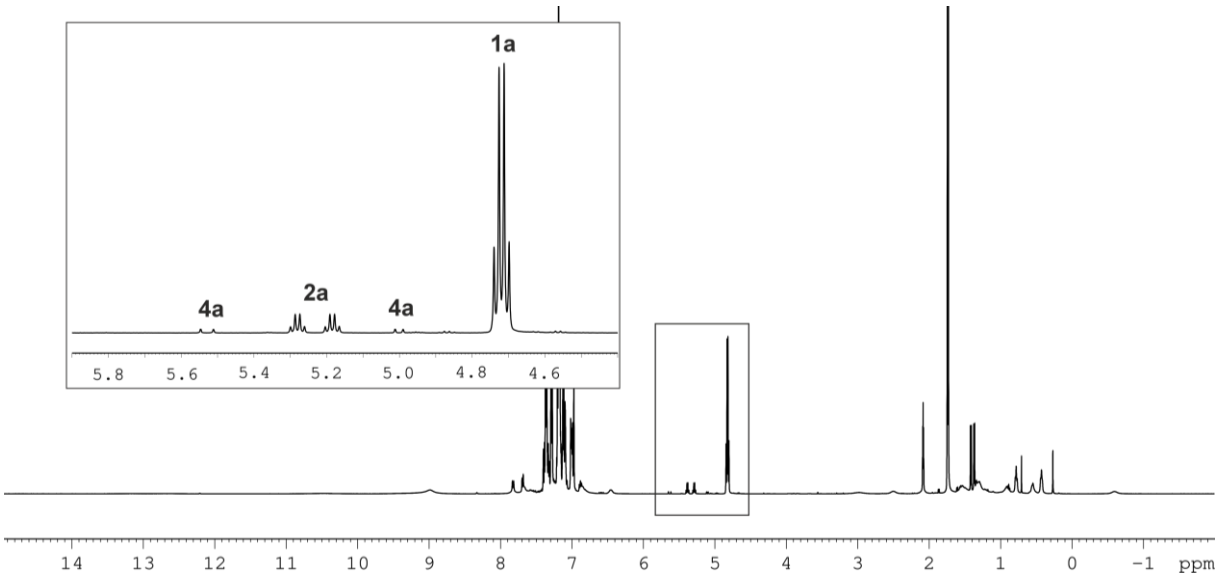

Figure 3.20: ^1H NMR of UPF (*S*)-**3u**: Ph_4P^+: F^- + **1a** following sonication (500 MHz, Toluene-d_8, 25 mM, 298 K)

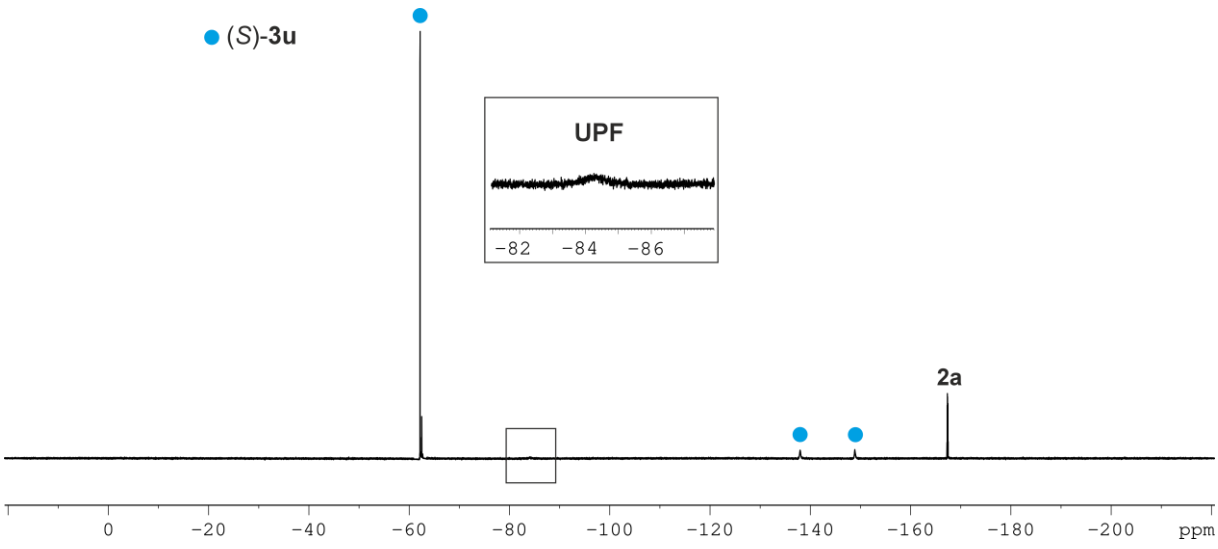

Figure 3.21: ^{19}F NMR of UPF (*S*)-**3u**: Ph_4P^+: F^- + **1a** following sonication (471 MHz, Toluene-d_8, 25 mM, 298 K)

UPF complexes could also be prepared and isolated as crystalline solids. Subjection of **1a** to pre-formed UPF complex (*S*)-**3u**: Ph_4P^+: F^- in *p*-xylene at 40 °C for 48 h allowed the formation of **2a** in 57 % yield and 87:13 e.r., as well as **4a** in 6 % yield. In comparison, catalytic conditions where (*S*)-**3u** and Ph_4P^+ I^- were employed at 10 mol% provided a higher yield of **2a** (83 %) at the same enantioselectivity (Scheme 3.5). These data are consistent with the ability of UPF complexes to act as fluorinating reagents.

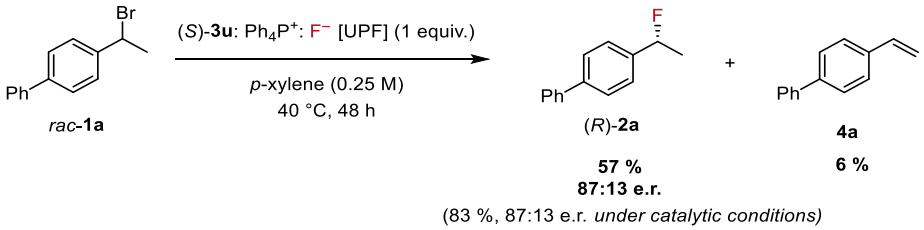

Scheme 3.5: Employing UPF (*S*)-**3u**: Ph_4P^+: F^- as a stochiometric reagent

3.3. Effect of Catalytic Iodide on Reaction Rate

The use of onium iodide salts as co-catalysts rather than onium bromides was paramount in achieving high yields of fluorinated products under S-HBPTC (*v. 2.4.1. Optimisation of Onium Salt Co-catalyst*). The optimal onium salt co-catalyst for the fluorination of benzylic bromides under S-HBPTC was Ph_4P^+ I^-, providing near a two-fold increase in yield compared to using the corresponding onium bromide salt (Table 3.2).

Table 3.2: Screening of tetraphenylphosphonium bromide versus iodide as a co-catalyst

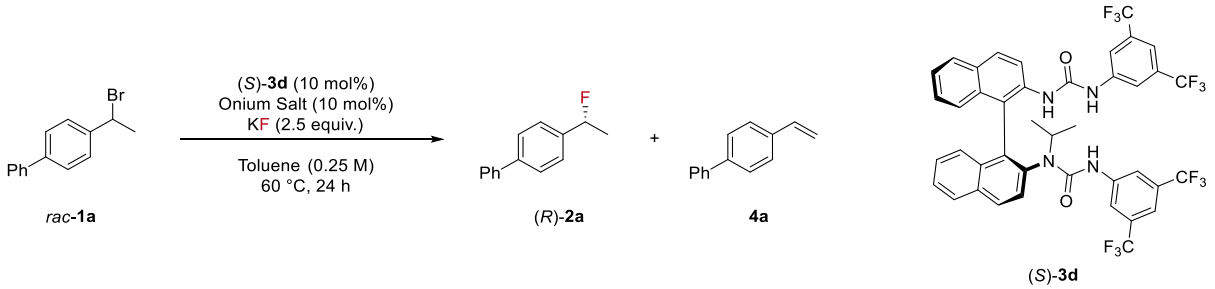

Entry	Onium Co-catalyst	Yield **2a** (%)[a]	Ratio **2a**: **4a**	e.r.[b]
1	Ph_4P^+ Br^-	33	6:1	76:24
2	Ph_4P^+ I^-	61	7:1	77:23

General conditions: 0.05 mmol substrate, stirring at 1200 rpm. [a]Determined by ^{19}F NMR using 4-fluoroanisole as internal standard, [b]e.r. determined by HPLC analysis using a chiral stationary phase

The rate of reaction was also found to double when $Ph_4P^+ I^-$ was used instead of $Ph_4P^+ Br^-$ for the fluorination of benzylic bromide **1a**. This conclusion was derived from parallel reactions conducted within NMR tubes (*v. infra 3.4.3. Design of Experimental Set-up*) and was calculated by tracking the consumption of **1a** over time (Figure 3.22).

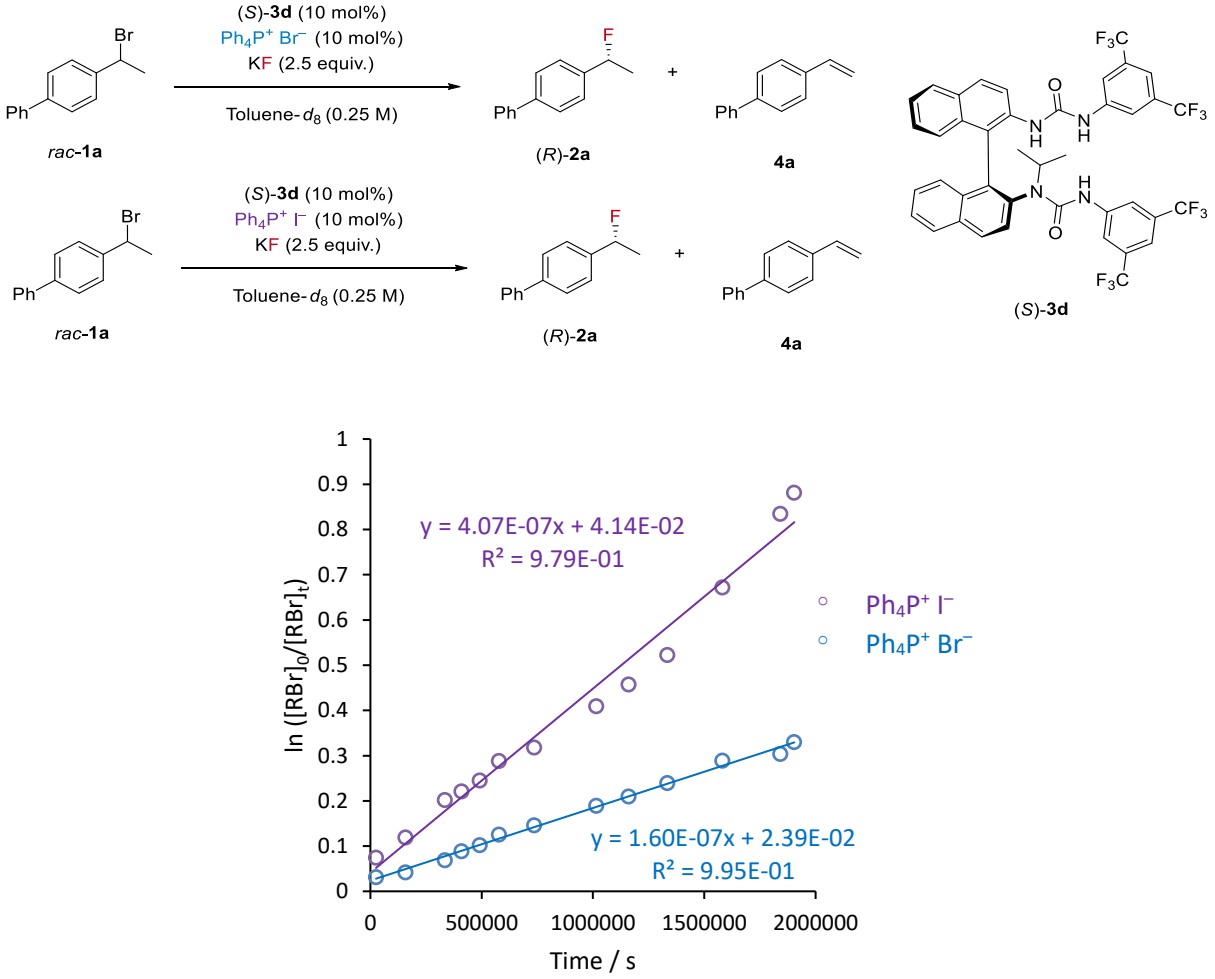

Figure 3.22: Reactions performed employing tetraphenylphosphonium bromide vs iodide as a co-catalyst following the rate of consumption of **1a**

Furthermore, the beneficial effect of catalytic iodide could also be achieved upon the addition of potassium iodide (KI) into reactions employing onium bromide salts as co-catalysts. A system comprising of urea (*S*)-**3d** with $Ph_4P^+ Br^-$ as a co-catalyst achieved increased yields of fluorinated product **2a** upon the addition of 10–20 mol% of KI compared to without (Table 3.3, entries 1–3).

Table 3.3: Screening of potassium iodide as an additive with $Ph_4P^+ Br^-$ co-catalyst

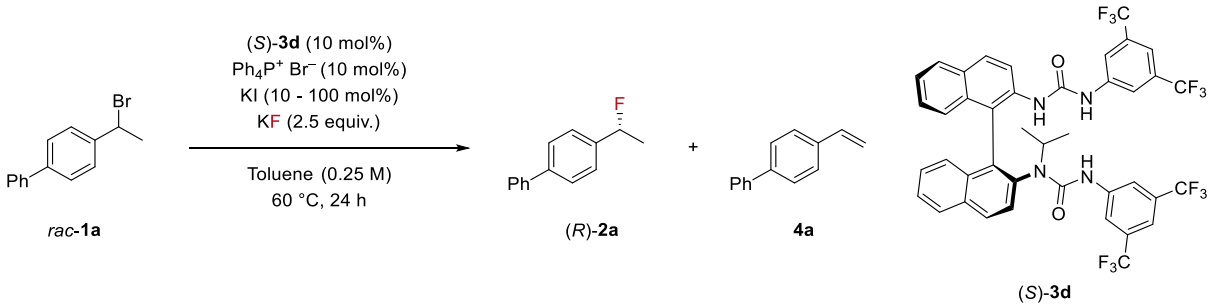

Entry	KI (mol %)	Yield **2a** (%)[a]	Ratio **2a**: **4a**	e.r.[b]
1	0	33	6:1	76:24
2	10	55	7:1	77:23
3	20	59	7:1	77:23
4	50	44	5:1	77:23
5	100	31	4:1	77:23

General conditions: 0.05 mmol substrate, stirring at 1200 rpm. [a]Determined by ^{19}F NMR using 4-fluoroanisole as internal standard, [b]e.r. determined by HPLC analysis using a chiral stationary phase

^1H spectroscopic analysis of the crude reaction mixture over time revealed that when $Ph_4P^+ I^-$ was employed as a co-catalyst, a benzylic iodide species (**5a**) could be detected. Control reactions elucidated that benzylic iodide **5a** was formed only in the presence of a urea catalyst ((*S*)-**3u**) (Figure 3.23) and increasing the loading of $Ph_4P^+ I^-$ to 50 mol%, at the same loading of urea (10 mol%) did not result in an increased concentration of **5a** (Figure 3.24); this suggests the participation of the urea for the solubilisation of $Ph_4P^+ I^-$ in order to displace the bromide anion of **1a**. This is consistent with the data showing that increased loading of $Ph_4P^+ I^-$ above the loading of urea catalyst (**3u**) did not further benefit reactivity (*v. 2.4.1. Optimisation of Onium Salt Co-catalyst*). Following the formation of **5a**, deshielding of the urea NH resonances was also observed ($\Delta\delta_{NH}$ ~ + 1–3 ppm) suggesting their coordination to the displaced bromide anions, presumably held within a UPBr ion pair.

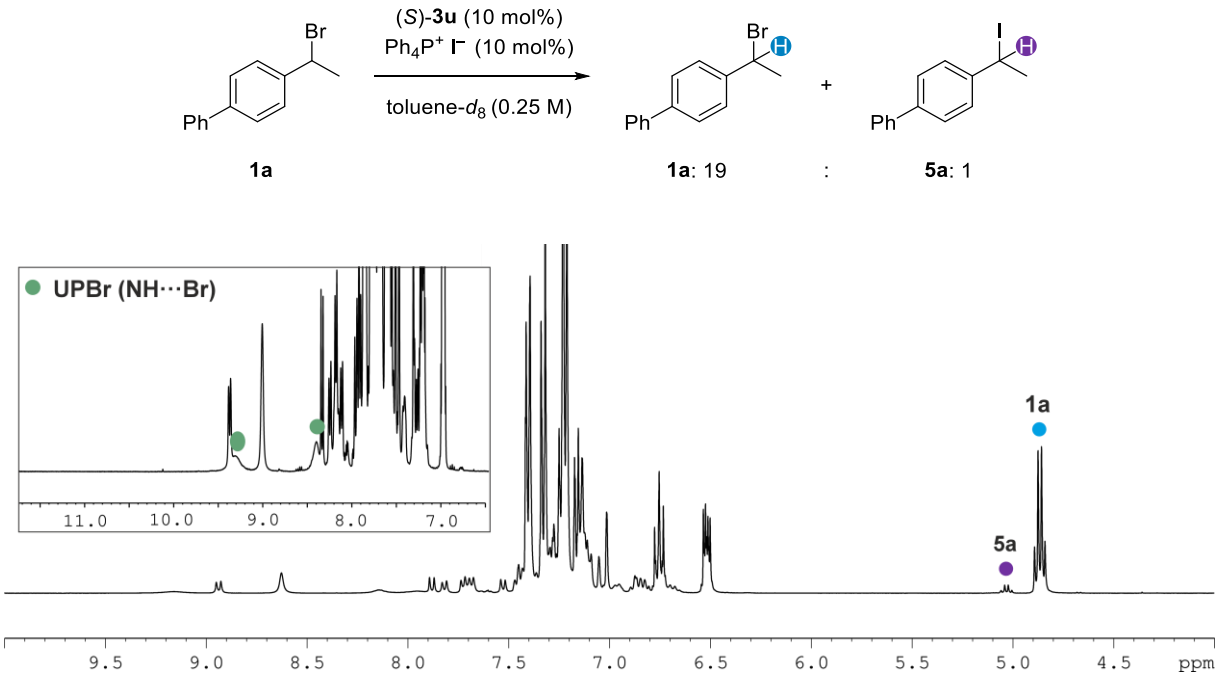

Figure 3.23: ^{1}H NMR spectra of **1a** + (*S*)-**3u** (10 mol%) + $Ph_4P^+ I^-$ (10 mol%) showing formation of iodide **5a** (5 %), (inset – evidence of UPBr complex) (500 MHz, Toluene-d_8, 25 mM, 298 K)

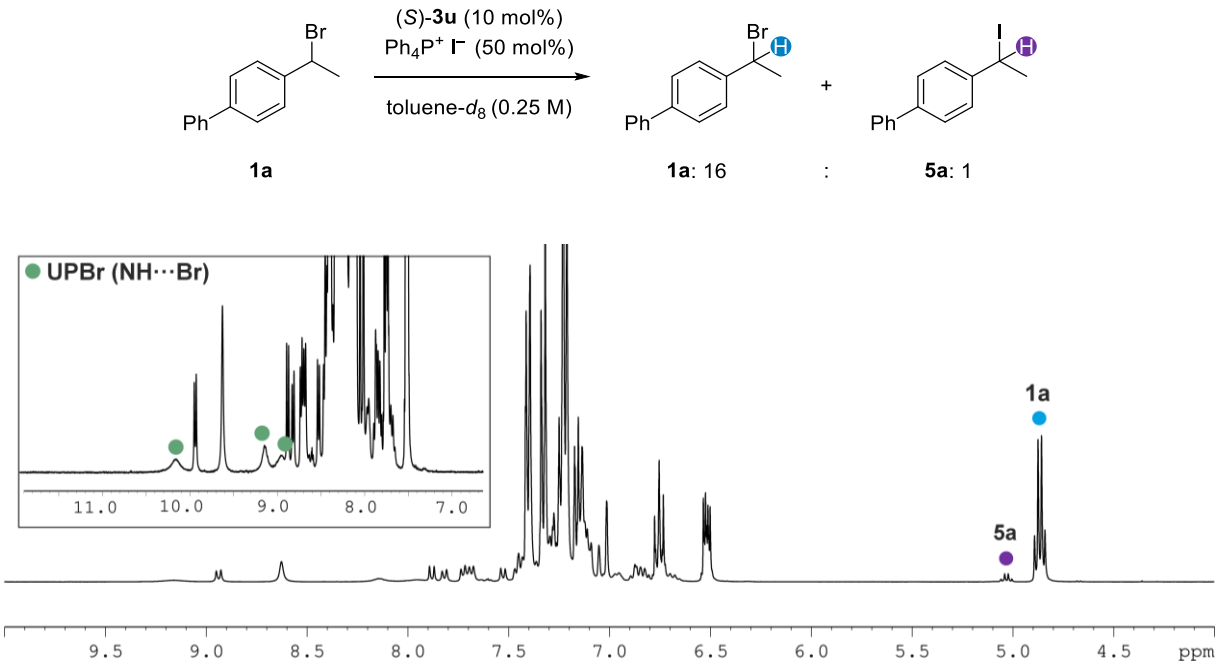

Figure 3.24: ^{1}H NMR spectra of **1a** + (*S*)-**3u** (10 mol%) + $Ph_4P^+ I^-$ (50 mol%) showing formation of iodide **5a** (6 %), (inset – evidence of UPBr complex) (500 MHz, Toluene-d_8, 25 mM, 298 K)

It was hypothesised that **5a** could act as an intermediate which increases the rate of reaction considering that iodide is known to be a better leaving group than bromide for fluorination.[13] Whilst attempt to isolate benzylic iodide **5a** were unsuccessful, due to their intrinsic instability upon

purification, α-iodoketone substrate **14a** was prepared and isolated quantitively.[14, 15] However, subjecting substrate **14a** to the optimised reaction conditions for α-bromoketone **12a** resulted in trace yields of fluorinated product **13a**, with the iodide starting material largely unreacted. In comparison, the reaction performed from **12a**, furnished fluorinated product **13a** in 60 % yield, 92:8 e.r. In contrast, the fluorination of α-iodoketone substrate **14a** was observed when the corresponding ammonium bromide co-catalyst (Et_4N^+ Br^-) was utilised, providing **13a** in 10 % yield, 90:10 e.r. (Scheme 3.6).

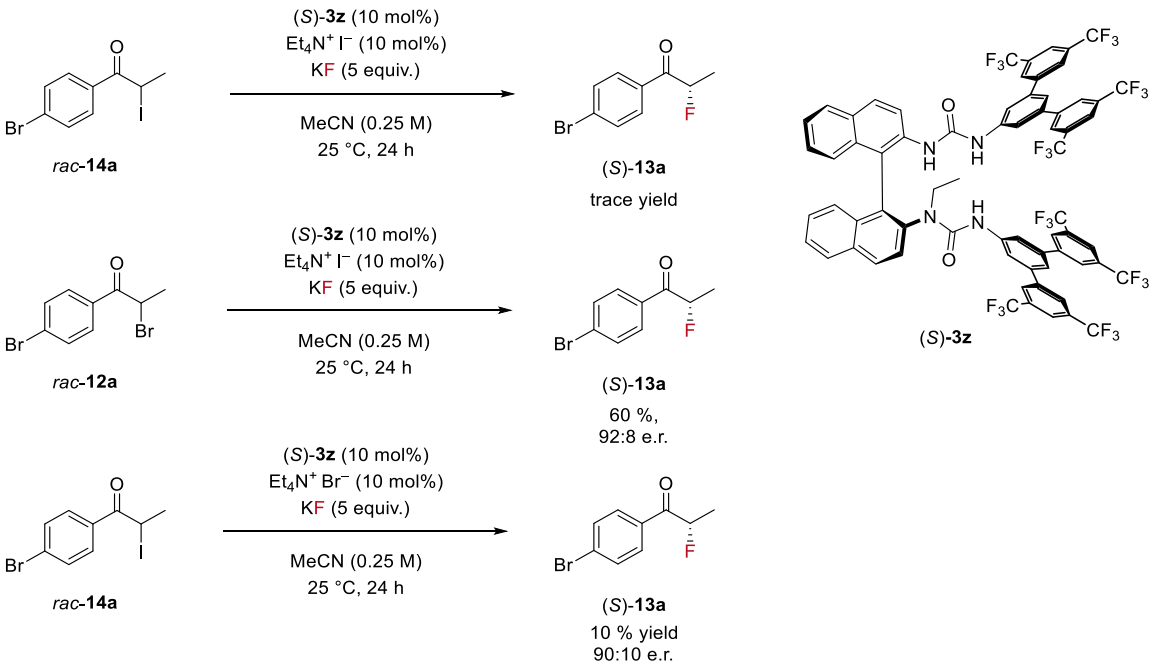

Scheme 3.6: Comparitive reactions performed from iodide **14a** and bromide **12a** substrates

It was hypothesised that the inability to fluorinate α-iodoketone substrate **14a** under the reaction conditions with urea catalyst (**3z**) and onium iodide (Et_4N^+ I^-) could stem from the increased solubility of KI compared to KBr (KBr lattice energy, 672 kJ mol^{-1} vs KI lattice energy, 632 kJ mol^{-1}),[16] which provides a reduced thermodynamic driving force within the catalytic cycle to compensate for the solubilisation of fluoride as a urea-onium-fluoride species.

To further investigate this hypothesis, the phase-transfer of fluoride by urea catalysts with either onium bromide and onium iodide co-catalysts was compared spectroscopically. Urea catalyst (*S*)-**3u** and KF were added to an NMR tube and dissolved in toluene-d_8 and either Ph_4P^+ Br^- or Ph_4P^+ I^- was

added and sonicated in attempt to form the corresponding UPF species. In the case of using Ph_4P^+ Br, the formation of a UPF species was observed, evidenced by substantial line-broadening of deshielded resonances in the ^{1}H NMR which, upon cooling to 273 K the spectra revealed three characteristic deshielded doublets ($\Delta\delta_{NH}$ = 6.0–4.0 ppm), denoting HBCs of the urea NH protons to fluoride (Figure 3.25, blue circles). Within the same ^{1}H NMR spectra there was also evidence for the formation of a UPBr species (Figure 3.25, green circles), indicated by a second set of urea NH resonances assigned by ^{1}H–^{13}C HSQC, which also experienced deshielding upon binding to the bromide anion ($\Delta\delta_{NH}$ = 2.5–4.0 ppm). The ^{19}F NMR spectrum further indicated the solubilisation of fluoride from the presence of a broad signal at -83 ppm characteristic of fluoride bound to urea HBD catalysts (Figure 3.25 (inset)).

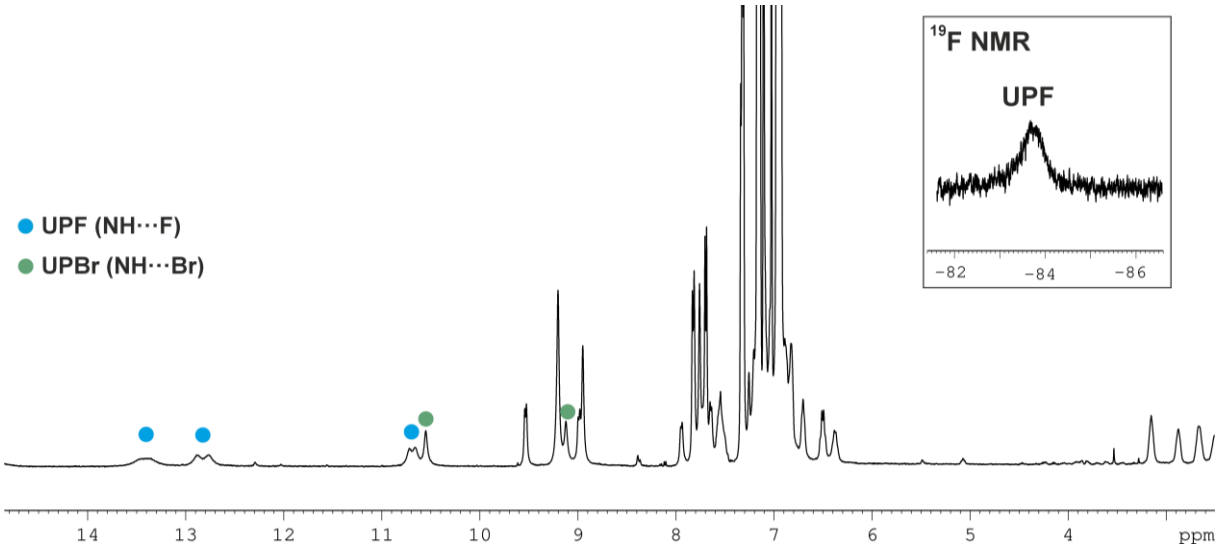

Figure 3.25: ^{1}H NMR of (*S*)-**3u** + Ph_4P^+ Br^- + KF multiple NH resonances indicating formation of both UPF (blue circles) and UPBr (green circles) complexes (inset – ^{19}F NMR showing fluoride solubilisation) (500 MHz, Toluene-d_8, 25 mM, 298 K).

In contrast, when Ph_4P^+ I^- was added to (*S*)-**3u** and KF in toluene-d_8, there was no evidence of UPF complex formation. No significant line broadening was observed and the urea NH resonances could be assigned as singlets deshielded ~ $\Delta\delta$ = 1.2–2.0 ppm, suggesting the binding of the less electronegative iodide anion and the formation of a urea-phosphonium-iodide complex [UPI] (Figure 3.26, purple circles). Furthermore, there was no signal in the expected chemical shift range of ^{19}F NMR spectrum which would indicate fluoride solubilisation (Figure 3.26 (inset)).

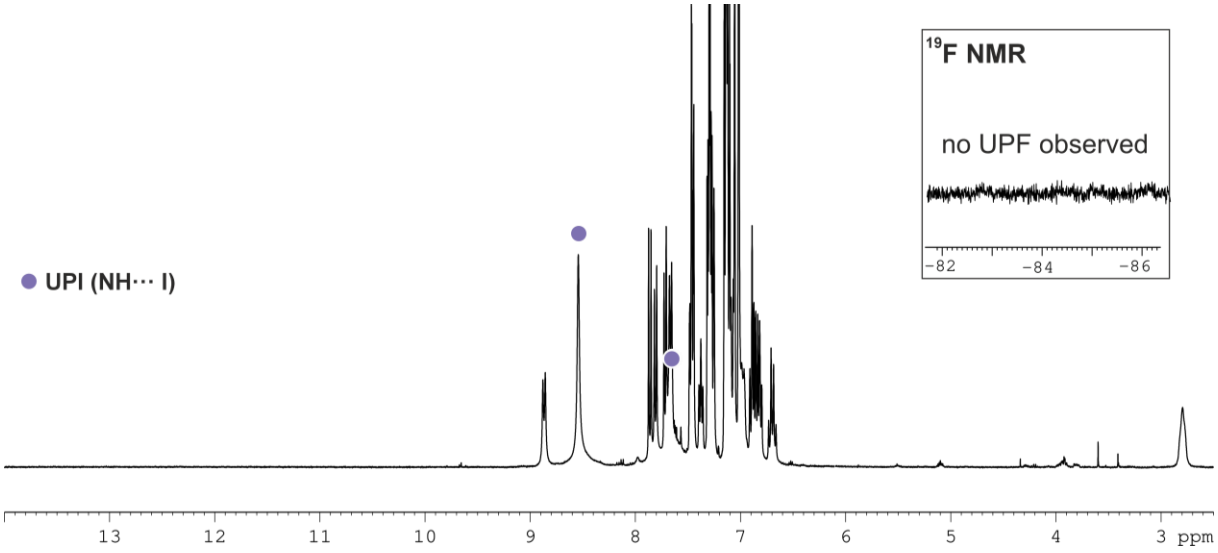

Figure 3.26: ^{1}H NMR of (*S*)-**3u** + $Ph_4P^+ I^-$ + KF, minor deshielding of NH resonances indicating formation of UPI complex (inset – ^{19}F NMR showing no fluoride solubilisation) (500 MHz, Toluene-d_8, 25 mM, 298 K).

These data suggest that the formation of UPF species within reactions occurs stepwise, through the initial formation of a UPBr species followed by an anion-exchange of the bromide ion by KF. In contrast, this is not observed through exchange of an iodide anion. Therefore, when reactions are performed directly from iodide substrates (**14a**), trace yields are observed (Scheme 3.6), consistent with minimal KF solubilisation by the catalysts (Figure 3.23). In the scenario where $Et_4N^+ Br^-$ was used a co-catalyst for the fluorination of α-iodoketone **14a**, a 10 % yield of fluorinated product **13a** was obtained, consistent with a single turnover of the ammonium bromide catalyst as the precipitation of KBr halts the phase-transfer of fluoride into solution by the urea and onium catalysts (Scheme 3.6).

When α-bromo- and α-iodoketone are subjected to reaction with pre-formed stochiometric urea-onium-fluoride complex (*S*)-**3z**: Et_4N^+: F^- the fluorinated product **13a** was formed in comparable yields of 56 and 53 % respectively (Scheme 3.7). This experiment demonstrates that bromide and iodide are both suitable leaving groups for substitution with urea-onium-fluoride species, however, it does not establish iodide as a superior leaving group. It is notable that for the α-haloketone substrate class, the use of an onium iodide co-catalyst, in lieu of an onium bromide, did not lead to substantially increased yields of the fluorinated product (*v. 2.5.2. Optimisation for the Fluorination of α-Bromoketones under S-HBPTC*).

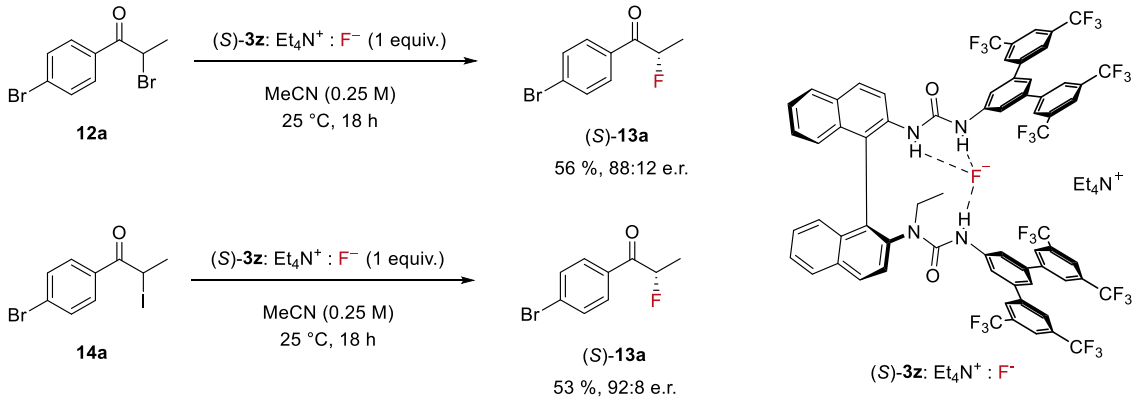

Scheme 3.7: Reactions performed comparing reactivity of bromide **12a** and iodide **14a** substrate with stochiometric urea-onium-fluoride species ((*S*)-**3z**: Et_4N^+: F^-)

In summary, these data suggest the necessity for the precipitation of KBr as a thermodynamic driving force, enabling the solubilisation of fluoride under this urea-onium catalysis platform. Whilst the distinction between the halide leaving groups was minimal for the fluorination of α-haloketones, for the benzylic substrate class, the beneficial effect of catalytic iodide in the system is hypothesised to stem from the increased reactivity of benzylic iodide species towards fluorination with UPF species.

3.4. Kinetics

3.4.1. Introduction to Kinetic Isotope Effects

Kinetic isotope effects refer to the phenomena which are associated with changes in reaction rates with isotopic substitution. First introduced in the 1940s, KIEs have become a powerful tool for organic chemists to decipher reaction mechanisms. KIEs are generally reported as a ratio of rate coefficients so that $k_{(\text{light isotopologue})}/k_{(\text{heavy isotopologue})}$ (e.g. KIE = $k(^1H)/k(^2H)$).[17] The observed rate change upon isotopic substitution can be rationalised considering the differences in vibrational energy of bonds as a factor of atomic mass. Bonds to heavier isotopes (^2H or D), vibrate at lower frequencies and therefore have lower zero-point energies (ZPE) compared to lighter isotopes (^1H). Consequently, more energy is required to break bonds to heavy isotopologues (Figure 3.27). The deuterium kinetic isotope effect is the most used and well understood type of KIE. This is the case for several reasons, including the commercial availability of, or facile syntheses towards, deuterated substrates. Additionally, the large

relative difference in mass between ^{1}H and ^{2}H and accompanying differences in vibrational frequencies mean that KIEs are easily observed and measured. In contrast KIEs for carbon ($^{12}C/^{13}C$) suffer from a much smaller difference in mass between isotopologues, resulting in intrinsically smaller observed KIEs which require high precision methods to ensure accurate measurements.[18]

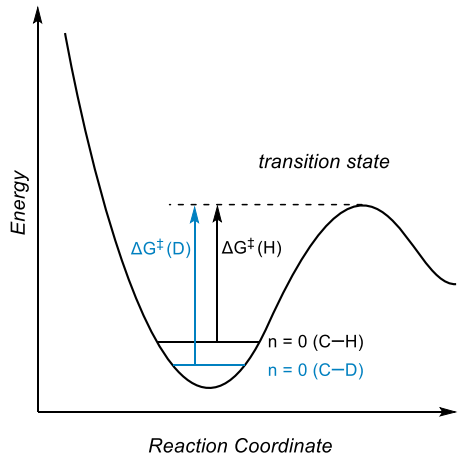

Figure 3.27: Differing zero-point energies for proteo- or deutero- substrates as the cause of a primary isotope effect

KIEs are classified as primary or secondary depending on the position of isotopic labelling. A primary KIE (PKIE) arises when a bond to the isotopically labelled atom is being broken or formed during the transition state of the rate determining step of a reaction. PKIEs have been investigated for leaving groups, nucleophiles and at the atom where substitution takes place. Secondary KIEs (SKIE) arise when bonds to the isotopically labelled atom themselves are not broken or formed but are in close proximity to the site of interest. This results in significantly smaller SKIE values compared to PKIEs. However, secondary deuterium effects are still widely used to elucidate reaction mechanism particularly in distinguishing between S_N1 and S_N2 pathways. Two types of SKIEs include the α-deuterium SKIE where hydrogen(s) on the α-carbon are replaced by deuterium and β-deuterium SKIE, where hydrogen(s) on the β-carbon are replaced by deuterium atom(s). These deuterium effects come from changes in hybridisation or hyperconjugation at the position of substitution.[19]

3.4.2. Aims of the Experiment

It was recognised that two scenarios for the substitution of benzylic bromides under S-HBPTC may be distinguished by means of a $^{1}H/^{2}H$ SKIE experiment. Understanding the pathway of substitution has mechanistic implications considering the possibility of forming an ion-pair between a carbocation and fluoride, which may be responsible for reactivity of the neutral electrophiles. Conversely, under the mild reaction conditions, the formation of a discrete carbocation for the α-bromoketone motif can be reasonably excluded and therefore investigations were not carried out on these substrates.[20]

If a reaction proceeds through the formation of a benzylic carbocation species following the departure of the bromide (or iodide) anion, one would expect a significant normal SKIE. This is in accordance with the change in the hybridisation of the benzylic carbon from sp^3 to sp^2 during the transition state, resulting in decreased resistance to out-of-plane bending modes. In contrast an S_N2 pathway, whereby C–F bond formation occurs concurrently with C–Br bond cleavage, would be indicated by a small normal or inverse SKIE value (Figure 3.28a). Moreover, the presence of a carbocation intermediate may be further determined through the presence of substantial β-SKIE, as hyperconjugative stabilisation weakens bonds to β-hydrogens, and this conjugative effect is lesser for compounds possessing β-deuterium atoms (Figure 3.28b).[19]

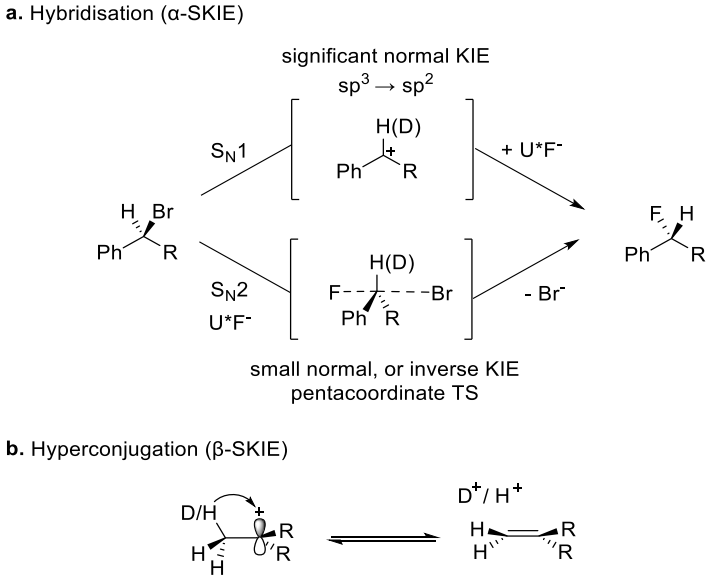

Figure 3.28: Mechanistic scenarios of substitution with fluoride showing a. changes in hybridisation which would give rise to a α-SKIE; b. Hyperconjugation effect which gives rise to β-SKIE

Accordingly, two deuterated substrates **1a-*d*$_1$** and **1a-*d*$_3$** were synthesised to allow for the measurement of both an α- and β- SKIE for fluorination. Moreover, the subjection of **1a-*d*$_3$** would also allow for the observation of a α-PKIE for the competitive elimination pathway. The deuterated substrates were prepared following literature procedures and isolated in good yields (Scheme 3.8).

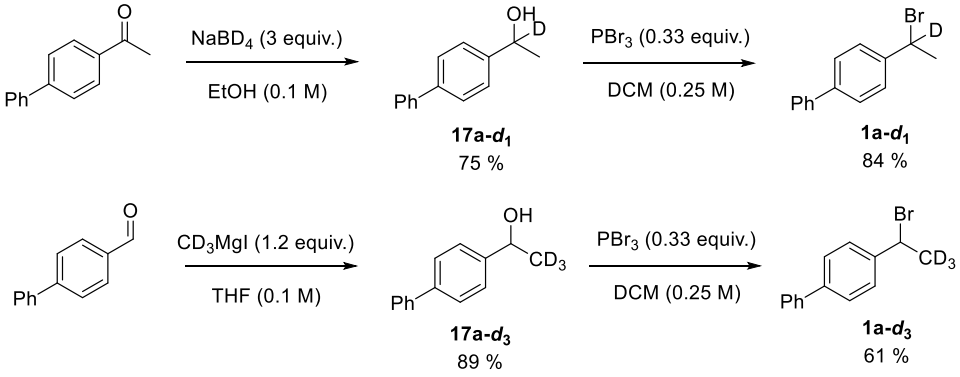

Scheme 3.8: Synthesis of deuterated substrates **1a-*d*$_1$** and **1a-*d*$_3$**

3.4.3. Design of Experimental Set-up

The heterogeneous nature of reactions performed under S-HBPTC required careful consideration of reaction set-up for kinetic analysis. An experiment was designed whereby a single reaction could be performed and multiple datapoints collected over an extended period of time. *In situ* spectroscopic analysis *via* NMR spectroscopy was desired, considering that performing *ex situ* parallel reactions could introduce experimental error and involve laborious set up and cost considering the amount of material required. Furthermore, a method which allowed for sufficient continuous mixing or agitation of solid KF within an NMR tube without manual manipulation was required (e.g. removing magnetic stirrers).

An experiment was devised based on 'periodic activation'.[21] Considering the importance of KF agitation for reactivity under S-HBPTC it was rationalised that a reaction could be performed within an NMR tube which is continuously rotated using a mechanical motor and halted upon the removal of this external stimulus. This approach is distinct and intrinsically more reproducible than an *ex situ* time course where individual experiments are sequentially quenched (e.g. KF is removed from the system

by filtration) as the reaction can be resumed directly after analysis through resubjecting the NMR tube to rotation (Scheme 3.9).[21]

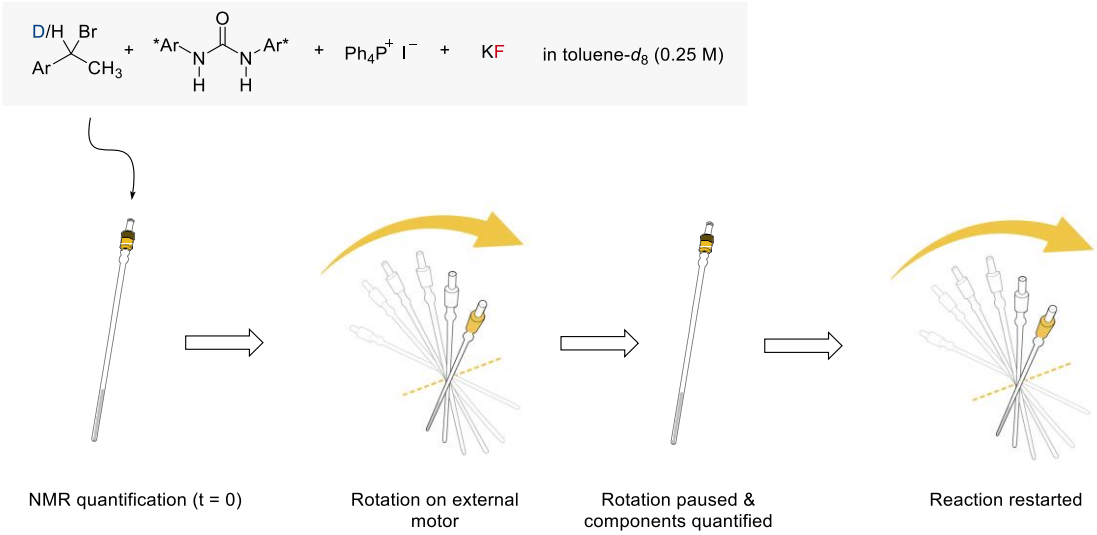

Scheme 3.9: Proposed reaction set up for periodic monitoring *via* rotation of an NMR tube

KIEs were determined through an intermolecular competition experiments where the proteo- and deutero- substrate were present in the same vessel and KIEs could be estimated from the relative concentrations of products formed.[22] This method has advantages over performing parallel reactions of proteo- and deutero- substrates, considering that both substrates are subjected to identical conditions eliminating the risk of unintentional errors in set up.

3.4.4. Results and Discussion

α- and β-SKIEs were determined *via* competition experiments between **1a** and **1a-*d*$_1$** and **1a** and **1a-*d*$_3$** with (*S*)-**3a** and $Ph_4P^+ I^-$ as catalysts. Following the initial quantification of the substrates, catalysts and KF were added to the NMR tube which was fastened onto the external motor and inverted continuously. The concentration of substrates and products were determined by quantitative ^{1}H and ^{19}F NMR. Spectroscopic analysis of the reaction of **1a** and **1a-*d*$_1$** allowed for the identification of fluoride (**2a** and **2a-*d*$_1$**) and elimination (**4a** and **4a-*d*$_1$**) products as well as iodide species (**5a** and **5a-*d*$_1$**),

employing 4-fluoroanisole as an internal standard (IS). Representative examples of spectra at the initial timepoint and 70 % conversion are shown in Figure 3.29.

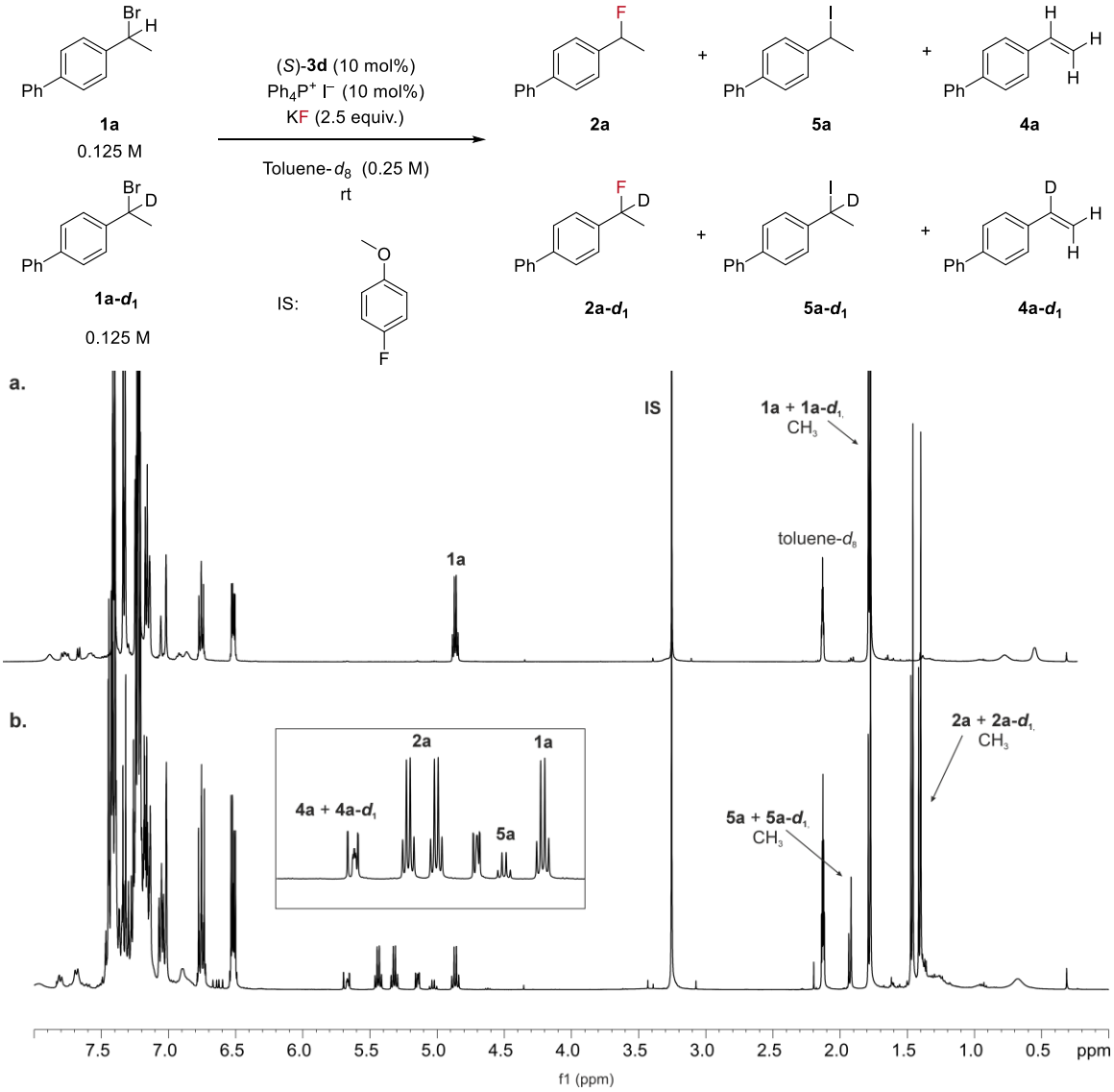

Figure 3.29: Typical ^{1}H NMR spectra of the reaction mixture a. before starting of the reaction; b. at 70% conversion

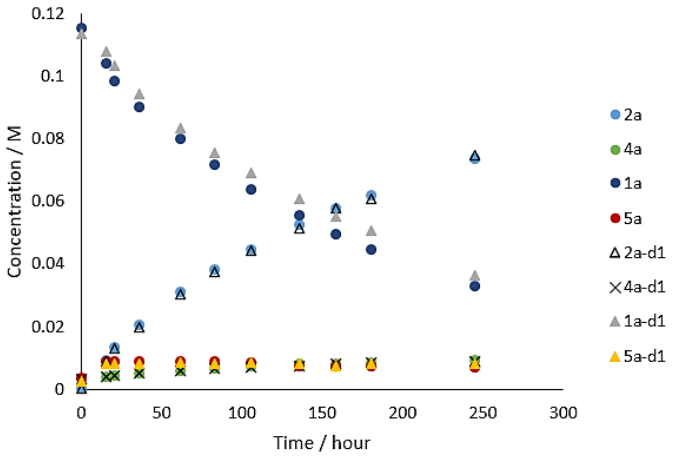

Figure 3.30: Kinetic profile of the competition experiment between **1a** and **1a-*d*$_1$**

Temporal concentration data demonstrated that the benzylic bromide substrates (**1a, 1a-*d*$_1$**) were consumed with approximately pseudo first-order kinetics generating fluoride (**2a, 2a-*d*$_1$**) and elimination products (**4a, 4a-*d*$_1$**) in a constant ratio (Figure 3.30). This allowed for the rate constants (k_{obs}(H) and k_{obs}(D)) to be estimated considering $\ln([A_0]/[A_t]) = k_{obs}t$; where A_0 is the initial concentration of benzylic bromide, and A_t is the concentration of benzylic bromide at time *t*. This determined an overall net α-SKIE calculated from kH/kD as ~ 1.1. It is notable that this value was the same taking into account the combined concentration of benzylic bromide (**1a**, **1a-*d*$_1$**) and iodide (**5a**, **5a-*d*$_1$**), which both may act as potential starting materials generating fluorination and elimination products (*v. infra 4.9.2.1. Calculation of Competition α-SKIE*).

An analogous competition reaction was performed for the β-SKIE, following the conversion of substrates **1a** and **1a-*d*$_3$** into products (fluorides: **2a**, **2a-*d*$_3$**, iodides: **5a**, **5a-*d*$_3$**, elimination: **4a**, **4a-*d*$_2$**). The concentration of species was followed spectroscopically (^{1}H and ^{19}F quantification) employing 1,2,3-trifluoroanisole as the IS. The signal corresponding to the vinylic proton of elimination products **4a** and **4a-*d*$_2$**, suffered from substantial overlap with the aromatic region of the spectra, and required regional baseline correction and deconvolution to allow for accurate quantification. Examples of spectra obtained from initial timepoints and at 90 % conversion can be seen in Figure 3.31. The consumption of **1a** and **1a-*d*$_3$** also followed pseudo first-order kinetics allowing for a net β-SKIE to be calculated as ~1.2 (Figure 3.32) (*v. infra 4.9.2.2. Calculation of Competition β-SKIE).*

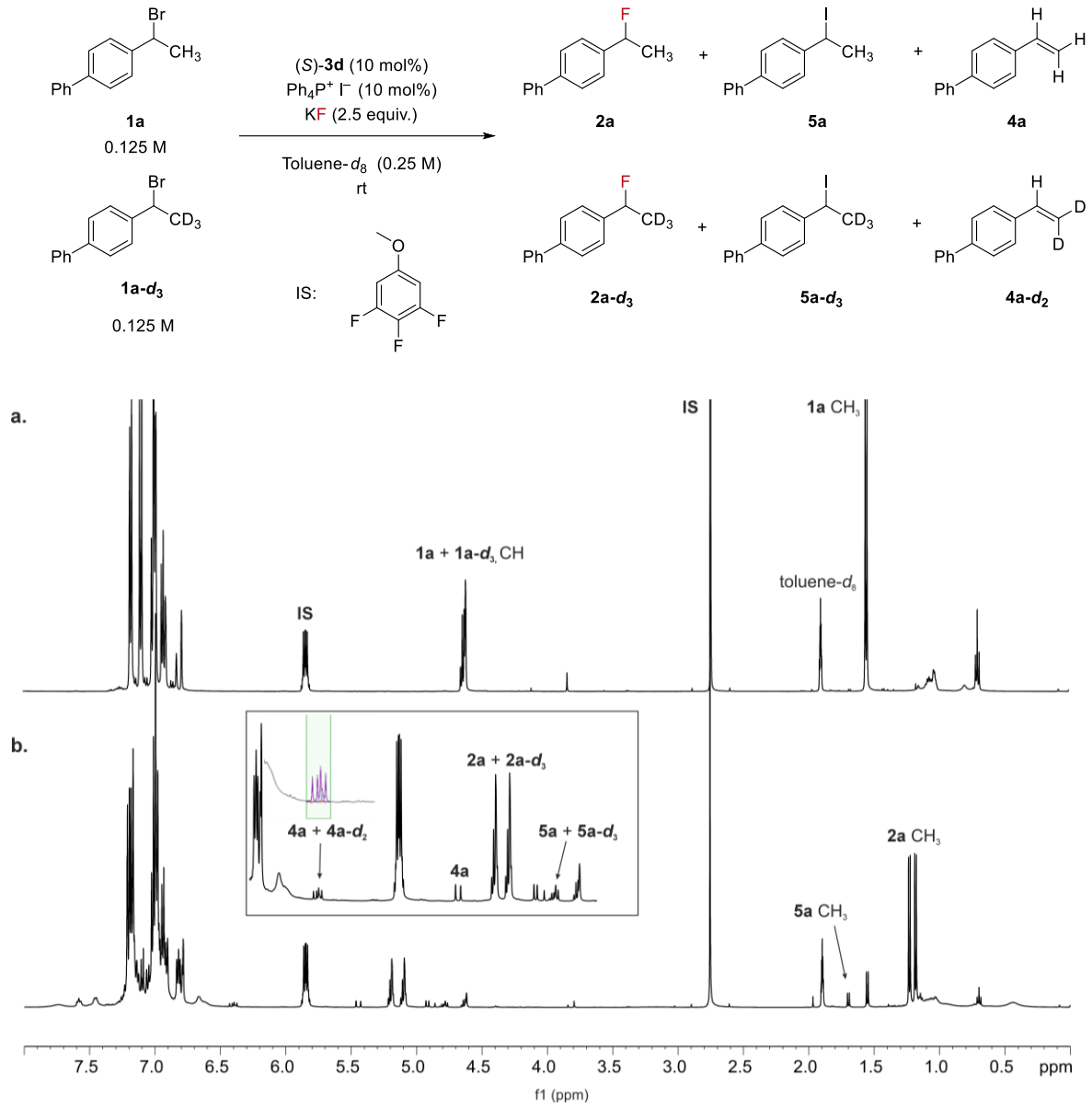

Figure 3.31: Typical ^{1}H NMR spectra of the reaction mixture a. before starting of the reaction; b. at 90% conversion

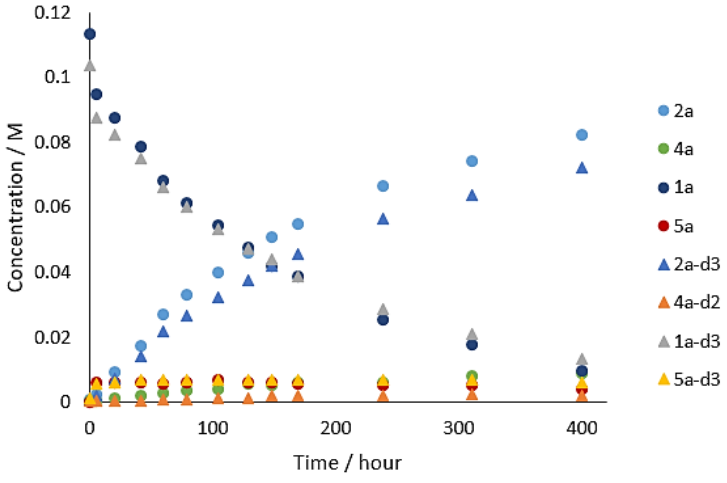

Figure 3.32: Kinetic profile of the competition experiment between **1a** and **1a-*d*$_3$**

The partitioning observed between fluorination and elimination was constant over the course of the reaction in both experiments (α- and β-SKIE), allowing for individual KIEs for fluorination and elimination to be estimated as α-SKIE ≈ 1.1, β-SKIE ≈ 1.1 (for fluoride addition), and β-SKIE ≈ 1.2, α-PKIE ≈ 3.0 (for elimination) (Figure 3.33 and 3.34).

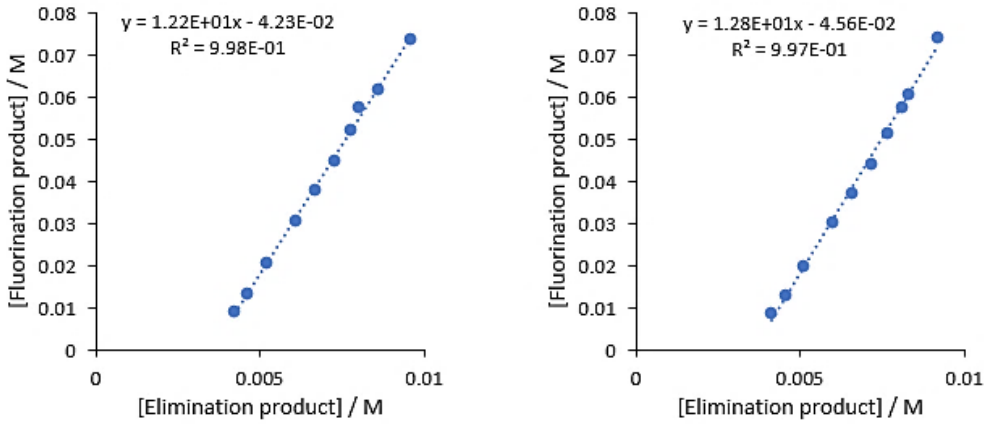

Figure 3.33: Partitioning between fluorination and elimination in α-SKIE experiment, left proteo components (**2a**/**4a**) right deutero components (**2a**-d_1/**4a**-d_1)

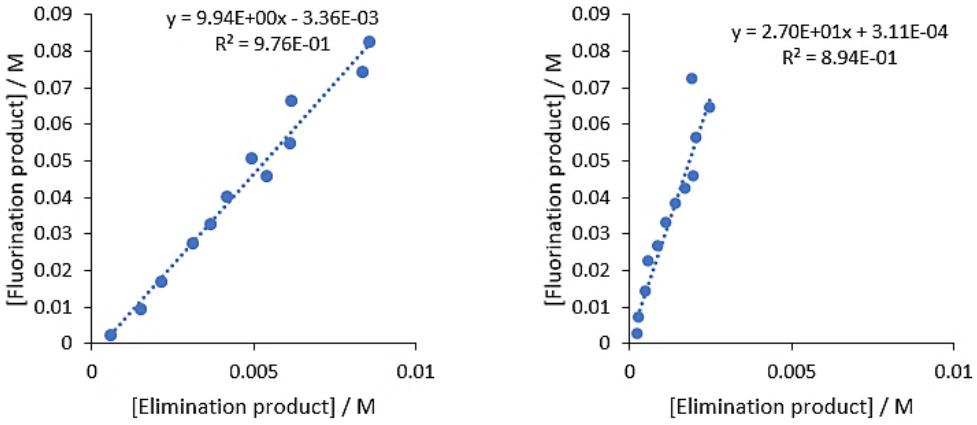

Figure 3.34: Partitioning between fluorination and elimination in β-SKIE experiment, left proteo components (**2a**/**4a**) right deutero components (**2a**-d_3/**4a**-d_3)

3.4.5. Kinetic Isotope Effect Employing TBAF as Fluoride Source

The homogenous fluorination of the benzylic substrate with TBAF in DCM-d_2 was performed to have a comparative datapoint to the β-SKIE measured for fluorination under S-HBPTC with KF. DCM was selected as the solvent for this experiment considering the insolubility of TBAF in toluene, which

prohibited accurate quantification. The periodic monitoring set-up was not required for this homogeneous reaction, as convection within the NMR tube allowed for the reaction to progress and measurements to be taken inside the spectrometer over 15 hours. Here, a fluorine-tagged substrate **1b** and **1b-*d*$_3$** was utilised, and all components were monitored exclusively by means of ^{19}F NMR analysis (Scheme 3.10).

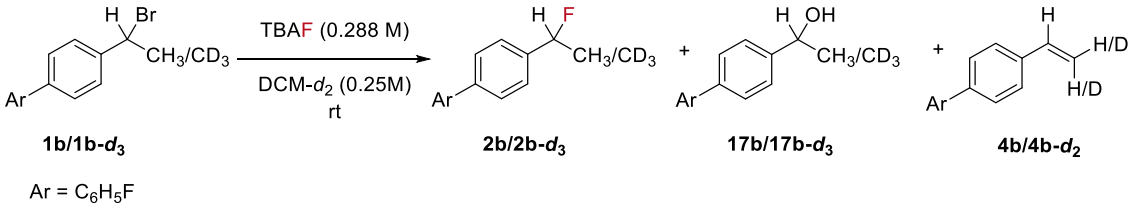

Scheme 3.10: Competition experiment of **1b**/**1b-*d*$_3$** with TBAF as a soluble fluoride source

Notably during the reaction, the formation of benzylic secondary alcohols **17b** and **17b-*d*$_3$** were observed and their identities were confirmed through spiking the NMR tube with authentic references. Furthermore, unlike the previous KIE experiments performed on S-HBPTC reactions, the decay of the substrates (**1b** and **1b-*d*$_3$**) for this homogeneous reaction did not correspond to simple first-order decay and the net KIE was calculated to be 1.93 (*v. infra 4.9.2.3. Calculation of Competition β-SKIE (TBAF)*).[23] Individual KIEs for fluorination and elimination were estimated here as ~1.5 and 5.8 respectively, higher than those for the β-SKIE calculated for fluorination under heterogeneous conditions with KF and catalysts ((*S*)-**3a** and $Ph_4P^+ I^-$) in toluene.

3.4.6. Summary of Results

In conclusion the KIEs measured for the fluorination of the benzylic substrate **1a** under S-HBPTC do not support significant ionisation or charge separation which would be indicative of carbocation formation, with the conclusion that they are more consistent with an S_N2-like process. In contrast a significantly higher β-SKIE value was measured for the fluorination of **1b** under the homogeneous conditions employing TBAF·3H_2O as a fluorinating reagent in DCM. This value is more consistent with an S_N1 mechanism which is further corroborated the generation of alcohols **17b**/**17b-*d*$_3$** likely formed by the

addition of water into a benzylic carbocation (Scheme 3.11). While PKIE values for the elimination product under the heterogeneous (S-HBPTC) and homogeneous (TBAF) systems are not directly comparable, due to differences in solvents and potential bases (KF or TBAOH), the consistent partitioning between fluorination and elimination in both systems suggests that both products arise from a common intermediate (or substrate). Therefore, as data for fluorinations performed under S-HBPTC is interpreted as S_N2-like, and data for fluorination with TBAF under homogeneous conditions as S_N1, the elimination products follow E2 and E1 pathways respectively.

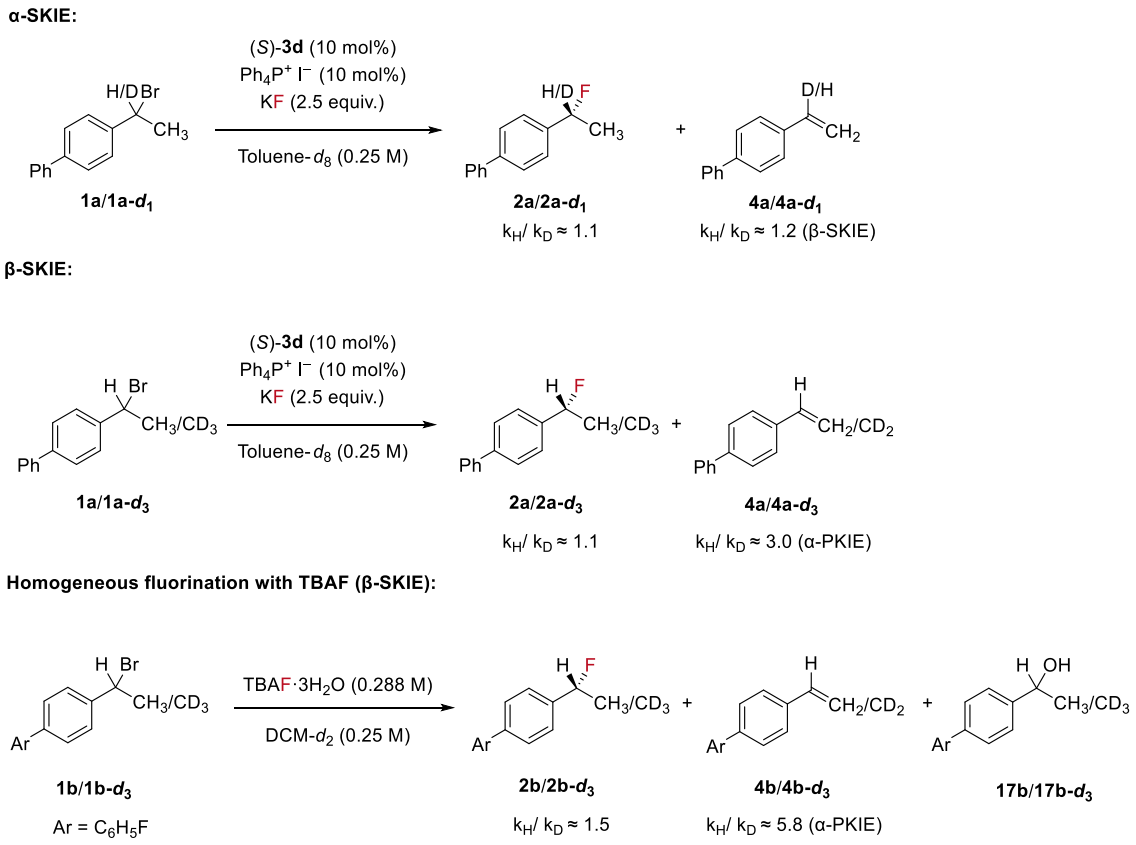

Scheme 3.11: Overview of KIE data

3.5. Mechanistic Investigations into Enantioconvergence

3.5.1 Introduction to Enantioconvergent Nucleophilic Substitution Reactions

Enantioconvergent substitution reactions which involve the simultaneous or consecutive departure of a leaving group and formation of a C–Nu bond, represent a powerful strategy in the synthesis of

enantiopure products, as they overcome the inherently low yields obtained from kinetic resolutions (KR) or chiral separation processes (Figure 3.35).[24] While organocatalytic enantioselective addition reactions of prochiral electrophiles have been extensively studied, nucleophilic substitutions of racemic electrophiles have received comparatively little attention.[25]

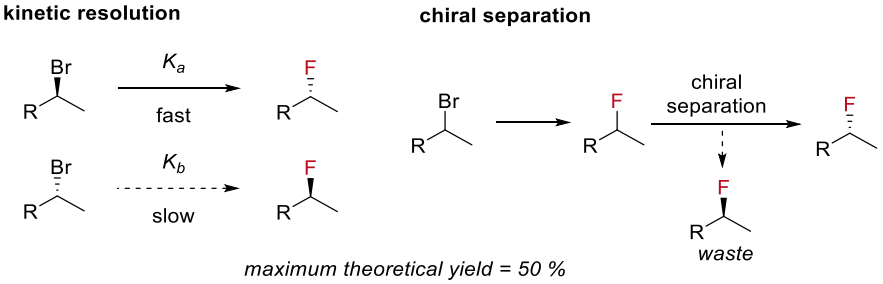

Figure 3.35: Preparation of single enantiomers *via* kinetic resolution, or chiral separation

Several mechanistic scenarios have been reported which achieve enantioconvergence nucleophilic substitutions, these include: (i) the generation of stabilised achiral cationic intermediates (e.g. carbocations, onium ions) which undergo enantioselective substitution by nucleophiles, (ii) the *in-situ* de-racemisation of substrates through dynamic processes, where interconversion of substrate enantiomers is faster than nucleophilic substitution (e.g. Dynamic Kinetic Resolution (DKR)), (iii) the formation of achiral intermediates under more unconventional approaches including halogenophilic or radical mechanisms which are merged with photoredox and/or transition metal catalysis.[26-28]

3.5.2.1. Generation of Achiral Cationic Intermediates

In the context of enantioconvergent processes employing organocatalysts, the generation of achiral cationic intermediates including onium cations or carbocations have been reported by the groups of Toste, Jacobsen and List. Critical to the control of stereoselectivity is developing strategies to establish efficient stabilisation of these reactive intermediates. The introduction of sulfur functionality on electrophile structure to stabilise cationic intermediates by means of neighbouring group participations (NGP) was first reported by Toste and co-workers and later by Jacobsen. Here, activation of substrates by organocatalysts generates *meso*-episulfonium electrophiles, which following

desymmetrisation by nucleophiles has provided a platform for the synthesis of enantiopure C–Nu bonds. Nucleophiles which were employed in these seminal works, included alcohols and indoles, forming corresponding addition products in excellent yields and enantioselectivities (up to 99 %, 95% *ee*) (Scheme 3.12).[29, 30]

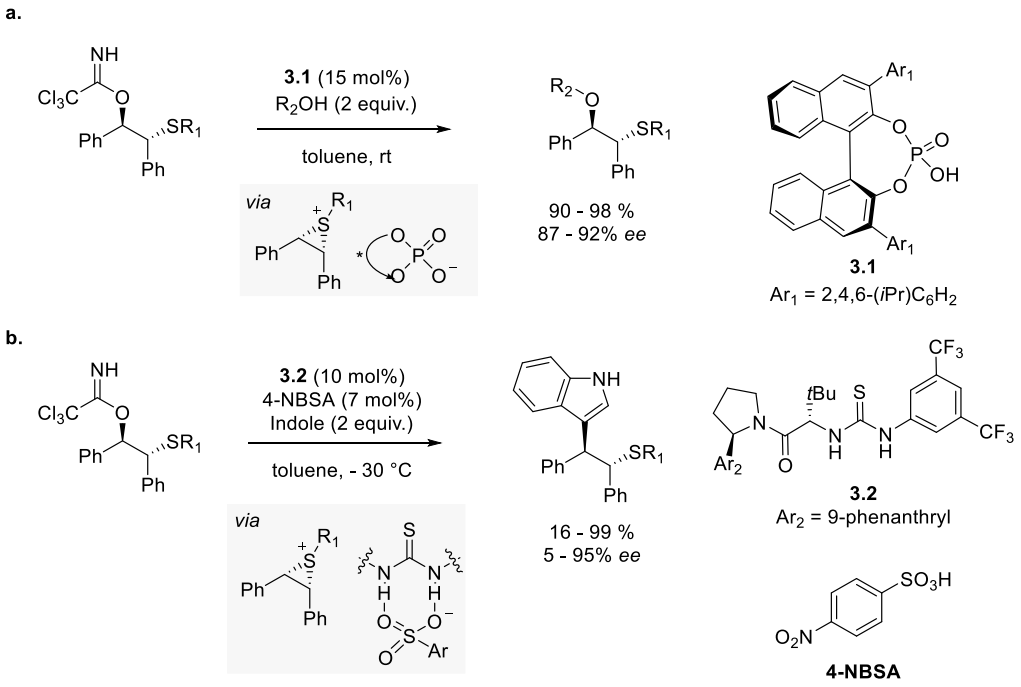

Scheme 3.12: Enantioconvergent nucleophilic substitution of *in situ* formed *meso*-episulfonium salts by a. Toste and co-workers; b. Jacobsen and co-workers

Jacobsen and co-workers further investigated the stereocontrol of non-heteroatom stabilised carbocations reporting an enantioconvergent S_N1 process of racemic propargyl acetates with allyltrimethylsilane.[31] Here, a chiral hydrogen-bond donor catalyst **3.3**, in combination with a strong Lewis acid (TMSOTf) generated a prochiral carbocation, which, held within a chiral environment, could be trapped by an allyl nucleophile, yielding quaternary stereocentres in excellent yields and enantioselectivities (up to 95 %, 98% *ee*) (Scheme 3.13a).

More recently, List and co-workers achieved a series of asymmetric S_N1 substitution reactions proceeding through highly reactive secondary benzylic carbocations held within the chiral pocket of an imidadiphosphorimidate (IDPi) catalyst **3.4**. This platform was initially shown amenable for the

conversion of secondary trichloroacetimidates with acetic acid as the nucleophile, giving desired products in up to 85 % yield and 92% *ee*. Minor modifications on the IDPi catalyst also allowed for the conversion of racemic trichloroacetimidate or acetate starting materials to fashion enantioenriched C–N and C–C bonds in up to 96 % yield and 92 % *ee* (Scheme 3.13b).[32]

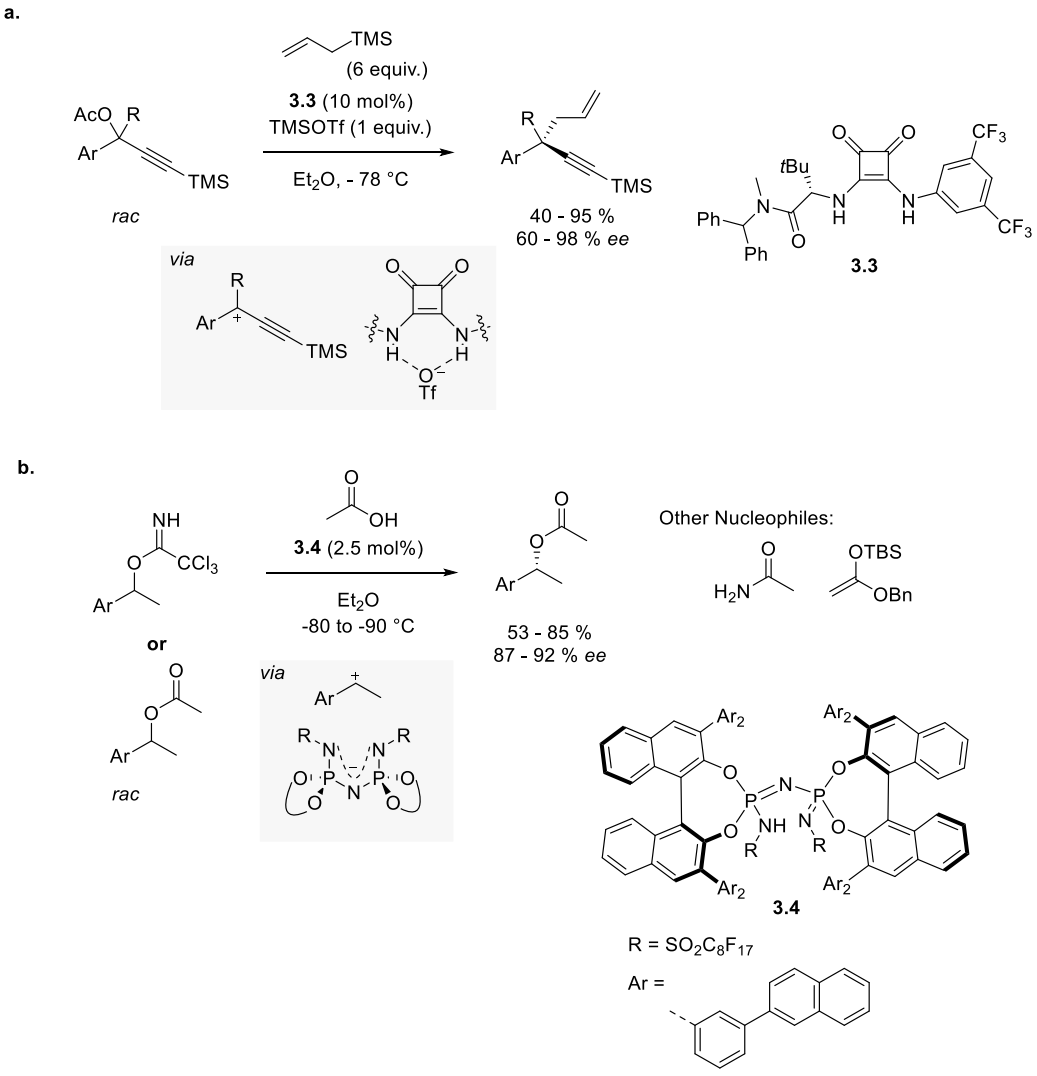

Scheme 3.13: Enantioconvergent nucleophilic substitution *via* S_N1 substitution by a. Jacobsen and co-workers; b. List and co-workers

3.5.2.2. Dynamic Kinetic Resolution Processes

Sun and co-workers reported an enantioconvergent S_N2 chlorination of α-ketosulfonium salts under a liquid-liquid phase transfer mechanism employing thiourea catalyst **3.6**, which yielded α-chloroketones in high yields and enantioselectivity (up to 96 %, 92% *ee*). Enantioconvergence was

achieved within this system considering the labile chirality of the α-proton on the bespoke sulfonium substrate **3.5** which underwent facile enolization. The lability of the α-proton was demonstrated by its deuteration upon addition of D_2O to the substrate, by virtue of rapid proton-deuterium exchange (Scheme 3.14).[33]

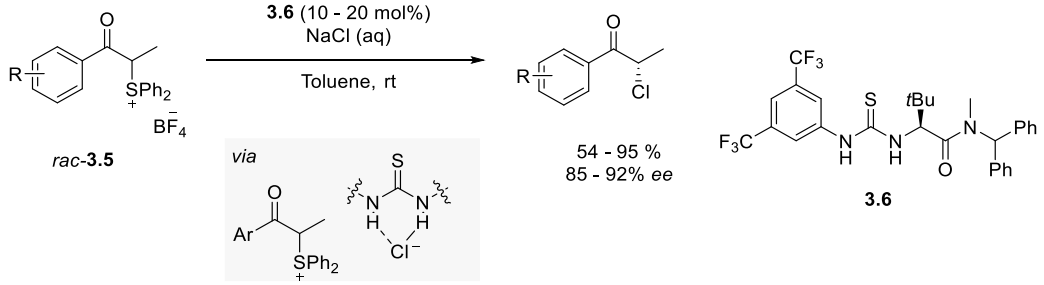

Scheme 3.14: Enantioconvergent S_N2 chlorination of α-ketosulfonium salts under DKR mechanism by Sun and co-workers

3.5.2.3. Halogenophilic S_N2X

An example of a more mechanistically distinct enantioconvergent process was reported by Lee, Tan and co-workers who described a halogenophilic nucleophilic S_N2X substitution.[34] Here, the nucleophile (thiocarboxylate or azide) interacts with the halogen leaving group on the substrate (tertiary alkyl bromide) to generate an electrophilic Nu–X species and a carbanion. This carbanion, held in an ion pair with a chiral cationic catalyst **3.8**, displaces the halogen from Nu–X species yielding an enantioenriched C–Nu bond. The occurrence of an S_N2X mechanism, rather than an S_N2 attack onto the tertiary bromide, was validated through experimental controls and further supported by DFT calculations (Scheme 3.15).

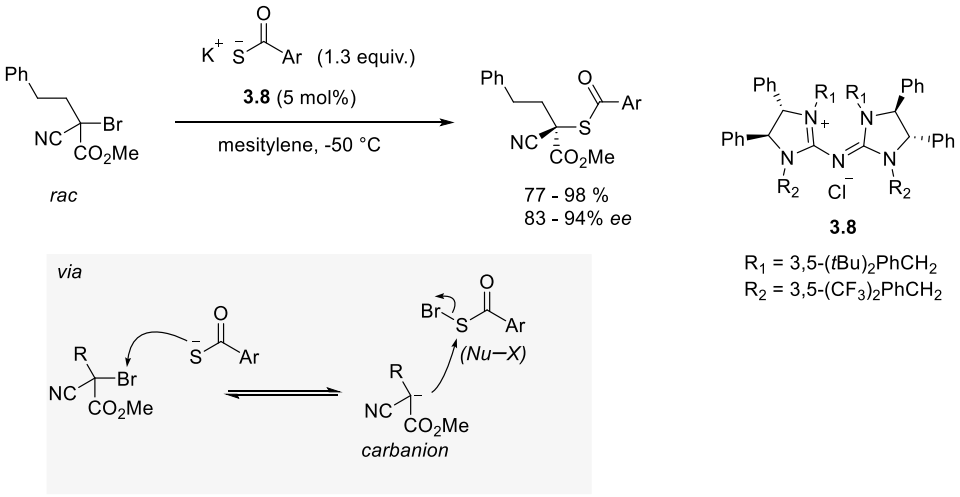

Scheme 3.15: Enantioconvergent nucleophilic substitution with thiocarboxylate nucleophile *via* S_N2X mechanism by Lee, Tan and co-workers

3.5.2. Monitoring Enantiomeric Ratios Over Time

The KIE studies performed on benzylic substrate **1a** indicated the likelihood of an S_N2 process for the fluorination of racemic electrophiles under S-HBPTC, discouraging the formation of an achiral carbocationic intermediate. Therefore, to achieve the high yields of fluorinated product observed at good enantioselectivity, efficient racemisation of substrates must occur. Whilst KIEs and accurate kinetic curves were constructed and determined through the *in situ* NMR experiments (*v. 3.4. Kinetics*), no information regarding the enantiomeric excess of either the fluoride product **2a** or bromide starting material **1a** over the course of the reaction was obtained from these studies**.** Therefore, to investigate this, an *ex situ* time course was performed, where reactions were sequentially quenched, and enantiomeric ratios determined using HPLC.

Monitoring of the reaction of bromide **1a** to fluorinated product **2a** demonstrated that the enantiomeric ratio of fluorinated product **2a** remained constant over reaction progression and the enantiomeric ratio of subtrate **1a** remained near racemic (51:49 e.r.) until final timepoints where some enantioenrichment was observed (~ 6% *ee*). These data suggest that the interconversion of the enantiomers of bromide **1a** occurred at a faster rate than fluorination, indicated by the stable enantiomeric ratio of the fluoride product (Table 3.5, Figure 3.36).

Table 3.5: *Ex situ* monitoring of the enantiomeric ratio of **1a** and **2a** over reaction time-course

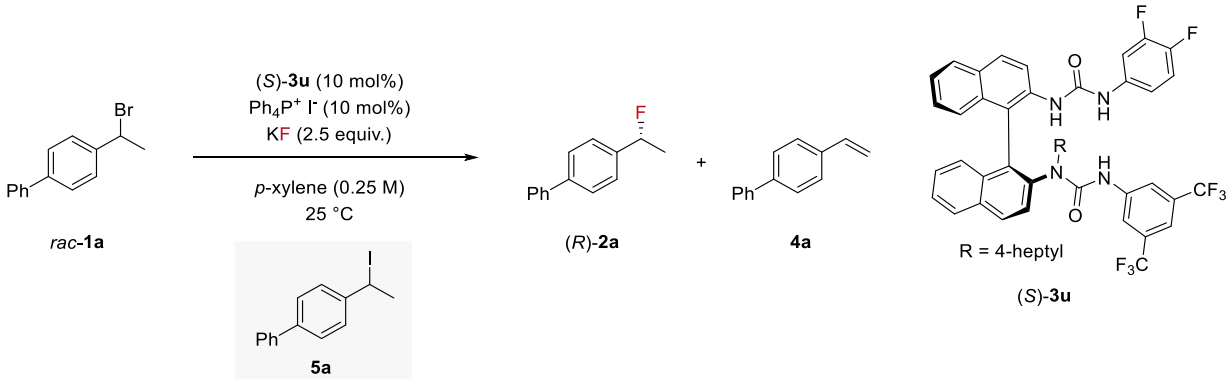

Entry	Time (h)	**2a** (%)[a]	**1a** (%)[a]	**5a** (%)[a]	**4a** (%)[a]	**2a** e.r.[b]	**1a** e.r.[b]
1	1	2	88	7	0	91:9	51:49
2	2	4	86	6	1	91:9	51:49
3	4	10	72	7	1	91:9	50:50
4	8	22	59	7	2	91:9	51:49
5	24	39	41	6	3	91:9	52:48
6	48	56	30	7	5	90.5:9.5	53:47
7	72	75	3	5	6	91:9	nd

General conditions: Substrate (0.05 mmol), urea catalyst (10 mol%), $Ph_4P^+ I^-$ (10 mol%), and KF (2.5 equiv.) in 200 µL of *p*-xylene stirred at 1200 rpm [a]Determined by ^1H and/or ^{19}F NMR using 4-fluoroanisole as internal standard, [b]e.r. was determined by HPLC analysis using a chiral stationary phase. nd = not determined

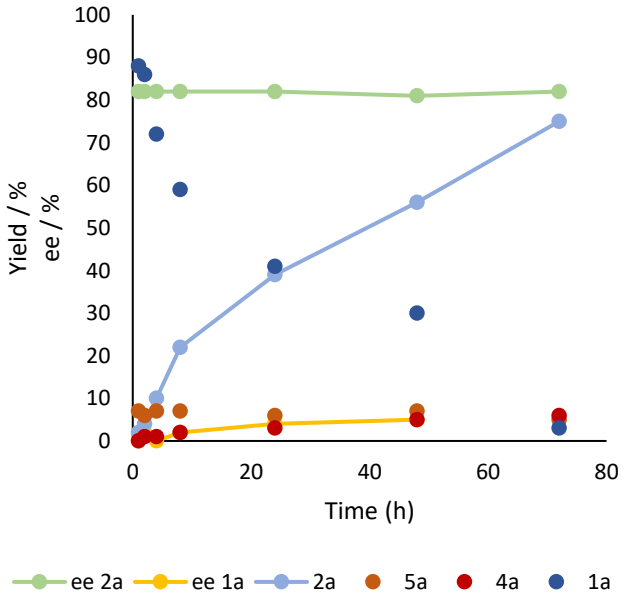

Figure 3.36: Graphical representation of reaction components and enantioselectivity over reaction time-course

The enantiomeric ratios over time for the reaction of bromide **1q** to fluoride **2q** were also investigated to validate whether the data obtained for **1a** was consistent across different benzylic scaffolds, particularly those where fluorinated products were isolated in lower yields and enantioselectivities. Analogously to previous data, the enantiomeric ratio of **2q** remained constant (87:13 e.r.) over the course of the reaction and the enantiomeric ratio of **1q** remained near racemic, with slight enantioenrichment observed at final timepoints (Table 3.6, Figure 3.37). These data suggest that the lower enantioselectivity measured for the fluorination of benzylic bromide **1q** was not the result of a kinetic resolution (KR) due to inefficient substrate racemisation, but more likely to stem from less-favourable catalyst-substrate interactions and enantiodiscrimination of this scaffold.

Table 3.6: *Ex situ* monitoring of the enantiomeric ratio of **1q** and **2q** over reaction time-course

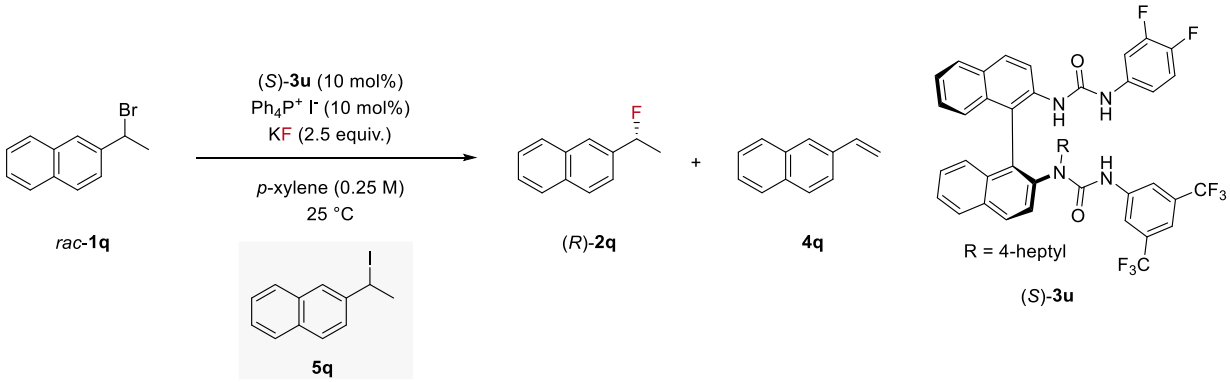

Entry	Time (h)	**2q** (%)[a]	**1q** (%)[a]	**5q** (%)[a]	**4q** (%)[a]	**2q e.r.**[b]	**1q** e.r.[b]
1	1	1	92	6	0	87:13	50:50
2	4	4	89	8	1	87:13	51:49
3	8	10	84	8	1	87:13	52:48
4	24	24	66	8	3	87:13	52:48
5	48	42	50	8	4	87:13	53:47
6	72	59	35	8	5	87:13	53:47
7	120	73	14	7	5	87:13	54:46

General conditions: Substrate (0.05 mmol), urea catalyst (10 mol%), $Ph_4P^+ I^-$ (10 mol%), and KF (2.5 equiv.) in 200 µL of *p*-xylene stirred at 1200 rpm [a]Determined by ^1H and/or ^{19}F NMR using 4-fluoroanisole as internal standard, [b]e.r. was determined by HPLC analysis using a chiral stationary phase.

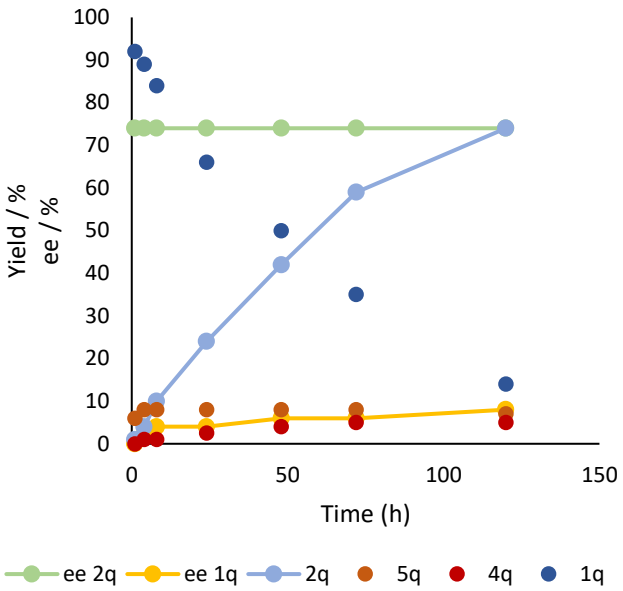

Figure 3.37: Graphical representation of reaction components and enantioselectivity over reaction time-course

Ex-situ reaction monitoring was also performed for the fluorination of α-bromoketone **12a**, which demonstrated that the enantiomeric ratio of the bromide starting material remained near racemic over the course of the reaction and the enantiomeric ratio of the product **13a** remained stable (Table 3.7, Figure 3.38). Once more these data suggest that the interconversion of bromide enantiomers occurs at a faster rate than subsequent fluorination, allowing for enantioconvergence of the starting material into the fluorinated product.

Table 3.7: *Ex situ* monitoring of the enantiomeric ratio of **1q** and **2q** over reaction time-course

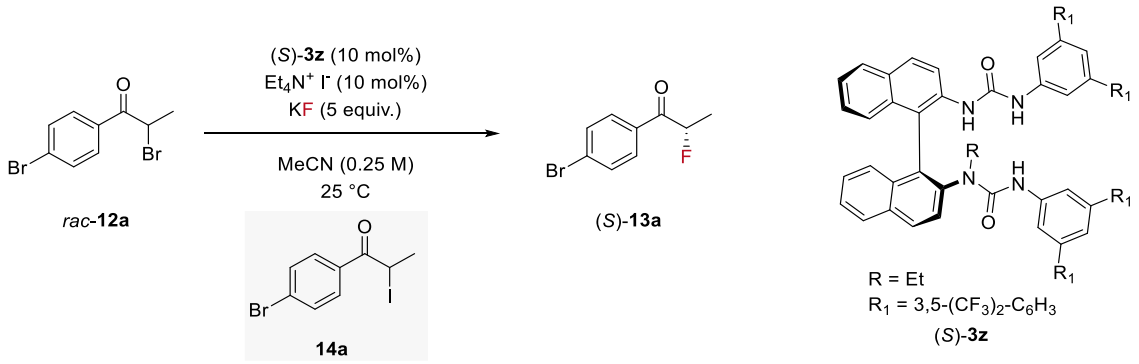

Entry	Time (h)	**13q** (%)[a]	**12a** (%)[a]	**14a** (%)[a]	**10a e.r.**[b]	**9a** e.r.[b]
1	1	6	81	10	92:8	50:50
2	2	10	76	10	93:7	51:49
3	4	15	71	10	92:8	52:48
4	6	19	70	10	92:8	52:48
5	8	26	60	10	92:8	53:47
6	24	65	20	10	92:8	54:46

General conditions: Substrate (0.05 mmol), urea catalyst (10 mol%), $Et_4N^+ I^-$ (10 mol%), and KF (5 equiv.) in 200 µL of MeCN stirred at 1200 rpm [a]Determined by ^1H and/or ^{19}F NMR using 4-fluoroanisole as internal standard, [b]e.r. was determined by HPLC analysis using a chiral stationary phase.

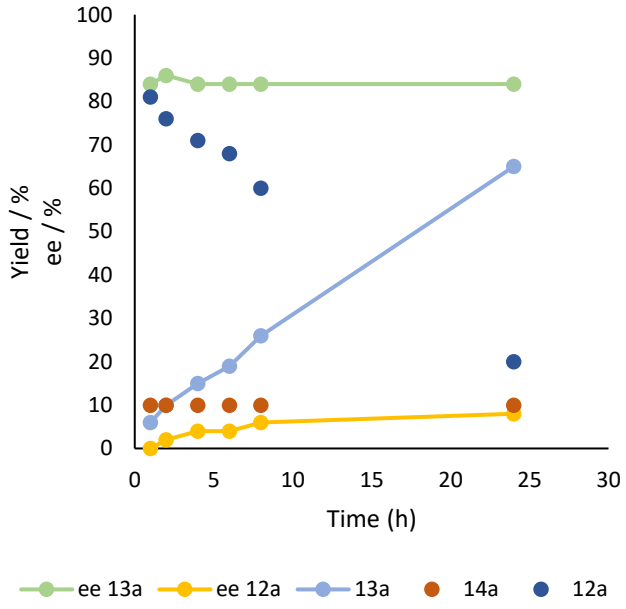

Figure 3.38: Graphical representation of reaction components and enantioselectivity over reaction time-course

The stability of both fluorinated products, benzylic (**2a**) and α-fluoroketone (**13a**), were further validated through their subjection to the standard reaction conditions. In both cases upon measuring the enantiomeric ratio, no racemisation was observed, and no further reactivity or degradation was seen by NMR spectroscopy (Scheme 3.16).

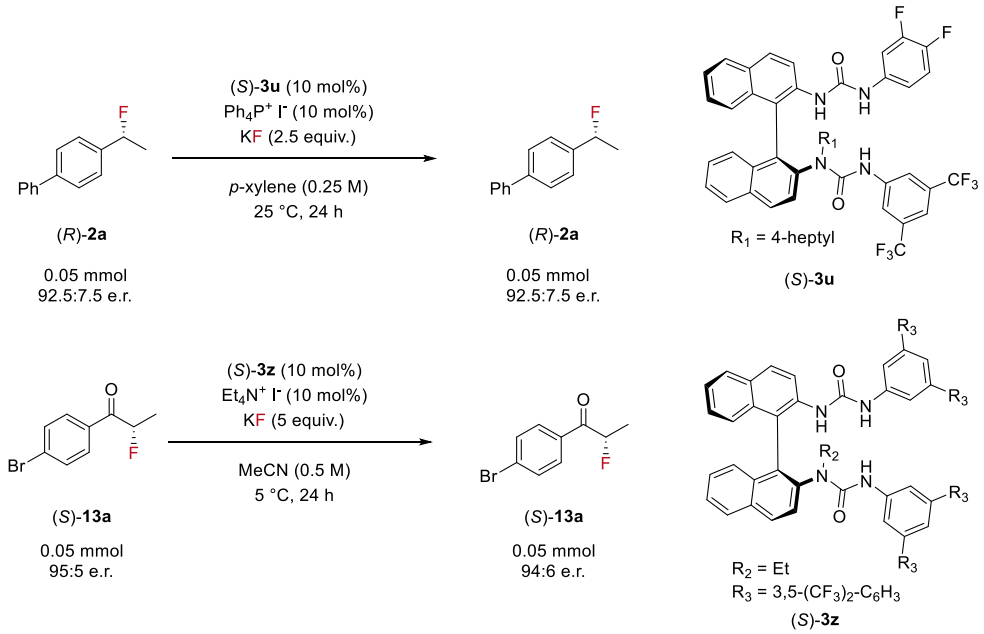

Scheme 3.16: Subjection of fluorinated products (**2a** and **13a**) to the reaction conditions.

3.5.3. Racemisation of Enantioenriched Substrate

Studies investigating the enantiomeric ratios over the time course of the reaction provided evidence that there is efficient interconversion of substrate enantiomers under the standard reaction conditions of S-HBPTC (**1a**, **1q**, **12a**). This eliminates the occurrence of a kinetic resolution (KR) process, where the theoretical yield of desired enantiomer of product cannot exceed 50 % (Figure 3.39a). These data however, do not provide insight into mechanism or pathways of interconversion of the substrate enantiomers. Specifically, the objective was to determine whether substrate enantiomers undergo independent racemisation which would denote a classical dynamic kinetic resolution (DKR) (Figure 3.39b), or whether catalyst participation aids the interconversion of enantiomers through diastereomeric intermediates, which would be considered a dynamic kinetic asymmetric transformation (DYKAT) (Figure 3.39c).

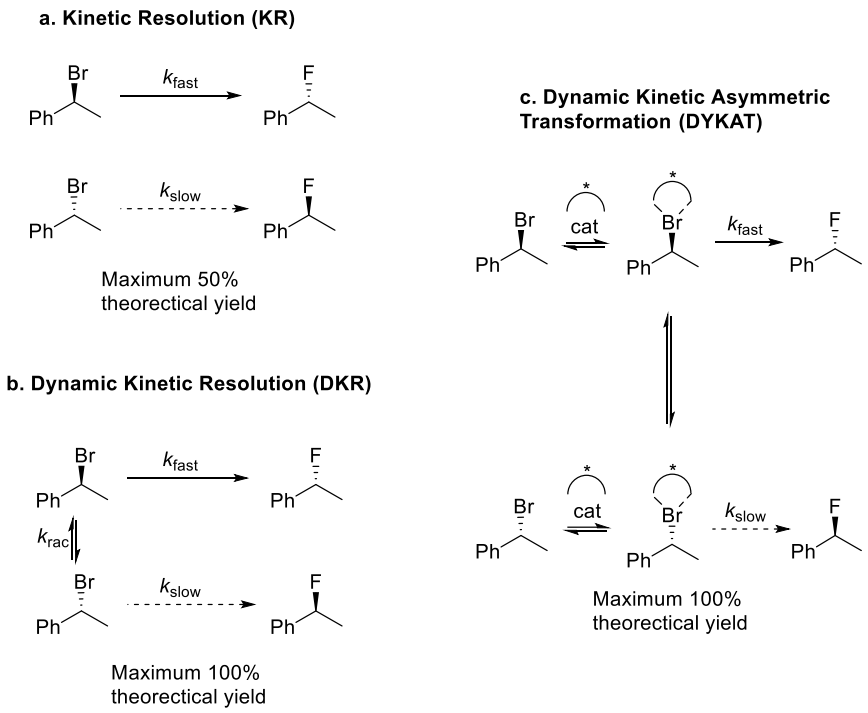

Figure 3.39: Possible mechanisms of enantioinduction a. KR; b. DKR; c. DYKAT processes

3.5.3.1. Synthesis of Enantioenriched Substrate

To perform control reactions investigating the racemisation of the substrate and the mechanism of enantioconvergence, an enantioenriched sample of **1a** was prepared following a two-step procedure. Suzuki-Miyaura cross-coupling of commercially available chiral alcohol (*R*)-4-bromo-α-methylbenzyl alcohol (**17am**) and phenylboronic acid provided enantiopure (*R*)-**17a** in 70 % yield. Deoxybromination of (*R*)-**17a** following a literature procedure provided an enantioenriched sample of bromide **1a**, in 63:37 e.r. (Scheme 3.17).[35]

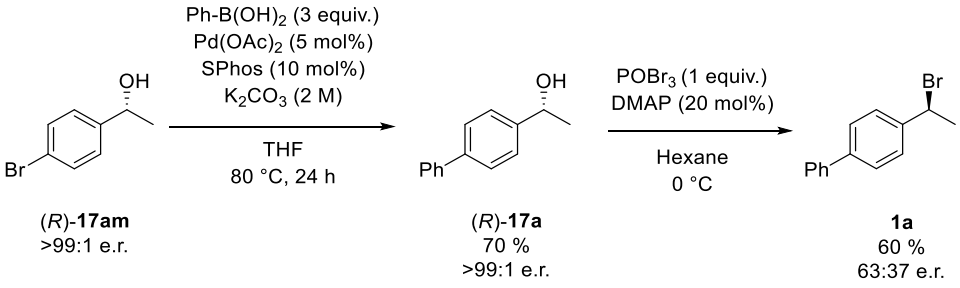

Scheme 3.17: Synthesis of enantioenriched sample of (*S*)-**1a**

The enantioenriched sample of **1a** was subjected to a series of control experiments whereby individual components of the reaction were added, and the enantiomeric ratio of **1a** was re-measured after a specified time. No racemisation of the enantioenriched sample of **1a** was detected in the absence of catalysts under the standard concentration of reactions (Scheme 3.18a). In contrast, racemisation of **1a** was observed upon the addition of urea catalyst (*S*)-**3k** (10 mol%) where a diminished enantiomeric ratio of 48:52 was measured after 24 hours (Scheme 3.18b). It is notable that racemisation was also observed, albeit to a lesser extent, when **1a** was subject to only to $Ph_4P^+ I^-$ (10 mol%) with a lower enantiomeric ratio measured after 24 h of 60.5:39.5 (Scheme 3.18c). Finally, when both (*S*)-**3k** and $Ph_4P^+ I^-$ were present in the reaction mixture full erosion of enantiomeric ratio was observed (50:50 e.r.), and the formation of a small amount of iodide **5a** was also detected by NMR and HPLC (Scheme 3.18d).

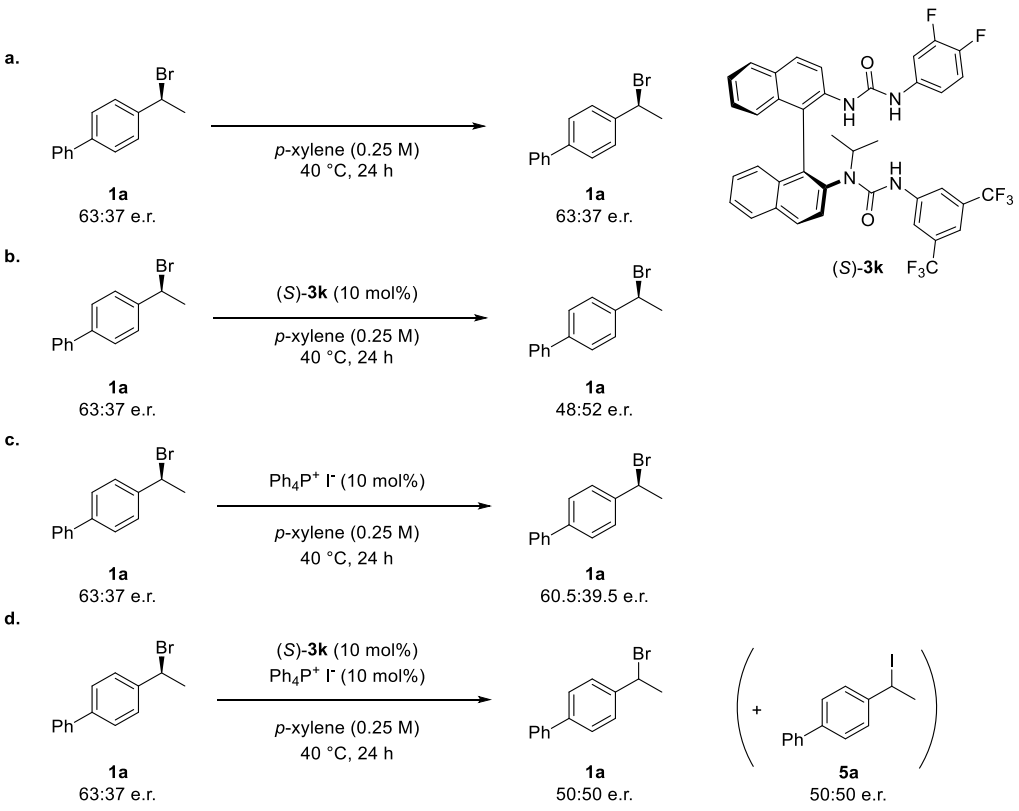

Scheme 3.18: Control reactions performed with enantioenriched bromide substrate **1a**

These data suggest that the interconversion of enantiomers of **1a** rely on the intervention of catalysts and primarily the urea HBD catalyst (**3k**). Therefore, fluorination of benzylic bromides under S-HBPTC is most appropriately denoted as a dynamic kinetic asymmetric transformation (DYKAT) since it involves the equilibration of diastereomeric (rather than enantiomeric) intermediates.[24]

3.5.4. Non-linear Effect Studies

Studying the relationship between the enantioselectivity of the product and the enantiopurity of the chiral catalyst is a classical experiment performed in enantioselective catalysis to elucidate reaction mechanism.[36] The detection of a non-linear relationship between product and chiral catalyst can indicate the presence of multiple chiral species in the enantiodetermining transition state, and therefore is critical to perform prior to initiating TS analysis. Scalemic mixtures of catalyst **3u** were prepared by diluting enantiopure (*S*)-**3u** with a racemic sample. These mixtures were dissolved in a small quantity of DCM and evaporated to dryness to ensure homogeneity. The enantiomeric ratio of catalyst batches were varied between 0–100 % *ee* and their enantiopurity was determined by chiral HPLC. The fluorination of **1a** was performed with different scalemic mixtures of **3u** and the enantioselectivity of product **2a** recorded. The enantioselectivity of **2a**, expressed as % *ee,* was seen to positively correlate in a linear relationship with the enantiopurity of the catalyst **3u**, thus suggesting that a single molecule of chiral catalyst is present in the enantiodetermining transition state (Table 3.8, Figure 3.40).

Table 3.8: Non-linear effect study for the fluorination of **1a** with catalyst **3u**

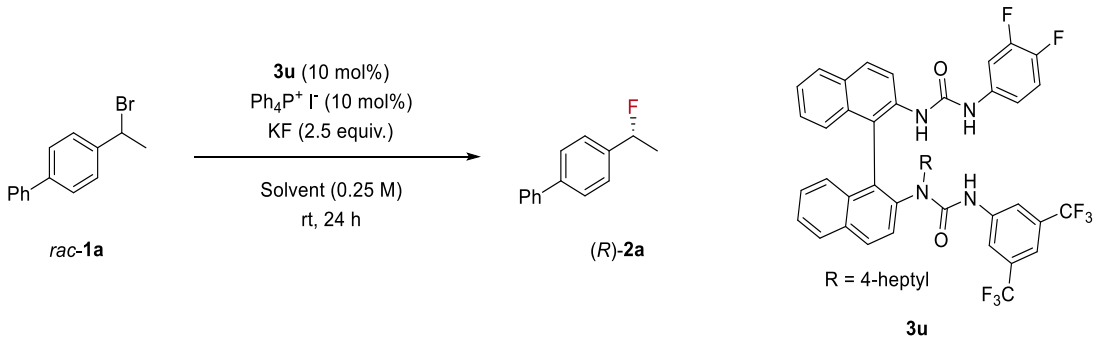

Entry	% *ee* catalyst **3u**	% *ee* product **2a**
1	0	0
2	21.5	18.2
3	39.7	38.3
4	60.1	58.7
5	79.6	70.5
6	100	82.0

Scalemic mixtures of catalyst **3u** were prepared by mixing (*S*)-**3u** with (*rac*)-**3u**, dissolving in DCM and evaporating to dryness. The enantiopurity of each catalyst batch was determined by chiral HPLC

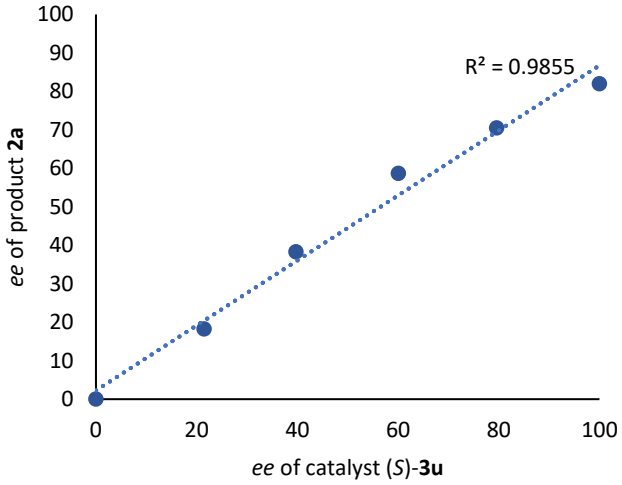

Figure 3.40: Graphical plot of enantiopurity of **2a** vs **3u**

An analogous study was also performed for the fluorination of α-bromoketone substrate **12a** employing batches of urea HBD catalyst **3d** varied between 5–100 % *ee*. Here, the enantiopurity of fluorinated product **13a** was also shown to correlate with the enantiopurity of the urea catalyst, again

consistent with a single molecule of chiral catalyst being involved in the enantiodetermining transition state (Table 3.9, Figure 3.41).

Table 3.9: Non-linear effect study for the fluorination of **12a** with catalyst **3d**

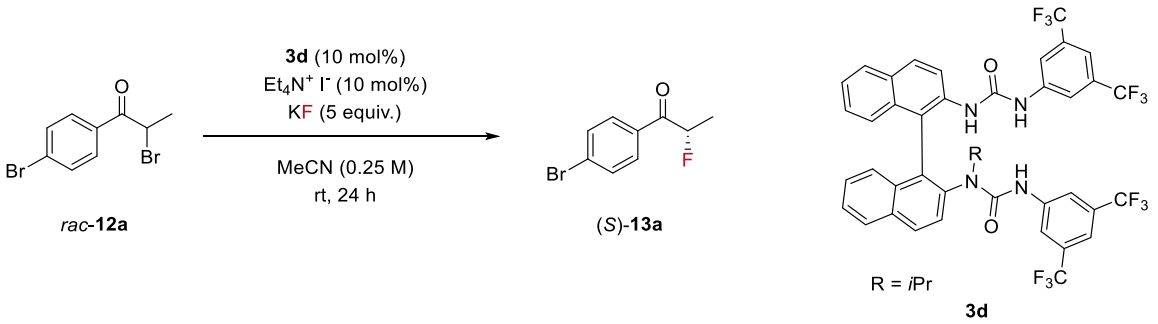

Entry	% *ee* catalyst **3d**	% *ee* product **13a**
1	5.0	4.1
2	41.1	23.0
3	59.4	29.2
4	80.3	40.1
5	100	50.5

Scalemic mixtures of catalyst **3d** were prepared by mixing (*S*)-**3d** with (*rac*)-**3d**, dissolving in CH_2Cl_2 and evaporating to dryness. The enantiopurity of each catalyst batch was determined by chiral HPLC.

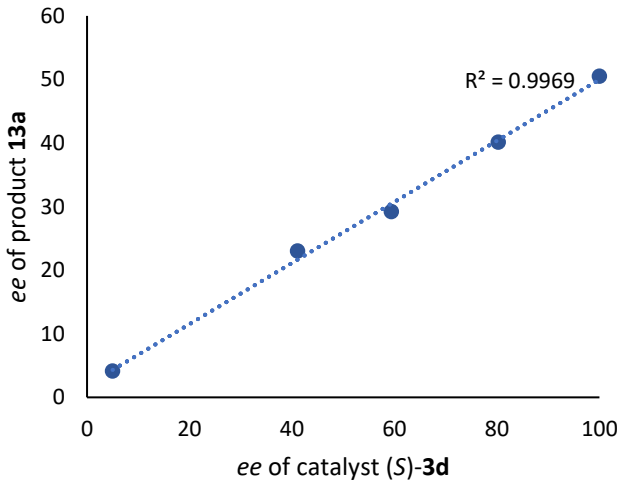

Figure 3.41: Graphical plot of enantiopurity of **13a** vs **3d**

3.5.5. Transition State Analyses

The diastereomeric transition state (TS) structures leading to the major and minor enantiomer of the fluorinated product **2a** with urea-fluoride complex derived from (*S*)-**3k** were optimised using DFT calculations to gain insight into the origin of enantioselectivity. TS analysis predicted the activation free energies leading to the formation of (*R*)-**2a** and (*S*)-**2a** as 81.7 and 88.9 kJ mol^{-1} respectively from **1a**, which provided a predicted enantioselectivity of 91:9 at 25 °C. This data is in good agreement with selectivity and absolute configuration of the fluorinated products achieved with catalyst (*S*)-**3k** under S-HBPTC. In both TSs, the stabilisation of the benzylic substrate occurred through weak, dispersion dominated interactions with the urea-motif and stabilising π–π interactions were observed between the aryl rings of the *bis*-urea structure. A notable difference between the two TS is the presence of a strong, direct C–H–π interaction between the benzylic proton on the substrate to the BINAM backbone of catalyst (*S*)-**3k**. For the major TS, this C–H–π interaction is short and direct (2.47 Å), whereas in the minor TS, the methyl group of the substrate is directed towards the backbone, with C–H–π distances of 3.30 Å. This important non-covalent interaction is thought to be responsible for the energetic difference ($\Delta\Delta G^{\ddagger}$) in TSs, differentiating the enantiomers of the bromide substrate for fluorination (Figure 3.42a).

Diastereomeric TSs were also calculated considering the benzylic iodide **5a**, which is formed *in situ*, as a substrate for fluorination. This predicted the activation free energies for the formation of (*R*)-**2a** and (*S*)-**2a** as 68.9 and 77.6 kJ mol^{-1} respectively, consistent with experimental data and lower than those calculated from bromide **1a** (~ 10 kJ mol^{-1}). The energy difference ($\Delta\Delta G^{\ddagger}$) between the major and minor pathways is similar considering both leaving groups, with the (*R*) enantiomer of the fluoride product favoured in all cases (7.2 kJ mol^{-1} when X = Br, and 8.7 kJ mol^{-1} when X = I). Catalyst-substrate non-covalent interactions were similar independent of leaving group, with the major TS presenting a stronger C–H–π interaction to the backbone of catalyst (*S*)-**3k** (Figure 3.24b).

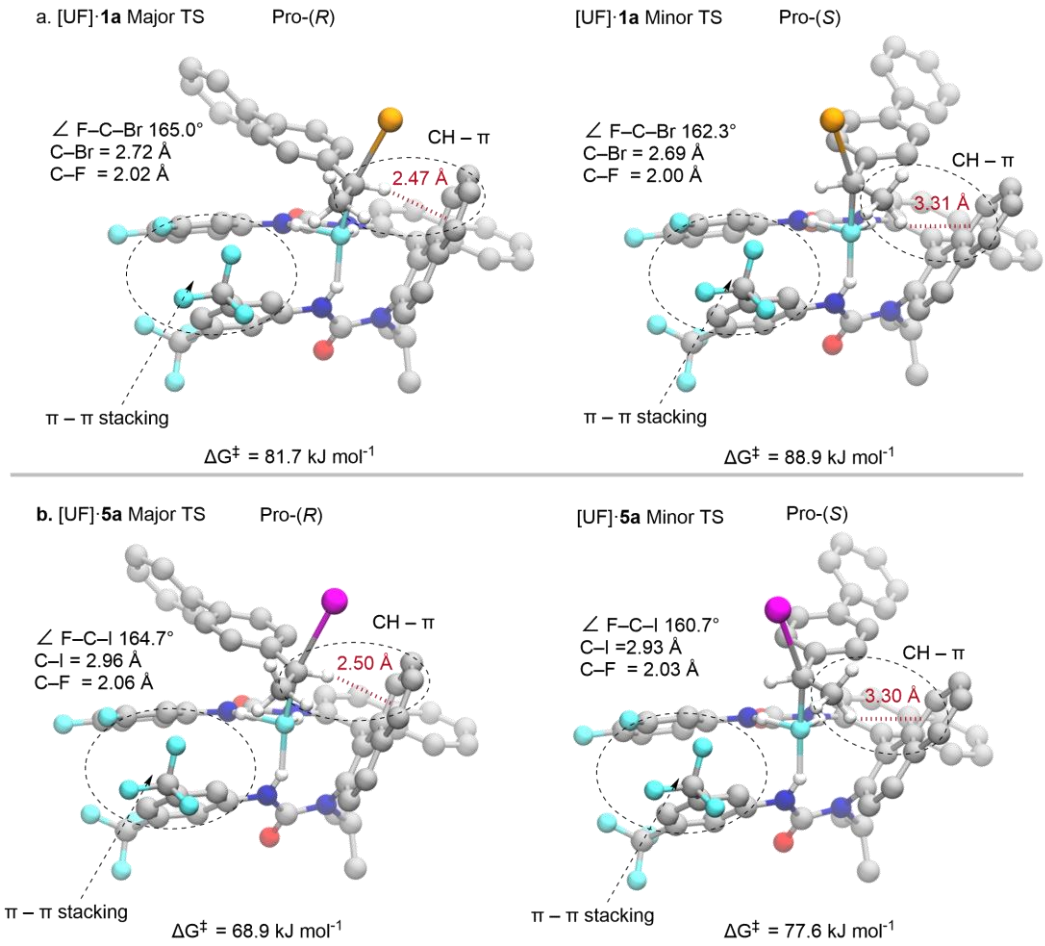

Figure 3.42: Major and minor TS computed using DFT calculation for a. substitution of the bromide substrate **1a**; b. substitution of the iodide substrate **5a** (Computational work performed by Dr. Christopher Goult and Professor Robert Paton)

3.6. Conclusions and Implications on Catalysis

Herein is described the mechanistic study performed to gain insights on the enantioconvergent fluorination of alkyl halides under S-HBPTC. A series of experiments were designed in order to answer key questions on this novel catalytic manifold, including the role of both catalysts, mode of fluoride substitution, and the mechanism allowing enantioconvergence.

Spectroscopic NMR investigations provided compelling evidence that the solubilisation of KF relies on the interaction of both the urea HBD catalyst and onium co-catalyst, forming a singular and stable urea-phosphonium-fluoride [UPF] species. Key evidence for complex formation between urea catalyst (**3u**), onium salt (**8i**) and the fluoride anion included the detection of hydrogen bond correlations between the urea NH protons and fluoride, characterised through scalar coupling constants ($^{1h}J_{NHc\cdots F^-}$ = 51, $^{1h}J_{NHa\cdots F^-}$ = 57 and $^{1h}J_{NHb\cdots F^-}$ = 31 Hz). Fluoride solubilisation was further observed within ^{19}F NMR as a broad singlet (-74.2 ppm) and this signal was used to probe through space correlations between the fluoride anion and proton resonances of the urea HBD catalyst and phosphonium cation demonstrating the close nature of the ion-pair formed. Furthermore, UPF complexes were shown to be capable fluorinating reagents allowing for the conversion of bromide substrates into products.

Together mechanistic investigations, undertaken primarily on the benzylic bromide substrate class, suggested a catalytic cycle that involves initial halogen exchange between the bromide and phosphonium iodide (Ph_4P^+ I^-) facilitated by the urea HBD catalyst (**3u**) forming an iodide species (**5**) and a urea-phosphonium-bromide [UPBr] complex. Ion metathesis between UPBr and KF occurs to form the key urea-phosphonium-fluoride [UPF] complex and KBr. It is notable that the phase-transfer of KF is spectroscopically observed from UPBr complexes, however not from corresponding urea-phosphonium-iodide [UPI] complex, which is rationalised considering that the precipitation of KBr may serve as an important thermodynamic driving force for ion metathesis. Fluoride delivery from UPF species is thought to substitute either bromide **1** or iodide **5** *via* an S_N2-like pathway generating the enantioenriched fluoride product **2** irreversibly, regenerating both catalysts (**3u** and Ph_4P^+ Br^- or Ph_4P

I^-) (Figure 3.43). Extensive investigations indicated that urea HBD catalyst participated in, and allowed, for efficient substrate racemisation, subsequently aiding enantioconvergence through a DYKAT mechanism. Moreover, TS analysis demonstrated the presence of favourable interactions between benzylic substrates and urea-fluoride complexes which allow for enantiodiscrimination between substrate enantiomers, forming fluoride products in high enantioselectivity.

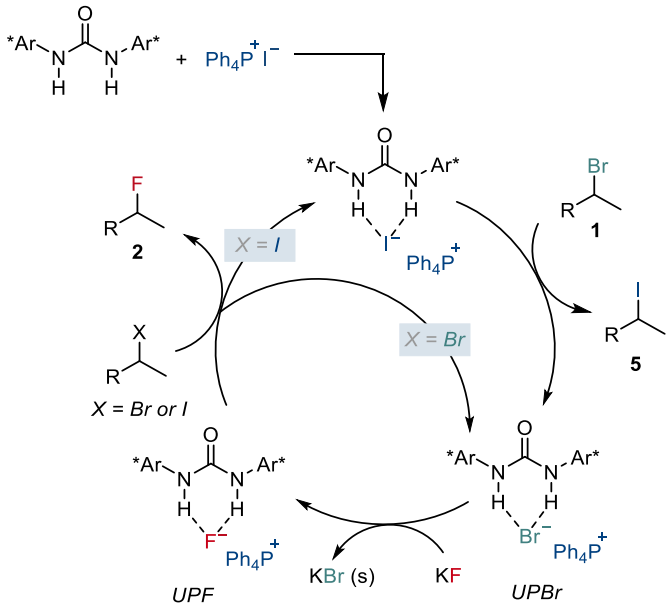

Figure 3.43: Proposed catalytic cycle for S-HBPTC

The information gained in this study represents a significant synthetic advance for the construction of enantioenriched benzylic fluorides and α-fluoroketones with KF, an industrially relevant reagent considering its low cost, abundance, and favourable safety profile. Moreover, from a fundamental perspective this study demonstrates the feasibly of applying the principles of HBPTC beyond the remits of ion-pairing between urea-fluoride species and cationic electrophiles. Here, onium halides served to fulfil the ion-pairing requirements permitting the solubilisation of KF as stabilised UPF species, which have been shown to fluorinate neutral electrophiles. It is hoped that this information gained on fluoride solubilisation by urea HBD catalysts and concept of synergistic catalysis will offer new opportunities to further expand the scope of enantioenriched alkyl fluorides that can be accessed directly using KF.

3.7. References

(1) Ibba, F.; Pupo, G.; Thompson, A. L.; Brown, J. M.; Claridge, T. D. W.; Gouverneur, V. Impact of Multiple Hydrogen Bonds with Fluoride on Catalysis: Insight from NMR Spectroscopy. *J. Am. Chem. Soc.* **2020**, *142* (46), 19731–19744.
(2) Roagna, G.; Ascough, D. M. H.; Ibba, F.; Vicini, A. C.; Fontana, A.; Christensen, K. E.; Peschiulli, A.; Oehlrich, D.; Misale, A.; Trabanco, A. A.; Paton, R. S.; Pupo, G.; Gouverneur, V. Hydrogen Bonding Phase-Transfer Catalysis with Ionic Reactants: Enantioselective Synthesis of γ-Fluoroamines. *J. Am. Chem. Soc.* **2020**, *142* (33), 14045–14051.
(3) Imrie, C.; Modro, T.; Rohwer, E.; Wagener, C. Photolysis of (Arylmethyl)triphenylphosphonium Salts - Substituent, Counterion, and Solvent Efects on Reaction-Products. *J. Org. Chem.* **1993**, *58* (21), 5643–5649.
(4) Wenzel, T.; Wilcox, J. Chiral Reagents for the Determination of Enantiomeric excess and Absolute Configuration Using NMR Spectroscopy. *Chirality* **2003**, *15* (3), 256–270.
(5) Enthart, A.; Freudenberger, J. C.; Furrer, J.; Kessler, H.; Luy, B. The CLIP/CLAP-HSQC: Pure Absorptive Spectra for the Measurement of One-Bond Couplings. *J. Magn. Reson.* **2008**, *192* (2), 314–322.
(6) Yu, C.; Levy, G. C. Two-Dimensional Heteronuclear NOE (HOESY) Experiments - Investigation of Dipolar Interactions Between Heteronuclei and Nearby Protons. *J. Am. Chem. Soc.* **1984**, *106* (22), 6533–6537.
(7) Claridge, T. D. W. *High-Resolution NMR Techniques in Organic Chemistry.* Elsevier Science & Technology, 2016.
(8) Pfeifer, L.; Engle, K.; Pidgeon, G.; Sparkes, H.; Thompson, A.; Brown, J.; Gouverneur, V. Hydrogen-Bonded Homoleptic Fluoride-Diarylurea Complexes: Structure, Reactivity, and Coordinating Power. *J. Am. Chem. Soc.* **2016**, *138* (40), 13314–13325.
(9) Iribarren, I.; Mates-Torres, E.; Trujillo, C. Revisiting Ion-Pair Interactions in Phase Transfer Catalysis: from Ionic Compounds to Real Catalyst Systems. *Dalton Trans.* **2024**, *53* (3), 1322–1335.
(10) Pupo, G.; Ibba, F.; Ascough, D. M. H.; Vicini, A. C.; Ricci, P.; Christensen, K. E.; Pfeifer, L.; Morphy, J. R.; Brown, J. M.; Paton, R. S.; Gouverneur, V. Asymmetric Nucleophilic Fluorination under Hydrogen Bonding Phase-Transfer Catalysis. *Science* **2018**, *360* (6389), 638–642.
(11) Ibba, F. Hydrogen Bonding Phase-Transfer Catalysis:A New Approach to Asymmetric Fluorination. DPhil Thesis, University of Oxford, 2020.
(12) Ascough, D. M. H. Novel Fluorination Methodology Through Computational Insight – Tuning Fluoride Through Hydrogen Bonding. DPhil Thesis, University of Oxford, 2019.
(13) Hamlin, T.; Swart, M.; Bickelhaupt, F. Nucleophilic Substitution S_N2: Dependence on Nucleophile, Leaving Group, Central Atom, Substituents, and Solvent. *ChemPhysChem* **2018**, *19* (11), 1315–1330.
(14) Bandgar, B.; Sadavarte, V.; Uppalla, L. An Expedient and Highly Selective Iodination of Alcohols Using a KI/BF_3·Et_2O System. *Tetrahedron Lett.* **2001**, *42* (5), 951–953.
(15) Kirsch, S.; Klahn, P.; Erhardt, H.; Kotthaus, A. The Synthesis of α-Azidoesters and Geminal Triazides. *Synthesis* **2014**, *46* (21), 147–149.
(16) Learner, R.; *CRC Handbook of Chemistry and Physics,* 84th Edition; Lide, D. R., Ed.; CRC Press, 2003.
(17) Lowry, T., H.; Richardson, K., S.; *Mechanism and Theory in Organic Chemistry*; Joanna Cotler Books, 1981.
(18) Dale, H. J. A.; Leach, A. G.; Lloyd-Jones, G. C. Heavy-Atom Kinetic Isotope Effects: Primary Interest or Zero Point? *J. Am. Chem. Soc.* **2021**, *143* (50), 21079–21099.
(19) Westaway, K. Determining Transition State Structure Using Kinetic Isotope Effects. *J. Label. Compd. Radiopharm.* **2007**, *50* (11–12), 989–1005.
(20) Kumar, A.; Mondal, S.; Sandeep; Venugopalan, P.; Kumar, A.; Banerjee, S. Destabilized Carbocations Caged in Water Microdroplets: Isolation and Real-Time Detection of α-Carbonyl Cation Intermediates. *J. Am. Chem. Soc.* **2022**, *144* (8), 3347–3352.

(21) Ben-Tal, Y.; Boaler, P. J.; Dale, H. J. A.; Dooley, R. E.; Fohn, N. A.; Gao, Y.; García-Domínguez, A.; Grant, K. M.; Hall, A. M. R.; Hayes, H. L. D.; Kucharski, M. M.; Wei, R.; Lloyd-Jones, G. C. Mechanistic Analysis by NMR Spectroscopy: A Users Guide. *Prog. Nucl. Magn. Reson. Spectrosc.* **2022**, 129, 28–106.
(22) Simmons, E.; Hartwig, J. On the Interpretation of Deuterium Kinetic Isotope Effects in C–H Bond Functionalizations by Transition-Metal Complexes. *Angew. Chem. Int. Ed.* **2012**, *51* (13), 3066–3072.
(23) Bigleisen, J.; Woldsberg, M. Theoretical and Experimental Aspects of Isotope Effects in Chemical Kinetics. *Adv. Chem. Phys.* **1958**, *1*, 15–76.
(24) Steinreiber, J.; Faber, K.; Griengl, H. De-racemization of Enantiomers versus De-epimerization of Diastereomers-Classification of Dynamic Kinetic Asymmetric Transformations (DYKAT). *Chem. Eur. J.* **2008**, *14* (27), 8060–8072.
(25) Kikuchi, J.; Terada, M. Enantioconvergent Substitution Reactions of Racemic Electrophiles by Organocatalysis. *Chem. Eur. J.* **2021**, *27* (40), 10215–10225.
(26) Bartoszewicz, A.; Matier, C.; Fu, G. Enantioconvergent Alkylations of Amines by Alkyl Electrophiles: Copper-Catalyzed Nucleophilic Substitutions of Racemic α-Halolactams by Indoles. *J. Am. Chem. Soc.* **2019**, *141* (37), 14864–14869.
(27) K Kainz, Q. M.; Matier, C. D.; Bartoszewicz, A.; Zultanski, S. L.; Peters, J. C.; Fu, G. C. Asymmetric Copper-Catalyzed C–N Cross-Couplings Induced by Visible Light. *Science* **2016**, *351* (6274), 681–684.
(28) Tian, Y.; Li, X.; Liu, J.; Cheng, J.; Gao, A.; Yang, N.; Li, Z.; Guo, K.; Zhang, W.; Wen, H.; Li, Z. L.; Gu, Q. S.; Hong, X.; Liu, X. Y. A general Copper-Catalysed Enantioconvergent C(sp^3)–S Cross-Coupling via Biomimetic Radical Homolytic Substitution. *Nat. Chem.* **2024**, *16* (3), 466–475.
(29) Hamilton, G.; Kanai, T.; Toste, F. Chiral Anion-Mediated Asymmetric Ring Opening of *meso*-Aziridinium and Episulfonium Ions. *J. Am. Chem. Soc.* **2008**, *130* (45), 14984–14986.
(30) Lin, S.; Jacobsen, E. Thiourea-Catalysed Ring Opening of Episulfonium Ions with Indole Derivatives by Means of Stabilizing Non-Covalent Interactions. *Nat. Chem.* **2012**, *4* (10), 817–824.
(31) Wendlandt, A. E.; Vangal, P.; Jacobsen, E. N. Quaternary Stereocentres via an Enantioconvergent Catalytic S_N1 Reaction. *Nature* **2018**, *556* (7702), 447–451.
(32) Singh, V. K.; Zhu, C.; Kanta De, C.; Leutzch, M.; Baldinelli, L.; Mitra, R.; Bistoni, G.; List, B. Taming Secondary Benzylic Cations in Catalytic Asymmetric S_N1 Reactions. *Science* **2023**, *382* (6668), 325–329.
(33) Li, Z. Y.; Wang, B. C.; Zhang, C. S.; Lo, W. Y.; Yang, L. L.; Sun, J. W. Catalytic Enantioselective Nucleophilic α-Chlorination of Ketones with NaCl. *J. Am. Chem. Soc.* **2024**, *146* (4), 2779–2788.
(34) Zhang, X.; Ren, J. Y.; Tan, S. M.; Tan, D.; Lee, R.; Tan, C. H. An Enantioconvergent Halogenophilic Nucleophilic Substitution (S_N2X) Reaction. *Science* **2019**, *363* (6425), 400–404.
(35) Li, C. X.; Zhang, Y. Y.; Sun, Q.; Gu, T. N.; Peng, H. N.; Tang, W. J. Transition-Metal-Free Stereospecific Cross-Coupling with Alkenylboronic Acids as Nucleophiles. *J. Am. Chem. Soc.* **2016**, *138* (34), 10774–10777.
(36) Benedetto, E.; Tredwell, M.; Hollingworth, C.; Khotavivattana, T.; Brown, J.; Gouverneur, V. Regio- and Stereoretentive Synthesis of Branched, Linear (*E*)- and (*Z*)-Allyl Fluorides from Allyl Carbonates under Ir-Catalysis. *Chem. Sci.* **2013**, *4*, 89–96.

4. Experimental

4.1. General Information

Unless stated reagents were purchased from commercial suppliers and used without further purification. Unless stated solvents were used without drying or degassing, all reactions that required anhydrous conditions were performed in flamed-dried glassware under an inert atmosphere of nitrogen and solvents from stills were used. CsF (99.9% trace metal basis from Sigma-Aldrich) was ground prior to reactions and used without pre-drying. KF (99.99% trace metal basis from Alfa Aesar) was ground prior to reactions and used without pre-drying. Reactions were performed in glass; and benzylic fluoride products were stable and isolated contained in PFA round bottom flasks and stored in polypropylene vials at -20 °C where they remained stable for several months. Reactions were monitored by thin layer chromatography (TLC) supplied by Merck (Kieselgel 60 F_{254} plates). Visualisation of reaction on TLC was accomplished by irradiation with UV light at 254 nm and/or cerium ammonium molybdate (CAM) stain and/or permanganate stain. Flash column chromatography (FCC) was performed on Merck silica gel (60, particle size 0.040-0.062 mm). Optical rotations were measured on an Autopol L 2000 (Schmidt-Haensh) at 589 nm, 25 °C. Data are reported as $[\alpha]^{D}_{25\,^{\circ}C}$ concentration (c in g/100 mL), and solvent. High resolution mass spectra (HRMS, *m/z*) were recorded on a Thermo Exactive mass spectrometer equipped with Waters Acquity liquid chromatography system using the heated electrospray (HESI-II) probe for positive electrospray ionization (ESI^{+}) or atmospheric pressure chemical ionization (APCI) or on an Agilent 7200 Q-TOF spectrometer equipped with a direct insertion probe supplied by Scientific Instrument Manufacturer (SIM) GmbH using electron ionization (EI – 20eV). Some compounds were found to be unstable under a variety of MS ionization methods (CI, EI, ESI, GC-MS) and therefore no HRMS could be obtained for them; this is stated for the relevant compounds. Infrared spectra were recorder as the neat compound or in liquid solution using a Bruker tensor 27 FT-IR spectrometer, absorptions are reported in wavenumber (cm^{-1}) Melting points of solids were measured on a Griffin apparatus and are uncorrected. All enantiomeric ratios (e.r.) were

determined by HPLC analysis on a Shimadzu *i*-Prominence LC-2030 (PDA detector), employing a chiral stationary phase, post purification and compared to traces of the racemic mixtures, which were independently prepared. All NMR spectra were recorded on Bruker AVIIIHD 400, AVIIIHD 500, AVII 500 or AVIII HD 600. Deuterated solvents were purchased from Sigma-Aldrich and used without purification. Toluene-d_8 and DCM-d_2 was stored at 4 °C over 3 Å molecular sieves, under nitrogen atmosphere. NMR spectra are recorded at 298 K, unless otherwise specified. NMR spectra are referenced to the residual solvent peak for ^{1}H and ^{13}C spectra, while ^{19}F NMR spectra are referenced relative to $CFCl_3$ in $CDCl_3$. Coupling constants, *J*, are reported in Hz to the nearest 0.1 Hz. Unless otherwise stated, ^{13}C spectra are ^{1}H decoupled. The following abbreviations are used to describe peak multiplicities: s = singlet, d = doublet, t = triplet, q = quartet, quin = quintet, sext = sextet, sept = septet, m = multiplet). ^{13}C NMR for (*S*)-**3g, k-l, s-y** and (*S*)-**16l, t-x** recorded with simultaneous proton and fluorine decoupling for clarity. Determination of absolute stereochemistry was achieved by comparison of the optical rotation value and chromatographic data for compounds **2ae** and **13a** with reported literature values and all other compounds were assigned by analogy.[1, 2]

4.2. Urea Catalyst Synthesis and Characterisation

4.2.1. Synthesis of Alkylated BINAM Intermediates

Alkylated *bis*-anilines were prepared according to general procedure described. Anilines **15a, 15b** and **15c** spectroscopic data are in accordance with those in literature.[3-5]

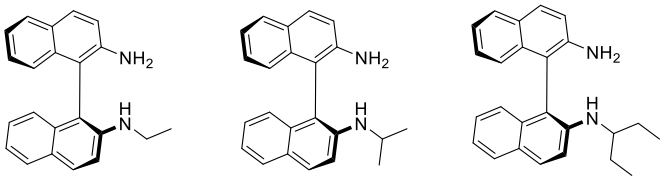

(*S*)-**15a** (*S*)-**15b** (*S*)-**15c**

General Procedure 1: In two neck round-bottom flask equipped with a stirrer bar, the appropriate ketone (1.4 equiv.) was dissolved in THF (0.25 M) and 20% aqueous H_2SO_4 solution (2 mL/$mmol_{substrate}$). (*S*)-(-)-1,1'-binapthalene-2,2'-diamine (1 equiv.) was added and after 5 minutes, the solution was cooled to 0 °C and $NaBH_4$ (10 equiv.) was added portion-wise. The mixture was brought up to room temperature and stirred for 1 hour, then quenched with 1 M KOH solution to a pH of 8 and diluted with EtOAc. The mixture was extracted with EtOAc and combined organic phases were washed with brine prior to drying with $MgSO_4$. The filter organic phase was concentrated under reduced pressure and the crude product purified by FCC.

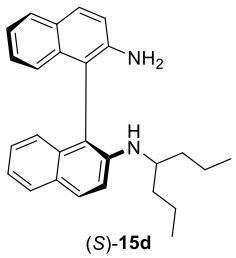

(*S*)-**15d**

(*S*)-*N*^{2} -heptan-5-yl-[1,1'-binaphthalene]-2,2'-diamine (15d)

Prepared according to General Procedure 1 from (*S*)-(-)-1,1'-binapthalene-2,2'-diamine (1.76 mmol, 1 equiv.) and 4-heptanone (1.4 equiv.). Following purification (FCC eluent pentane:Et_2O 95:5 to 90:10), the product was isolated as a as an off-white solid in 38 % yield.

^{1}H NMR (500 MHz, $CDCl_3$, 298 K) δ = 7.98 (d, *J* = 9.0 Hz, 1H), 7.95 – 7.84 (m, 3H), 7.37 (d, *J* = 5.2 Hz, 1H), 7.37 – 7.23 (m, 5H), 7.20 (d, *J* = 8.4, 1H), 7.16 – 7.04 (m, 1H), 3.80 (br s, 2H), 3.73 – 3.60 (m, 1H), 3.56 (br s, 1H), 1.58 – 1.40 (m, 5H), 1.40 – 1.28 (m, 2H), 1.28 – 1.17 (m, 1H), 0.98 (t, *J* = 7.0 Hz, 3H), 0.85 (t, *J* = 7.3 Hz, 3H); **^{13}C NMR** (126 MHz, $CDCl_3$, 298 K) δ = 144.5, 143.2, 134.1, 134.0, 129.6, 129.5, 128.6,

128.2, 128.1, 127.4, 126.8, 126.7, 124.4, 123.7, 122.5, 121.6, 118.3, 114.5, 112.6, 111.7, 52.4, 37.6, 37.5, 19.1, 18.7, 14.3, 14.16; **HRMS** (ESI^+) m/z calculated for $C_{27}H_{31}N_2$ $(M+H)^+$ 383.2482, found 383.2480; **IR** (neat) v = 3057, 2981, 2971, 1620, 1598, 1512, 1463, 1380, 1350, 1249, 1152, 956, 813, 660 cm^{-1}; **mp** 153 – 154 ˚C; **$[\alpha]^D_{25\,°C}$** = -121.0 ° (c = 1.0, $CHCl_3$).

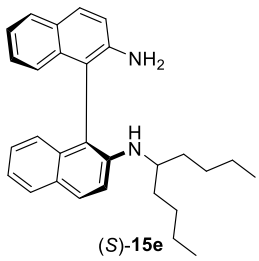

(*S*)-**15e**

(*S*)-*N*^{2} -nonan-7-yl-[1,1'-binaphthalene]-2,2'-diamine (15e)

Prepared according to General Procedure 1 from (*S*)-(-)-1,1'-binapthalene-2,2'-diamine (7.0 mmol, 1 equiv.) and 5-nonanone (1.4 equiv.). Following purification (FCC eluent 95:5 –pentane:Et_2O 90:10), the product was isolated as a viscous yellow oil in 21 % yield.

^{1}H NMR (500 MHz, $CDCl_3$, 298 K) δ = 7.88 (d, *J* = 9.0 Hz, 1H), 7.83 (d, *J* = 8.7 Hz, 1H), 7.79 – 7.76 (m, 2H), 7.28 – 7.11 (m, 6H), 7.10 (dd, *J* = 8.4, 1.2 Hz, 1H), 7.03– 6.99 (m, 1H), 3.69 (br s, 2H), 3.53 – 3.51 (m, 1H), 1.52 – 1.23 (m, 8H), 1.23 – 1.00 (m, 4H), 0.87 – 0.80 (t, *J* = 6.9 Hz, 3H), 0.70 (t, *J* = 7.1 Hz, 3H).**^{13}C NMR** (126 MHz, $CDCl_3$, 298 K) δ = 144.4, 143.2, 134.1, 134.0, 129.6, 129.5, 128.6, 128.2, 128.1, 127.3, 126.8, 126.8, 124.4, 123.8, 122.5, 121.6, 118.3, 114.5, 112.6, 111.8, 53.0, 35.0, 34.8, 28.1, 27.7, 22.9, 22.8, 14.2, 14.1 ; **HRMS** (ESI^+) m/z calculated for $C_{29}H_{35}N_2$ $(M+H)^+$ 411.2975, found 411.2789; **IR** (neat) v = 3371, 3056, 2956, 2930, 2859, 1619, 1597, 1511, 1467, 1426, 1379, 1350, 1302, 1248, 1212, 1146, 1119, 1024, 930, 860, 811, 746, 666, 639 cm^{-1}; **$[\alpha]^D_{25\,°C}$** = -87.7 ° (c = 1.0, $CHCl_3$).

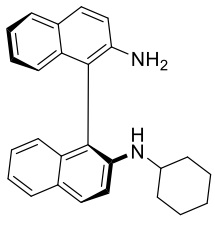

(*S*)-**15f**

(*S*)-*N*^{2} -cyclohexyl-[1,1'-binaphthalene]-2,2'-diamine (15f)

Prepared according to General Procedure 1 from (*S*)-(-)-1,1'-binapthalene-2,2'-diamine (7.0 mmol, 1 equiv.) and cyclohexanone (1.4 equiv.). Following purification (FCC eluent pentane:EtOAc 90:10), the product was isolated as an off-white solid in 30 % yield.

^{1}H NMR (500 MHz, $CDCl_3$) δ = 7.86 (d, *J* = 9.0 Hz, 1H), 7.84 – 7.78 (m, 2H), 7.77 (d, *J* = 7.6 Hz, 1H), 7.28 (d, *J* = 9.1 Hz, 1H), 7.23 (ddd, *J* = 8.0, 6.7, 1.3 Hz, 1H), 7.20 – 7.12 (m, 4H), 7.05 (dd, *J* = 8.4, 1.2 Hz, 1H), 6.97 (dd, *J* = 7.8, 1.7 Hz, 1H), 3.66 (br s, 2H), 3.53 – 3.50 (m, 1H), 3.41 (br s, 1H), 1.99 – 1.91 (m, 1H),

1.91 – 1.83 (m, 1H), 1.66 – 1.60 (m, 1H), 1.58 – 1.50 (m, 2H), 1.36 – 1.22 (m, 2H), 1.09 – 0.97 (m, 1H), 0.98 – 0.88 (m, 1H), 0.81 (tdd, *J* = 12.8, 10.2, 3.5 Hz, 1H).**^{13}C NMR** (126 MHz, $CDCl_3$, 298 K) δ = 144.0, 143.0, 134.1, 133.9, 129.6, 129.5, 128.6, 128.2, 128.1, 127.7, 126.8, 126.7, 124.3, 123.9, 122.5, 121.9, 118.4, 115.4, 112.7, 112.5, 52.3, 33.9, 33.8, 25.8, 25.2, 25.1; **HRMS** (ESI^+) m/z calculated for $C_{29}H_{26}N_2$ $(M+H)^+$ 367.2169, found 367.2166; **IR** (neat) ν = 3460, 3367, 3051, 2931, 2846, 1947, 1618, 1596, 1513, 1488, 1449, 1425, 1382, 1348, 1291, 1250, 1216, 1147, 1110, 1052, 1022, 962, 920, 813, 774, 754, 687, 671, 634, 623 cm^{-1}; **mp** 138 – 140 ˚C; **$[\alpha]^D_{25\,°C}$** = -143.5 ° (c = 1.0, $CHCl_3$).

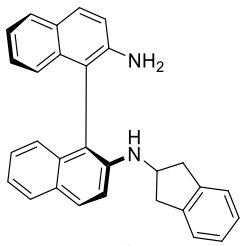

(*S*)-**15g**

(*S*)-*N*^{2}-(2,3-dihydro-1*H*-inden-2-yl)-[1,1'-binaphthalene]-2,2'-diamine 15g)

Prepared according to General Procedure 1 from (*S*)-(-)-1,1'-binapthalene-2,2'-diamine (3.5 mmol, 1 equiv.) and 2-indanone. Following purification (FCC eluent: DCM:pentane 50:50 to 80:20), the product was isolated as an off-white solid in 78 % yield.

^{1}H NMR (600 MHz, $CDCl_3$) δ = 7.93 (d, *J* = 9.0 Hz, 1H), 7.81 (dd, *J* = 8.0, 1.7 Hz, 1H), 7.78 – 7.72 (m, 2H), 7.40 (d, *J* = 9.0 Hz, 1H), 7.25 – 7.13 (m, 4H), 7.11 – 6.99 (m, 7H), 4.54 (p, *J* = 7.0 Hz, 1H), 3.80 – 3.56 (br s, 3H), 3.29 (ddd, *J* = 28.1, 15.8, 7.2 Hz, 2H), 2.67 (dd, *J* = 15.7, 6.7 Hz, 1H), 2.51 (dd, *J* = 15.9, 6.7 Hz, 1H); **^{13}C NMR** (151 MHz, $CDCl_3$) δ = 144.0, 142.9, 141.1, 141.1, 134.0, 133.8, 129.8, 129.7, 128.6, 128.3, 128.2, 128.1, 127.0, 126.9, 126.7, 126.6, 124.8, 124.6, 124.1, 124.0, 122.5, 122.4, 118.3, 115.4, 113.8, 112.1, 55.5, 40.5, 40.4; **HRMS** (ESI^+) m/z calculated for $C_{29}H_{25}N_2$ $(M+H)^+$ 401.2012, found 401.2005; **IR** (neat) ν = 3365, 2923, 2865, 2364, 1685, 1618, 1508, 1379, 1347, 1281, 1263, 1182, 1133, 1055, 1033, 1015, 926, 817, 742 cm^{-1}; **mp** 169 – 171 ˚C; **$[\alpha]^D_{25\,°C}$** = -100.0 ° (c = 1.0, $CHCl_3$).

4.2.2. Catalyst Synthesis

Catalysts (*S*)-**3a-e** and **z** were synthesised according to literature procedure and spectroscopic data matches literature.[3-5]

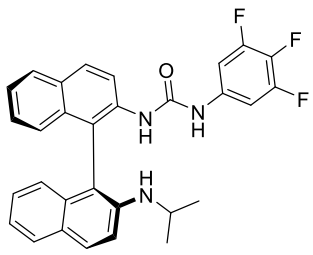

(*S*)-**16l**

(*S*)-1-(3,4,5-trifluoromethylphenyl)-3-(2'-(isopropylamino)-[1,1'-binaphthalen]-2-yl)urea (16l)

In a flame-dried Schlenk under inert atmosphere, triphosgene (148 mg, 0.5 mmol, 0.33 equiv) was dissolved in dry DCM (0.8 mL). To this solution, a 0.2 M solution 3,4,5-trifluoroaniline in dry DCM was added at 0 °C. Triethylamine (0.43 mL, 3.1 mmol, 2 equiv) was added dropwise at 0 °C and the reaction mixture was stirred at room temperature for 2 hours under nitrogen. Aniline (*S*)-**15b** was then added as a solid and the reaction mixture was stirred at room temperature for 24 hours (until TLC showed no further conversion). The reaction was quenched by the addition of water and the aqueous phase was extracted with DCM (3 x 10 mL). Combined organic extracts were washed with brine, dried with $MgSO_4$ and solvent was removed under reduced pressure. The crude mixture was purified (FCC eluent: DCM:pentane 80:20) to afford the desired product as off-white solid in 63 % yield.

^{1}H NMR (500 MHz, $CDCl_3$, 298 K) δ = 8.45 (d, *J* = 9.1 Hz, 1H), 8.01 (d, *J* = 9.1 Hz, 1H), 7.90 (t, *J* = 7.3 Hz, 2H), 7.78 (d, *J* = 7.9 Hz, 1H), 7.44–7. 38 (m, 1H), 7.26–7.23 (m, 2H), 7.21 (d, *J* = 7.42 Hz, 1H), 7.17–7.12 (m, 1H), 7.10 (d, *J* = 8.5 Hz, 1H), 6.81 (m, 3H), 6.48 (br s, 1H), 6.26 (br s, 1H), 3.76 (br s, 1H), 3.26 (br s, 1H), 0.97 (dd, J = 23.2, 6.3 Hz, 6H); **^{19}F NMR** (471 MHz, $CDCl_3$, 298 K) δ = - 134.49 (br s), - 164.54 (br s); **^{13}C NMR{^{1}H, ^{19}F}** (125 MHz, $CDCl_3$, 298 K) δ = 152.7, 151.0, 143.9, 136.5, 135.1, 134.2, 133.6, 133.3, 132.9, 132.7, 131.1, 130.3, 130.0, 129.5, 128.2, 128.1, 127.3, 127.0, 125.2, 125.1, 123.3, 122.4, 120.5, 115.0 (br), 105.5, 44.7 (br), 23.1, 22.9; **HRMS** (ESI^+) m/z calculated for $C_{30}H_{25}N_3OF_3^+$ $(M+H)^+$ 500.1944, found 500.1941; **IR** (liquid film) ν = 3658, 2980, 2888, 2665, 1768, 1631, 1598, 1526, 1473, 1462, 1383, 1252, 1152, 1073, 955, 814, 772 cm^{-1}; **mp** 222 – 223 ˚C; **$[\alpha]_D^{25\,°C}$** = -95.0 ° (c = 1.0, $CHCl_3$).

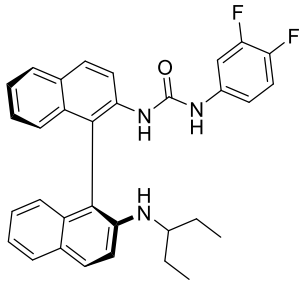
(*S*)-**16t**

(*S*)-1-(3,4-difluoromethylphenyl)-3-(2'-(pentylamino)-[1,1'-binaphthalen]-2-yl)urea (16t)

In a flame-dried Schlenk under inert atmosphere, aniline (*S*)-**15c** (300 mg, 0.92 mmol, 1 equiv.) was dissolved in dry DCM (0.4 M) and 3,4-difluorophenyl isocyanate (1 equiv.) was added dropwise. The mixture was stirred for 30 minutes until full consumption of starting material was seen by TLC. The reaction was quenched with MeOH and solvent was removed under reduced pressure. The crude mixture was purified (FCC eluent: DCM:pentane 90:10 – 100:0) to afford the desired product as a white solid in 92 % yield.

^{1}H NMR (500 MHz, $CDCl_3$) δ = 8.50 (d, *J* = 9.1 Hz, 1H), 7.98 (d, *J* = 9.1 Hz, 1H), 7.89 (d, *J* = 8.1 Hz, 1H), 7.82 (d, *J* = 9.0 Hz, 1H), 7.73 (d, *J* = 7.9 Hz, 1H), 7.41 – 7.36 (m, 1H), 7.25 – 7.19 (m, 1H), 7.19 – 7.07 (m, 4H), 6.86 (br t, *J* = 7.9 Hz, 1H), 6.75 (d, *J* = 8.2 Hz, 1H), 6.71 (q, *J* = 9.6 Hz, 1H), 6.55 (s, 1H), 6.47 – 6.37 (m, 1H), 6.33 (br s, 1H), 3.47 – 3.30 (m, 1H), 3.27 (br s, 1H), 1.45 – 1.27 (m, 2H), 1.27 – 1.10 (m, 2H), 0.73 (t, *J* = 7.4 Hz, 3H), 0.57 (t, *J* = 7.4 Hz, 3H); **^{19}F NMR** (471 MHz, $CDCl_3$, 298 K) δ = -134.5 (br), - 141.4 (br); **^{13}C NMR{^{1}H, ^{19}F}** (126 MHz, $CDCl_3$) [overlapping signals] δ = 153.2, 150.1, 147.7, 144.2 (br), 135.6, 133.8, 133.5, 132.8, 131.0, 130.3, 129.5, 128.3, 127.3, 127.2, 126.9, 125.4, 125.0, 123.2, 122.1, 120.3, 119.7, 118.9, 117.4, 114.4, 112.5, 109.5 (br), 55.5 (br), 27.2, 27.1, 10.1, 9.9; **IR** (liquid film) ν = 3649, 3353, 3021, 2943, 2761, 1645, 1609, 1541, 1510, 1447, 1409, 1215, 996, 752; **HRMS** (ESI^+) m/z calculated for $C_{32}H_{30}F_2N_3O$ $(M+H)^+$ 510.2351, found 510.2346; **mp** 171 – 175 ˚C; **$[\alpha]^{D}_{25\,°C}$** = -104.1 ° (c = 0.5, $CHCl_3$).

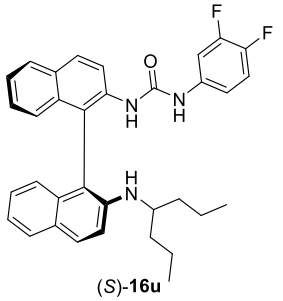
(*S*)-**16u**

(*S*)-1-(3,4-difluoromethylphenyl)-3-(2'-(heptylamino)-[1,1'-binaphthalen]-2-yl)urea (16u)

In a flame-dried Schlenk under inert atmosphere, aniline (*S*)-**15d** (300 mg, 0.92 mmol, 1 equiv.) was dissolved in dry DCM (0.4 M) and 3,4-difluorophenyl isocyanate (1 equiv.) was added dropwise. The mixture was stirred for 30 minutes at room

temperature until full conversion of starting material was seen by TLC. The reaction was quenched with MeOH and solvent was removed under reduced pressure. The crude mixture was purified (FCC eluent: pentane: Et_2O 90:10) to afford the desired product as a white solid in 95 % yield.

^{1}H NMR (500 MHz, $CDCl_3$, 298 K) δ = 8.50 (d, *J* = 9.0 Hz, 1H), 7.98 (d, *J* = 9.1 Hz, 1H), 7.89 (d, *J* = 8.2 Hz, 1H), 7.82 (d, *J* = 9.0 Hz, 1H), 7.73 (d, *J* = 7.8 Hz, 1H), 7.39 (t, *J* = 7.5 Hz, 1H), 7.22 (t, *J* = 7.5 Hz, 1H), 7.18 – 7.07 (m, 4H), 6.89 (ddd, *J* = 10.6, 7.0, 2.6 Hz, 1H), 6.75 (dd, *J* = 16.6, 8.7 Hz, 1H), 6.70 (q, *J* = 8.8 Hz, 1H), 6.56 (s, 1H), 6.42 (dd, *J* = 8.7, 4.0 Hz, 1H), 6.28 (s, 1H), 3.50 – 3.42 (m, 1H), 3.20 (s, 1H), 1.35 – 0.95 (m, 8H), 0.77 (t, *J* = 6.7 Hz, 3H), 0.68 (t, *J* = 6.7 Hz, 3H); **^{19}F NMR** (471 MHz, $CDCl_3$, 298 K) δ = - 134.5 (br), -141.5 (br); **^{13}C NMR{^{1}H, ^{19}F}** (125 MHz, $CDCl_3$, 298 K) δ = 153.2, 150.1, 147.7, 146.7, 144.5, 139.6, 135.6, 133.9, 133.6, 132.8, 131.0, 130.3, 129.5, 128.3, 127.3, 126.9, 125.4, 125.0, 123.1, 122.0, 120.3, 120.0, 118.5, 118.3, 117.4, 116.8, 114.2, 52.3, 37.5, 37.4, 19.2, 18.7, 14.2, 14.1; **HRMS** (ESI^+) m/z calculated for $C_{34}H_{34}F_2N_3O$ $(M+H)^+$ 538.2664, found 538.2657; **IR** (liquid film) ν = 3350, 3104, 2873, 1744, 1716, 1684, 1621, 1599, 1503, 1451, 1231, 1023, 939, 747 cm^{-1}; **mp** 108 – 110 ˚C; **$[\alpha]^D_{25\,°C}$** = -64.4 ° (c = 1.0, $CHCl_3$).

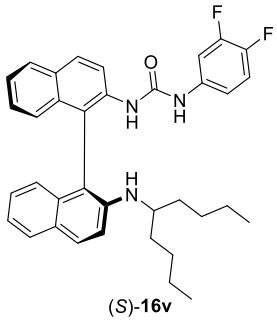

(*S*)-**16v**

(*S*)-1-(3,4-difluorophenyl)-3-(2'-(nonan-5-ylamino)-[1,1'-binaphthalen]-2-yl)urea (16v)

In a flame-dried Schlenk under inert atmosphere, aniline (*S*)-**15e** (200 mg, 0.92 mmol, 1 equiv.) was dissolved in dry DCM (0.4 M) and 3,4-difluorophenyl isocyanate (1 equiv.) was added dropwise. The mixture was stirred for 30 minutes at room temperature until full conversion of starting material was seen by TLC. The reaction was quenched with MeOH and solvent was removed under reduced pressure. The crude mixture was purified (FCC eluent: pentane: Et_2O 90:10) to afford the desired product as a white solid in 68 % yield.

^{1}H NMR (500 MHz, $CDCl_3$) δ = 8.56 (dd, *J* = 9.1, 3.2 Hz, 1H), 7.99 (d, *J* = 9.1 Hz, 1H), 7.89 (d, *J* = 8.1 Hz, 1H), 7.85 (d, *J* = 9.0 Hz, 1H), 7.75 (d, *J* = 8.0 Hz, 1H), 7.38 (ddd, *J* = 8.0, 6.6, 1.2 Hz, 1H), 7.25 – 7.07 (m, 5H), 6.95 (s, 1H), 6.80 – 6.70 (m, 2H), 6.54 (s, 1H), 6.49 (s, 1H), 6.35 (s, 1H), 3.43 (br s, 1H), 3.23 (br s,

1H), 1.42 – 1.31 (m, 2H), 1.31 – 1.24 (m, 4H), 1.22 – 1.17 (m, 2H), 1.17 – 1.07 (m, 2H), 1.06 – 0.91 (m, 1H), 0.90 – 0.81 (m, 1H), 0.78 (t, *J* = 6.7 Hz, 3H), 0.65 (t, *J* = 7.2 Hz, 3H); **^{19}F NMR** (471 MHz, $CDCl_3$) δ = -134.6, -141.6; **^{13}C NMR{^{1}H, ^{19}F}** (125 MHz, $CDCl_3$, 298 K) δ = [overlapping signals] 153.1, 150.1, 147.4, 143.3 (br), 135.9, 133.9, 133.8, 132.9, 130.9, 130.5, 129.7, 128.3, 127.7 (br), 127.5, 126.9, 125.3, 125.0, 123.5, 122.6 (br), 120.3, 119.2, 117.8, 117.3, 114.9, 111.7, 53.8 (br), 34.5 (br), 34.3 (br), 28.2, 27.4, 22.8, 22.6, 14.1, 14.0; **HRMS** (ESI$^+$) m/z calculated for $C_{36}H_{38}F_2N_3O$ $(M+H)^+$ 566.2977, found 566.2964; **IR** (neat) ν = 2958, 2928, 2857, 1740, 1720, 1658, 1621, 1599, 1563, 1516, 1498, 1465, 1429, 1379, 1330, 1281, 1262, 1227, 1206, 1153, 1115, 1024, 908, 864, 811, 807, 745, 654, 623 cm^{-1}; **mp** =112 – 114 ˚C; **$[\alpha]^{D}_{25\,°C}$** = -64.18° (c = 0.4, $CHCl_3$).

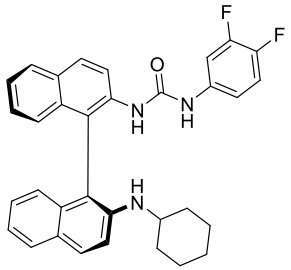

(*S*)-**16w**

(*S*)-1-(2'-(cyclohexylamino)-[1,1'-binaphthalen]-2- yl)-3-(3,4-difluoropheyl)urea (16w)

In a flame-dried Schlenk under inert atmosphere, aniline (*S*)-**15f** (300 mg, 0.92 mmol, 1 equiv.) was dissolved in dry DCM (0.4 M) and 3,4-difluorophenyl isocyanate (1 equiv.) was added dropwise. The mixture was stirred for 30 minutes at room temperature until full conversion of starting material was seen by TLC. The reaction was quenched with MeOH and solvent was removed under reduced pressure. The crude mixture was purified (FCC eluent: pentane: Et_2O 90:10) to afford the desired product as a white solid in 95 % yield.

^{1}H NMR (500 MHz, $CDCl_3$) δ = 8.50 (d, *J* = 9.1, 1H), 7.98 (d, *J* = 9.1 Hz, 1H), 7.89 (d, *J* = 8.1 Hz, 1H), 7.86 (d, *J* = 9.1 Hz, 1H), 7.77 (d, *J* = 7.9, 1H), 7.39 (t, *J* = 7.6 Hz, 1H), 7.25 – 7.18 (m, 3H), 7.12 (t, *J* = 7.5 Hz, 1H), 7.08 (d, *J* = 8.4 Hz, 1H), 6.96 – 6.92 (m, 1H), 6.78 (d, *J* = 8.2 Hz, 1H), 6.77 – 6.71 (m, 1H), 6.55 – 6.43 (m, 3H), 3.57 (br s, 1H), 3.39 – 3.31 (m, 1H), 1.84 (d, *J* = 11 Hz, 1H), 1.78 (d, *J* = 11 Hz, 1H) 1.59 – 1.48 (m, 3H), 1.24 – 1.15 (m, 2H), 1.05 – 0.95 (m, 1H), 0.91 – 0.81 (m, 2H), 0.80– 0.70 (m, 1H); **^{19}F NMR** (471 MHz, $CDCl_3$) δ = -134.8, -141.9; **^{13}C NMR{^{1}H, ^{19}F}** (125 MHz, $CDCl_3$, 298 K) δ = 153.0, 150.1, 147.6, 142.9, 135.7, 133.7, 133.7, 132.8, 130.9, 130.4, 129.7, 128.3, 128.3, 127.9, 127.4, 127.0, 125.3, 125.0, 123.6,

122.7, 120.2, 119.2, 118.2, 117.4, 115.3, 112.0, 111.3, 52.6, 33.5, 33.2, 25.5, 24.9, 24.9; **HRMS** (ESI^+) m/z calculated for $C_{33}H_{30}F_2N_3O$ $(M+H)^+$ 522.2351, found 522.2342; **IR** (neat) ν = 2969, 2932, 2581, 2849, 1739, 1719, 1657, 1620, 1599, 1567, 1518, 1502, 1452, 1428, 1378, 1367, 1347, 1287, 1262, 1230, 1214, 1207, 1150, 1113, 957, 867, 810, 772, 747, 665, 646, 623 cm^{-1}; **mp** 110 – 113 ˚C; **$[\alpha]^D_{25\,°C}$** = -81.6° (c = 0.4, $CHCl_3$).

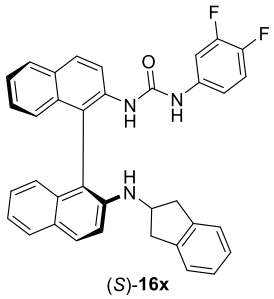
(*S*)-**16x**

(*S*)-1-(3,4-difluorophenyl)-3-(2'-((2,3-dihydro-1*H*-inden-2-yl)amino)-[1,1'-binapthalen]-2-yl)urea (16x)

In a flame-dried Schlenk under inert atmosphere, aniline (*S*)-**15g** (200 mg, 0.5 mmol, 1 equiv.) was dissolved in dry DCM (0.4 M) and 3,4-difluorophenyl isocyanate (1 equiv.) was added dropwise. The mixture was stirred for 4 hours at room temperature until full conversion of starting material was seen by TLC. The reaction was quenched with MeOH and solvent was removed under reduced pressure. The crude mixture was purified (FCC eluent: DCM:pentane 80:20 to 100:0) to afford the desired product as a white solid in 96 % yield.

^{1}H NMR (500 MHz, $CDCl_3$) δ = 8.47 (d, *J* = 9.2 Hz, 1H), 7.96 (d, *J* = 9.0 Hz, 1H), 7.94 (d, *J* = 9.0 Hz, 1H), 7.87 (d, *J* = 7.2 Hz, 1H), 7.82 (dd, *J* = 8.2, 1.6 Hz, 1H), 7.38 (ddd, *J* = 8.1, 6.7, 1.2 Hz, 1H), 7.34 (d, *J* = 9.2 Hz, 1H), 7.27 – 7.22 (m, 2H), 7.19 (ddd, *J* = 15.1, 7.2, 1.4 Hz, 1H), 7.14 – 7.00 (m, 5H), 6.97 (ddd, *J* = 11.6, 7.0, 2.6 Hz, 1H), 6.87 – 6.83 (m, 1H), 6.83 – 6.76 (m, 1H), 6.50 (s, 2H), 6.45 (s, 1H), 4.46 (t, *J* = 7.0 Hz, 1H), 3.73 (s, 1H), 3.25 (dd, *J* = 15.7, 7.2 Hz, 2H), 2.50 (ddd, *J* = 15.9, 11.3, 6.6 Hz, 2H); **^{19}F NMR** (471 MHz, $CDCl_3$) δ = -134.7, -141.8; **^{13}C NMR{^{1}H, ^{19}F}** (126 MHz, $CDCl_3$) δ = 153.0, 150.1, 147.5, 144.0, 140.7, 140.5, 135.6, 133.8, 133.6, 132.7, 131.0, 130.5, 129.7, 128.4, 128.3, 127.8, 127.5, 127.1, 126.8, 126.8, 125.0, 125.0, 124.8, 124.6, 123.6, 122.8, 120.4, 119.5, 118.0, 117.4, 115.0, 111.9, 111.5, 55.1, 40.5; **HRMS** (ESI^+) m/z calculated for $C_{36}H_{28}F_2N_3O$ $(M+H)^+$ 556.2195, found 556.2186; **IR** (neat) ν = 3600, 3338, 3057, 2924, 2360, 1658, 1621, 1558, 1515, 1500, 1428, 1377, 1334, 1284, 1263, 1208, 1136, 1093, 1056, 1033, 957, 927, 864, 812, 774, 744, 707, 624, 609 cm^{-1}; **mp** 143 – 146 ˚C**; $[\alpha]^D_{25\,°C}$** = -59.7 ° (c = 0.6, $CHCl_3$).

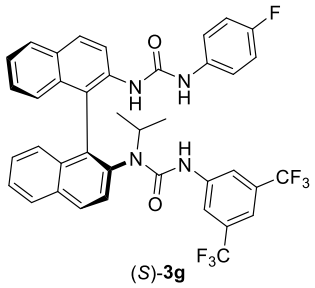
(*S*)-**3g**

(*S*)-3-(3,5-bis(trifluoromethyl)phenyl)-1-isopropyl-1-(2'-(3-(4-fluorophenyl)ureido)-[1,1'-binaphthalen]-2- yl)urea (3g)

In a flame-dried Schlenk under inert atmosphere, aniline (*S*)-**15b** (300 mg, 0.92 mmol, 1 equiv.) was dissolved in dry DCM (0.4 M) and 4-fluorophenyl isocyanate (1 equiv.) was added dropwise. The mixture was stirred for 10 minutes at room temperature until full conversion of starting material was seen by TLC. 3,5-bistrifluoromethylphenyl isocyanate (1 equiv.) was added dropwise and mixture was stirred at reflux for 24 h. The reaction was quenched with MeOH and solvent was removed under reduced pressure. The crude mixture was purified (FCC eluent: 1st column pentane: EtOAc 80:20, 2nd column 100% DCM) and following recrystallisation in MeCN the desired product was afforded as a white solid in 63 % yield.

^{1}H NMR (500 MHz, $CDCl_3$) δ = 8.49 (d, *J* = 8.9 Hz, 1H), 8.10 (d, *J* = 8.4 Hz, 1H), 7.98 (d, *J* = 9.0 Hz, 2H), 7.89 (d, *J* = 8.1 Hz, 1H), 7.78 (br s, 2H), 7.55 (t, *J* = 7.3 Hz, 1H), 7.51 (d, *J* = 8.8 Hz, 1H), 7.46 (s, 1H), 7.35 (t, *J* = 7.5 Hz, 1H), 7.31 (t, *J* = 7.4 Hz, 1H), 7.24–7.05 (m, 3H), 6.93 – 6.80 (m, 3H), 6.79 – 6.53 (m, 4H), 3.53 (br s, 1H), 1.02 (br s, 3H), 0.67 (br s, 3H); **^{19}F NMR** (471 MHz, $CDCl_3$, 298 K) δ = -62.9 (s), - 120.4 (br s); **^{13}C NMR{^{1}H, ^{19}F}** (125 MHz, $CDCl_3$, 298 K) δ = 158.8 (br), 155.3 (br), 152.8, 140.1, 139.8, 136.1 (br), 133.8, 133.2, 132.3, 132.1, 130.8, 130.3, 129.9, 128.7, 128.4, 128.2, 127.9, 127.8, 127.5, 127.0, 126.9 (br), 125.0 (br), 124.6, 123.2, 120.9 (br), 120.2, 120.0, 119.8, 116.9 (br), 115.5 (br), 53.7 (br), 20.8 (br), 20.6; **HRMS** (ESI^+) m/z calculated for $C_{39}H_{30}N_4O_2F_7$ $(M+H)^+$ 719.2252, found 719.2252; **IR** (neat) ν = 3658, 2981, 2888, 1665, 1545, 1504, 1473, 1439, 1385, 1278, 1216, 1178, 1138, 1073, 966, 940, 884, 825, 754, 701, 682 cm^{-1}; **mp** 151 – 154 ˚C; **$[\alpha]^{D}_{25\,°C}$** = -49.8 ° (c = 1.0, $CHCl_3$).

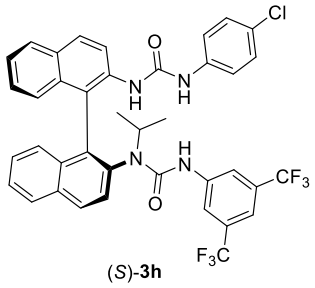
(*S*)-**3h**

(*S*)-3-(3,5-bis(trifluoromethyl)phenyl)-1-isopropyl-1-(2'-(3-(4-chlorophenyl)ureido)-[1,1'-binaphthalen]-2- yl)urea (3h)

In a flame-dried Schlenk under inert atmosphere, aniline (*S*)-**15b** (300 mg, 0.92 mmol, 1 equiv.) was dissolved in dry DCM (0.4 M) and 4-chlorophenyl isocyanate (1 equiv.) was added dropwise. The mixture was stirred for 4 hours at room temperature

until full conversion of starting material was seen by TLC. 3,5-bistrifluoromethylphenyl isocyanate (1 equiv.) was added dropwise and mixture was stirred at reflux for 24 h. The reaction was quenched with MeOH and solvent was removed under reduced pressure. The crude mixture was purified (FCC eluent: 1st column pentane: EtOAc 90:10, 2nd column 100% DCM) to afford the desired product as a white solid in 55 % yield.

^{1}H NMR (600 MHz, $CDCl_3$) δ = 8.52 (d, *J* = 9.1 Hz, 1H), 8.11 (d, *J* = 8.7 Hz, 1H), 7.99 (d, *J* = 8.9 Hz, 2H), 7.89 (d, *J* = 8.3 Hz, 1H), 7.82 – 7.75 (m, 2H), 7.55 (t, *J* = 7.9 Hz, 1H), 7.51 (d, *J* = 8.6 Hz, 1H), 7.47 (s, 1H), 7.36 (t, *J* = 7.6 Hz, 1H), 7.31 (t, *J* = 7.7 Hz, 1H), 7.19 (d, *J* = 8.6 Hz, 3H), 7.00 (d, *J* = 8.8 Hz, 2H), 6.95 – 6.92 (m, 3H), 6.87 (d, *J* = 8.5 Hz, 1H), 6.77 (s, 1H), 3.57 (s, 1H), 1.03 (s, 3H), 0.66 (s, 3H); **^{19}F NMR** (565 MHz, $CDCl_3$) δ = -62.9; **^{13}C NMR** (151 MHz, $CDCl_3$) δ = [overlapping signals]155.6 (br), 152.4, 140.1, 139.7, 136.7, 136.1, 133.9, 133.2, 132.3 (q, $J_{C\text{-}F}$ = 33.6 Hz), 132.0, 130.7, 130.3, 129.9, 128.8, 128.7, 128.4, 128.0, 127.7, 127.5, 127.0, 125.1, 124.6, 123.2 (q, $J_{C\text{-}F}$ = 272.9 Hz), 120.1, 119.9, 117.0, 53.7, 20.9, 20.7; **HRMS** (ESI$^+$) m/z calculated for $C_{39}H_{30}ClF_6N_4O_2$ $(M+H)^+$ 735.1956, found 735.1956; **IR** (neat) ν = 3680, 2923, 2865, 2844, 2362, 1684, 1540, 1378, 1346, 1279, 1181, 1135, 1055, 1033, 1014, 819, 683 cm^{-1}; **mp** 141 – 144 ˚C; **$[\alpha]^{D}_{25\,°C}$** = -53.0 ° (c = 1.0, $CHCl_3$).

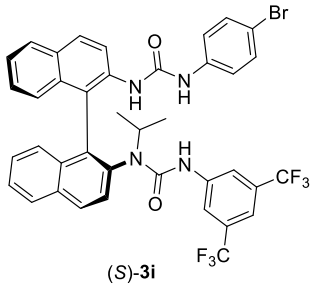

(*S*)-**3i**

(*S*)-3-(3,5-bis(trifluoromethyl)phenyl)-1-isopropyl-1-(2'-(3-(4-bromophenyl)ureido)-[1,1'-binaphthalen]-2- yl)urea (3i)

In a flame-dried Schlenk under inert atmosphere, aniline (*S*)-**15b** (300 mg, 0.92 mmol, 1 equiv.) was dissolved in dry DCM (0.4 M) and 4-bromophenyl isocyanate (1 equiv.) was added dropwise. The mixture was stirred for 4 hours at room temperature until full conversion of starting material was seen by TLC. 3,5-bistrifluoromethylphenyl isocyanate (1 equiv.) was added dropwise and mixture was stirred at reflux for 24 h. The reaction was quenched with MeOH and solvent was removed under reduced pressure. The crude mixture was purified (FCC eluent: DCM:pentane 80:20) and following recrystallisation in MeCN the desired product was afforded as a white solid in 88 % yield.

^{1}H NMR (600 MHz, $CDCl_3$) δ = 8.50 (d, *J* = 9.1 Hz, 1H), 8.11 (d, *J* = 8.8 Hz, 1H), 7.99 (dd, *J* = 8.8, 3.3 Hz, 2H), 7.89 (d, *J* = 8.1 Hz, 1H), 7.79 (s, 2H), 7.55 (t, *J* = 7.5 Hz, 1H), 7.51 (d, *J* = 8.7 Hz, 1H), 7.47 (s, 1H), 7.36 (t, *J* = 7.5 Hz, 1H), 7.30 (t, *J* = 7.7 Hz, 1H), 7.19 (m, 3H), 7.14 (d, *J* = 8.8 Hz, 2H), 6.87 (d, *J* = 8.4 Hz, 2H), 6.77 (br s, 3H), 3.57 (s, 1H), 1.04 – 1.00 (m, 3H), 0.66 (s, 3H); **^{19}F NMR** (565 MHz, $CDCl_3$) δ -62.9; **^{13}C NMR** (151 MHz, $CDCl_3$) δ [overlapping signals] 155.6 (br), 152.4, 140.1, 139.7, 137.3, 136.1, 133.9, 133.2, 133.2, 132.3 (q, *J* = 33.6 Hz), 132.1, 131.7, 130.7, 130.2, 129.9, 128.7, 128.4, 128.0, 127.7, 127.4, 127.0, 127.0 (br), 125.1, 124.6, 123.1 (d, *J* = 272.9 Hz), 120.4, 120.1, 119.9, 117.0, 115.3, 53.6, 20.9, 20.7; **HRMS** (ESI^+) m/z calculated for $C_{39}H_{30}BrF_6N_4O_2$ $(M+H)^+$ 779.1451, found 779.1434; **IR** (neat) ν = 3680, 3364, 2923, 2865, 2844, 2361, 1685, 1535, 1379, 1346, 1279, 1181, 1134, 1055, 1033, 1014, 819, 683 cm^{-1}; **mp** 148 – 150 ˚C; **$[\alpha]^{D}_{25\,°C}$** = -49.4 ° (c = 1.0, $CHCl_3$).

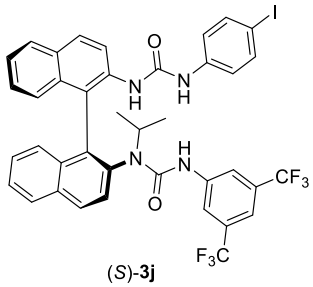
(*S*)-**3j**

(*S*)-3-(3,5-bis(trifluoromethyl)phenyl)-1-isopropyl-1-(2'-(3-(4-iodophenyl)ureido)-[1,1'-binaphthalen]-2- yl)urea (3j)

In a flame-dried Schlenk under inert atmosphere, aniline (*S*)-**15b** (200 mg, 0.61 mmol, 1 equiv.) was dissolved in dry DCM (0.4 M) and 4-iodophenyl isocyanate (1 equiv.) was added dropwise. The mixture was stirred for 30 minutes at room temperature until full conversion of starting material was seen by TLC. 3,5-bistrifluoromethylphenyl isocyanate (1 equiv.) was added dropwise and mixture was stirred at reflux for 24 h. The reaction was quenched with MeOH and solvent was removed under reduced pressure. The crude mixture was purified (FCC eluent: DCM:pentane 80:20) and recrystallised in MeCN to afford the desired product as a white solid in 83 % yield.

^{1}H NMR (600 MHz, $CDCl_3$) δ = 8.51 (d, *J* = 9.1 Hz, 1H), 8.12 (d, *J* = 8.7 Hz, 1H), 7.99 (m, 2H), 7.89 (d, *J* = 8.2 Hz, 1H), 7.79 (s, 2H), 7.55 (t, *J* = 7.5 Hz, 1H), 7.51 (d, *J* = 8.6 Hz, 1H), 7.47 (s, 1H), 7.36 (t, *J* = 7.5 Hz, 1H), 7.32 (t, *J* = 9.0 Hz, 3H), 7.19 (d, *J* = 8.5 Hz, 2H), 6.87 (d, *J* = 8.5 Hz, 1H), 6.85 – 6.49 (m, 6H), 3.57 (s, 1H), 1.04 – 1.00 (m, 3H), 0.66 (s, 3H); **^{19}F NMR** (565 MHz, $CDCl_3$) δ = -62.9; **^{13}C NMR** (151 MHz, $CDCl_3$) δ = 155.6, 152.3, 140.1, 139.7, 138.2, 137.7, 136.1, 133.9, 133.2 (br), 133.2, 132.3 (q, *J* = 33.6 Hz), 132.0,

130.7, 130.3, 129.9, 128.7, 128.4, 128.0, 127.7, 127.5, 127.0, 125.1, 124.6, 123.2 (q, *J* = 272.9 Hz), 120.7 (br), 120.1, 119.9, 117.0, 85.6, 53.6, 20.9, 20.7; **HRMS** (ESI$^+$) m/z calculated for $C_{39}H_{30}IF_6N_4O_2$ $(M+H)^+$ 827.1312, found 827.1289; **IR** (neat) ν = 3680, 1923, 2865, 2844, 2358, 1685, 1507, 1381, 1346, 1279, 1181, 1135, 1055, 1033, 1014, 818, 683 cm^{-1}; **mp** 163 – 165 ˚C; **$[\alpha]^D_{25\,°C}$** = -38.4 ° (c = 1.0, $CHCl_3$).

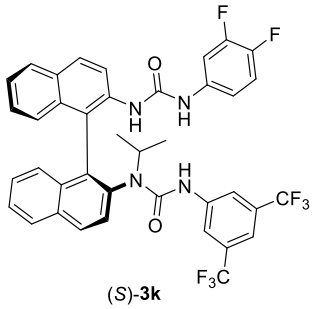
(*S*)-**3k**

(*S*)-3-(3,5-bis(trifluoromethyl)phenyl)-1-isopropyl-1-(2'-(3-(3,4-difluorophenyl)ureido)-[1,1'-binaphthalen]-2- yl)urea (3k)

In a flame-dried Schlenk under inert atmosphere, aniline (*S*)-**15b** (300 mg, 0.92 mmol, 1 equiv.) was dissolved in dry DCM (0.4 M) and 3,4-difluorophenyl isocyanate (1 equiv.) was added dropwise. The mixture was stirred for 30 minutes at room temperature until full conversion of starting material was seen by TLC. 3,5-bistrifluoromethylphenyl isocyanate (1 equiv.) was added dropwise and mixture was stirred at reflux for 24 hours. The reaction was quenched with MeOH and solvent was removed under reduced pressure. The crude mixture was purified (FCC eluent: DCM:pentane 80:20) and following recrystallisation in MeCN the desired product was afforded as a white solid in 64 % yield.

^{1}H NMR (500 MHz, $CDCl_3$, 298 K) δ = 8.50 (d, *J* = 8.9 Hz, 1H), 8.11 (d, *J* = 8.7 Hz, 1H), 8.00 (d, *J* = 9.1 Hz, 1H), 7.99 (d, *J* = 8.1 Hz, 1H), 7.90 (d, *J* = 8.1 Hz, 1H), 7.80 (br s, 2H), 7.57 – 7.45 (m, 2H), 7.47 (s, 1H), 7.37 (t, *J* = 7.2 Hz, 1H), 7.29 (t, *J* = 7.7 Hz, 1H), 7.21 (t, *J* = 7.4 Hz, 1H), 7.18 (d, *J* =8.6 Hz, 1H), 7.09 (br s, 1H), 6.92 (br s, 1H), 6.86 (d, *J* = 8.5 Hz, 2H), 6.85 – 6.73 (m, 2H), 6.54–6.45 (m, 1H), 3.58 (br s, 1H), 1.03 (d, *J* = 6.2 Hz, 3H), 0.66 (br s, 3H), **^{19}F NMR** (471 MHz, $CDCl_3$, 298 K) δ = -63.0 (s), - 136.6 (br s), - 145.4 (br s); **^{13}C NMR{^{1}H, ^{19}F}** (125 MHz, $CDCl_3$, 298 K) [overlapping signals] δ = 155.6 (br), 152.3, 150.0, 146.2 (br), 140.0, 139.6, 136.0, 134.8 (br), 133.9, 133.3, 133.2, 132.4, 132.0, 130.7, 130.3, 129.9, 128.7, 128.3, 128.1, 127.7, 127.4, 127.1, 127.0, 125.2, 124.6, 123.2, 120.1, 120.0, 117.1, 116.9, 114.3 (br), 108.5 (br), 53.5 (br), 20.9 (br), 20.7; **HRMS** (ESI$^+$) m/z calculated for $C_{39}H_{29}N_4O_2F_8$ $(M+H)^+$ 759.1977, found 759.1976; **IR** (liquid film) ν = 3337, 2981, 2882, 2351, 1722, 1681, 1462, 1382, 1285, 1250, 1151, 1072,

955, 863, 802, 774, 712, 690, 577, 668, 653, 643, 622, 607 cm^{-1}; **mp** 149 – 150 ˚C; **$[\alpha]^{D}_{25\,°C}$** = -67.7 ° (c = 1.0, $CHCl_3$).

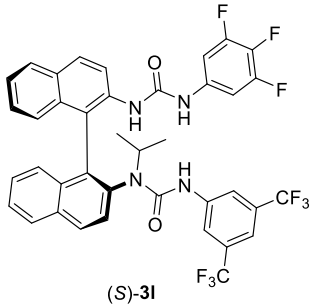
(*S*)-**3l**

(*S*)-3-(3,5-bis(trifluoromethyl)phenyl)-1-isopropyl-1-(2'-(3-(3,4,5-trifluorophenyl)ureido)-[1,1'-binaphthalen]-2- yl)urea (3l)

In a flame-dried Schlenk under inert atmosphere, intermediate (*S*)-**16l** (350 mg, 0.7 mmol, 1 equiv.) was dissolved in dry DCM (0.4 M) and 3,5-bis(trifluoromethyl)phenyl isocyanate (1 equiv.) was added dropwise. The mixture was stirred at reflux for 24 hours. The reaction was quenched with MeOH and solvent was removed under reduced pressure. The crude mixture was purified (FCC eluent: 90:10 pentane:EtOAc) and following recrystallisation in MeCN the desired product was afforded as a white solid in 85 % yield.

^{1}H NMR (500 MHz, $CDCl_3$, 298 K) δ = 8.54 (d, *J* = 9.0 Hz, 1H), 8.13 (d, *J* = 8.8 Hz, 1H), 8.01 (d, *J* = 9.2 Hz, 2H), 8.00 (d, *J* = 8.0 Hz, 1H), 7.91 (d, *J* = 8.1 Hz, 1H), 7.80 (br s, 2H), 7.56 (t, *J* = 7.5 Hz, 1H), 7.54–7.50 (m, 2H), 7.38 (t, *J* = 7.3 Hz, 1H), 7.31 (t, *J* = 7.6 Hz, 1H), 7.22 (t, *J* = 7.9 Hz, 1H), 7.17 (d, *J* = 8.4 Hz, 1H), 6.90 (br s, 1H), 6.87 (d, *J* = 8.7 Hz, 1H), 6.80–6.68 (m, 3H), 3.64 (m, 1H), 1.04 (d, *J* = 6.8 Hz, 3H), 0.67 (br s, 3H); **^{19}F NMR** (471 MHz, $CDCl_3$, 298 K) δ = -63.03 (s), - 134.50 (br s), - 164.54 (br s); **^{13}C NMR{^{1}H, ^{19}F}** (125 MHz, $CDCl_3$, 298 K) δ = 171.8, 155.9 (br), 152.0, 151.0 (br), 135.9, 135.5 (br), 134.4, 134.1, 133.3, 133.2, 132.4, 131.9, 130.7, 130.3, 129.9, 128.7, 128.5, 128.3, 128.1, 127.6, 127.4, 127.1, 127.0, 126.9, 125.3, 124.7, 123.0, 120.2, 119.8, 117.3, 102.8 (br), 53.4 (br), 21.0 (br), 20.7 (br); **HRMS** (ESI^{+}) m/z calculated for $C_{39}H_{28}N_4O_2F_9$ $(M+H)^{+}$ 755.2063, found 755.2061; **IR** (liquid film) ν = 3658, 2980, 2889, 1712, 1632, 1528, 1505, 1474, 1461, 1437, 1387, 1277, 1252, 1172, 1149, 1073, 966, 940, 829, 805, 755, 646 cm^{-1}; **mp** 145–147 ˚C; **$[\alpha]_{D}^{25\,°C}$** = -68.6 ° (c = 0.5, $CHCl_3$).

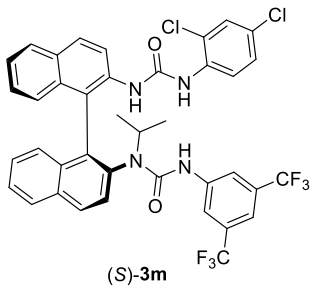
(*S*)-**3m**

(*S*)-3-(3,5-bis(trifluoromethyl)phenyl)-1-isopropyl-1-(2'-(3-(2,4-dichlorophenyl)ureido)-[1,1'-binaphthalen]-2- yl)urea (3m)

In a flame-dried Schlenk under inert atmosphere, aniline (*S*)-**15b** (200 mg, 0.61 mmol, 1 equiv.) was dissolved in dry DCM (0.4 M) and 2,4-

dichlorophenyl isocyanate (1 equiv.) was added dropwise. The mixture was stirred for 4 hours at room temperature until full conversion of starting material was seen by TLC. 3,5-bistrifluoromethylphenyl isocyanate (1 equiv.) was added dropwise and mixture was stirred at reflux for 48 h. The reaction was quenched with MeOH and solvent was removed under reduced pressure. The crude mixture was purified (FCC eluent: 80:20 DCM:hexane) and recrystallised in DCM/hexane to afford the desired product as a white solid in 79 % yield.

^{1}H NMR (600 MHz, $CDCl_3$) δ = 8.26 – 8.22 (m, 1H), 8.10 (d, *J* = 8.8 Hz, 1H), 8.03 (d, *J* = 9.0 Hz, 1H), 7.98 (d, *J* = 8.2 Hz, 1H), 7.93 (d, *J* = 8.2 Hz, 1H), 7.76 (s, 2H), 7.53 (dd, *J* = 11.7, 7.8 Hz, 2H), 7.42 (s, 2H), 7.30 (t, *J* = 7.7 Hz, 1H), 7.26 – 7.23 (m, 1H), 7.20 (d, *J* = 8.5 Hz, 1H), 7.17 – 7.14 (m, 1H), 7.08 (s, 1H), 6.93 (t, *J* = 7.3 Hz, 2H), 6.74 (br s, 3H), 3.43 (s, 1H), 1.11 (br s, 3H), 0.57 (br s, 3H); **^{19}F NMR** (565 MHz, $CDCl_3$) δ -62.9; **^{13}C NMR** (151 MHz, $CDCl_3$) δ 154.7, 152.2, 140.3, 139.9, 135.0, 133.8, 133.3, 133.1, 132.2 (q, *J* = 33.6 Hz), 132.1, 130.9, 130.9, 130.0, 128.7, 128.6, 128.5, 127.8, 127.5, 127.4, 127.2, 126.7, 125.4, 125.2, 123.2 (d, *J* = 272.9 Hz), 121.8, 120.9 (d, *J* = 16.0 Hz), 119.6, 116.6, 54.6, 20.6, 20.3; **HRMS** (ESI^+) m/z calculated for $C_{39}H_{29}Cl_2F_6N_4O_2$ $(M+H)^+$ 769.1566, found 769.1566; **IR** (neat) ν = 3680, 3366, 2923, 2865, 2844, 2359, 1679, 1507, 1439, 1386, 1339, 1278, 1181, 1136, 1055, 1033, 1014, 883, 818, 750, 683 cm^{-1}; **mp** 138 – 141˚C; **$[\alpha]^{D}_{25\,°C}$** = -123.2 ° (c = 1.0, $CHCl_3$).

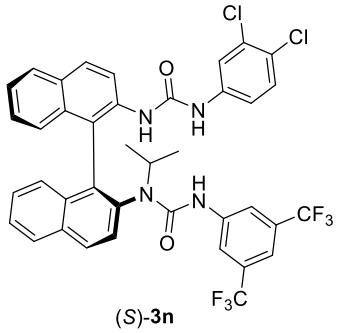

(*S*)-**3n**

(*S*)-3-(3,5-bis(trifluoromethyl)phenyl)-1-isopropyl-1-(2'-(3-(3,4-dichlorophenyl)ureido)-[1,1'-binaphthalen]-2- yl)urea (3n)

In a flame-dried Schlenk under inert atmosphere, aniline (*S*)-**15b** (200 mg, 0.61 mmol, 1 equiv.) was dissolved in dry DCM (0.4 M) and 3,4-dichlorophenyl isocyanate (1 equiv.) was added dropwise. The mixture was stirred for 10 minutes at room temperature until full conversion of starting material was seen by TLC. 3,5-bistrifluoromethylphenyl isocyanate (1 equiv.) was added dropwise and mixture was stirred at reflux for 48 h. The reaction was quenched with MeOH and solvent was removed under reduced

pressure. The crude mixture was purified (FCC eluent: 80:20 pentane:EtOAc) and following recrystallisation in DCM/hexane the desired product was afforded as a white solid in 73 % yield.

^{1}H NMR (600 MHz, $CDCl_3$) δ = 8.49 (d, *J* = 9.1 Hz, 1H), 8.12 (d, *J* = 8.7 Hz, 1H), 7.99 (dd, *J* = 8.4, 4.3 Hz, 2H), 7.90 (d, *J* = 8.0 Hz, 1H), 7.79 (s, 2H), 7.57 – 7.50 (m, 2H), 7.49 (s, 1H), 7.37 (t, *J* = 7.5 Hz, 1H), 7.33 (s, 1H), 7.32 – 7.27 (m, 1H), 7.20 (dd, *J* = 24.1, 8.3 Hz, 1H), 7.08 (d, *J* = 8.8 Hz, 1H), 6.96 (s, 1H), 6.87 (d, *J* = 8.5 Hz, 1H), 6.84 – 6.78 (m, 1H), 6.76 (dd, *J* = 8.7, 2.8 Hz, 1H), 5.32 (br s, 2H), 3.60 (s, 1H), 1.03 (d, *J* = 7.1 Hz, 3H), 0.66 (s, 3H); **^{19}F NMR** (565 MHz, $CDCl_3$) δ -62.9; **^{13}C NMR** (151 MHz, $CDCl_3$) δ = 155.7 (br), 152.1, 140.0, 139.6, 137.9, 133.9, 133.3, 133.2, 132.5, 132.4 (q, *J* = 33.6 Hz), 132.0, 130.7, 130.3, 130.1, 129.9, 128.7, 128.3, 128.1, 127.7, 127.4, 127.1, 127.0, 125.8, 125.2, 124.7, 123.1 (q, *J* = 272.9 Hz), 120.1, 120.0, 118.0, 117.2, 53.5 (br), 21.0, 20.7; **HRMS** (ESI^+) m/z calculated for $C_{39}H_{29}Cl_2F_6N_4O_2$ $(M+H)^+$ 769.1566, found 769.1547; **IR** (neat) ν = 3375, 2923, 2844, 2357, 1683, 1620, 1501, 1429, 1378, 1332, 1283, 1262, 1208, 1133, 1054, 1033, 927, 865, 813, 744 cm^{-1}; **mp** 180 – 181 ˚C; **$[\alpha]^D_{25\,°C}$** = -35.2 ° (c = 0.5, $CHCl_3$).

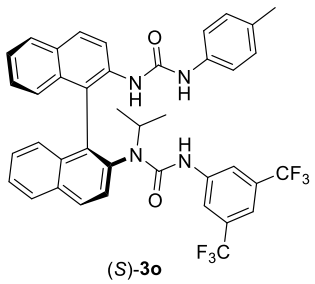
(*S*)-**3o**

(*S*)-3-(3,5-bis(trifluoromethyl)phenyl)-1-isopropyl-1-(2'-(3-(4-methylphenyl)ureido)-[1,1'-binaphthalen]-2- yl)urea (3o)

In a flame-dried Schlenk under inert atmosphere, aniline (*S*)-**15b** (450 mg, 1.37 mmol, 1 equiv.) was dissolved in dry DCM (0.4 M) and 4-methylphenyl isocyanate (1 equiv.) was added dropwise. The mixture was stirred for 24 hours at room temperature until full conversion of starting material was seen by TLC. 3,5-bis(trifluoromethyl)phenyl isocyanate (1 equiv.) was added dropwise and mixture was stirred at reflux for 24 hours. The reaction was quenched with MeOH and solvent was removed under reduced pressure. The crude mixture was purified (FCC eluent: 1st column: pentane:EtOAc 80:20, 2nd column 100% DCM) and following recrystallisation in Et_2O/hexane the desired product was afforded as a white solid in 57 % yield.

^{1}H NMR (500 MHz, $CDCl_3$, 323 K) δ = 8.52 (d, *J* = 8.9 Hz, 1H), 8.07 (d, *J* = 8.7 Hz, 1H), 7.99 (d, *J* = 8.8 Hz, 2H), 7.88 (d, *J* = 8.5 Hz, 1H), 7.70 (br s, 2H), 7.57 (t, *J* = 7.4 Hz, 1H), 7.49 (d, *J* = 8.7 Hz, 1H), 7.43 (s, 1H),

7.38–7.29 (m, 2H), 7.23 (d, *J* = 8.4 Hz, 1H), 7.19–7.08 (m, 1H), 6.87 (d, 8.5 Hz, 2H), 6.80–6.70 (m, 2H), 6.70 (br s, 2H), 6.55 (br s, 1H), 6.46 (br s, 1H), 3.39 (br s, 1H), 2.22 (s, 3H), 1.01 (d, *J* = 4.7 Hz, 3H), 0.84 (br s, 3H), **^{19}F NMR** (471 MHz, $CDCl_3$, 323 K) δ = -63.01 (s), **^{13}C NMR** (126 MHz, $CDCl_3$, 323 K) δ = 154.4 (br), 153.0, 140.4, 140.2, 136.1, 134.8 (br), 133.9, 133.3, 133.2, 132.6, 132.3, 132.3 (q, *J* = 33.4 Hz), 130.8, 130.5, 129.9, 129.6, 128.7, 128.4, 127.9, 127.8, 127.5, 126.9, 126.8, 124.8 (br), 124.6, 123.3 (q, *J* = 272.3 Hz), 120.7, 120.3 (br), 119.7 (br), 116.6, 116.3, 54.9, 20.8, 20.5, 20.4 (br); **HRMS** (ESI^+) m/z calculated for $C_{40}H_{33}N_4O_2F_6$ $(M+H)^+$ 715.2502, found 715.2502; **IR** (neat) ν = 3656, 3353, 2981, 2887, 1683, 1599, 1539, 1505, 1473, 1438, 1384, 1278, 1178, 1135, 955, 883, 817, 751, 700, 682, 642, 621, 610 cm^{-1}; **mp** 153–155 ˚C; **$[\alpha]_D^{25\,°C}$** = -11.9 ° (c = 1.0, $CHCl_3$).

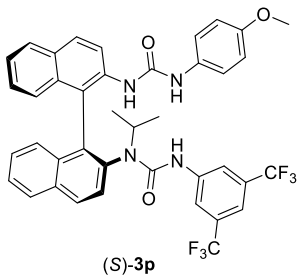
(*S*)-**3p**

(*S*)-3-(3,5-bis(trifluoromethyl)phenyl)-1-isopropyl-1-(2'-(3-(4-methoxyphenyl)ureido)-[1,1'-binaphthalen]-2- yl)urea (3p)

In a flame-dried Schlenk under inert atmosphere, aniline (*S*)-**15b** (450 mg, 1.37 mmol, 1 equiv.) was dissolved in dry DCM (0.4 M) and 4-methoxyphenyl isocyanate (1 equiv.) was added dropwise. The mixture was stirred for 24 hours at room temperature until full conversion of starting material was seen by TLC. 3,5-bis(trifluoromethyl)phenyl isocyanate (1 equiv.) was added dropwise and mixture was stirred at reflux for 24 hours. The reaction was quenched with MeOH and solvent was removed under reduced pressure. The crude mixture was purified (FCC eluent: DCM:Et_2O 98:2 to 95:5) and following recrystallisation in DCM/hexane the desired product was afforded as a white solid in 61 % yield.

^{1}H NMR (500 MHz, $CDCl_3$, 323 K) δ = 8.55 (d, *J* = 9.0 Hz, 1H), 8.05 (d, *J* = 8.4 Hz, 1H), 8.00 (d, *J* = 9.1 Hz, 1H), 7.99 (d, *J* = 8.0 Hz, 1H), 7.88 (d, *J* = 8.1 Hz, 1H), 7.68 (br s, 2H), 7.57 (t, *J* = 7.5 Hz, 1H), 7.47 (d, *J* = 8.6 Hz, 1H), 7.43 (br s, 1H), 7.38–7.28 (m, 2H), 7.24 (d, *J* = 8.5 Hz, 1H), 7.16–7.06 (m, 1H), 6.87 (d, *J* = 8.4 Hz, 1H), 6.66 (br s, 2H), 6.49 (d, *J* = 8.2 Hz, 3H), 6.31 (br s, 1H), 3.75 (s, 3H), 3.35 (br s, 1H), 0.99 (br s, 3H), 0.88 (br s, 3H), **^{19}F NMR** (471 MHz, $CDCl_3$, 323 K) δ = -63.0 (s), **^{13}C NMR** (126 MHz, $CDCl_3$, 323 K) [overlapping signals] δ = 157.2 (br), 154.2 (br), 153.4, 140.5, 140.2, 136.0, 133.8, 133.3, 133.1, 132.3,

132.3 (q, *J* = 33.5 Hz), 130.9, 130.6, 130.0, 128.8, 128.5, 128.0, 127.8, 127.5, 126.8, 126.7, 124.7, 123.3 (q, *J* = 272.4 Hz), 120.5, 120.2 (br), 120.1, 119.6, 116.5, 114.5, 55.6, 55.2 (br), 20.6, 20.3 (br); **HRMS** (ESI^+) m/z calculated for $C_{40}H_{32}N_4O_3F_6Na$ $(M+Na)^+$ 753.2271, found 753.2268; **IR** (neat) ν = 3657, 2981, 2887, 1683, 1599, 1504, 1473, 1438, 1386, 1278, 1243, 1178, 1108, 1036, 967, 939, 883, 824, 752, 682, 647, 625 cm-1; **mp** 152 – 154 ˚C; $[\alpha]_D^{25\,°C}$ = +18.0 ° (c = 1.0, $CHCl_3$).

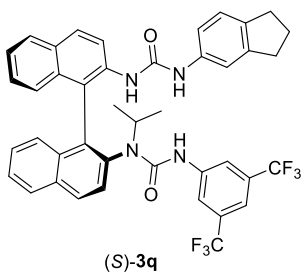
(*S*)-**3q**

(*S*)-3-(3,5-bis(trifluoromethyl)phenyl)-1-(2'-(3-(2,3-dihydro-1*H*-iden-5-yl)ureido)-[1,1'-binaphthalen]-2-yl)-1-isopropylurea (3q)

In a flame-dried Schlenk under inert atmosphere, aniline (*S*)-**15b** (500 mg, 1.53 mmol, 1 equiv.) was dissolved in dry DCM (0.4 M) 5-indanyl isocyanate (1 equiv.) was added dropwise. The mixture was stirred for 24 hours at room temperature until full conversion of starting material was seen by TLC. 3,5-bis(trifluoromethyl)phenyl isocyanate (1 equiv.) was added dropwise and mixture was stirred at reflux for 48 hours. The reaction was quenched with MeOH and solvent was removed under reduced pressure. The crude mixture was purified (FCC eluent: pentane:EtOAc 90:10 to 80:20) and following recrystallisation in DCM/hexane the desired product was afforded as a white solid in 76 % yield.

^{1}H NMR (600 MHz, $CDCl_3$) δ = 8.52 (d, *J* = 10.0 Hz, 1H), 8.07 (s, 1H), 7.98 (dd, *J* = 8.7, 3.3 Hz, 2H), 7.88 (d, *J* = 8.2 Hz, 1H), 7.74 (s, 1H), 7.56 (t, *J* = 7.6 Hz, 1H), 7.49 (s, 1H), 7.41 (s, 1H), 7.33 (t, *J* = 7.7 Hz, 2H), 7.23 (d, *J* = 8.4 Hz, 1H), 7.14 (s, 1H), 6.85 (d, *J* = 8.4 Hz, 1H), 6.77 (s, 2H), 6.52 (s, 2H), 3.45 (s, 1H), 2.77 (t, *J* = 7.5 Hz, 2H), 2.69 (hept, *J* = 7.9 Hz, 2H), 2.03 – 1.96 (m, 2H), 1.64 (s, 3H), 1.15 – 0.81 (m, 3H); **^{19}F NMR** (565 MHz, $CDCl_3$) δ = -62.9 (s); **^{13}C NMR** (151 MHz, $CDCl_3$) [overlapping signals] δ = 154.9 (br), 145.2, 140.2, 140.0, 139.2 (br), 136.0, 133.8, 133.1, 132.2, 132.1 (q, *J* = 33.6 Hz), 130.8, 130.3, 129.9, 128.7, 128.3, 127.8, 127.5, 126.8, 126.7, 124.6, 123.2 (q, *J* = 272.9 Hz), 120.5, 120.5, 120.0 (br), 119.6, 119.3 (br), 117.7 (br), 116.6, 116.4, 54.2 (br), 32.8, 32.4, 25.6, 20.5**,** 20.2 (br); **HRMS** (ESI^+) m/z calculated for $C_{42}H_{35}F_6N_4O_2$ $(M+H)^+$ 741.2659, found 741.2635; **IR** (neat) ν = 3680, 3404, 2923, 2865,

2365, 1681, 1541, 1439, 1378, 1346, 1278, 1180, 1133, 1055, 1033, 1015, 929, 880, 818, 751, 628 cm^{-1}; **mp** 140 – 143 ˚C; **$[\alpha]^{D}_{25\,°C}$** = +0.2 ° (c = 1.0, $CHCl_3$).

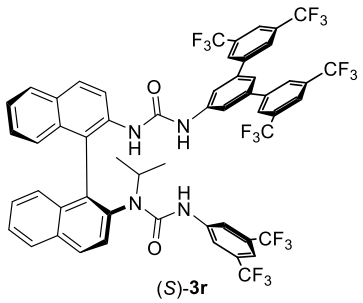
(*S*)-**3r**

3-(3,5-bis(trifluoromethyl)phenyl)-1-isopropyl-1-(2'-(3-(3,3'',5,5''-tetrakis(trifluoromethyl)-[1,1':3',1''-terphenyl]-5'-yl)ureido)-[1,1'-binaphthalen]-2-yl)urea (3r)

In a flame-dried Schlenk under inert atmosphere, aniline (*S*)-**15b** (500 mg, 1.53 mmol, 1 equiv.) was dissolved in dry DCM (0.4 M) and 5'-isocyanato-3,3'',5,5''-tetrakis(trifluoromethyl)-1,1':3',1''-terphenyl (1 equiv.) was added dropwise. The mixture was stirred for 1 hour at room temperature until full conversion of starting material was seen by TLC. 3,5-bis(trifluoromethyl)phenyl isocyanate (1 equiv.) was added dropwise and mixture was stirred at reflux for 24 hours. The reaction was quenched with MeOH and solvent was removed under reduced pressure. The crude mixture was purified (FCC eluent: pentane:EtOAc 90:10) and following recrystallisation in DCM/hexane the desired product was afforded as a white solid in 65 % yield.

^{1}H NMR (500 MHz, $CDCl_3$) δ = 8.49 (d, *J* = 9.8 Hz, 1H), 8.14 (d, *J* = 8.7 Hz, 1H), 8.04 (d, *J* = 9.2 Hz, 1H), 8.00 (d, *J* = 7.9 Hz, 1H), 7.98 – 7.90 (m, 6H), 7.88 (s, 2H), 7.80 (s, 2H), 7.59 – 7.51 (m, 2H), 7.47 (d, *J* = 1.7 Hz, 2H), 7.41 (ddd, *J* = 8.1, 6.7, 1.1 Hz, 1H), 7.32 (ddd, *J* = 8.4, 6.1, 2.6 Hz, 2H), 7.29 – 7.19 (m, 4H), 7.01 (s, 1H), 6.91 (d, *J* = 8.2 Hz, 1H), 6.77 (s, 1H), 3.68 – 3.57 (m, 1H), 1.11 (d, *J* = 6.9 Hz, 3H), 0.68 – 0.63 (m, 3H); **^{19}F NMR** (471 MHz, $CDCl_3$) δ = -62.8, -63.3; **^{13}C NMR** (126 MHz, $CDCl_3$) δ = 155.7 (br), 152.5, 142.8, 140.3, 140.2, 140.0, 139.6, 135.7, 133.9, 133.4, 133.2, 132.3, 132.2, 132.1, 130.8, 130.6, 130.1, 128.7, 128.4, 127.9, 127.8, 127.6, 127.5, 127.3, 127.1, 125.4, 124.9, 123.4, 123.2, 123.0, 121.5, 120.8, 120.7, 119.9, 117.9, 116.9, 53.7 (br), 21.0, 20.6; **HRMS** (ESI^+) m/z calculated for $C_{55}H_{34}F_{18}N_4O_2$ $(M+H)^+$ 1125.2467, found 1125.2437; **IR** (neat) ν = 3367, 2925, 2854, 1686, 1599, 1542, 1506, 1471, 1368, 1278, 1177, 1131, 901, 844, 819, 751, 706, 683, 640 cm^{-1}; **mp** 136 – 138 ˚C; **$[\alpha]^{D}_{25\,°C}$** = -24.0 ° (c = 1.0, $CHCl_3$).

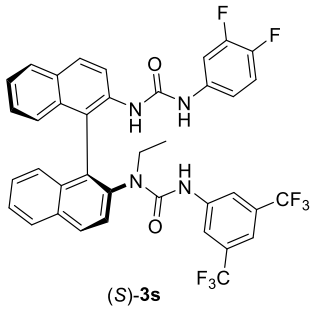

(*S*)-**3s**

(*S*)-3-(3,5-bis(trifluoromethyl)phenyl)-1-(2'-(3-(3,4-difluorophenyl)ureido)-[1,1'-binapthalen]-2-yl)-1-ethylurea (3s)

In a flame-dried Schlenk under inert atmosphere, aniline (*S*)-**15a** (500 mg, 1.60 mmol, 1 equiv.) was dissolved in dry DCM (0.4 M) and 3,4-difluorophenyl isocyanate (1 equiv.) was added dropwise. The mixture was stirred for 10 minutes at room temperature until full conversion of starting material was seen by TLC. 3,5-bistrifluoromethylphenyl isocyanate (1 equiv.) was added dropwise and mixture was stirred at reflux for 24 h. The reaction was quenched with MeOH and solvent was removed under reduced pressure. The crude mixture was purified (FCC eluent: 80:20 pentane:EtOAc) and following recrystallisation in DCM/hexane the desired product was afforded as a white solid in 59 % yield.

^{1}H NMR (500 MHz, $CDCl_3$) δ = 8.13 (s, 1H), 7.84 (d, *J* = 8.7 Hz, 1H), 7.70 (d, *J* = 8.2 Hz, 1H), 7.67 (d, *J* = 9.0 Hz, 1H), 7.62 (d, *J* = 8.2 Hz, 1H), 7.55 (br s, 1H), 7.26 (t, *J* = 7.6 Hz, 2H), 7.21 (s, 1H), 7.10 (t, *J* = 7.8 Hz, 1H), 7.06 – 6.97 (m, 2H), 6.95 (br s, 1H), 6.83 (d, *J* = 8.5 Hz, 2H), 6.71 (br s, 2H), 6.61 (d, *J* = 8.4 Hz, 1H), 6.54 (q, *J* = 9.0 Hz, 1H), 6.25 (d, *J* = 8.7 Hz, 1H), 2.94 (s, 1H), 2.81 (s, 1H), 0.70 (t, *J* = 7.2 Hz, 3H); **^{19}F NMR** (471 MHz, $CDCl_3$) δ = -63.0, -136.5, -145.2; **^{13}C NMR{^{1}H, ^{19}F}** (126 MHz, $CDCl_3$) δ = 155.6 (br), 152.4, 150.0, 146.3, 139.7, 138.8, 135.8, 134.7, 133.8, 133.3, 133.1, 132.3, 131.7, 130.7, 130.2, 129.8, 128.7, 128.4, 128.0, 127.6, 127.4, 127.2, 126.7, 124.9, 124.7, 123.1, 120.1 (br), 120.0, 119.6 (br), 117.1, 116.9, 114.6, 108.6, 44.4, 13.5; **HRMS** (ESI^+) m/z calculated for $C_{38}H_{26}F_8N_4O_2$ $(M+H)^+$ 723.2001, found 723.1983; **IR** (neat) ν = 3680, 3339, 2923, 2866, 2844, 2362, 1683, 1502, 1430, 1374, 1346, 1281, 1263, 1208, 1133, 1054, 1033, 1016, 813, 744, 683 cm^{-1}; **mp** 147 – 149 ˚C; **$[\alpha]^{D}_{25\,°C}$** = -81.4 ° (c = 1.0, $CHCl_3$).

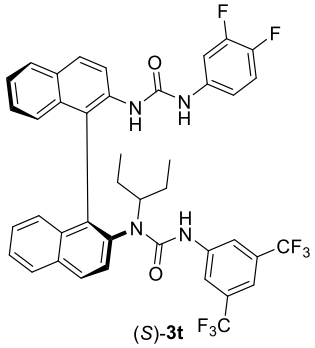

(*S*)-**3t**

(*S*)-3-(3,5-bis(trifluoromethyl)phenyl)-1-pentyl-1-(2'-(3-(3,4-difluorophenyl)ureido)-[1,1'-binaphthalen]-2- yl)urea (3t)

In a flame-dried Schlenk under inert atmosphere, intermediate (*S*)-**16t** was dissolved in dry DCM (0.4 M) and 3,5-*bis*(trifluoromethyl)phenyl isocyanate (1 equiv.) was added dropwise. The mixture was refluxed for

72 hours. The reaction was quenched with MeOH and solvent was removed under reduced pressure. The crude reaction was (FCC eluent: 1st column 95:5 pentane:Et_2O to 80:20, 2nd column 100% $CHCl_3$) to afford the desired product as a white solid in 48 % yield.

^{1}H NMR (500 MHz, $CDCl_3$, 298 K) δ = 8.57 (d, *J* = 9.1 Hz, 1H), 8.10 (d, *J* = 8.8 Hz, 1H), 8.01 (d, *J* = 9.2 Hz, 1H), 7.97 (d, *J* = 8.1 Hz, 1H), 7.92 (d, *J* = 8.1 Hz, 1H), 7.82 (s, 2H), 7.62 (d, *J* = 8.8 Hz, 1H), 7.57 – 7.50 (m, 2H), 7.38 (ddd, *J* = 8.0, 6.7, 1.1 Hz, 1H), 7.32 – 7.26 (m, 2H), 7.25 – 7.15 (m, 2H), 7.13 (d, *J* = 8.5 Hz, 1H), 6.94 (d, *J* = 8.4 Hz, 1H), 6.91 (br s, 1H), 6.88 – 6.75 (m, 2H), 6.57 (d, *J* = 8.9 Hz, 1H), 2.97 (s, 1H), 1.74 (s, 1H), 1.64 (m, 1H), 0.98 (s, 3H), 0.87 (s, 1H), 0.53 (s, 1H), -0.21 (s, 3H); **^{19}F NMR** (471 MHz, $CDCl_3$, 298 K) δ = -63.0 (s), -136.6 (br s), -145.4 (br s); **^{13}C NMR{^{1}H, ^{19}F}** (126 MHz, $CDCl_3$) [overlapping signals] δ = 156.0 (br), 152.1, 150.1, 146.2, 142.1, 139.5, 136.2, 134.9, 133.8, 133.2, 133.1, 132.5, 130.8, 130.4, 130.3, 130.0, 128.8, 128.3, 127.5, 127.3, 127.3, 127.0, 125.2, 124.7, 123.1, 119.9, 119.8, 117.3, 116.9, 114.2 (br), 108.3 (br), 66.7, 28.9 (br), 26.4, 12.9, 11.1; **HRMS** (ESI$^+$) m/z calculated for $C_{41}H_{33}F_8N_4O_2$ $(M+H)^+$ 765.2470, found 765.2462; **IR** (liquid film) ν = 3649, 2067, 2994, 2954, 1685, 1602, 1541, 1520, 1475, 1279, 1252, 1118, 970, 886 cm^{-1}; **mp** 119-122 ˚C; **$[\alpha]^D_{25\,°C}$** = -88.6 ° (c = 0.5, $CHCl_3$).

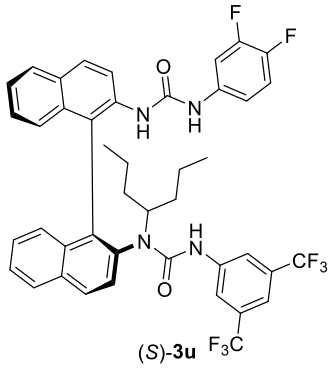

(*S*)-**3u**

(*S*)-3-(3,5-bis(trifluoromethyl)phenyl)-1-heptyl-1-(2'-(3-(3,4-difluorophenyl)ureido)-[1,1'-binaphthalen]-2- yl)urea (3u)

In a flame-dried Schlenk under inert atmosphere, intermediate (*S*)-**16u** was dissolved in dry DCM (0.4 M) and 3,5-*bis*(trifluoromethyl)phenyl isocyanate (1 equiv.) was added dropwise. The mixture was refluxed for 72 hours. The reaction was quenched with MeOH and solvent was removed under reduced pressure. The crude reaction was purified (FCC eluent: 1st column 95:5 pentane:Et_2O to 80:20, 2nd column 100% $CHCl_3$) to afford the desired product as a white solid in 40 % yield.

^{1}H NMR (600 MHz, $CDCl_3$, 298 K) δ = 8.60 (d, *J* = 9.1 Hz, 1H), 8.10 (d, *J* = 8.8 Hz, 1H), 8.02 (d, *J* = 9.1 Hz, 1H), 7.98 (d, *J* = 8.2 Hz, 1H), 7.91 (d, *J* = 8.2 Hz, 1H), 7.84 (s, 2H), 7.60 (d, J = 8.8 Hz, 1H), 7.57 – 7.51 (m, 2H), 7.38 (t, *J* = 7.3 Hz, 1H), 7.34 – 7.26 (m, 2H), 7.26 – 7.16 (m, 2H), 7.14 (d, *J* =8.5 Hz, 1H), 7.00 – 6.89

(m, 2H), 6.88 – 6.70 (m, 2H), 6.58 (d, *J* = 8.9 Hz, 1H), 3.15 – 3.00 (m, 1H), 1.78 (s, 1H), 1.52 – 1.45 (m, 2H), 1.30 (s, 2H), 0.78 (t, *J* = 6.9 Hz, 3H), 0.57 (s, 1H), 0.34 (m, 4H), -0.69 (s, 1H); **^{19}F NMR** (565 MHz, $CDCl_3$, 298 K) δ = -62.9 (s), -136.6 (br s), -145.5 (br s); **^{13}C NMR{^{1}H, ^{19}F}** (125 MHz, $CDCl_3$, 298 K) [overlapping signals] δ = 155.9 (br), 152.2, 150.1, 146.2, 142.1, 139.6, 136.2, 135.0, 133.8, 133.2, 133.1, 132.5, 130.8, 130.4, 130.3, 129.9, 128.7, 128.3, 128.2, 127.5, 127.3, 127.3, 127.1, 125.7, 125.2, 124.7, 124.3, 123.2, 122.0, 119.9 (br), 117.3, 116.9, 114.2, 108.3 (br), 63.8 (br), 38.7 (br), 36.3, 22.8, 20.5, 14.3, 14.0; ; **HRMS** (ESI^+) m/z calculated for $C_{43}H_{37}F_8N_4O_2$ $(M+H)^+$ 793.2783, found 793.2770; **IR** (neat) ν = 3367, 2926, 2872, 2855, 1717, 1686, 1620, 1519, 1505, 1472, 1432, 1381, 1278, 1209, 1180, 1133, 1037, 1016, 936, 882, 817, 752, 700, 683, 610 cm^{-1}; **mp** 142–144 ˚C **$[\alpha]^{D}_{25\,°C}$** = -83.2° (c = 1.0, $CHCl_3$).

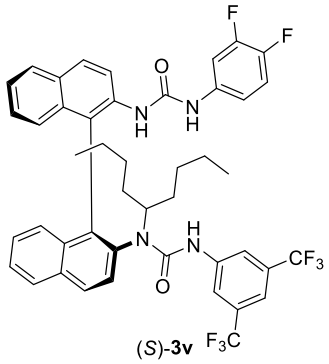

(*S*)-**3v**

(*S*)-3-(3,5-bis(trifluoromethyl)phenyl)-1-nonan-5-yl-1-(2'-(3-(3,4-difluorophenyl)ureido)-[1,1'-binaphthalen]-2- yl)urea (3v)

In a flame-dried Schlenk under inert atmosphere, intermediate (*S*)-**16v** was dissolved in dry DCM (0.4 M) and 3,5-*bis*(trifluoromethyl)phenyl isocyanate (1 equiv.) was added dropwise. The mixture was refluxed for 72 hours. The reaction was quenched with MeOH and solvent was removed under reduced pressure. The crude reaction was (FCC eluent: 1st column 95:5 pentane:Et_2O to 80:20, 2nd column 100% $CHCl_3$) to afford the desired product as a white solid 26 % yield.

^{1}H NMR (500 MHz, $CDCl_3$) δ = 8.57 (d, *J* = 9.1 Hz, 1H), 8.10 (d, *J* = 8.8 Hz, 1H), 8.01 (d, *J* = 9.2 Hz, 1H), 7.97 (d, *J* = 8.1 Hz, 1H), 7.90 (d, *J* = 8.1 Hz, 1H), 7.84 (s, 2H), 7.60 (d, *J* = 8.8 Hz, 1H), 7.57 – 7.49 (m, 2H), 7.44 – 7.32 (m, 2H), 7.31 – 7.26 (m, 2H), 7.24 – 7.17 (m, 1H), 7.12 (d, *J* = 8.5 Hz, 1H), 7.03 -6.91 (m, 2H), 6.90 – 6.77 (m, 2H), 6.57 (d, *J* = 8.9 Hz, 1H), 3.08 (s, 1H), 1.78 (br s, 1H), 1.60 (br s, 1H), 1.58 -1.50 (m, 1H), 1.43 (br s, 1H), 1.21 – 1.05 (m, 2H), 0.96 – 0.85 (m, 1H), 0.82 (t, *J* = 7.2 Hz, 3H), 0.80 – 0.67 (m, 1H) 0.66 – 0.52 (m, 4H), 0.50 – 0.27 (m, 2H), -0.71 (br s, 1H); **^{19}F NMR** (471 MHz, $CDCl_3$) δ = -63.0, -136.5, -145.3; **^{13}C NMR{^{1}H, ^{19}F}** (125 MHz, $CDCl_3$, 298 K) δ = 156.0 (br), 152.2, 150.1, 146.2, 142.2, 140.3, 139.5, 136.1, 134.9, 133.8, 133.2, 133.1, 132.6, 132.2, 130.8, 130.4, 130.0, 128.8, 128.3, 128.2, 127.5, 127.3,

127.1, 125.3, 124.7, 123.1, 119.8, 118.8, 117.3, 116.9, 116.2, 114.2, 108.4, 63.9 (br), 36.7, 33.4, 30.2, 29.9, 22.8, 22.5, 14.0, 13.9; **HRMS** (ESI$^+$) m/z calculated for $C_{45}H_{41}F_8N_4O_2$ 821.3096, 821.3083; **IR** (neat) ν = 3814, 3692, 3335, 1711, 1688, 1659, 1623, 1505, 1474, 1437, 1383, 1280, 1211, 1182, 1137, 882, 757, 683, 671, 657, 646, 620 cm^{-1}; **mp** 108 – 109 ˚C; **[α]^D $_{25\,°C}$** = -53.7° (c = 0.2, $CHCl_3$).

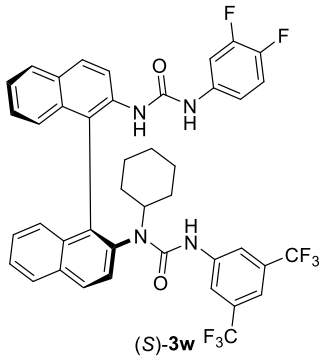

(*S*)-**3w**

(*S*)-3-(3,5-bis(trifluoromethyl)phenyl)-1-cyclohexyl-1-(2'-(3-(3,4-difluorophenyl)ureido)-[1,1'-binaphthalen]-2- yl)urea (3w)

In a flame-dried Schlenk under inert atmosphere, intermediate (*S*)-**16w** was dissolved in dry DCM (0.4 M) and 3,5-*bis*(trifluoromethyl)phenyl isocyanate (1 equiv.) was added dropwise. The mixture was refluxed for 72 hours. The reaction was quenched with MeOH and solvent was removed under reduced pressure. The crude reaction was (FCC eluent: 1st column 90:10 pentane:Et_2O to 80:20, 2nd column 100% $CHCl_3$) to afford the desired product as a white solid in 50 % yield.

^{1}H NMR (500 MHz, $CDCl_3$) δ = 8.42 (d, *J* = 9.1 Hz, 1H), 8.09 (d, *J* = 8.7 Hz, 1H), 7.98 (d, *J* = 9.2 Hz, 1H), 7.96 (d, *J* = 8.0 Hz, 1H), 7.92 (d, *J* = 8.2 Hz, 1H), 7.81 (s, 2H), 7.57 – 7.52 (m, 2H), 7.51 (br s, 1H), 7.42 (t, *J* = 7.5 Hz, 1H), 7.38 – 7.26 (m, 3H), 7.25 (d, *J* = 8.3 Hz, 1H), 7.10 (br s, 1H), 7.02 – 6.90 (m, 3H), 6.82 (q, *J* = 9.2 Hz, 1H), 6.49 (d, *J* = 8.6 Hz, 1H), 3.16 (br s, 1H), 1.80 (s, 1H), 1.54 (d, *J* = 12.5 Hz, 1H), 1.40 (s, 1H), 1.33 – 1.18 (m, 3H), 0.99 – 0.82 (m, 1H), 0.80 – 0.51 (m, 2H), 0.06 (br s, 1H); **^{19}F NMR** (471 MHz, $CDCl_3$) δ = -62.9, -136.6, -145.3; **^{13}C NMR{^{1}H, ^{19}F}** (125 MHz, $CDCl_3$, 298 K) δ = 155.7 (br), 152.4, 149.9, 146.2, 140.2, 139.7, 135.9, 134.7, 133.9, 133.1, 133.1, 132.3, 131.7, 130.6, 130.4, 129.8, 128.7, 128.3, 128.2, 127.6, 127.3, 127.0, 126.9, 125.5, 124.7, 123.2, 120.4, 120.2, 120.1, 117.0, 116.8, 114.4, 108.4, 62.5 (br), 31.7, 30.8, 26.1, 25.7, 25.0; **HRMS** (ESI$^+$) m/z calculated for $C_{42}H_{33}F_8N_4O_2$ $(M+H)^+$ 777.2470, found 777.2449; **IR** (neat) ν = 3359, 2933, 2860, 2360, 1683, 1621, 1539, 1505, 1473, 1432, 1383, 1339, 1278, 1209, 1180, 1134, 1040, 1003, 909, 882, 844, 804, 750, 735, 701, 682, 650, 627 cm^{-1}; **mp** 154 – 155 ˚C; **[α]^D $_{25\,°C}$** = -80.2° (c = 0.5, $CHCl_3$).

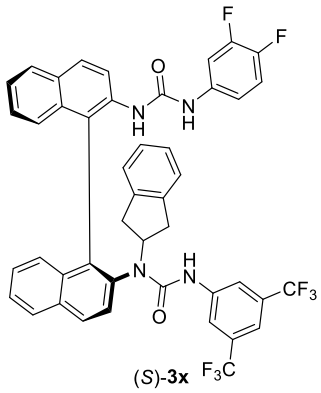

(*S*)-**3x**

(*S*)-3-(3,5-bis(trifluoromethyl)phenyl)-1-(2'-(3,4-difluorophenyl)ureido)-[1,1'-binaphthalen]-2-yl)-1-(2,3-dihydro-1*H*-inden-2-yl)urea (3x)

In a flame-dried Schlenk under inert atmosphere, intermediate (*S*)-**16x** (267 mg, 0.48 mmol, 1 equiv.) was dissolved in dry DCM (0.4 M) and 3,5-*bis*(trifluoromethyl)phenyl isocyanate (1 equiv.) was added dropwise. The mixture was refluxed for 72 hours. The reaction was quenched with MeOH and solvent was removed under reduced pressure. The crude reaction was (FCC eluent: 1st column 90:10 pentane:Et_2O to 80:20, 2nd column 100% $CHCl_3$) to afford the desired product as a white solid in 41 % yield.

^{1}H NMR (500 MHz, $CDCl_3$) δ 8.70 (d, *J* = 9.2 Hz, 1H), 8.15 (d, *J* = 8.7 Hz, 1H), 8.08 (d, *J* = 9.2 Hz, 1H), 8.01 (d, *J* = 7.6 Hz, 1H), 7.98 – 7.90 (m, 1H), 7.64 – 7.49 (m, 3H), 7.43 – 7.27 (m, 6H), 7.26 – 7.19 (m, 2H), 7.10 (dd, *J* = 5.3, 3.6 Hz, 1H), 6.93 (td, *J* = 18.8, 10.3 Hz, 5H), 6.68 (dd, *J* = 8.9, 4.1 Hz, 1H), 6.62 (s, 1H), 4.26 (tt, *J* = 10.4, 2.6 Hz, 1H), 3.55 (dd, *J* = 18.1, 10.5 Hz, 1H), 3.33 (dd, *J* = 18.1, 2.7 Hz, 1H), 2.06 – 1.95 (m, 1H), 1.87 (dd, *J* = 18.7, 10.3 Hz, 1H); **^{19}F NMR** (471 MHz, $CDCl_3$) δ = -63.12, -136.5, -145.3; **^{13}C NMR** (126 MHz, $CDCl_3$) δ 155.4 (br), 152.1, 150.1, 146.2, 142.6, 140.4, 139.9, 139.5, 136.5, 135.1, 133.8, 133.3, 133.1, 132.3, 130.9, 130.8, 130.0, 129.9, 128.8, 128.8, 128.7, 128.3, 127.6, 127.4, 127.4, 127.1, 127.0, 125.8, 124.6, 124.4, 123.0, 119.5, 118.6, 118.0, 116.9, 116.5, 114.4, 108.5, 60.4 (br), 39.6, 38.4; **IR** (neat) ν = 3680, 2923, 2865, 2844, 1684, 1505, 1382, 1346, 1279, 1263, 1181, 1134, 1055, 1033, 1014, 816, 683 cm^{-1}; **HRMS** (ESI^+) m/z calculated for $C_{45}H_{30}F_6N_4O_2$ $(M+H)^+$ 811.2314, found 811.2295; **mp** 147 – 150 ˚C; **$[\alpha]^D_{25\,°C}$** = -53.0 ° (c = 1.0, $CHCl_3$).

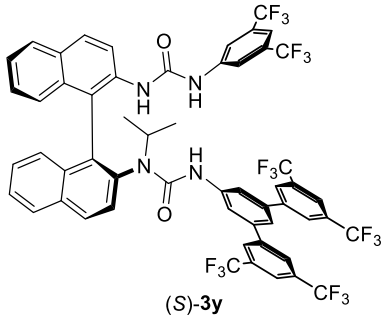

(*S*)-**3y**

1-(2'-(3-(3,5-bis(trifluoromethyl)phenyl)ureido)-[1,1'-binaphthalen]-2-yl)-1-isopropyl-3-(3,3'',5,5''-tetrakis(trifluoromethyl)-[1,1':3,1''-terphenyl]-5'-yl)urea (3y)

Synthesised by C. Palladino

In a flame-dried Schlenk under inert atmosphere, aniline (*S*)-**15b** (500 mg, 1.53 mmol, 1 equiv.) was dissolved in dry DCM (0.4 M) and 3,5-bis(trifluoromethyl)phenyl

isocyanate (1 equiv.) was added dropwise. The mixture was stirred for 1 hour at room temperature until full conversion of starting material was seen by TLC. 5'-isocyanato-3,3'',5,5''-tetrakis(trifluoromethyl)-1,1':3',1''-terphenyl (1 equiv.) was added and mixture was stirred at reflux for 72 hours. The reaction was quenched with MeOH and solvent was removed under reduced pressure. The crude mixture was purified (FCC eluent: pentane:Et_2O 90:10) to afford the desired product as a white solid in 60 % yield.

^{1}H NMR (500 MHz, $CDCl_3$) δ = 8.66 (d, *J* = 9.2 Hz, 1H), 8.15 (d, *J* = 8.7 Hz, 1H), 8.05 (d, *J* = 9.2 Hz, 1H), 7.99 (d, *J* = 8.1 Hz, 1H), 7.94 (d, *J* = 1.7 Hz, 5H), 7.88 (s, 2H), 7.62 (d, *J* = 8.7 Hz, 1H), 7.59 (s, 2H), 7.54 (ddd, *J* = 8.1, 6.8, 1.2 Hz, 1H), 7.48 (s, 2H), 7.43 (s, 1H), 7.42 – 7.38 (m, 1H), 7.35 (s, 2H), 7.29 (ddd, *J* = 8.4, 6.8, 1.4 Hz, 1H), 7.27 – 7.23 (m, 1H), 7.21 (s, 1H), 7.18 (d, *J* = 8.5 Hz, 1H), 6.90 (d, *J* = 8.4 Hz, 1H), 6.76 (s, 1H), 3.84 – 3.65 (m, 1H), 1.04 (d, *J* = 6.9 Hz, 3H), 0.77 (d, *J* = 6.9 Hz, 3H); **^{19}F NMR** (471 MHz, $CDCl_3$) δ = -62.8, -63.3; **^{13}C NMR{^{1}H, ^{19}F}** (126 MHz, $CDCl_3$) δ 157.0 (br), 151.9, 141.7, 140.5, 140.1, 139.8, 139.3, 136.0, 134.0, 133.5, 133.2, 132.5, 132.0, 131.7, 130.8, 130.3, 130.1, 128.7, 128.5, 128.4, 127.6, 127.4, 127.3, 127.2, 127.2, 125.5, 124.7, 123.3, 123.0, 122.7, 122.0, 121.7, 120.0, 119.4, 117.9, 115.6, 53.2 (br), 21.2, 20.9; **HRMS** (ESI^+) m/z calculated for $C_{55}H_{34}F_{18}N_4O_2$ $(M+H)^+$ 1125.2467, found 1125.2439; **IR** (neat) ν = 3379, 2923, 2853, 1719, 1636, 1509, 1474, 1389, 1367, 1279, 1180, 1128, 1180, 1128, 951, 921, 870, 846, 821, 747, 705, 683, 641 cm^{-1}; **mp** 218 – 220 ˚C; **$[\alpha]^D_{25\,°C}$** = -57.0 ° (c = 1.0, $CHCl_3$).

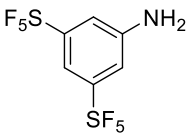

10

3,5-bis(pentafluorosulfanyl)aniline (10)

Compound **10** was prepared according to literature procedure in 55 % yield. Spectroscopic data are in accordance with those in literature.[6]

^{1}H NMR (400 MHz, $CDCl_3$) δ = 7.48 (s, 1H), 7.17 (s, 2H), 4.16 (s, 2H); **^{19}F NMR** (377 MHz, $CDCl_3$) δ = 62.3 (d, J_{FF} = 150.0 Hz), 82.7 (m); **^{13}C NMR** (101 MHz, $CDCl_3$) δ = 154.6 (quin, J_{CF} = 19.6 Hz), 142.2, 120.3, 119.9.

4.3. Substrate Synthesis and Characterisation

4.3.1. Synthesis of Benzylic Bromide Precursors

General Procedure 2

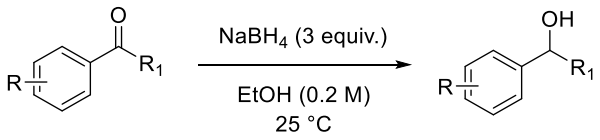

Alcohols were prepared by reduction of corresponding ketone (1 equiv.) with $NaBH_4$ (3 equiv.) in EtOH (0.2 M) at 25 °C. The reactions were monitored by TLC and quenched with H_2O when the ketone was fully consumed. Following work up in EtOAc/H_2O the organic extracts were washed with brine and dried with $MgSO_4$, solvent was removed under reduced pressure to give the corresponding alcohol. When required the mixture was purified by FCC.

General Procedure 3

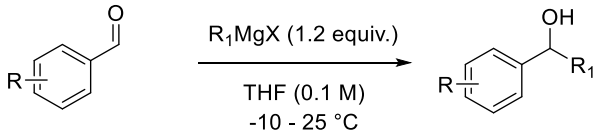

Alcohols were prepared by Grignard addition (1.2 equiv.) to the corresponding aldehyde (1 equiv.) in THF (0.25 M) at -10 °C. The reactions were monitoring by TLC and quenched with saturated NH_4Cl solution when the aldehyde was fully consumed. Following work up in Et_2O/H_2O the organic extracts were washed with brine and dried with $MgSO_4$, solvent was removed under reduced pressure to give the corresponding alcohol. When required the mixture was purified by FCC.

Alcohols *rac*-**17a** (CAS: 3562-73-0), *rac*-**17h** (CAS: 1517-72-2), *rac*-**17q** (CAS: 7228-47-9) were commercially available.

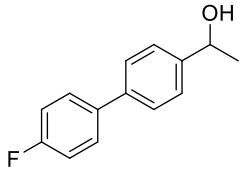

rac-**17b**

1-(4'-fluoro-[1,1'-biphenyl]-4-yl)ethan-1-ol (17b)

Compound *rac*-**6b** was prepared according to General Procedure 2, the product was isolated as a white solid in in 88 % yield. Spectroscopic data are in accordance with those in literature.[7]

^{1}H NMR (400 MHz, $CDCl_3$) δ = 7.59 – 7.49 (m, 4H), 7.49 – 7.41 (m, 2H), 7.18 – 7.07 (m, 2H), 4.96 (q, *J* = 6.4 Hz, 1H), 1.54 (d, *J* = 6.4 Hz, 3H); **^{19}F NMR** (377 MHz, $CDCl_3$) δ = -115.8; **^{13}C NMR** (126 MHz, $CDCl_3$) δ = 162.6 (d, J_{CF} = 246.3 Hz), 145.0, 139.5, 137.1 (d, J_{CF} = 3.2 Hz), 128.7 (d, J_{CF} = 8.1 Hz), 127.2, 126.0, 115.7 (d, J_{CF} = 21.6 Hz), 70.2, 25.3.

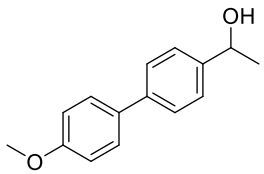

rac-**17c**

1-(4'-methoxy-[1,1'-biphenyl]-4-yl)ethan-1-ol (17c)

Compound *rac*-**6c** was prepared according to General Procedure 2, the product was isolated as a white solid in 75 % yield. Spectroscopic data are in accordance with those in literature.[8]

^{1}H NMR (400 MHz, $CDCl_3$) δ = 7.58 – 7.48 (m, 4H), 7.46 – 7.39 (m, 2H), 7.04 – 6.94 (m, 2H), 4.94 (q, *J* = 6.5 Hz, 1H), 3.85 (s, 3H), 1.54 (d, *J* = 6.4 Hz, 3H); **^{13}C NMR** (101 MHz, $CDCl_3$) δ = 159.3, 144.3, 140.2, 133.5, 128.2, 127.0, 126.0, 114.4, 70.3, 55.5, 25.3.

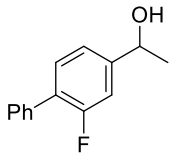

rac-**17d**

1-(2-fluoro-[1,1'-biphenyl]-4-yl)ethan-1-ol (17d)

Compound *rac*-**6d** was prepared according to General Procedure 2, following purification (FCC eluent: 90:10 pentane:EtOAc) the product was isolated as a white solid in 85 % yield. Spectroscopic data are in accordance with those in literature.[9]

^{1}H NMR (500 MHz, $CDCl_3$) δ = 7.58 – 7.53 (m, 2H), 7.44 (dt, *J* = 14.4, 7.6 Hz, 3H), 7.37 (t, *J* = 7.4 Hz, 1H), 7.24 – 7.17 (m, 2H), 4.94 (q, *J* = 6.5 Hz, 1H), 1.54 (d, *J* = 6.5 Hz, 3H); **^{19}F NMR** (377 MHz, $CDCl_3$) δ = -117.7; **^{13}C NMR** (126 MHz, $CDCl_3$) δ = 159.9 (d, *J* = 248.4 Hz), 147.6 (d, *J* = 6.9 Hz), 135.7, 130.9 (d, *J* = 3.7 Hz), 129.1 (d, *J* = 2.8 Hz), 128.6, 128.1 (d, J_{CF} = 13.6 Hz), 127.8, 121.4 (d, J_{CF} = 3.3 Hz), 113.2 (d, J_{CF} = 23.6 Hz), 69.7 (d, J_{CF} = 1.5 Hz), 25.3.

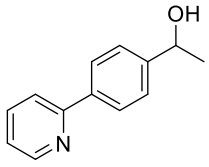

rac-**17e**

1-(4-(pyridine-2-yl)phenyl)ethan-1-ol (17e)

Compound *rac*-**6e** was prepared according to General Procedure 2, following purification (FCC eluent: 95:5 – 80:20 pentane: EtOAc) the product was isolated as a white solid in 72 % yield.

^{1}H NMR (400 MHz, $CDCl_3$) δ = 8.68 (dt, *J* = 5.0, 1.5 Hz, 1H), 8.00 – 7.93 (m, 1H), 7.81 – 7.68 (m, 2H), 7.60 – 7.54 (m, 1H), 7.46 (dd, *J* = 12.0, 8.3 Hz, 2H), 7.28 – 7.19 (m, 1H), 5.01 – 4.90 (m, 1H), 1.53 (d, *J* = 6.5, 3H); **^{13}C NMR**[a] (101 MHz, $CDCl_3$) δ = 157.2, 149.6, 146.9, 145.0, 140.2, 137.1, 127.3 (minor), 127.3 (major), 126.0 (minor), 126.0 (major), 122.3, 120.7, 70.3, 25.4 (major), 25.3 (minor); **HRMS** (ESI^+) m/z calculated for $C_{13}H_{13}NO$ $(M+H)^+$ 200.1070, found 200.1068; **IR** (neat) ν = 3271, 2971, 2925, 2867, 1591, 1561, 1473, 1436, 1403, 1363, 1344, 1288, 1207, 1158, 1121, 1091, 1061, 1035, 1013, 994, 907, 850, 519, 785, 752, 736, 721, 626 cm^{-1}; **mp** 109-110 ˚C. [a]Mixture of rotamers reported.

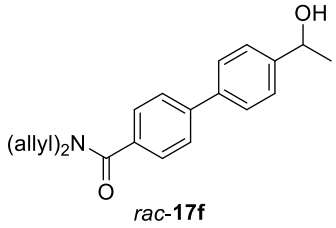

rac-**17f**

***N,N*-diallyl-4'-(1-hydroxyethyl)-[1,1'biphenyl]-4-carboxamide (17f)**

Compound *rac*-**6f** was prepared according to General Procedure 2, following purification (FCC eluent: 90:10 – 70:30 pentane:EtOAc) the product was isolated as a viscous pale yellow oil in 81 % yield.

^{1}H NMR (400 MHz, $CDCl_3$) δ = 7.54 (ddd, *J* = 13.2, 8.3, 2.2 Hz, 4H), 7.47 (dd, *J* = 8.3, 2.1 Hz, 2H), 7.41 (dd, *J* = 8.3, 2.3 Hz, 2H), 5.87 (br s, 1H), 5.76 (br s, 1H), 5.28 – 5.16 (m, 4H), 4.90 (qd, *J* = 6.4, 2.9 Hz, 1H), 4.16 – 4.07 (m, 2H), 3.88 (s, 2H), 1.50 (dd, *J* = 6.5, 2.4 Hz, 3H); **^{13}C NMR** (101 MHz, $CDCl_3$) [overlapping signals] δ = 171.7, 145.8, 142.3, 139.1, 134.8, 133.2, 132.8, 127.2, 127.1, 127.0, 126.0, 117.8, 69.8, 50.9, 47.2, 25.3; **HRMS** (ESI^+) m/z calculated for $C_{21}H_{23}BrNO$ $(M+H)^+$ 384.0958, found 384.0955; **IR** (neat) ν = 3373, 3082, 3031, 2983, 2926, 2243, 1915, 1620, 1525, 1511, 1414, 1365, 1344, 1261, 1209, 1187, 1114, 1091, 1005, 910, 859, 827, 790, 758, 732, 647, 637, 628, 621 cm^{-1}.

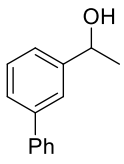

rac-**17g**

1-([1,1'-biphenyl]-3-yl)ethan-1-ol (17g)

Compound *rac*-**6g** was prepared according to General Procedure 2, the product was isolated as a white solid in 92 % yield. Spectroscopic data are in accordance with those in literature.[10]

^{1}H NMR (400 MHz, $CDCl_3$) δ = 7.68 (dd, *J* = 7.9, 1.4 Hz, 1H), 7.47 – 7.27 (m, 7H), 7.22 (dd, *J* = 7.6, 1.4 Hz, 1H), 4.99 (q, *J* = 6.0 Hz, 1H), 1.42 (d, *J* = 6.4 Hz, 3H); **^{13}C NMR** (101 MHz, $CDCl_3$) δ = 143.2, 141.1, 140.5, 130.1, 129.4, 128.3, 128.1, 127.3, 127.2, 125.5, 66.6, 25.0.

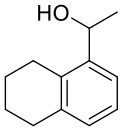

rac-**17i**

1-(5,6,7,8-tetrahydronaphthalen-1-yl)ethan-1-ol (17i)

Compound *rac*-**6i** was prepared according to General Procedure 3 from 5,6,7,8-tetrahydronaphalene-1-carbaldehyde and MeMgBr, following purification (FCC eluent: 95:5 – 80:20 pentane:Et_2O) the product was isolated as an off-white solid in 64 % yield.

^{1}H NMR (400 MHz, $CDCl_3$) δ 7.37 (d, *J* = 7.6 Hz, 1H), 7.16 (t, *J* = 7.6 Hz, 1H), 7.01 (d, *J* = 7.5 Hz, 1H), 5.14 (q, *J* = 6.4 Hz, 1H), 2.90 – 2.77 (m, 3H), 2.66 (dt, *J* = 16.7, 6.5 Hz, 1H), 1.89 – 1.72 (m, 4H), 1.46 (d, *J* = 6.4 Hz, 3H); **^{13}C NMR** (101 MHz, $CDCl_3$) δ = 144.0, 137.5, 133.5, 128.7, 125.9, 121.9, 66.2, 30.3, 25.7, 24.1, 23.4, 22.8; **IR** (neat) ν = 3347, 2980, 2930, 2589, 1451, 1369, 1266, 1108, 1066, 1014, 903, 831, 779, 737 cm^{-1}; No HRMS obtained.

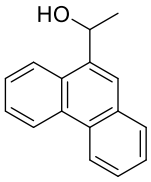

rac-**17j**

1-(phenanthrene-9-yl)ethan-1-ol (17j)

Compound *rac*-**6j** was prepared according to General Procedure 3 from phenanthrene-9-carbaldehyde and MeMgCl, the product was isolated as a white solid in 95 % yield.

^{1}H NMR (400 MHz, $CDCl_3$) δ = 8.46 – 8.36 (m, 1H), 8.36 – 8.28 (m, 1H), 7.86 – 7.75 (m, 1H), 7.59 (s, 1H), 7.58 – 7.50 (m, 1H), 7.39 – 7.21 (m, 4H), 5.33 (qd, *J* = 6.4, 0.9 Hz, 1H), 1.39 (d, *J* = 6.4 Hz, 3H); **^{13}C NMR** (101 MHz, $CDCl_3$) δ = 139.6, 131.6, 130.9, 130.1, 129.7, 128.9, 126.9, 126.7, 126.7, 126.4, 124.0, 123.5, 122.8, 122.6, 67.3, 24.2; **HRMS** (ESI^+) m/z calculated for $C_{16}H_{15}O$ $(M+H)^+$ 223.1117, found 223.0649; **IR** (neat) ν = 3269, 2981, 2955, 2924, 2853, 1691, 1635, 1608, 1484, 1455, 1392, 1373, 1269, 1250, 1176, 1077, 910, 726 cm^{-1}; **mp** 120-123 ˚C.

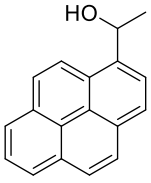

rac-**17k**

1-(pyren-1-yl)ethan-1-ol (17k)

Compound *rac*-**6j** ws prepared according to General Procedure 2, the product was isolated as an off-white solid in 92 % yield. Spectroscopic data are in accordance with those in literature.[11]

^{1}H NMR (500 MHz, $CDCl_3$) δ = 8.36 (d, *J* = 9.3 Hz, 1H), 8.25 (d, *J* = 8.0 Hz, 1H), 8.23 – 8.16 (m, 3H), 8.12 (d, *J* = 9.3 Hz, 1H), 8.05 (s, 2H), 8.01 (t, *J* = 7.6 Hz, 1H), 6.01 (q, *J* = 6.5 Hz, 1H), 1.79 (d, *J* = 6.5 Hz, 3H); **^{13}C NMR** (126 MHz, $CDCl_3$) δ = 139.2, 131.5, 130.8, 127.8, 127.6, 127.4, 127.4, 126.1, 125.4, 125.3, 125.2, 125.1, 125.0, 122.7, 122.6, 67.5, 25.2.

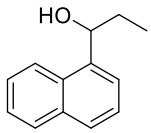

rac-**17l**

1-(napthalen-1-yl)propan-1-ol (17l)

Compound *rac*-**6k** was prepared according to General Procedure 3 from 1-napthaldehyde and EtMgBr, following purification (FCC eluent: 50:50 – 100:0 DCM:pentane) the product was isolated as viscous colourless oil in 87 % yield. Spectroscopic data are in accordance with those in literature.[12]

^{1}H NMR (400 MHz, $CDCl_3$) δ = 8.17 – 8.08 (m, 1H), 7.93 – 7.84 (m, 1H), 7.79 (dt, *J* = 8.2, 1.1 Hz, 1H), 7.64 (dt, *J* = 7.1, 1.0 Hz, 1H), 7.57 – 7.43 (m, 3H), 5.40 (td, *J* = 6.0, 2.1 Hz, 1H), 2.05 – 2.02 (m, 1H), 2.03 – 1.87 (m, 2H), 1.04 (t, *J* = 7.4 Hz, 3H); **^{13}C NMR** (101 MHz, $CDCl_3$) δ = 140.4, 134.0, 130.6, 129.0, 128.0, 126.1, 125.6, 125.5, 123.4, 123.0, 72.7, 31.2, 10.7.

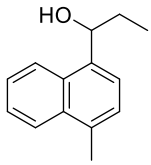

rac-**17m**

1-(4-methylnaphthalen-1-yl)propan-1-ol (17m)

Compound *rac*-**6l** was prepared according to General Procedure 3 from 4-methyl-1-napthaldehyde and EtMgBr, following purification (FCC eluent: 100% DCM) the product was isolated as a viscous colourless oil in 79 % yield.

^{1}H NMR (400 MHz, $CDCl_3$) δ = 8.15 (dt, *J* = 7.8, 2.7 Hz, 1H), 8.09 – 8.00 (m, 1H), 7.60 – 7.48 (m, 3H), 7.33 (dd, *J* = 7.3, 1.1 Hz, 1H), 5.38 (dd, *J* = 7.6, 5.0 Hz, 1H), 2.70 (d, *J* = 0.9 Hz, 3H), 2.10 – 1.85 (m, 2H), 1.04 (t, *J* = 7.4 Hz, 3H); **^{13}C NMR** (101 MHz, $CDCl_3$) δ = 138.5, 134.1, 133.0, 130.8, 126.3, 125.7, 125.5, 125.1, 123.9, 122.8, 72.7, 31.2, 19.8, 10.7; **HRMS** (ESI^+) m/z calculated for $C_{14}H_{17}O$ $(M+H)^+$ 201.1274, 201.1094; **IR** (neat) ν = 3375, 3074, 2966, 2932, 2875, 1598, 1516, 1457, 1381, 1244, 1216, 1164, 1035, 979, 837, 759 cm^{-1}.

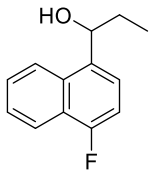

rac-**17n**

1-(4-fluoronaphthalen-1-yl)propan-1-ol (17n)

Compound *rac*-**6m** was prepared according to General Procedure 3 from 4-fluoro-1-napthaldehyde and EtMgBr, following purification (FCC eluent: 100% DCM) the product was isolated as a viscous colourless oil in 78 % yield.

^{1}H NMR (400 MHz, $CDCl_3$) δ = 8.19 – 8.07 (m, 2H), 7.61 – 7.49 (m, 3H), 7.12 (dd, *J* = 10.3, 8.0 Hz, 1H), 5.31 (dd, *J* = 7.6, 5.2 Hz, 1H), 2.06 – 1.82 (m, 3H), 1.01 (t, *J* = 7.4 Hz, 3H); **^{19}F NMR** (377 MHz, $CDCl_3$) δ = -124.0; **^{13}C NMR** (101 MHz, $CDCl_3$) δ = 158.4 (d, *J* = 251.3 Hz), 136.1 (d, *J* = 4.4 Hz), 131.9 (d, *J* = 4.2 Hz), 127.0, 125.9 (d, *J* = 2.0 Hz), 124.0 (d, *J* = 16.0 Hz), 123.4 (d, *J* = 2.8 Hz), 123.1 (d, *J* = 8.4 Hz), 121.4 (d, *J* = 6.0 Hz), 108.9 (d, *J* = 19.7 Hz), 72.5, 31.2, 10.6; **HRMS** (ESI^+) m/z calculated for $C_{12}H_{11}FO$ $(M+H)^+$ 191.0867, found 191.0773; **IR** (neat) ν = 3365, 3072, 2970, 2935, 2876, 1635, 1604, 1585, 1513, 1465, 1396, 1322, 1261, 1143, 1049, 966, 835, 761, 710 cm^{-1}.

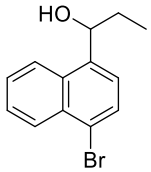

rac-**17o**

1-(4-bromonaphthalen-1-yl)propan-1-ol (17o)

Compound *rac*-**6n** was prepared according to General Procedure 3 from 4-bromo-1-napthaldehyde and EtMgBr, following purification (FCC eluent: 95:5-80:20 pentane:Et_2O) the product was isolated as a white solid in 76 % yield.

^{1}H NMR (500 MHz, $CDCl_3$) δ = 8.31 (dd, *J* = 8.5, 1.4 Hz, 1H), 8.10 – 8.06 (m, 1H), 7.77 (d, *J* = 7.8 Hz, 1H), 7.59 (dddd, *J* = 25.7, 8.3, 6.8, 1.3 Hz, 2H), 7.47 (d, *J* = 7.8 Hz, 1H), 5.35 (dd, *J* = 7.6, 4.8 Hz, 1H), 2.02 – 1.83 (m, 2H), 1.02 (t, *J* = 7.4 Hz, 3H); **^{13}C NMR** (126 MHz, $CDCl_3$) δ = 140.5, 132.1, 131.8, 129.7, 128.2, 127.0, 126.8, 123.67 123.6, 122.6, 72.4, 31.3, 10.5; **HRMS** (ESI^+) m/z calculated for $C_{13}H_{14}BrO$ $(M+H)^+$ 265.0223, found 264.9896; **IR** (liquid film) ν = 3207, 3123, 2931, 1944, 1915, 1868, 1834, 1795, 1594, 1567, 1509, 1455, 1367, 1250, 1202, 1106, 1047, 972, 911, 876, 725, 802, 773, 750, 697, 648 cm^{-1}; **mp** 67-68 ˚C.

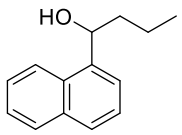

rac-**17p**

1-(naphthalen-1-yl)butan-1-ol (17p)

Compound *rac*-**6p** was prepared according to General Procedure 3 from 1-napthaldehyde and *n*PropylMgBr, following purification, (FCC eluent: 95:5 – 85:15 pentane:Et_2O) the product was isolated as viscous colourless oil in 75 % yield.

^{1}H NMR (400 MHz, $CDCl_3$) δ = 8.16 – 8.07 (m, 1H), 7.94 – 7.84 (m, 1H), 7.79 (dt, *J* = 8.2, 1.1 Hz, 1H), 7.63 (dt, *J* = 7.2, 1.0 Hz, 1H), 7.58 – 7.42 (m, 3H), 5.44 (dd, *J* = 7.6, 5.1 Hz, 1H), 2.00 – 1.82 (m, 2H), 1.66 – 1.38 (m, 2H), 0.99 (t, *J* = 7.4 Hz, 3H); **^{13}C NMR** (101 MHz, $CDCl_3$) δ = 140.7, 133.9, 130.5, 129.0, 127.9, 126.0, 125.5, 125.5, 123.3, 122.9, 71.0, 40.6, 19.5, 14.1; **HRMS** (ESI^+) m/z calculated for $C_{14}H_{17}O$ $(M+H)^+$ 201.1274, found 201.1073; **IR** (liquid film) ν = 3585, 3050, 2957, 2872, 1942, 1834, 1511, 1457, 1395, 1353, 1261, 1229, 1168, 1120, 1081, 1062, 1029, 909, 860, 800, 778, 734, 633 cm^{-1}.

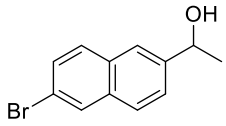

rac-**17r**

1-(6-bromonaphthalen-2-yl)ethan-1-ol (17r)

Compound *rac*-**6r** was prepared according to General Procedure 2, following purification (FCC eluent: 95:5 – 80:20 pentane:Et_2O) the product was isolated as an off-white solid in 97 % yield. Spectroscopic data are in accordance with those in literature.[13]

^{1}H NMR (500 MHz, $CDCl_3$) δ = 7.74 (d, *J* = 1.9 Hz, 1H), 7.54 – 7.46 (m, 2H), 7.43 (d, *J* = 8.7 Hz, 1H), 7.33 – 7.24 (m, 2H), 4.80 (q, *J* = 6.5 Hz, 1H), 1.33 (d, *J* = 6.5 Hz, 3H); **^{13}C NMR** (126 MHz, $CDCl_3$) δ = 143.8, 134.0, 131.8, 129.8, 129.7, 129.6, 127.5, 125.0, 123.8, 119.8, 70.4, 25.3.

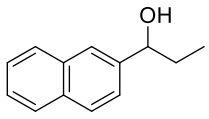

rac-**17s**

1-(naphthalen-2-yl)propan-1-ol (17s)

Compound *rac*-**6k** was prepared according to General Procedure 3 from 2-naphthaldehyde and EtMgBr, following purification (FCC eluent: 90:10 – 80:20 pentane: EtOAc) the product was isolated as a white solid in 62 % yield. Spectroscopic data are in accordance with those in literature.[14]

^{1}H NMR (400 MHz, $CDCl_3$) δ = 7.87 – 7.81 (m, 3H), 7.80 – 7.77 (m, 1H), 7.53 – 7.42 (m, 3H), 4.78 (td, *J* = 6.6, 3.1 Hz, 1H), 1.96 (d, *J* = 3.2 Hz, 1H), 1.95 – 1.78 (m, 2H), 0.95 (t, *J* = 7.4 Hz, 3H); **^{13}C NMR** (101 MHz, $CDCl_3$) δ = 142.1, 133.4, 133.1, 128.4, 128.1, 127.8, 126.3, 125.9, 124.9, 124.3, 76.3, 31.9, 10.3.

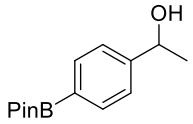

rac-**17t**

1-(4-(4,4,5,5-tetramethyl-1,3,2-dioxaborolan-2-yl)phenyl)ethan-1-ol (17t)

Compound *rac*-**6t** was prepared according to General Procedure 3 from 4-(4,4,5,5-Tetramethyl-1,3,2-dioxaborolan-2-yl)-benzaldehyde and MeMgBr, following purification (FCC eluent: 100:0 – 90:10 DCM:EtOAc) product was isolated as a white solid in 59 % yield. Spectroscopic data are in accordance with those in literature.[15]

^{1}H NMR (400 MHz, $CDCl_3$) δ = 7.83 – 7.76 (m, 2H), 7.41 – 7.33 (m, 2H), 4.91 (q, *J* = 6.4 Hz, 1H), 1.48 (d, *J* = 6.5 Hz, 3H), 1.34 (s, 12H); **^{13}C NMR** (101 MHz, $CDCl_3$) δ = 149.1, 135.2, 124.8, 83.9, 70.5, 25.3, 25.0. (*ipso*-carbon bound to boron not observed by ^{13}C NMR).

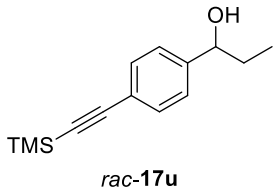

rac-**17u**

1-(4-((trimethylsilyl)ethynyl)phenyl)propan-1-ol (17u)

Compound *rac*-**17u** was prepared according to General Procedure 3 from 4-[(trimethylsilyl)ethynyl]benzaldehyde and EtMgBr Following purification (FCC eluent: 90:10 – 80:20 pentane: Et_2O) product was isolated as a colourless oil in 82 % yield.

^{1}H NMR (400 MHz, $CDCl_3$) δ = 7.47 – 7.42 (m, 2H), 7.30 – 7.24 (m, 2H), 4.59 (t, *J* = 6.5 Hz, 1H), 1.83 – 1.68 (m, 2H), 0.89 (t, *J* = 7.4 Hz, 3H), 0.25 (s, 9H); **^{13}C NMR** (101 MHz, $CDCl_3$) δ = 145.1, 132.2, 125.9, 122.3, 105.1, 94.2, 75.7, 32.0, 10.1, 0.1; **HRMS** (ESI^+) m/z calculated for $C_{14}H_{21}OSi$ $(M+H)^+$ 233.1356, found 233.1509; **IR** (neat) ν = 3375, 2963, 2934, 2876, 2158, 1724, 1566, 1503, 1457, 1411, 1379, 1250, 1223, 1200, 1097, 1044, 1016, 976, 864, 842, 760, 702, 650, 639, 625 cm^{-1}.

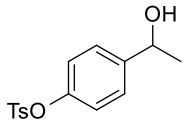

rac-**17v**

4-(1-hydroxyethyl)phenyl-4-methylbenzenesulfonate (17v)

Compound *rac*-**17v** was prepared according to General Procedure 2, following purification (FCC eluent: 90:10 – 80:20 pentane: Et_2O) product was isolated as an off-white solid in 74 % yield. Spectroscopic data are in accordance with those in literature.[16]

^{1}H NMR (400 MHz, $CDCl_3$) δ = 7.74 – 7.68 (m, 2H), 7.34 – 7.25 (m, 4H), 6.99 – 6.91 (m, 2H), 4.87 (q, *J* = 6.5 Hz, 1H), 2.45 (s, 3H), 1.83 (s, 1H), 1.45 (dd, *J* = 6.5, 0.7 Hz, 3H); **^{13}C NMR** (101 MHz, $CDCl_3$) δ = 148.9, 145.5, 144.8, 132.6, 129.9, 128.6, 126.8, 122.5, 69.8, 25.4, 21.9.

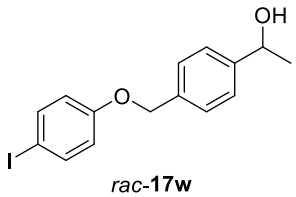

rac-**17w**

1-(4-((4-iodophenoxy)methyl)phenyl)ethan-1-ol (17w)

Compound *rac*-**17w** was prepared according to General Procedure 2, yielding product as white solid in 93 % yield.

^{1}H NMR (500 MHz, $CDCl_3$) δ = 7.59 – 7.52 (m, 2H), 7.40 (s, 4H), 6.78 – 6.71 (m, 2H), 5.02 (s, 2H), 4.92 (q, *J* = 6.5 Hz, 1H), 1.59 (br s, 1H), 1.50 (d, *J* = 6.5 Hz, 3H); **^{13}C NMR** (151 MHz, $CDCl_3$) δ = 158.7, 145.9, 138.4, 135.9, 127.8, 125.9, 117.4, 83.2, 70.3, 70.0, 25.4; **HRMS** (ESI^+) m/z calculated for $C_{15}H_{16}IO_2$

(M+H)$^+$ 355.0190, found 355.0681; **IR** (neat) ν = 2962, 2927, 2854, 1776, 1702, 1587, 1486, 1464, 1400, 1383, 1339, 1282, 1246, 1177, 1072, 1014, 997, 872, 832, 809, 760 cm^{-1}; **mp** 110-112 ˚C.

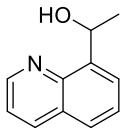

rac-**17x**

1-(quinoline-8-yl)ethan-1-ol (17x)

Compound *rac*-**17x** was prepared according to General Procedure 3 from quinoline-8-carbaldehyde and MeMgBr, following purification (FCC eluent: 90:10 – 80:20 pentane: EtOAc) affording product as a yellow viscous oil in 80 % yield.

^{1}H NMR (400 MHz, $CDCl_3$) δ = 8.85 (dd, *J* = 4.3, 1.8 Hz, 1H), 8.19 (dd, *J* = 8.3, 1.8 Hz, 1H), 7.73 (dd, *J* = 8.1, 1.5 Hz, 1H), 7.59 (ddd, *J* = 7.1, 1.6, 0.7 Hz, 1H), 7.50 (dd, *J* = 8.1, 7.1 Hz, 1H), 7.43 (dd, *J* = 8.3, 4.2 Hz, 1H), 5.47 (q, *J* = 6.6 Hz, 1H), 1.74 (d, *J* = 6.6 Hz, 3H); **^{13}C NMR** (101 MHz, $CDCl_3$) δ = 148.5, 146.6, 142.0, 137.2, 128.8, 127.2, 126.6, 126.5, 121.0, 70.3, 24.3; **HRMS** (ESI$^+$) m/z calculated for $C_{11}H_{12}NO$ (M+H)$^+$ 174.0913, found 174.0912; **IR** (liquid film) ν = 3373, 3054, 2969, 2922m 1616, 1596, 1580, 1500, 1418, 1367, 1326, 1283, 1242, 1168, 1114, 1069, 1055, 1020, 1001, 988, 901, 831, 794, 763, 667, 636, 621 cm^{-1}.

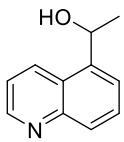

rac-**17y**

1-(quinoline-5-yl)ethan-1-ol (17y)

Compound *rac*-**17y** was prepared according to General Procedure 3 from quinoline-5-carbaldehyde and MeMgBr, following purification (FCC eluent: 100:0 -90:10 DCM:EtOAc) the product was isolated as a white solid in 87 % yield.

^{1}H NMR (400 MHz, $CDCl_3$) δ = 8.79 (dd, *J* = 4.2, 1.7 Hz, 1H), 8.51 (ddd, *J* = 8.7, 1.7, 0.9 Hz, 1H), 7.96 (dt, *J* = 8.0, 1.2 Hz, 1H), 7.67 – 7.62 (m, 2H), 7.35 (dd, *J* = 8.6, 4.2 Hz, 1H), 5.57 (q, *J* = 6.3 Hz, 1H), 1.65 (d, *J* = 6.5 Hz, 3H); **^{13}C NMR** (101 MHz, $CDCl_3$) δ = 149.9, 148.5, 142.0, 132.3, 129.2, 129.1, 125.7, 123.0, 120.8, 67.2, 24.7; **HRMS** (ESI$^+$) m/z calculated for $C_{11}H_{11}NO$ (M+H)$^+$ 174.0913, found 174.0913; **IR** (liquid film) ν = 3170, 2987, 2973, 2873, 1742, 1505, 1448, 1365, 1313, 1284, 1245, 1170, 1119, 1072, 1011, 905, 833, 805, 716 cm^{-1}; **mp** 95-96 ˚C.

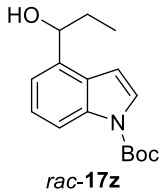

rac-**17z**

***tert*-butyl-4-(1-hydroxypropyl)-1*H*-indole-1-carboxylate (17z)**

Compound *rac*-**17z** was prepared according to General Procedure 3 from *tert*-butyl-4-formyl-1*H*-indole-1-carboxylate and EtMgBr. Following purification (FCC eluent: 95:5-70:30 pentane:Et_2O) the product was isolated as a viscous colourless oil in 62 % yield.

^{1}H NMR (400 MHz, $CDCl_3$) δ = 8.11 (d, *J* = 8.2 Hz, 1H), 7.62 (d, *J* = 3.8 Hz, 1H), 7.31 (t, *J* = 7.9 Hz, 1H), 7.25 – 7.23 (m, 1H), 6.75 (dd, *J* = 3.8, 0.8 Hz, 1H), 4.95 (t, *J* = 6.6 Hz, 1H), 1.96 (ddt, *J* = 15.1, 13.6, 7.3 Hz, 2H), 1.70 (s, 9H), 0.94 (t, *J* = 7.4 Hz, 3H); **^{13}C NMR** (101 MHz, $CDCl_3$) δ = 149.8, 136.9, 135.5, 128.1, 125.7, 124.2, 119.6, 114.4, 105.8, 83.8, 74.4, 31.2, 28.2, 10.4; **HRMS** (ESI^+) m/z calculated for $C_{16}H_{22}NO_3$ $(M+H)^+$ 276.1594, found 276.1591; **IR** (liquid film) ν = 2981, 2964, 2933, 2873, 1734, 1602, 1538, 1481, 1457, 1430, 1386, 1347, 1283, 1157, 1134, 1105, 1045, 910, 853, 761, 733 cm^{-1}.

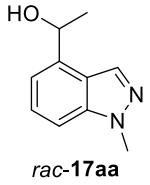

rac-**17aa**

1-(1-methyl-1*H*-indazol-4-yl)ethan-1-ol (17aa)

Compound *rac*-**17aa** was prepared according to General Procedure 3 from 1-methyl-1*H*-indazole-4-carbaldehyde and MeMgBr, following purification (FCC eluent: 90:10-60:40 DCM:EtOAc) the product was isolated as a colourless oil in 69 % yield.

^{1}H NMR (400 MHz, $CDCl_3$) δ = 8.11 (d, *J* = 1.0 Hz, 1H), 7.41 – 7.27 (m, 2H), 7.13 (dt, *J* = 6.9, 0.9 Hz, 1H), 5.29 (q, *J* = 6.5, 1H), 4.07 (s, 3H), 1.63 (d, *J* = 6.5 Hz, 3H); **^{13}C NMR** (101 MHz, $CDCl_3$) δ = 140.5, 139.5, 131.8, 126.5, 121.4, 116.4, 108.4, 69.6, 35.7, 24.9; **HRMS** (ESI^+) m/z calculated for $C_{10}H_{13}N_2O$ $(M+H)^+$ 177.1022, found 177.1023; **IR** (liquid film) ν = 3367, 2947, 2877, 2829, 1701, 1613, 1510, 1449, 1411, 1271, 1203, 1165, 1110, 1080, 1013, 964, 899, 850, 789, 745, 631 cm^{-1}.

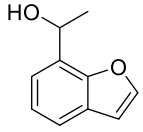

rac-**17ab**

1-(benzofuran-7-yl)ethan-1-ol (17ab)

Compound *rac*-**17ab** was prepared according to General Procedure 3 from benzofuran-7-carbaldehyde and MeMgBr, following purification (FCC eluent: 100% DCM) the product was isolated as a colourless oil in 71 % yield.

^{1}H NMR (500 MHz, $CDCl_3$) δ = 7.63 (d, *J* = 2.2 Hz, 1H), 7.52 (dd, *J* = 7.7, 1.3 Hz, 1H), 7.33 (dt, *J* = 7.3, 1.0 Hz, 1H), 7.23 (t, *J* = 7.6 Hz, 1H), 6.78 (d, *J* = 2.2 Hz, 1H), 5.37 (q, *J* = 6.5 Hz, 1H), 2.51 (s, 1H), 1.65 (d, *J* = 6.5 Hz, 3H); **^{13}C NMR** (126 MHz, $CDCl_3$) δ = 151.9, 144.8, 129.6, 127.6, 123.1, 120.7, 120.4, 106.8, 66.4,

23.7; **HRMS** (ESI$^+$) m/z calculated for $C_{10}H_{11}O_2$ $(M+H)^+$ 163.0754, found 163.0389; **IR** (liquid film) ν = 3400, 2975, 2930, 1482, 1447, 1427, 1369, 1324, 1259, 1163, 1118, 1031, 892, 868, 854, 831, 799, 742 cm^{-1}.

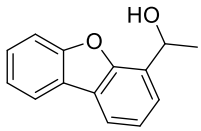

rac-**17ac**

1-(dibenzo[*b*,*d*]furan-4-yl)ethan-1-ol (17ac)

Compound *rac*-**17ac** was prepared according to General Procedure 3 from dibenzofuran-4-carbaldehyde and MeMgBr, following purification (FCC eluent: 100% DCM) the product was isolated as a colourless oil in 95 % yield.

^{1}H NMR (500 MHz, $CDCl_3$) δ = 7.96 (dt, *J* = 7.6, 0.9 Hz, 1H), 7.87 (dd, *J* = 7.6, 1.3 Hz, 1H), 7.60 (d, *J* = 8.2 Hz, 1H), 7.52 (dt, *J* = 7.5, 0.9 Hz, 1H), 7.47 (ddd, *J* = 8.4, 7.3, 1.3 Hz, 1H), 7.39 – 7.32 (m, 2H), 5.49 (qd, *J* = 6.5, 4.6 Hz, 1H), 1.71 (d, *J* = 6.5 Hz, 3H); **^{13}C NMR (**126 MHz, $CDCl_3$) δ = 156.2, 153.1, 129.9, 127.3, 124.5, 124.3, 123.7, 123.1, 123.0, 120.8, 119.8, 111.9, 66.5, 23.9; **HRMS** (ESI$^+$) m/z calculated for $C_{14}H_{13}O_2$ $(M+H)^+$ 213.0910, found 213.0553; **IR** (liquid film) ν = 3393, 3066, 3048, 2956, 1722, 1588, 1495, 1475, 1452, 1422, 1267, 1188, 1125, 1058, 1010, 916, 867, 755, 643, 626 cm^{-1}.

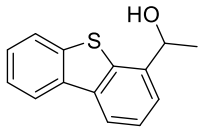

rac-**17ad**

1-(dibenzo[*b*,*d*]thiophen-4-yl)ethan-1-ol (17ad)

Compound *rac*-**17ad** was prepared according to General Procedure 3 from dibenzothiophene-4-carbaldehyde and MeMgBr, following purification (FCC eluent: 100% DCM) the product was isolated as a colourless oil in 94% yield.

^{1}H NMR (400 MHz, $CDCl_3$) δ = 8.20 – 8.11 (m, 1H), 8.07 (dd, *J* = 7.7, 1.4 Hz, 1H), 7.91 – 7.82 (m, 1H), 7.56 – 7.41 (m, 4H), 5.25 (q, *J* = 6.5 Hz, 1H), 1.66 (d, *J* = 6.5 Hz, 3H); **^{13}C NMR** (126 MHz, $CDCl_3$) δ = 140.2, 139.6, 136.5, 136.4, 135.6, 127.0, 125.0, 124.5, 123.0, 122.8, 121.7, 120.8, 70.1, 23.4; **HRMS** (ESI$^+$) m/z calculated for $C_{14}H_{13}SO$ $(M+H)^+$ 229.0682, found 229.0495; **IR** (neat) ν = 3381, 3063, 2975, 2927, 2871, 1584, 1561, 1444, 1404, 1368, 1304, 1252, 1171, 1121, 1069, 911, 752 cm^{-1}.

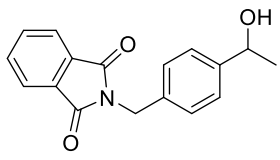

rac-**17ae**

2-(4-(1-hydroxyethyl)benzyl)isoindoline-1,3-dione (17ae)

Compound *rac*-**17ae** was prepared according to General Procedure 3, from 4-((1,3-dioxoisoindolin-2-yl)methyl)benzaldehyde and MeMgBr, following

purification (FCC eluent: 100:0 - 90:10 DCM:EtOAc) the product was isolated as a white solid in 90 % yield.

^{1}H NMR (400 MHz, $CDCl_3$) δ = 7.84 (dd, *J* = 5. 4, 3.1 Hz, 2H), 7.70 (dd, *J* = 5.5, 3.0 Hz, 2H), 7.46 – 7.38 (m, 2H), 7.36 – 7.28 (m, 2H), 4.91 – 4.84 (m, 1H), 4.83 (s, 2H), 1.45 (d, *J* = 6.4 Hz, 3H); **^{13}C NMR** (101 MHz, $CDCl_3$) δ = 168.2, 145.6, 135.7, 134.1, 132.3, 129.0, 125.9, 123.5, 70.2, 41.5, 25.3; **HRMS** (ESI^+) m/z calculated for $C_{17}H_{16}NO_3$ $(M+H)^+$ 282.1125, found 282.1121; **IR** (neat) ν = 3496, 2925, 2856, 2361, 1768, 1708, 1612, 1499, 1468, 1428, 1394, 1364, 1298, 1261, 1202, 1170, 1111, 1089, 1017, 959, 938, 904, 854, 813, 739, 616 cm^{-1}; **mp** 102-103 ˚C.

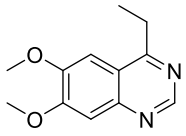

17af

4-ethyl-6,7-dimethoxyquinazoline (17af)

Compound **17af** was prepared following a modified literature procedure[17], 6,7-dimethoxy-4-chloroquinazoline (3.0 mmol) and $Fe(acac)_2$ (5 mol%) were added into a flamed-dried Schlenk flask, THF (20 mL) and NMP (2 mL) were added followed by dropwise addition of EtMgBr (3.0 M solution in Et_2O) at 0 °C. The reaction was left to stir at room temperature for 16 h after which it was quenched with H_2O and extracted with EtOAc. Organic extracts were dried with $MgSO_4$, and solvent removed under reduced pressure. The crude mixture was purified (FCC eluent 80:20 – 60:40 DCM:EtOAc) to afford product as a white solid in 66 % yield.

^{1}H NMR (400 MHz, $CDCl_3$) δ = 9.01 (s, 1H), 7.27 (s, 1H), 7.20 (s, 1H), 4.01 (s, 3H), 4.01 (s, 3H), 3.18 (q, *J* = 7.5 Hz, 2H), 2.24 (t, *J* = 7.6 Hz, 3H); **^{13}C NMR** (101 MHz, $CDCl_3$) δ = 168.9, 155.6, 153.6, 150.2, 147.9, 119.3, 107.3, 101.8, 56.4, 56.2, 27.9, 12.6; **HRMS** (ESI^+) m/z calculated for $C_{12}H_{14}N_2O_2$ $(M+H)^+$ 219.1128, found 219.1127; **IR** (neat) ν = 3009, 2974, 2935, 1668, 1619, 1581, 1556, 1507, 1482, 1464, 1429, 1414, 1373, 1341, 1305, 1282, 1234, 1211, 1176, 1131, 1079, 1027, 1000, 968, 913, 887, 859, 847, 744 cm^{-1}; **mp** 152-153 ˚C.

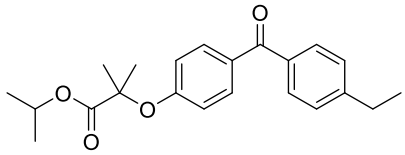

17ag

Isopropyl-2-(4-(4-ethylbenzoyl)phenoxy-3-methylpropanoate (17ag)

Compound **17ag** was prepared following a modified literature procedure[18], fenofibrate (2.0 mmol), Cs_2CO_3 (6.0 mmol) and $Pd(dppf)Cl_2$ (2 mol%) were added to a flamed-dried Schlenk tube under N_2 atmosphere and dry THF was added (4 mL). To the stirred suspension, triethylborane (3 mmol, 1.0 M solution in hexanes) was added dropwise at 0 °C and mixture was refluxed for 16 h. The reaction was cooled to 0 °C and quenched with H_2O and extracted with EtOAc, organic extracts were combined, washed with brine and dried with $MgSO_4$. Solvent was removed under reduced pressure and the crude reaction mixture was purified (FCC eluent 90:10 – 80:20 pentane: Et_2O) to afford product as white solid in 40 % yield.

^{1}H NMR (400 MHz, $CDCl_3$) δ = 7.80 – 7.72 (m, 2H), 7.72 – 7.64 (m, 2H), 7.35 – 7.27 (m, 2H), 6.90 – 6.80 (m, 2H), 5.09 (hept, *J* = 6.3 Hz, 1H), 2.73 (q, *J* = 7.6 Hz, 2H), 1.66 (d, *J* = 1.3 Hz, 6H), 1.28 (t, *J* = 7.6 Hz, 3H), 1.20 (d, *J* = 6.3 Hz, 6H); **^{13}C NMR** (101 MHz, $CDCl_3$) δ = 195.5, 173.4, 159.5, 149.0, 135.7, 132.1, 131.1, 130.2, 127.8, 117.3, 79.5, 69.4, 29.1, 25.5, 21.7, 15.4; **HRMS** (ESI^+) m/z calculated for $C_{22}H_{17}O_4$ $(M+H)^+$ 355.1904, found 355.1898; **IR** (liquid film) ν = 2984, 2938, 2875, 1732, 1655, 1601, 1574, 1530, 1502, 1467, 1416, 1385, 1252, 1178, 1149, 1104, 1062, 1013, 974, 930, 899, 855, 765 cm^{-1}; **mp** 82-83 ˚C.

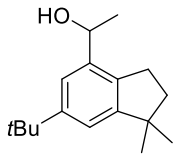

rac-**17ah**

1-(6-(*tert*-butyl)-1,1-dimethyl-2,3-dihydro-1*H*-inden-4-yl)ethan-1-ol (17ah)

Compound *rac*-**17ah** was prepared according to General Procedure 2, product isolated as a white solid in 95 % yield. Spectroscopic data are in accordance with those in literature.[19]

^{1}H NMR (600 MHz, $CDCl_3$) δ = 7.35 – 7.32 (m, 1H), 7.10 (d, *J* = 1.8 Hz, 1H), 5.00 (q, *J* = 6.5 Hz, 1H), 2.86 (qt, *J* = 15.7, 7.2 Hz, 2H), 1.94 (t, *J* = 7.2 Hz, 2H), 1.73 (s, 1H), 1.49 (d, *J* = 6.5 Hz, 3H), 1.34 (s, 9H), 1.26 (d, *J* = 1.6 Hz, 6H); **^{13}C NMR** (151 MHz, $CDCl_3$) δ = 152.9, 150.5, 140.8, 136.7, 119.5, 118.1, 68.8, 44.0, 41.6, 35.0, 31.8, 28.9, 28.9, 27.9, 23.9.

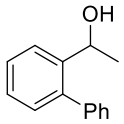

rac-**17ai**

1-([1,1'-biphenyl]-2-yl)ethan-1-ol (17ai)

Compound *rac*-**17ai** was prepared according to General Procedure 2, affording product as an off-white solid in 89 % yield. Spectroscopic data are in accordance with those in literature.[20]

^{1}H NMR (400 MHz, $CDCl_3$) δ = 7.68 (dd, *J* = 7.8, 1.4 Hz, 1H), 7.47 – 7.27 (m, 7H), 7.21 (dd, *J* = 7.7, 1.5 Hz, 1H), 4.99 (qd, *J* = 6.4, 3.2 Hz, 1H), 1.42 (d, *J* = 6.4 Hz, 3H); **^{13}C NMR** (101 MHz, $CDCl_3$) δ = 143.2, 141.0, 140.5, 130.1, 128.3, 128.1, 127.2, 125.5, 66.6, 25.0.

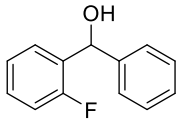

rac-**17aj**

(2-fluorophenyl)(phenyl)methanol (17aj)

Compound *rac*-**17aj** was prepared according to General Procedure 2, following purification (FCC eluent: 100% DCM), the product was isolated as a colourless oil in 55 % yield. Spectroscopic data are in accordance with those in literature.[21]

^{1}H NMR (500 MHz, $CDCl_3$) δ = 7.53 (td, *J* = 7.6, 1.8 Hz, 1H), 7.43 (d, *J* = 7.2 Hz, 2H), 7.36 (dd, *J* = 8.5, 6.8 Hz, 2H), 7.32 – 7.23 (m, 2H), 7.17 (td, *J* = 7.6, 1.2 Hz, 1H), 7.04 (ddd, *J* = 10.5, 8.2, 1.2 Hz, 1H), 6.16 (s, 1H); **^{13}C NMR** (126 MHz, $CDCl_3$) δ = 160.0 (d, *J* = 246.2 Hz), 142.9, 131.1 (d, *J* = 13.1 Hz), 129.2 (d, *J* = 8.3 Hz), 128.6, 127.8, 127.8, 126.5, 124.4 (d, *J* = 3.4 Hz), 115.5 (d, *J* = 21.6 Hz), 70.1 (d, *J* = 3.3 Hz).

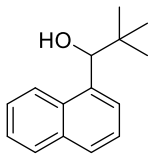

rac-**17ak**

2,2-dimethyl-1-(naphthalen-1-yl)propan-1-ol (17ak)

Compound *rac*-**17ak** was prepared according to General Procedure 3 from 1-naphthaldehyde and *t*BuMgCl, following purification (FCC eluent: 100% DCM) the product was isolated as a white solid in 51 % yield.

^{1}H NMR (400 MHz, $CDCl_3$) δ = 8.16 (d, *J* = 8.2 Hz, 1H), 7.94 – 7.83 (m, 1H), 7.80 – 7.76 (m, 1H), 7.70 – 7.68 (m, 1H), 7.54 – 7.40 (m, 3H), 5.43 (s, 1H), 1.00 (s, 9H); **^{13}C NMR** (151 MHz, $CDCl_3$) δ = 138.9, 133.6, 132.0, 129.0, 128.0, 125.7, 125.6 (br), 125.3, 125.1, 124.1 (br), 76.3 (br), 37.1, 26.6; **HRMS** (EI) m/z calculated for $C_{15}H_{18}O$ $(M)^{+\cdot}$ 214.13522, found 214.13577; **IR** (liquid film) ν = 3368, 3349, 3320, 1835, 1780, 1631, 1597, 1550, 1513, 1481, 1393, 1375, 1300, 1281, 1258, 1165, 1102, 1063, 998, 898, 843, 752, 627 cm^{-1}; **mp** 70-73 ˚C.

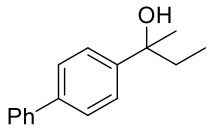

rac-**17al**

2-([1,1'-biphenyl]-4-yl)butan-2-ol (17al)

Compound *rac*-**17al** was prepared according to General Procedure 3 from 4-acetylbiphenyl and EtMgBr, following purification (FCC eluent: 90:10 – 100:0 DCM:Pentane), affording product as white solid, 34 % yield.

^{1}H NMR (500 MHz, $CDCl_3$) δ = 7.66 – 7.54 (m, 4H), 7.54 – 7.51 (m, 2H), 7.50 – 7.40 (m, 2H), 7.37 – 7.30 (m, 1H), 1.96 – 1.81 (m, 2H), 1.59 (s, 3H), 0.85 (t, *J* = 7.4 Hz, 3H); **^{13}C NMR** (126 MHz, $CDCl_3$) δ = 147.0, 141.0, 139.5, 128.9, 127.3, 127.2, 127.0, 125.5, 75.0, 36.8, 29.8, 8.5; **HRMS** (ESI^+) m/z calculated for $C_{16}H_{18}O$ $(M+H)^+$ 227.1641, found 227.1642; **IR** (neat) ν = 3568, 3030, 2247, 1670, 1602, 1488, 1401, 1353, 1267, 1039, 1007, 909, 840, 766, 732, 678 cm^{-1}; **mp** 33-34 ˚C.

4.3.2. Synthesis of Benzylic Bromides

General Procedure 4

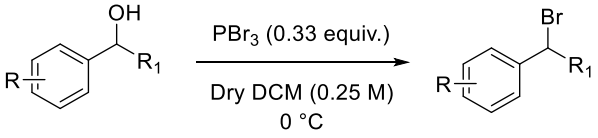

Bromide substrates were prepared from corresponding alcohols (0.5 – 1.0 mmol) via bromination with PBr_3 (0.33 equiv.) in dry DCM (0.5 M) at 0 °C following a literature procedure.[22] After completion the reaction was quenched with ice-cold H_2O. The aqueous layer was extracted with Et_2O (3 x 10mL) and combined organic extracts were washed with brine, dried with $MgSO_4$ and concentrated in vacuo to give pure products or subsequently purified by FCC.

General Procedure 5

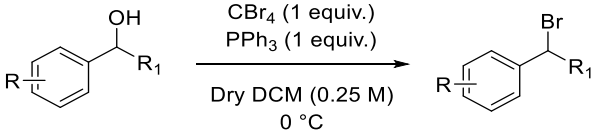

Bromide substrates were prepared from corresponding alcohols via bromination (0.5 – 1.0 mmol) with CBr_4 (1 equiv.) and PPh_3 (1 equiv.) in dry DCM (0.25 M). After completion, monitored by TLC, the reactions were filtered over celite and washed with Et_2O (3 x 10mL). The combined organic extracts

were washed with brine, dried with $MgSO_4$ and concentrated in vacuo. Triphenylphosphine oxide (PPh_3O) was removed using $CaBr_2$ (3 equiv.) in Et_2O following literature procedure[23] and following filtration and concentration under reduced pressure, pure products were obtained or subsequently purified by FCC.

General Procedure 6

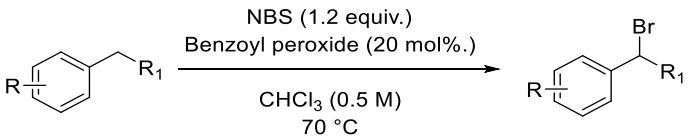

Bromide substrates were prepared from corresponding alkyl precursors through NBS bromination. Alkyl substrates (0.5 – 1.0 mmol) were dissolved in $CHCl_3$ (0.5 M), NBS (1.2 equiv.) and benzoyl peroxide (20 mol%) were added, and the reaction mixture was brought to reflux for 16 h. Following which the reaction was partitioned between H_2O and Et_2O and combined organic extracts were washed with brine and dried with $MgSO_4$ and concentrated under reduced pressure. Reaction mixtures were purified by FCC to give product.

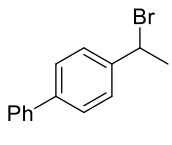

rac-**1a**

4-(1-bromoethyl)-1,1'-biphenyl (1a)

Compound *rac*-**1a** was prepared according to General Procedure 4, scaled up to 5 mmol of *rac*-**17a** (CAS: 3562-73-0). The product was isolated as a white solid in 98 % yield. Spectroscopic data are in accordance with those in literature.[22]

^{1}H NMR (500 MHz, $CDCl_3$) δ = 7.62 – 7.55 (m, 4H), 7.55 – 7.49 (m, 2H), 7.45 (dd, *J* = 8.3, 6.9 Hz, 2H), 7.40 – 7.33 (m, 1H), 5.28 (q, *J* = 6.9 Hz, 1H), 2.10 (d, *J* = 6.9 Hz, 3H); **^{13}C NMR** (126 MHz, $CDCl_3$) δ = 142.3, 141.5, 140.6, 129.0, 127.7, 127.6, 127.4, 127.3, 49.5, 26.9.

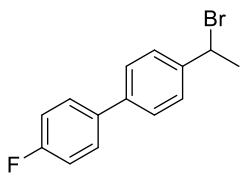

rac-**1b**

4-(1-bromoethyl)-4'-fluoro-1,1'biphenyl (1b)

Compound *rac*-**1b** was prepared according to General Procedure 4 from *rac*-**17b.** The product was isolated as a white solid in 84 % yield.

^{1}H NMR (500 MHz, $CDCl_3$) δ = 7.56 – 7.51 (m, 6H), 7.18 – 7.10 (m, 2H), 5.27 (q, *J* = 6.9 Hz, 1H), 2.09 (d, *J* = 6.9 Hz, 3H); **^{19}F NMR** (471 MHz, $CDCl_3$) δ = -115.3; **^{13}C NMR** (126 MHz, $CDCl_3$) δ = 162.7 (d, *J* = 246.8 Hz), 142.4, 140.4, 136.7, 136.7, 128.8 (d, *J* = 8.1 Hz), 127.4 (d, *J* = 7.2 Hz), 115.8 (d, *J* = 21.5 Hz), 49.4, 26.8; **IR** (neat) ν = 2990, 2979, 1914, 1834, 1601, 1528, 1496, 1443, 1398, 1251, 1237, 1199, 1067, 1046, 1006, 963, 910, 821, 738, 663 cm^{-1}; **mp** 61-62 ˚C; No HRMS obtained.

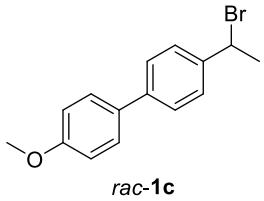

rac-**1c**

4-(1-bromoethyl)-4'-methoxy-1,1'-biphenyl (1c)

Compound *rac*-**1c** was prepared according to General Procedure 4 from *rac*-**17c**. The product was isolated as a white solid in 97 % yield.

^{1}H NMR (500 MHz, $CDCl_3$) δ = 7.57 – 7.46 (m, 6H), 7.01 – 6.95 (m, 2H), 5.28 (q, *J* = 7.0 Hz, 1H), 3.85 (s, 3H), 2.09 (dd, *J* = 6.9, 1.1 Hz, 3H); **^{13}C NMR** (126 MHz, $CDCl_3$) δ = 159.5, 141.7, 141.1, 133.2, 128.3, 127.4, 127.1, 114.4, 55.5, 49.7, 26.9; **IR** (neat) ν = 2955, 2925, 2853, 1713, 1607, 1496, 1465, 1433, 1400, 1367, 1289, 1276, 1221, 1178, 1110, 1050, 1021, 1005, 971, 958, 833, 794, 773, 733, 700, 647 cm^{-1}; **mp** 97-99 ˚C; No HRMS obtained.

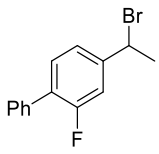

rac-**1d**

4-(1-bromoethyl)-2-fluoro-1,1'-biphenyl (1d)

Compound *rac*-**1d** was prepared according to General Procedure 4 from *rac*-**17d**. Following purification (FCC eluent 80:20 pentane: Et_2O) the product was isolated as a white solid in 61 % yield.

^{1}H NMR (600 MHz, $CDCl_3$) δ = 7.58 (dt, *J* = 8.1, 1.5 Hz, 2H), 7.52 – 7.46 (m, 2H), 7.44 – 7.42 (m, 1H), 7.42 – 7.39 (m, 1H) 7.34 – 7.26 (m, 2H), 5.25 (q, *J* = 6.9 Hz, 1H), 2.11 (d, *J* = 6.9 Hz, 3H); **^{19}F NMR** (565 MHz, $CDCl_3$) δ = -117.1; **^{13}C NMR** (151 MHz, $CDCl_3$) δ = 159.7 (d, *J* = 249.0 Hz), 144.6 (d, *J* = 7.6 Hz), 135.4, 131.1 (d, *J* = 3.9 Hz), 129.2 (d, *J* = 13.7 Hz), 129.1 (d, *J* = 3.0 Hz), 128.6, 128.02, 122.9 (d, *J* = 3.3 Hz), 114.8 (d, *J* = 24.1 Hz), 48.0 (d, *J* = 1.7 Hz), 26.7; **HRMS** (EI) m/z calculated for $C_{14}H_{12}{}^{79}BrF$ $(M)^{+\cdot}$ 278.01009, found 278.01064; **IR** (neat) ν = 3051, 2962, 2924, 2852, 1969, 1910, 1779, 1664, 1622, 1581, 1562, 1513, 1485, 1453, 1417, 1377, 1330, 1267, 1221, 1184, 1130, 10772, 1044, 1011, 956, 911, 873, 738, 651 cm^{-1}; **mp** 56-57 ˚C.

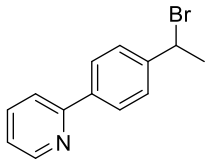

rac-**1e**

2-(4-(1-bromoethyl)phenyl)pyridine (1e)

Compound *rac*-**1e** was prepared according to General Procedure 4 from *rac*-**17e**. The product was isolated as a viscous colourless oil in 89 % yield.

^{1}H NMR (400 MHz, $CDCl_3$) δ = 8.71 (ddd, *J* = 5.0, 1.8, 0.9 Hz, 1H), 8.00 – 7.95 (m, 1H), 7.85 – 7.72 (m, 2H), 7.61 – 7.40 (m, 3H), 7.26 (ddd, *J* = 7.4, 5.0, 1.2 Hz, 1H), 5.27 (q, *J* = 6.9, 2.4 Hz, 1H), 2.09 (d, *J* = 7.0, 1.4 Hz, 3H); **^{13}C NMR**[a] (101 MHz, $CDCl_3$)[a] δ = 156.8, 149.7, 144.1, 142.6, 140.7, 139.3, 137.1, 127.5 (minor), 127.4 (major), 127.4 (major), 122.5, 120.8, 49.4 (minor), 49.2 (major), 30.5 (minor), 29.9 (major); **HRMS** (ESI^+) m/z calculated for $C_{13}H_{13}{}^{79}BrN$ $(M+H)^+$ 262.0226, found 262.0222; **IR** (neat) ν = 2973, 2925, 2855, 1624, 1540, 1467, 1411, 1380, 1341, 1380, 1341, 1305, 1162, 1130, 1109, 1010, 951, 896, 851, 816, 781, 720, 647, 622 cm^{-1}. [a]Mixture of rotamers reported.

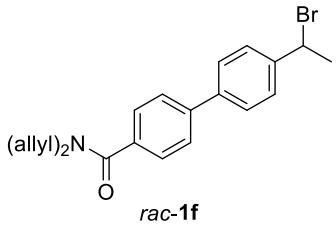

rac-**1f**

***N,N*-diallyl-4'-(1-bromoethyl)-[1,1'-biphenyl]-4-carboxamide (1f)**

Compound *rac*-**1f** was prepared according to General Procedure 4 from *rac*-**17f**. The product was isolated as a viscous pale-yellow oil in 63 % yield.

^{1}H NMR (400 MHz, $CDCl_3$) δ = 7.65 – 7.55 (m, 4H), 7.54 – 7.47 (m, 4H), 5.89 (br s, 1H), 5.78 (br s, 1H), 5.33 – 5.17 (m, 5H), 4.15 (br s, 2H), 3.90 (br s, 2H), 2.08 (d, *J* = 6.9 Hz, 3H); **^{13}C NMR** (101 MHz, $CDCl_3$) [overlapping signals] δ = 171.6, 142.8, 141.9, 140.4, 135.4, 133.3, 132.9, 127.5, 127.5, 127.4, 127.1, 117.8, 50.9 (br), 49.2, 47.2 (br), 26.8; **HRMS** (ESI^+) m/z calculated for $C_{21}H_{23}{}^{79}BrNO$ $(M+H)^+$ 384.0958, found 384.0950; **IR** (neat) ν = 2979, 2924, 1715, 1647, 1630, 1608, 1527, 1458, 1412, 1340, 1261, 1180, 1114, 1099, 1046, 1005, 986, 926, 862, 828, 772, 738 cm^{-1}.

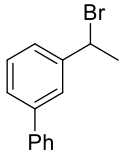

rac-**1g**

3-(1-bromoethyl)-1,1'-biphenyl (1g)

Compound *rac*-**1g** was prepared according to General Procedure 4 from *rac*-**17g**. The product was isolated as a viscous yellow oil in 88 % yield.

^{1}H NMR (600 MHz, $CDCl_3$) δ = 7.68 (q, *J* = 1.4 Hz, 1H), 7.65 – 7.58 (m, 2H), 7.58 – 7.49 (m, 1H), 7.51 – 7.43 (m, 4H), 7.43 – 7.35 (m, 1H), 5.28 (q, *J* = 6.9 Hz, 1H), 2.10 (d, *J* = 6.9 Hz, 3H); **^{13}C NMR** (151 MHz, $CDCl_3$) [overlapping signal] δ = 143.9, 141.9, 140.9, 129.3, 129.0, 127.7, 127.4, 125.9, 125.8, 49.6, 27.1; **HRMS** (EI) m/z calculated for $C_{14}H_{13}{}^{79}Br$ $(M)^{+\cdot}$ 260.01951, found 260.02006; **IR** (neat) ν = 3060, 3033, 2969, 2921, 2866, 1599, 1480, 1454, 1422, 1376, 1198, 1101, 1075, 1042, 968, 893, 801, 758, 700, 639 cm^{-1}.

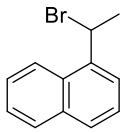

rac-**1h**

1-(1-bromoethyl)naphthalene (1h)

Compound *rac*-**1h** was prepared according to General Procedure 4 from *rac*-**17h** (CAS: 57605-95-5). The product was isolated as an off-white solid in 90 % yield. Spectroscopic data are in accordance with those in literature.[24]

^{1}H NMR (500 MHz, $CDCl_3$) δ = 8.28 (d, *J* = 8.4 Hz, 1H), 7.93 (d, *J* = 8.1 Hz, 1H), 7.87 (d, *J* = 8.2 Hz, 1H), 7.79 (d, *J* = 7.2 Hz, 1H), 7.66 (ddq, *J* = 8.4, 6.8, 1.4 Hz, 1H), 7.60 – 7.48 (m, 2H), 6.05 (q, *J* = 6.8 Hz, 1H), 2.31 (dd, *J* = 6.9, 1.5 Hz, 3H); **^{13}C NMR** (126 MHz, $CDCl_3$) δ = 138.1, 134.0, 130.4, 129.4, 129.0, 126.5, 126.0, 125.5, 123.6, 123.3, 45.1, 25.5.

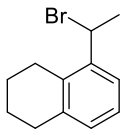

rac-**1i**

5-(1-bromoethyl)-1,2,3,4-tetrahydronaphthalene (1i)

Compound *rac*-**1i** was prepared according to General Procedure 4 from *rac*-**17i**. The product was isolated as a pale-yellow viscous oil in 64 % yield.

^{1}H NMR (400 MHz, $CDCl_3$) δ = 7.41 (dd, *J* = 7.8, 1.3 Hz, 1H), 7.15 (t, *J* = 7.7 Hz, 1H), 7.04 (dd, *J* = 7.6, 1.3 Hz, 1H), 5.45 (q, *J* = 6.9 Hz, 1H), 2.95 (dt, *J* = 16.9, 6.1 Hz, 1H), 2.90 – 2.58 (m, 2H), 2.08 (d, *J* = 6.9 Hz, 3H), 1.96 – 1.67 (m, 4H); **^{13}C NMR** (101 MHz, $CDCl_3$) δ = 140.8, 138.0, 134.5, 129.8, 125.9, 123.5, 45.9, 30.3, 25.9, 25.4, 23.3, 22.7; **IR** (neat) ν = 2981, 2931, 2860, 2663, 1459, 1436, 1376, 1243, 1164, 1039, 972, 779, 717 cm^{-1}; No HRMS obtained.

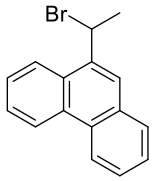

rac-**1j**

9-(1-bromoethyl)phenanthrene (1j)

Compound *rac*-**1j** was prepared according to General Procedure 4 from *rac*-**17j**. The product was isolated as a pale-yellow viscous oil in 64 % yield.

^{1}H NMR (400 MHz, $CDCl_3$) δ = 8.79 – 8.71 (m, 1H), 8.66 (ddt, *J* = 8.8, 1.3, 0.7 Hz, 1H), 8.36 – 8.26 (m, 1H), 8.00 (s, 1H), 7.91 (dd, *J* = 7.8, 1.5 Hz, 1H), 7.77 – 7.57 (m, 4H), 5.99 (q, *J* = 6.9 Hz, 1H), 2.37 (d, *J* = 6.9 Hz, 3H); **^{13}C NMR** (101 MHz, $CDCl_3$) δ = 136.3, 131.3, 131.0, 130.7, 129.5, 129.2, 127.5, 127.1, 126.9, 126.8, 124.8, 124.2, 123.4, 122.7, 45.4, 25.3; **IR** (neat) ν = 2981, 2925, 1735, 1448, 1379, 1252, 1157, 1065, 951, 903, 767, 748, 723 cm^{-1}; No HRMS obtained.

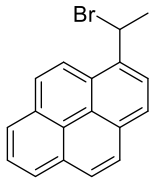

rac-**1k**

1-(1-bromoethyl)pyrene (1k)

Compound *rac*-**1k** was prepared according to General Procedure 4 from *rac*-**17k**. The product was isolated as a off white solid in 78 % yield.

^{1}H NMR (400 MHz, $CDCl_3$) δ = 8.45 (d, *J* = 9.3 Hz, 1H), 8.30 – 8.18 (m, 5H), 8.12 – 7.97 (m, 3H), 6.37 (q, *J* = 6.9 Hz, 1H), 2.41 (d, *J* = 6.9 Hz, 3H); **^{13}C NMR** (101 MHz, $CDCl_3$) δ = 135.6, 131.6, 131.5, 130.8, 128.2, 128.1, 127.9, 127.5, 126.4, 125.8, 125.6, 125.3, 125.1, 124.9, 123.6, 122.4, 45.8, 26.3; **IR** (neat) ν = 2984, 2882, 2880, 1607, 1517, 1400, 1381, 1189, 1073, 1035, 839, 800, 755, 613 cm^{-1}; **mp** 82-85˚C, No HRMS obtained.

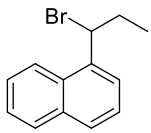

rac-**1l**

1-(1-bromopropyl)naphthalene (1l)

Compound *rac*-**1l** was prepared according to General Procedure 4 from *rac*-**17l**. The product was isolated as a colourless oil in 90 % yield.

^{1}H NMR (500 MHz, $CDCl_3$) δ = 8.24 (d, *J* = 7.7 Hz, 1H), 7.95 – 7.88 (m, 1H), 7.85 (dd, *J* = 8.6, 3.4 Hz, 1H), 7.75 (t, *J* = 5.8 Hz, 1H), 7.62 (ddq, *J* = 8.7, 5.3, 1.7 Hz, 1H), 7.57 – 7.46 (m, 2H), 5.75 – 5.72 (m, 1H), 2.66 – 2.52 (m, 1H), 2.51 – 2.38 (m, 1H), 1.21 – 1.14 (m, 3H); **^{13}C NMR** (126 MHz, $CDCl_3$) δ = 137.3, 134.1, 130.7, 129.2, 129.1, 126.5, 126.0, 125.6, 124.6, 123.1, 53.2, 32.1, 13.4; **IR** (neat) ν = 3052, 2958, 2872,

1699, 1598, 1511, 1464, 1208, 1180, 1105, 1020, 798, 775, 750, 733, 656, 630, 616 cm^{-1}; No HRMS obtained.

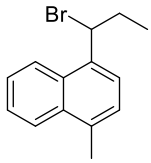

rac-**1m**

1-(1-bromopropyl)-4-methylnaphthalene (1m)

Compound *rac*-**1l** was prepared according to General Procedure 4 from *rac*-**17l**. The product was isolated as a colourless oil in 90 % yield

^{1}H NMR (400 MHz, $CDCl_3$) δ = 8.22 (d, *J* = 8.4 Hz, 1H), 8.09 – 8.02 (m, 1H), 7.65 – 7.48 (m, 3H), 7.32 (d, *J* = 7.4 Hz, 1H), 5.71 (t, *J* = 7.3 Hz, 1H), 2.69 (s, 3H), 2.64 – 2.34 (m, 2H), 1.14 (t, *J* = 7.2 Hz, 3H); **^{13}C NMR** (101 MHz, $CDCl_3$) δ = 135.6, 135.5, 133.2, 130.7, 126.5, 126.2, 125.9, 125.1, 124.3, 123.7, 53.6, 32.0, 19.9, 13.5; **IR** (neat) ν = 2980, 2884, 1597, 1517, 1457, 1381, 1179, 1073, 1035, 962, 833, 800, 755 cm^{-1}; No HRMS obtained.

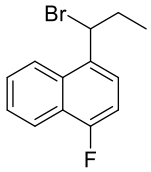

rac-**1n**

1-(1-bromopropyl)-4-fluoronaphthalene (1n)

Compound *rac*-**1m** was prepared according to General Procedure 4 from *rac*-**17m**. The product was isolated as a white solid in 85 % yield

^{1}H NMR (400 MHz, $CDCl_3$) δ = 8.23 – 8.14 (m, 2H), 7.70 – 7.53 (m, 3H), 7.13 (dd, *J* = 10.0, 8.1 Hz, 1H), 5.64 (dd, *J* = 8.4, 6.2 Hz, 1H), 2.67 – 2.26 (m, 2H), 1.14 (t, *J* = 7.2 Hz, 3H); **^{19}F NMR** (376 MHz, $CDCl_3$) δ = -121.4; **^{13}C NMR** (101 MHz, $CDCl_3$) δ = 158.9 (d, *J* = 254.2 Hz), 133.4 (d, *J* = 4.8 Hz), 132.1 (d, *J* = 4.7 Hz), 127.5, 126.4 (d, *J* = 2.1 Hz), 124.8 (d, *J* = 8.7 Hz), 124.2 (d, *J* = 16.0 Hz), 123.3, 121.5 (d, *J* = 6.1 Hz), 109.2 (d, *J* = 20.5 Hz), 52.7, 32.1, 13.4; **IR** (neat) ν = 2981, 2888, 1607, 1512, 1464, 1393, 1256, 1158, 961, 807, 770 cm^{-1}; **mp** 43-44 ˚C. No HRMS obtained.

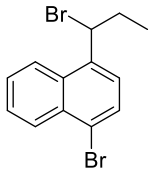

rac-**1o**

1-bromo-4-(1-bromopropyl)naphthalene (1o)

Compound *rac*-**1n** was prepared according to General Procedure 4 from *rac*-**17n**. The product was isolated as a white solid in 89 % yield.

^{1}H NMR (500 MHz, $CDCl_3$) δ = 8.37 – 8.30 (m, 1H), 8.20 (d, *J* = 8.0 Hz, 1H), 7.79 (d, *J* = 7.8 Hz, 1H), 7.69 – 7.60 (m, 2H), 7.56 (d, *J* = 7.9 Hz, 1H), 5.65 (t, *J* = 7.3 Hz, 1H), 2.53 (ddt, *J* = 14.5, 8.5, 7.1 Hz, 1H), 2.39 (dqd, *J* = 14.4, 7.2, 5.9 Hz, 1H), 1.14 (t, *J* = 7.2 Hz, 3H); **^{13}C NMR** (126 MHz, $CDCl_3$) δ = 137.5, 132.4,

131.9, 129.8, 128.3, 127.5, 127.3, 125.0, 124.0, 123.6, 52.2 (br), 32.0, 13.4; **IR** (neat) ν = 3081, 2909, 2841, 1806, 1565, 1508, 1450, 1385, 1353, 1326, 1203, 1176, 1153, 1120, 1034, 934, 884, 834, 799, 777, 756, 744, 638 cm^{-1}; **mp** 81-83 ˚C; No HRMS obtained.

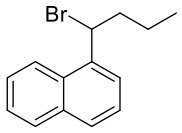

rac-**1p**

1-(1-bromobutyl)naphthalene (1p)

Compound *rac*-**1** was prepared according to General Procedure 4 from *rac*-**17p**. The product was isolated as a colourless oil in 95 % yield.

^{1}H NMR (500 MHz, $CDCl_3$) δ = 8.20 (d, *J* = 8.5 Hz, 1H), 7.92 – 7.86 (m, 1H), 7.86 – 7.78 (m, 1H), 7.73 (d, *J* = 7.1 Hz, 1H), 7.60 (ddd, *J* = 8.5, 6.8, 1.4 Hz, 1H), 7.57 – 7.40 (m, 2H), 5.88 – 5.68 (m, 1H), 2.59 – 2.48 (m, 1H), 2.40 – 2.31 (m, 1H), 1.74 – 1.60 (m, 1H), 1.54 – 1.45 (m, 1H), 1.01 (t, *J* = 7.4 Hz, 3H); **^{13}C NMR** (126 MHz, $CDCl_3$) δ = 137.5, 134.1, 130.6, 129.2, 129.1, 126.5, 126.0, 125.6, 124.7, 123.1, 50.9, 40.9, 21.8, 13.6; **IR** (neat) ν = 3050, 2961, 2872, 1701, 1597, 1511, 1463, 1180, 1151, 1110, 1034, 936, 863, 799, 776, 733 cm^{-1}; No HRMS obtained.

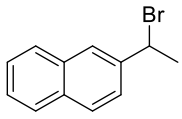

rac-**1q**

2-(1-bromoethyl)naphthalene (1q)

Compound *rac*-**1q** was prepared according to General Procedure 4 from *rac*-**17q** (CAS: 7228-47-9). The product was isolated as an off-white solid in 95 % yield. Spectroscopic data are in accordance with those in literature.[25]

^{1}H NMR (500 MHz, $CDCl_3$) δ = 7.88 – 7.80 (m, 4H), 7.61 (dd, *J* = 8.4, 1.9 Hz, 1H), 7.55 – 7.45 (m, 2H), 5.41 (q, *J* = 6.9 Hz, 1H), 2.16 (d, *J* = 6.9 Hz, 3H); **^{13}C NMR** (126 MHz, $CDCl_3$) δ = 140.6, 133.3, 133.2, 128.8, 128.2, 127.8, 126.6, 126.6, 125.3, 125.2, 50.1, 26.9.

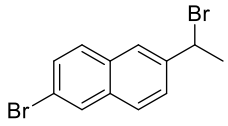

rac-**1r**

2-bromo-6-(1-bromoethyl)naphthalene (1r)

Compound *rac*-**1r** was prepared according to General Procedure 4 from *rac*-**17r**. The product was isolated as an off-white solid in 97 % yield.

^{1}H NMR (400 MHz, $CDCl_3$) δ = 7.99 (d, *J* = 1.9 Hz, 1H), 7.79 (d, *J* = 1.8 Hz, 1H), 7.75 (d, *J* = 8.6 Hz, 1H), 7.73 – 7.65 (m, 1H), 7.61 (dd, *J* = 8.6, 1.9 Hz, 1H), 7.56 (dd, *J* = 8.7, 2.0 Hz, 1H), 5.36 (q, *J* = 6.9 Hz, 1H), 2.13 (d, *J* = 6.9 Hz, 3H); **^{13}C NMR** (126 MHz, $CDCl_3$) δ = 141.1, 134.3, 131.6, 130.0, 129.9, 129.8, 127.9,

126.4, 125.2, 120.7, 49.6, 26.7; **IR** (neat) ν = 2980, 2918, 2850, 128, 1588, 1497, 1462, 1438, 1375, 1338, 1302, 1253, 1195, 1162, 1132, 1061, 1038, 968, 948, 896, 884, 821, 809, 791, 763, 725, 665, 642 cm^{-1}; **mp** 85-86 ˚C; No HRMS obtained.

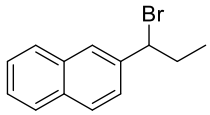

rac-**1s**

2-(1-bromopropyl)naphthalene (1s)

Compound *rac*-**1s** was prepared according to General Procedure 4 from *rac*-**17s**. The product was isolated as an off-white solid in 89 % yield.

^{1}H NMR (400 MHz, $CDCl_3$) δ = 7.89 – 7.77 (m, 4H), 7.57 (dt, *J* = 8.6, 1.9 Hz, 1H), 7.54 – 7.45 (m, 2H), 5.08 (t, *J* = 7.5 Hz, 1H), 2.50 – 2.21 (m, 2H), 1.04 (t, *J* = 7.2 Hz, 3H); **^{13}C NMR** (101 MHz, $CDCl_3$) [overlapping signal] δ = 139.5, 133.3, 133.2, 128.8, 128.2, 127.8, 126.6, 126.2, 125.3, 58.1, 33.3, 13.2; **HRMS** (EI) m/z calculated for $C_{13}H_{13}Br$ $(M)^{+\cdot}$ 248.01951, found 248.02006; **IR** (neat) ν = 3057, 2969, 2933, 2874, 1739, 1722, 1599, 1509, 1453, 1381, 1367, 1278, 1231, 1216, 1187, 1126, 1096, 1067, 1018, 904, 861, 825, 797, 750, 658 cm^{-1}; **mp** 52-53 ˚C.

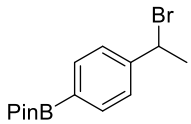

rac-**1t**

2-(4-(1-bromoethyl)phenyl)-4,4,5,5-tetramethyl-1,3,2-dioxaborolane (1t)

Compound *rac*-**1t** was prepared according to General Procedure 4 from *rac*-**17t**. The product was isolated as a colourless oil in 80 % yield.

^{1}H NMR (500 MHz, $CDCl_3$) δ = 7.82 – 7.76 (m, 2H), 7.46 – 7.41 (m, 2H), 5.20 (q, *J* = 6.9 Hz, 1H), 2.04 (d, *J* = 6.9 Hz, 3H), 1.34 (s, 12H); **^{13}C NMR** (126 MHz, $CDCl_3$) δ = 146.2, 135.3, 126.3, 84.0, 49.4, 26.8, 25.0; **IR** (liquid film) ν = 2981, 2929, 2248, 1612, 1517, 1443, 1400, 1361, 1324, 1297, 1271, 1144, 1092, 1065, 1042, 1020, 963, 910, 859, 837, 768, 735, 658 cm^{-1}; No HRMS obtained.

(*ipso*-carbon bound to boron not observed by ^{13}C NMR).

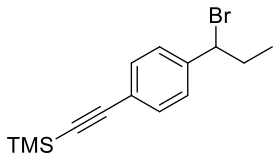

rac-**1u**

((4-(1-bromopropyl)phenyl)ethynyl)trimethylsilane (1u)

Compound *rac*-**1u** was prepared according to General Procedure 4 from *rac*-**17u**. Following purification (FCC eluent: 100% DCM) the product was isolated as a colourless oil in 64 % yield.

^{1}H NMR (500 MHz, $CDCl_3$) δ = 7.46 – 7.35 (m, 2H), 7.34 – 7.27 (m, 2H), 4.84 (dd, *J* = 7.9, 6.9 Hz, 1H), 2.33 – 2.21 (m, 1H), 2.14 (dp, *J* = 14.3, 7.2 Hz, 1H), 0.98 (t, *J* = 7.3 Hz, 3H), 0.25 (s, 9H); **^{13}C NMR** (126 MHz, $CDCl_3$) δ = 142.5, 132.4, 127.4, 123.2, 104.7, 95.1, 56.8, 33.2, 13.0, 0.1; **HRMS** (EI) m/z calculated for $C_{14}H_{19}{}^{79}BrSi$ $(M)^{+\cdot}$ 294.04339, found 294.04394; **IR** (neat) ν = 2966, 2917, 2849, 2159, 1508, 1463, 1409, 1393, 1352, 1250, 1221, 1116, 1088, 1018, 866, 844, 760, 672, 640 cm^{-1}.

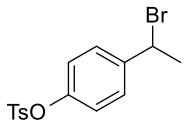

rac-**1v**

4-(1-bromoethyl)phenyl-4-methylbenzenesulfonate (1v)

Compound *rac*-**1v** was prepared according to General Procedure 4 from *rac*-**17v**. The product was isolated as a colourless oil in 87 % yield.

^{1}H NMR (500 MHz, $CDCl_3$) δ = 7.72 (dt, *J* = 8.9, 1.6 Hz, 2H), 7.39 – 7.30 (m, 4H), 6.99 – 6.92 (m, 2H), 5.14 (q, *J* = 6.9 Hz, 1H), 2.46 (s, 3H), 2.00 (dd, *J* = 6.9, 1.1 Hz, 3H); **^{13}C NMR** (126 MHz, $CDCl_3$) δ = 149.3, 145.6, 142.3, 132.5, 130.0, 128.6, 128.3, 122.7, 48.1, 26.9, 21.9; **IR** (neat) ν = 2985, 2958, 2859, 1599, 1503, 1443, 1375, 1216, 1199, 1177, 1154, 1119, 1093, 1044, 1018, 956, 943, 867, 846, 813, 785, 755, 707, 682, 659 cm^{-1}; No HRMS obtained.

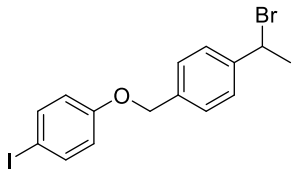

rac-**1w**

1-(1-bromoethyl)-4-((4-iodophenoxy)methyl)benzene (1w)

Compound *rac*-**1w** was prepared according to General Procedure 4 from *rac*-**17w**. The product was isolated as a white solid in 78 % yield.

^{1}H NMR (500 MHz, $CDCl_3$) δ = 7.59 – 7.52 (m, 2H), 7.49 – 7.43 (m, 2H), 7.41 – 7.32 (m, 2H), 6.79 – 6.71 (m, 2H), 5.22 (q, *J* = 6.9 Hz, 1H), 5.02 (s, 2H), 2.05 (d, *J* = 7.0 Hz, 3H); **^{13}C NMR** (126 MHz, $CDCl_3$) δ = 158.6, 143.3, 138.4, 136.8, 127.8, 127.3, 117.4, 83.3, 69.7, 49.1, 26.9; **IR** (neat) ν = 2919, 2865, 1585, 1572, 1515, 1486, 1459, 1422, 1381, 1280, 1242, 1173, 115, 1042, 1015, 1000, 967, 874, 823, 751, 719, 634 cm^{-1}; **mp** 92-93 ˚C; No HRMS obtained.

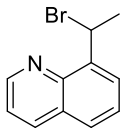

rac-**1x**

8-(1-bromoethyl)quinoline (1x)

Compound *rac*-**1x** was prepared according to General Procedure 4, scaled up to 5 mmol of *rac*-**17x**. The product was isolated as a yellow viscous oil in 40 % yield.

^{1}H NMR (400 MHz, $CDCl_3$) δ = 8.99 (dd, *J* = 4.2, 1.8 Hz, 1H), 8.17 (dd, *J* = 8.3, 1.8 Hz, 1H), 8.03 (dd, *J* = 7.3, 1.4 Hz, 1H), 7.78 (dd, *J* = 8.2, 1.4 Hz, 1H), 7.58 (dd, *J* = 8.2, 7.3 Hz, 1H), 7.44 (dd, *J* = 8.3, 4.2 Hz, 1H), 6.80 (q, *J* = 7.0 Hz, 1H), 2.20 (d, *J* = 7.0 Hz, 3H); **^{13}C NMR** (101 MHz, $CDCl_3$) δ = 149.9, 144.6, 141.3, 136.6, 128.4, 128.3, 127.6, 126.7, 121.5, 43.5, 26.4; **HRMS** (ESI^+) m/z calculated for $C_{11}H_{11}{}^{79}BrN$ $(M+H)^+$ calculated 236.0069, found 236.0069; **IR** (neat) ν = 3039, 2921, 2861, 1947, 1820, 1596, 1576, 1497, 1441, 1375, 1322, 1253, 1193, 1165, 1134, 1089, 1041, 1008, 963, 910, 856, 831, 794, 760, 733 cm^{-1}.

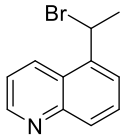

rac-**1y**

5-(1-bromoethyl)quinoline (1y)

Compound *rac*-**1y** was prepared according to General Procedure 4 from *rac*-**17y**. The product was isolated as a pale-yellow solid in 70 % yield.

^{1}H NMR (400 MHz, $CDCl_3$) δ = 9.36 (d, *J* = 8.5 Hz, 1H), 9.18 (m, 1H), 8.94 (dd, *J* = 6.8, 2.8 Hz, 1H), 8.14 – 8.12 (m, 1H), 8.08 – 8.05 (m, 2H), 5.87 (q, *J* = 6.8 Hz, 1H), 2.31 (d, *J* = 6.8 Hz, 3H); **^{13}C NMR** (101 MHz, $CDCl_3$) δ = 142.8, 142.5, 140.2, 138.7, 134.9, 127.4, 127.0, 122.3, 121.3, 41.1, 24.8; **HRMS** (ESI^+) m/z calculated for $C_{11}H_{11}{}^{79}BrN$ $(M+H)^+$ calculated 236.0069, found 236.0069; **IR** (neat) ν = 2627, 2852, 2620, 1630, 1597, 1554, 1410, 1372, 1293, 1225, 1194, 1027, 1007, 991, 919, 825, 803, 704, 660 cm^{-1}; **mp** 183-184 ˚C.

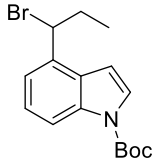

rac-**1z**

***tert*-butyl-4-(1-bromopropyl)-1*H*-indole-1-carboxylate (1z)**

Compound *rac*-**1z** was prepared according to General Procedure 5 from *rac*-**17z**. The product was isolated as a yellow oil in 45 % yield.

^{1}H NMR (500 MHz, $CDCl_3$) δ = 8.12 (d, *J* = 7.3 Hz, 1H), 7.67 (d, *J* = 3.8 Hz, 1H), 7.32 – 7.27 (m, 2H), 6.78 (dd, *J* = 3.8, 0.9 Hz, 1H), 5.26 (dd, *J* = 8.2, 6.8 Hz, 1H), 2.52 – 2.28 (m, 2H), 1.67 (s, 9H), 1.04 (t, *J* = 7.3 Hz, 3H); **^{13}C NMR** (126 MHz, $CDCl_3$) δ = 149.8 (br), 134.0, 128.8, 126.1, 125.2, 124.5, 120.9, 115.5, 105.5, 84.1, 55.2, 32.5, 28.3, 13.3; **HRMS** (ESI^+) m/z calculated for $C_{16}H_{21}{}^{79}BrNO_2$ $(M+H)^+$ 338.0750, found 338.1078; **IR** (liquid film) ν = 3008, 2926, 2854, 2360, 2340, 1740, 1537, 1426, 1382, 1371, 1349, 1284, 1258, 1158, 1135, 1048, 913, 758, 734, 646 cm^{-1}.

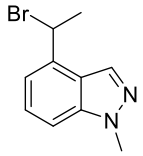

rac-**1aa**

4-(1-bromoethyl)-1-methyl-1*H*-indazole (1aa)

Compound *rac*-**1aa** was prepared according to General Procedure 4 from *rac*-**17aa**. The product was isolated as a colourless oil in 88 % yield.

^{1}H NMR (400 MHz, $CDCl_3$) δ = 8.22 (d, *J* = 0.9 Hz, 1H), 7.41 – 7.28 (m, 2H), 7.26 – 7.17 (m, 1H), 5.57 (q, *J* = 7.0 Hz, 1H), 4.09 (s, 3H), 2.21 (d, *J* = 7.0 Hz, 3H); **^{13}C NMR** (101 MHz, $CDCl_3$) δ = 140.5, 136.3, 131.6, 126.3, 121.9, 117.8, 109.6, 47.0, 35.9, 26.2; **HRMS** (ESI^+) m/z calculated for $C_{10}H_{12}BrN_2$ $(M+H)^+$ 239.0178, found 239.0179; **IR** (neat) ν = 2917, 2851, 1611, 1509, 1452, 1409, 1376, 1276, 1182, 1074, 1030, 987, 942, 912, 836, 789, 735, 660, 641, 629 cm^{-1}.

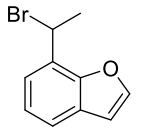

rac-**1ab**

7-(1-bromoethyl)benzofuran (1ab)

Compound *rac*-**1ab** was prepared according to General Procedure 4 from *rac*-**17ab**. The product was isolated as a colourless oil in 66 % yield.

^{1}H NMR (400 MHz, $CDCl_3$) δ =7.69 (d, *J* = 2.2 Hz, 1H), 7.56 (dd, *J* = 7.8, 1.2 Hz, 1H), 7.41 (dd, *J* = 7.5, 1.2 Hz, 1H), 7.24 (t, *J* = 7.7 Hz, 1H), 6.80 (d, *J* = 2.2 Hz, 1H), 5.73 (q, *J* = 7.0 Hz, 1H), 2.20 (d, *J* = 7.0 Hz, 3H); **^{13}C NMR** (101 MHz, $CDCl_3$) δ = 151.8, 145.2, 128.1, 127.2, 123.2, 122.1, 121.6, 106.9, 43.3, 25.7; **IR** (neat) ν =3063, 2818, 1542, 1430, 1377, 1314, 1267, 1198, 1169, 1125, 1091, 1030, 949, 872, 838, 799, 738, 680, 660, 635 cm^{-1}; No HRMS obtained.

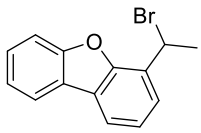

rac-**1ac**

4-(1-bromoethyl)dibenzo[*b*,*d*]furan (1ac)

Compound *rac*-**1ac** was prepared according to General Procedure 4 from *rac*-**17ac**. The product was isolated as a colourless oil in 46 % yield.

^{1}H NMR (400 MHz, $CDCl_3$) δ = 7.96 (d, *J* = 0.6 Hz, 1H), 7.90 (dd, *J* = 7.6, 1.2 Hz, 1H), 7.65 (dt, *J* = 8.3, 0.9 Hz, 1H), 7.61 (dd, *J* = 7.7, 1.2 Hz, 1H), 7.50 (ddd, *J* = 8.3, 7.2, 1.4 Hz, 1H), 7.42 – 7.31 (m, 2H), 5.87 (q, *J* = 7.0 Hz, 1H), 2.26 (d, *J* = 7.0 Hz, 3H); **^{13}C NMR** (101 MHz, $CDCl_3$) δ = 156.2, 152.8, 127.5, 127.4, 124.9, 124.8, 124.1, 123.2, 123.0, 120.8, 120.8, 112.0, 42.8, 25.9; **IR** (neat) ν = 3063, 2818, 1542, 1430, 1377, 1314, 1267, 1125, 1091, 1030, 949, 872, 838, 799, 738, 680, 660, 635 cm^{-1}; No HRMS obtained.

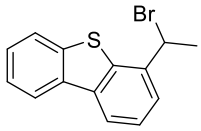

rac-**1ad**

4-(1-bromoethyl)dibenzo[*b*,*d*]thiophene (1ad)

Compound *rac*-**1ad** was prepared according to General Procedure 4 from *rac*-**17ad**. Following purification (FCC eluent: 50:50 pentane:DCM) the product was isolated as a yellow oil in 44 % yield.

^{1}H NMR (400 MHz, $CDCl_3$) δ = 8.21 – 8.14 (m, 1H), 8.11 (dd, *J* = 7.9, 1.1 Hz, 1H), 7.94 – 7.84 (m, 1H), 7.63 (dd, *J* = 7.7, 1.1 Hz, 1H), 7.54 – 7.45 (m, 3H), 5.53 (q, *J* = 6.9 Hz, 1H), 2.26 (d, *J* = 6.9 Hz, 3H); **^{13}C NMR** (101 MHz, $CDCl_3$) δ = 139.2, 138.3, 137.2, 136.6, 135.7, 127.2, 125.2, 124.7, 124.2, 122.9, 121.9, 121.7, 47.4, 25.4; **IR** (liquid film) ν = 2973, 2931, 1657, 1468, 1408, 1380, 1301, 1163, 1130, 1036, 953, 818, 753, 682, 627 cm^{-1}; No HRMS obtained.

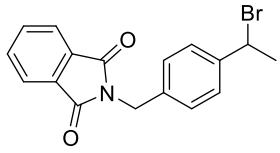

rac-**1ae**

2-(4-(1-bromoethyl)benzyl)isoindoline-1,3-dione (1ae)

Compound *rac*-**1ae** was prepared according to General Procedure 4 from *rac*-**17ae**. The product was isolated as a white solid in 92 % yield.

^{1}H NMR (500 MHz, $CDCl_3$) δ = 7.86 (dd, *J* = 5.4, 3.0 Hz, 2H), 7.71 (dd, *J* = 5.5, 3.0 Hz, 2H), 7.44 – 7.35 (m, 4H), 5.17 (q, *J* = 6.9 Hz, 1H), 4.83 (s, 2H), 2.00 (d, *J* = 6.9 Hz, 3H); **^{13}C NMR** (126 MHz, $CDCl_3$) δ = 168.1, 143.0, 136.6, 134.2, 132.2, 129.2, 127.3, 123.5, 49.1, 41.3, 26.9; **HRMS** (ESI^+) m/z calculated for $C_{17}H_{15}{}^{79}BrNO_2$ $(M+H)^+$ 344.0281, found 344.0276; **IR** (neat) ν = 2923, 2854, 1765, 1718, 1613, 1511, 1466, 1426, 1392, 1342, 1328, 1298, 1260, 1211, 1186, 1096, 1067, 1047, 1018, 976, 940, 752, 727, 812, 765, 715, 692, 627 cm^{-1}; **mp** 79-81 ˚C.

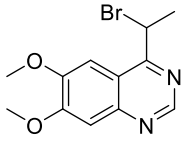

rac-**1af**

4-(1-bromoethyl)-6,7-dimethoxyquinazoline (1af)

Compound *rac*-**1af** was prepared according to General Procedure 6 from *rac*-**17af**. Following purification (FCC eluent: 90:10 – 85:15 DCM:EtOAc) the product was isolated as an off-white solid in 51 % yield.

^{1}H NMR (400 MHz, $CDCl_3$) δ = 9.14 (s, 1H), 7.38 (s, 1H), 7.36 (s, 1H), 5.78 (q, *J* = 6.7 Hz, 1H), 4.08 (s, 3H), 4.07 (s, 3H), 2.24 (d, *J* = 6.7 Hz, 3H); **^{13}C NMR** (101 MHz, $CDCl_3$) δ = 164.3, 156.3, 153.3, 150.6, 149.0, 118.0, 107.2, 101.4, 56.7, 56.5, 42.8, 22.7; **HRMS** (ESI^+) m/z calculated for $C_{12}H_{14}{}^{79}BrN_2O_2$ $(M+H)^+$

297.0233, found 297.0233; **IR** (neat) ν = 2941, 2834, 2363, 1713, 1620, 1553, 1507, 1476, 1434, 1372, 1372, 1343, 1291, 1238, 1214, 1166, 1133, 1021, 991, 889, 868, 842, 824, 779, 735 cm^{-1}; **mp** 149-150 ˚C.

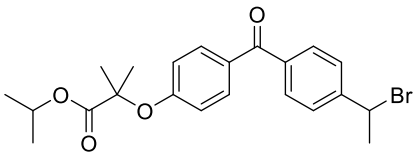

rac-**1ag**

isopropyl-2-(4-(4-(1-bromoethyl)benzoyl)phenoxy)-2-methylpropanoate (1ag)

Compound *rac*-**1ag** was prepared according to General Procedure 6 from *rac*-**17ag**. Following purification (FCC eluent: 100% DCM) the product was isolated as a viscous colourless oil in 77 % yield.

^{1}H NMR (400 MHz, $CDCl_3$) δ = 7.80 – 7.65 (m, 4H), 7.58 – 7.49 (m, 2H), 6.95 – 6.77 (m, 2H), 5.23 (q, *J* = 6.9 Hz, 1H), 5.08 (hept, *J* = 6.3 Hz, 1H), 2.06 (d, *J* = 6.9 Hz, 3H), 1.65 (s, 6H), 1.20 (d, *J* = 6.3 Hz, 6H); **^{13}C NMR** (101 MHz, $CDCl_3$) δ = 194.9, 173.2, 159.8, 147.1, 138.1, 132.1, 130.5, 130.3, 126.8, 117.3, 79.5, 69.4, 48.3, 26.7, 25.5, 21.6; **HRMS** (ESI^+) m/z calculated for $C_{22}H_{26}{}^{79}BrO_4$ $(M+H)^+$ 433.1009, found 433.1008; **IR** (liquid film) ν = 3042, 2945, 2908, 2361, 1731, 1655, 1600, 1505, 1444, 1287, 1253, 1179, 1102, 1044, 930, 857, 771, 690, 617 cm^{-1}.

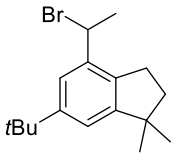

rac-**1ah**

4-(1-bromoethyl)-6-(*tert*-butyl)-1,1-dimethyl-2,3-dihydro-1*H*-indene (1ah)

Compound *rac*-**1ah** was prepared according to General Procedure 4 from *rac*-**17ah**. The product was isolated as an off-white solid in 82 % yield.

^{1}H NMR (400 MHz, $CDCl_3$) δ = 7.35 (d, *J* = 1.8 Hz, 1H), 7.12 (d, *J* = 1.8 Hz, 1H), 5.33 (q, *J* = 6.9 Hz, 1H), 3.06 – 2.80 (m, 2H), 2.09 (d, *J* = 7.0 Hz, 3H), 2.02 – 1.94 (m, 2H), 1.35 (s, 9H), 1.27 (s, 3H), 1.26 (s, 3H); **^{13}C NMR** (101 MHz, $CDCl_3$) δ = 153.1, 150.5, 137.9, 137.7, 120.8, 119.3, 48.3, 44.2, 41.4, 35.0, 31.7, 28.9, 28.8, 27.9, 25.9; **IR** (neat) ν = 3000, 2945, 1769, 1609, 1479, 1462, 1394, 1362, 1318, 1254, 1224, 1189, 1144, 1055, 1014, 933, 907, 878, 773, 722, 655, 641, 630 cm^{-1}; **mp** 61-63 ˚C; No HRMS obtained.

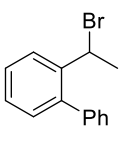

rac-**1ai**

2-(1-bromoethyl)-1,1'-biphenyl (1ai)

Compound *rac*-**1ai** was prepared according to General Procedure 4 from *rac*-**17ai**. The product was isolated as an off-white solid in 98 % yield.

^{1}H NMR (400 MHz, $CDCl_3$) δ = 7.78 (dd, *J* = 7.9, 1.3 Hz, 1H), 7.51 – 7.37 (m, 6H), 7.33 (td, *J* = 7.5, 1.3 Hz, 1H), 7.20 (dd, *J* = 7.6, 1.5 Hz, 1H), 5.28 (q, *J* = 6.9 Hz, 1H), 1.98 (d, *J* = 6.9 Hz, 3H); **^{13}C NMR** (101 MHz, $CDCl_3$) δ = 140.9, 140.5, 140.3, 130.2, 129.2, 128.5, 128.3, 128.1, 127.6, 127.5, 47.0, 27.6; **IR** (neat) ν = 3022, 2947, 2924, 2850, 1708, 1595, 1479, 1438, 1338, 1266, 1198, 1172, 1122, 1070, 1037, 1010, 970, 913, 791, 765, 753, 721, 702 cm^{-1}; **mp** 35-36 ˚C; No HRMS obtained.

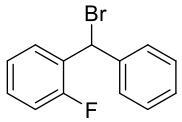

rac-**1aj**

1-(bromo(phenyl)methyl)-2-fluorobenzene (1aj)

Compound *rac*-**1i** was prepared according to General Procedure 4 from *rac*-**17aj**. The product was isolated as a colourless oil in 61 % yield.

^{1}H NMR (500 MHz, $CDCl_3$) δ = 7.57 (td, *J* = 7.8, 1.8 Hz, 1H), 7.49 (d, *J* = 7.6 Hz, 2H), 7.41 (t, *J* = 7.5 Hz, 2H), 7.27 (qd, *J* = 7.3, 3.3 Hz, 2H), 7.14 (t, *J* = 7.6 Hz, 1H), 7.03 (dd, *J* = 10.3, 8.2 Hz, 1H), 6.57 (s, 1H); **^{19}F NMR** (471 MHz, $CDCl_3$) δ = -118.4; **^{13}C NMR** (126 MHz, $CDCl_3$) δ = 159.2 (d, *J* = 248.9 Hz), 140.0, 130.8 (d, *J* = 2.6 Hz), 130.1 (d, *J* = 8.3 Hz), 128.7, 128.7, 128.4, 128.3, 124.5 (d, *J* = 3.7 Hz), 115.7 (d, *J* = 21.7 Hz), 47.1 (d, *J* = 4.4 Hz); **IR** (neat) ν = 3034, 2249, 1615, 1542, 1493, 1456, 1330, 1268, 1224, 1191, 1151, 1078, 1023, 909, 865, 806, 758, 732, 698, 650 cm^{-1}; No HRMS obtained.

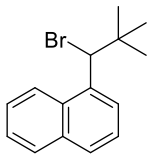

rac-**1ak**

1-(1-bromo-2,2-dimethylpropyl)naphthalene (1ak)

Compound *rac*-**1p** was prepared according to General Procedure 4 from *rac*-**17p**. The product was isolated as a colourless oil in 42 % yield.

^{1}H NMR (500 MHz, $CDCl_3$) δ = 8.10 (d, *J* = 8.6 Hz, 1H), 7.94 (d, *J* = 7.4 Hz, 1H), 7.87 (d, *J* = 8.1 Hz, 1H), 7.79 (d, *J* = 8.1 Hz, 1H), 7.57 – 7.44 (m, 3H), 5.99 (s, 1H), 1.15 (s, 9H); **^{13}C NMR** (126 MHz, $CDCl_3$) δ = 136.7, 133.5, 131.1, 129.7, 129.2, 128.5, 126.4, 125.5, 125.1, 123.1, 62.1, 38.4, 28.0; **HRMS** (EI) m/z calculated for $C_{15}H_{17}{}^{79}Br$ $(M)^{+\cdot}$ 276.05081, found 276.05136; **IR** (neat) ν = 3049, 2961, 2874, 1701, 1596, 1511, 1462, 1181, 1152, 1111, 1034, 962, 776, 736 cm^{-1}.

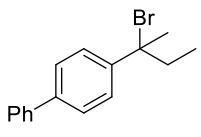

rac-**1al**

4-(2-bromobutan-2-yl)-1,1'-biphenyl (1al)

Compound *rac*-**1r** was prepared according to General Procedure 5 from *rac*-**17r**. The product was isolated as a colourless oil in 57 % yield.

^{1}H NMR (400 MHz, $CDCl_3$) δ = 7.67 – 7.55 (m, 4H), 7.54 – 7.49 (m, 2H), 7.49 – 7.38 (m, 2H), 7.38 – 7.29 (m, 1H), 1.88 (p, *J* = 7.3 Hz, 2H), 1.59 (s, 3H), 0.84 (t, *J* = 7.4 Hz, 3H); **^{13}C NMR** (101 MHz, $CDCl_3$) δ = 147.0, 141.0, 139.5, 128.9, 127.3, 127.2, 127.0, 125.5, 75.0, 36.8, 29.8, 8.5; **IR** (liquid film) ν = 3059, 3030, 2926, 2851, 1682, 1604, 1487, 1450, 1402, 1273, 1172, 1094, 1077, 1008, 916, 842, 767, 734, 699 cm^{-1}; No HRMS obtained

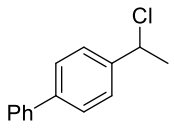

rac-**1a-Cl**

4-(1-chloroethyl)-1,1'-biphenyl (1a-Cl)

Compound *rac*-**1a-Cl** was prepared through the dropwise addition of thionyl chloride (1.5 equiv.) to a solution of 1-([1,1'-biphenyl)-4-yl)ethan-1-ol (1 equiv.) in Et_2O (0.1 M) at 0 °C. The reaction mixture was stirred at 25 °C for 16 h. Upon completion, monitored by TLC, the reaction mixture was quenched with ice-cold water and washed with $NaHCO_3$ (sat). The aqueous phase was extracted with Et_2O, dried with $MgSO_4$ and concentrated under reduced pressure. Following purification (95:5 -80:20 pentane:Et_2O) the product was isolated as a white solid in 89 % yield. Spectroscopic data are in accordance with those in literature.[26]

^{1}H NMR (400 MHz, $CDCl_3$) δ = 7.69 – 7.58 (m, 4H), 7.57 – 7.45 (m, 4H), 7.45 – 7.35 (m, 1H), 5.19 (q, *J* = 6.8 Hz, 1H), 1.94 (d, *J* = 6.8 Hz, 3H); **^{13}C NMR** (101 MHz, $CDCl_3$) δ = 141.9, 141.4, 140.7, 128.9, 127.6, 127.5, 127.2, 127.1, 58.7, 26.6.

4.3.3. Synthesis of α-Bromoketones

General procedure 7

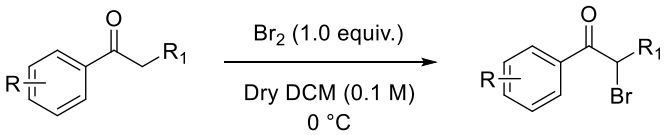

Bromide substrates were prepared from corresponding ketones via bromination with Br_2 (2.5 mmol, 1 equiv.) in dry DCM (0.1 M) at 0°C following a literature procedure.[27] After the completion of the reaction (18 h) the mixture was quenched slowly with $Na_2S_2O_3$ (sat aq.) and the aqueous layer was

extracted with DCM (3 x 20 mL). The combined organic extracts were dried with Na_2SO_4 and concentrated under reduced pressure. Products were subsequently purified by FCC.

General procedure 8

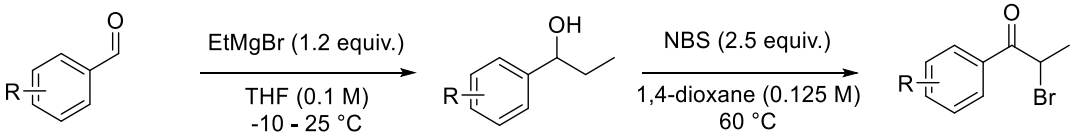

Bromide substrates were prepared via a two-step protocol following a literature procedure.[28] Alcohol intermediates were prepared through Grignard addition to the corresponding aldehydes in THF at -10 °C. The reactions were monitoring by TLC and quenched with saturated NH_4Cl solution when the aldehyde was fully consumed. Following work up in Et_2O/H_2O the organic extracts were washed with brine and dried with $MgSO_4$, solvent was removed under reduced pressure to give the corresponding alcohol. The alcohol was dissolved in 1,4-dioxane (0.125 M), NBS (2.5 equiv.) was added, and the reaction was stirred at 60 °C. The reaction was monitored by TLC and upon completion quenched with $Na_2S_2O_3$ (sat aq.), aqueous layer the extracted with Et_2O (15 mL x 3). The combined organic extracts were washed with brine and dried with $MgSO_4$. After concentration under reduced pressure the products were purified by FCC.

Bromides *rac*-**12a** (CAS: 38786-67-3), *rac*-**12b** (CAS: 877-37-2), *rac*-**12c** (CAS: 345-94-8), *rac*-**12i** (CAS: 2114-00-3), *rac*-**12j** (CAS: 1451-82-7), *rac*-**12k** (CAS 21086-33-9) were commercially available.

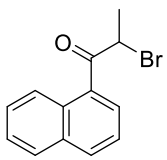

rac-**12d**

2-bromo-1-(naphthalen-1-yl)propan-1-one (12d)

Compound *rac*-**12d** was prepared according to General Procedure 8. Following purification (FCC eluent: pentane:DCM 80:20) the product was isolated as a white solid in 84 % yield.

^{1}H NMR (400 MHz, $CDCl_3$) δ = 8.44 (d, *J* = 8.6, 1H), 8.02 (dt, *J* = 8.2, 1.1 Hz, 1H), 7.93 – 7.83 (m, 2H), 7.67 – 7.46 (m, 3H), 5.37 (q, *J* = 6.7 Hz, 1H), 1.98 (d, *J* = 6.7 Hz, 3H); **^{13}C NMR** (101 MHz, $CDCl_3$) δ = 196.7,

134.0, 133.8, 133.2, 130.9, 128.5, 128.2, 126.7, 126.7, 125.6, 124.2, 45.6, 20.5; **HRMS** (ESI^+) m/z calculated for $C_{13}H_{12}{}^{79}BrO$ $(M+H)^+$ 263.0066, found 263.0065; **IR** (neat) ν = 3059, 2975, 2879, 2360, 1954, 1681, 1604, 1560, 1529, 1478, 1450, 1407, 1368, 1324, 1300, 1273, 1227, 1205, 1165, 1132, 1114, 1068, 1004, 951, 931, 901, 854, 806, 738, 696, 643 cm^{-1}; **mp** 81-83 ˚C.

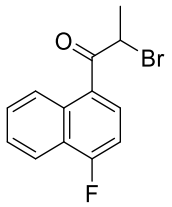

rac-**12e**

2-bromo-1-(4-fluoronaphthalen-1-yl)propan-1-one (12e)

Synthesised by C. Palladino

Compound *rac*-**12e** was prepared according to General Procedure 8. Following purification (FCC eluent: pentane:DCM 70:30) the product was isolated as a white solid in 86 % yield.

^{1}H NMR (600 MHz, $CDCl_3$) δ = 8.58 (m, 1H), 8.21 – 8.15 (m, 1H), 7.91 (dd, *J* = 8.1, 5.2 Hz, 1H), 7.69 (ddd, *J* = 8.5, 6.8, 1.4 Hz, 1H), 7.63 (ddd, *J* = 8.1, 6.8, 1.1 Hz, 1H), 7.17 (dd, *J* = 9.7, 8.1 Hz, 1H), 5.36 (q, *J* = 6.6 Hz, 1H), 1.97 (d, *J* = 6.6 Hz, 3H); **^{19}F NMR** (565 MHz, $CDCl_3$) δ = - 131.5; **^{13}C NMR** (151 MHz, $CDCl_3$) δ = 195.3, 161. (d, $J_{C\text{-}F}$ = 260.7 Hz), 133.1 (d, $J_{C\text{-}F}$ = 5.5 Hz), 129.6 (d, $J_{C\text{-}F}$ = 4.5 Hz), 129.3, 128.1 (d, $J_{C\text{-}F}$ = 10.0 Hz), 127.1 (d, $J_{C\text{-}F}$ = 2.2 Hz), 125.9 (d, $J_{C\text{-}F}$ = 2.7 Hz), 124.3 (d, $J_{C\text{-}F}$ = 15.9 Hz), 120.9 (d, $J_{C\text{-}F}$ = 6.3 Hz), 108.1 (d, $J_{C\text{-}F}$ = 21.3 Hz), 45.0, 20.5; **HRMS** (ESI^+) m/z $C_{13}H_{11}{}^{79}BrFO$ $(M+H)^+$ 280.9972, found 280.9969; **IR** (neat) ν = 3346, 3075, 2966, 2936, 2869, 1855, 1683, 1630, 1602, 1578, 1509, 1466, 1424, 1394, 1379, 1338, 1230, 1186, 1168, 1143, 1109, 1061, 1044, 1019, 979, 898, 832, 706, 636 cm^{-1}; **mp** 80-81 ˚C.

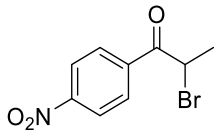

rac-**12f**

2-bromo-1-(4-nitrophenyl)propan-1-one 9 (12f)

Synthesised by C. Palladino

Compound *rac*-**12f** was prepared according to General Procedure 7. Following purification (FCC eluent: pentane:DCM 60:40) the product was isolated as a yellow solid in 86 % yield. **^{1}H NMR** (400 MHz, $CDCl_3$) δ = 8.37 – 8.29 (m, 2H), 8.22 – 8.14 (m, 2H), 5.26 (q, J = 6.6 Hz, 1H), 1.94 (d, J = 6.6 Hz, 3H).8.35-8.31 (m, 2H); **^{13}C NMR** (101 MHz, $CDCl_3$) δ = 191.7, 150.5, 138.8, 130.0, 123.9, 41.4, 19.8; **HRMS** (ESI^+) m/z calculated for $C_9H_8{}^{79}BrNO_3$ $(M+H)^+$ 257.9760, found 257.9948; **IR** (neat) ν = 2954, 2928, 2855, 1691, 1606, 1531, 1448, 1340, 1319, 1236, 1165, 1112, 997, 951, 854, 755, 714 cm^{-1}; **mp** 45-46 ˚C.

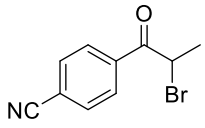

rac-**12g**

4-(2-bromopropanoyl)benzonitrile (12g)

Synthesised by C. Palladino

Compound *rac*-**12g** was prepared according to General Procedure 7. Following purification (FCC eluent: pentane:DCM 60:40) as a white solid in 85 % yield.

^{1}H NMR (400 MHz, $CDCl_3$) δ = 8.15 – 8.08 (m, 2H), 7.81 – 7.78 (m, 2H), 5.23 (q, J = 6.6 Hz, 1H), 1.92 (dd, J = 6.5, 1.7 Hz, 3H); **^{13}C NMR** (101 MHz, $CDCl_3$) δ= 191.9, 137.3, 132.5, 129.4, 117.8, 116.9, 41.2, 19.8; **HRMS** (ESI^+) m/z calculated for $C_{10}H_9{}^{79}BrNO$ $(M+H)^+$ 237.9862, found 237.9998; **IR** (neat) ν = 2988, 2356, 2228, 1934, 1692, 1566, 1439, 1407, 1376, 1339, 1294, 1241, 1152, 1119, 1056, 997, 951, 851, 756, 711, 688, 651 cm^{-1}; **mp** 75-76 ˚C.

2-bromo-1-(4-(trifluoromethyl)phenyl)propan-1-one (12h)

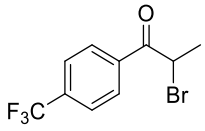

rac-**12h**

Synthesised by C. Palladino

Compound *rac*-**12h** was prepared according to General Procedure 7. Following purification (FCC eluent: pentane:DCM, 70:30) the product was isolated as a white solid in 91 % yield.

^{1}H NMR (400 MHz, $CDCl_3$) δ = 8.17-8.09 (m, 2H), 7.79 – 7.72 (m, 2H), 5.26 (q, J = 6.6 Hz, 1H), 1.93 (d, J = 6.6 Hz, 3H); **^{19}F NMR** (376 MHz, $CDCl_3$) δ= -63.2; **^{13}C NMR** (101 MHz, $CDCl_3$) δ = 192.3, 136.9, 134.9 (q, $J_{C\text{-}F}$ =32.8 Hz) 129.3, 125.80 (q, $J_{C\text{-}F}$ = 3.7 Hz), 123.5, (q, $J_{C\text{-}F}$ = 272.8 Hz), 41.3, 19.9; **HRMS** (ESI^+) m/z calculated for $C_{10}H_8{}^{79}BrF_3O$ $(M+H)^+$ 280.9783, found 280.9403; **IR** (neat) ν = 2982, 2933, 2871, 1687, 1529, 1446, 1411, 1382, 1324, 1242, 1165, 1126, 1069, 1016, 998, 953, 861, 807, 768, 737, 701, 668 cm^{-1}; **mp** 40-42 ˚C.

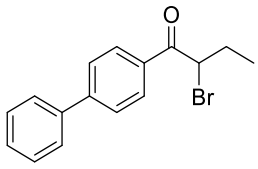

rac-**12l**

1-([1,1'-biphenyl]-4-yl)-2-bromobutan-1-one (12l)

Compound *rac*-**12l** was prepared according to General Procedure 7. Following purification (FCC eluent: pentane:DCM 80:20) the product was isolated as a pale-yellow solid in 87 % yield.

^{1}H NMR (400 MHz, $CDCl_3$) δ = 8.12 – 8.09 (m, 2H), 7.73 – 7.70 (m, 2H), 7.65 – 7.62 (m, 2H), 7.51 – 7.39 (m, 2H), 7.48 – 7.37 (m, 1H), 5.11 (dd, *J* = 7.7, 6.4 Hz, 1H), 2.34 – 2.12 (m, 2H), 1.11 (t, *J* = 7.3 Hz, 3H); **^{13}C NMR** (101 MHz, $CDCl_3$) δ = 192.8, 146.4, 139.7, 133.2, 129.5, 129.0, 128.4, 127.4, 127.3, 49.2, 27.0,

12.2; **HRMS** (ESI$^+$) m/z calculated for $C_{16}H_{16}{}^{79}BrO$ $(M+H)^+$ 303.0379, found 303.0377; **IR** (neat) ν = 3340, 2975, 2939, 2879, 1680, 1604, 1560, 1529, 1487, 1450, 1407, 1324, 1300, 1273, 1226, 1206, 1164, 1133, 1068, 1004, 951, 901, 855, 801, 772, 738, 716, 696, 642 cm^{-1}; **mp** 66-68 ˚C.

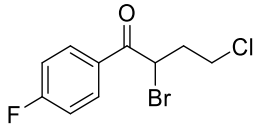

rac-**12m**

2-bromo-4-chloro-1-(4-fluorophenyl)butan-1-one (12m)

Synthesised by C. Palladino

Compound *rac*-**12m** was prepared according to General Procedure 7. Following purification (FCC eluent: pentane:DCM 90:10) the product was isolated as a white solid in 73 % yield. **^{1}H NMR** (400 MHz, $CDCl_3$) 8.12 – 8.03 (m, 2H), 7.23 – 7.13 (m, 2H), 5.43 (dd, *J* = 8.1, 5.8 Hz, 1H), 3.88 – 3.71 (m, 2H), 2.65 – 2.48 (m, 2H); **^{19}F NMR** (376 MHz, $CDCl_3$) δ= -103.2; **^{13}C NMR** (101 MHz, $CDCl_3$) δ = 191.0, 166.2 (d, $J_{C\text{-}F}$ = 256.8 Hz), 131.8 (d, $J_{C\text{-}F}$ = 9.5 Hz), 130.4 (d, $J_{C\text{-}F}$ = 3.0 Hz), 116.1 (d, $J_{C\text{-}F}$ = 22.0 Hz), 43.5, 42.4, 35.7; **HRMS** (ESI$^+$) m/z calculated for $C_{10}H_{10}{}^{79}BrClFO$ $(M+H)^+$ 278.9582 found 279.0056; **IR** (neat) ν = 3355, 2973, 2880, 1683, 1602, 1560, 1529, 1507, 1487, 1448, 1408, 1372, 1322, 1300, 1260, 1228, 1205, 1158, 1129, 1023, 1004, 945, 901, 862, 844, 818, 772, 752, 739, 697, 652 cm^{-1}; **mp** 42-43 ˚C.

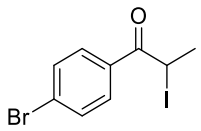

rac-**14a**

1-(4-bromophenyl)-2-iodopropan-1-one (14a)

Compound *rac*-**14a** was prepared by the addition of KI (3 equiv.) to **12a** in MeCN (0.25 M). Following filtration over celite the product was isolated as an off-white solid in 85 % yield. Spectroscopic data are in accordance with those in literature.[29]

^{1}H NMR (400 MHz, $CDCl_3$) δ 7.92 – 7.82 (m, 2H), 7.68 – 7.56 (m, 2H), 5.42 (q, *J* = 6.7 Hz, 1H), 2.07 (d, *J* = 6.7 Hz, 3H); **^{13}C NMR** (101 MHz, $CDCl_3$) δ 193.9, 132.5, 132.2, 130.3, 128.8, 22.0, 17.9;

4.4. Synthesis of Onium Salts

Onium salts **8b** (CAS: 30537-09-8), **8c** (CAS: 2750-90-8), **8d** (CAS: 2065-67-0), **8e** (1779-49-3), **8f** (1449-46-3), **8g** (1243-97-6), **8h** (1100-88-5), **8j** (1519-46-6), **8k** (3115-68-2), **8l** (1643-19-2), **8m** (311-28-4) were commercially available.

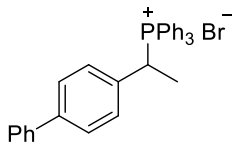

8a

(1-([1,1'-biphenyl]-4-yl)ethyl)triphenylphosphonium bromide (8a)

Compound **8a** was prepared by the addition of PPh_3 (1 equiv.) to **1a** in dioxane (0.25 M) the reaction was heated to 80 °C and left to stir until precipitate formed. The solution was then cooled and following filtration and washing with Et_2O, the product was isolated as a white solid in 80 % yield.

^{1}H NMR (400 MHz, $CDCl_3$, 298 K) δ = 7.90–7.78 (m, 6H), 7.82–7.72 (m, 3H), 7.69 – 7.62 (m, 6H), 7.54–7.49 (m, 2H), 7.45-7.38 (m, 4H), 7.37–7.30 (m, 1H), 7.28 (d, *J* = 2.4 Hz, 2H), 7.01 (sext, *J* = 7.2 Hz, 1H), 1.85 (dd, *J* = 19.0, 7.3 Hz, 3H); **^{13}C NMR** (151 MHz, $CDCl_3$, 298 K) δ = 141.4, 140.0, 135.0 (d, *J* = 8.9 Hz), 134.8 (d, *J* = 3.2 Hz), 132.6 (d, *J* = 5.7 Hz) 131.2 (d, *J* = 6.0 Hz), 130.3 (d, *J* = 12.3 Hz), 129.0, 127.9, 127.3 (br), 127.1, 118.2, 34.4 (d, *J* = 41.8 Hz), 17.2; **^{31}P{^{1}H} NMR** (203 MHz, $CDCl_3$, 298 K) δ = 27.4; ; **HRMS** (ESI$^+$) m/z calculated for $C_{32}H_{28}P^+$ $(M\text{-}Br)^+$ 443.1923, found 443.1920; **IR** (neat) ν = 3658, 3455. 2981, 2888, 1485, 1473, 1462, 1438, 1382, 1253, 1153, 1109, 1080, 99 6, 955, 889, 871, 838, 765, 725, 697, 617 cm^{-1}; **mp** 166–167 ˚C

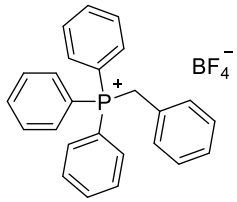

8i

Benzyltriphenylphosphonium tetrafluoroborate (8n)

Compound **8n** was prepared by the addition of $NaBF_4$ (1 equiv.) to benzyltriphenylphosphonium chloride (CAS: 1100-88-5) in H2O (0.04 M) the reaction was left to stir at room temperature until a precipitate formed. Following filtration **8n** was isolated as a white solid in 85 % yield. Spectroscopic data are in accordance with those in literature.[30]

^{1}H NMR (500 MHz, $CDCl_3$) δ = 7.82 – 7.74 (m, 3H), 7.63 (td, *J* = 7.9, 3.6 Hz, 6H), 7.55 (ddt, *J* = 12.5, 6.6, 1.3 Hz, 6H), 7.27 – 7.20 (m, 1H), 7.13 (t, *J* = 7.7 Hz, 2H), 6.96 – 6.90 (m, 2H), 4.70 (d, *J* = 14.2 Hz, 2H); **^{19}F NMR** (471 MHz, $CDCl_3$) δ = -151.9; **^{31}P NMR** (202 MHz, $CDCl_3$) δ = -21.9; **^{13}C NMR** (126 MHz, $CDCl_3$) δ 135.3 (d, *J* = 2.7 Hz), 134.2 (d, *J* = 9.5 Hz), 131.4 (d, *J* = 5.4 Hz), 130.4, 130. 3, 129.2 (d, *J* = 3.6 Hz), 128.8 (d, *J* = 3.6 Hz), 126.8 (d, *J* = 8.6 Hz), 117.5 (d, *J* = 85.8 Hz).

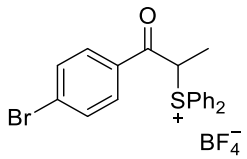

rac-1**8a**

(1-(4-bromophenyl)-1-oxopropan-2-yl)diphenylsulfonium tetrafluoroborate (18a)

Compound **18a** was prepared according to literature procedure in 69 % yield. Spectroscopic data are in accordance with those in literature.[27]

^{1}H NMR (400 MHz, $CDCl_3$) δ = 8.29 – 8.19 (m, 2H), 8.14 – 8.02 (m, 4H), 7.76 (tt, *J* = 6.0, 3.1 Hz, 3H), 7.72 – 7.66 (m, 2H), 7.66 – 7.54 (m, 3H), 7.00 (q, *J* = 7.2 Hz, 1H), 1.75 (d, *J* = 7.1 Hz, 3H); **^{19}F NMR** (377 MHz, $CDCl_3$) δ -150.8; **^{13}C NMR** (101 MHz, $CDCl_3$) δ = 193.1, 135.5, 134.8, 133.1, 132.4, 132.1, 131.8, 131.8, 131.3, 131.1, 130.6, 125.0, 121.8, 63.6, 16.3;

4.5. General Procedure for Fluorination under S-HBPTC

For reaction optimisation: In a 1.75 mL screw-cap vial equipped with a magnetic stirring bar pre-ground potassium fluoride (2.5 – 5 equiv.), the appropriate substrate (0.05 mmol, 1 equiv.), urea catalyst (10–20 mol%), onium co-catalyst (0 – 100 mol%) and solvent (0.25 – 0.5M) were sequentially added. The vial was sealed, and reaction was stirred at 1200 rpm at the specified temperature for 24 – 72 h. The crude reaction mixture was filtered over celite, solvent removed under reduced pressure in a polypropylene vial. Samples were dissolved in deuterated solvent and analysed by ^{1}H and ^{19}F NMR (4-fluoroanisole used as an internal standard).

4.5.1. General Procedure for Enantioselective Benzylic Fluorination

General Procedure 9: In a 7 mL screw-cap vial equipped with a magnetic stirring bar pre-ground potassium fluoride (2.5 equiv.), the appropriate substrate (0.16 – 0.38 mmol, 1 equiv.), (*S*)-**3u** (10 mol%), $Ph_4P^+ I^-$ (10 mol%) and *p*-xylene (0.25 M) were sequentially added. The vial was sealed, and reaction was stirred at 1200 rpm at the specified temperature and time. The crude reaction mixture was directly purified by FCC to give product. Solvent was removed in PFA round bottom flask and products were stored in polypropylene vials at -20 °C.

4.5.2. General Procedure for Enantioselective Fluorination of α-Haloketones

General Procedure 10: In a 7 mL screw-cap vial equipped with a magnetic stirring bar were sequentially added, pre-ground potassium fluoride (2.5 equiv.), the appropriate substrate (0.4 mmol, 1 equiv.), (*S*)-**3z** (10 mol%), $Et_4N^+ I^-$ (10 mol%) and MeCN (0.5 M). The vial was sealed, and reaction was stirred at 1200 rpm at the appropriate temperature for 96 h. The crude reaction mixture was directly purified by FCC to give product.

4.5.3. General Procedure for Synthesis of Racemic Standards

Racemic standards for all products were prepared by either (i) deoxyfluorination from corresponding alcohol or (ii) TBAF fluorination of corresponding bromide to produce racemic fluoride products – these were purified by preparative TLC for HPLC.

4.5.4. Synthesis and Characterisation of Benzylic Fluoride Products

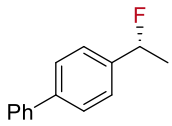

(*R*)-**2a**

(*R*)-4-(1-fluoroethyl)-1,1'-biphenyl (2a)

(*R*)-**2a** was prepared according to General Procedure 9 employing 0.38 mmol of *rac*-**1a** (100 mg), the reaction was stirred at 15 °C at 1200 rpm for 72 h. Following purification (FCC eluent: 100:0 – 98:2 pentane:DCM) the product was isolated as a white solid, 54 mg, 76 % yield, 92.5:7.5 e.r.

^{1}H NMR (400 MHz, $CDCl_3$) δ = 7.63 – 7.60 (m, 4H), 7.50 – 7.40 (m, 4H), 7.40 – 7.31 (m, 1H), 5.70 (dq, *J* = 47.7, 6.4 Hz, 1H), 1.71 (dd, *J* = 23.8, 6.4 Hz, 3H). **^{19}F NMR** (376 MHz, $CDCl_3$) δ = -166.6; **^{13}C NMR** (126 MHz, $CDCl_3$) δ = 141.4 (d, $J_{C\text{-}F}$ = 2.2 Hz), 140.8, 140.5 (d, $J_{C\text{-}F}$ = 20.1 Hz), 129.0, 127.6, 127.4, 127.3, 125.9 (d, $J_{C\text{-}F}$ = 6.6 Hz), 90.93 (d, $J_{C\text{-}F}$ = 167.3 Hz), 23.0 (d, $J_{C\text{-}F}$ = 25.2 Hz); **HRMS** (EI) m/z calculated for $C_{14}H_{12}F$ $(M)^{+\cdot}$ 200.09958**,** found 200.10013; **IR** (liquid film) ν = 2955, 2928, 1487, 1376, 1260, 1219, 1076, 1009, 841, 763, 698 cm^{-1}; **mp** 72-73 ˚C; **$[\alpha]^{D}_{25\ °C}$** = +17.7 ° (c = 0.5, $CHCl_3$); **HPLC separation:** DAICEL CHIRALPAK® OJ-3, Heptane: iPrOH = 99:1, 1 mL/min; t_1 = 12.3 (minor), t_2 = 13.7 min (major).

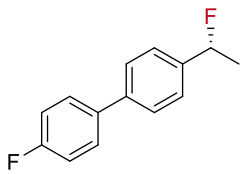

(*R*)-**2b**

(*R*)-4-fluoro-4'-(1-fluoroethyl)-1,1'-biphenyl (2b)

(*R*)-**2b** was prepared according to General Procedure 9 employing 0.38 mmol of *rac*-**1b** (106 mg), the reaction was stirred at 25 °C at 1200 rpm for 72 h. Following purification (FCC eluent: 100% pentane) the product was isolated as an off-white solid, 75 mg, 89 % yield, 92:8 e.r.

^{1}H NMR (400 MHz, $CDCl_3$) δ = 7.58 – 7.50 (m, 4H), 7.46 – 7.39 (m, 2H), 7.18 – 7.08 (m, 2H), 5.68 (dq, *J* = 47.6, 6.4 Hz, 1H), 1.68 (dd, *J* = 23.8, 6.4 Hz, 3H); **^{19}F NMR** (377 MHz, $CDCl_3$) δ = -115.5, -166.8; **^{13}C NMR** (126 MHz, $CDCl_3$) δ = 162.7 (d, $J_{C\text{-}F}$ = 246.6 Hz), 140.6 (d, $J_{C\text{-}F}$ = 19.7 Hz), 140.3 (d, $J_{C\text{-}F}$ = 2.2 Hz), 136.9 (d, $J_{C\text{-}F}$ = 3.3 Hz), 128.8 (d, $J_{C\text{-}F}$ = 7.9 Hz), 127.2, 125.9 (d, $J_{C\text{-}F}$ = 6.7 Hz), 115.8 (d, $J_{C\text{-}F}$ = 21.5 Hz), 90.9 (d, $J_{C\text{-}F}$ = 167.5 Hz), 23.0 (d, $J_{C\text{-}F}$ = 25.3 Hz); **HRMS** (EI) m/z calculated for $C_{14}H_{12}F_2$ $(M)^{+\cdot}$ 218.09016, found 218.09071; **IR** (liquid film) ν = 3021, 2981, 2892, 1616, 1605, 1586, 1216, 1069, 825, 754, 669 cm^{-1}; **mp**

56-58 ˚C; **[α]$^{D}_{25\,°C}$** = +14.1 ° (c = 1.0, $CHCl_3$); **HPLC separation:** DAICEL CHIRALPAK® OJ-3, Heptane: iPrOH = 99.5:0.5, 1 mL/min; t_1 = 25.9 (major), t_2 = 30.4 min (minor).

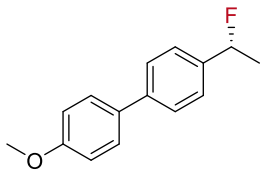

(*R*)-**2c**

(*R*)-4-(1-fluoroethyl)-4'-methoxy-1,1'-biphenyl (2c)

(*R*)-**2c** was prepared according to General Procedure 9 employing 0.3 mmol of *rac*-**1c** (87 mg), the reaction was stirred at 25 °C at 1200 rpm for 72h. Following purification (FCC eluent: 100:0 – 95:5 pentane:EtOAc) the product was isolated as a white solid, 44 mg, 64 % yield, 92:8 e.r.

^{1}H NMR (600 MHz, $CDCl_3$) δ = 8.14 – 8.09 (m, 2H), 7.69 – 7.61 (m, 4H), 7.48 – 7.43 (m, 2H), 5.69 (dq, *J* = 47.6, 6.5 Hz, 1H), 3.94 (s, 3H), 1.69 (dd, *J* = 23.9, 6.5 Hz, 3H); **^{19}F NMR** (565 MHz, $CDCl_3$) δ = -167.7; **^{13}C NMR** (151 MHz, $CDCl_3$) δ = 145.2, 141.6 (d, $J_{C\text{-}F}$ = 19.8 Hz), 140.1 (d, $J_{C\text{-}F}$ = 2.2 Hz), 130.3, 129.2, 127.5, 127.2, 125.9 (d, $J_{C\text{-}F}$ = 6.9 Hz), 90.8 (d, $J_{C\text{-}F}$ = 167.8 Hz), 52.3, 23.1 (d, $J_{C\text{-}F}$ = 25.2 Hz); **IR** (liquid film) ν = 3018, 2931, 1721, 1609, 1437, 1399, 1283, 1218, 1184, 1114, 1070, 1007, 867, 833, 700 cm^{-1}; **mp** 95-96 ˚C; **[α]$^{D}_{25\,°C}$** = +21.7 ° (c = 0.4, $CHCl_3$); **HPLC separation:** DAICEL CHIRALPAK® OJ-3 Heptane: iPOH = 97:3, 1 mL/min; t_1 = 21.5 (minor), t_2 = 26.1 min (major). No HRMS obtained.

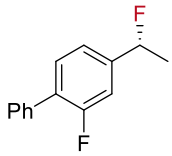

(*R*)-**2d**

(*R*)-2-fluoro-4-(1-fluoroethyl)-1,1'-biphenyl (2d)

(*R*)-**2d** was prepared according to General Procedure 9 employing 0.38 mmol of *rac*-**1d** (106 mg), the reaction was stirred at 25 °C at 1200 rpm for 72 hours. Following purification (FCC eluent: 100% pentane) the product was isolated as a colourless oil, 44 mg, 53 % yield, 92:8 e.r.

^{1}H NMR (600 MHz, $CDCl_3$) δ = 7.55 (dt, *J* = 7.9, 1.5 Hz, 2H), 7.45 (td, *J* = 7.8, 1.7 Hz, 3H), 7.41 – 7.35 (m, 1H), 7.18 (t, *J* = 10.5 Hz, 2H), 5.66 (dq, *J* = 47.5, 6.4 Hz, 1H), 1.68 (dd, *J* = 23.9, 6.5 Hz, 3H); **^{19}F NMR** (565 MHz, $CDCl_3$, 298 K) δ = -177.5, -168.3; **^{13}C NMR** (151 MHz, $CDCl_3$) δ = 159.8 (d, $J_{C\text{-}F}$ = 248.4 Hz), 143.1 (dd, $J_{C\text{-}F}$ = 20.2, 7.4 Hz), 135.5, 131.0 (d, $J_{C\text{-}F}$ = 3.5 Hz), 129.1 (d, $J_{C\text{-}F}$ = 2.9 Hz), 128.6, 127.9, 121.2 (dd, $J_{C\text{-}F}$ = 6.7, 3.4 Hz), 113.2 (d, $J_{C\text{-}F}$ = 7.4 Hz), 113.1 (d, $J_{C\text{-}F}$ = 7.4 Hz), 90.1 (d, $J_{C\text{-}F}$ = 169.2 Hz), 23.0 (d, $J_{C\text{-}F}$ = 24.9 Hz); **HRMS** (EI) m/z calculated for $C_{14}H_{12}F_2$ $(M)^{+\cdot}$ 218.09016, found 218.09071; **IR** (liquid film) ν = 3813,

3421, 2921, 1651, 1486, 1419, 1273, 1217, 1072, 1011, 837, 833, 759, 644 cm^{-1}; **$[\alpha]^{D}_{25\,°C}$** = +6.1° (c = 1.2, $CHCl_3$); **HPLC separation:** DAICEL CHIRALPAK® IB-3, Heptane 100%, 0.5 mL/min; t_1 = 14.3 (major), t_2 = 17.5 min (minor).

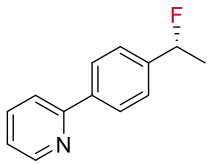

(*R*)-**2e**

(*R*)-2-(4-(1-fluoroethyl)phenylpyridine (2e)

(*R*)-**2e** was prepared according to General Procedure 9 employing 0.29 mmol of *rac*-**1e** (75 mg), the reaction was stirred at 25 °C at 1200 rpm for 72 h. Following purification (FCC eluent: 1st column: 90:10 pentane:EtOAc, 2nd column: 100% DCM) the product was isolated as a colourless oil, 40 mg, 70 % yield, 89:11 e.r.

^{1}H NMR (500 MHz, $CDCl_3$) δ = 8.73 (ddd, *J* = 4.8, 1.8, 1.0 Hz, 1H), 8.04 – 8.01 (m, 2H), 7.81 – 7.73 (m, 2H), 7.51 – 7.46 (m, 2H) 7.26 – 7.22 (m, 1H), 5.72 (dq, *J* = 47.7, 6.5 Hz, 1H), 1.70 (dd, *J* = 23.9, 6.5 Hz, 3H); **^{19}F NMR** (377 MHz, $CDCl_3$, 298 K) δ = -168.1; **^{13}C NMR** (126 MHz, $CDCl_3$) δ = 157.1, 149.8, 142.4 (d, $J_{C\text{-}F}$ = 19.5 Hz), 139.3, 137.1, 127.2, 125.7 (d, $J_{C\text{-}F}$ = 6.8 Hz), 122.4, 120.7, 90.9 (d, $J_{C\text{-}F}$ = 168.0 Hz), 23.1 (d, $J_{C\text{-}F}$ = 25.3 Hz); **HRMS** (ESI^+) m/z calculated for $C_{13}H_{14}FN$ $(M+H)^+$ 201.1027, found 202.1025; **IR** (liquid film) ν = 3769, 3743, 2980, 2929, 1590, 1469, 1437, 1375, 1260, 1155, 1018, 951, 785 cm^{-1}; **$[\alpha]^{D}_{25\,°C}$** = +16.7 ° (c = 0.15, $CHCl_3$); **HPLC separation:** DAICEL CHIRALPAK® OJ-3, Heptane: iPrOH = 90:10, 1 mL/min; t_1 = 12.2 (minor), t_2 = 19.4 min (major).

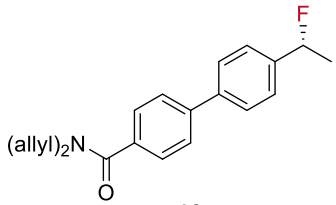

(*R*)-**2f**

(*R*)-*N,N*-diallyl-4'-(1-fluoroethyl)-[1,1'-biphenyl]-4-carboxamide (2f)

(*R*)-**2f** was prepared according to General Procedure 9 employing 0.25 mmol of *rac*-**1f** (96 mg), the reaction was stirred at 25 °C at 1200 rpm for 72 h. Following purification (FCC eluent: 100:0 – 95:5 DCM:EtOAc) the product was isolated as a yellow oil, 61 mg, 63 % yield, 92:8 e.r.

^{1}H NMR (400 MHz, $CDCl_3$) δ = 7.66 – 7.57 (m, 4H), 7.55 – 7.49 (m, 2H), 7.44 (dd, *J* = 8.1, 1.3 Hz, 2H), 5.89 (br s, 1H), 5.78 (br s, 1H), 5.68 (dq, *J* = 47.8, 6.4 Hz, 1H), 5.30 – 5.18 (m, 4H), 4.16 (s, 2H), 3.90 (s, 2H), 1.68 (dd, *J* = 23.8, 6.4 Hz, 3H); **^{19}F NMR** (377 MHz, $CDCl_3$) δ = -168.1; **^{13}C NMR** (101 MHz, $CDCl_3$) δ = 171.7, 142.1, 141.1 (d, $J_{C\text{-}F}$ = 19.6 Hz), 140.4 (d, $J_{C\text{-}F}$ = 2.1 Hz), 135.3, 133.4 (br), 133.0 (br), 127.4, 127.2,

125.9 (d, $J_{C\text{-}F}$ = 6.6 Hz), 117.8, 90.8 (d, $J_{C\text{-}F}$ = 167.8 Hz), 50.9 (br), 47.2 (br), 23.1 (d, $J_{C\text{-}F}$ = 25.2 Hz); **HRMS** (ESI$^+$) m/z calculated for $C_{21}H_{23}FNO$ $(M+H)^+$ 324.1758, found 324.1748; **IR** (liquid film) ν = 3078, 2925, 2857, 1636, 1457, 1414, 1288, 1261, 1217, 1112, 1069, 1007, 927, 885, 830, 769, 647 cm^{-1}; **[α]^D $_{25\,°C}$** = +13.3 ° (c = 0.4, $CHCl_3$); **HPLC separation:** DAICEL CHIRALPAK® IC-3, Heptane: iPOH = 90:10, 1mL/min; t_1 = 38.5 (minor), t_2 = 42.8 min (major).

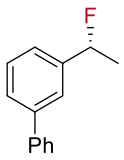

(*R*)-**2g**

(*R*)-3-(1-fluoroethyl)-1,1'-biphenyl (2g)

(*R*)-**2g** was prepared according to General Procedure 9 employing 0.38 mmol of *rac*-**1g** (50 mg), the reaction was stirred at 25 °C at 1200 rpm for 72 h. Following purification (FCC eluent: 100% pentane) the product was isolated as a colourless oil, 61 mg, 80 % yield, 90.5:9.5 e.r.

^{1}H NMR (400 MHz, $CDCl_3$) δ = 7.67 – 7.51 (m, 4H), 7.51 – 7.42 (m, 3H), 7.42 – 7.31 (m, 2H), 5.71(dq, *J* = 47.7, 6.4 Hz, 1H), 1.70 (dd, *J* = 23.9, 6.4 Hz, 3H); **^{19}F NMR** (377 MHz, $CDCl_3$, 298 K) δ = -167.3; **^{13}C NMR** (101 MHz, $CDCl_3$) δ = 142.2 (d, $J_{C\text{-}F}$ = 19.6 Hz), 141.7, 141.1, 129.1, 128.9, 127.6, 127.4, 127.2 (d, $J_{C\text{-}F}$ = 1.9 Hz), 124.2 (d, $J_{C\text{-}F}$ = 6.1 Hz), 124.2 (d, $J_{C\text{-}F}$ = 6.9 Hz), 91.1 (d, $J_{C\text{-}F}$ = 168.0 Hz), 23.2 (d, $J_{C\text{-}F}$ = 25.3 Hz); **HRMS** (EI) m/z calculated for $C_{14}H_{13}F$ $(M)^{+\cdot}$ 200.09958, found 200.10013; **IR** (liquid film) ν = 3020, 2982, 1600, 1482, 1376, 1216, 1068, 896, 703, 668 cm^{-1}; **[α]^D $_{25\,°C}$** = +14.6 ° (c = 0.25, $CHCl_3$); **HPLC separation:** DAICEL CHIRALPAK® OJ-3, Heptane: iPrOH = 99.5:0.5, 1 mL/min; t_1 = 12.2 (minor), 13.2 min (major).

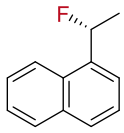

(*R*)-**2h**

(*R*)-1-(1-fluoroethyl)naphthalene (2h)

(*R*)-**2h** was prepared according to General Procedure 9 employing 0.38 mmol of *rac*-**1h** (89 mg), the reaction was stirred at 25 °C at 1200 rpm for 24 h. Following purification (FCC eluent: 100% pentane) the product was isolated as a colourless oil, 63 mg, 95 % yield, 95.5:4.5 e.r.

^{1}H NMR (600 MHz, $CDCl_3$) δ = 8.04 – 7.99 (m, 1H), 7.91 – 7.85 (m, 1H), 7.83 (dd, *J* = 8.2, 1.2 Hz, 1H), 7.61 (dd, *J* = 7.1, 1.0 Hz, 1H), 7.57 – 7.47 (m, 3H), 6.36 (dq, *J* = 46.7, 6.4 Hz, 1H), 1.84 (dd, *J* = 23.8, 6.5 Hz, 3H); **^{19}F NMR** (565 MHz, $CDCl_3$, 298 K) δ = -169.8; **^{13}C NMR** (151 MHz, $CDCl_3$) δ = 137.1 (d, $J_{C\text{-}F}$ = 18.1 Hz), 133.9, 129.8 (d, $J_{C\text{-}F}$ = 160.7 Hz), 128.9, 128.9, 126.5, 125.9, 125.5, 123.3, 122.7 (d, $J_{C\text{-}F}$ = 10.2 Hz), 89.0 (d, $J_{C\text{-}F}$ = 167.4 Hz), 22.6 (d, $J_{C\text{-}F}$ = 25.2 Hz); **HRMS** (EI) m/z calculated for $C_{12}H_{11}F$ $(M)^{+\cdot}$ 174.08393,

found 174.08448; **IR** (liquid film) ν = 2924, 2850, 1599, 1510, 1146, 1054, 851, 801, 645, 638 cm^{-1}; **[α]^{D} $_{25\ °C}$** = +17.6 ° (c = 0.3, $CHCl_3$); **HPLC separation:** DAICEL CHIRALPAK® OJ-3, Heptane: iPrOH = 99:1, 1 mL/min; t_1 = 6.2 (major), t_2 = 7.0 min (minor).

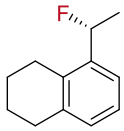

(*R*)-**2i**

5-(1-fluoroethyl)-1,2,3,4-tetrahydronaphthalene (2i)

(*R*)-**2i** was prepared according to General Procedure 9 employing 0.25 mmol of *rac*-**1i** (60 mg), the reaction was stirred at 25 °C at 1200 rpm for 72 h. Following purification (FCC eluent: 100:0 – 95:5 pentane:DCM) the product was isolated as a white solid, 38 mg, 87% yield, 95:5 e.r.

^{1}H NMR (400 MHz, $CDCl_3$) δ = 7.39 – 7.27 (m, 1H), 7.17 (t, *J* = 7.6 Hz, 1H), 7.10 – 7.03 (m, 1H), 5.85 (dq, *J* = 46.9, 6.4 Hz, 1H), 2.82 (dq, *J* = 11.8, 5.4 Hz, 3H), 2.62 (dt, *J* = 16.8, 6.4 Hz, 1H), 1.90 – 1.71 (m, 4H), 1.62 (dd, *J* = 23.9, 6.4 Hz, 3H); **^{19}F NMR** (376 MHz, $CDCl_3$) δ = -169.3; **^{13}C NMR** (101 MHz, $CDCl_3$) δ = 139.6 (d, $J_{C\text{-}F}$ = 18.2 Hz), 137.6, 133.5 (d, $J_{C\text{-}F}$ = 4.8 Hz), 129.4 (d, $J_{C\text{-}F}$ = 2.2 Hz), 125.7, 122.2 (d, $J_{C\text{-}F}$ = 9.1 Hz), 87.9 (d, $J_{C\text{-}F}$ = 165.7 Hz), 30.2, 25.7, 23.3, 22.8, 22.1 (d, $J_{C\text{-}F}$ = 26.0 Hz); **HRMS** (EI) m/z calculated for $C_{12}H_{15}F$ $(M)^{+\cdot}$ 178.11523 found 178.11578; **IR** (liquid film) ν = 2972, 2930, 2887, 1469, 1380, 1310, 1252, 1162, 953, 818 cm^{-1}; **mp** 61-62 ˚C; **[α]^{D} $_{25\ °C}$** = +16.3 ° (c = 0.3, $CHCl_3$); **HPLC separation:** DAICEL CHIRALPAK® IB-3, Heptane 100%, 1 mL/min; t_1 = 4.5 (minor), t_2 = 4.8 min (major).

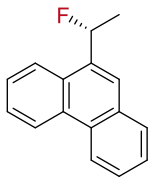

(*R*)-**2j**

(*R*)-9-(1-fluoroethyl)phenanthrene (2j)

(*R*)-**2j** was prepared according to General Procedure 9 employing 0.25 mmol of *rac*-**1j** (71 mg), the reaction was stirred at 25 °C at 1200 rpm for 72 h. Following purification (FCC eluent: 100:0 – 95:5 pentane:DCM) the product was isolated as a white solid, 49 mg, 88 % yield, 96:4 e.r.

^{1}H NMR (400 MHz, $CDCl_3$) δ = 8.82 – 8.72 (m, 1H), 8.71 – 8.62 (m, 1H), 8.11 – 8.02 (m, 1H), 7.95 – 7.91 (m, 1H), 7.89 (s, 1H), 7.75 – 7.58 (m, 4H), 6.39 (dq, *J* = 46.6, 0.9 Hz, 1H), 1.92 (dd, *J* = 23.8, 6.4 Hz, 3H); **^{19}F NMR** (376 MHz, $CDCl_3$) δ = -170.5; **^{13}C NMR** (101 MHz, $CDCl_3$) δ = 135.3 (d, $J_{C\text{-}F}$ = 17.7 Hz), 131.3, 130.8, 130.5 (d, $J_{C\text{-}F}$ = 1.3 Hz), 129.2 (d, $J_{C\text{-}F}$ = 3.0 Hz), 129.1, 127.2, 127.0, 126.9, 126.6, 124.0 (d, $J_{C\text{-}F}$ =

1.7 Hz), 123.7 (d, $J_{C\text{-}F}$ = 10.9 Hz), 123.5, 122.6, 89.1 (d, $J_{C\text{-}F}$ = 168.1 Hz), 22.3 (d, $J_{C\text{-}F}$ = 25.0 Hz); **IR** (liquid film) ν = 3021, 2981, 2892, 1616, 1609, 1584, 1500, 1216, 1070, 826, 854 cm^{-1}; **mp** 63-64 ˚C; **$[\alpha]^{D}_{25\,°C}$** = +21.2 ° (c = 0.5, $CHCl_3$); **HPLC separation:** DAICEL CHIRALPAK® IF-3, Heptane: iPrOH = 99.5:0.5, 1 mL/min; t_1 = 5.8 (minor), t_2 = 6.6 min (major). No HRMS obtained.

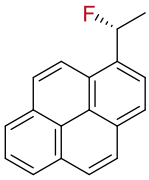
(*R*)-**2k**

1-(1-fluoroethyl)pyrene (2k)

(*R*)-**2k** was prepared according to General Procedure 9 employing 0.25 mmol of *rac*-**1k** (77 mg), the reaction was stirred at 25 °C at 1200 rpm for 72 h. Following purification – plugged over short silica column (FCC eluent: 100:0 – 90:10 pentane:DCM) the product was isolated as a viscous pale-yellow oil, 37 mg, 60 % yield, 96:4 e.r.

^{1}H NMR (500 MHz, $CDCl_3$) δ = 8.26 (d, *J* = 9.3 Hz, 1H), 8.22 (dd, *J* = 7.8, 5.0 Hz, 2H), 8.16 (s, 1H), 8.08 (m, 2H), 8.06 – 8.00 (m, 2H), 6.68 (dq, *J* = 46.8, 6.6 Hz, 1H), 1.95 (dd, *J* = 23.7, 6.5 Hz, 3H); **^{19}F NMR** (470 MHz, $CDCl_3$) δ = -168.4; **^{13}C NMR** (126 MHz, $CDCl_3$) δ = 139.1, 134.8, 134.7, 131.5, 130.7, 128.1, 127.7 (d, $J_{C\text{-}F}$ = 23.4 Hz), 127.6 (d, $J_{C\text{-}F}$ = 11.2 Hz), 127.1 (d, $J_{C\text{-}F}$ = 8.4 Hz), 126.2, 126.0, 125.6 (d, $J_{C\text{-}F}$ = 26.1 Hz), 125.1, 125.0, 122.7 (d, $J_{C\text{-}F}$ = 9.5 Hz), 122.4, 89.2 (d, $J_{C\text{-}F}$ = 167.6 Hz), 23.3 (d, $J_{C\text{-}F}$ = 25.5 Hz); **IR** (liquid film) ν = 2941, 2934, 2262, 1558, 1476, 1372, 1243, 1291, 1166, 1021, 991, 889, 867, 620 cm^{-1}; **$[\alpha]^{D}_{25\,°C}$** = +22.6 ° (c = 0.3, $CHCl_3$); **HPLC separation:** DAICEL CHIRALPAK® IB-3, Heptane 100%, 0.5 mL/min; t_1 = 14.2 (minor), t_2 = 16.0 min (major). No HRMS obtained.

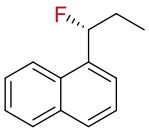
(*R*)-**2l**

(*R*)-1-(1-fluoropropyl)naphthalene (2l)

(*R*)-**2l** was prepared according to General Procedure 9 employing 0.3 mmol of *rac*-**1l** (75 mg), the reaction was stirred at 25 °C for at 1200 rpm 48 hours. Following purification (FCC eluent: 100% Pentane) the product was isolated as a colourless oil, 53 mg, 94 % yield, 93:7 e.r.

^{1}H NMR (400 MHz, $CDCl_3$) δ = 8.04 – 7.95 (m, 1H), 7.94 – 7.84 (m, 1H), 7.65 – 7.57 (m, 1H), 7.57 – 7.42 (m, 3H), 6.10 (ddd, 46.8, 7.2, 5.3 Hz 1H), 2.25 – 2.04 (m, 2H), 1.10 (t, *J* = 7.4 Hz, 3H); **^{19}F NMR** (377 MHz, $CDCl_3$, 298 K) δ = -179.4; **^{13}C NMR** (101 MHz, $CDCl_3$) δ = 136.1 (d, $J_{C\text{-}F}$ = 18.4 Hz), 133.9, 130.2 (d, $J_{C\text{-}F}$ = 3.7 Hz), 129.1, 128.8 (d, $J_{C\text{-}F}$ = 1.9 Hz), 126.3, 125.8, 125.4, 123.3 (d, $J_{C\text{-}F}$ = 10.5 Hz), 123.3 (d, $J_{C\text{-}F}$ = 1.3

Hz), 93.9 (d, $J_{C\text{-}F}$ = 171.1 Hz), 29.8 (d, $J_{C\text{-}F}$ = 23.9 Hz), 10.0 (d, $J_{C\text{-}F}$ = 4.7 Hz); **HRMS** (EI) m/z calculated for $C_{13}H_{13}F(M)^{+\cdot}$ 188.09958, found 188.10013; **IR** (liquid film) ν = 3019, 2976, 1599, 1513, 1463, 1217, 1095, 1044, 958, 912, 762 cm^{-1}; **$[\alpha]^{D}_{25\,°C}$** = +10.8 ° (c = 1.0, $CHCl_3$); **HPLC separation:** DAICEL CHIRALPAK® OJ-3, Heptane: iPrOH = 99:1, 0.5 mL/min; t_1 = 9.1 (major), 9.9 min (minor).

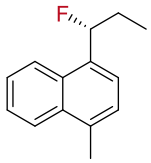
(*R*)-**2m**

(*R*)-1-(1-fluoropropyl)-4-methylnaphthalene (2m)

(*R*)-**2m** was prepared according to General Procedure 9 employing 0.25 mmol of *rac*-**1m** (66 mg), the reaction was stirred at 25 °C for at 1200 rpm 48 hours. Following purification (FCC eluent: 100% Hexane) the product was isolated as a colourless oil, 31 mg, 62 % yield, 92:8 e.r.

^{1}H NMR (400 MHz, $CDCl_3$) δ = 8.10 – 7.97 (m, 2H), 7.59 – 7.50 (m, 2H), 7.47 (d, *J* = 7.3 Hz, 1H), 7.34 (d, *J* = 7.3 Hz, 1H), 6.16 – 5.96 (m, 1H), 2.71 (t, *J* = 1.1 Hz, 3H), 2.22 – 2.02 (m, 2H), 1.09 (t, *J* = 7.4 Hz, 3H); **^{19}F NMR** (376 MHz, $CDCl_3$) δ = -178.1; **^{13}C NMR** (101 MHz, $CDCl_3$) δ = 135.0 (d, $J_{C\text{-}F}$ = 1.9 Hz), 134.2 (d, $J_{C\text{-}F}$ = 18.6 Hz), 133.0, 130.4 (d, $J_{C\text{-}F}$ = 3.6 Hz), 126.2, 126.0, 125.6, 125.1, 123.8, 123.2 (d, $J_{C\text{-}F}$ = 10.2 Hz), 94.0 (d, $J_{C\text{-}F}$ = 170.4 Hz), 29.8 (d, $J_{C\text{-}F}$ = 23.9 Hz), 19.8, 10.1 (d, $J_{C\text{-}F}$ = 4.7 Hz); **IR** (liquid film) ν = 3077, 2931, 2874, 1634, 1603, 1583, 1513, 1464, 1398, 1320, 1254, 1223, 1143, 1108, 1050, 916, 832, 763, 710, 644, 618 cm^{-1}; **$[\alpha]^{D}_{25\,°C}$** = +10.1 ° (c = 0.2, $CHCl_3$); **HPLC separation:** DAICEL CHIRALPAK® IF-3, Heptane 100%, 0.8 mL/min; t_1 = 9.5 (minor), 10.7 min (major). No HRMS obtained.

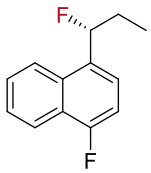
(*R*)-**2n**

(*R*)-1-fluoro-4-(1-fluoropropyl)naphthalene (2n)

(*R*)-**2n** was prepared according to General Procedure 9 employing 0.25 mmol of *rac*-**1n** (67 mg), the reaction was stirred at 25 °C for at 1200 rpm 48 hours. Following purification (FCC eluent: 100% Hexane) the product was isolated as a colourless oil, 38 mg, 74 % yield, 95:5 e.r.

^{1}H NMR (400 MHz, $CDCl_3$) δ = 8.22 – 8.10 (m, 1H), 8.06 – 7.97 (m, 1H), 7.64 – 7.54 (m, 2H), 7.53 – 7.47 (m, 1H), 7.15 (dd, *J* = 10.2, 8.0 Hz, 1H), 6.03 (ddd, *J* = 46.8, 7.4, 5.1 Hz, 1H), 2.31 – 1.95 (m, 2H), 1.08 (t, *J* = 7.4 Hz, 3H); **^{19}F NMR** (376 MHz, $CDCl_3$) δ = -122.7, -177.6; **^{13}C NMR** (101 MHz, $CDCl_3$) δ = 158.9 (d,

$J_{C\text{-}F}$ = 254.6 Hz), 132.2 – 131.5 (m), 127.3, 126.2 (d, $J_{C\text{-}F}$ = 2.1 Hz), 124.0 (d, $J_{C\text{-}F}$ = 16.3 Hz), 123.6 (d, $J_{C\text{-}F}$ = 8.9 Hz), 123.5 (d, $J_{C\text{-}F}$ = 8.7 Hz), 123.4 – 123.3 (m), 121.5 (d, $J_{C\text{-}F}$ = 6.0 Hz), 108.8 (d, $J_{C\text{-}F}$ = 20.2 Hz), 93.7 (d, $J_{C\text{-}F}$ = 171.1 Hz), 29.7 (d, $J_{C\text{-}F}$ = 24.0 Hz), 10.0 (d, $J_{C\text{-}F}$ = 4.9 Hz); **IR** (liquid film) ν = 3073, 2965, 2929, 2874, 1722, 1634, 1603, 1583, 1513, 1464, 1427, 1395, 1321, 1253, 1223, 1145, 1108, 1050, 1008, 832, 764, 711, 637 cm^{-1}; **$[\alpha]^{D}_{25\,°C}$** = +15.4 ° (c = 0.3, $CHCl_3$); **HPLC separation:** DAICEL CHIRALPAK® IB-3, Heptane 100%, 0.8 mL/min; t_1 = 5.5 (minor), 9.4 min (major). No HRMS obtained.

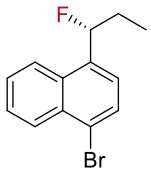

(*R*)-**2o**

(*R*)- 1-bromo-4-(1-fluoropropyl)naphthalene (2o)

(*R*)-**2o** was prepared according to General Procedure 9 employing 0.3 mmol of *rac*-**1o** (98 mg), the reaction was stirred at 25 °C at 1200 rpm for 72 h. Following purification (FCC eluent: 100% pentane) the product was isolated as a pale-yellow oil, 69 mg, 86 % yield, 96:4 e.r.

^{1}H NMR (400 MHz, $CDCl_3$) δ = 8.4 – 8.3 (m, 1H), 8.0 – 7.9 (m, 1H), 7.8 (d, *J* = 7.8 Hz, 1H), 7.7 – 7.5 (m, 2H), 7.4 (d, *J* = 7.8 Hz, 1H), 6.3 – 5.8 (m, 1H), 2.2 – 2.0 (m, 2H), 1.1 (t, *J* = 7.4 Hz, 3H); **^{19}F NMR** (377 MHz, $CDCl_3$, 298 K) δ = -180.2; **^{13}C NMR** (101 MHz, $CDCl_3$) δ = 136.2 (d, $J_{C\text{-}F}$ = 18.7 Hz), 132.1, 131.3 (d, $J_{C\text{-}F}$ = 3.9 Hz), 129.6, 128.3, 127.2, 127.2, 123.8 (d, $J_{C\text{-}F}$ = 11.1 Hz), 123.6 (d, $J_{C\text{-}F}$ = 1.3 Hz), 123.5 (d, $J_{C\text{-}F}$ = 2.3 Hz), 93.4 (d, $J_{C\text{-}F}$ = 172.1 Hz), 29.8 (d, $J_{C\text{-}F}$ = 23.8 Hz), 9.9 (d, $J_{C\text{-}F}$ = 4.6 Hz); **HRMS** (EI) m/z calculated for $C_{13}H_{12}BrF$ $(M)^{+\cdot}$ 266.01009, found 266.01064; **IR** (liquid film) ν = 3552, 3092, 3049, 2931, 1727, 1568, 1510, 1458, 1385, 1200, 1125, 961, 922, 835, 761, 641 cm^{-1}; **$[\alpha]^{D}_{25\,°C}$** = +27.2 ° (c = 0.35, $CHCl_3$); **HPLC separation:** DAICEL CHIRALPAK® OJ-3 Heptane 100%, 0.5 mL/min; t_1 = 10.8 (minor) t_2 = 11.7 min (major).

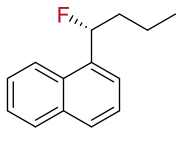

(*R*)-**2p**

(*R*)-1-(1-fluorobutyl)naphthalene (2p)

(*R*)-**2p** was prepared according to General Procedure 9 employing 0.3 mmol of *rac*-**1p** (79 mg), the reaction was stirred at 25 °C at 1200 rpm for 48 h. Following purification (FCC eluent: 100% pentane) the product was isolated as a yellow oil, 36 mg, 59 % yield, 88:12 e.r.

^{1}H NMR (400 MHz, $CDCl_3$) δ = 7.99 (d, *J* = 8.0 Hz, 1H), 7.92 – 7.86 (m, 1H), 7.85 – 7.80 (m, 1H), 7.58 (dd, *J* = 7.2, 1.3 Hz, 1H), 7.57 – 7.36 (m, 3H), 6.18 (ddd, *J* = 47.2, 8.3, 4.2 Hz, 1H), 2.22 – 1.92 (m, 2H), 1.72 – 1.46 (m, 2H), 1.07 – 0.94 (m, 3H); **^{19}F NMR** (377 MHz, $CDCl_3$) δ = -178.5; **^{13}C NMR** (101 MHz, $CDCl_3$) δ = 136.4 (d, *J* = 18.4 Hz), 133.9, 130.1 (d, *J* = 3.7 Hz), 129.1, 128.7 (d, *J* = 1.8 Hz), 126.4, 125.8, 125.4, 123.3 (d, *J* = 3.1 Hz), 123.2 (d, *J* = 6.6 Hz), 92.6 (d, *J* = 170.7 Hz), 39.1 (d, *J* = 24.2 Hz), 19.0 (d, *J* = 3.7 Hz), 14.0; **IR** (liquid film) ν = 2959, 2926, 2873, 2853, 2614, 2002, 1832, 1649, 1597, 1514, 1432, 1335, 1274, 1192, 1062, 1025, 1003, 944, 916, 864, 799, 756, 670, 620 cm^{-1}; **HRMS** (EI) m/z calculated for $C_{14}H_{15}F$ $(M)^{+\cdot}$ 202.11523, found 202.11578; **$[\alpha]^{D}_{25\ °C}$** = +9.9 ° (c = 0.9, $CHCl_3$); **HPLC separation:** DAICEL CHIRALPAK® IB-3 Heptane: iPOH 99:1, 1 mL/min; t_1 = 3.8 (minor), t_2 = 4.7 min (major).

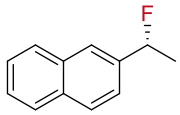

(*R*)-**2q**

(*R*)- 2-(1-fluoroethyl)naphthalene (2q)

(*R*)-**2q** was prepared according to General Procedure 9 employing 0.38 mmol of *rac*-**1q** (89 mg), the reaction was stirred at 15 °C at 1200 rpm for 72 h. Following purification (FCC eluent: 100:0 – 97:3 pentane: DCM) the product was isolated as a white solid, 38 mg, 57 % yield, 89:11 e.r.

^{1}H NMR (400 MHz, $CDCl_3$) δ = 8.00 – 7.72 (m, 4H), 7.64 – 7.41 (m, 3H), 5.81 (dq, *J* = 47.6, 6.4 Hz, 1H), 1.74 (dd, *J* = 23.8, 6.4 Hz, 3H); **^{19}F NMR** (377 MHz, $CDCl_3$, 298 K) δ = -167.0; **^{13}C NMR** (126 MHz, $CDCl_3$) δ = 139.0 (d, *J* = 19.5 Hz), 133.3 (d, *J* = 1.6 Hz), 133.2, 128.5, 128.2, 127.9, 126.5, 126.3, 124.3 (d, *J* = 8.1 Hz), 123.3 (d, *J* = 5.6 Hz), 91.3 (d, *J* = 167.7 Hz), 23. 1 (d, *J* = 25.2 Hz); **HRMS** (EI) m/z calculated for $C_{12}H_{11}F$ $(M)^{+\cdot}$ 174.08393, found 174.08448; **IR** (neat) ν = 3036, 2961, 2952, 2918, 1573, 1543, 1522, 1451, 1420, 1377, 1100, 1027, 973, 943, 899, 692 cm^{-1}; **mp** 58-60 ˚C; **$[\alpha]^{D}_{25\ °C}$** = +13.3 ° (c = 0.5, $CHCl_3$); **HPLC separation:** DAICEL CHIRALPAK® OJ-3, Heptane: iPrOH = 99:1, 1 mL/min; t_1 = 9.2 (minor), t_2 = 10.6 min (major).

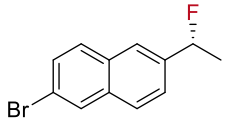

(*R*)-**2r**

(*R*)-2-bromo-6-(1-fluoroethyl)naphthalene (2r)

(*R*)-**2r** was prepared according to General Procedure 9 employing 0.38 mmol of *rac*-**1r** (119 mg), the reaction was stirred at 25 °C at 1200 rpm for 72 h. Following

purification (FCC eluent: 100% pentane) the product was isolated as a white solid, 82 mg, 85 % yield, 92:8 e.r.

^{1}H NMR (400 MHz, $CDCl_3$) δ = 8.01 (d, *J* = 2.0 Hz, 1H), 7.84 – 7.74 (m, 2H), 7.72 (d, *J* = 8.7 Hz, 1H), 7.57 (dd, *J* = 8.7, 2.0 Hz, 1H), 7.49 (dd, *J* = 8.6, 1.6 Hz, 1H), 5.78 (dq, *J* = 47.5, 6.4 Hz, 1H), 1.73 (dd, *J* = 23.8, 6.4 Hz, 3H); **^{19}F NMR** (377 MHz, $CDCl_3$, 298 K) δ = -167.8; **^{13}C NMR** (101 MHz, $CDCl_3$) δ = 139.5 (d, $J_{C\text{-}F}$ = 19.5 Hz), 134.3, 134.3, 131.7, 129.9, 129.9, 127.6, 124.3 (d, $J_{C\text{-}F}$ = 5.8 Hz), 124.2 (d, $J_{C\text{-}F}$ = 8.0 Hz), 120.3, 91.0 (d, $J_{C\text{-}F}$ = 168.4 Hz), 23.0 (d, $J_{C\text{-}F}$ = 25.1 Hz); **IR** (neat) ν = 2998, 2982, 2955, 2918, 2849, 1631, 1589, 1499, 1463, 1391, 1366, 1315, 1257, 1220, 1169, 1135, 1061, 1021, 956, 898, 808, 773, 728, 615 cm^{-1}; **mp** 69-71 ˚C; **$[\alpha]^{D}_{25\,°C}$** = +21.6 ° (c = 0.3, $CHCl_3$); **HPLC separation:** DAICEL CHIRALPAK® OJ-3, Heptane: iPrOH = 99:1, 1 mL/min; t_1 = 9.0 (minor), t_2 = 10.9 min (major). No HRMS obtained.

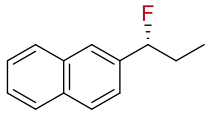

(*R*)-**2s**

(*R*)-1-(2-fluoropropyl)naphthalene (2s)

(*R*)-**2s** was prepared according to General Procedure 9 employing 0.38 mmol of *rac*-**1s** (94 mg), the reaction was stirred at 25 °C at 1200 rpm for 72 h. Following purification (FCC eluent: 100% pentane) the product was isolated as a colourless oil, 52 mg, 73 % yield, 94:6 e.r.

^{1}H NMR (400 MHz, $CDCl_3$) δ = 7.90 – 7.80 (m, 3H), 7.78 (br s, 1H), 7.53 – 7.48 (m, 2H), 7.45 (dd, *J* = 8.5, 1.8 Hz, 1H), 5.54 (ddd, *J* = 47.6, 7.5, 5.4 Hz, 1H), 2.18 – 1.87 (m, 2H), 1.02 (t, *J* = 7.4 Hz, 3H); **^{19}F NMR** (377 MHz, $CDCl_3$, 298 K) δ = -175.3; **^{13}C NMR** (126 MHz, $CDCl_3$) δ 137.7 (d, $J_{C\text{-}F}$ = 19.8 Hz), 133.2, 133.1, 128.3, 128.1, 127.7, 126.3, 126.2, 124.8 (d, $J_{C\text{-}F}$ = 8.2 Hz), 123.5 (d, $J_{C\text{-}F}$ = 5.8 Hz), 96.0 (d, $J_{C\text{-}F}$ = 170.8 Hz), 30.1 (d, $J_{C\text{-}F}$ = 24.1 Hz), 9.4 (d, $J_{C\text{-}F}$ = 5.8 Hz); **HRMS** (EI) m/z calculated for $C_{13}H_{13}F\,(M)^{+\cdot}$ 188.09958, found 188.10013; **IR** (liquid film) ν = 3061, 2971, 2922, 1464, 1380, 1177, 966, 918, 819, 632 cm^{-1}; **$[\alpha]^{D}_{25\,°C}$** = +15.7 ° (c = 1.0, $CHCl_3$); **HPLC separation:** DAICEL CHIRALPAK® OJ-3, Heptane: iPrOH = 99.5:0.5, 1 mL/min; t_1 = 10.6 (minor), t_2 = 12.2 min (major).

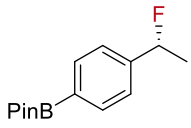

(*R*)-**2t**

(*R*)-2-(4-(1-fluoroethyl)phenyl)-4,4,5,5-tetramethyl-1,3-dioxolane (2t)

(*R*)-**2t** was prepared according to General Procedure 9 employing 0.24 mmol of *rac*-**1t** (75 mg), the reaction was stirred at 25 °C at 1200 rpm for 72 h. Following purification (FCC eluent: 100:0 – 97:3 pentane:EtOAc) the product was isolated as a white solid, 43 mg, 71 % yield, 91.5:8.5 e.r.

^{1}H NMR (500 MHz, $CDCl_3$) δ = 7.83 (d, *J* = 7.6 Hz, 2H), 7.35 (d, *J* = 7.6 Hz, 2H), 5.64 (dq, *J* = 47.7, 6.4 Hz, 1H), 1.63 (dd, *J* = 24.0, 6.4 Hz, 3H), 1.35 (s, 12H); **^{19}F NMR** (471 MHz, $CDCl_3$) δ = -169.6; **^{13}C NMR** (126 MHz, $CDCl_3$) δ = 144.7 (d, *J* = 19.5 Hz), 135.1, 124.5, 124.4, 91.0 (d, *J* = 168.2 Hz), 84.0, 25.0, 23.2 (d, *J* = 25.0 Hz); **HRMS** (EI) m/z calculated for $C_{14}H_{20}BFO_2$ $(M)^{+\cdot}$ 249.15712, found 249.15767; **IR** (liquid film) ν = 2983, 1733, 1616, 1519, 1401, 1364, 1324 1273, 1215, 1146, 1092, 1071, 1022, 963, 887, 860 cm^{-1}; **mp** 52-54 ˚C; **$[\alpha]^{D}_{25\,°C}$** = +14.4 ° (c = 0.15, $CHCl_3$); **HPLC separation:** DAICEL CHIRALPAK® IB-3, Heptane: iPOH 99.8:0.2, 0.8 mL/min; t_1 = 3.7 (major), t_2 = 4.1 min (minor).

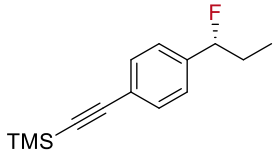

(*R*)-**2u**

(*R*)-((4-(1-fluoropropyl)phenyl)ethynyl)trimethylsilane (2u)

(*R*)-**2u** was prepared according to General Procedure 9 employing 0.3 mmol of *rac*-**1u** (89 mg), the reaction was stirred at 40 °C at 1200 rpm for 72 h. Following purification (FCC eluent: 100% pentane) the product was isolated as a colourless oil, 48 mg, 68 % yield, 92:8 e.r.

^{1}H NMR (500 MHz, $CDCl_3$) δ = 7.50 – 7.43 (m, 2H), 7.26 – 7.22 (m, 2H), 5.35 (ddd, *J* = 47.6, 7.5, 5.2 Hz, 1H), 2.02 – 1.78 (m, 2H), 0.96 (t, *J* = 7.4 Hz, 3H), 0.25 (s, 9H); **^{19}F NMR** (377 MHz, $CDCl_3$) δ = -177.4; **^{13}C NMR** (126 MHz, $CDCl_3$) δ = 140.7 (d, *J* = 19.2 Hz), 132.1, 125.5 (d, *J* = 7.0 Hz), 123.0, 104.8, 95.4 (d, *J* = 171.6 Hz), 94.7, 30.2 (d, *J* = 24.0 Hz), 9.3, 0.1; **IR** (liquid film) ν = 3735, 2959, 2929, 2856, 2161, 1731, 1511, 1502, 1464, 1412, 1379, 1362, 1306, 1251, 1222, 1208, 1088, 1078, 1046, 1019, 1002, 963, 867, 845, 762, 701, 646, 629 cm^{-1}; **$[\alpha]^{D}_{25\,°C}$** = +10.1 ° (c = 0.2, $CHCl_3$); **HPLC separation:** DAICEL CHIRALPAK® OJ-3 Heptane: iPOH 99:1, 0.5 mL/min; t_1 = 5.2 (minor), t_2 = 5.6 min (minor). No HRMS obtained.

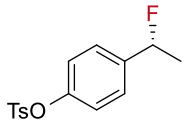

(*R*)-**2v**

(*R*)-4-(1-fluoroethyl)phenyl-4-methylbenzenesulfonate (2v)

(*R*)-**2v** was prepared according to General Procedure 9 employing 0.3 mmol of *rac*-**1v** (89 mg) and the reaction was stirred at 40 °C at 1200 rpm for 72 h. Following purification (FCC eluent: 100:0 – 95-5 pentane:EtOAc) the product was isolated as a colourless oil, 47 mg, 64 % yield, 81:19 e.r.

1H NMR (500 MHz, $CDCl_3$) δ = 7.75 – 7.67 (m, 2H), 7.32 (d, *J* = 8.0 Hz, 2H), 7.29 – 7.25 (m, 2H), 7.02 – 6.95 (m, 2H), 5.59 (dq, *J* = 47.4, 6.4 Hz, 1H), 2.45 (s, 3H), 1.60 (dd, *J* = 23.9, 6.4 Hz, 3H); **^{19}F NMR** (377 MHz, $CDCl_3$, 298 K) δ = -167.5; **^{13}C NMR** (101 MHz, $CDCl_3$) δ = 149.4 (d, $J_{C\text{-}F}$ = 2.2 Hz), 145.6, 140.5 (d, $J_{C\text{-}F}$ = 20.0 Hz), 132.5, 129.9, 128.6 (d, $J_{C\text{-}F}$ = 1.9 Hz), 126.6 (d, $J_{C\text{-}F}$ = 6.8 Hz), 122.6, 90.3 (d, $J_{C\text{-}F}$ = 168.6 Hz), 23.0 (d, $J_{C\text{-}F}$ = 25.0 Hz), 21.8; **HRMS** (EI) m/z calculated for $C_{15}H_{15}FO_3S$ $(M)^{+\cdot}$ 294.07204, found 294.07259; **IR** (liquid film) ν = 2928, 1599, 1505, 1377, 1295, 1200, 1180, 1158, 1095, 1070, 1019, 870, 817, 779, 709, 659 cm^{-1}; **$[\alpha]^{D}_{25\,°C}$** = +15.0 ° (c = 0.4, $CHCl_3$); **HPLC separation:** DAICEL CHIRALPAK® AS-3, Heptane: iPOH 98:2, 1 mL/min; t_1 = 22.0 (major), t_2 = 23.9 min (minor).

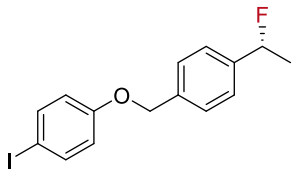

(*R*)-**2w**

(*R*)-1-(1-fluoroethyl)-4-((4-iodophenoxy)methyl)benzene (2w)

(*R*)-**2w** was prepared according to General Procedure 9 employing 0.3 mmol *rac*-**1w** (125 mg), the reaction was stirred at 25 °C at 1200 rpm for 72 h. Following purification (FCC eluent: 100:0 – 90:10 pentane: DCM) the product was isolated as a white solid, 55 mg, 52 % yield, 89:11 e.r.

^{1}H NMR (400 MHz, $CDCl_3$) δ = 7.60 – 7.51 (m, 2H), 7.45 – 7.39 (m, 2H), 7.39 -7.34 (d, 2H), 6.79 – 6.70 (m, 2H), 5.64 (dd, *J* = 47.6, 6.4 Hz, 1H), 5.04 (s, 2H), 1.64 (dd, *J* = 23.9, 6.5 Hz, 3H); **^{19}F NMR** (377 MHz, $CDCl_3$) δ = -167.5; **^{13}C NMR** (101 MHz, $CDCl_3$) δ = 158.7, 141.6 (d, $J_{C\text{-}F}$ = 19.7 Hz), 138.4, 136.7 (d, $J_{C\text{-}F}$ = 2.0 Hz), 127.7, 125.7 (d, $J_{C\text{-}F}$ = 6.7 Hz), 117.4, 90.8 (d, $J_{C\text{-}F}$ = 167.8 Hz), 83.3, 69.9, 23.1 (d, $J_{C\text{-}F}$ = 25.2 Hz); **IR** (neat) ν = 2959, 2925, 2853, 1584, 1467, 1380, 1280, 1235, 1177, 1060, 1009, 861, 809, 741, 633 cm^{-1}; **mp** 45-47 ˚C; **$[\alpha]^{D}_{25\,°C}$** = +7.3 ° (c = 0.4, $CHCl_3$); **HPLC separation:** DAICEL CHIRALPAK® OJ-3, Heptane:iPOH 98.0:2.0, 1 mL/min; t_1 = 24.1 (major), t_2 = 29.0 min (minor). No HRMS obtained.

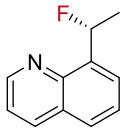

(*R*)-**2x**

(*R*)-8-(1-fluoroethyl)quinoline (2x)

(*R*)-**2x** was prepared according to General Procedure 9 employing 0.3 mmol of *rac*-**1x** (71 mg), the reaction was stirred at 25 °C at 1200 rpm for 72 h. Following purification (FCC eluent: 80:20 – 50:50 pentane:DCM) the product was isolated as a pale yellow oil, 42 mg, 79 % yield, 93:7 e.r.

Scale up: A 100 mL round bottom flask was charged with 4.7 mmol of *rac*-**1u** (1.1 g), catalyst (*S*)-**3u** (10 mol%), Ph_4P^+ I (10 mol%) and KF (2.5 equiv.). *p*-Xylene was added (20 mL) and the reaction was stirred at 25 °C at 1200 rpm for 72 h. The crude was filtered and washed with DCM was removed under reduced pressure. Following purification (FCC eluent: 80:20 – 50:50 pentane:DCM), the product was isolated as a pale yellow oil (576 mg, 70% yield, 6:94 e.r.) and (*S*)-**3u** was recovered eluting off the column in 50:50 DCM:pentane (98 % recovered).

^{1}H NMR (400 MHz, $CDCl_3$) δ = 8.91 (dd, *J* = 4.2, 1.8 Hz, 1H), 8.17 (dd, *J* = 8.3, 1.8 Hz, 1H), 7.87 (dt, *J* = 7.2, 1.2 Hz, 1H), 7.78 (dd, *J* = 8.2, 1.5 Hz, 1H), 7.59 (dd, *J* = 8.2, 7.2 Hz, 1H), 7.47 – 7.38 (m, 1H), 6.82 (dq, *J* = 47.4, 6.4 Hz, 1H), 1.81 (dd, *J* = 24.5, 6.4 Hz, 3H); **^{19}F NMR** (377 MHz, $CDCl_3$, 298 K) δ = -177.5; **^{13}C NMR** (151 MHz, $CDCl_3$) δ = 149.7, 144.8 (d, $J_{C\text{-}F}$ = 5.4 Hz), 140.4 (d, $J_{C\text{-}F}$ = 19.3 Hz), 136.4, 128.1, 127.7, 126.6, 125.0 (d, $J_{C\text{-}F}$ = 10.8 Hz), 121.26, 88.2 (d, $J_{C\text{-}F}$ = 166.2 Hz), 23.3 (d, $J_{C\text{-}F}$ = 24.8 Hz); **HRMS** (ESI^+) m/z calculated for $C_{11}H_{11}FN$ $(M+H)^+$ 176.0870, found 176.0869; **IR** (liquid film) ν = 3650, 2981, 2890, 1732, 1714, 1466, 1378, 1291, 1259, 1194, 1092, 1028, 891, 842, 793, 667 cm^{-1}; **$[\alpha]^D_{25\,°C}$** = +11.6 ° (c = 0.2, $CHCl_3$); **HPLC separation:** DAICEL CHIRALPAK® IB-3, Heptane: iPrOH = 99.5:0.5, 1 mL/min; t_1 = 4.0 (minor), t_2 = 4.3 min (major).

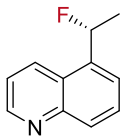

(*R*)-**2y**

(*R*)-5-(1-fluoroethyl)quinoline (2y)

(*R*)-**2y** was prepared according to General Procedure 9 employing 0.35 mmol of *rac*-**1y** (82 mg), the reaction was stirred at 25 °C at 1200 rpm for 48 h. Following purification (FCC eluent: 100:0 – 90:10 DCM: EtOAc) the product was isolated as a yellow oil, 60 mg, 99 % yield, e.r. 97:3.

^{1}H NMR (400 MHz, $CDCl_3$) δ = 8.95 (dd, *J* = 4.2, 1.7 Hz, 1H), 8.44 (ddt, *J* = 8.7, 1.8, 1.0 Hz, 1H), 8.11 (dq, *J* = 8.5, 1.1 Hz, 1H), 7.72 (ddd, *J* = 8.3, 7.2, 0.8 Hz, 1H), 7.67 – 7.59 (m, 1H), 7.45 (dd, *J* = 8.6, 4.2 Hz, 1H), 6.28 (dq, *J* = 46.8, 6.5 Hz, 1H), 1.84 (dd, *J* = 23.6, 6.5 Hz, 3H); **^{19}F NMR** (377 MHz, $CDCl_3$, 298 K) δ = -167.6; **^{13}C NMR** (126 MHz, $CDCl_3$) δ = 150.4, 148.7, 137.3 (d, $J_{C\text{-}F}$ = 18.4 Hz), 132.1, 130.5, 129.0, 125.6 (d, $J_{C\text{-}F}$ = 2.7 Hz),123.6 (d, $J_{C\text{-}F}$ = 8.8 Hz), 121.3, 88.8 (d, $J_{C\text{-}F}$ = 168.1 Hz), 22.4 (d, $J_{C\text{-}F}$ = 24.9 Hz); **HRMS** (ESI^+) m/z calculated for $C_{11}H_{11}FN$ $(M+H)^+$ 176.0870, found 176.0868; **IR** (liquid film) ν = 3659, 2981, 2889, 1599, 1505, 1462, 1378, 1316, 1252, 1165, 1075, 1054, 952, 829 cm^{-1}; **$[\alpha]^D_{25\,°C}$** = +17.9 ° (c = 0.5, $CHCl_3$); **HPLC separation:** DAICEL CHIRALPAK® OJ-3, Heptane: iPrOH = 90:10, 1 mL/min; t_1 = 6.2 (major), 6.8 min (minor).

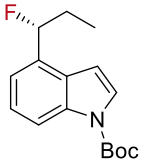

(*R*)-**2z**

(*R*)-*tert*-butyl-4-(1-fluoropropyl)-1*H*-indole-1-carboxylate (2z)

(*R*)-**2z** was prepared according to General Procedure 9 employing 0.2 mmol of *rac*-**1z** (66 mg) and the reaction was stirred at 25 °C at 1200 rpm for 72 h. Following purification (FCC eluent: 100:0 – 80:20 pentane:DCM) the product was isolated as a colourless oil, 35 mg, 65 % yield, e.r. 87:13.

^{1}H NMR (400 MHz, $CDCl_3$) δ = 8.14 (d, *J* = 8.3 Hz, 1H), 7.62 (d, *J* = 3.8 Hz, 1H), 7.31 (ddd, *J* = 8.3, 7.3, 1.0 Hz, 1H), 7.19 (dq, *J* = 7.6, 1.1 Hz, 1H), 6.68 (ddd, *J* = 3.8, 1.3, 0.8 Hz, 1H), 5.69 (ddd, *J* = 47.2, 7.6, 5.4 Hz, 1H), 2.21 – 1.88 (m, 2H), 1.67 (s, 9H), 1.00 (t, *J* = 7.4 Hz, 3H); **^{19}F NMR** (377 MHz, $CDCl_3$, 298 K) δ = -176.7; **^{13}C NMR** (126 MHz, $CDCl_3$) δ = 149.8, 135.6, 132.5 (d, $J_{C\text{-}F}$ = 20.1 Hz), 127.8, 126.2, 124.2, 119.8 (d, $J_{C\text{-}F}$ = 7.7 Hz), 115.2, 105.6 (d, $J_{C\text{-}F}$ = 1.9 Hz), 95.1 (d, $J_{C\text{-}F}$ = 170.6 Hz), 84.0, 29.9 (d, $J_{C\text{-}F}$ = 24.4 Hz), 28.3, 9.8 (d, $J_{C\text{-}F}$ = 5.8 Hz); **HRMS** (ESI^+) m/z calculated for $C_{16}H_{21}FNO_2$ $(M+H)^+$ calculated 278.1551, found 278.1812; **IR** (liquid film) ν = 3021, 2936, 2843, 1737, 1536, 1432, 1389, 1371, 1349, 1324, 1285, 1261, 1217, 1139, 1031, 810, 764 cm^{-1}; **$[\alpha]^D_{25\,°C}$** = +20.6 ° (c = 0.2, $CHCl_3$); **HPLC separation:** DAICEL CHIRALPAK® IC-3 Heptane:iPOH = 99.8:0.2, 1mL/min; t_1 = 10.7 (minor), t_2 = 11.3 min (major).

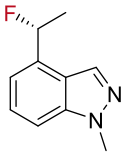

(*R*)-**2aa**

(*R*)-4-(1-fluoroethyl)-1-methyl-1*H*-indazole (2aa)

(*R*)-**2aa** was prepared according to General Procedure 9 employing 0.3 mmol of *rac*-**1aa** (71 mg), the reaction was stirred at 25 °C at 1200 rpm for 72 h. Following purification (FCC eluent: 100% DCM) the product was isolated as a pale-yellow oil, 37 mg, 70 % yield, 91.5:8.5 e.r.

^{1}H NMR (400 MHz, $CDCl_3$) δ = 8.12 – 8.07 (m, 1H), 7.55 – 7.24 (m, 2H), 7.13 – 7.05 (m, 1H), 5.99 (dqd, *J* = 47.1, 6.5, 0.8 Hz, 1H), 4.09 (s, 3H), 1.78 (dd, *J* = 23.9, 6.5 Hz, 3H); **^{19}F NMR** (377 MHz, $CDCl_3$, 298 K) δ = -169.7; **^{13}C NMR** (101 MHz, $CDCl_3$) δ = 140.4, 135.0 (d, $J_{C\text{-}F}$ = 20.6 Hz), 131.7 (d, $J_{C\text{-}F}$ = 2.9 Hz), 126.2, 121.0 (d, $J_{C\text{-}F}$ = 3.8 Hz), 116.6 (d, $J_{C\text{-}F}$ = 8.3 Hz), 109.1 (d, $J_{C\text{-}F}$ = 1.5 Hz), 90.4 (d, $J_{C\text{-}F}$ = 167.8 Hz), 35.7, 22.8 (d, $J_{C\text{-}F}$ = 25.0 Hz); **HRMS** (EI) m/z calculated for $C_{10}H_{11}FN_2$ $(M)^{+\cdot}$ 178.09008, found 178.09063; **IR** (liquid film) ν = 2934, 1726, 1676, 1613, 1513, 1452, 1411, 1375, 1345, 1275, 1204, 1169, 1111, 1080, 1038, 996, 847, 789, 652 cm^{-1}; **$[\alpha]^D_{25\,°C}$** = +17.4 ° (c = 0.4, $CHCl_3$); **HPLC separation:** DAICEL CHIRALPAK® IB-3, Heptane: iPrOH = 99:1, 1 mL/min; t_1 = 7.4 (minor), t_2 = 7.9 min (major).

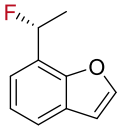

(*R*)-**2ab**

(*R*)-7-(1-fluoroethyl)benzofuran (2ab)

(*R*)-**2ab** was prepared according to General Procedure 9 employing 0.3 mmol of *rac*-**1ab** (67 mg), the reaction was stirred at 25 °C at 1200 rpm for 72 h. Following purification (FCC eluent: 100% pentane) the product was isolated as a colourless oil, 36 mg, 74 % yield, 91:9 e.r.

^{1}H NMR (400 MHz, $CDCl_3$) δ = 7.65 (d, *J* = 2.2 Hz, 1H), 7.59 (dt, *J* = 7.7, 1.1 Hz, 1H), 7.36 (dq, *J* = 7.5, 1.1 Hz, 1H), 7.30 – 7.22 (m, 1H), 6.80 (d, *J* = 2.2 Hz, 1H), 6.13 (dq, *J* = 47.0, 6.5 Hz, 1H), 1.81 (dd, *J* = 24.0, 6.5 Hz, 3H); **^{19}F NMR** (377 MHz, $CDCl_3$, 298 K) δ = -171.3; **^{13}C NMR** (151 MHz, $CDCl_3$) δ = 151.6 (d, $J_{C\text{-}F}$ = 5.0 Hz), 145.1, 127.9, 125.4 (d, $J_{C\text{-}F}$ = 20.9 Hz), 123.0, 121.4 (d, *J* = 2.3 Hz), 120.9 (d, $J_{C\text{-}F}$ = 7.6 Hz), 106.8, 87.3 (d, $J_{C\text{-}F}$ = 167.7 Hz), 21.9 (d, $J_{C\text{-}F}$ = 25.2 Hz); **IR** (liquid film) ν = 2929, 1721, 1428, 1325, 1262, 1217, 1032, 867, 832, 764, 668 cm^{-1}; **$[\alpha]^D_{25\,°C}$** = +19.4 ° (c = 0.4, $CHCl_3$); **HPLC separation:** DAICEL CHIRALPAK® ID-3, Heptane 100%, 1 mL/min, t_1 = 6.2 (minor), t_2 = 9.1 min (major). No HRMS obtained.

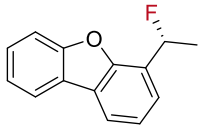

(*R*)-**2ac**

(*R*)-4-(1-fluoroethyl)dibenzo[*b*,*d*]furan (2ac)

(*R*)-**2ac** was prepared according to General Procedure 9 employing 0.16 mmol of *rac*-**1ac** (45 mg) and the reaction was stirred at 25 °C at 1200 rpm for 72 h. Following purification (FCC eluent: 100% pentane) the product was isolated as a colourless oil, 30 mg, 85 % yield, 92:8 e.r.

^{1}H NMR (400 MHz, $CDCl_3$) δ = 8.00 – 7.89 (m, 2H), 7.60 (dt, *J* = 8.3, 0.9 Hz, 1H), 7.57 – 7.51 (m, 1H), 7.48 (ddd, *J* = 8.3, 7.3, 1.4 Hz, 1H), 7.45 – 7.31 (m, 2H), 6.24 (dq, *J* = 47.0, 6.5 Hz, 1H), 1.89 (dd, *J* = 24.0 Hz, 6.5 Hz, 3H); **^{19}F NMR** (377 MHz, $CDCl_3$, 298 K) δ = -171.9; **^{13}C NMR** (126 MHz, $CDCl_3$) δ = 156.3, 152.7 (d, $J_{C\text{-}F}$ = 5.1 Hz), 127.5, 125.9, 125.7, 124.6, 124.1, 123.6 (d, $J_{C\text{-}F}$ = 7.7 Hz), 123.0 (d, $J_{C\text{-}F}$ = 2.2 Hz), 120.9, 120.6 (d, $J_{C\text{-}F}$ = 1.9 Hz), 111.9, 87.0 (d, $J_{C\text{-}F}$ = 168.1 Hz), 22.1 (d, $J_{C\text{-}F}$ = 25.0 Hz); **HRMS** (EI) m/z calculated for $C_{14}H_{11}FO$ $(M)^{+\cdot}$ 214.07884, found 214.07939; **IR** (liquid film) ν = 3500, 3444, 1453, 1425, 1343, 1219, 1191, 1127, 1056, 1009, 910, 861, 757 cm^{-1}; **$[\alpha]^{D}_{25\,°C}$** = +7.6 ° (c = 0.8, $CHCl_3$); **HPLC separation:** DAICEL CHIRALPAK® OJ-3 Heptane: iPOH = 99:1, 1mL/min; t_1 = 5.9 (major), t_2 = 6.7 min (minor).

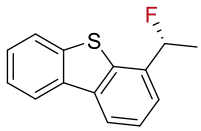

(*R*)-**2ad**

(*R*)-4-(1-fluoroethyl)dibenzo[*b*,*d*]thiophene (2ad)

(*R*)-**2ad** was prepared according to General Procedure 9 employing 0.25 mmol of *rac*-**1ad** (73 mg) and the reaction was stirred at 25 °C at 1200 rpm for 72 h. Following purification (FCC eluent: 100% pentane) the product was isolated as a pale-yellow oil, 54 mg, 94 % yield, 92:8 e.r.

^{1}H NMR (500 MHz, $CDCl_3$) δ = 8.21 – 8.09 (m, 2H), 7.92 – 7.84 (m, 1H), 7.55 – 7.44 (m, 4H), 5.97 (dq, *J* = 46.7, 6.5 Hz, 1H), 1.82 (dd, *J* = 24.0, 6.5 Hz, 3H); **^{19}F NMR** (470 MHz, $CDCl_3$) δ = -170.6; **^{13}C NMR** (126 MHz, $CDCl_3$) δ = 139.4 (d, $J_{C\text{-}F}$ = 1.5 Hz), 136.5, 136.2 (d, $J_{C\text{-}F}$ = 3.8 Hz), 136.1 (d, $J_{C\text{-}F}$ = 20.5 Hz), 135.5, 127.1, 124.9, 124.7, 123.0 (d, $J_{C\text{-}F}$ = 8.0 Hz), 122.8, 121.8, 121.5 (d, $J_{C\text{-}F}$ = 1.6 Hz), 90.3 (d, $J_{C\text{-}F}$ = 170.1 Hz), 21.5 (d, $J_{C\text{-}F}$ = 25.0 Hz); **IR** (liquid film) ν = 3066, 2985, 2926, 1707, 1561, 1444, 1407, 1375, 1348, 1304, 1256, 1176, 1122, 1074, 1041, 1022, 1005, 904, 831, 780, 752, 723, 706, 625 cm^{-1}; **$[\alpha]^{D}_{25\,°C}$** = +9.0 ° (c

= 0.3, $CHCl_3$); **HPLC separation:** DAICEL CHIRALPAK® OJ-3, Heptane:iPOH 99:1, 1mL/min; t_1 = 12.7 (major), t_2 = 18.8 min (minor). No HRMS obtained.

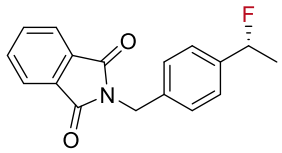

(*R*)-**2ae**

(*R*)-2-(4-(1-fluoroethyl)benzyl)isoindoline-1,3-dione (2ae)

(*R*)-**2ae** was prepared according to General Procedure 9 employing 0.25 mmol of *rac*-**1ae** (93 mg) and the reaction was stirred at 40 °C at 1200 rpm for 72 h. Following purification (FCC eluent: 90:10 pentane: EtOAc), 42 mg, 59 % yield, 90:10 e.r.

^{1}H NMR (500 MHz, $CDCl_3$) δ = 7.85 (dd, *J* = 5.4, 3.1 Hz, 2H), 7.75 – 7.67 (m, 2H), 7.45 (d, *J* = 7.9 Hz, 2H), 7.30 (d, *J* = 7.7 Hz, 2H), 5.59 (dq, *J* = 47.6, 6.5 Hz, 1H), 4.85 (s, 2H), 1.60 (dd, *J* = 23.9, 6.4 Hz, 3H); **^{19}F NMR** (471 MHz, $CDCl_3$) δ = -167.5; **^{13}C NMR** (151 MHz, $CDCl_3$) δ = 168.2, 141.3 (d, *J* = 19.6 Hz), 136.5 (d, *J* = 2.1 Hz), 134.2, 132.3, 128.9, 125.7 (d, *J* = 6.6 Hz), 123.5, 90.8 (d, *J* = 167.8 Hz), 41.4, 23.0 (d, *J* = 25.0 Hz); **HRMS** (ESI^+) m/z calculated for $C_{17}H_{14}FNO_2$ $(M+H)^+$ 284.1081, found 284.0734; **IR** (liquid film) ν = 2991, 2953, 2926, 2854, 1770, 1719, 1612, 1462, 1428, 1395, 1354, 1262, 1150, 1087, 1024, 939, 895, 808, 738, 677, 653, 638, 624, 613 cm^{-1}; **$[\alpha]^D_{25\,°C}$** = +17.4° (c = 0.2, $CHCl_3$); **mp** 88-90 ˚C; **HPLC separation:** DAICEL CHIRALPAK® OJ-3, Heptane:iPOH 90:10, 1 mL/min; t_1 = 15.8 (major), t_2 = 17.5 min (minor).

Absolute configuration was determined by comparing optical rotation and chromatograph of **2ae** to that of literature values.[1]

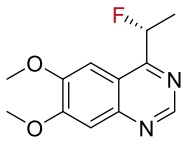

(*R*)-**2af**

(*R*)-4-(1-fluoroethyl)-6,7-dimethoxyquinazoline (2af)

(*R*)-**2af** was prepared according to modified General Procedure 9 using 1,4-difluorobenzene (0.25 M) as solvent, employing 0.24 mmol of *rac*-**1af** (71 mg), the reaction was stirred at 40 °C at 1200 rpm for 96 h. Following purification (FCC eluent: 80:20 – 50:50 pentane:EtOAc) the product was isolated as an off-white solid, 65 % yield, 78:22 e.r.

^{1}H NMR (500 MHz, $CDCl_3$) δ 9.11 (d, *J* = 0.9 Hz, 1H), 7.55 (s, 1H), 7.36 (s, 1H), 6.14 (dq, *J* = 48.0, 6.6 Hz, 1H), 4.07 (s, 3H), 4.05 (s, 3H), 1.89 (dd, *J* = 24.3, 6.6 Hz, 3H); **^{19}F NMR** (471 MHz, $CDCl_3$) δ = -174.1; **^{13}C NMR** (151 MHz, $CDCl_3$) δ = 163.5 (d, $J_{C\text{-}F}$ = 20.7 Hz), 156.1, 153.1, 150.5, 149.5, 118.1, 107.3, 102.2 (d,

$J_{C\text{-}F}$ = 9.2 Hz), 91.7 (d, $J_{C\text{-}F}$ = 171.1 Hz), 56.5, 56.4, 20.5 (d, $J_{C\text{-}F}$ = 23.3 Hz); **IR** (neat) ν = 3011, 2989, 2940, 2838, 2363, 1711, 1619, 1503, 1476, 1430, 1352, 1303, 1286, 1237, 1209, 1182, 1135, 1086, 1032, 1014, 979, 890, 872, 817, 784, 761, 633 cm^{-1}; **HRMS** (ESI^+) m/z calculated for $C_{12}H_{14}FN_2O_2$ $(M+H)^+$ 237.1034, found 237.1030; **mp** 105-106 ˚C; **$[\alpha]^D_{25\,°C}$** = +14.6 ° (c = 0.4, $CHCl_3$); **HPLC separation:** DAICEL CHIRALPAK® OJ-3 Heptane: iPOH 92:8, 1 mL/min; t_1 = 9.9 (major), t_2 = 10.8 min (minor).

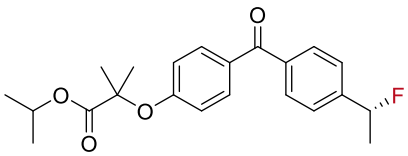

(*R*)-**2ag**

isopropyl (*R*)-2-(4-(4-(1-fluoroethyl)benzoyl)phenoxy)-2-methylpropanoate (2ag)

(*R*)-**2ag** was prepared according to General Procedure 9 employing 0.3 mmol of *rac*-**1ag** (130 mg), the reaction was stirred at 40 °C at 1200 rpm for 72 h. Following purification (FCC eluent: 1st column: 100% DCM, 2nd column: 100:0 – 90:10 pentane:EtOAc) the product was isolated as an colourless oil, 60 mg, 54 % yield, 93:7 e.r.

^{1}H NMR (600 MHz, $CDCl_3$) δ = 7.76 (dd, *J* = 8.6, 1.9 Hz, 4H), 7.47 – 7.40 (m, 2H), 6.91 – 6.83 (m, 2H), 5.70 (dq, *J* = 47.6, 6.5 Hz, 1H), 5.09 (hept, *J* = 6.3 Hz, 1H), 1.72 – 1.62 (m, 9H), 1.21 (s, 3H), 1.20 (s, 3H); **^{19}F NMR** (565 MHz, $CDCl_3$) δ = -170.4; **^{13}C NMR** (151 MHz, $CDCl_3$) δ = 195.2, 173.3, 159.8, 145.6 (d, $J_{C\text{-}F}$ = 19.4 Hz), 138.1, 132.2, 130.7, 130.2, 125.0 (d, $J_{C\text{-}F}$ = 7.1 Hz), 117.3, 90.6 (d, $J_{C\text{-}F}$ = 169.4 Hz), 79.5, 69.5, 25.5, 23.2 (d, $J_{C\text{-}F}$ = 24.9 Hz), 22.5; **IR** (liquid film) ν = 3130, 2973, 2884, 2825, 2356, 2338, 1746, 1625, 1575, 1503, 1476, 1380, 1338, 1225, 1162, 1050, 952, 817, 784, 643 cm^{-1}; **HRMS** (ESI^+) m/z calculated for $C_{22}H_{16}FO_4$ $(M+H)^+$ 373.1810, found 373.1806; **$[\alpha]^D_{25\,°C}$** = +9.2 ° (c = 0.2, $CHCl_3$); **HPLC separation:** DAICEL CHIRALPAK® OJ-3, Heptane:iPOH 97:3, 0.8 mL/min; t_1 = 13.1 (minor), t_2 = 14.0 min (major).

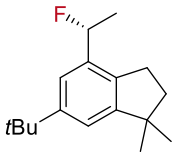

(*R*)-**2ah**

(*R*)-6-(*tert*-butyl)-4-(1-fluoroethyl)-1,1-dimethyl-2,3-dihydro-1*H*-indene (2ah)

(*R*)-**2ah** was prepared according to General Procedure 9 employing 0.3 mmol of *rac*-**1ah** (93 mg), the reaction was stirred at 25 °C at 1200 rpm for 48 h. Following purification (FCC eluent: 100% pentane) the product was isolated as a colourless oil, 62 mg, 83 % yield, 93.5:6.5 e.r.

^{1}H NMR (400 MHz, $CDCl_3$) δ = 7.25 – 7.24 (m, 1H), 7.16 (br s, 1H), 5.71 (dq, *J* = 47.3, 6.5 Hz, 1H), 2.97 – 2.77 (m, 2H), 1.95 (t, *J* = 7.2 Hz, 2H), 1.65 (dd, *J* = 23.5, 6.5 Hz, 3H), 1.34 (s, 9H), 1.27 (s, 3H), 1.26 (s, 3H); **^{19}F NMR** (377 MHz, $CDCl_3$, 298 K) δ = -168.7; **^{13}C NMR** (101 MHz, $CDCl_3$) δ = 153.1, 150.4, 136.7 (d, $J_{C\text{-}F}$ = 4.7 Hz), 136.4 (d, $J_{C\text{-}F}$ = 18.9 Hz), 119.8 (d, $J_{C\text{-}F}$ = 7.4 Hz), 118.9 (d, $J_{C\text{-}F}$ = 2.0 Hz), 90.0 (d, $J_{C\text{-}F}$ = 166.5 Hz), 43.9, 41.6, 35.0, 31.8, 28.9, 27.9, 22.1 (d, $J_{C\text{-}F}$ = 25.8 Hz); **IR** (liquid film) ν = 2864, 1629, 1480, 1395, 1375, 1216, 1073, 755, 670, 643 cm^{-1}; **$[\alpha]^{D}_{25\,°C}$** = +18.4° (c = 0.2, $CHCl_3$); **HPLC separation:** DAICEL CHIRALPAK® DAICEL CHIRALPAK® IB-3, Heptane:iPOH 99.8:0.2, 0.4 mL/min; t_1 = 5.3 (major), t_2 = 5.8 min (minor). No HRMS obtained.

4.5.5. Synthesis and Characterisation of α-Fluoroketone Products

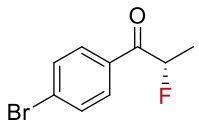

(*S*)-**13a**

(*S*)-1-(4-bromophenyl)-2-fluoropropan-1-one (13a)

(S)-**13a** was prepared according to General Procedure 10 employing 0.4 mmol of *rac*-**12a** (117 mg), the reaction was stirred at 5 °C at 1200 rpm for 96 h. Following purification (FCC eluent: pentane:DCM 70:30) the product was isolated as an off-white solid in 65 % yield, 60 mg, 95:5 e.r.

^{1}H NMR (600 MHz, $CDCl_3$) δ = 7.90 – 7.82 (m, 2H), 7.67 – 7.60 (m, 2H), 5.62 (dq, *J* = 48.5, 6.8 Hz, 1H), 1.66 (dd, *J* = 24.1, 6.8 Hz, 3H); **^{19}F NMR** (565 MHz, $CDCl_3$) δ = -180.5; **^{13}C NMR** (151 MHz, $CDCl_3$) δ = 196.3 (d, $J_{C\text{-}F}$ = 20.4 Hz), 132.9 (d, $J_{C\text{-}F}$ = 2.2 Hz), 132.2, 130.7 (d, $J_{C\text{-}F}$ = 5.0 Hz), 129.3, 90.8 (d, $J_{C\text{-}F}$ = 180.5 Hz), 18.3 (d, $J_{C\text{-}F}$ = 22.6 Hz); **HRMS** (ESI^+) m/z calculated for C_9H_9BrFO $(M+H)^+$ 230.9815, found 230.9815; **IR** (neat) ν = 2991, 2901, 1701, 1586, 1567, 1486, 1445, 1399, 1378, 1280, 1239, 1132, 1072, 1037, 1012, 974, 887, 840, 774, 738, 702, 643 cm^{-1}; **mp** 39-42 ˚C; **$[\alpha]^{D}_{25\,°C}$** = -5.0 (c = 0.5, $CHCl_3$); **HPLC separation:** DAICEL CHIRALPAK® ID-3, Heptane: iPOH = 99.2:0.8, 1 mL/min; t_1 = 5.0 (major), t_2= 5.7 min (minor).

Absolute configuration was determined by comparing optical rotation and chromatograph of **10a** to that of literature values[2].

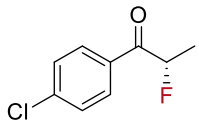

(*S*)-**13b**

(*S*)-1-(4-chlorophenyl)-2-fluoropropan-1-one (13b)

Synthesised by C. Palladino

(*S*)-**13b** was prepared according to General Procedure 10 employing 0.4 mmol of *rac*-**12b** (99 mg), the reaction was stirred at 5 °C at 1200 rpm for 96 h. Following purification (FCC eluent: pentane:DCM 70:30) the product was isolated as a white solid in 68 % yield, 48 mg, 95:5 e.r. **^{1}H NMR** (600 MHz, $CDCl_3$) δ = 7.97 – 7.91 (m, 2H), 7.49 – 7.43 (m, 2H), 5.63 (dq, *J* = 48.6, 6.8 Hz, 1H), 1.66 (dd, *J* = 24.1, 6.8 Hz, 3H); **^{19}F NMR** (565 MHz, $CDCl_3$) δ = -180.46 (m); **^{13}C NMR** (151 MHz, $CDCl_3$) δ = 195.9 (d, $J_{C\text{-}F}$ = 20.3 Hz), 140.3, 132.3 (d, $J_{C\text{-}F}$ = 2.4 Hz), 130.5 (d, $J_{C\text{-}F}$ = 4.4 Hz), 129.1, 90.6 (d, $J_{C\text{-}F}$ = 180.5 Hz), 18.2 (d, $J_{C\text{-}F}$ = 22.6 Hz); **HRMS** (ESI^+) m/z calculated for C_9H_9ClFO $(M+H)^+$ 187.0321, found 187.0554; **IR** (neat) ν = 3379, 2996, 1929, 1978, 1698, 1591, 1571, 1489, 1447, 1403, 1379, 1283, 1230, 1132, 1092, 1038, 1014, 974, 889, 843, 778, 742, 672, 651 cm^{-1}; **mp** 33-34 ˚C; **$[\alpha]^{D}_{25\,°C}$** = -5.4 (c = 0.5, $CHCl_3$); **HPLC separation:** DAICEL CHIRALPAK® ID-3, Heptane: iPOH = 99.2:0.8 mL/min; t_1 = 4.4 (major), t_2= 5.0 min (minor).

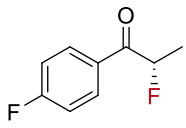

(*S*)-**13c**

(*S*)-2-fluoro-1-(4-fluorophenyl)propan-1-one (13c)

Synthesised by C. Palladino

(*S*)-**13c** was prepared according to General Procedure 10 employing 0.4 mmol of *rac*-**12c** (92 mg), the reaction was stirred at 5 °C at 1200 rpm for 96 h. Following purification (FCC eluent: pentane:DCM 70:30) the product was isolated as a colourless oil in 55 % yield, 37 mg, 96:4 e.r. (the product is highly volatile).

^{1}H NMR (600 MHz, $CDCl_3$) δ = 8.08 – 8.01 (m, 2H), 7.20 – 7.12 (m, 2H), 5.63 (dq, *J* = 48.6, 6.8 Hz, 1H), 1.66 (dd, *J* = 24.1, 6.8 Hz, 3H); **^{19}F NMR** (565 MHz, $CDCl_3$) δ = -103.6, -180.2; **^{13}C NMR** (151 MHz, $CDCl_3$) δ = 194.4 (d, $J_{C\text{-}F}$ = 20.0 Hz), 165.0 (d, $J_{C\text{-}F}$ = 256.1 Hz), 130.8 (dd, $J_{C\text{-}F}$ = 9.4, 4.6 Hz), 129.4 (dd, $J_{C\text{-}F}$ = 2.7, 1.5 Hz), 114.9 (d, $J_{C\text{-}F}$ = 22.0 Hz), 89.6 (d, $J_{C\text{-}F}$ = 180.3 Hz), 17.2 (d, $J_{C\text{-}F}$ = 22.6 Hz); **HRMS** (ESI^+) m/z calculated for $C_9H_9F_2O$ $(M+H)^+$ 171.0616, found 171.0617; **IR** (neat) ν = 3380, 2981, 2902, 1699, 1600, 1508, 1450, 1413, 1381, 1381, 1302, 1231, 1161, 1130, 1082, 1037, 974, 889, 847, 818, 767, 671 cm^{-1};

$[\alpha]^{D}_{25\,°C}$ = -3.2 (c = 0.2, $CHCl_3$); **HPLC separation:** DAICEL CHIRALPAK® ID-3, Heptane: iPOH = 99.2:0.8, 1 mL/min; t_1 = 4.1 (major), t_2= 4.6 min (minor).

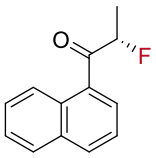

(*S*)-**13d**

(*S*)-2-fluoro-1-(naphthalen-1-yl)propan-1-one (13d)

(*S*)-**13d** was prepared according to General Procedure 10 employing 0.4 mmol of *rac*-**12d** (105 mg), the reaction was stirred at 25 °C at 1200 rpm for 96 h Following purification (FCC eluent: pentane:DCM 80:20) the product was isolated as a colourless oil in 96 % yield, 77 mg, 98:2 e.r.

^{1}H NMR (600 MHz, $CDCl_3$) δ = 8.48 – 8.43 (m, 1H), 8.03 (dd, *J* = 8.2, 1.2 Hz, 1H), 7.90 (ddd, *J* = 8.1, 1.4, 0.7 Hz, 1H), 7.84 (dt, *J* = 7.2, 1.3 Hz, 1H), 7.61 (ddd, *J* = 8.5, 6.8, 1.5 Hz, 1H), 7.56 (ddd, *J* = 8.1, 6.8, 1.2 Hz, 1H), 7.52 (dd, *J* = 8.2, 7.2 Hz, 1H), 5.77 (dq, *J* = 48.9, 6.9 Hz, 1H), 1.67 (dd, *J* = 23.5, 6.9 Hz, 3H); **^{19}F NMR** (565 MHz, $CDCl_3$) δ = - 179.8; **^{13}C NMR** (151 MHz, $CDCl_3$) δ = 200.9 (d, $J_{C\text{-}F}$ = 20.0 Hz), 134.0, 133.2, 132.5, 130.5, 128.6, 128.2, 127.9 (d, $J_{C\text{-}F}$ = 4.4 Hz), 126.7, 125.3, 124.2, 90.7 (d, $J_{C\text{-}F}$ = 182.7 Hz), 18.2 (d, $J_{C\text{-}F}$ = 22.6 Hz); **HRMS** (ESI^+) m/z calculated for $C_{13}H_{12}FO$ $(M+H)^+$ 203.0867, found 203.0868; **IR** (neat) ν = 2981, 2899, 1699, 1594, 1574, 1509, 1440, 1375, 1263, 1241, 1184, 1140, 1085, 1067, 1031, 942, 889, 805, 780, 760, 647 cm^{-1}; **$[\alpha]^{D}_{25\,°C}$** = +43.2 (c = 0.5, $CHCl_3$); **HPLC separation:** DAICEL CHIRALPAK® IC-3, Heptane: iPOH = 99.5:0.5, 1 mL/min; t_1 = 15.4 (major), t_2= 15.8 min (minor).

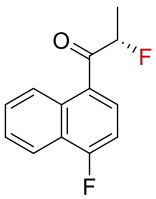

(*S*)-**13e**

(*R*)-2-fluoro-1-(4-fluoronaphthalen-1-yl)propan-1-one (13e)

(*S*)-**13e** was prepared according to General Procedure 10 employing 0.4 mmol of *rac*-**12e** (112 mg), the reaction was stirred at 25 °C at 1200 rpm for 96 h. Following purification (FCC eluent: pentane:DCM 80:20) the product was isolated as a colourless oil in 97 % yield, 85 mg, 96:4 e.r.

^{1}H NMR (600 MHz, $CDCl_3$) δ = 8.59 (ddt, *J* = 8.7, 1.9, 0.9 Hz, 1H), 8.20 – 8.15 (m, 1H), 7.90 (ddd, *J* = 8.1, 5.4, 1.4 Hz, 1H), 7.68 (ddd, *J* = 8.5, 6.9, 1.4 Hz, 1H), 7.63 (ddd, *J* = 8.1, 6.8, 1.1 Hz, 1H), 7.18 (dd, *J* = 9.7, 8.1 Hz, 1H), 5.74 (dq, *J* = 48.8, 6.9 Hz, 1H), 1.68 (dd, *J* = 23.6, 6.8 Hz, 3H); **^{19}F NMR** (565 MHz, $CDCl_3$) δ = -178.7, -113.3; **^{13}C NMR** (151 MHz, $CDCl_3$) δ = 199.4 (d, $J_{C\text{-}F}$ = 20.3 Hz), 161.5 (d, $J_{C\text{-}F}$ = 260.8 Hz), 132.8 (d, $J_{C\text{-}F}$ = 5.5 Hz), 129.5 (dd, $J_{C\text{-}F}$ = 10.1, 5.7 Hz), 129.3, 128.4 (d, $J_{C\text{-}F}$ = 4.4 Hz), 127.1 (d, $J_{C\text{-}F}$ = 2.1 Hz), 125.6

(d, $J_{C\text{-}F}$ = 2.6 Hz), 124.3 (d, $J_{C\text{-}F}$ = 15.6 Hz), 120.9 (d, $J_{C\text{-}F}$ = 6.4 Hz), 108.2 (d, $J_{C\text{-}F}$ = 21.0 Hz), 90.7 (d, $J_{C\text{-}F}$ = 182.7 Hz), 18.3 (d, $J_{C\text{-}F}$ = 22.6 Hz); **HRMS** (ESI$^+$) m/z calculated for $C_{13}H_{11}F_2O$ $(M+H)^+$ 221.0773, found 221.0772; **IR** (neat) ν = 2981, 1692, 1630, 1602, 1576, 1511, 1488, 1465, 1427, 1376, 1263, 1230, 1178, 1133, 1073, 1053, 1032, 969, 917, 864, 832, 793, 768, 747, 967, 644, 616 cm^{-1}; **[α]^D $_{25\,°C}$** = +27.8 (c = 0.5, $CHCl_3$); **HPLC separation:** DAICEL CHIRALPAK® IC-3, Heptane: iPOH = 99.5:0.5, 1 mL/min; t_1 =8.8 (major), t_2= 9.4 min (minor).

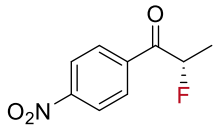

(*S*)-**13f**

(*S*)-2-fluoro-1-(4-nitrophenyl)propan-1-one (13f)

Synthesised by C. Palladino

(*S*)-**13f** was prepared according to General Procedure 10 employing 0.4 mmol of *rac*-**12f** (103 mg), the reaction was stirred at 5 °C at 1200 rpm for 96 h. Following purification (FCC eluent: pentane:DCM 70:30) the product was isolated as a yellow solid in 91 % yield, 72 mg, 91.5:8.5 e.r.

^{1}H NMR (600 MHz, $CDCl_3$) δ = 8.36 – 8.31 (m, 2H), 8.19 – 8.14 (m, 2H), 5.64 (dq, *J* = 48.3, 6.8 Hz, 1H), 1.70 (dd, *J* = 24.1, 6.8 Hz, 3H); **^{19}F NMR** (565 MHz, $CDCl_3$) δ = - 181.7; **^{13}C NMR** (151 MHz, $CDCl_3$) δ = 196.0 (d, $J_{C\text{-}F}$ = 21.6 Hz), 150.6, 138.7 (d, $J_{C\text{-}F}$ = 2.2 Hz), 130.3 (d, $J_{C\text{-}F}$ = 5.0 Hz), 123.8, 91.0 (d, $J_{C\text{-}F}$ = 180.9 Hz), 17.9 (d, $J_{C\text{-}F}$ = 22.5 Hz); **HRMS** (ESI$^+$) m/z calculated for $C_9H_8FNO_3$ $(M+H)^+$ 198.0561, found 198.0141; **IR** (neat) ν = 2980, 2887, 1703, 1601, 1526, 1509, 1450, 1413, 1344, 1301, 1263, 1240, 1160, 1128, 1087, 1041, 974, 938, 889, 871, 851, 810, 742, 712, 669 cm^{-1}; **mp** 44-45 ˚C; **[α]^D $_{25\,°C}$** = -15.2 (c = 0.5, $CHCl_3$); **HPLC separation:** DAICEL CHIRALPAK® ID-3, Heptane: iPOH = 99.2:0.8, 1 mL/min; t_1 = 13.5 (major), t_2= 20.0 min (minor).

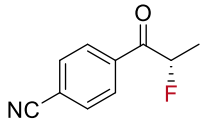

(*S*)-**13g**

(*S*)-4-(2-fluoropropanoyl)benzonitrile (13g)

Synthesised by C. Palladino

(*S*)-**13g** was prepared according to General Procedure 10 employing 0.4 mmol of *rac*-**12g** (95 mg), the reaction was stirred at 5 °C at 1200 rpm for 96 h. Following purification (FCC eluent: pentane:DCM 70:30) the product was isolated as a white solid in 86 % yield, 61 mg, 93:7 e.r.

^{1}H NMR (600 MHz, $CDCl_3$) δ = 8.11 – 8.05 (m, 2H), 7.81 – 7.75 (m, 2H), 5.63 (dq, *J* = 48.3, 6.8 Hz, 1H), 1.67 (dd, *J* = 24.1, 6.8 Hz, 3H); **^{19}F NMR** (565 MHz, $CDCl_3$) δ = -180.5; **^{13}C NMR** (151 MHz, $CDCl_3$) δ = 196.1 (d, J_{C-F} = 21.4 Hz), 137.2 (d, J_{C-F} = 2.2 Hz), 132.5, 129.6 (d, J_{C-F} = 4.6 Hz), 117.3 (d, J_{C-F} = 123.3 Hz), 90.9 (d, J_{C-F} = 180.9 Hz), 17.9 (d, J_{C-F} = 22.3 Hz); **HRMS** (ESI^+) m/z calculated for $C_{10}H_9FNO$ $(M+H)^+$ 178.0663, found 178.1073; **IR** (neat) ν = 2980 1685, 1599, 1508, 1447, 1411, 1372, 1321, 1292, 1258, 1236, 1192, 1179, 1157, 1132, 1097, 1022, 973, 943, 862, 844, 819, 771, 752, 689, 657 cm^{-1}; **mp** 55-56 ˚C; **$[\alpha]^D_{25\,°C}$** = -2.0 (c = 0.2, $CHCl_3$); **HPLC separation:** DAICEL CHIRALPAK® ID-3, Heptane: iPOH = 99.2:0.8, 1 mL/min; t_1 = 16.2 (major), t_2= 19.5 min (minor).

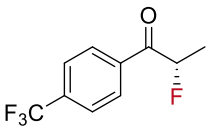

(*S*)-**13h**

(*S*)-2-fluoro-1-(4-(trifluoromethyl)phenyl)propan-1-one (13h)

Synthesised by C. Palladino

(*S*)-**13h** was prepared according to General Procedure 10 employing 0.4 mmol of *rac*-**12h** (112 mg), the reaction was stirred at 5 °C at 1200 rpm for 96 h. Following purification (FCC eluent: pentane:DCM 70:30) the product was isolated as a white solid in 78 % yield, 69 mg, 92:8 e.r. **^{1}H NMR** (600 MHz, $CDCl_3$) δ = 8.10 (m, 2H), 7.79 – 7.72 (m, 2H), 5.66 (dq, *J* = 48.4, 6.8 Hz, 1H), 1.68 (dd, *J* = 24.1, 6.8 Hz, 3H); **^{19}F NMR** (565 MHz, $CDCl_3$) δ = -63.3, -180.7; **^{13}C NMR** (151 MHz, $CDCl_3$) δ = 196.3 (d, J_{C-F} = 20.9 Hz), 136.8, 134.9 (q, J_{C-F} = 32.8 Hz), 129.5 (d, J_{C-F} = 4.4 Hz), 125.7 (q, J_{C-F} = 3.9 Hz), 123.5 (q, J_{C-F} = 272.7 Hz), 90.8 (d, J_{C-F} = 180.6 Hz), 18.0 (d, J_{C-F} = 22.4 Hz); **HRMS** (ESI^+) m/z calculated for $C_{10}H_9F_4O$ $(M+H)^+$ 221.0584, found 221.0836; **IR** (neat) ν = 2981, 2918, 1702, 1601, 1508, 1449, 1413, 1381, 1327, 1263, 1233, 1162, 1132, 1068, 1038, 1018, 975, 890, 853, 818, 766, 694, 672 cm^{-1}; **mp** 41-42 ˚C; **$[\alpha]^D_{25\,°C}$** = -4.6 (c = 0.5, $CHCl_3$); **HPLC separation:** DAICEL CHIRALPAK® ID-3, Heptane: iPOH = 99.5:0.5, 1 mL/min; t_1 = 3.7 (major), t_2 = 4.1 min (minor).

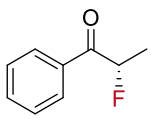

(*S*)-**13i**

(*S*)-2-fluoro-1-phenylpropan-1-one (13i)

Synthesised by C. Palladino

(*S*)-**13i** was prepared according to General Procedure 10 employing 0.4 mmol of *rac*-**12i** (85 mg), the reaction was stirred at 25 °C at 1200 rpm for 96 h. Following purification (FCC eluent:

pentane:DCM 80:20) the product was isolated as a colourless oil in 91 % yield, 55 mg, 87:13 e.r. (the product is highly volatile).

^{1}H NMR (600 MHz, $CDCl_3$) δ = 8.00 – 7.95 (m, 2H), 7.62 – 7.58 (m, 1H), 7.52 – 7.46 (m, 2H), 5.71 (dq, *J* = 48.6, 6.8 Hz, 1H), 1.67 (dd, *J* = 24.0, 6.8 Hz, 3H); **^{19}F NMR** (565 MHz, $CDCl_3$) δ = -181.4; **^{13}C NMR** (151 MHz, $CDCl_3$) δ =196.9 (d, $J_{C\text{-}F}$ = 19.4 Hz), 137.8, 129.0 (d, $J_{C\text{-}F}$ = 3.8 Hz), 128.7, 90.3 (d, $J_{C\text{-}F}$ = 180.2 Hz), 18.4 (d, $J_{C\text{-}F}$ = 22.6 Hz); **HRMS** (ESI$^+$) m/z calculated for C_9H_9FO $(M+H)^+$ 153.0710, found 153.0711; **IR** (neat) ν = 2981, 2889, 1702, 1598, 1579, 1451, 1380, 1318, 1281, 1234, 1132, 1085, 1036, 1002, 951, 887, 793, 742, 699, 659 cm^{-1}; **$[\alpha]^{D}_{25\,°C}$** = +3.2 (c = 0.5, $CHCl_3$); **HPLC separation:** DAICEL CHIRALPAK® ID-3, Heptane: iPOH = 99.2:0.8, 1 mL/min; t_1 = 4.7 (major), t_2= 5.4 min (minor).

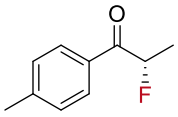

(*S*)-**13j**

(*S*)-2-fluoro-1-(p-tolyl)propan-1-one (13j)

Synthesised by C. Palladino

(*S*)-**13j** was prepared according to General Procedure 10 employing 0.4 mmol of *rac*-**12j** (91 mg), the reaction was stirred at 25 °C at 1200 rpm for 96 h. Following purification (FCC eluent: pentane:DCM 80:20) the product was isolated as a colourless oil in 83 % yield, 55 mg, 92:8 e.r.

^{1}H NMR (600 MHz, $CDCl_3$) δ = 7.88 (d, *J* = 8.1 Hz, 2H), 7.31 – 7.26 (m, 2H), 5.69 (dq, *J* = 48.7, 6.8 Hz, 1H), 2.43 (s, 3H), 1.66 (dd, *J* = 24.0, 6.8 Hz, 3H); **^{19}F NMR** (565 MHz, $CDCl_3$) δ = -181.3; **^{13}C NMR** (151 MHz, $CDCl_3$) δ = 196.6 (d, $J_{C\text{-}F}$ = 19.3 Hz), 144.9, 131.6, 129.6, 129.2 (d, $J_{C\text{-}F}$ = 3.9 Hz), 90.4 (d, $J_{C\text{-}F}$ = 179.9 Hz), 21.9, 18.6 (d, $J_{C\text{-}F}$ = 23.1 Hz); **HRMS** (ESI$^+$) m/z calculated for $C_{10}H_{12}FO$ $(M+H)^+$ 167.0867, found 167.0867; **IR** (neat) ν = 2981, 1698, 1608, 1571, 1447, 1411, 1379, 1282, 1262, 1239, 1212, 1887, 1132, 1085, 1037, 971, 887, 826, 760, 645 cm^{-1}; **$[\alpha]^{D}_{25\,°C}$** = +2.1 (c = 0.5, $CHCl_3$); **HPLC separation:** DAICEL CHIRALPAK® ID-3, Heptane: iPOH = 99.2:0.8, 1 mL/min; t_1 = 5.1 (major), t_2= 5.8 min (minor).

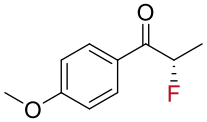

(*S*)-**13k**

(*S*)-2-fluoro-1-(4-methoxyphenyl)propan-1-one (13k)

Synthesised by C. Palladino

(*S*)-**13k** was prepared according to General Procedure 10 employing 0.4 mmol of *rac*-**12k** (97 mg), the reaction was stirred at 25 °C at 1200 rpm for 96 h. Following purification (FCC eluent: pentane:DCM 70:30) the product was isolated as a colourless oil in 90 % yield, 65 mg, 92:8 e.r.

^{1}H NMR (600 MHz, $CDCl_3$) δ = 8.03 – 7.95 (m, 2H), 7.01 – 6.90 (m, 2H), 5.65 (dq, *J* = 48.8, 6.8 Hz, 1H), 3.88 (s, 3H), 1.65 (dd, *J* = 24.2, 6.8 Hz, 3H). **^{19}F NMR** (565 MHz, $CDCl_3$) δ = -180.4; **^{13}C NMR** (151 MHz, $CDCl_3$) δ = 195.3 (d, $J_{C\text{-}F}$ = 19.6 Hz), 164.0, 131.4 (d, $J_{C\text{-}F}$ = 4.0 Hz), 126.9, 114.0, 90.4 (d, $J_{C\text{-}F}$ = 179.6 Hz), 55.5, 18.5 (d, $J_{C\text{-}F}$ = 22.7 Hz); **HRMS** (ESI^+) m/z calculated for $C_{10}H_{12}FO_2$ $(M+H)^+$ 183.0816, found 183.0816; **IR** (neat) ν = 2981, 2907, 1689, 1601, 1574, 1512, 1460, 1422, 1379, 1313, 1264, 1242, 1177, 1130, 1083, 1030, 972, 887, 844, 805, 775, 762 cm^{-1}; **$[\alpha]^D_{25\,°C}$** = +1.4 (c = 0.5, $CHCl_3$); **HPLC separation:** DAICEL CHIRALPAK® ID-3, Heptane: iPOH = 99.5:0.5, 0.8 mL/min; t_1 = 21.2 (major), t_2= 23.7 (minor).

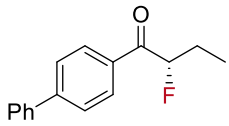

(*S*)-**13l**

(*S*)-1-([1,1'-biphenyl]-4-yl)-2-fluorobutan-1-one (13l)

Synthesised by C. Palladino

(*S*)-**13l** was prepared according to General Procedure 10 employing 0.4 mmol of *rac*-**12l** (121 mg), the reaction was stirred at 40 °C at 1200 rpm for 96 h. Following purification (FCC eluent: pentane:DCM 80:20) the product was isolated as a white solid in 83 % yield, 80 mg, 92:8 e.r.

^{1}H NMR (600 MHz, $CDCl_3$) δ = 8.08 – 8.04 (m, 2H), 7.73 – 7.68 (m, 2H), 7.65 – 7.62 (m, 2H), 7.51 – 7.45 (m, 2H), 7.45 – 7.39 (m, 1H), 5.54 (ddd, *J* = 49.3, 7.8, 4.5 Hz, 1H), 2.16 – 1.96 (m, 2H), 1.11 (t, *J* = 7.4 Hz, 3H); **^{19}F NMR** (565 MHz, $CDCl_3$) δ = -190.5; **^{13}C NMR** (151 MHz, $CDCl_3$) δ = 196.4 (d, $J_{C\text{-}F}$ = 19.7 Hz), 146.4, 139.7, 133.1 (d, $J_{C\text{-}F}$ = 1.4 Hz), 129.5 (d, $J_{C\text{-}F}$ = 3.9 Hz), 129.0, 128.4, 127.3 (d, $J_{C\text{-}F}$ = 6.6 Hz), 95.0 (d, $J_{C\text{-}F}$ = 183.6 Hz), 26.2 (d, $J_{C\text{-}F}$ = 21.5 Hz), 9.1 (d, $J_{C\text{-}F}$ = 4.5 Hz); **HRMS** (ESI^+) m/z calculated for $C_{16}H_{16}FO$ $(M+H)^+$ 243.1180, found 243.1180; **IR** (neat) ν = 2980, 2885, 1954, 1690, 1604, 1561, 1488, 1459, 1407, 1383, 1264, 1229, 1208, 1131, 1095, 1052, 1026, 1006, 968, 896, 842, 808, 768, 745, 692, 643 cm^{-1}; **mp** 51-52 ˚C; **$[\alpha]^D_{25\,°C}$** = +17.0 (c = 0.5, $CHCl_3$); **HPLC separation:** DAICEL CHIRALPAK® ID-3, Heptane: iPOH = 99.2:0.8, 1 mL/min; t_1 = 7.5 (major), t_2= 8.5 min (minor).

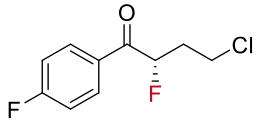

(*S*)-**13m**

(*S*)-4-chloro-2-fluoro-1-(4-fluorophenyl)butan-1-one (13m)

Synthesised by C. Palladino

(*S*)-**13m** was prepared according to General Procedure 10 employing 0.4 mmol of *rac*-**12m** (112 mg), the reaction was stirred at 40 °C at 1200 rpm for 96 h. Following purification (FCC eluent: pentane:DCM 80:20) the product was isolated as a white solid in 78 % yield, 68 mg, 84:16 e.r.

^{1}H NMR (600 MHz, $CDCl_3$) δ = 8.04 (m, 2H), 7.20 – 7.15 (m, 2H), 5.90 – 5.78 (m, 1H), 3.84 – 3.74 (m, 2H), 2.46 – 2.34 (m, 2H); **^{19}F NMR** (565 MHz, $CDCl_3$) δ = -182.8, -191.9; **^{13}C NMR** (151 MHz, $CDCl_3$) δ = 193.9 (d, $J_{C\text{-}F}$ = 18.8 Hz), 166.2 (d, $J_{C\text{-}F}$ = 256.9 Hz), 131.8 (dd, $J_{C\text{-}F}$ = 9.5, 4.1 Hz), 130.4, 116.1 (d, $J_{C\text{-}F}$ = 22.0 Hz), 89.9 (d, $J_{C\text{-}F}$ = 183.3 Hz), 40.0 (d, $J_{C\text{-}F}$ = 3.8 Hz), 35.1 (d, $J_{C\text{-}F}$ = 21.4 Hz); **HRMS** (ESI^+) m/z calculated for $C_{10}H_{10}ClF_2O$ $(M+H)^+$ 219.0383, found 219.0382; **IR** (neat) ν = 2980, 2890, 1688, 1601, 1509, 1459, 1415, 1382, 1312, 1264, 1243, 1177, 1159, 1131, 1086, 1032, 972, 845, 809, 653 cm^{-1}; **mp** 40-42 ˚C; **$[\alpha]^{D}_{25\,°C}$** = +5.8 (c = 0.5, $CHCl_3$); **HPLC separation:** DAICEL CHIRALPAK® ID-3, Heptane: iPOH = 99.2:0.8, 1 mL/min; t_1 = 5.5 (major), t_2= 7.6 min (minor).

4.6. Synthesis of Deuterated Precursors and Substrates

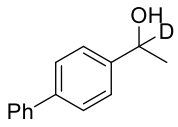

17a-d_1

1-([1,1'-biphenyl)-4-yl)ethan-1-*d*-1-ol (17a-d_1)

Compound **17a-d_1** was prepared according to a literature procedure[31] – 4-acetylbiphenyl (1 equiv.) was added to a round bottom flask and dissolved in EtOH (0.1 M), $NaBD_4$ (2 equiv.) was added and the reaction was stirred for 2 hours at 25 °C. Upon completion, monitored by TLC, the reaction was quenched with H_2O and diluted with EtOAc. The aqueous phase was washed with EtOAc (3 x 10 mL) and organic extracts were washed with brine and dried with $MgSO_4$. Solvent was removed under reduced pressure and following purification (FCC eluent: 100% DCM), the product was isolated as a white solid in 75 % yield. Spectroscopic data are in accordance with those in the literature.[31]

^{1}H NMR (400 MHz, $CDCl_3$) δ = 7.65 – 7.56 (m, 4H), 7.46 (ddd, *J* = 7.9, 4.4, 2.1 Hz, 4H), 7.41 – 7.32 (m, 1H), 1.55 (s, 3H); **^{13}C NMR** (126 MHz, $CDCl_3$) δ = 142.3, 141.4, 140.6, 129.0, 127.7, 127.6, 127.4, 127.2, 49.2 (t, $J_{C\text{-}D}$ = 22.1 Hz), 26.8.

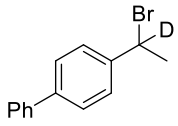

1a-d_1

4-(1-bromoethyl-1-*d*)-1,1'-biphenyl (1a-d_1)

Compound **1a-d_1 was** prepared according to General procedure 3 from *rac*-**17a-d_1**. The product was isolated as a white solid in 84 % yield.

^{1}H NMR (500 MHz, $CDCl_3$) δ = 7.62 – 7.56 (m, 4H), 7.53 (d, *J* = 8.4 Hz, 2H), 7.46 (t, *J* = 7.7 Hz, 2H), 7.41 – 7.34 (m, 1H), 2.12 (s, 3H); **^{13}C NMR** (126 MHz, $CDCl_3$) δ = 142.3, 141.4, 140.6, 129.0, 127.7, 127.6, 127.4, 127.2, 49.2 (t, $J_{C\text{-}D}$ = 23.2 Hz), 26.8; **IR** (neat) ν = 3030, 2927, 2854, 1739, 1564, 1486, 1404, 1376, 1258, 1231, 1205, 1072, 1044, 1006, 884, 938, 813, 765, 726, 692, 640 cm^{-1}; **mp** 68-69 ˚C; No HRMS obtained.

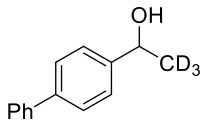

17a-d_3

1-([1,1'-biphenyl]-4-yl)ethan-2,2,2-d_3-1-ol (17a-d_3)

Compound **17a-d_3** was prepared through dropwise addition of CD_3MgI (1.2 equiv.) to a solution of 4-phenylbenzaldehyde (1 equiv.) in dry THF (0.5 M) at -10 °C. The

reaction was then stirred at 25 °C for 2 hours. Upon completion of the reaction, monitored by TLC, the reaction mixture was quenched with NH_4Cl (sat) and diluted with Et_2O. The organic extracts were washed with brine and dried with $MgSO_4$. Solvent was removed under reduced pressure and the following purification (FCC eluent: 100% DCM) the product was isolated as a white solid in 98 % yield.

^{1}H NMR (600 MHz, $CDCl_3$) δ = 7.63 – 7.56 (m, 4H), 7.48 – 7.42 (m, 4H), 7.40 – 7.32 (m, 1H), 4.95 (s, 1H); **^{13}C NMR** (151 MHz, $CDCl_3$) δ = 144.9, 141.0, 140.6, 128.9, 127.4, 127.2, 126.0, 70.2, 24.4 (sept, $J_{C\text{-}D}$ = 19.3 Hz); **IR** (neat) ν = 3386, 3059, 3034, 2958, 2926, 1599, 1566, 1524, 1487, 1404, 1334, 1304, 1274, 1241, 1168, 1039, 1005, 965, 902, 833, 788, 623 cm^{-1}; **mp** 92-93 ˚C; No HRMS obtained.

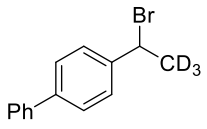

1a-*d*$_3$

4-(1-bromoethyl-2,2,2-*d*$_3$)-1,1'-biphenyl (1a-*d*$_3$)

Compound **1a-*d*$_3$** was prepared according to General procedure 3 from *rac*-**17a-*d*$_3$**. The product was isolated as a white solid in 84 % yield.

^{1}H NMR (600 MHz, $CDCl_3$) δ = 7.66 – 7.56 (m, 4H), 7.56 – 7.47 (m, 2H), 7.46 (tt, *J* = 6.6, 1.0 Hz, 2H), 7.42 – 7.30 (m, 1H), 5.28 (s, 1H); **^{13}C NMR** (151 MHz, $CDCl_3$) δ = 142.3, 141.4, 140.6, 129.0, 127.7, 127.6, 127.4, 127.2, 49.3, 26.0 (sept, $J_{C\text{-}D}$ = 19.3 Hz); **IR** (neat) ν = 3030, 2970, 2924, 1739, 1722, 1600, 1486, 1452, 1410, 1377, 1367, 1350, 1231, 1216, 1203, 1160, 1041, 1006, 901, 920, 765, 725, 692 cm^{-1}; **mp** 68-69 ˚C; No HRMS obtained.

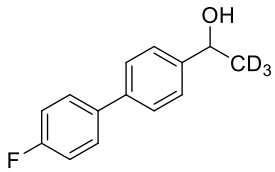

17b-*d*$_3$

1-(4'-fluoro-[1,1'-biphenyl]-4-yl)ethan-2,2-2,2-*d*$_3$-1-ol (17b-*d*$_3$)

Compound **17b-*d*$_3$** was prepared through dropwise addition of CD_3MgI (1.2 equiv.) to a solution of 4-(4-fluorophenyl)benzaldehyde (1 equiv.) in dry THF (0.5 M) at -10 °C. The reaction was then stirred at 25 °C for 2 hours. Upon completion of the reaction, monitored by TLC, the reaction mixture was quenched with NH_4Cl (sat) and extracted with Et_2O. The organic extracts were washed with brine, dried with $MgSO_4$. Solvent was removed under reduced pressure and the following purification (FCC eluent: 100% DCM) the product was isolated as a white solid in 63 % yield.

^{1}H NMR (400 MHz, $CDCl_3$) δ = 7.60 – 7.49 (m, 4H), 7.49 – 7.41 (m, 2H), 7.18 – 7.07 (m, 2H), 4.95 (s, 1H); **^{19}F NMR** (376 MHz, $CDCl_3$) δ = -115.8; **^{13}C NMR** (101 MHz, $CDCl_3$) δ = 162.6 (d, *J* = 246.3 Hz), 145.0, 139.6, 137.1 (d, *J* = 3.3 Hz), 128.8 (d, *J* = 8.0 Hz), 127.3, 126.1, 115.8 (d, *J* = 21.4 Hz), 70.1, 24.2 (sept, $J_{C\text{-}D}$ = 19.3 Hz); **IR** (neat) ν = 3314, 2891, 2225, 1894, 1603, 1528, 1497, 1395, 1344, 1252, 1190, 1163, 1120, 1100, 1061, 1038, 1025, 1006, 964, 911, 821, 741, 649 cm^{-1}; **mp** 94-96 ˚C; No HRMS obtained.

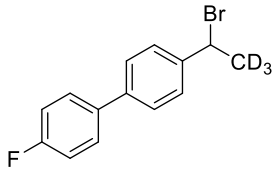

1b-*d*$_3$

4-(1-bromoethyl-2,2,2-*d*$_3$)-4'-fluoro-1,1'-biphenyl (1b-*d*$_3$)

Compound **1b-*d*$_3$** was prepared according to General procedure 3 from *rac*-**17a-*d*$_3$**. The product was isolated as a white solid in 71 % yield.

^{1}H NMR (600 MHz, $CDCl_3$) δ = 7.60 – 7.43 (m, 6H), 7.18 – 7.08 (m, 2H), 5.26 (s, 1H); **^{19}F NMR** (565 MHz, $CDCl_3$) δ = -115.3; **^{13}C NMR** (151 MHz, $CDCl_3$) δ = 162.7 (d, *J* = 246.8 Hz), 142.4, 140.4, 136.7 (d, *J* = 3.3 Hz), 128.8 (d, *J* = 8.0 Hz), 127.5, 127.4, 115.9 (d, *J* = 21.5 Hz), 49.1, 26.0 (sept, $J_{C\text{-}D}$ = 19.6 Hz); **IR** (neat) ν = 3002, 2952, 1600, 1498, 1240, 1196, 1163, 1041, 1006, 935, 813, 656, 637 cm^{-1}; **mp** 58-59 ˚C; No HRMS obtained.

4.7. Synthesis of Enantioenriched Precursors and Substrates

Alcohol (*R*)-**17am** (CAS: 76155-78-7) was commercially available.

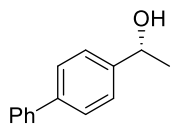

(*R*)-**17a**

(*R*)-1-([1,1'-biphenyl]-4-yl)ethan-1-ol (17a)

Compound **17a** was prepared *via* a Suzuki-Miyaura cross-coupling. Alcohol (*R*)-**17am** and phenyl boronic acid (3 equiv.) were added to a solution of degassed THF (0.1 M) and K_2CO_3 in H_2O (2 M), followed by the addition of SPhos (10 mol%) and $Pd(OAc)_2$ (5 mol%). The reaction mixture was heated to 70 °C for 24 h. Upon completion, the reaction was cooled and H_2O was added and the organic layer was extracted with Et2O. The organic extracts were combined and washed with brine and concentrated under reduced pressure. Following purification (FCC eluent: 80:20 pentane: EtOAc) the product was isolated as a white solid in 70 % yield, > 99:1 e.r. Spectroscopic data are in accordance with those in the literature.[32]

^{1}H NMR (400 MHz, $CDCl_3$) δ = 7.66 – 7.55 (m, 4H), 7.49 – 7.38 (m, 4H), 7.38 – 7.30 (m, 1H), 4.96 (q, *J* = 6.4 Hz, 1H), 1.55 (d, *J* = 6.5 Hz, 3H); **^{13}C NMR** (101MHz, $CDCl_3$) δ = 144.8, 140.8, 140.4, 128.7, 127.2, 127.0, 125.8, 70.11, 25.1.

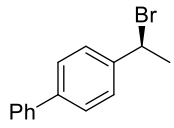

(*S*)-**1a**

4-(1-bromoethyl)-1,1'-biphenyl (1a)

Compound **1a** was prepared following literature procedure employing 1.5 mmol of (*R*)-**17a**. The product was isolated as an off-white solid in 60 % yield, 63:37 e.r. Spectroscopic data are in accordance with those in literature.[22]

^{1}H NMR (500 MHz, $CDCl_3$) δ = 7.62 – 7.55 (m, 4H), 7.55 – 7.49 (m, 2H), 7.45 (dd, *J* = 8.3, 6.9 Hz, 2H), 7.40 – 7.33 (m, 1H), 5.28 (q, *J* = 6.9 Hz, 1H), 2.10 (d, *J* = 6.9 Hz, 3H); **^{13}C NMR** (126 MHz, $CDCl_3$) δ = 142.3, 141.5, 140.6, 129.0, 127.7, 127.6, 127.4, 127.3, 49.5, 26.9.

4.8. NMR Investigations

4.8.1. Assignment of Urea Catalyst (S)-**3u** and Copies of NMR spectra

Sample preparation: (*S*)-**3u** (0.125 mmol) was weighted into an NMR tube and dissolved in toluene-d_8.

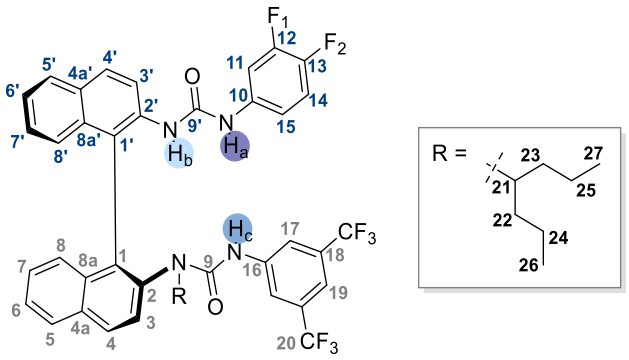

Scheme 4.1: Structure and numbering of (*S*)-**3u**

Table 4.1: Assignment of (*S*)-**3u**

^{1}H	**δ [ppm]**	**Multiplicity ^{n}J [Hz]**	**^{13}C**	**δ [ppm]**	**Multiplicity $^{n}J_{CF}$ [Hz]**
NH(b)	7.04	very br s	9	155.5	br s
NH(c)	6.71	br s	9’	151.9	s
NH(a)	6.41	br s	13	150.2	dd $^{2}J_{CF}$ = 245.5; $^{3}J_{CF}$ =13.2
3’	8.68	br d, ^{3}J = 8.5	12	146.4	dd $^{2}J_{CF}$ = 242.6; $^{3}J_{CF}$ =12.9
17	7.87	s	2	142.6	s
4’	7.70	d, ^{3}J = 9.1	16	140.6	s
4	7.67	d, ^{3}J = 8.9	2’	136.8	s
5’	7.60	d, ^{3}J = 8.2	10	135.4	d, $^{3}J_{CF}$ = 7.8
5	7.54	d, ^{3}J = 8.2	8a	134.3	s
3	7.43	d, ^{3}J = 8.9	8a’	133.7	s
19	7.41	s	4a or 1	133.2	s
8	7.14	d, overlapping	18	132.6	q, $^{3}J_{CF}$ = 33.4
6’ or 6	7.09 or 7.08	t, overlapping	4a or 1	131.1	s
11	7.03	overlapping	1’ or 4a’	130.9	s
8’	6.92	d, overlapping	4	130.2	s
7’ or 7	6.88 or 6.83	t, ^{3}J = 8.0	4’	130.0	s
14	6.52	q, $^{2}J_{HF}$ = 9.1	3	128.9	overlapping
15	6.42	overlapping	5’	128.8	overlapping
21	2.94	m	3	128.4	overlapping
22, 23	1.60 and 1.21	br s and m	7’ or 7	127.6	s
24 or 25	1.30 and 1.11	m	8’ or 8	127.3	s
26 or 27	0.64 or 0.37	t, ^{3}J = 7.1 or br s	6’ or 6	127.2	s
^{19}F	**δ [ppm]**	**Multiplicity ^{n}J [Hz]**	8’ or 8	127.1	s
CF_3	-62.8	s	20	123.7	q, $^{1}J_{CF}$ = 273.1
F_1	-138.8	br s	3’	121.6	s
F_2	-145.6	br s	17	119.7	s
			14	116.7	d, $^{3}J_{CF}$ = 17.8 overlapping
			19	116.7	s overlapping
			15	114.2	br s
			11	108.2	d, $^{3}J_{CF}$ = 17.9
			21	64.1	s
			22 or 23	36.3	s
			24 or 25	21.6	s
			26 or 27	14.0 or 14.1	s

*overlapping signals masked by solvent peaks

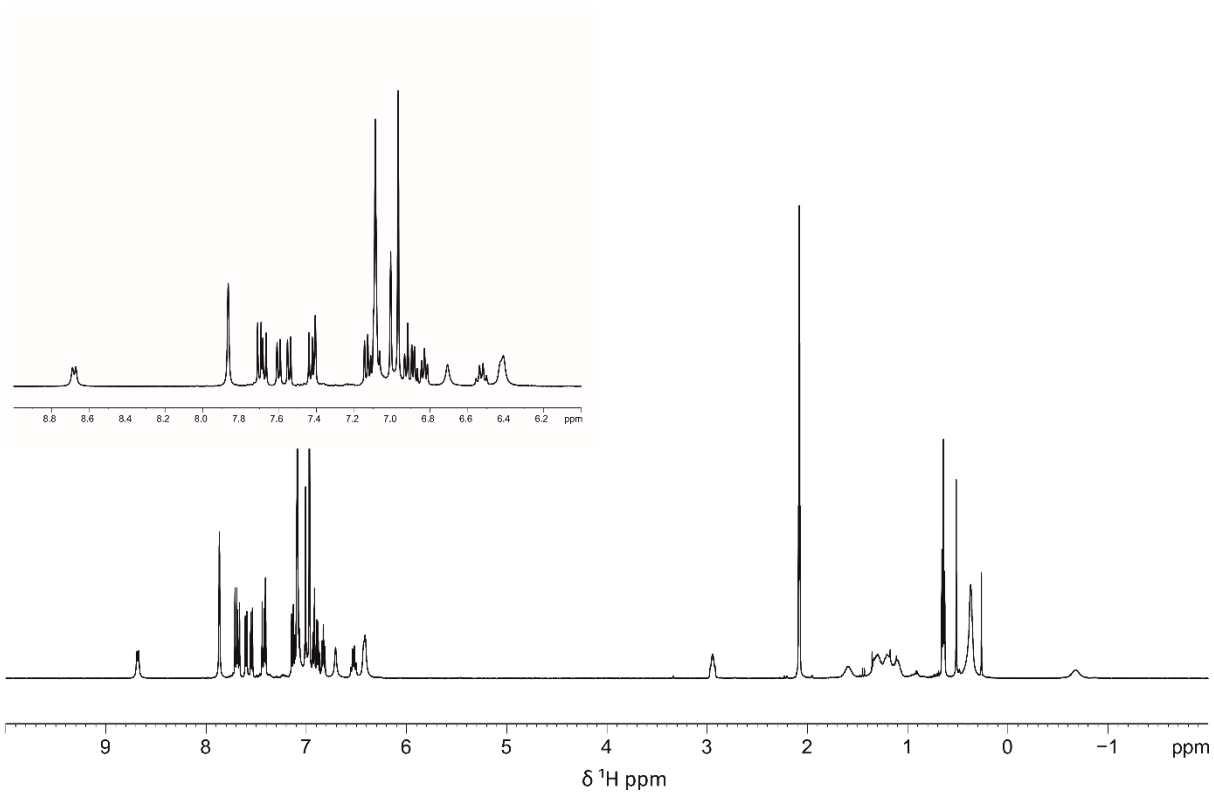

Figure 4.1: ^{1}H NMR of (*S*)-**3u** (500 MHz, Toluene-d_8, 25 mM, 298 K).

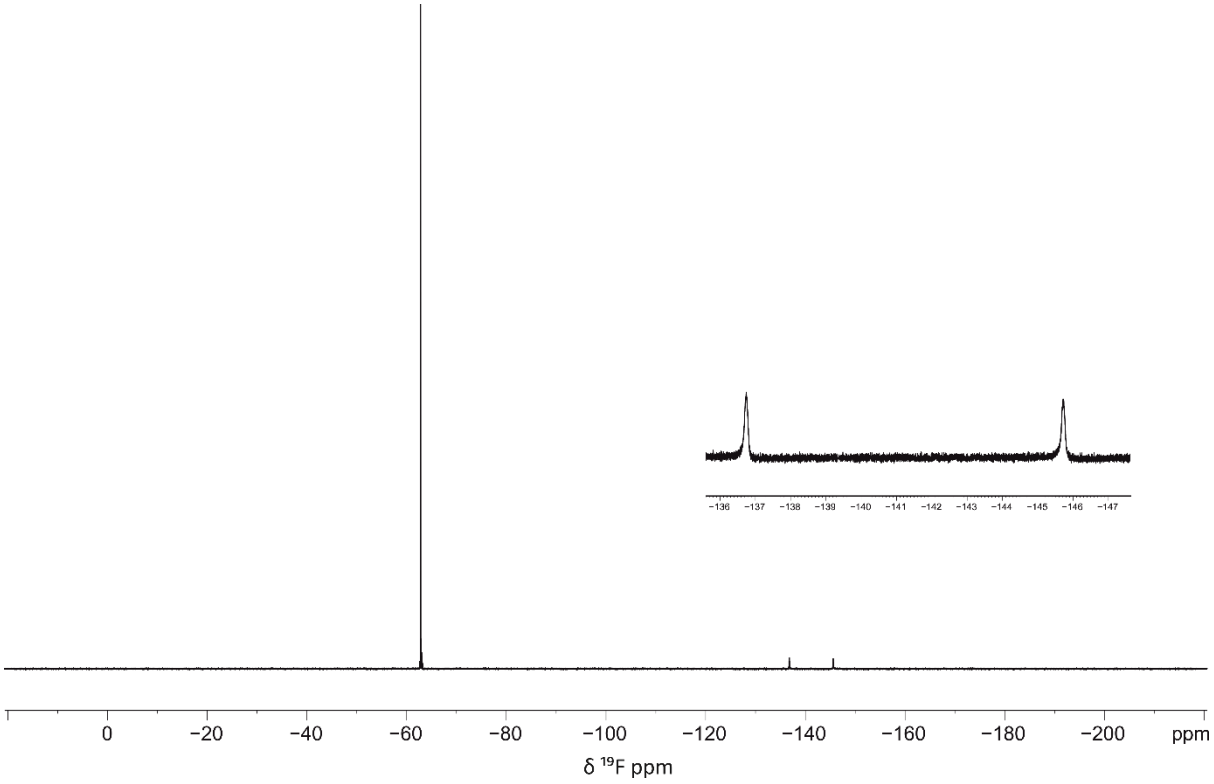

Figure 4.2: ^{19}F NMR of (*S*)-**3u** (471 MHz, Toluene-d_8, 25 mM, 298 K).

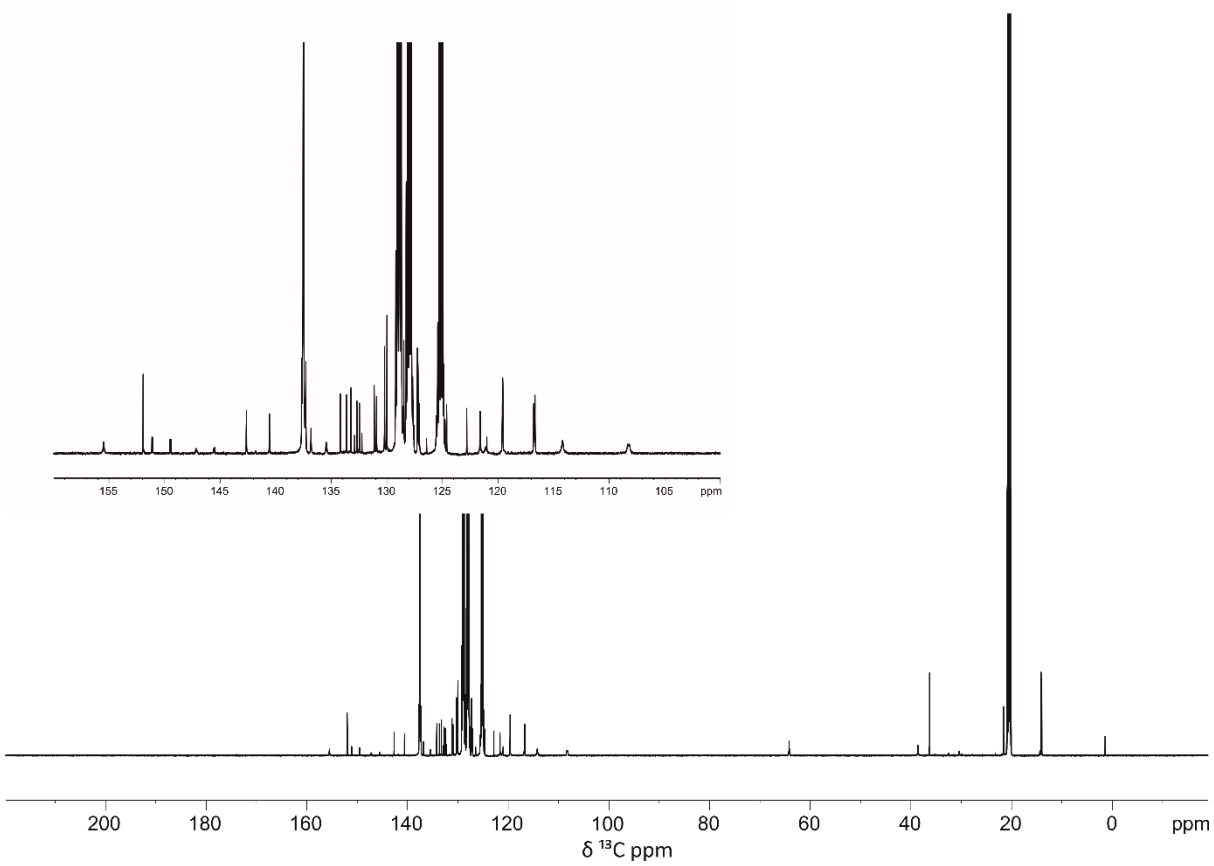

Figure 4.3: ^{13}C NMR of (*S*)-**3u** (151 MHz, Toluene-d_8, 25 mM, 298 K).

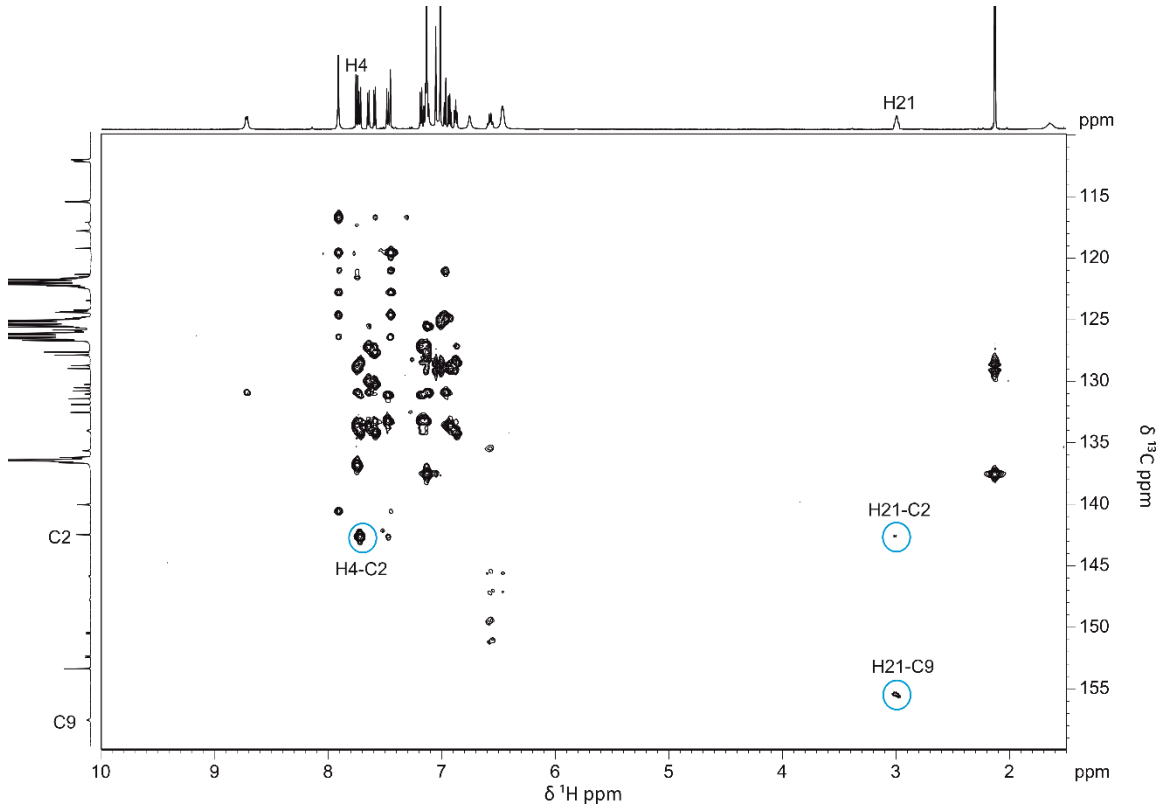

Figure 4.4: ^{1}H-^{13}C HMBC of (*S*)-**3u** (600 MHz, Toluene-d_8, 25 mM, 298 K).

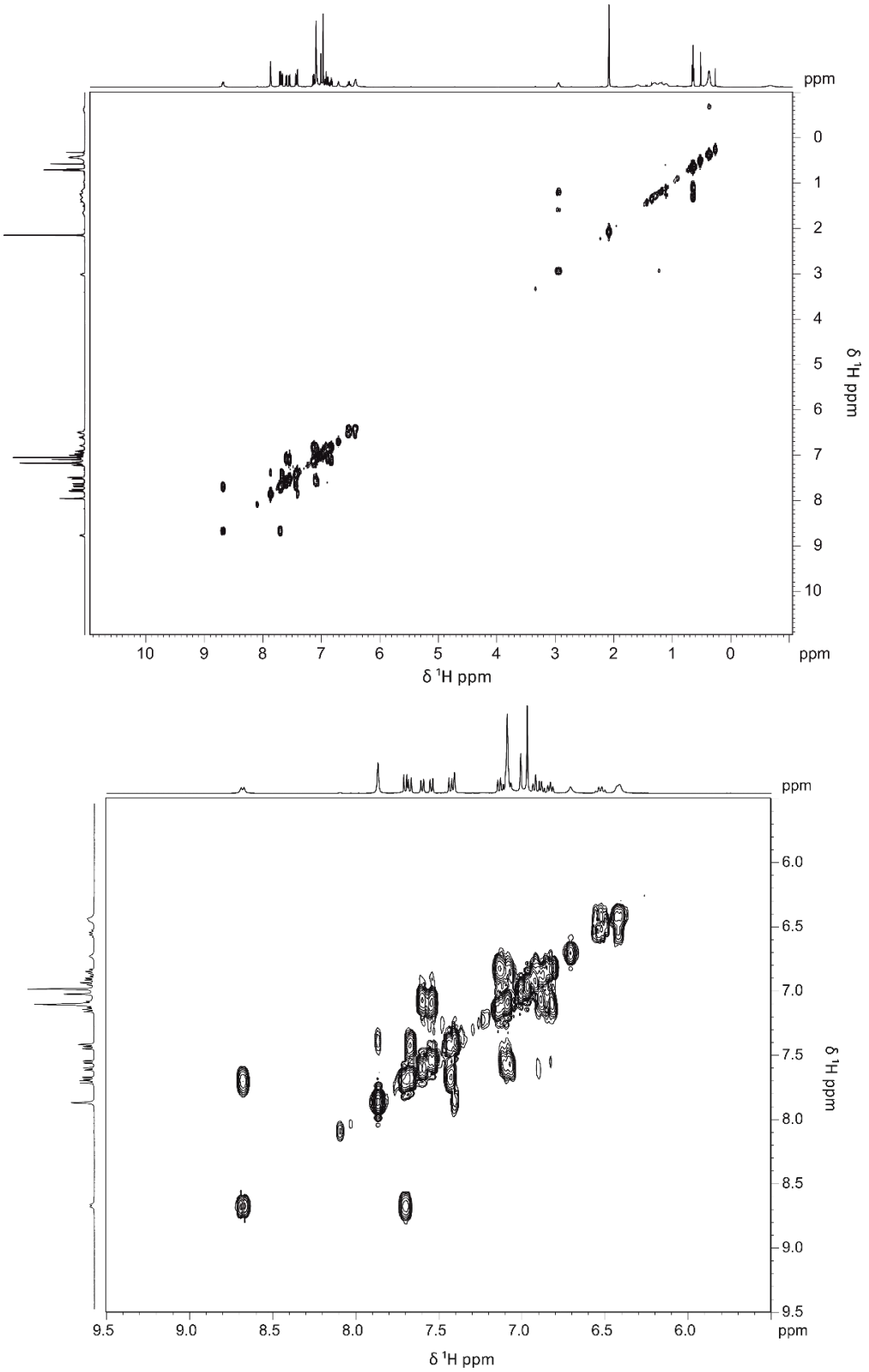

Figure 4.5: ^{1}H COSY of (*S*)-**3u** (500 MHz, Toluene-d_8, 25 mM, 298 K).

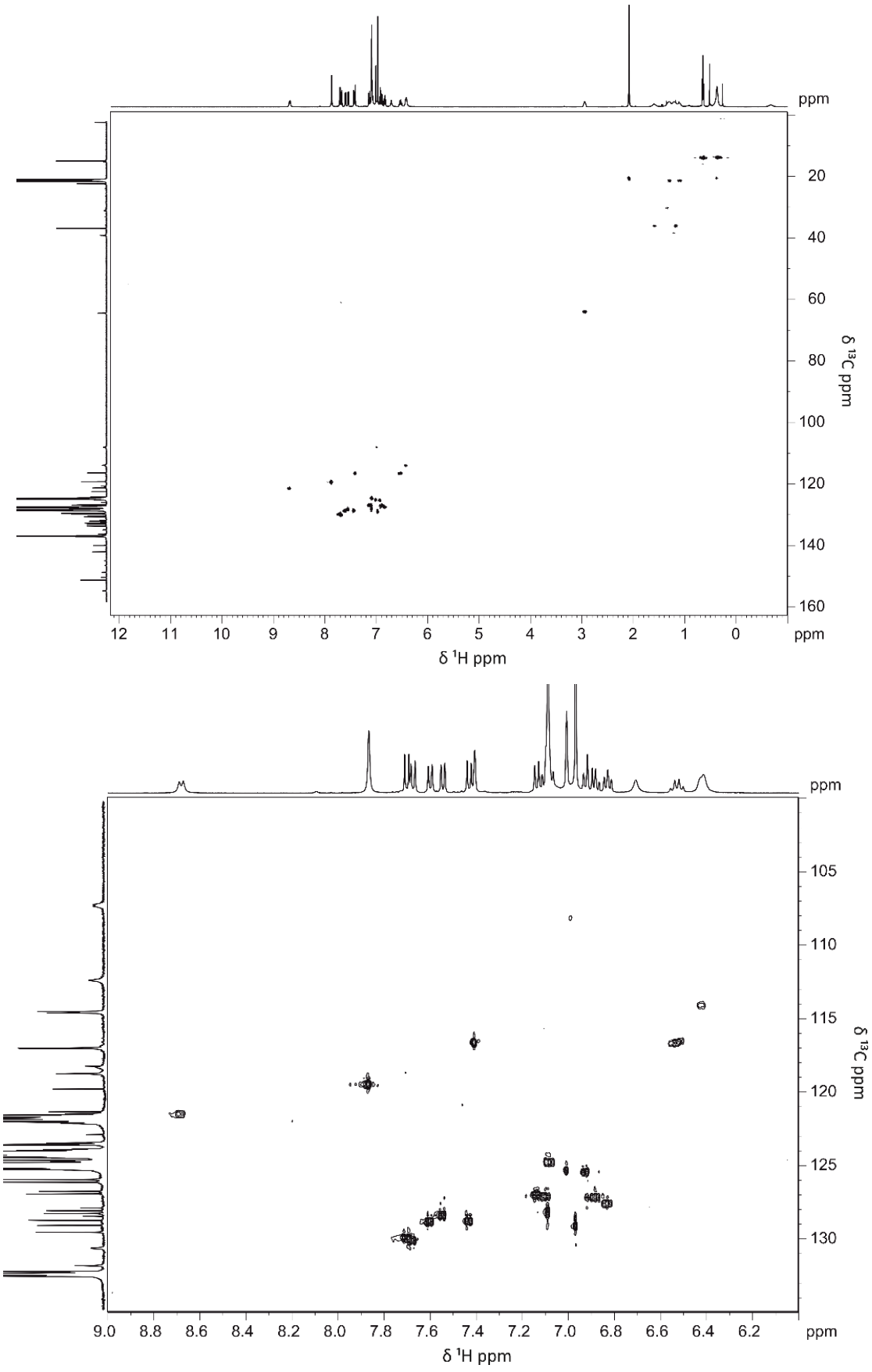

Figure 4.6: ^{1}H-^{13}C HSQC of (*S*)-**3u** (500 MHz, Toluene-d_8, 25 mM, 298 K).

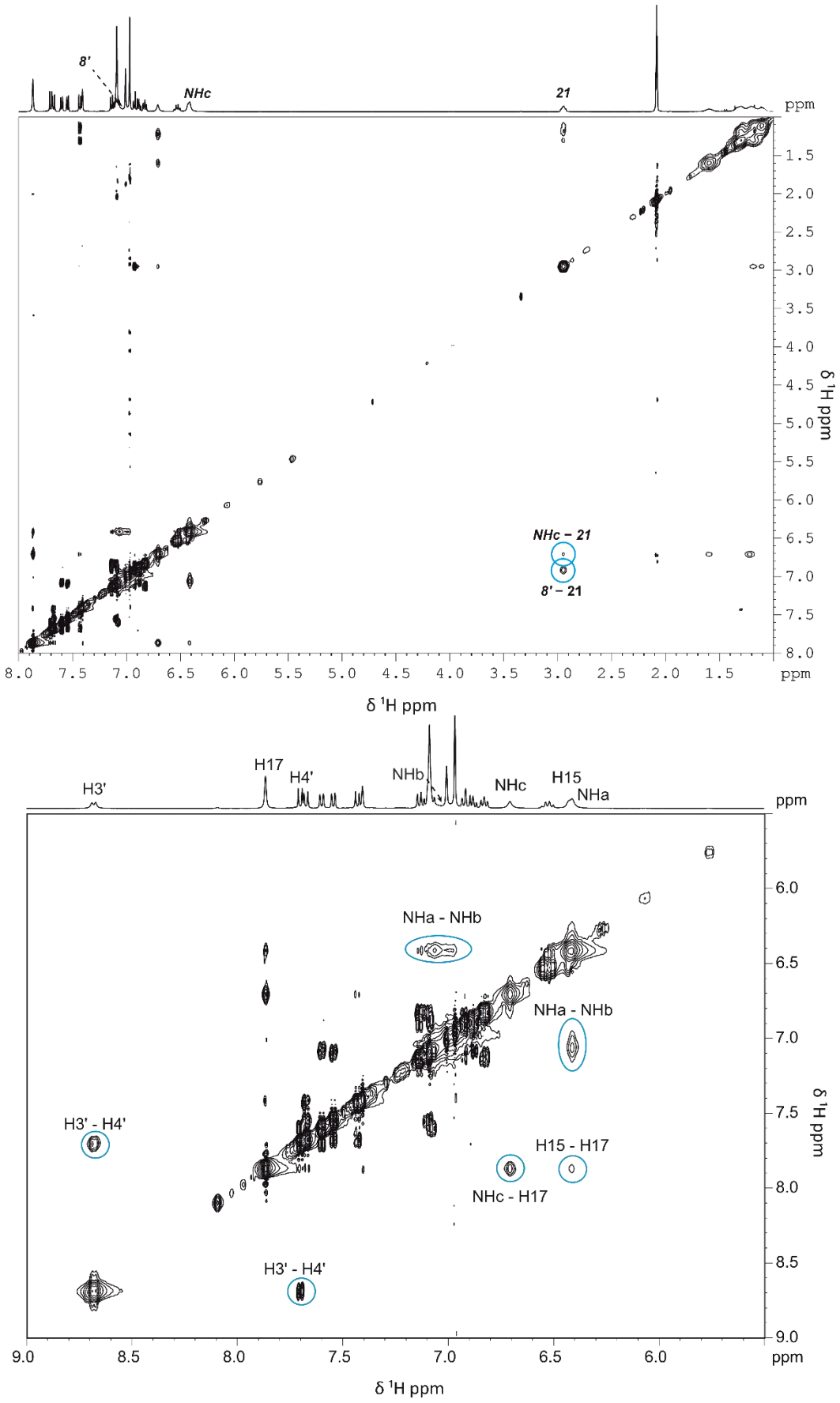

Figure 4.7: ^{1}H NOESY of (*S*)-**3u** (600 MHz, Toluene-d_8, 25 mM, 298 K).

4.8.2. Assignment of UPF Complex and Copies of Spectra

Sample Preparation: (*S*)-**3u** (0.125 mmol), $BnPh_3P^+$ BF_4^- and KF (2.5 equiv.) was weighted into a J Young Norell 5mm NMR tube and toluene-d_8 (0.5 mL) was added. The tube was sealed and sonicated for 45 minutes allowing for the formation of the complex. The sample remained stable for several months stored at 253 K.

NMR spectra of (*S*)-**3u**: $BnPh_3P^+$: F^- complexes were recorded on an AVIII HD 500 or AVIII HD 600 spectrometer.

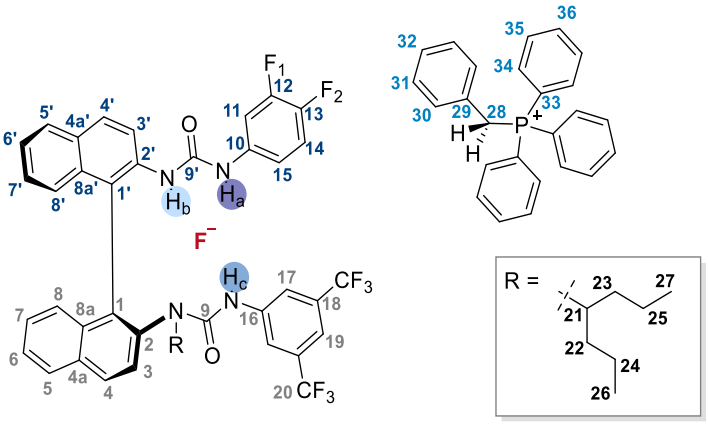

Scheme 4.2: Structure and numbering of (*S*)-**3u**: $BnPh_3P^+$: F^- (UPF) complex

Table 4.2: Assignment of (*S*)-**3u**: $BnPh_3P^+$: F^- [UPF]

^{1}H	**δ [ppm]**	**Multiplicity ^nJ [Hz]**	**^{13}C**	**δ [ppm]**	**Multiplicity $^nJ_{CF}$ [Hz]**
NH(c)	12.7	d, $^{1h}J_{FH}$ = 51	9 or 9’	155.6 or 154.7	s
NH(a)	12.4	d, $^{1h}J_{FH}$ = 57	12 or 13	150.2	dd, $^1J_{CF}$ =243.3 $^3J_{CF}$ = 12.4
NH(b)	10.6	d, $^{1h}J_{FH}$ = 31	16	145.5	s
3’	9.72	d, $^3J_{HH}$ = 9.2	8a	145.0	s
17	9.09	s	12 or 13	144.9	dd, $^1J_{CF}$ =238.5 $^3J_{CF}$ = 13.5
4’	7.84	d, $^3J_{HH}$ 9.2	2’	139.4	s
5’	7.61	d, $^3J_{HH}$	10	138.6	d, $^3J_{CF}$= 8.9
3 or 4	7.59 or 7.34	d, $^3J_{HH}$	8	135.6	s
11	7.51	m	P36	134.9	d, J_{CP} = 2.4
19	7.46	s	8a’	134.3	s
5	7.32	d, $^3J_{HH}$	P34	133.9	d, J_{CP} = 9.8
6’	7.03	t, overlapping	1	132.7	s
8, 8’ and 6	7.01-6.95	overlapping	P31	132.3	d, J_{CP} = 8.0
P31	6.86	overlapping	4a	131.8	s
15	6.84	overlapping	P32	131.6	d, $^4J_{CP}$ = 2.4
30	6.68	br d	P30	131.4	d, $^3J_{CP}$ = 4.7
7 or 7’	6.63	t, J = 8.0	3 or 4	130.5	s
14	6.54	q $^2J_{HF}$ = 9.3	P35	130.0	d, $^3J_{CP}$ = 10.4
28	4.25 and 3.82	dd, $^2J_{HH}$ = 15.1, $^2J_{HP}$ = 14.8	4’	129.5	s
30	6.68	br d	3 or 4	129.4	s
21	3.03	br s	5’	128.5	overlapping
22 or 23	2.59	br m	5	128.4	overlapping
22 or 23	2.10	overlapping	P29	127.9	overlapping
22 or 23	1.59	br m	1’	126.5	s
24 or 25	1.47	br m	20	124.7	q, $^1J_{CF}$ = 273.1
24 or 25	1.22	br m	3’	120.4	s
22 or 23	0.81	br m	17	119.4	s
26 or 27	0.79	t $^3J_{HH}$ = 6.9	P33	118.1	d, $^1J_{CP}$ = 85.5
24 or 25	0.52	br m	14	116.4	d, $^2J_{CF}$ = 17.5
26 or 27	0.49	t $^3J_{HH}$ = 6.3	15	113.6	s
24 or 25	-0.40	br s	19	113.3	s
^{19}F	**δ [ppm]**	**Multiplicity ^nJ [Hz]**	11	107.3	d
CF_3	-62.1	s	21	65.7	s
F^-	-74.2	br s	22 or 23	36.6	s
F1	-137.4	m	22 or 23	35.5	s
F2	-148.5	m	P28	28.5	d, $^2J_{CP}$ = 46.8
			24 or 25	22.1	s
^{31}P	**δ [ppm]**	**Multiplicity ^nJ [Hz]**	24 or 25	20.4	overlapping
P^+	22.3	br s	26 or 27	14.7	s
			26 or 27	14.4	s

*overlapping signals masked by solvent peaks, phosphonium protons 32, 34, 35, 36 overlapping with solvent peaks, urea carbons 2, 6, 7, 6’, 7’, 8’ indistinguishable

(*S*)-**3u**: $BnPh_3P^+$: F^- (UPF) complex Spectra in Toluene-d_8

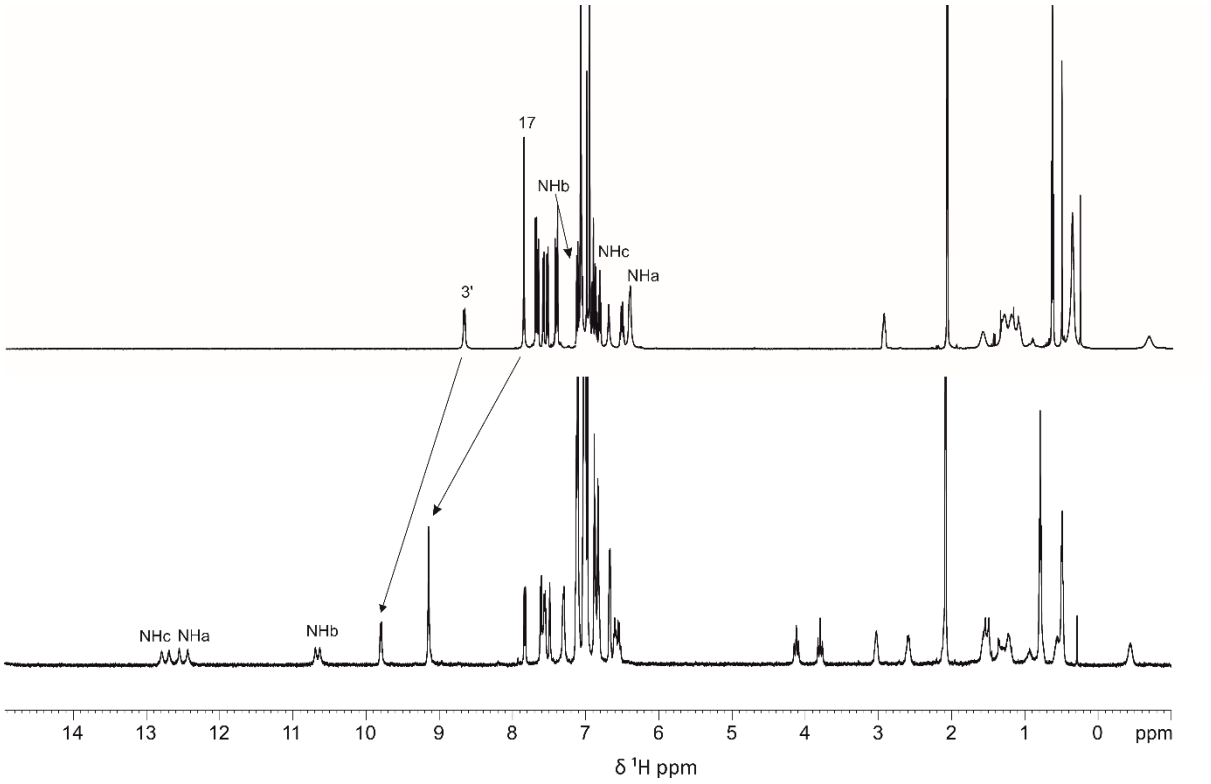

Figure 4.8: Overlapping 1H of (*S*)-**3u** unbound and (*S*)-**3u**: $BnPh_3P^+$: F^- complex (500 MHz, Toluene-d_8, 25 mM, 298 K).

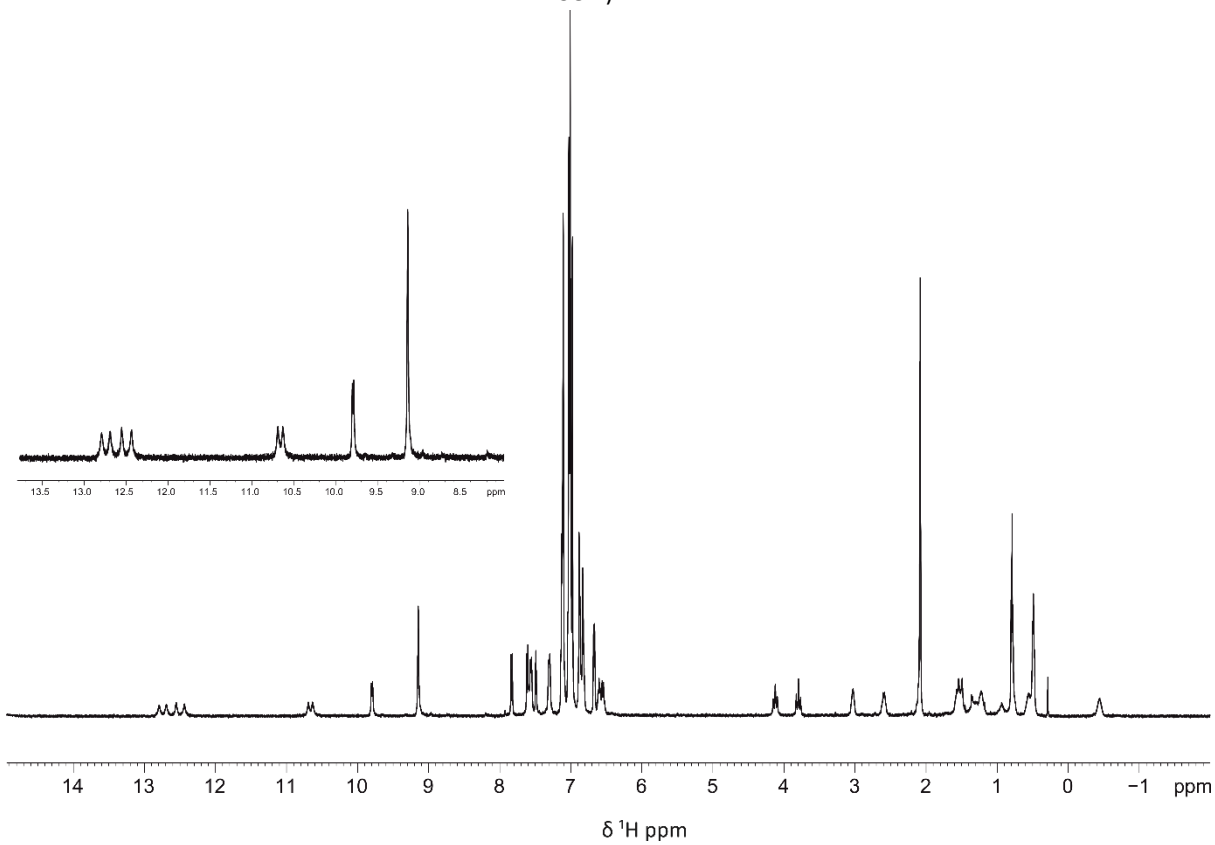

Figure 4.9: ^1H NMR of (*S*)-**3u**: $BnPh_3P^+$: F^- Complex (500 MHz, Toluene-d_8, 25 mM, 298 K).

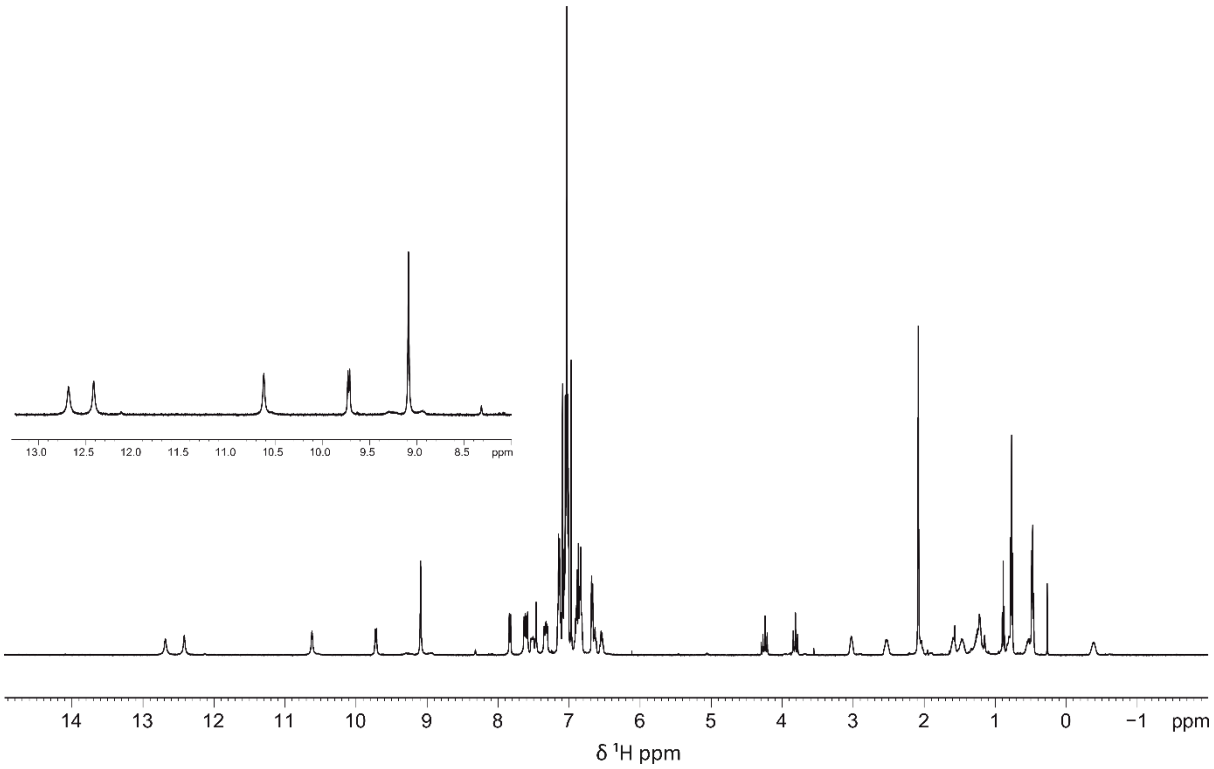

Figure 4.10: $^{1}H\{^{19}F\}$ NMR of (*S*)-**3u**: $BnPh_3P^+$: F^- Complex (500 MHz, Toluene-d_8, 25 mM, 298 K).

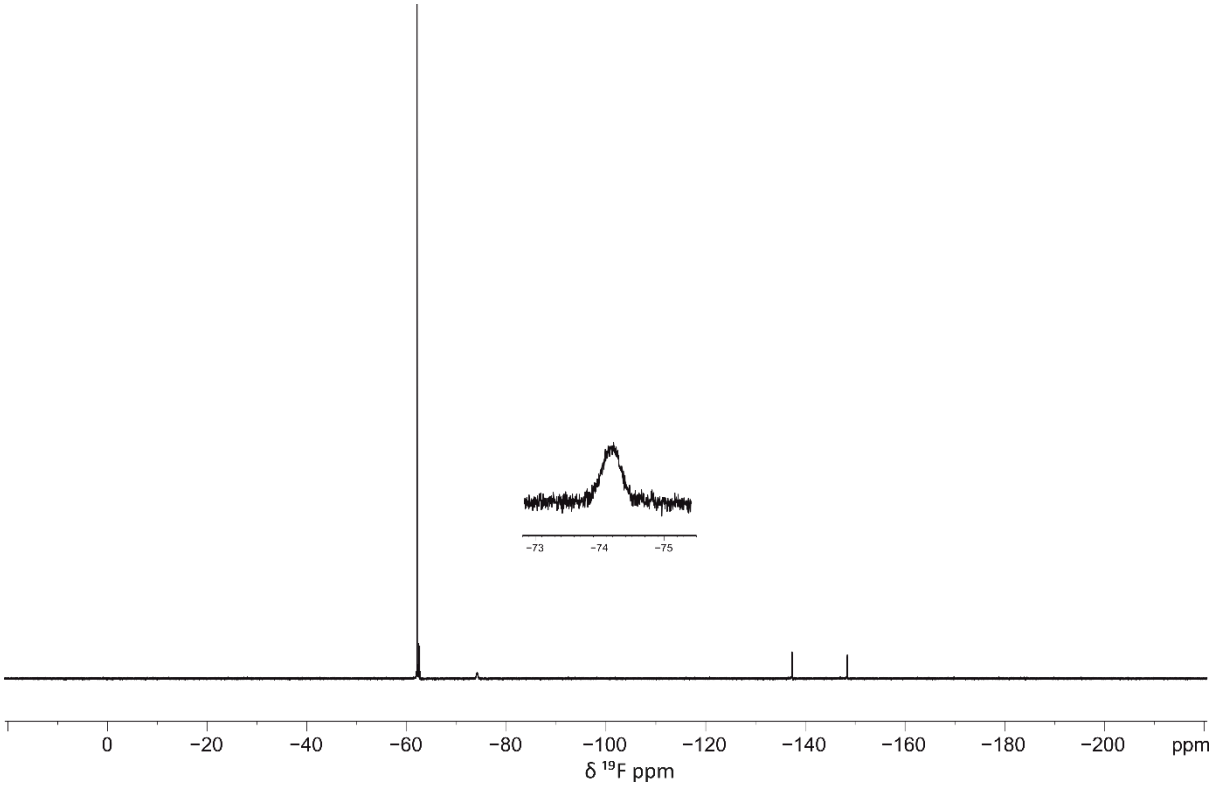

Figure 4.11: ^{19}F NMR of (*S*)-**3u**: $BnPh_3P^+$: F^- Complex (471 MHz, Toluene-d_8, 25 mM, 298 K).

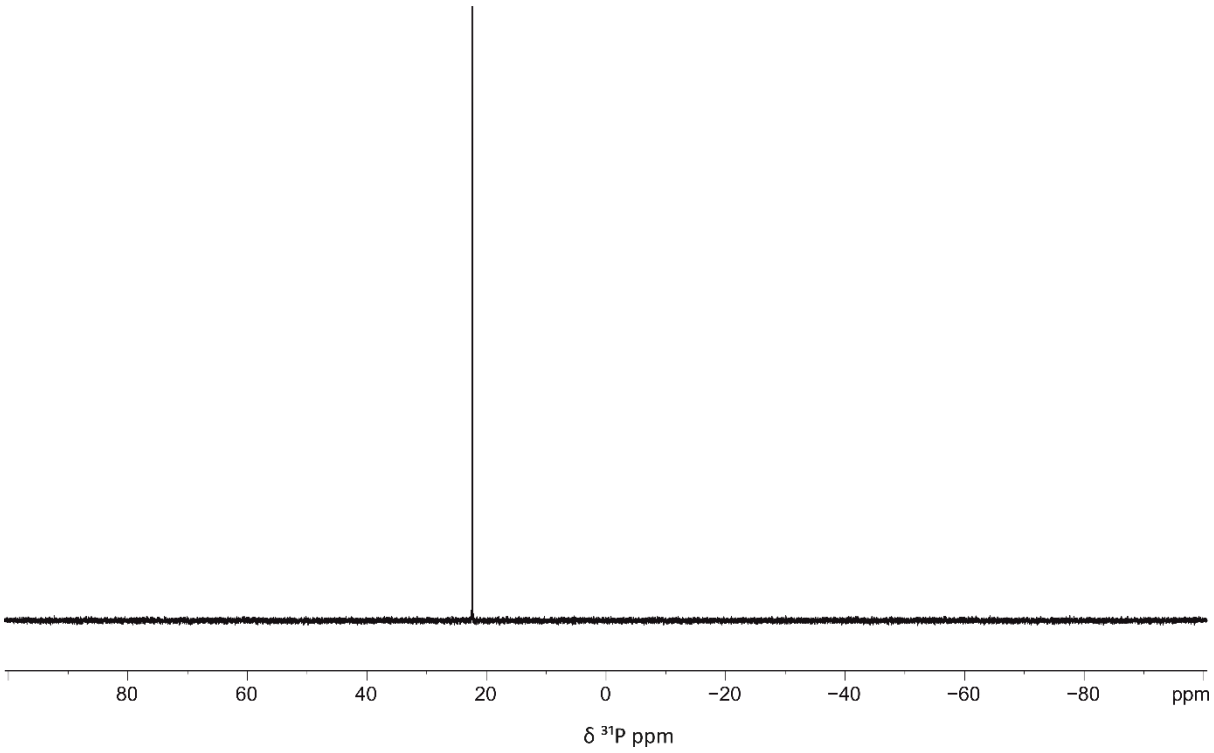

Figure 4.12: ^{31}P NMR of (*S*)-**3u**: $BnPh_3P^+$: F^- Complex (203 MHz, Toluene-d_8, 25 mM, 298 K).

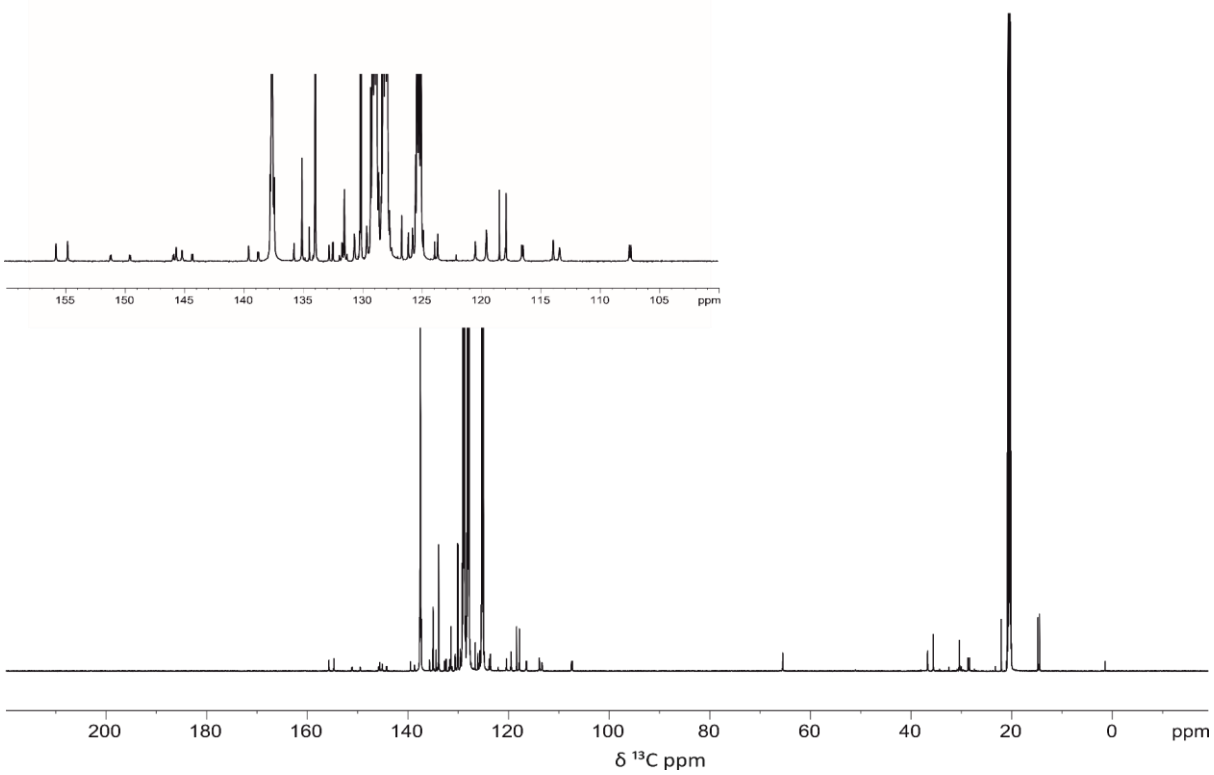

Figure 4.13: ^{13}C NMR of (*S*)-**3u**: $BnPh_3P^+$: F^- Complex (151 MHz, Toluene-d_8, 25 mM, 298 K).

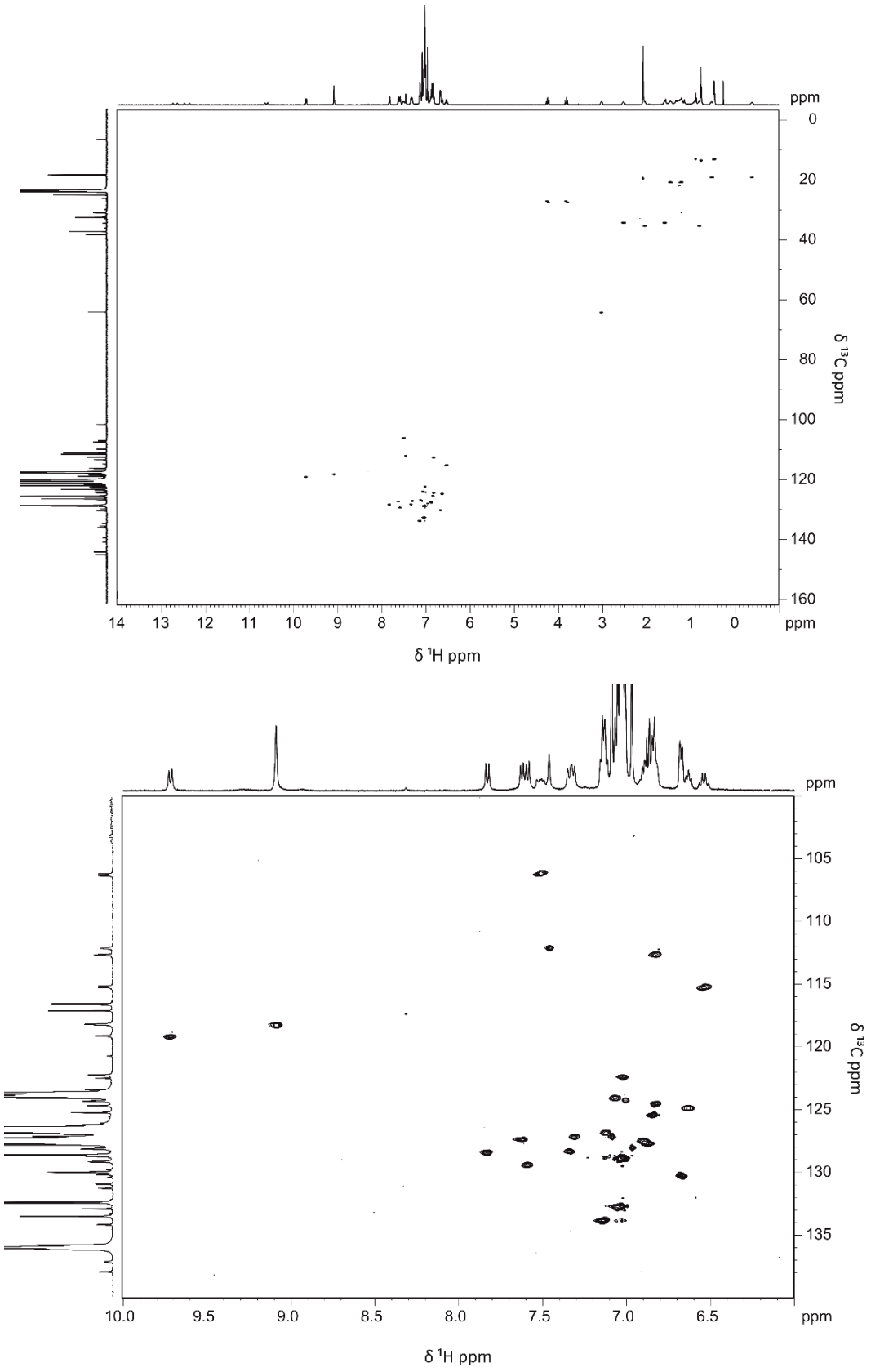

Figure 4.14: ^{1}H-^{13}C HSQC of (*S*)-**3u**: $BnPh_3P^+$: F^- Complex (500 MHz, Toluene-d_8, 25 mM, 298 K).

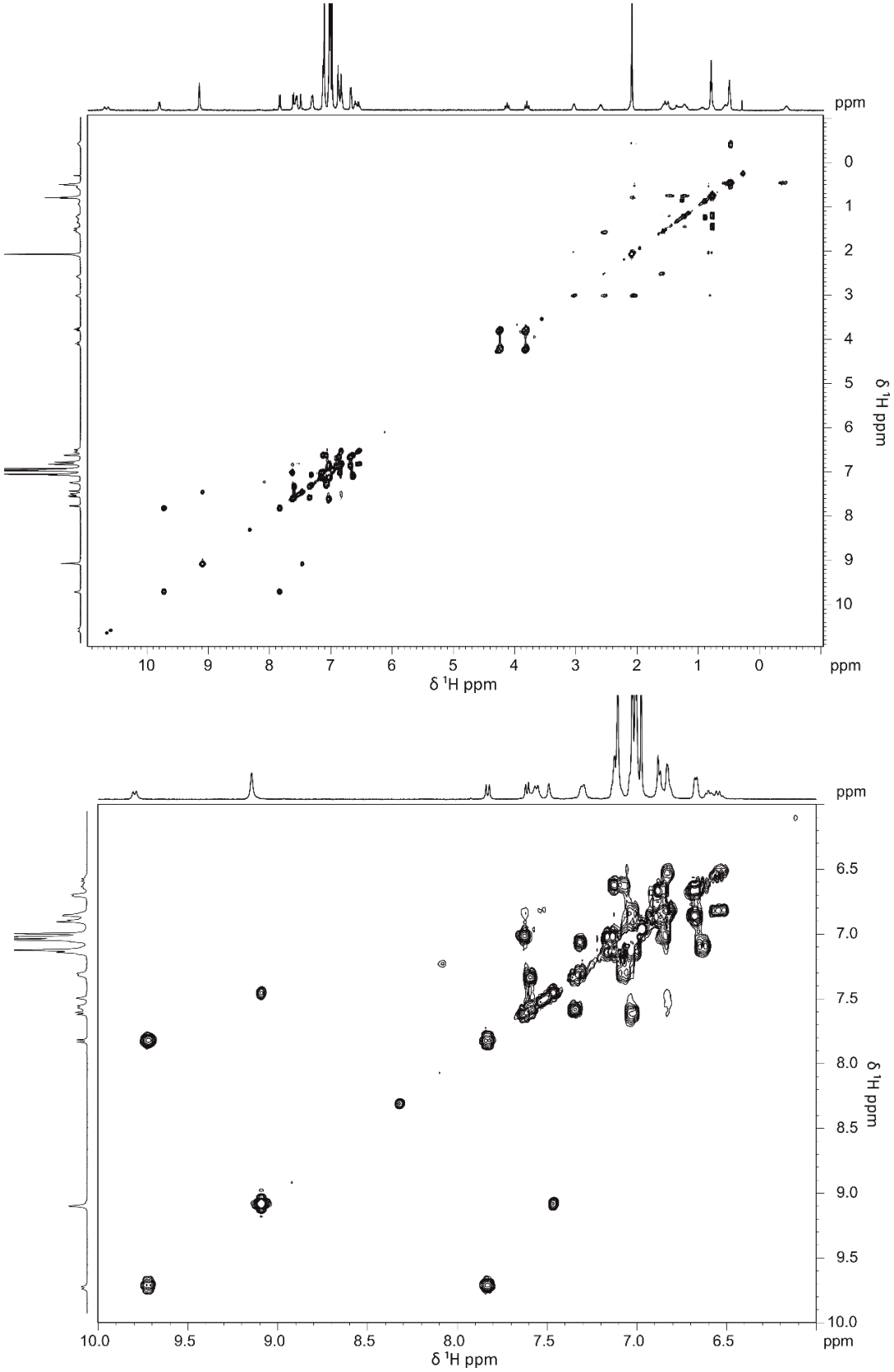

Figure 4.15: ^{1}H COSY of (*S*)-**3u**: $BnPh_3P^+$: F^- Complex (500 MHz, Toluene-d_8, 25 mM, 298 K).

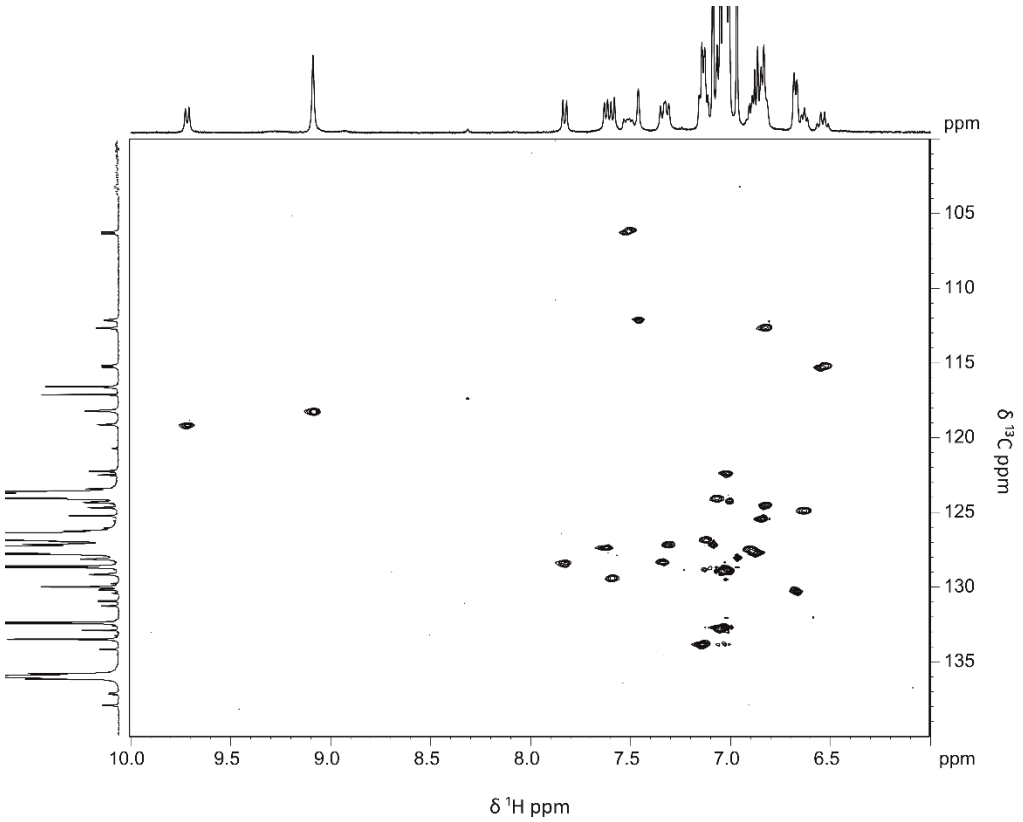

Figure 4.16: ^{1}H- ^{13}C HMBC of (*S*)-**3u**: $BnPh_3P^+$: F^- Complex (500 MHz, Toluene-d_8, 25 mM, 298 K).

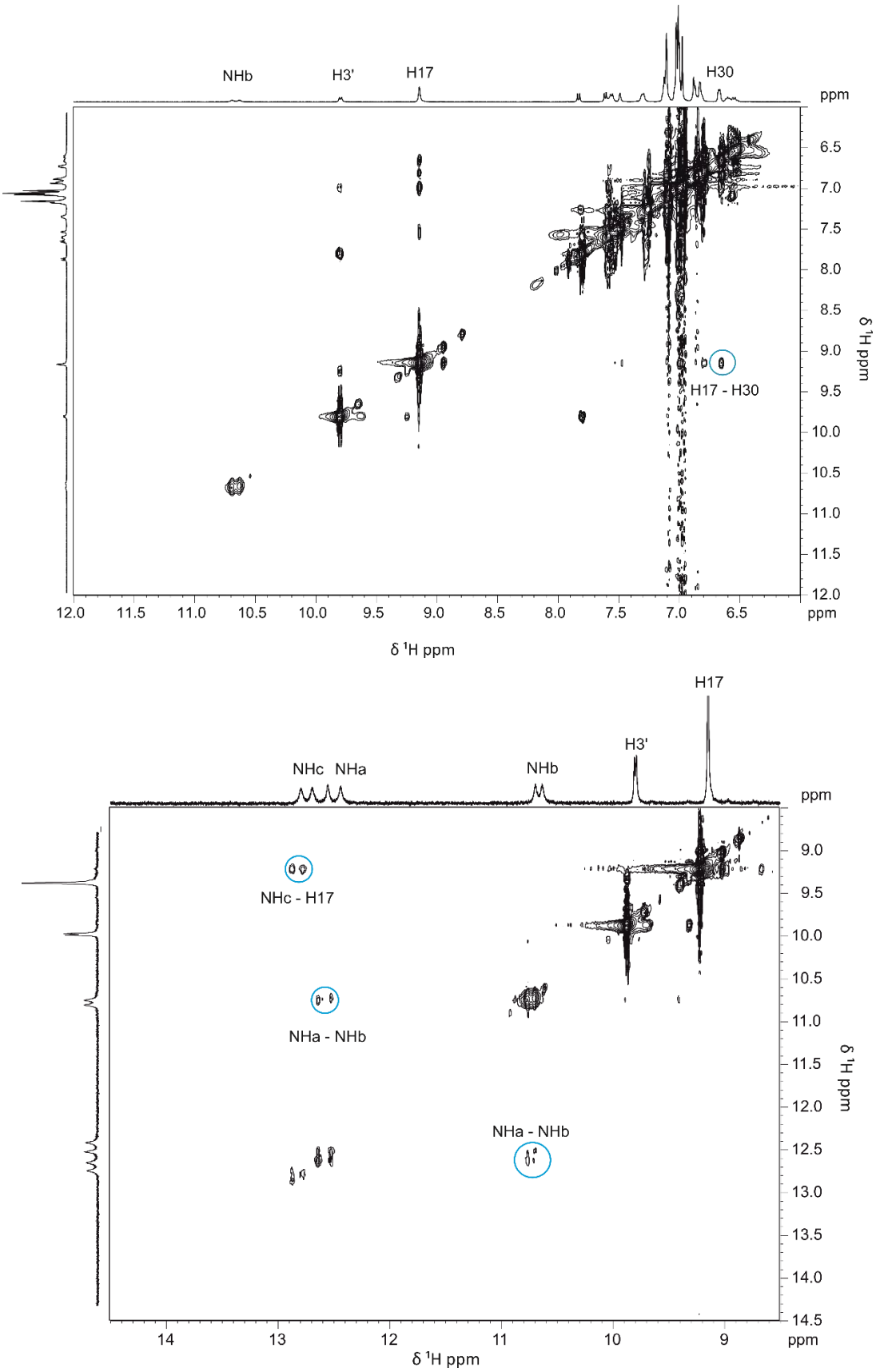

Figure 4.17: ^{1}H ROESY of (*S*)-**3u**: $BnPh_3P^+$: F^- Complex spin lock pulse (P15) = 100 ms (500 MHz, Toluene-d_8, 25 mM, 298 K).

4.8.3 HOESY

Relative and absolute distance determination:

Sample preparation: A sample of (*S*)-**3u:** Ph_3BnP^+: F^- was prepared in toluene-d_8 (25 mM).

1D heteronuclear $^1H—^{19}F$ nOe experiments (HOESY) utilising ^{19}F inversion and ^1H detection, were acquired on an AVIII HD 500 with a previously developed pulse sequence (hoesyfhgpsp1d_v2cpd.wvm)[33] set to the parameters below.

Table 4.3: Parameters for $^1H—^{19}F$ nOe experiments (HOESY):

Parameter	Value
TD	16384
SW	20 ppm
o1p/ o2p	4.7/ -74
NS (DS)	256
relaxation delay d1	3 s
mixing time τ_m	10-600 ms

Build-up curves for nOe's developed between fluoride and N-H or C-H were used to calculate the relative distances according to equation 1.

Equation 1:

$$\eta_{\mathrm{H}}\{F^-\} \propto r_{H-F}^{-6}$$

$\eta_{\mathrm{NH}}\{F^-\}$ = H—F nOe build up rate

r_{NH-F} = H—F distance

Table 4.4: Determination of relative distances:

nOe correlation	nOe build up rate	$\sqrt[6]{\frac{1}{\eta}}$	Distance relative to H(a)-F = 1.0
NH(a)-F	63.704	0.500	1.00
NH(b)-F	40.905	0.538	1.08
NH(c)-F	74.290	0.488	0.98
CH(17)-F	15.075	0.636	1.27
P-CH(34/35)-F	16.200	0.629	1.26
P-CH(30)-F	3.137	0.827	1.65
P-CH(28)-F	20.985	0.602	1.20

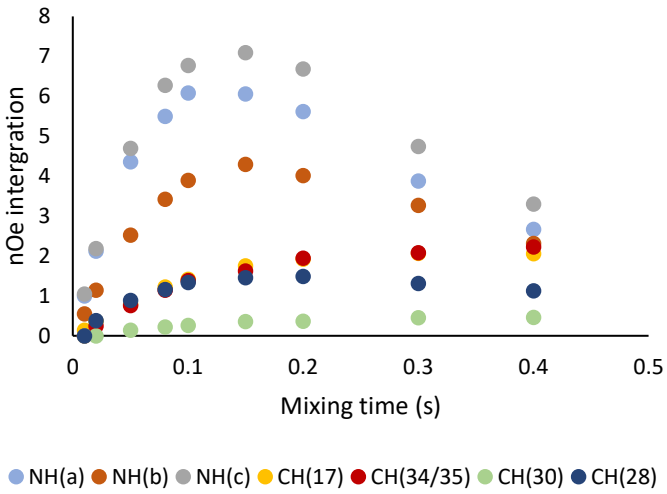

Figure 4.18: ^{1}H—^{9}F nOe build-up curves of (*S*)-**3u:** Ph_3BnP^+: F^-.

Absolute Distance Determination:

1D heteronuclear ^{1}H—^{19}F nOe experiments (HOESY) utilising ^{19}F inversion and ^{1}H detection, were acquired on an AVIII HD 500 with pulse sequence (hoesyfhgpsp1d_v2cpd.wvm) under parameters listed in Table 4.3.

An additional set of experiments were performed irradiating a fluorine atom (F2) on the catalyst (*S*)-**3u** (F2 = -148 ppm) and observing the nOe build up to H14. The distance between F2 and H14 has been previously measured by X-ray crystallography to be 2.60 Å.[5] A mixing time of 50 ms was selected as this lay within the linear region of growth for both this reference and the signals of interest. Absolute distances were calculated using equation 2.

Equation 2:

$$r_{NH-F} = \sqrt[6]{\frac{I_{H-F\ ref.}}{I_{H-F}}}\ r_{H-F\ ref.}$$

r_{NH-F} = NH-F distance

$r_{NH-F\ ref}$ = H-F distance reference = 2.60 Å

$I_{NH\text{-}F}$ = nOe intensity between H-F

Table 4.5: Determination of absolute distances for (*S*)-**3u**: Ph_3BnP^+: F^-

nOe correlation	I_{NH-F}	Absolute H-F distance (Å)
NH(a)–F	1.00	1.72
NH(b)–F	0.59	1.88
NH(c)–F	1.08	1.70
CH(17)–F	0.18	2.28
P-CH(30)–F	0.03	3.05
P-CH(28)–F	0.20	2.24
CH(14)–F_2 *(Reference)*	0.08	2.60

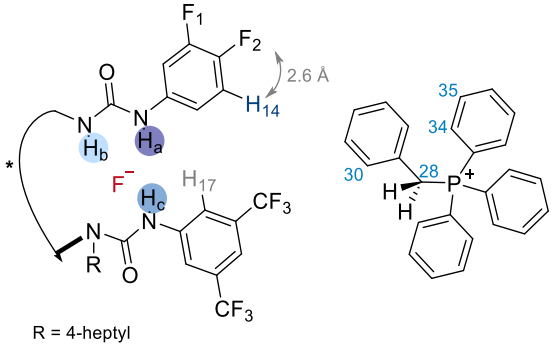

Figure 4.19: ^1H–^{19}F HOESY correlations of (*S*)-**3u:** Ph_3BnP^+: F^-.

4.8.4. ^1H—^{19}F CLIP-HSQC

^1H—^{19}F CLIP-HSQC experiments were recorded on an AVIII HD 500 using a 25 mM sample of (*S*)-**3u:** Ph_3BnP^+: F^- in toluene-d_8 at 298 K. The experiment was acquired using pulse sequence (*hsqcetgpclip)*[34] under the following parameters:

Table 4.6: Parameters for ^1H—^{19}F CLIP-HSQC experiments:

Parameter	Value
TD	2048 (f2) x 128 (f1)
SW	8 (f2) x 25 (f1)
o1p/ o2p	12/ -75.5 ppm
NS (DS)	4 (4)
relaxation delay d1	2 s
delay for evolution of coupling CNST[2]	50

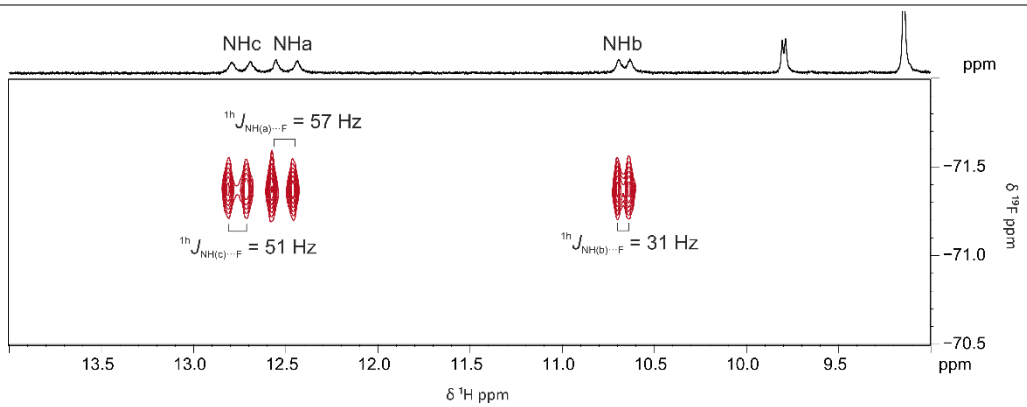

Figure 4.20: ^1H–^{19}F CLIP-HSQC of (*S*)-**3u**: Ph_3BnP^+: F^-

4.9. Kinetics

4.9.1. Kinetic Isotope Effect Study

General Procedures and Reaction Assembly

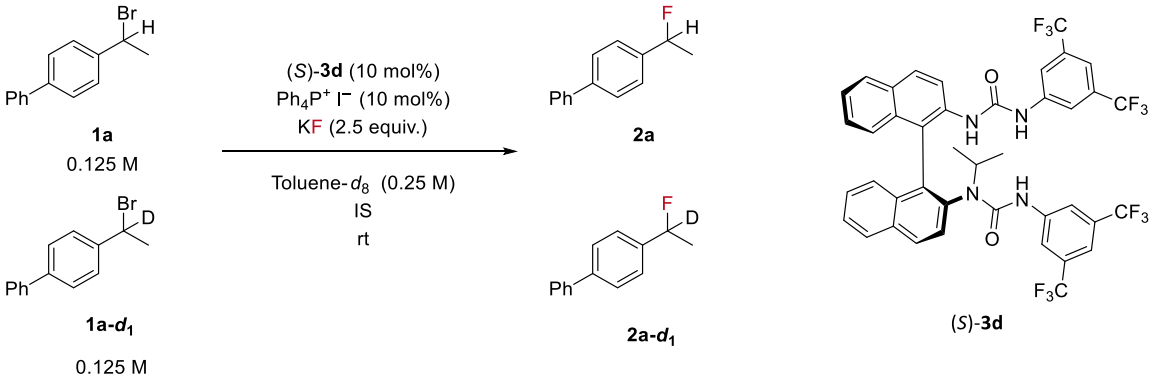

Benzylic bromides **1a** (0.0625 mmol) and **1a-*d*$_1$** (or **1a-*d*$_3$**) (0.0625 mmol) and anhydrous toluene-d_8 (0.5 mL) were loaded into a J. Young Norell 5mm NMR tube and 4-fluoroanisole (0.044 mmol), or 1,2,3-trifluoro-5-methoxybenzene (0.0396 mmol), was added as an internal standard. The NMR tube was then sealed and a reference spectrum was taken using ^{1}H NMR with a 90° excitation pulse (zg) and a relaxation delay of t_{D1} = 30.0 s, NS(DS) = 8(0). Following that, (*S*)-**3d** (0.0125 mmol), Ph_4P^+ I^- (0.0125 mmol) and KF (0.3125 mmol) were added to the NMR tube to initiate the reaction, and the time was recorded. The initial timepoint was analysed immediately with quantitative ^{1}H NMR (zg) and ^{19}F{^{1}H} NMR (90° excitation pulse (zgig), a relaxation delay of t_{D1} = 30.0 s, NS(DS)= 12(4), o1p = -146 ppm, SW = 100 ppm).

Following initial quantification NMR tubes were secured on an external motor (Figure 4.21) and rotated at 5 rpm at ambient temperature. The reaction was rotated for specified time before being swiftly transferred back to spectrometer where quantitative ^{1}H and ^{19}F{^{1}H} spectra (following the same parameters) were taken. This was repeated over the course of reaction monitoring to build kinetic curves.

All NMR spectra were recorded on AVIIIHD 500 NMR spectrometer at 298 K. All spectra acquired were processed using Mestrenova version 14.0, with 128 K points zero filling, manual phase correction and baseline correction. In some cases, regional baseline correction and line fitting were performed to get

a more accurate estimation of the integral of the peak. Each peak was integrated, and concentrations of species were calculated by comparison of the corresponding integral to that of internal standard.

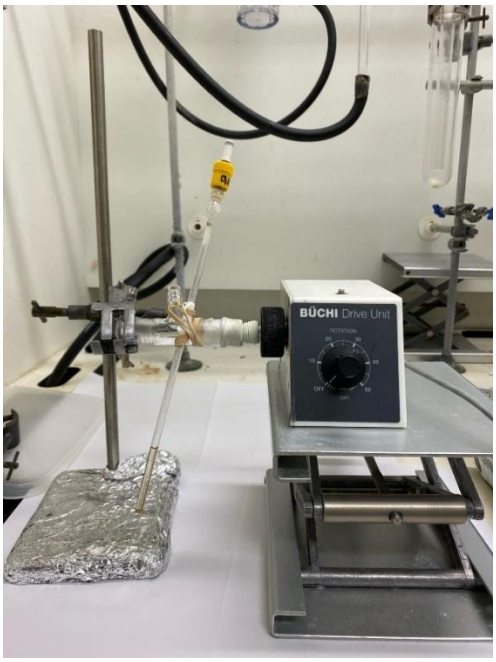

Figure 4.21: External motor set up for the periodic rotation of NMR tubes

4.9.1.1. T_1 Measurements

The longitudinal relaxation time constants T_1 of the benzylic fluoride product **2a**, benzylic bromide substrate **1a** and internal standards, 4-fluoroanisole and 1,2,3-trifluoroanisole, were measured *via* ^{1}H and ^{19}F inversion recovery experiments (t1ir) on an AVIII 500. T_1 values were calculated by non-linear fitting using Dynamic centre on Topspin version 4.1.1. The results are summarised in Table 4.9.

Sample preparation: A 0.25 M sample of bromide **1a** (0.0625 mmol), fluoride **2a** (0.0625 mmol), and Ph_4P^+ I^- (0.0125 mmol) was prepared in toluene-d_8 and 5 µL of internal standard was added (4-fluoroanisole or 1,2,3-trifluoroanisole). The experiment was acquired with the following parameters set.

Table 4.7: Parameters for ^{1}H T_1 measurements –bromide **1a**, fluoride **2a** and internal standards (IS):

Parameter	**Value**
TD	65536
SW	18
O1P	5.0
NS (DS)	4 (0)
Relaxation delay d1	60 s
Variable delay d1	0.001-60 s (15)

Table 4.8: Parameters for ^{19}F T_1 measurement –fluoride **2a** and internal standards (IS):

Parameter	**Value**
TD	65536
SW	10
O1P	-124.2 (IS)/ -167.5 (2a)
NS (DS)	2 (2)
Relaxation delay d1	45 s
Variable delay d1	0.001-60 s (15)

Table 4.9: Summary of T_1 measurements

Compound	**^{1}H T_1 (s)**	**^{19}F T_1 (s)**
1a	3.564	-
2a	3.944	3.820
4-fluoroanisole (OMe)	3.914	4.828
1,2,3-trifluoro-5-methoxybenzene (OMe)	2.975	2.798 (-134 ppm)

t_{D1} value of 30.0 s was selected for quantitative ^{1}H and ^{19}F NMR.

4.9.1.2. Kinetic Curves and Spectra - α-Secondary Kinetic Isotope Effect

Competition experiment between **1a** and **1a-*d*$_1$**

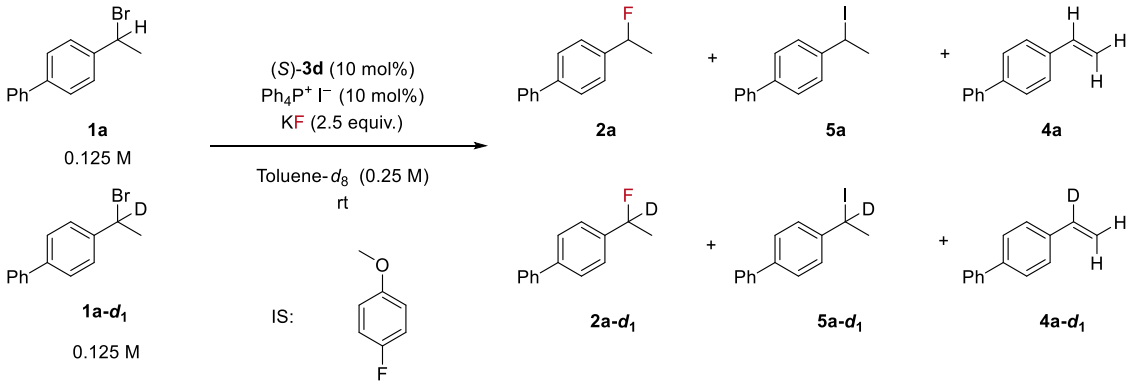

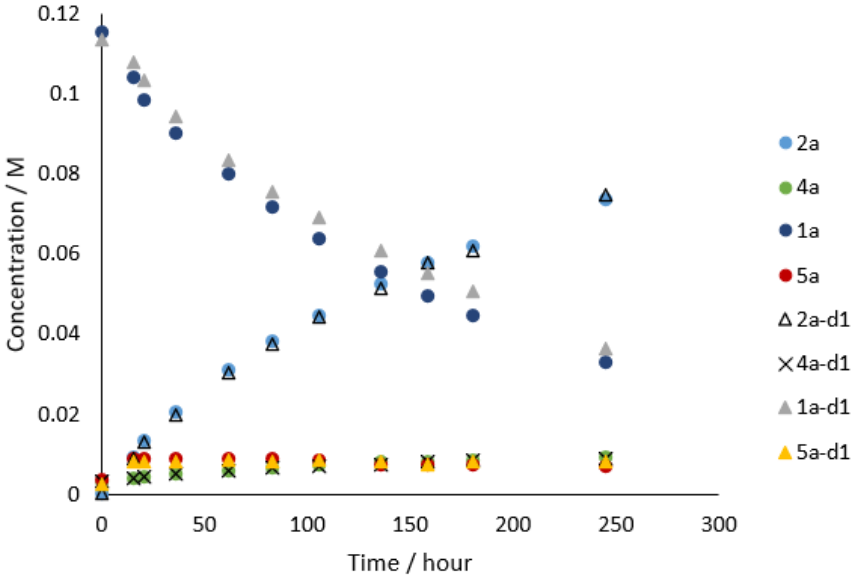

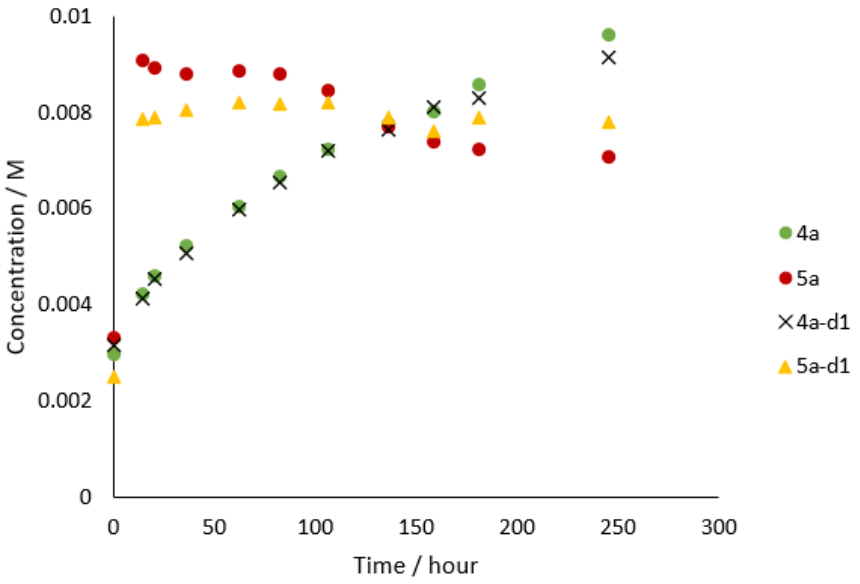

Figure 4.22: Kinetic profile of the competition experiment between **1a** and **1a-*d*$_1$**

All spectra acquired within the same experiment were processed via the same method to minimise error. Typical ^{1}H NMR spectra following manual phase correction and baseline correction are shown. By referring to the integral of the internal standard (4-fluoroanisole), the concentrations of benzylic bromides, iodides and eliminated side products were calculated. The concentrations of fluorinated products were calculated based on $^{19}F\{^{1}H\}$ NMR due to peak overlap in the ^{1}H NMR spectra. Typical $^{19}F\{^{1}H\}$ NMR spectra after processing are shown in Figure 4.25.

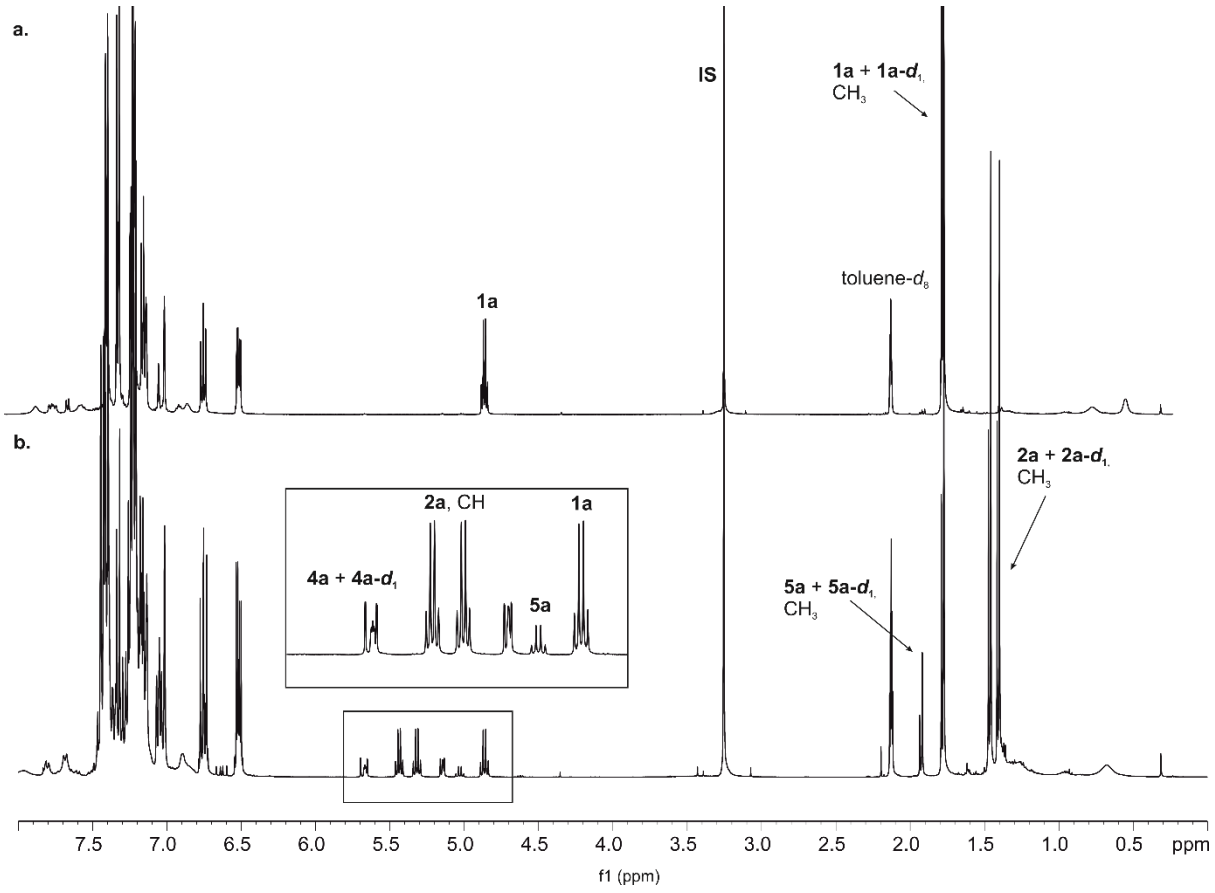

Figure 4.23: Typical ^{1}H NMR spectra of the reaction mixture; a. before the reaction was started; b. at ~70% conversion.

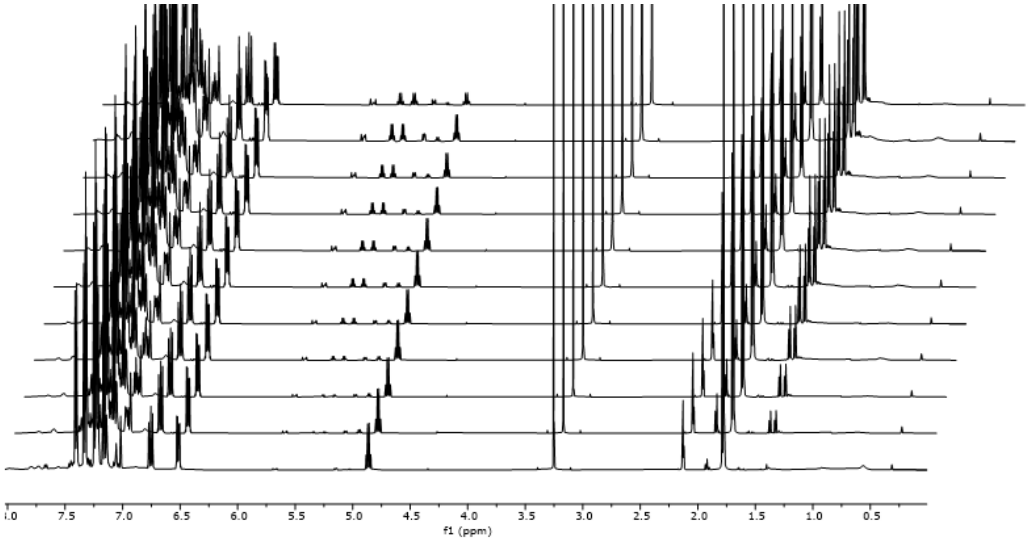

Figure 4.24: Stacked ^{1}H NMR spectra for competition experiment between **1a** and **1a-*d*$_1$**

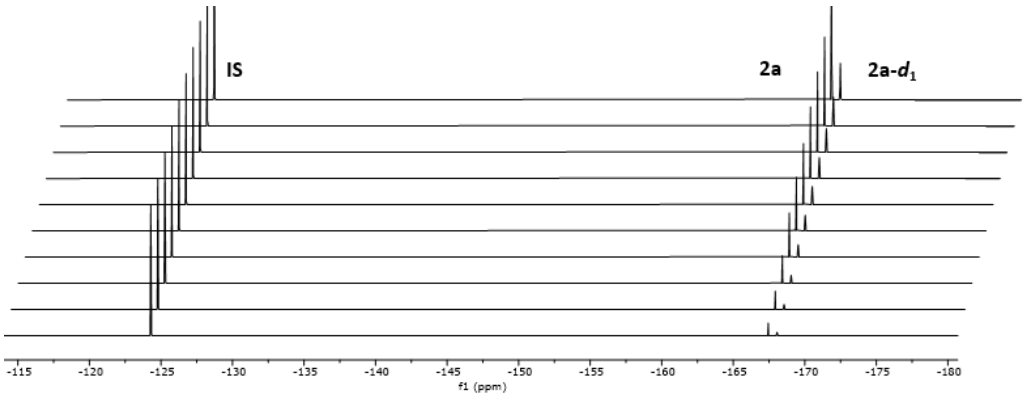

Figure 4.25: Stacked ^{19}F{^{1}H} NMR spectra for the competition experiment between **1a** and **1a-*d*$_1$**

4.9.1.3. Kinetic Curves and Spectra - β-Secondary Kinetic Isotope Effect

Competition experiment between **1a** and **1a-d$_3$**

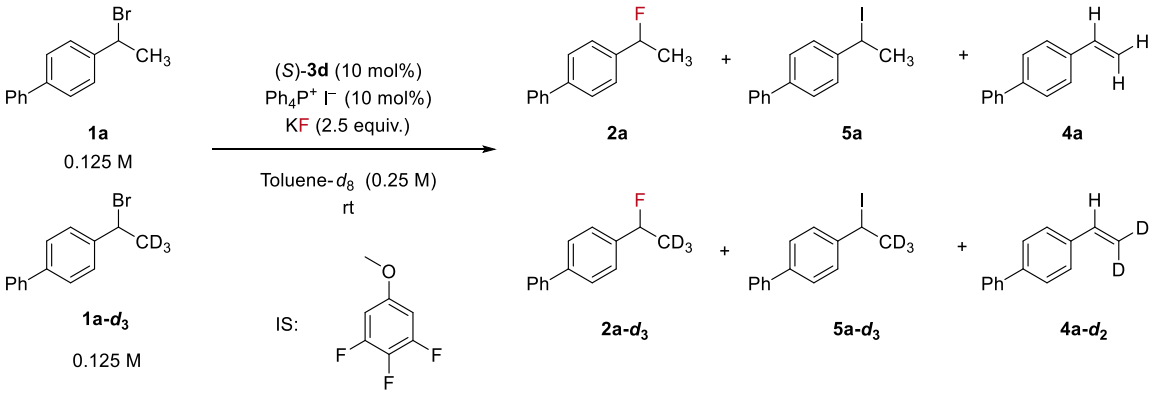

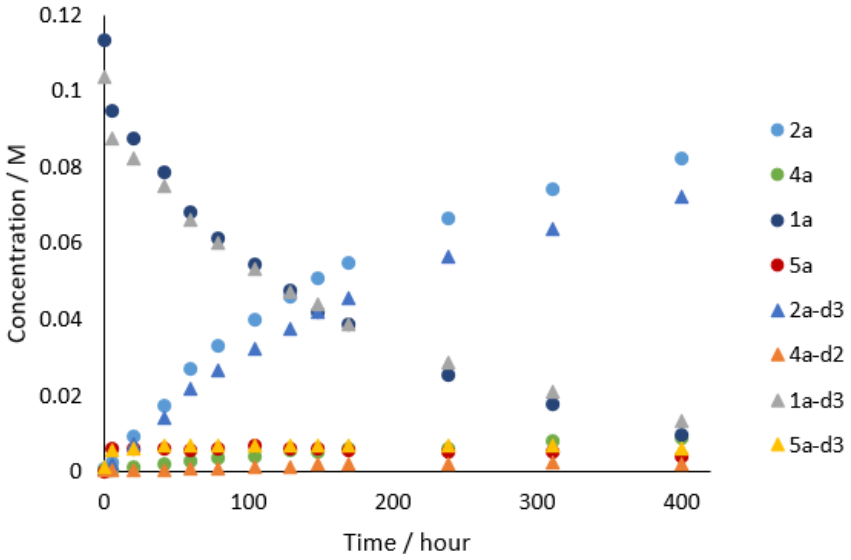

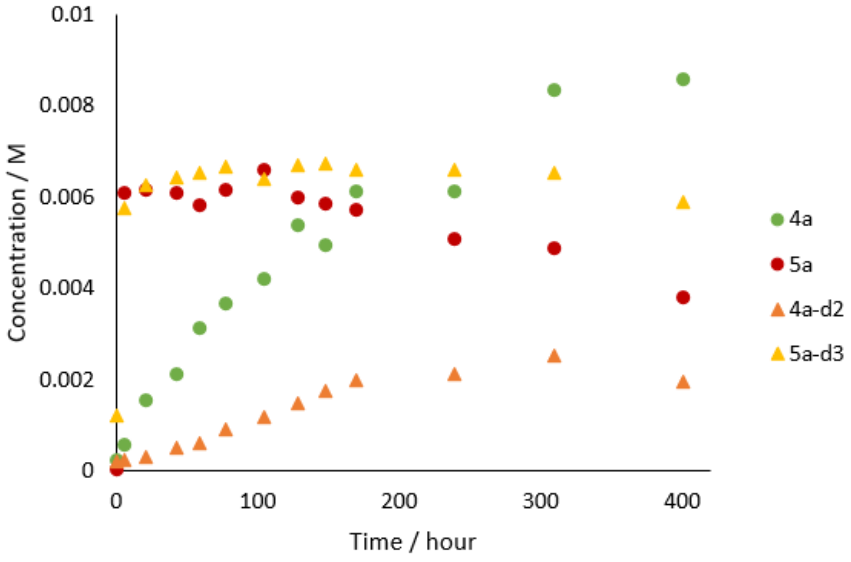

Figure 4.26: Kinetic profile of the competition experiment between **1a** and **1a-*d*$_3$**.

AS before, all spectra acquired within the same experiment were processed by the same method to minimise error. Typical ^{1}H NMR spectra after manual phase correction and baseline correction are shown. By referring to the integral of the internal standard (1,2,3-trifluoromethoxybenzene), the concentrations of benzylic bromides and iodides were calculated. The concentrations of fluorinated products were calculated based on ^{19}F{^{1}H} NMR due of peak overlap in the ^{1}H NMR spectra. Typical ^{19}F{^{1}H} NMR spectra after processing are shown in Figure 4.29. In this experiment, regional baseline correction (Whittaker smoother, filter 3.81 Hz, from 4 to 10 ppm) was required to minimise the effect of neighbouring signals to allow for the integration of elimination species. After performing line fitting on the region of 6.35 to 6.45 ppm, the peaks of the vinylic protons in **4a** (doublet of doublets) and **4a-*d*$_2$** (singlet) could be deconvoluted and their concentrations were calculated (Figure 4.30).

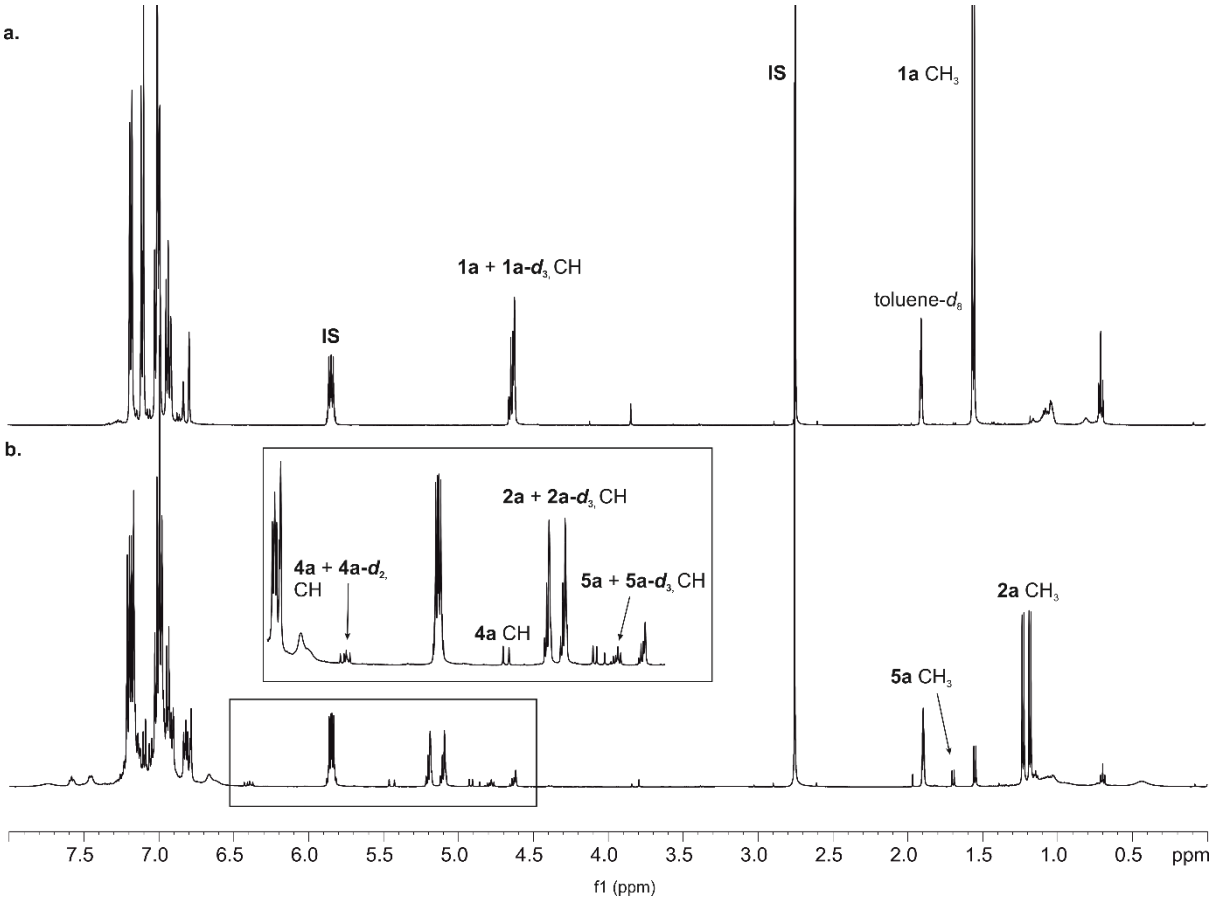

Figure 4.27: Typical ^{1}H NMR spectra of the reaction mixture; a. before the reaction was started, b. when the reaction reached ~90% conversion.

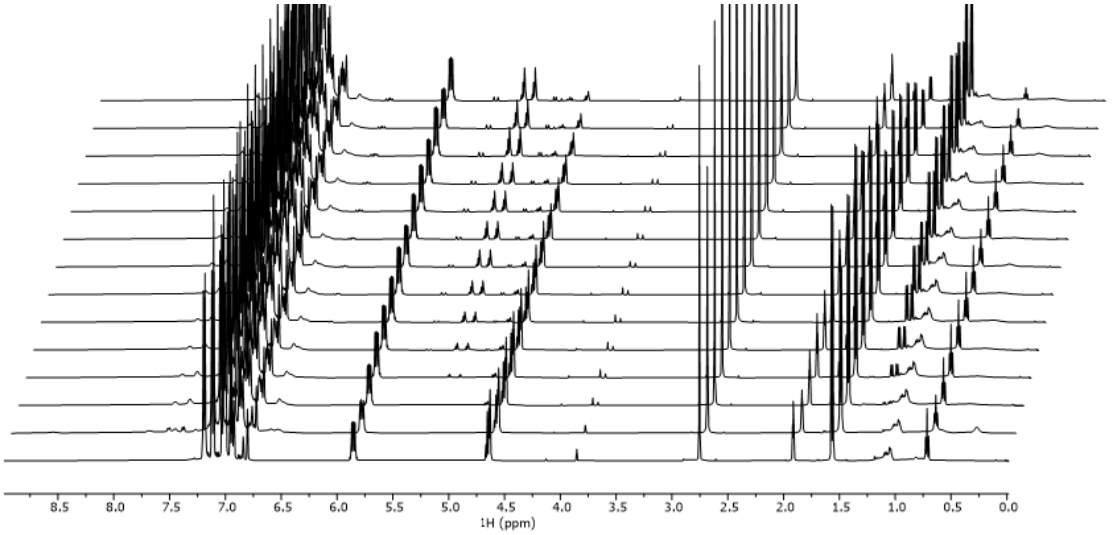

Figure 4.28: Stacked ^{1}H NMR spectra for competition experiment between **1a** and **1a-*d*$_3$**.

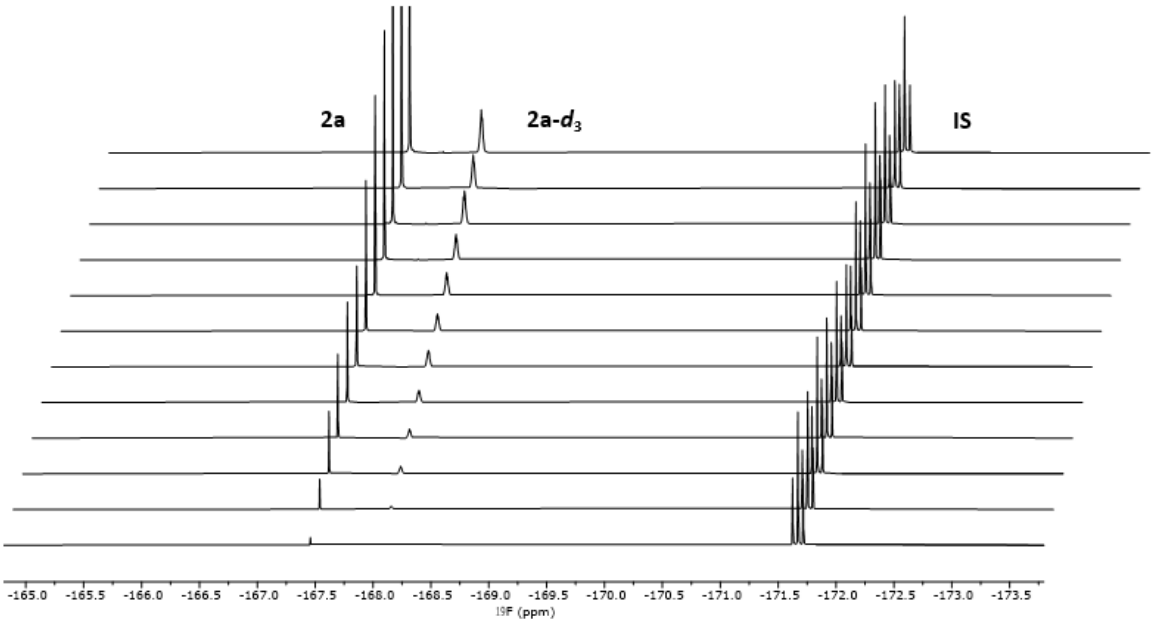

Figure 4.29: Stacked $^{19}F\{^{1}H\}$ NMR spectra for competition experiment between **1a** and **1a-*d*$_3$**.

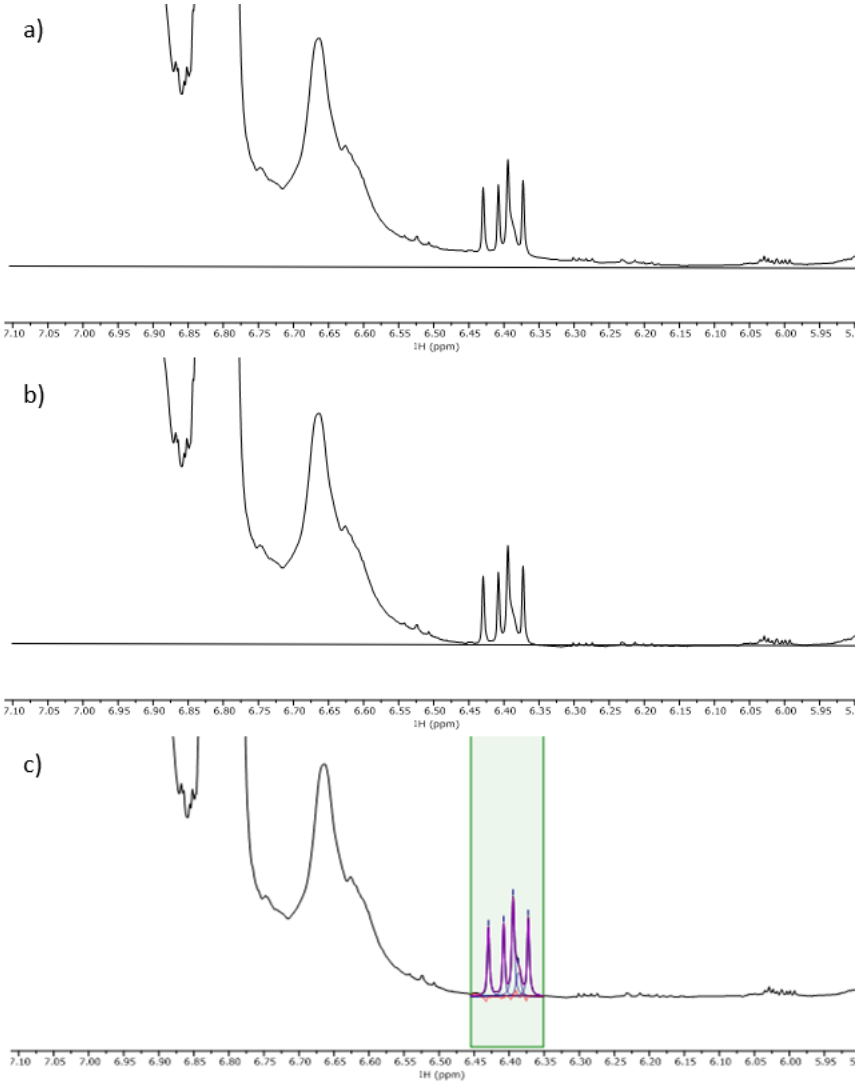

Figure 4.30: An example of ^{1}H NMR spectra for overlapping vinylic **4a** (dd) and **4a-*d*$_2$** (s); a. before regional baseline correction, b. following regional baseline correction, c. after line fitting.

(Regional baseline correction and deconvolution performed by Y. Gao)

4.9.2. Calculation of KIE Values

4.9.2.1. Calculation of Competition α-SKIE

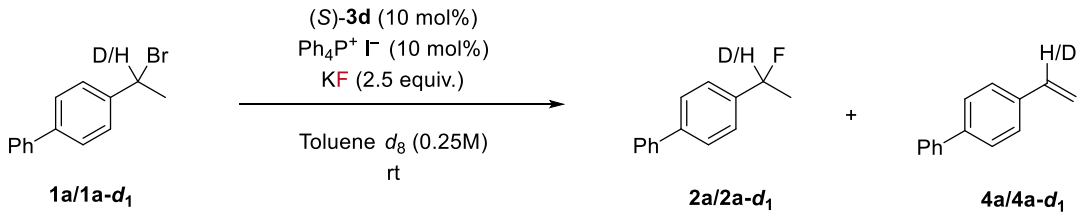

1a/1a-d_1 **2a/2a-d_1** **4a/4a-d_1**

The pseudo first-order rate constants, $k_{obs(H)}$ and $k_{obs(D)}$ for the conversion of **1a** and **1a-d_1** were estimated semi-logarithmically, $\ln([A_0]/[A_t]) = k_{obs}\,t$; where A_0 is the initial concentration of benzylic bromide (**1**), and A_t is the concentration of benzylic bromide at time *t*. The same calculation could be performed by considering both benzylic bromide (**1**) and benzylic iodides (**5**) as reactants, i.e., A_0 is the initial concentration of benzylic bromide, and A_t is the total concentration of benzylic bromide and benzylic iodide at time *t*. These plots are shown in Figure 4.31.

Elimination side products (**4a**, **4a-d_1**) were formed during the reaction and it was found that the partition between fluorination and elimination was approximately constant (Figure 4.31 e-f). By using these partition ratios, $r_{A(H)}$ and $r_{A(D)}$, and $KIE_{net} = k_{obs(H)} / k_{obs(D)}$ (Equations 3-5), the KIEs for the fluorination and the elimination were be estimated as shown below, with the results summarised in Table 4.10.

Equation 3:

$$KIE_{\text{net}} = \frac{k_{\text{F(H)}} + k_{\text{Elim(H)}}}{k_{\text{F(D)}} + k_{\text{Elim(D)}}}\ ;\ r_{\text{AH}} = \frac{k_{\text{F(H)}}}{k_{\text{Elim(H)}}}\ and\ r_{\text{AD}} = \frac{k_{\text{F(D)}}}{k_{\text{Elim(D)}}}$$

Equation 4:

$$\text{KIE (F}-\text{addition)} \approx KIE_{\text{net}} \left(\frac{1 + \frac{1}{r_{\text{AD}}}}{1 + \frac{1}{r_{\text{AH}}}}\right) = \left(\frac{1.38}{1.27}\right)\left(\frac{1 + \frac{1}{13}}{1 + \frac{1}{12}}\right) = 1.1$$

Equation 5:

$$\text{KIE (elimination)} \approx KIE_{\text{net}} \left(\frac{1 + r_{\text{AD}}}{1 + r_{\text{AH}}}\right) = \left(\frac{1.38}{1.27}\right)\left(\frac{1 + 13}{1 + 12}\right) = 1.2$$

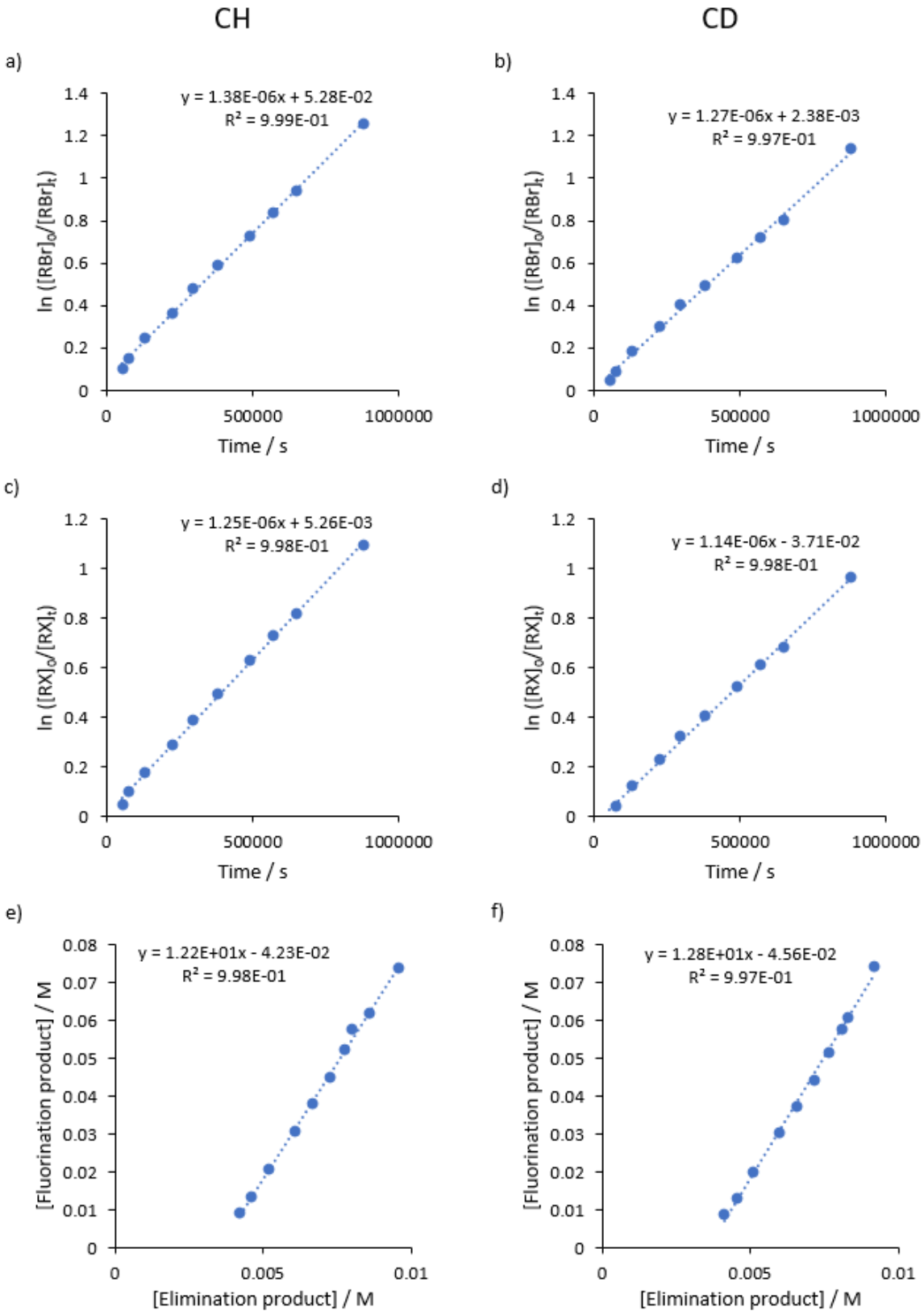

Figure 4.31: Plots of ln([A_0]/[A_t]) against time for non-deuterated (a,c) and deuterated substrate (b,d); [RX] = [RBr]+[RI]. Partitions $r_{A(H)}$ and $r_{A(D)}$ for addition versus elimination for non-deuterated (e) and deuterated substrate (f).

4.9.2.2. Calculation of Competition β-SKIE

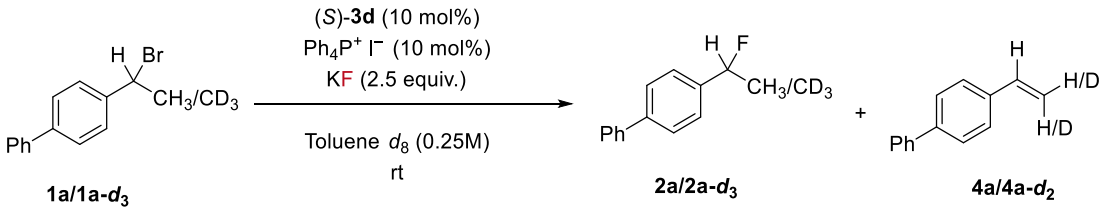

An analogous method that was applied to the α-SKIE was used for calculation of β-SKIE, and key plots shown in Figure 4.32. The results for the KIE are summarised in Table 4.10.

Independent experiments performing the reaction from the non-labelled (**1a**) and the labelled substrate (**1a-*d*$_3$**) were also performed, with the partition ratios, $r_{A(H)}$ and $r_{A(D)}$, for fluorination over elimination were found to be 10 and 27 respectively, i.e. the same as what was observed in the competition β-SKIE experiment.

Equation 3:

$$KIE_{\text{net}} = \frac{k_{\text{F(H)}} + k_{\text{Elim(H)}}}{k_{\text{F(D)}} + k_{\text{Elim(D)}}} \; ; \; r_{\text{AH}} = \frac{k_{\text{F(H)}}}{k_{\text{Elim(H)}}} \; and \; r_{\text{AD}} = \frac{k_{\text{F(D)}}}{k_{\text{Elim(D)}}}$$

Equation 4:

$$\text{KIE (F– addition)} \approx KIE_{\text{net}} \left(\frac{1 + \frac{1}{r_{\text{AD}}}}{1 + \frac{1}{r_{\text{AH}}}} \right) = \left(\frac{1.56}{1.31} \right) \left(\frac{1 + \frac{1}{27}}{1 + \frac{1}{10}} \right) = 1.1$$

Equation 5:

$$\text{KIE (elimination)} \approx KIE_{\text{net}} \left(\frac{1 + r_{\text{AD}}}{1 + r_{\text{AH}}} \right) = \left(\frac{1.56}{1.31} \right) \left(\frac{1 + 27}{1 + 10} \right) = 3.0$$

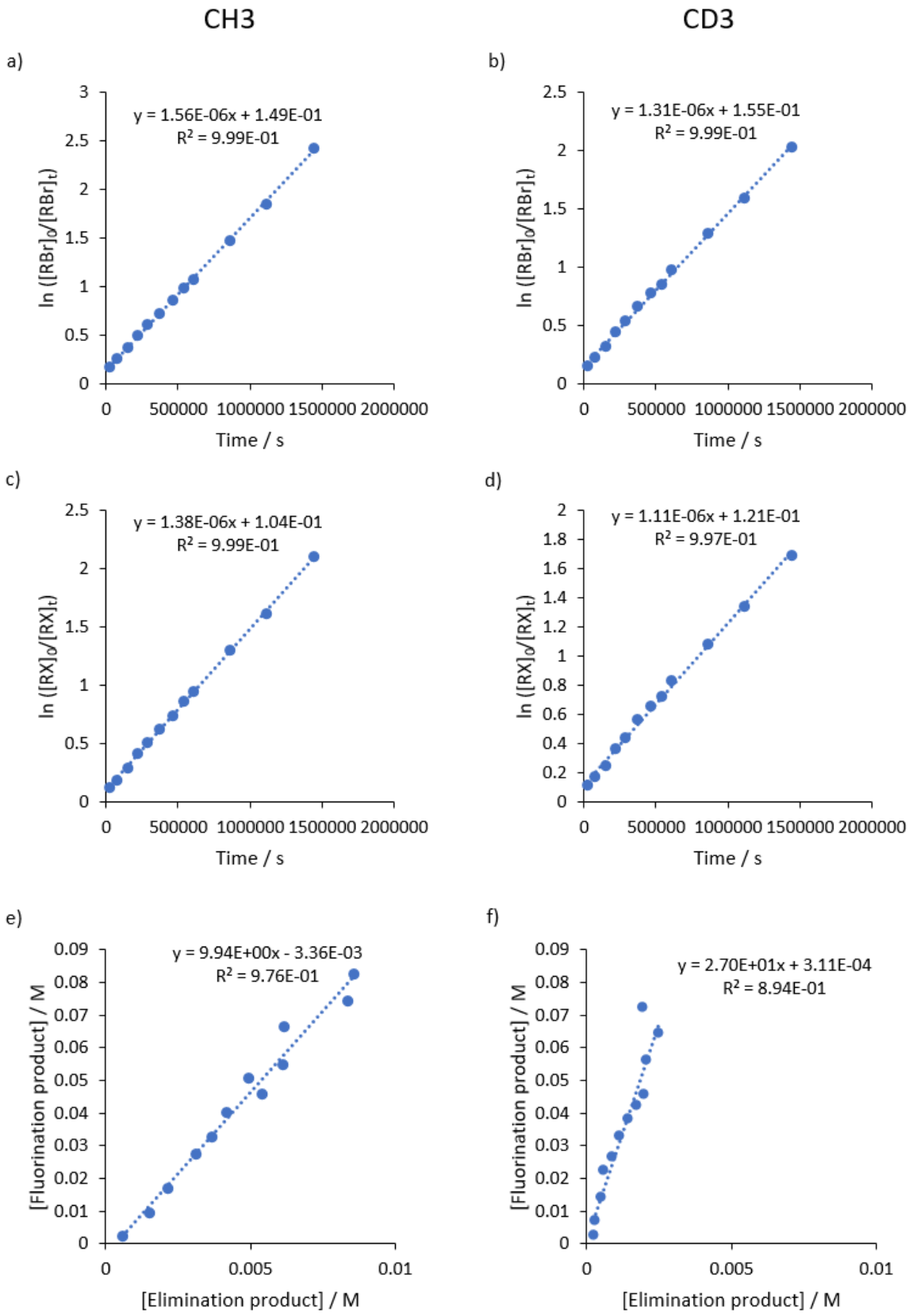

Figure 4.32: Plots of ln([A_0]/[A_t]) against time for non-deuterated (a,c) and deuterated substrate (b,d); [RX] = [RBr]+[RI]. Partitions $r_{A(H)}$ and $r_{A(D)}$ for addition versus elimination for non-deuterated (e) and deuterated substrate (f).

4.9.2.3. Calculation of Competition β-SKIE (TBAF)

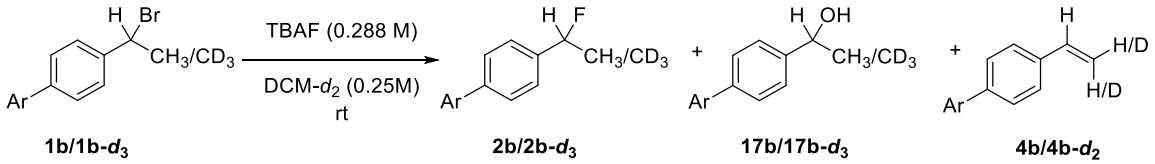

1b/1b-d_3 **2b/2b-d_3** **17b/17b-d_3** **4b/4b-d_2**

Ar = C_6H_5F

In this experiment, tetra-n-butylammonium fluoride trihydrate (TBAF·$3H_2O$) was used as a fluorinating reagent in the place of KF and catalysts (**3d** and $Ph_4P^+ I^-$) for comparison. The reaction was performed in DCM-d_2 due to the poor solubility of TBAF in toluene. This homogeneous reaction was set up in a sealed J. Young Norell 5mm NMR tube and was left in the spectrometer taking quantitative ^1H and ^{19}F spectra hourly over the course of the reaction. During the reaction, the formation of secondary alcohols **17b** and **17b-d_3** was observed, and their identities were confirmed through spiking of authentic references.

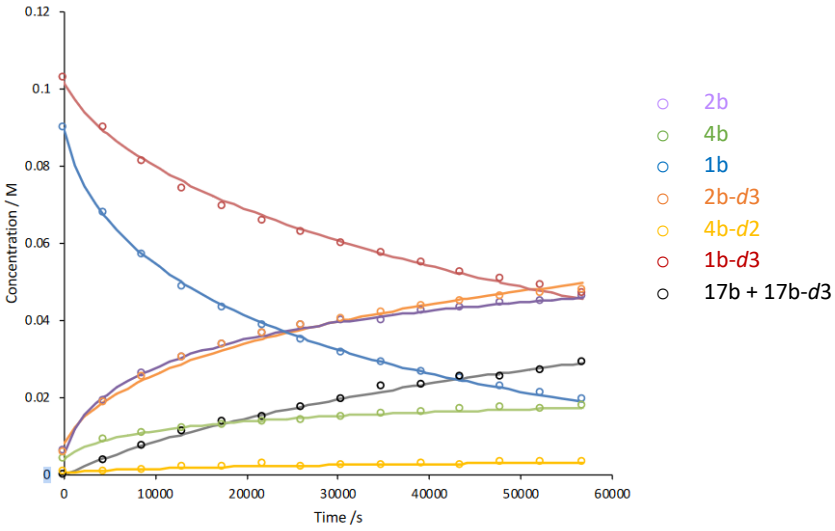

Figure 4.43: Kinetic profile for competition between **1b** and **1b-d_3** under homogeneous fluorination conditions with TBAF

The data obtained for this reaction did not correspond to simple pseudo first order decay of the substrate, and the net KIE was calculated using the Bigeleisen-Wolfsberg equation (Equation 6),[35, 36] in which F is the total fractional conversion of the substrates (**1b** + **1b-d_3**) to products (**2b**, **2b-d_3**, **4b**, **4b-**

***d*₂**, **17b**, **17b-*d*₂**), R_0 is the initial ratio of labelled to unlabelled substrate ([**1a-*d*₃**]$_0$/[**1a**]$_0$) and R the same ratio measured after a given fractional conversion, F.

Equation 6:

$$\frac{k_H}{k_D} = \frac{\ln\left((1-F)\left(\frac{1+R_0}{1+R}\right)\right)}{\ln\left((1-F)\left(\frac{R}{R_0}\right)\left(\frac{1+R_0}{1+R}\right)\right)}$$

The Bigeleisen-Wolfsberg equation (Equation 6) can be rearranged to an equation that defines F, and the KIE then calculated by non-linear regression of R/R_0 versus F using the KIE as the fitting parameter. The fitting for R/R_0 against F is shown in Figure 4.34. The overall KIE was estimated to be 1.93.

$$F = 1 - \left(\frac{1+R}{1+R_0}\right)\left(\frac{R}{R_0}\right)^{\frac{\frac{k_H}{k_D}}{1-\frac{k_H}{k_D}}}$$

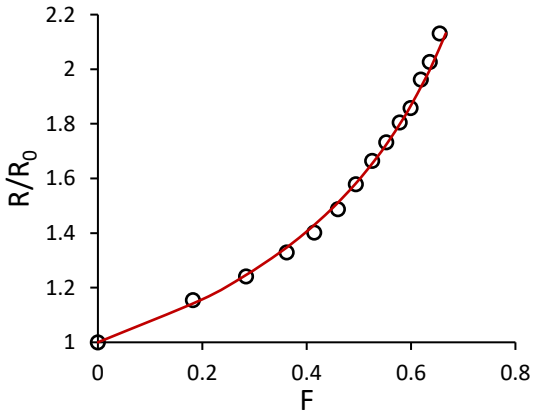

Figure 4.34: R/R_0 versus fractional conversion, F, for the intermolecular competition of [**1a-*d*₃**] against [**1a**] for reaction with TBAF·3H$_2$O in DCM. Experimental data (black open circles) and fitting of the Bigeleisen-Wolfsberg equation, when KIE_{net} = 1.93 (red line).

The fluorination / elimination partition ratios, r_H and r_D, were also estimated by plotting the temporal concentrations of the addition products (**2b**, **2b-*d*₃**, **17b**, **17b-*d*₂**) against those of the elimination products (**4b**, **4b-*d*₂**), and fluoride addition / water addition partition ratios, r_{FH} and r_{FD}, were estimated by plotting the temporal concentrations of (**2b**, **2b-*d*₃**) against those of (**17b**, **17b-*d*₂**) (Figure 4.35).

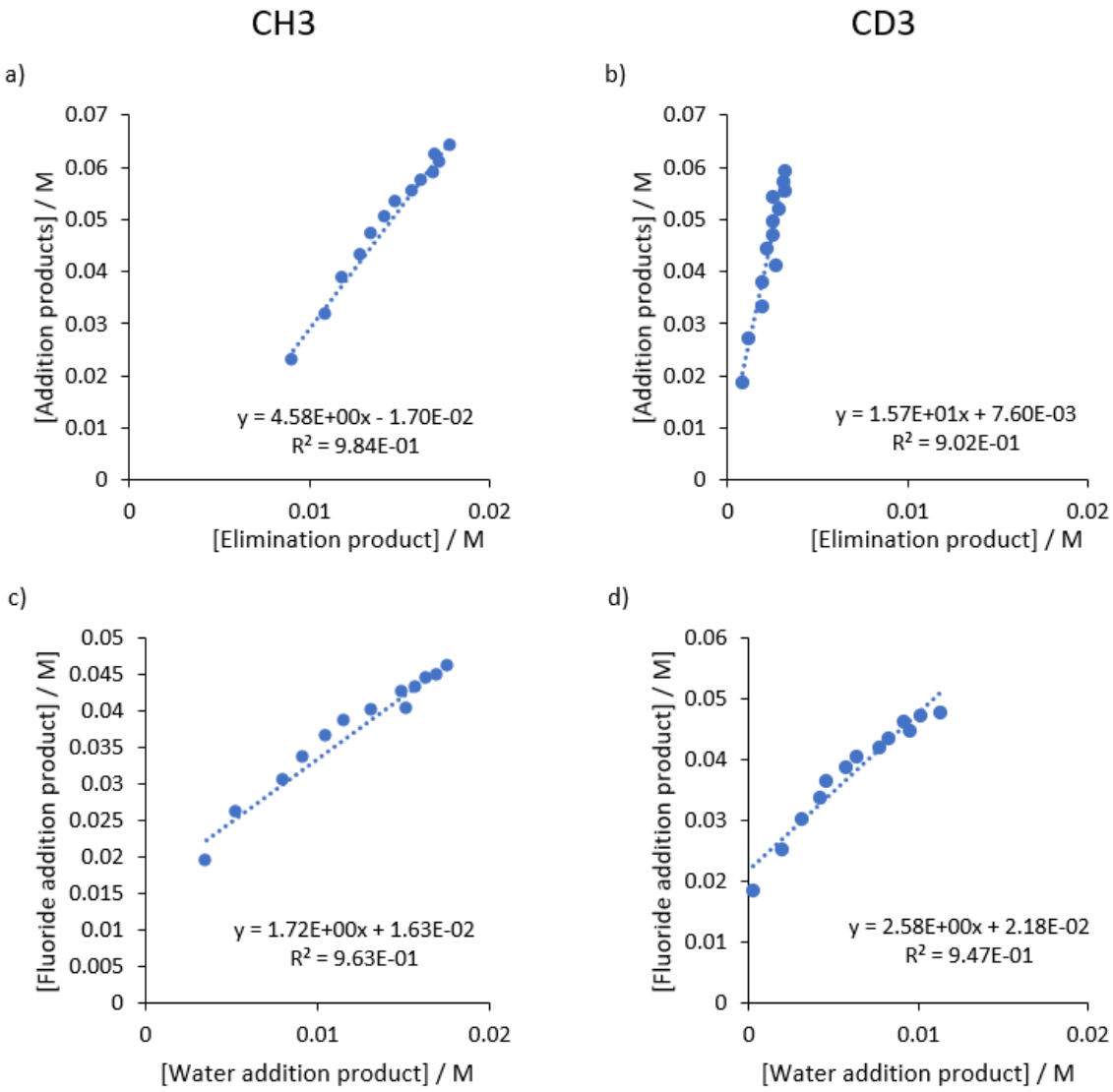

Figure 4.35: Partitions $r_{A(H)}$ and $r_{A(D)}$ for addition versus elimination for non-deuterated (a) and deuterated substrate (b). Partitions $r_{F(H)}$ and $r_{F(D)}$ for fluoride addition versus water addition for non-deuterated (c) and deuterated substrate (d).

The value of KIE_{net} calculated from the Bigeleisen-Wolfsberg analysis was used to estimate the KIE values for fluoride addition and elimination, based on the relationships below (Equations 7 – 10).

Equation 7:

$$r_{\mathrm{FH}} = \frac{k_{\mathrm{F(H)}}}{k_{\mathrm{H2O(H)}}}; r_{\mathrm{AH}} = \frac{k_{\mathrm{F(H)}} + k_{\mathrm{H2O(H)}}}{k_{\mathrm{Elim(H)}}}; r_{\mathrm{FD}} = \frac{k_{\mathrm{F(D)}}}{k_{\mathrm{H2O(D)}}}; r_{\mathrm{AD}} = \frac{k_{\mathrm{F(D)}} + k_{\mathrm{H2O(D)}}}{k_{\mathrm{Elim(D)}}}$$

Equation 8:

$$KIE_{\mathrm{net}} = \frac{k_{\mathrm{F(H)}} + k_{\mathrm{H2O(H)}} + k_{\mathrm{Elim(H)}}}{k_{\mathrm{F(D)}} + k_{\mathrm{H2O(D)}} + k_{\mathrm{Elim(D)}}}$$

Equation 9:

$$\mathrm{KIE\ (F-addition)} \approx KIE_{\mathrm{net}} \frac{1+\left(\frac{1+\frac{1}{r_{\mathrm{FD}}}}{r_{\mathrm{AD}}}\right)+\left(\frac{1}{r_{\mathrm{FD}}}\right)}{+\left(\frac{1+\frac{1}{r_{\mathrm{FH}}}}{r_{\mathrm{AH}}}\right)+\left(\frac{1}{r_{\mathrm{FH}}}\right)} = 1.93 \frac{1+\left(\frac{1+\frac{1}{2.6}}{15.7}\right)+\left(\frac{1}{2.6}\right)}{1+\left(\frac{1+\frac{1}{1.7}}{4.6}\right)+\left(\frac{1}{1.7}\right)} = 1.5$$

Equation 10:

$$\mathrm{KIE\ (elimination)} \approx KIE_{\mathrm{net}} \left(\frac{1+r_{\mathrm{AD}}}{1+r_{\mathrm{AH}}}\right) = 1.93\left(\frac{1+15.7}{1+4.6}\right) = 5.8$$

It should be noted that the analysis assumes first-order competition between the labelled and unlabelled substrate, that the competing reactions are irreversible, and the net KIE is constant with conversion. The competing hydrolysis and the potential impact of an accumulating bromide common ion-effect on fluoride addition and elimination S_N1/E1-like pathways, may therefore affect the validity of these assumptions.

Table 4.10: A summary of KIEs:

		KIE
Competition α-SKIE	Fluorination	1.1
	Elimination	1.2
Competition β-SKIE	Fluorination	1.1
	Elimination	3.0
Competition β-SKIE (with TBAF)	Fluorination	1.5
	Elimination	5.8

4.10. References

(1) Yin, X. M.; Chen, B.; Qiu, F.; Wang, X. H.; Liao, Y.; Wang, M.; Lei, X. X.; Liao, J. Enantioselective Palladium-Catalyzed Hydrofluorination of Alkenylarenes. *ACS Catal.* **2020**, *10* (3), 1954–1960.
(2) Phipps, R. J.; Hiramatsu, K.; Toste, F. D. Asymmetric Fluorination of Enamides: Access to α-Fluoroimines Using an Anionic Chiral Phase-Transfer Catalyst. *J. Am. Chem. Soc.* **2012**, *134* (20), 8376–8379.
(3) Pupo, G.; Ibba, F.; Ascough, D. M. H.; Vicini, A. C.; Ricci, P.; Christensen, K. E.; Pfeifer, L.; Morphy, J. R.; Brown, J. M.; Paton, R. S.; Gouverneur, V. Asymmetric Nucleophilic Fluorination under Hydrogen Bonding Phase-Transfer Catalysis. *Science* **2018**, *360* (6389), 638–642.
(4) Pupo, G.; Vicini, A. C.; Ascough, D. M. H.; Ibba, F.; Christensen, K. E.; Thompson, A. L.; Brown, J. M.; Paton, R. S.; Gouverneur, V. Hydrogen Bonding Phase-Transfer Catalysis with Potassium Fluoride: Enantioselective Synthesis of beta-Fluoroamines. *J. Am. Chem. Soc.* **2019**, *141* (7), 2878–2883.
(5) Ibba, F.; Pupo, G.; Thompson, A. L.; Brown, J. M.; Claridge, T. D. W.; Gouverneur, V. Impact of Multiple Hydrogen Bonds with Fluoride on Catalysis: Insight from NMR Spectroscopy. *J. Am. Chem. Soc.* **2020**, *142* (46), 19731–19744.
(6) Yang, Y.; Tokunaga, E.; Akiyama, H.; Saito, N.; Shibata, N. Bis(pentafluorosulfanyl)phenyl Azide as an Expeditious Tool for Click Chemistry toward Antitumor Pharmaceuticals. *ChemMedChem* **2014**, *9* (5), 913–917.
(7) Adak, L.; Yoshikai, N. Cobalt-Catalyzed Preparation of Arylindium Reagents from Aryl and Heteroaryl Bromides. *J. Am. Chem. Soc.* **2011**, *76* (18), 7563–7568.
(8) Sato, T. Estrogenic Biphenyls 8. Preparation and Estrogenic Activity of 4'-(1-hydroxyalkyl)-4-methoxybiphenyls. *BCJS* **1960**, *33* (1), 5–7.
(9) Min, S. Y.; Song, H. X.; Yan, S. S.; Yuan, R.; Ye, J. H.; Wang, B. Q.; Gui, Y. Y.; Yu, D. G. Photocatalytic Defluorocarboxylation using Formate Salts as Both a Reductant and a Carbon Dioxide Source. *Green Chem.* **2023**, *25* (16), 6194–6199.
(10) Fialho, D. M.; Etemadi-Davan, E.; Langner, O. C.; Takale, B. S.; Gadakh, A.; Sambasivam, G.; Lipshutz, B. H. Copper-Catalyzed Asymmetric Reductions of Aryl/Heteroaryl Ketones under Mild Aqueous Micellar Conditions. *Org. Lett.* **2021**, *23* (9), 3282–3286.
(11) Helberg, J.; Marin-Luna, M.; Zipse, H. Chemoselectivity in Esterification Reactions - Size Matters after All. *Synth.* **2017**, *49* (15), 3460–3470.
(12) Tanaka, K.; Tomihama, M.; Yamamoto, K.; Matsubara, N.; Harada, T. Method for Catalytic Enantioselective Alkylation of Aldehydes Using Grignard Reagents as Alkyl Sources. *J. Org. Chem.* **2018**, *83* (11), 6127–6132.
(13) Ehrlich, R. S.; Shiao, A. L.; Li, M. H.; Teppang, K. L.; Jeoung, K. Y.; Theodorakis, E. A.; Yang, J. Exploring the Effect of Aliphatic Substituents on Aryl Cyano Amides on Enhancement of Fluorescence upon Binding to Amyloid-β Aggregates. *ACS Chem. Neurosci.* **2021**, *12* (15), 2946–2952.
(14) Balakrishnan, V.; Murugesan, V.; Chindan, B.; Rasappan, R. Nickel-Mediated Enantiospecific Silylation via Benzylic C-OMe Bond Cleavage. *Org. Lett.* **2021**, *23* (4), 1333–1338.
(15) Andrade, L. H.; Barcellos, T. Lipase-Catalyzed Highly Enantioselective Kinetic Resolution of Boron-Containing Chiral Alcohols. *Org. Lett.* **2009**, *11* (14), 3052–3055.
(16) Mai, W. P.; Wang, H. H.; Li, Z. C.; Yuan, J. W.; Xiao, Y. M.; Yang, L. R.; Mao, P.; Qu, L. B. *n*Bu_4N I-catalyzed direct synthesis of α-ketoamides from aryl methyl ketones with dialkylformamides in water using TBHP as oxidant. *Chem. Commun.* **2012**, *48* (81), 10117–10119.
(17) Danahy, K. E.; Cooper, J. C.; Van Humbeck, J. F. Benzylic Fluorination of Aza-Heterocycles Induced by Single-Electron Transfer to Selectfluor. *Angew. Chem. Int. Ed.* **2018**, *57* (18), 5134–5138.
(18) Wang, B.; Sun, H. X.; Sun, Z. H.; Lin, G. Q. Direct B-Alkyl Suzuki-Miyaura Cross-Coupling of Trialkylboranes with Aryl Bromides in the Presence of Unmasked Acidic or Basic Functions and Base-Labile Protections under Mild Non-Aqueous Conditions. *ACS.* **2009**, *351* (3), 415–422.
(19) Tang, S. Z.; Xiang, K.; Ye, R.; Chen, M. E.; Yu, J. C.; He, Z. J.; Zhang, F. M. Preparation of Thioamides from Alkyl Bromides, Nitriles, and Hydrogen Sulfide Through a Thio-Ritter-Type Reaction. *Chem. Commun.* **2022**, *58* (81), 11430–11433.

(20) Liardo, E.; Ríos-Lombardía, N.; Morís, F.; González-Sabín, J.; Rebolledo, F. A Straightforward Deracemization of *sec*-Alcohols Combining Organocatalytic Oxidation and Biocatalytic Reduction. *Eur. J. Org. Chem.* **2018**, *2018* (23), 3031–3035.
(21) Kline, R. H.; Izenwasser, S.; Katz, J. L.; Joseph, D. B.; Bowen, W. D.; Newman, A. H. 3'-chloro-3 Alpha-(diphenylmethoxy)tropane but Not 4'-chloro-3 Alpha-(diphenylmethoxy)tropane Produces a Cocaine-Like Behavioral Profile. *J. Med. Chem.* **1997**, *40* (6), 851–857.
(22) Kuang, C. W.; Zhou, X.; Xie, Q. Q.; Ni, C. F.; Gu, Y. C.; Hu, J. B. Generation of Carbocations under Photoredox Catalysis: Electrophilic Aromatic Substitution with 1-Fluoroalkylbenzyl Bromides. *Org. Lett.* **2020**, *22* (21), 8670–8675.
(23) Hergueta, A. R. Easy Removal of Triphenylphosphine Oxide from Reaction Mixtures by Precipitation with $CaBr_2$. *OPR&D.* **2022**, *26* (6), 1845–1853.
(24) Chen, H. J.; Teo, R. H. X.; Li, Y. X.; Pullarkat, S. A.; Leung, P. H. Stereogenic Lock in 1-Naphthylethanamine Complexes for Catalyst and Auxiliary Design: Structural and Reactivity Analysis for Cycloiridated Pseudotetrahedral Complexes. *Organometallics* **2018**, *37* (1), 99–106.
(25) Yang, W.; Chen, C.; Chan, K. S. Hydrodebromination of Allylic and Benzylic Bromides with Water Catalyzed by a Rhodium Porphyrin Complex. *Dalton Trans.* **2018**, *47* (37), 12879–12883.
(26) Wang, F.; Nishimoto, Y.; Yasuda, M. Indium-Catalyzed Formal Carbon-Halogen Bond Insertion: Synthesis of α-Halo-α,α-disubstituted Esters from Benzylic Halides and Diazo Esters. *Org. Lett.* **2022**, *24* (8), 1706–1710.
(27) Li, Z. Y.; Wang, B. C.; Zhang, C. S.; Lo, W. Y.; Yang, L. L.; Sun, J. W. Catalytic Enantioselective Nucleophilic α-Chlorination of Ketones with NaCl. *J. Am. Chem. Soc.* **2024**, *146* (4), 2779–2788.
(28) Zhu, M.; Wei, W.; Yang, D.; Cui, H.; Cui, H.; Sun, X.; Wang, H. NBS/DBU mediated one-pot synthesis of α-acyloxyketones from benzylic secondary alcohols and carboxylic acids. *Org. Biomol. Chem*. **2016**, *14* (46), 10998–11001.
(29) Yamauchi, T.; Hattori, K.; Nakao, K.; Tamaki, K. A Facile and Efficient Preparative Method of Methyl 2-Arylpropanoates by Treatment of Propiophenones and Their Derivatives with Iodine or Iodine Chlorides. *J. Org. Chem.* **1988**, *53* (20), 4858–4859.
(30) Müller, M.; Albrecht, M.; Sackmann, J.; Hoffmann, A.; Dierkes, F.; Valkonen, A.; Rissanen, K. CH-Anion *vs* Anion-π Interactions in the Crystal and in Solution of Pentafluorobenzyl Phosphonium Salts. *Dalton Trans.* **2010**, *39* (47), 11329–11334.
(31) Stridfeldt, E.; Lindstedt, E.; Reitti, M.; Blid, J.; Norrby, P. O.; Olofsson, B. Competing Pathways in O-Arylations with Diaryliodonium Salts: Mechanistic Insights. *Chem. Eur. J.* **2017**, *23* (53), 13249–13258.
(32) Zhang, B.; Li, T.; Mao, Z.; Jiang, M.; Zhang, Z.; Zhao, K.; Qu, W.; Xiao, W.; Chen, J. Enantioselective Cyanofunctionalization of Aromatic Alkenes via Radical Anions. *J. Am. Chem. Soc.* **2024**, *146* (2), 1410–1422.
(33) Yu, C.; Levy, G. C. Two-Dimensional Heteronuclear NOE (HOESY) Experiments - Investigation of Dipolar Interactions Between Heteronuclei and Nearby Protons. *J. Am. Chem. Soc.* **1984**, *106* (22), 6533–6537.
(34) Enthart, A.; Freudenberger, J. C.; Furrer, J.; Kessler, H.; Luy, B. The CLIP/CLAP-HSQC: Pure Absorptive Spectra for the Measurement of One-Bond Couplings. *J. Magn. Reson.* **2008**, *192* (2), 314–322.
(35) Bigeleisen, J.; Wolfsberg, M. Theoretical and Experimental Aspects of Isotope Effects in Chemical Kinetics. *Adv. Chem. Phys.* **1958**, *1*, 15–76.
(36) Ben-Tal, Y.; Boaler, P. J.; Dale, H. J. A.; Dooley, R. E.; Fohn, N. A.; Gao, Y.; García-Domínguez, A.; Grant, K. M.; Hall, A. M. R.; Hayes, H. L. D.; Kucharski, M. M.; Wei, R.; Lloyd-Jones, G. C. Mechanistic Analysis by NMR Spectroscopy: A Users Guide. *Prog. Nucl. Magn. Reson. Spectrosc.* **2022**, *129*, 28–106.